1986

SIMULATION OF POLLUTANT TRANSPORT RESPONSES TO LOADING AND WEATHER VARIATIONS IN LAKE ST. CLAIR AND THE CONNECTING CHANNELS.

KAMAL ABOU EL-HASSAN ALY. IBRAHIM
University of Windsor

SIMULATION OF POLLUTANT TRANSPORT RESPONSES TO LOADING AND WEATHER VARIATIONS IN LAKE ST.CLAIR AND THE CONNECTING CHANNELS

by

© Kamal Abou El-Hassan Aly Ibrahim

A Dissertation
Submitted to the Faculty of Graduate Studies through the Department of Civil Engineering in Partial Fulfillment of the Requirements for the Degree of
Doctor of Philosophy at the
University of Windsor

Windsor, Ontario, Canada

1988

ISBN 0-315-29299-7

I hereby declare that I am the sole author of this thesis. I authorize the University of Windsor to lend this thesis to other institutions or individuals for the purpose of scholarly research.

KAMAL ABOU EL-HASSAN ALY IBRAHIM

I further authorize the University of Windsor to reproduce this thesis by photocopying or by other means, in total or in part, at the request of other institutions or individuals for the purpose of scholarly research.

KAMAL ABOU EL-HASSAN ALY IBRAHIM

The University of Windsor requires the signatures of all persons using or photocopying this thesis. Please sign below, and give address and date.

To my parents, Hala and Dina

ABSTRACT

Within the past decade, declining water quality in the Great Lakes has motivated an accelerated interest in both modelling techniques and extensive programs of field observations. This dissertation presents a mathematical modelling framework which can be used to simulate the transport of toxic and conventional substances in surface waters for the Huron-Erie corridor of the Great Lakes. In modelling the fate of a toxic chemical in a natural water system it is necessary to include the dynamic relationship between all phases of the environment (atmospheric, water and sediment). Moreover, it is important to calibrate and verify the numerical models before applying a prediction. The simulation in this study is presented for the transport in rivers as well as the transport in shallow lakes.

In simulating the transport of conventional pollutants in the rivers, a simple hydrodynamic submodel, which includes flow around islands, diversions and confluences, is used to establish the velocity fields. Then, a stream function form of the transport equation is coupled with the k-ε equations in order to obtain the turbulent dispersion coefficients.

The submodel uses a variable grid finite difference scheme. Once the velocity fields and dispersion coefficients have been obtained, the EPA (JOXIWASP) model is used to simulate the interaction between sediments and contaminants. The model was verified by comparing the simulated results with measured levels of HCB in St.Clair River and similarly with measured concentrations of cadmium in the Detroit River.

In an attempt to include the effects of the seasonal variations on the circulation patterns in Lake St.Clair, a three dimensional finite element model which includes wind stress, bottom friction, Coriolis force, inflow, outflow and the bottom topography of the lake was developed and verified with field data. The overall root mean square differences between predicted and measured current magnitudes and directions were 1.3 $cm.s^{-1}$ and 22.5°, respectively, whereas the correlation coefficients were 0.99 and 0.95, respectively. The Hydrodynamic submodel was tested for stability, convergence, and sensitivity to parameters such as wind shear, wind direction, slip-coefficient for bottom friction and vertical eddy viscosity effects.

This submodel was used to generate the typical lake circulation patterns for different steady state wind and ice conditions which are required for the long-term pollutant simulation study by the EPA (TOXIWASP) model. The depth averaged velocities were also used in finite element pollutant and suspended sediment transport models. An upwind finite element formulation was used to obtain a stable solution for the steady state convective transport phenomena. The predicted pollutant (chloride ion) and the suspended solids concentration patterns were compared with observed field data and fairly good agreement was obtained. By allowing a variable resuspension velocity for the sediments in bed segments, the EPA (TOXIWASP) model appeared to be able to reasonably simulate the transport of toxic chemicals for representative weather conditions in Lake St.Clair. A long-term simulation in Lake St.Clair was implemented in order to roughly predict the loading of PCBs during the period of 1970 to 1974.

In general, this framework can offer the basis for quantifying the water quality responses to the man-made and natural changes in loading and climate. The models were used to study four toxic contaminants-lead, cadmium, PCBs and octachlorostyrene in this region. Specifically, the models were used to predict the best estimates for these contaminant loads. Furthermore, investigations were carried out using hypothetical loads released from selected locations to make interferences about the distribution patterns or even to show how the concentrations would change with time if a particular contaminant load is changed in the region.

ACKNOWLEDGEMENTS

My sincere thanks and gratitude are due to HIS ALMIGHTY, ALLAH, WHO helped and blessed me during the course of my studies.

This dissertation is the culmination of much work and I would like to take this opportunity to thank those who helped make it possible. Heading the list is my advisor Dr. J.A. McCorquodale who suggested the basic theme of this research and who has been a continuous source of support and creative insight throughout the duration of this work. Several other people deserve special mention. I would particularly like to thank Dr. Bewtra for his deep interest. The remaining of my committee, Dr. S. P. Chee and Dr. A. C. Smith were responsible for valuable improvements in the manuscript. P. Nettleton is a fellow graduate student and a good friend, who has helped me collect the required data.

Acknowledgement should also be given to Dr. M. Sanderson, Director of the Great Lakes Institute, University of Windsor, to the department of Civil Engineering and the Natural Science and Engineering Research Council of Canada for their financial support during this research. I am grateful to the Civil Engineering Department, Cairo University for having provided with study leave.

With deep sincerity, I am highly grateful to my wife Hala and my family for their encouragement, continued support and patience during my educational career.

TABLE OF CONTENTS

DEDICATION vi

ABSTRACT vii

ACKNOWLEDGEMENTS x

LIST OF FIGURES xvi

LIST OF TABLES xxv

I: INTRODUCTION 1

Objective 1
Statement of the Problem 2
Site Description 4
Lake St.Clair 5
St.Clair River 6
Detroit River 6
General Approach 7
Simulation of River Transport 9
Simulation of Lake Transport 11

II: BACKGROUND AND REVIEW OF LITERATURE 13

General 13
Dispersion of Pollutant in Rivers 13
Lake Circulation Models 17
Toxic Chemicals 23
Speciation Processes 24
Acid-Base Effects 24
Sorption on Suspended Sediments 25
Transport Processes 28
Volatilization 28
Sediment Transport 29
Bed Sedimentation 30
Transformation Processes 31
Biodegradation 31
Photolysis and Hydrolysis 32

Part 1: SIMULATION OF RIVER TRANSPORT

III: THEORETICAL DEVELOPMENTS 35
General 35
Hydrodynamic Submodel 36
Model Description 38
Pollutant Transport Model 39
Numerical Method 41
Boundary Conditions 45
Outfalls and Source Streams 46
Turbulence Model 47
Toxic Chemical Model 50
River Segmentation 53

IV: RIVER MODELS CALIBRATION AND VALIDATION 54
General 54
St.Clair River 55
The Hydrodynamics For St.Clair River 56
HCB Simulation 58
Pollutant Transport Submodel In St.Clair River 59
Toxic Chemical Model For HCB 60
Simulation Results For HCB 62
Detroit River 65
Hydrodynamics Of Detroit River 65
Cadmium Calibration In Detroit River 66
Pollutant Transport Submodel For Detroit River 67
Toxic Chemical Model For Cadmuim 67
Calibration Results For Cadmium 68

Part 2: SIMULATION OF LAKE TRANSPORT

V: THEORETICAL DEVELOPMENTS 71
General 71
Hydrodynamic Submodel 71
Mathematical Formulation 72
Formulation of the Numerical Schemes 82
Pollutant Transport Model 89
Governing Equations 89
Finite Element Formulations 91
The Convective Transport Problem 92
Suspended Solids Transport 95
Model Structure 96
Numerical Solution 97
Statistical Model 99
Toxic Chemical Model 100

VI: LAKE MODELS CALIBRATION AND VALIDATION 103
General 103
Hydrodynamic Submodel 104

The Effect of Inertia on Flow Pattern 105
Sensitivity Analysis 108
Wind Stresses 108
Vertical Eddy Viscosity 111
Bottom Boundary Conditions 112
Velocity Measurement 113
Pollutant Submodel 115
Suspended Solids 116
PCBs: Calibration, 1970 to 1974 119
Loading Estimates 120
Suspended Sediments 120
Atmospheric Loads 121
Tributaries and Point Sources 121
Currents and Wind Stresses 122
PCBs Simulation Results 123

Part 3: MODEL APPLICATIONS AND CONCLUSIONS

VII: MODEL APPLICATIONS 127
General 127
Simulation Procedure 128
Sediment Balance 130
Octachlorostyrene 131
Simulation Parameters 132
Simulation Results 133
Analysis 138
Polychlorinated Biphenyls 139
PCBs Simulation Parameters 141
Simulation Results 142
Analysis 143
Lead 144
Simulation Parameters 145
Simulation Results 146
Analysis 148
Cadmium 149
Simulation Parameters 150
Simulation Results 151
Evaluations of Model Performance 153

VIII: CONCLUSIONS AND RECOMMENDATIONS 155
General 155
Specific Conclusions 158
Recommendations 161
Measurements 161
Parameter Estimation 162
Theoretical Developments 163

Appendix A: COEFFICIENTS OF THE LAKE CIRCULATION EQUATIONS 164

Appendix B: TOXIWASP MODEL SEGMENT PARAMETERS 169

General 170

Appendix C: FLOW CHARTS AND LISTING OF THE COMPUTER PROGRAMS 189

Users Guide for River Pollutant Transport Model . . 190
Listing of the (k-ε) Computer Program 191
The Computer Flow Chart for the Finite Element Model 211
Listing of the Finite Element Subroutines 215

Appendix D: FIGURES 241

Appendix E: TABLES 392

Appendix F: NOMENCLATURE 418

REFERENCES 427

VITA AUCTORIS 436

LIST OF FIGURES

1.1	Environmental Fate of a Toxic Pollutant (After Haque, 1980)	242
1.2	The Study Region, Including Surface Water Outfalls and Disposal Sites (Source: GLI, March, 1984, Annual Report)	243
1.3	Typical Ice Conditions in January, February and March in Lake St.Clair (Source: Great Lakes Atlas, 1971)	244
1.4	The Proposed Structure of The Overall Water Quality Modelling For Lake Huron-Erie Corridor	245
2.1	Typical Discharge into a River Indicating Near and Far Fields	246
2.2	The Transport and Transformation Processes of TOXIWASP Model	247
2.3	Isotherms For Adsorption of a Hydrophobic Pollutant on Sediments (Source: Mills et al., 1982)	248
3.1	Discretization of St.Clair River	249
3.2	Discretization of Detroit River	250
3.3	Orthogonal Curvilinear Coordinate System For Natural Channels	251
4.1	Predicted Distribution of Velocity (U), Dispersion Coefficient ($\mathcal{E}$) at 5,000 m from the Inlet of St.Clair River, and the Measured Surface Velocities by Corps of Engineers, For Reach No. 1	252
4.2	Predicted Distribution of Velocity (U), Dispersion Coefficient ($\mathcal{E}$) at 10,000 m from the Inlet of St.Clair River with the Measured Surface Velocities by Corps of Engineers, For Reach No. 1	253
4.3	Predicted Distribution of Velocity (U), Dispersion Coefficient ($\mathcal{E}$) and the Measured Surface Velocities by Corps of Engineers, For Reach No. 2 in St.Clair River	254

4.4 Predicted Distribution of Velocity (U), Dispersion Coefficient ($\mathcal{E}$) and the Measured Surface Velocities by Corps of Engineers, For Reach No. 3 in St.Clair River 255

4.5 Predicted Distribution of Velocity (U), Dispersion Coefficient ($\mathcal{E}$) and the Measured Surface Velocities by Corps of Engineers, For Reach No. 4 in St.Clair River 256

4.6 Segmentation For The Upper St.Clair River For the 48 Segments Model 257

4.7 Segmentation For the Lower St.Clair River 258

4.8 St.Clair River Model Segment Flow Pattern (all flows are percent of total flow) 259

4.9 Segmentation Grid For The Upper St.Clair River Showing the Locations of HCB Point Sources . 260

4.10 Upper St.Clair River Model Segment Flow Pattern (all flows are percent of total flow) 261

4.11 HCB Levels in Water Along The Canadian Shoreline as Measured by MOE and Predicted From the k-$\mathcal{E}$ Model 262

4.12 Comparison of Predicted and Measured HCB Concentrations in Bed Sediments in the Upper Part of St.Clair River 263

4.13 Predicted HCB Concentrations in Bed Sediment Along the Canadian Shoreline Segments, Extrapolated Results up to Six Years 264

4.14 Predicted HCB Concentrations in Water and Bed Sediments Along With Measured Concentrations at Station No. SR 33.4 in the Upper Part of St.Clair River 265

4.15 Predicted Distribution of Velocity (U), Dispersion Coefficient ($\mathcal{E}$) and the Measured Surface Velocities by Corps of Engineers, For Reach No. 4 in Detroit River 266

4.16 Predicted Distribution of Velocity (U), Dispersion Coefficient ($\mathcal{E}$) and the Measured Surface Velocities by Corps of Engineers, For Reach No. 5 in Detroit River 267

4.17 Predicted Distribution of Velocity (U), Dispersion Coefficient ($\mathcal{E}$) and the Measured Surface Velocities by Corps of Engineers, For Reach No. 6 in Detroit River 268

4.18 Segmentation For The Upper Detroit River . . . 269

4.19 Segmentation For the Lower Detroit River 270

4.20 Detroit River Model Segment Flow Pattern (all flows are percent of total flow) 271

4.21 The Estimated Distribution of Cadmium Levels in Water and Suspended Solids in Detroit River 272

5.1 Boundary Conditions and Definitions For Shallow Water Flow 273

5.2 Instantaneous Streamlines in a Two Dimensional Flow 274

5.3 The Finite Element Model for Lake St.Clair . . . 275

5.4 Types of Boundary Conditions for the Finite Element Pollutant Model. 276

5.5 The Displacement Distance Along The Streamline in R* and R Elements 277

5.6 Cell Layout for TOXIWASP Model for Lake St.Clair 278

6.1 The Finite Element Scheme with Interlacing Elements 279

6.2 Vertically Integrated Velocities for 8 $m.s^{-1}$ Wind Speed From Southwest Direction 280

6.3 Surface Velocities For 8 $m.s^{-1}$ Wind Speed From Southwest Direction 281

6.4 Velocities 0.2 Depth Below Water Surface for 8 $m.s^{-1}$ Wind Speed From Southwest Direction . . 282

6.5 Velocities 0.6 Depth Below Water Surface For 8 $m.s^{-1}$ Wind Speed From Southwest Direction . . 283

6.6 Vertically Integrated Velocities for 8 $m.s^{-1}$ Wind Speed From Northwest Direction 284

6.7 Surface Velocities For 8 $m.s^{-1}$ Wind Speed From Northwest Direction 285

6.8 Velocities 0.2 Depth Below Water Surface for 8 $m.s^{-1}$ Wind Speed From Northwest Direction . . 286

6.9 Velocities 0.6 Depth Below Water Surface For 8 $m.s^{-1}$ Wind Speed From Northwest Direction . . 287

6.10 Vertically Integrated Velocities for 8 $m.s^{-1}$ Wind Speed From Northeast Direction 288

6.11 Surface Velocities For 8 $m.s^{-1}$ Wind Speed From Northeast Direction 289

6.12 Velocities 0.2 Depth Below Water Surface for 8 $m.s^{-1}$ Wind Speed From Northeast Direction . . 290

6.13 Velocities 0.6 Depth Below Water Surface For 8 $m.s^{-1}$ Wind Speed From Northeast Direction . . 291

6.14 Vertically Integrated Velocities for 8 $m.s^{-1}$ Wind Speed From West Direction 292

6.15 Surface Velocities For 8 $m.s^{-1}$ Wind Speed From West Direction 293

6.16 Velocities 0.2 Depth Below Water Surface for 8 $m.s^{-1}$ Wind Speed From West Direction 294

6.17 Velocities 0.6 Depth Below Water Surface For 8 $m.s^{-1}$ Wind Speed From West Direction 295

6.18 The Effect of Vertical Eddy Viscosity on the Velocity Profile in Element No. 36, in Lake St.Clair 296

6.19 The Effect of Vertical Eddy Viscosity on the Velocity Profile in Element No. 145, in Lake St.Clair 297

6.20 The Effect of Bottom Boundary Condition on the Velocity Profile in Element No. 36, in Lake St.Clair 298

6.21 The Effect of Bottom Boundary Condition on the Velocity Profile in Element No. 145, in Lake St.Clair 299

6.22 Location of Measuring Sites in Lake St.Clair . . 300

6.23 Flow Measurement Techniques 301

6.24 Comparison of the Observed and Calculated Currents in Lake St.Clair 302

6.25 The Measured and Simulated Horizontal Distribution of the Mean Chloride Concentration in Lake St.Clair 305

6.26 The Measured and Simulated Horizontal Distribution of the Mean Chloride Concentration in Lake St.Clair 306

6.27 Wind Speed Variations From Windsor Airport in 1983 307

6.28 Turbidity Data From Windsor Water Treatment Plant in 1983 308

6.29a Correlation of Suspended Solids and Wind Speed in Lake St.Clair 309

6.29b Correlation of Suspended Solids and Turbidity data in Lake St.Clair 310

6.30 Measured and Simulated Horizontal Distribution of the Mean Suspended Solids Concentration in Lake St.Clair 311

6.31 Measured and Simulated Horizontal Distribution of the Mean Suspended Solids Concentration in Lake St.Clair 312

6.32 Distributed PCBs in Bed Sediment in 1970 and 1974 in Lake St.Clair (after, Frank et al., 1977) 313

6.33 Piecewise Approximation For Wind Speed and Direction 314

6.34 Piecewise Approximation For Sediment and PCBs Loads 314

6.35 Vertically Integrated Velocities Under Complete Ice Cover 315

6.36 Predicted and Measured Concentrations of PCBs in Bed Sediments 316

6.37 Total PCBs Concentration in Water Segments in Lake St.Clair 317

6.38 Total PCBs Concentration in Water Segments in Lake St.Clair 318

6.39 PCBs Sorbed onto Suspended Sediments in Water Segments 319

6.40 PCBs Sorbed onto Suspended Sediments in Water Segments 320

6.41 Suspended Solids Concentrations in Water Segments 321

6.42 Suspended Solids Concentrations in Water Segments 322

6.43 PCBs Sorbed onto Sediments in Bed Segments 323

6.44 PCBs Sorbed onto Bed Sediment Segments 324

6.45 Cumulative Mass of PCBs Lost From Water Segments by Volatilization 325

6.46 Cumulative Mass of PCBs Lost From Water Segments by Volatilization 326

6.47 Total Mass of PCBs in Surface Bed Segments . . . 327

6.48 Total Mass of PCBs in Surface Bed Segments . . . 328

7.1 Assumed Wind Time Function Over Lake St.Clair . 329

7.2 Suspended Solids Concentrations in Water Segments in Lake St.Clair 330

7.3 Suspended Solids Concentrations in Water Segments in Lake St.Clair 331

7.4 The Main Drainage Basins in the Huron-Erie Corridor 332

7.5 The Concentrations of OCS in Bed Sediment in 1984 (After, Pugsley et al., 1985). 333

7.6 Predicted and Measured Concentrations of OCS in Bed Sediment Based on 2.5 cm Surface Bed Layer 334

7.7 Predicted and Measured Concentrations of OCS in Bed Sediment Based on 10 cm Surface Bed Layer 335

7.8 Total OCS Concentration in Water Segments in Lake St.Clair 336

7.9 Total OCS Concentration in Water Segments in Lake St.Clair 337

7.10 OCS Sorbed onto Suspended Sediments in Water Segments 338

7.11 OCS Sorbed onto Suspended Sediments in Water Segments 339

7.12 OCS Sorbed onto Sediments in Bed Segments . . . 340

7.13 OCS Sorbed onto Bed Sediment Segments in Lake St.Clair 341

7.14 Cumulative Mass of OCS Lost From Water Segments by Volatilization 342

7.15 Cumulative Mass of OCS Lost From Water Segments by Volatilization 343

7.16 Total Mass of OCS in Surface Bed Segments in Lake St.Clair 344

7.17 Total Mass of OCS in Surface Bed Segments in Lake St.Clair 345

7.18 Predicted OCS Concentrations in Bed Sediment Along the Canadian Shoreline Segments, in St.Clair River 346

7.19 Predicted OCS Concentrations in Bed Sediment in Lake St.Clair (Constant Loads) 347

7.20 Predicted OCS Concentrations in Bed Sediment in Lake St.Clair (Constant Loads) 348

7.21 Predicted OCS Concentrations in Bed Sediment in Lake St.Clair (No External Loads) 349

7.22 Predicted OCS Concentrations in Bed Sediment in Lake St.Clair (No External Loads) 350

7.23 Predicted Concentrations of PCBs in Water Segments and on Suspended Solids Under Ice Cover in Lake St.Clair 351

7.24 Total PCBs Concentration in Water Segments in Lake St.Clair 352

7.25 Total PCBs Concentration in Water Segments in Lake St.Clair 353

7.26 PCBs Sorbed onto Suspended Sediments in Water Segments 354

7.27 PCBs Sorbed onto Suspended Sediments in Water Segments 355

7.28 PCBs Sorbed onto Sediments in Bed Segments in Lake St.Clair 356

7.29 PCBs Sorbed onto Bed Sediment Segments in Lake St.Clair 357

7.30 Total Mass of PCBs in Surface Bed Segments in Lake St.Clair 358

7.31 Total Mass of PCBs in Surface Bed Segments . . . 359

7.32 Cumulative Mass of PCBs Lost From Water Segments by Volatilization 360

7.33 Cumulative Mass of PCBs Lost From Water Segments by Volatilization 361

7.34 Predicted Concentrations of PCBs in Water Segments and on Suspended Solids in St.Clair River 362

7.35 Predicted Concentrations of PCBs in Water Segments and on Suspended Solids in Detroit River 364

7.36 Predicted and Measured Concentrations of Lead in Bed Sediments in Lake St.Clair 366

7.37 Total Lead Concentration in Water Segments in Lake St.Clair 367

7.38 Total Lead Concentration in Water Segments in Lake St.Clair 368

7.39 Lead Sorbed onto Suspended Sediments in Water Segments 369

7.40 Lead Sorbed onto Suspended Sediments in Water Segments 370

7.41 Lead Sorbed onto Sediments in Bed Segments in Lake St.Clair 371

7.42 Lead Sorbed onto Bed Sediment Segments in Lake St.Clair 372

7.43 Total Mass of Lead in Surface Bed Segments in Lake St.Clair 373

7.44 Total Mass of Lead in Surface Bed Segments in Lake St.Clair 374

7.45 Predicted Concentrations of Lead in Water Segments and on Suspended Solids in St.Clair River 375

7.46 Predicted Lead Concentrations in Bed Sediment in Lake St.Clair (Reduced Loads) 377

7.47 Predicted and Measured Concentrations of Cadmium in Bed Sediments in Lake St.Clair . . 379

7.48 Total Cadmium Concentration in Water Segments in Lake St.Clair 380

7.49 Total Cadmuim Concentration in Water Segments in Lake St.Clair 381

7.50 Cadmium Sorbed onto Suspended Sediments in Water Segments 382

7.51 Cadmium Sorbed onto Suspended Sediments in Water Segments 383

7.52 Cadmium sorbed onto Sediments in Bed Segments in Lake St.Clair 384

7.53 Cadmium Sorbed onto Bed Sediment Segments in Lake St.Clair 385

7.54 Total Mass of Cadmium in Surface Bed Segments in Lake St.Clair 386

7.55 Total Mass of Cadmium in Surface Bed Segments . 387

7.56 Predicted Concentrations of Cadmium in Water Segments and on Suspended Solids in St.Clair River 388

7.57 Predicted Concentrations of Cadmium in Water Segments and on Suspended Solids in Detroit River 390

LIST OF TABLES

B.1 Segment Data for 48 SEGMENT MODEL 171

B.2 Segment Data for 48 SEGMENT MODEL (CONT.) 172

B.3 Segment Volumes (MCF) for 48 SEGMENT MODEL . . . 173

B.4 Segment Flow Rates (CFS) for 48 SEGMENT MODEL . 173

B.5 Segment Data for 52 SEGMENT MODEL 174

B.6 Segment Data for 52 SEGMENT MODEL (CONT.) . . . 175

B.7 Segment Volumes (MCF) for 52 SEGMENT MODEL . . . 176

B.8 Segment Flow Rates (CFS) for 52 SEGMENT MODEL . 176

B.9 Segment Data for 24 SEGMENT MODEL 177

B.10 Segment Volumes (MCF) for 24 SEGMENT MODEL . . . 178

B.11 Segment Flow (CFS)- Time (DAYS) Functions for 24 SEGMENT MODEL 178

B.12 Segment Flow (CFS)- Time (DAYS) Functions for 24 SEGMENT MODEL 179

B.13 Segment Flow (CFS)- Time (DAYS) Functions for 24 SEGMENT MODEL 180

B.14 Segment Flow (CFS)- Time (DAYS) Functions for 24 SEGMENT MODEL 181

B.15 Segment Flow (CFS)- Time (DAYS) Functions for 24 SEGMENT MODEL 182

B.16 Segment Flow (CFS)- Time (DAYS) Functions for 24 SEGMENT MODEL 183

B.17 Segment Flow (CFS)- Time (DAYS) Functions for 24 SEGMENT MODEL 184

B.18 Segment Flow (CFS)- Time (DAYS) Functions for 24 SEGMENT MODEL 185

B.19 Segment Data for 46 SEGMENT MODEL 186

B.20 Segment Data for 46 SEGMENT MODEL (CONT.) 187

B.21 Segment Volumes (MCF) for 46 SEGMENT MODEL . . . 187

B.22 Segment Flow Rates (CFS) for 46 SEGMENT MODEL . 188

4.1 The Hydraulic Parameters for St.Clair River . . . 393

4.2 HCB Industrial Point Loads into St.Clair River . 394

4.3 Non point HCB Loads into St.Clair River 395

4.4 HCB Parameters Required by The EPA (TOXIWASP) Model 396

4.5 The Hydraulic Parameters for Detroit River, (k-$\mathcal{E}$) Model 397

4.6 Suspended Solid and Cadmium Loads into the Upper Part of Detroit River 398

4.7 Cadmium Parameters Required by TOXIWASP Model . 399

6.1 The Effects of Vertical Eddy Viscosity on Depth Averaged Velocity 400

6.1 (CONTINUE) 401

6.2 The Effects of Slip Coefficient on Depth Averaged Velocity 402

6.2 (CONTINUE) 403

6.3 Parameters for Lake St.Clair Finite Element Model 404

6.4 Parameters for Suspended Solids Finite Element Model in Lake St.Clair 405

6.5 Average Concentrations of the Total PCBs in Lake St.Clair 406

6.6 Estimates of Average PCBs and S.S. Loads During Free Water Surface 406

6.7 Estimates of Average PCBs and Suspended Solid Loads During Ice Cover 407

6.8 Frequency of Occurrence of Winds in Hours per Year 408

6.9 Interchange Flow Rates Between Water Segments in CFS for Different Steady State Wind

Conditions in Lake St.Clair 409

6.10 PCBs Parameters Required by TOXIWASP Model . . . 410

7.1 Hydrologic Data for Canadian Streams in the Study Area 411

7.2 Hydrologic Data for U.S. Streams in the Study Region 412

7.3 OCS Parameters Required by the TOXIWASP Model . 413

7.4 Lead Parameters Required by the TOXIWASP Model . 414

7.5 The Estimated Lead and Cadmium Loading Rates into the Study Region 415

7.6 Comparison of Predicted and Measured Contaminants in Sediments 416

CHAPTER I

INTRODUCTION

1.1 Objective

In recent years the quantity of toxic substances reaching surface waters via wet and dry deposition from the atmosphere or through direct stream loading has led to concern regarding the quality of water in the Great Lakes. Both the contaminant distribution and variability are uncertain. Therefore, the primary objective of this dissertation is to develop a mathematical modelling framework which can be used to:

1. Identify the sources, where possible, by tracking the fate and transport of the pollutants as a function of space and time;
2. Evaluate the relative importance of existing inputs by relating mass inputs of trace pollutant to observed concentrations;
3. Clarify the role of the various factors and major processes which control the transport and transformation of pollutants;
4. Assess the impact of contaminants on the ecosystem;

5. Give further insight into the future needs for water quality modelling research.

This study includes the simulation of four selected toxic substances, the isomers of polychlorinated biphenyls (PCB), octachlorostyrene (OCS), lead (Pd) and cadmium (Cd), in the water column and in the sediments. Furthermore, chloride as a conservative ion and suspended solids are simulated in the waterway throughout the Huron-Erie corridor. However, the models are generalized to be flexible enough to provide the mechanisms to describe the kinetic process and the transport processes to simulate other contaminants in this region and in similar regions.

1.2 Statement of the Problem

The manufacture and use of industrial chemicals have led to the contamination of water, sediment and atmosphere. The level or concentration of a contaminant in the environment depends on three major mechanisms as shown in Figure 1.1. First, the amount of contaminant added to the environment; secondly, the transport processes which distribute the contaminant among different phases of the environment, and finally the transformation processes which alter or degrade the contaminant within each phase.

It is worthwhile to mention some fundamental distinctions between toxic substances and conventional pollutants. Many conventional pollutants are transported in dissolved/conservative form, without apparent adverse effects on the ecosystem. The mean residence times of the conventional pollutants are equivalent to the hydraulic detention times of the water in the system. On the other hand, many toxic chemicals are strongly sorbed to suspended and bed sediments and become part of the bed sediments. Consequently, the residence time of such chemicals can be in the order of years. Toxic chemicals can cause adverse effects even at very low concentrations.

The traditional physical models used for prediction present scaling and construction difficulties. Therefore, it is obvious that a mathematical model along with extensive field data is the only feasible approach to describe the relationship between aquatic sources of contaminants, their dispersion through surface waters, their deposition in sediments and their accumulation in aquatic organisms, birds and humans. The mathematical model permits the abstraction of a highly complex real world. Moreover, a mathematical model can forecast and evaluate the effects of changes in the surrounding environment on water quality.

However, accurate contaminant dynamics simulation requires both reliable models and detailed long-term meteorological, loading and field concentration data. Since sufficient loading data to permit an accurate calibration is not yet available, the emphasis on loading data is placed upon obtaining, where possible, both the flow and concentration data rather than accepting sparse data sets. In some instances where data is not available, procedures must be derived to provide better loading estimates designed for long-term mass balance, calibration and verification of contaminant and sediment transport models.

1.3 Site Description

This study involves the Huron-Erie corridor of the Great Lakes which extends from the beginning of St. Clair River to the outlet of Detroit River. The Huron-Erie waterway is a major navigational route for commercial vessels. Cargoes move nationally between Canadian or American ports, and internationally between Canadian, American and overseas ports. This waterway serves six ports out of the 13 main ports located in Ontario. The six ports handle over 40 million tonnes of cargo per year. In addition to commercial fishing and water supply for cities and industries, the waterway provides for extensive recreational uses including canoeing, pleasure boating, swimming and sport fishing. The nature of these water-oriented recreational areas creates strong focus for tourism. In total, this waterway significantly contributes to economic and social prosperity. As shown in Figure 1.2, the region can be distinctly divided into the following three basins .

1.3.1 Lake St.Clair

Lake St.Clair lies between Lakes Huron and Erie. The physiography of Lake St.Clair is unique among the Great Lakes, as it is the smallest and the shallowest of the Great Lakes. Lake St.Clair can be circumscribed by a diameter of 45 km. It has a surface area of 1250 km^2 of which 750 km^2 are in Ontario, and an average depth of only 3.6 m. The extreme long term fluctuation in the lake level of ±1 m is also very large by comparison with its depth. The lake has a large hydraulic flow-through (5400 m^3s^{-1}) which reduces the detention time of water to approximately one week.

On the other hand, Lake St.Clair is affected by strong and unstable wind conditions especially during the Spring and Fall periods. The speed and direction of wind-generated currents can change very rapidly. Although these weather systems may increase the mixing in the vertical water column, the wind-driven circulation, in general, creates distinctly different distributions of water quality in the horizontal direction. During the cold period of the year, (January, February and March), Lake St.Clair may be completely or partially covered by ice as shown in Figure 1.3. In addition to wind, the following factors also contribute to the dynamics of the lake: runoff, atmospheric precipitation and the inflow from the St.Clair River and the outflow to the Detroit River.

1.3.2 St.Clair River

The St.Clair River is 66 km long and also the main feed for Lake St.Clair with an average discharge of 5300 $m^3 \cdot s^{-1}$. The river has three distinct reaches. The upper reach, extends downstream from Lake Huron to a point about 5 km below the Blue Water Bridge. The reach is on average narrow, (up to 270 m), and includes many outfalls from industrial activities in Sarnia. The middle reach which extends downriver for the next 43 km is approximately 800 m wide. The lower reach, continues downstream for the next 14 km to Lake St.Clair.

The distribution of the river water into Lake St.Clair takes place through numerous delta branches. The average velocities of the river water through these branches are strongly variable depending upon the discharge and controlling characteristics.

1.3.3 Detroit River

Detroit River is the outlet for Lake St.Clair with a mean flow of 5400 $m^3 s^{-1}$ and a length of 52 km. The river is characterized by two distinct reaches. The upper reach extends downstream from Lake St.Clair about 21 km to the head of Fighting Island with an unbroken cross-section, except for Peche Island at its head. The water flows fast and is generally deep with steep banks. Gravel and sand dominate the river sediments in the upper reach, due to moderate to high current velocities which carry the fine particles to the depositional zones in Lake Erie.

The lower reach tends to be very wide, (up to 2,000 m), exhibiting a few islands and shallow expanses. It is subdivided in many places, around island headland, dikes and through shipping channels. As a result, depositional areas are mainly found in this reach, particularly, in the Trenton channel and along the river outlet to the western basin of Lake Erie. Heavy industry is located on the U.S. side from Zug Island, downstream through the Trenton Channel, as far south as the river mouth. Sediments of the lower reach of the river are composed of coarse material, mainly sand which constitutes about 60% of the sediment's composition. However, there is a slight decrease in mean grain size at areas with low river current velocities.

1.4 General Approach

The main objective of this thesis is to model the fate of toxic and conventional pollutants in surface waters. In principle, the fully three-dimensional analysis is the obvious starting point for a comprehensive calculation. However, such a detailed approach involves a large number of unknowns under relatively complicated boundary conditions and is time-consuming to run. The problem, therefore, is to choose the proper complexity for the model .

Recognizing that it is not possible to detail all the physical phenomena that comprise our natural world, the alternative is to keep the complexity as low as possible by applying simulation submodels with appropriate spatial complexity for individual limnological processes. These submodels will attempt to identify and include only the phenomena that are relevant to the water quality problem under consideration. Thus, instead of simulating all variables with the same grid resolution, some (e.g. toxic chemicals) are simulated with a coarse grid and, some (e.g. currents and suspended solids), with a fine grid. In addition, these submodels can be calibrated where possible with short-term observed data, and then combined to determine the distribution of the selected pollutants. However, the successful application of these submodels to a physical system depends greatly on the available data such as the historical levels, sources and distribution patterns of the pollutant.

Briefly, the analysis in this study is divided into the following two general parts, simulation of river transport and simulation of lake transport. The study for each part is carried out using the following four-step approach:

1. Description of the submodels development and selectting the numerical scheme,

2. The application of these submodels to the physical system, including the use of the necessary data for this study,
3. Model calibration and verification processes,
4. Finally, a discussion of the results and comparison to other studies.

A schematic diagram of this approach is shown in Figure 1.4. The details of the various interactions are described below.

1.4.1 Simulation of River Transport

The purpose of this simulation is to present simplified but representative models which can be used to predict responses of the rivers to the impact of pollutants. To do this, a sequential approach is taken. First, a simplified hydrodynamic submodel is introduced to establish the velocity profiles at different sections along the longitudinal direction. The proposed model is generalized to include flow around islands and the effect of curvature on the velocity distribution and on secondary flow.

Then, a stream function form of the convection-diffusion equation from Lau and Krishnappan (1981) was solved using an implicit finite difference scheme with variable grid model to simulate the transport of conventional pollutants. However, in order to obtain a better value for the turbulent dispersion coefficient, the k-ε equations from Rastogi and Rodi, (1978) are solved by the variable grid approach which was used for the mass transport equation and coupled with the transport model. Multiple inputs from either side of the river can be included in the model.

Finally, to account for contaminant adsorption by and desorption from sediments and to study the long-term levels and distribution of toxic chemicals, the EPA (TOXIWASP) model by Ambrose et al. (1983) is linked after some modifications with the outputs from the foregoing submodels. However, the complexity of the transport and transformation processes, (Richardson, et al., 1982), which influence a toxic chemical in natural streams require information concerning:

1. The loading processes such as inputs of suspended solids and chemical from tributaries and the atmosphere as a time-variable.
2. The transport of dissolved chemical within the water or adsorbed to sediments. This process strongly depends upon chemical speciation.
3. The bioaccumulation.
4. The sediment-water interface as a function of wind shear stresses, time and velocity patterns.
5. The biodegradation processes.
6. The volatilization of the dissolved chemical.

The TOXIWASP model includes the transport and transformation processes and contributions to the river system from wastewater discharges, overland runoff flow, fallout and underground leakage from old landfills.

1.4.2 Simulation of Lake Transport

Although the representation of the advection or flow of water in a lake is different from that in a river, the previous methodology for assessing river water quality will be very helpful in expanding our understanding of the various processes. Therefore, a finite element hydrodynamic circulation submodel is presented to generate representative flow patterns due to different specified wind speeds and directions as well as ice conditions.

The depth average velocities from the hydrodynamic submodel are used in a finite element model to simulate the transport of conventional pollutants. An upwind finite element formulation is used to obtain a stable solution for the convective transport phenomena.

Because Lake St.Clair is very shallow, much of the sediment deposited on the bottom can be resuspended by the large bottom shear stresses arising from the high-wind conditions that are most frequent in the Spring and Fall. Therefore, to understand qualitatively the various processes of sediment dispersion, a finite element transport model is linked with a statistical regression model. The purpose of this statistical model is to offer a simple and quick method that can be used to give a reasonable calibration for the fast response of the sediment resuspension in the lake due to the meteorological changes. In addition, the model can be used to simulate the mechanisms of deposition and resuspension of sediment as a function of a specified boundary conditions at the bed and the contributions from point/ nonpoint sources.

Finally, the EPA (TOXIWASP) model which is based on the conservation of mass principle is applied in order to simulate the coupled response of the sediment-water system. Since there was a significant source of chemicals from resuspended bed sediment, it was decided to include, in the model, a time variable resuspension mechanism as a function of bottom stresses.

CHAPTER II

BACKGROUND AND REVIEW OF LITERATURE

2.1 General

Predicting the aquatic fate of toxic chemicals involves both scientific-technical knowledge and engineering judgement. One must understand first the basic scientific principles which are operative in governing the water quality behavior. Equally important is making the necessary approximations, or assumptions, about scientific reality. Because this study covers the transport of toxic chemicals in two different but related areas, the two rivers and a small shallow lake, the literature review herein will deal with the work on: (1) Dispersion of Pollutant in Rivers, (2) Lake Circulation Models and (3) Basic Definitions and Processes of Toxic Chemicals in Surface Water.

2.2 Dispersion of Pollutant in Rivers

The discharge of chemically polluted water from industrial plants into rivers is becoming an increasing threat to our water resources. In general pollutants are convected by the mean fluid motion in the river and they are diffused by the turbulent motion. The flow phenomena occurring in the river in the vicinity of a waste water outfall is illustrated in Figure 2.1 for the case of a shore based outfall discharging perpendicular to the river direction; this is the case that prevails in both the St.Clair and Detroit Rivers. The discharge jet is deflected by the river cross-flow. The jet entrainment on the near-bank side may be restricted by the presence of the solid boundary, causing a recirculation. Apart from the occurrence of reverse flow, the flow in the vicinity of the discharge is usually complicated further by three-dimensional effects which are due either to the discharge geometry or due to buoyancy effects arising from a density difference between the waste water and the river water.

The discharged jet influences the flow field in the river for a certain distance downstream from the outlet. This region is called the near-field, and here the turbulences stem partly from generation at the river bed and partly from generation within shear layers induced by the outflow discharge. Therefore, the turbulent flow in the near field is particularly difficult to simulate in a mathematical model. Unfortunately, most of the near-field models use integral methods, which are difficult to use for discharges into rivers, (Motz and Benedict, 1972, Shirazi and Davis, 1974, and Stolzenbach and Harleman, 1973). The reason for this is that they cannot account completely for the interaction between the jet flow and solid surfaces or the secondary currents in the river. Demuren and Rodi, 1983, presented a three-dimensional numerical model for the near-field problem. They employed the k-ε turbulence model for determining the turbulent stresses. The model performed well for isothermal discharges, i.e., they did not include the buoyancy terms.

Beyond the near field the flow in the river is no longer influenced by the outfall discharge, this region is called the far-field. Here the turbulence is governed entirely by the shear at the river bed and the channel geometry. The development and application of a mathematical model for the region far downstream of the discharge, where the velocity field has returned to its normal state, is the aim of this study. However, one has to realize that, the far field model is dependent on an accurate input of the starting profiles, and starting initial conditions which are governed by the near field.

Taylor (1921) established a direct link between the Lagrangian turbulence characteristics of the flow, and the diffusion of a cloud of marked particles within that flow. Taylor (1953, 1954) has shown that after an initial convective period during which the tracer spreads over the entire cross section, the dispersion process may be simplified by the following one-dimensional diffusion equation:

$$\frac{\partial c}{\partial t} + V \frac{\partial c}{\partial x} = E \frac{\partial^2 c}{\partial x^2} \qquad [2.1]$$

where t is the time, c is the cross sectional average concentration, x is the distance along the stream, V is the cross sectional average velocity and E is the overall longitudinal dispersion coefficient. This dispersion coefficient represents the interaction between transverse diffusion and differential convection.

Aris (1956) extended Taylor's work to a general cross sectional diffusion coefficient. Fischer (1967,1968) estimated the value of E for natural streams and also presented an extension to the previous analysis to the case of infinitely long series of uniform bends in alternate directions. Although this approach remains a useful tool for the prediction of large-scale mixing in streams having relatively uniform flow it yields no information on local variations of concentration within the cross section.

Because of the complexity involved in the process of environmental diffussion, hardly a single theory can interpret or predict the entire pattern of contamination. An extensive review of literature indicates that numerous models for predicting the dispersion in natural streams are available, in varying degrees of complexity, (Fischer 1973, Jirka et al., 1975 and Akhtar, 1978). It is pertinent to note that while increased model accuracy usually implies increased complexity, increased complexity does not necessarily yield increased accuracy. Many models neglect the hydrodynamic aspect of the simulation and rather assume constant, parabolic or logarithmic velocity distributions. Some of them use empirical formulae to express the dispersion coefficient and some deal with only conservative type of pollutants.

2.3 Lake Circulation Models

A primary requirement for numerical modelling of circulation in lakes is an understanding of the basic physical processes which must be sufficiently understood for formulation in strict laws. Generally, the large-scale circulations in a lake can be described using the conservation of momentum and conservation of mass principles. Hydrodynamic lake models vary from simple models, in which the lake is represented by one homogeneous layer, to three-dimensional time dependent models with variable density. Simons (1980) presented a state-of-the-art review on models for large scale water circulations in lakes and seas. However, for the sake of clarity and brevity, the derivation of the fundamental equations and the approximations used in this study will not duplicate the literature reviewed by Simons. Therefore, to aid in the following discussion we list here the equations of motion and the continuity equation.

Using the Reynolds averaging procedure, the three-dimensional momentum equation for turbulent flow in vector form and after introducing the eddy viscosity concept using Boussinseq analogy, Hinze (1959), reads:

$$\frac{\partial \bar{V}}{\partial t} + (\bar{V}.\nabla)\bar{V} + \bar{\Omega} = -\frac{1}{\rho}\,\text{grad}\,(p+\rho g z) + \varepsilon_0 \nabla^2 \bar{V} \qquad [2.2]$$

and the continuity equation is:

$$\frac{\partial \rho}{\partial t} + \text{div}\,\rho\,\bar{V} = 0 \qquad [2.3]$$

where :

$\bar{V} = (u,v,w)$; $\bar{\Omega} = (-fv, fu, 0)$;

$$\text{and} \quad \nabla^2 = \frac{\partial^2}{\partial x^2} + \frac{\partial^2}{\partial y^2} + \frac{\partial^2}{\partial z^2} \qquad [2.4]$$

in which u,v,w = x-, y-, z-components of velocity respectively; p = pressure; t = time; ε_0 = eddy viscosity; ρ = density of water; f = Coriolis coefficient due to the rotation of the earth and g = the acceleration due to gravity.

However, the application of the equation of motion to specific situations in natural waters with their nonlinear and turbulent behaviour presents some difficulties. Therefore, instead of solving the equations fully, some approximations can be introduced to simplify the solution by including only the mechanisms that have a controlling influence on the circulation, and neglecting other terms.

The basic equations in the general form cannot be solved analytically and they must therefore be treated numerically. Some of the earlier efforts in hydrodynamics are the works of Hansen (1956) and Welander (1957). Although both were looking at shallow water circulation and employed vertically averaged equations, two widely different approaches have evolved from their work.

Hansen (1956) outlined the vertically averaged formulation for the equations of motion almost as we know it today (Laevastu et al.,1974). This model did not include the variations in surface atmospheric pressure or density. However, a horizontal virtual viscosity term with constant eddy viscosity coefficient was included in the momentum equations. The formulated problem was solved by the finite difference method using a staggered grid in space and time. This particular scheme allows the use of central differences in space and time, which is desirable for accuracy and numerical stability while keeping the number of variables low and partly uncoupled. However, the physical boundaries have remained as major problem which needs special treatment to avoid errors and instability.

Simons (1971) presented a finite difference model based on the vertically integrated equations using two space and time staggered grids simultaneously to avoid problems with the convective terms. Several variations on the treatment of bottom friction and convective terms were tried. Since high resolution was desired and the time integration scheme was explicit, considerable computation time was required.

Schwab et al. (1981) developed two finite difference lake models: (i) A free surface model to calculate water level fluctuations and (ii) A rigid lid model to simulate the circulation patterns for the Great Lakes including Lake St.Clair. Their models are depth averaged, two dimensional and unsteady. The one-and two-layer models have been extensively used to simulate lake hydrodynamics, Bengtsson, (1973,1978), Falkenmark (1973), Gedney (1971) and Gedney and Lick (1972).

The approach initiated by Welander (1957) based on the earlier work of Ekman (1905) is specifically designed for wind driven currents. In this method, the equations of motion are simplified by the hydrostatic approximation, that the water density is constant except in the buoyancy term since maximum density variation is likely to be of the order of 0.2%. Furthermore, the nonlinear inertia terms are neglected to linearize the equations. Thus, the dependence on the vertical z-coordinate can be determined analytically while the equations are integrated numerically in the horizontal directions and in the time domain. Because one of the assumptions is that changes in depth are small or the water surface is fixed, it is often called the 'rigid lid' method and is primarily used to predict wind circulation in lakes. For steady flow, this assumption is exact if the depths are taken as the actual depth under the imposed wind stress. For unsteady flow models, this assumption eliminates all surface waves, long as well as short waves. Thus, lake currents which result directly from wind can be calculated but those currents which result from external seiche modes are not computed, Liggett (1969). Simons (1980) showed that the rigid-lid approximation is valid only if $f^2L^2/gD \ll 1$, where L and D are the characteristic length and depth respectively. The applications of this approach have been carried out by Heaps (1973), and Graf (1978).

In this study, the above approach has been chosen to simulate the steady wind-driven three-dimensional circulation for Lake St.Clair. Since Lake St.Clair is very shallow, the following assumptions and restrictions are useful, Liggett and Hadjtheodorou (1969), including:

1. Stratification can be neglected;

2. The horizontal momentum transfer has very small influence on the solution since the horizontal diffusivity is less than 10^7 cm^2s^{-1} (Hamblin, 1969);
3. The geostrophic wind is assumed to be nearly uniform over the lake due to the relatively small size of the lake;
4. The "spin up time", i.e., time to reach to a nearly steady state condition is very short (about 3 hours);
5. The Coriolis force is considered constant over the lake, because of its small size.
6. The vertical eddy viscosity has been assumed constant, Csanady (1967, 1968) and Bowden et al. (1974).

Under the foregoing assumptions, the x, y and z momentum and continuity equations are respectively reduced to the following linear forms:

$$-fv = -\frac{1}{\rho}\frac{\partial p}{\partial x} + \varepsilon_0\frac{\partial^2 u}{\partial z^2} \qquad [2.5]$$

$$fu = -\frac{1}{\rho}\frac{\partial p}{\partial y} + \varepsilon_0\frac{\partial^2 v}{\partial z^2} \qquad [2.6]$$

$$g = -\frac{1}{\rho}\frac{\partial P}{\partial z} \qquad [2.7]$$

$$\frac{\partial u}{\partial x} + \frac{\partial v}{\partial y} + \frac{\partial w}{\partial z} = 0 \qquad [2.8]$$

This set of equations takes only the balance of Coriolis force, pressure gradient, and the vertical momentum exchange. It is therefore called an Ekman-type model. A combined analytical-numerical solution for these governing equations is presented in a subsequent chapter.

2.4 Toxic Chemicals

The development and use of a water quality model involves some fundamental concepts such as the transformation, transport and speciation processes which are of potential importance in a surface water body. Of course, changes in concentrations of a contaminant in any compartment of the environment depend not only on inputs from external sources, but also on the movement of contaminants between compartments, as well as the production within each compartment.

As mentioned earlier, the transport and transformation processes were implemented using the EPA (TOXIWASP) model, which is a planning/design model primarily for organic pollutants. The TOXIWASP is a dynamic chemical and sediment model which can be applied in streams, lakes and coastal waters. Figure 2.2 illustrates the available transport and transformation processes. It is not the intent of this chapter to present a detailed or complete review on these processes. The purpose is to give a greater appreciation of the complex sediment, chemical and physical interactions which take place in rivers and lakes.

2.4.1 Speciation Processes

2.4.1.1 Acid-Base Effects

Toxic organics exist in very low concentrations and therefore have little influence on the pH values of the water. The pH of natural water, however determines the fraction of an organic acid or base in neutral or ionic states. Since only electrically neutral species are directly volatile, values of pH for natural waters can strongly influence toxicant volatilization.

The hydrogen ion concentration also influences rates of biodegradation. Thus, at different pH values, a given species may metabolize the pollutant at different rates. However, there are no general rules available now for predicting pH effects. Therefore, biodegradation rates are assumed in this study to be independent of pH value in the range of, 5-9 pH, and decrease outside this range.

2.4.1.2 Sorption on Suspended Sediments

Sorption is a process which refers to the accumulation of dissolved chemical on the boundary of solids (adsorption). Also, it includes the interpenetration of substances with solids (absorption). Sorption occurs when the net sorbing solids (sorbent) attraction overcomes the water attraction. The substance that are sorbed (sorbates) are usually protected from many processes such as volatilization, biodegradation and photolysis, which would otherwise affect the solute. Adsorption results in the removal of solutes from solution and their concentration at the surface of the solid, to such time until the concentration of the solute remaining in solution is in a dynamic equilibrium with that at the surface. At this position of equilibrium there is a defined distribution of solute between the liquid and solid phases. The preferred form for depicting this distribution is to express the amount of solute adsorbed per unit weight of solid adsorbent as a function of the concentration of solute remaining in solution at a fixed temperature. An expression of this type is termed an adsorption isotherm.

The adsorption isotherm is a functional expression for the variation of adsorption with concentration of adsorbate in bulk solution at constant temperature. Since sorption reactions are more likely to achieve rapid equilibrium, the kinetics of sorption and desorption can be described using isotherms that relate the amount sorbed to the equilibrium solution concentration. In general, the isotherms increase with increasing solute concentration. The most commonly used isotherms, as shown in Figure 2.3, are :

(1) Langmuir adsorption isotherm which is expressed as :

$$X = \frac{m_0 \, b \, C_0}{1 + b \, C_0} \qquad [2.9]$$

(2) Freundlich adsorption isotherm expressed as:

$$X = K_f \, C_0^{1/n'} \qquad [2.10]$$

At low concentrations, both the Freundlich and Langmuir isotherms can be approximated as a linear function given by:

$$X = K_p \, C_0 \qquad [2.11]$$

where X= amount of sorbed chemical per mass of sediment; C_0= amount of dissolved chemical per volume of water; K_f, K_p, n', m_0 and b are unknown parameters.

The maximum amount of a toxic chemical which can be held in the water under equilibrium conditions is the aqueous equilibrium solubility, plus the amount of solute sorbed on suspended solids. The use of linear sorption isotherms is adequate at pollutant concentrations which are equal to or less than one half of the equilibrium solubility. Since organic chemicals usually exist in very low concentrations, linear isotherm is generally valid. This approach can only evaluate one parameter at a time. It was found by Karickhoff et al. (1979), that the partition coefficient (K_p) can be related to the organic carbon content of the sediments as follows:

$$K_p = K_{oc} \cdot X_{oc} \qquad [2.12]$$

$$K_{oc} = 0.63\ K_{ow} \qquad [2.13]$$

$$K_{oc} = -0.54 \log S_w + 0.44 \qquad [2.14]$$

where K_{oc}=partition coefficient expressed on an organic carbon basis; X_{oc} = mass fraction of organic carbon in sediment; K_{ow}= octanol-water partition coefficient which is the concentration of chemical in octanol divided by concentration of chemical in water at equilibrium and S_w= water solubility of sorbate expressed as a mole fraction.

The relative amount of pollutant sorbed and dissolved depends on both the suspended sediment concentration and the partition coefficient. The TOXIWASP model allows for three sorption possibilities, dissolved, sediment sorbed and biota sorbed for the unionized form of the chemical.

2.4.2 Transport Processes

2.4.2.1 Volatilization

Volatilization is the transfer of matter from the dissolved to the gaseous phase. Volatilization rate is usually modeled according to the following relationship:

$$R_v = (K_v/h)[C_o - C_g/H_o] \qquad [2.15]$$

Where R_v = net volatilization transfer rate; K_v = mass transfer coefficient; h = mixing depth of water; C_g = concentration of the chemical in the bulk gas phase and H_o = Henry's law constant. For many applications the concentrations of organic toxicant in the atmosphere is almost zero, so that Equ. 2.15 can be simplified to:

$$R_v = K_v C_o \qquad [2.16]$$

The values of the mass transfer coefficient, K_v, which depends on turbulence level in water and in the overlaying atmosphere, can be estimated using the two-resistance principle. The two film theory of volatilization assumes that two thin films, a liquid film and a gas film, are bounded on either side by well mixed compartments. The dissolved chemical moves upward through diffusion in the liquid film due to concentration gradient. Then, it passes through the gas film due to pressure differences before reaching the bulk vapor phase.

2.4.2.2 Sediment Transport

Sediment transport is an important process in determining the extent of sorption and the sorbed pollutant transport. Sediment movement is affected by many factors such as suspension and settling characteristics, hydraulic conditions within the water phase and other field conditions. The task of keeping track of all possible ecosystem variables to quantify these combined effects on suspended solids is too complex and would occupy too much computer space in the simulation model. Also, the CPU time would be excessive. Meanwhile, suspended solids and sediments are assumed to settle and resuspend from the bed to the water at spatially variable velocities.

Although the particle size of the sediments is influential, Rao and Davidson (1980) have shown that the organic matter content of each size fraction is the controlling factor. Therefore sediment is treated as a single size fraction that is advected and dispersed in the water.

2.4.2.3 Bed Sedimentation

Sedimentation will be referred to as either net deposition, positive sedimentation, where deposition exceeds sediment scour, or net erosion, negative sedimentation, where scour exceeds sediment deposition. The deposition of suspended sediments containing sorbed pollutants leads to the accumulation of sediments on the bed. However, the force of gravity squeezes the pore water out through compaction and decreases the porosity. This process can lead to a rising bed surface and the sorbed chemicals being buried. The concentration gradients of chemical between bed surface and water column will result in sorption or desorption and thus the bed sediment can act either as a sink or a source of contaminant to the water column.

Another process that can redistribute chemicals within the sediments is pore water diffusion which will exchange the dissolved chemicals. Infiltration can leach chemicals down through the bed, while percolation will move dissolved chemical up into the water. The mixing of sediments by organisms, bioturbation, which is dependent on the types and numbers of organisms, should accelerate this chemical exchange process.

2.4.3 Transformation Processes

2.4.3.1 Biodegradation

Microbial organisms metabolize pollutants and chemically altering their toxicity in different ways such as mineralization which refers to the complete degradation of an organic compound to inorganic products. While in detoxication reactions, microbes convert a toxic substance into an innocuous compound. Microorganisms also degrade compounds which they cannot use as a nutrient or growth substrate through cometabolism. Consequently, cometabolism has no effect on the population size.

Before the utilization of a compound can begin, the microbial community must adapt itself to the chemical. This lag-time depends on several biological and environmental constraints. Then, the degradation rate of a compound can be expressed in a second-order equation by:

$$R_b = K_b \, C_b \, C \qquad [2.17]$$

$$K_b = \frac{U_0}{Y \; K_0} \qquad [2.18]$$

Where R_b = net microbial degradation rate; K_b = second-order biodegradation rate constant; C_b =concentration of the bacteria; C = pollutant concentration; U_0= maximum specific growth rate; Y = biomass produced per mass of chemical degraded; K_0= half saturation constant. However, practical utilization of Equ. 2.17 is mathematically complex. As a simple alternative, the first-order kinetics is applied where Equ. 2.17 is reduced to:

$$R_b = K_B C \qquad [2.19]$$

Where K_B = first-order biodegradation rate constant. This expression is desirable for several reasons. One is that the toxicant is not going to be the predominant source for substrate. It is not possible either at this time to predict whether a toxic compound is a potential source of energy and carbon solely on the basis of its chemical structure. Also, there is high uncertainty in measuring the populations of microorganisms.

2.4.3.2 Photolysis and Hydrolysis

Photolysis and hydrolysis can be very important processes in an ecosystem. Photolysis which is driven by sunlight is truly a pollutant decay process. In some photochemical reactions, the absorption of light leads to the decomposition of a molecule. However, the products of the photochemical decomposition of a toxic chemical may still be toxic.

Other toxic compounds can be altered by direct reaction with water. This chemical reaction is called hydrolysis. Generally, in hydrolysis reactions hydroxide replaces another chemical group. Hydrolysis products are usually more volatile and more readily biodegraded than the original compounds, although there are some exceptions.

However, the photolysis processes are not evaluated in this study, because they are not likely to be an important influencing process in the water column for the chemicals included in the study.

PART 1

SIMULATION OF RIVER TRANSPORT

CHAPTER III

THEORETICAL DEVELOPMENTS

3.1 General

Two kinds of contaminants are included in this simulation, (i) conventional pollutants, (ii) toxic substances. Each component will be discussed separately. Since Detroit and St.Clair Rivers are fed by water from three Great lakes, they have a fairly steady flow of considerable volume. Therefore, a steady state depth averaged representation is considered to be adequate in this phase of the study. This often restricts the simulation to the transport of conventional pollutants which have a short duration over the period of interest. But, in order to account for the long-term buildup of concentrations and the sediment/water interactions of toxic substances, the unsteady EPA (TOXIWASP) model will be applied instead.

In modelling the mass transport of toxic chemicals in surface water, it is necessary to develop a mass balance for the suspended solids as well, (Dolan and Bierman, 1982; Richardson, et al., 1982). The reason is that both adsorption and desorption of toxic chemicals onto and from the suspended solid particles can occur. Consequently, the chemical can exist both in dissolved and particulate form, (Dolan and Bierman, 1982). Furthermore, for proper simulation, the hydrodynamics are solved to establish the required advection and turbulent diffusion mechanisms.

Due to the high velocity and short residence time in the connecting channels, and because the shipping channels are often dredged, the net sedimentation is assumed to be close to zero, i.e., no long-term sedimentation in the shipping channels of the rivers. However, there could be local sedimentation near the shores and in St.Clair River Delta as well as at the mouth of the Detroit River, i.e., downstream of Grosse Isle. The following sections describe the formulation as well as the solution procedure of the selected interrelated models.

3.2 Hydrodynamic Submodel

A numerical model based on the simplified equation derived by McCorquodale et al.,(1983) is introduced. The model is modified to include the effect of curvature by an analytical approach used by Chang (1983). The principle assumptions used are that the lateral and longitudinal depth profiles and river flow rates are available. However, due to multiple channels and flow around islands, the computational flow domain in the rivers is subdivided into reaches. It is also assumed that the channel is wide with constant slope within each reach.

This approach utilizes the Manning's equation to account for the effect of vertical momentum transfer and a shape function to account for side effects. Thus, the vertically averaged longitudinal velocity profile, at different sections is given by:

$$U(z) = \frac{X(z)}{n_0} h^{2/3} S_0^{1/2} \sqrt{\frac{r_0}{r}} \qquad [3.1]$$

Where $U(z)$ = the vertically averaged longitudinal velocity ; z=lateral distance from shore; T_0 = channel width; n_0 = Manning's roughness factor; h = water depth at a grid point; S_0= constant slope; r_0= radius of curvature to the middle of the channel and r = local radius of curvature $= r_0 - (T_0/h) + z$.

Thus, the boundary conditions in Equ. 3.1 are chosen so that $U(z)=0$ when $z=0$ and again when $z=T_0$. The proposed equation for the shape factor is defined as :

$$X(z) = \{-(\frac{z}{T_0} - \frac{1}{2})^2 + \frac{1}{4}\}^{n_1} \qquad [3.2]$$

The value of the empirical exponent, n_1, is chosen to best fit the available current data.

3.2.1 Model Description

In order to include every possible bifurcation or confluence in the flow, St.Clair River as shown in Figure 3.1, is subdivided into 13 reaches, while Detroit River is subdivided into 16 reaches as shown in Figure 3.2. The solution starts by assigning the values of water surface slopes for the various reaches while the roughness coefficient for that reach is estimated from a hydraulic study made by Quinn and Hagman (1977). Then the flow in each reach is established based upon actual flow measurements made by the Corps of Engineers (1974,1982).

After that, each reach is discretized by cross sections at a distance of 150 m apart where the radius of curvature and the depth profiles of the river are calculated using U.S. Department of Commerce, National Ocean Survey, Lake Survey Center, navigation chart No. 400, scale 1:15,000.

Finally, several computer runs were made using different values of the empirical exponent n_1. Then, a comparison between the calculated and observed data of the velocity was used to adjust n_1. In addition, the transport velocity should also obey the hydraulic flow continuity constraint, i.e.,

$$Q = \int_0^{T_0} U(z)\ h\ dz \qquad [3.3]$$

Using the measurements of depth and velocities, the discharge through each small segment of the river, 0.01 of the width, is calculated. From these, the cumulative discharge with its cross-river width are calculated at each cross section, by numerically integrating, using the trapezoidal role, the area of the segment times the average velocity at this segment.

3.3 Pollutant Transport Model

The transport and dispersion of contaminant in the turbulent flow will be described in a manner similar to that used for the transport of heat. The concentrations of the pollutant are sufficiently small so that they do not significantly alter the density of the water.

A modified model based on Lau and Krishnappan (1981) has been developed to simulate the dispersion of conventional pollutants discharged along the rivers. The model has been modified and applied to the Niagara River and St.Clair River by McCorquodale and Ibrahim (1983, 1985). A reasonable agreement between the computed and observed concentration values was reported. The proposed model predicts the concentrations of various non-conservative pollutants discharged from multiple outfalls into the river. This method was derived by writing the continuity and advection diffusion equations in a general orthogonal curvilinear coordinate system for a steady state case as:

$$\frac{\partial}{\partial x}(m_1 h U) + \frac{\partial}{\partial z}(m_2 h V) = 0 \qquad [3.4]$$

$$m_1 h U \frac{\partial c}{\partial x} + m_2 h V \frac{\partial c}{\partial z} = \frac{\partial}{\partial z}\left(\frac{m_2}{m_1} h \varepsilon_0 \frac{\partial c}{\partial z}\right) \qquad [3.5]$$

In which x,z= longitudinal and transverse distance coordinates . The x-axis has been chosen to coincide with the Canadian side of the river while z-axis is measured across the stream, orthogonal to the x-axis. U,V= depth-averaged velocity components ; h = local flow depth; c = depth averaged concentration; ε_0= turbulent mixing coefficient and m_1,m_2= coefficients for the coordinate system .

The lateral distance coordinate z is replaced by the dimensionless stream function η, Equ. 3.5 can then be written as:

$$\frac{\partial c}{\partial x} = \frac{1}{Q^2}\frac{\partial}{\partial \eta}\left[D_0(x,\eta)\frac{\partial c}{\partial \eta}\right] \qquad [3.6]$$

Where :

$$\eta = \frac{1}{Q}\int_0^z m_1 h\, U\, dz \qquad [3.7]$$

$$D_0 = U\, h^2\, m_2\, \varepsilon_0 \qquad [3.8]$$

In which Q= the total discharge of the river and D_0= the diffusion factor, which reflects local changes in channel width, depth, velocity and eddy viscosity. Equ. 3.6 is the same equation presented by Yotsukura and Sayre (1976), which is particularly suitable for natural streams and can be rearranged in the following form:

$$\frac{\partial c}{\partial x} + E\frac{\partial c}{\partial \eta} = D'\frac{\partial^2 c}{\partial \eta^2} \qquad [3.9]$$

Where :

$$E = -\frac{1}{Q^2}\frac{\partial D_0}{\partial \eta} \qquad [3.10]$$

$$\text{and} \quad D' = D_0/Q^2 \qquad [3.11]$$

At the left bank, η=0 and at the right bank, η=1. If D_0 is assumed to be constant, then Equ. 3.9 can be solved analytically. However, for accurate simulation it is necessary to use local values for D_0 then solve Equ. 3.9 numerically.

3.3.1 Numerical Method

The computational domain representing a natural stream is usually a rectangle with large ratio of length to width. Therefore, a finite difference scheme is considered more simpler and appropriate for the numerical simulation.

However, in order to reduce the number of required nodes, without sacrificing the high resolution needed in regions where flow and concentration gradients are expected to change rapidly. The variable size mesh system which was proposed by Roach, (1976) is selected for this study.

Thus, the total channel discharge Q is divided into 15 unequal increments. Lines of constant η are used as grid lines, as shown in Figure 3.3, causing the grid to expand and contract automatically with the river width T_o. The basis of this method is to replace the partial derivatives in Equ. 3.9 by their finite difference representations. In the case of a variable size mesh, the finite difference expressions for the first and second derivatives of any function, f, at node o are given, Imam (1981), in terms of the values of the function at the neighbouring nodes as follows:

$$\left(\frac{\partial f}{\partial \eta}\right) = \left(\frac{\Delta f}{\Delta \eta}\right)_o = \left(\frac{f_2 - f_o}{z_2}\right)\left(\frac{z_1}{z_1 + z_2}\right) + \left(\frac{f_o - f_1}{z_1}\right)\left(\frac{z_2}{z_1 + z_2}\right) \qquad [3.12]$$

$$\left(\frac{\partial^2 f}{\partial \eta^2}\right) = \left(\frac{\Delta^2 f}{\Delta \eta^2}\right)_o = \left(\frac{f_2 z_2 - (z_1 + z_2) f_o + f_1 z_1}{z_2 z_1 \ (z_1 + z_2)/2}\right) \qquad [3.13]$$

where z_1 = the change in stream function between nodes 1 and 0, z_2 = the change in stream function between nodes 2 and 0.

The implicit finite difference procedure of Stone and Brian (1963) is adopted for the present study. Therefore, the finite difference representation of Equ. 3.9 corresponding to Figure 3.3 is:

$$\{a_2[c_{i+1}^{j} - c_{i}^{j}] + a_3[c_{i+1}^{j-1} - c_{i}^{j-1} + c_{i+1}^{j+1} - c_{i}^{j+1}]\}/\Delta x$$

$$+ (2a_1 B_i^j)\{(c_i^{j+1} - c_i^{j})[\frac{z_1}{z_2(z_1+z_2)}] + (c_i^{j} - c_i^{j-1})[\frac{z_2}{z_1(z_1+z_2)}]$$

$$+ (c_{i+1}^{j+1} - c_{i+1}^{j})[\frac{z_1}{z_2(z_1+z_2)}] + (c_{i+1}^{j} - c_{i+1}^{j-1})[\frac{z_2}{z_1(z_1+z_2)}]\}$$

$$= [D_i'^{j}/z_1 z_2(z_1+z_2)]\{z_1 c_i^{j+1} - (z_1+z_2)c_i^{j} + z_2 c_i^{j-1}$$

$$+ z_1 c_{i+1}^{j+1} - (z_1+z_2)c_{i+1}^{j} + z_2 c_{i+1}^{j-1}\} \qquad [3.14]$$

where the derivative of c with respect to η is approximated using a set of weighting coefficients which have been recommended by Stone and Brian and are listed as follows:

$$a_1 = 1/4; \quad a_2 = 2/3; \quad \text{and} \quad a_3 = 1/6 \qquad [3.15]$$

Rearranging Equ. 3.14, Lau and Krishnappan (1981), to obtain the following system of equations:

$$p_j c_{i+1}^{j-1} + q_j c_{i+1}^{j} + r_j c_{i+1}^{j+1} = s_j \qquad [3.16]$$

Where :

$$p_j = \frac{1}{6\Delta x} - [E_i^j (z_2/2) + D'^j_i]/[z_1(z_1+z_2)] \qquad [3.17]$$

$$q_j = \frac{2}{3\Delta x} + (E_i^j/2)\left[\frac{z_2}{z_1(z_1+z_2)} - \frac{z_1}{z_2(z_1+z_2)}\right] + D'^j_i/z_1 z_2 \qquad [3.18]$$

$$r_j = \frac{1}{6\Delta x} + [E_i^j (z_1/2) - D'^j_i]/[z_1(z_2+z_2)] \qquad [3.19]$$

$$s_j = \left[\frac{1}{6\Delta x} + [E_i^j (z_2/2) + D'^j_i]/[z_1(z_1+z_2)]\right] c_i^{j-1}$$

$$+ \left[\frac{2}{3\Delta x} + (E_i^j/2)\left[\frac{z_2}{z_1(z_1+z_2)} - \frac{z_1}{z_2(z_1+z_2)}\right] - D'^j_i/z_1 z_2\right] c_i^{j}$$

$$+ \left[\frac{1}{6\Delta x} - [E_i^j (z_1/2) - D'^j_i]/[z_1(z_2+z_2)]\right] c_i^{j+1} \qquad [3.20]$$

Where j=2,3,...,M-1 and M is the number of nodes per cross section.

3.3.2 Boundary Conditions

At the inflow boundary, for i=1, the concentration is an input parameter and has to be determined from field measurements at the inlet of each river. The sidewalls of the river are treated as reflecting boundaries implying no penetration of pollutants. This is expressed by a central difference formula using the concentrations c(j,M-1) and c(j,M+1) at the external mesh points. The boundary condition can then be represented by:

i.e., for $$\frac{\partial c}{\partial \eta} = 0 \qquad [3.21]$$

$$c_i^{2} = c_i^{-1} \qquad [3.22]$$

and $$c_i^{M-1} = c_i^{M+1} \qquad [3.23]$$

at node J=1

$$q_1=[2/3\Delta x]+[D_1/\Delta\eta^2] \qquad [3.24]$$

$$r_1=[1/3\Delta x]-[D_1/\Delta\eta^2] \qquad [3.25]$$

$$s_1=[2/3\Delta x-D_1/\Delta\eta^2]c_1+[1/3\Delta x-D_1/\Delta\eta^2]c_2 \qquad [3.26]$$

at node J=15

$$p_{15}=[1/3\Delta x + D_{15}/\Delta\eta^2] \quad [3.27]$$

$$q_{15}=[2/3\Delta x]-[D_{15}/\Delta\eta^2] \quad [3.28]$$

$$s_{15}=[2/3\Delta x-D_{15}/\Delta\eta^2]c_{15}+[1/3\Delta x+D_{15}/\Delta\eta^2]c_{14} \quad [3.29]$$

The system of equations, Equ. 3.16, is then solved using the relaxation method. However, the solution requires as input the velocity component, which appears as a coefficient of a concentration gradient, and the turbulent eddy viscosity. The velocity field may be steady but it is seldom uniform. Thus, the hydrodynamic submodel yields the velocity components, U(i,j), at all the computational nodes. The turbulent eddy viscosity is also a function of space and will be considered in section 3.4 where the turbulence model is presented.

3.3.3 Outfalls and Source Streams

The model described by Equ. 3.9 treats outfalls and tributary sources as being mass sources. These sources are thus considered to bring no flow into the river just mass. This is usually a reasonable approximation since these source flows are usually small compared to the bulk river flow. The model will predict an increase in the concentration due to these sources at specified nodes where they discharge as follows:

$$\Delta c_j = c_0 Q_0 / [\; Q\; (z_1 + z_2)/2] \qquad [3.30]$$

where Δc_j = the increase in the concentration; c_0=input concentration of the source and Q_0= input discharge assigned to the specified node.

3.4 Turbulence Model

In developing any mathematical model for the transport of pollutants in natural streams, it is necessary to specify proper values for the dispersive mechanisms. A brief review of literature, showed that the Kinetic Energy-Dissipation (k-ε) model is one of the most promising turblence models which has been successfully applied in many fields of engineering. The model determines the value of the eddy viscosity directly from the structure of the flow field and boundary conditions . Therefore, the k-ε model, which was disscused earlier in Section 2.2, is selected for the present work.

Thus, the adapted equations, which have been proposed by Rastogi and Rodi (1978), for the depth-average calculations determine the variation of k and ε from the following transport equations:

$$U\frac{\partial k}{\partial x} + V\frac{\partial k}{\partial z} = \{\frac{1}{S_1}\frac{\partial}{\partial x}(\varepsilon_o\frac{\partial k}{\partial x})\} + \frac{\partial}{\partial z}(\varepsilon_o\frac{\partial k}{\partial z}) + G' + P_k - \varepsilon \qquad [3.31]$$

$$U\frac{\partial \varepsilon}{\partial x} + V\frac{\partial \varepsilon}{\partial z} = \{\frac{1}{S_2}\frac{\partial}{\partial x}(\varepsilon_o\frac{\partial \varepsilon}{\partial x})\} + \frac{\partial}{\partial z}(\varepsilon_o\frac{\partial \varepsilon}{\partial z})$$

$$+ b_1\frac{\varepsilon}{k}G' + P_\varepsilon - b_2\frac{\varepsilon^2}{k} \qquad [3.32]$$

$$\varepsilon_o = b_3\frac{k^2}{\varepsilon} \qquad [3.33a]$$

$$P_k = C_k\ (U_*^3 / h) \qquad [3.33b]$$

$$P_\varepsilon = C_k\ (U_*^4 / h^2) \qquad [3.33c]$$

$$U_*^2 = C_f\ (U^2 + V^2) / \cos\theta \qquad [3.33d]$$

Where k=turbulent kinetic energy; ε= turbulent dissipation rate; ε_o= eddy viscosity; G'= production of k due to interaction of turbulent stresses with horizontal mean velocity gradients which depends on the bottom roughness; P_k and P_ε= effective production of k and ε respectively due to non-uniformity of vertical profiles; and the empirical constants C_k and C_f were determined by Rastogi and Rodi (1978) from the rates of energy dissipation and the dye spreading in undisturbed normal channel flow. While the other empirical constants S_1, S_2, b_1, b_2 and b_3 are given by Rodi (1980).

The bottom and depth-average turbulent stresses are interrelated as given below :

$$T_{xz} = \delta_0 \left(\frac{\partial U}{\partial x} + \frac{\partial V}{\partial z} \right) - \frac{2}{3} k \qquad [3.34]$$

$$T_{bx} = C_f \rho U^2 \qquad [3.35]$$

Where ρ = fluid density and C_f = empirical coefficient.

The transformation of Equ. 3.32 to a more compacted and convenient form, Yotsukura and Cobb (1972), can be accomplished by aligning the longitudinal coordinate surfaces properly in the direction of the depth-averaged local velocity vectors, so that they form stream tube surfaces. Under this condition, the mean flow will be in the longitudinal, x, direction and the lateral flow is very small, or V=0 everywhere. Furthermore, the longitudinal dispersion term, in Equ. 3.5 has very little influence on the transverse mixing, except near the sources and can be neglected. Then, Equ. 3.31 and similarly Equ. 3.32 can be transformed into:

$$U \frac{\partial k}{\partial x} = \{\frac{1}{S_1} \frac{\partial}{\partial z}(\varepsilon_0 \frac{\partial k}{\partial z})\} + G' + P_k - \varepsilon \qquad [3.36]$$

$$U \frac{\partial \varepsilon}{\partial x} = \frac{1}{S_2} \frac{\partial}{\partial z}(\varepsilon_0 \frac{\partial \varepsilon}{\partial z}) + b_1 \frac{\varepsilon}{k} G' + P_\varepsilon - b_2 \frac{\varepsilon^2}{k} \qquad [3.37]$$

The k-ε equations are similar to the transport equation, Equ. 3.9, except in the appearance of the source/sink term. Accordingly, the finite difference analogies of the various terms in the transport equation are used. The k-ε equations are cast in the x-η independent variables and solved by the variable grid approach used for the mass transport equation, (McCorqudale et al., 1983). The program solves the k-equation before the ε-equation and then calculates the eddy viscosity ε_0. The source/sink term is decoupled from the solution to permit an analytical solution.

3.5 Toxic Chemical Model

As expressed previously, the basic computer program used for toxic chemicals is the EPA (TOXIWASP) model. This model includes the main mass transfer mechanisms to account for the interactions between dissolved chemical both with suspended solids and with stationary sediments in the riverbed. These mechanisms were discussed earlier in Section 2.4, and represent:

1. Advection and dispersion of dissolved contaminants,
2. Settlement or resuspension of sediment,
3. Direct contributions from point/nonpoint sources of solids and contaminants to the water,
4. Volatilization and biological degradation.

The model allows for time-variable input which is very important in the multi-year analysis. The model uses the compartment modelling approach whereby segments can be arranged in one, two or three dimensional configurations. The control volume method is very useful for the numerical solution techniques, because it conserves mass and is capable of handling various segment sizes and shapes.

The model solves two differential equations in the form of Equ. 3.40 to calculate chemical and sediment concentrations in surface water, surface bed and subsurface bed segments.

$$\frac{\partial C_1}{\partial t} = u \frac{\partial C_1}{\partial x} + \frac{\partial}{\partial x} (E \frac{\partial C_1}{\partial x}) + \frac{W_1}{V} - K + Q_1 \qquad [3.38]$$

$$\frac{\partial C_2}{\partial t} = u \frac{\partial C_2}{\partial x} + \frac{\partial}{\partial x} (E \frac{\partial C_2}{\partial x}) + \frac{W_2}{V} + Q_2 \qquad [3.39]$$

Where C_1, C_2= concentration of chemical and sediment; u= water velocity; W_1, W_2= mass loading of chemical and sediment; Q_1, Q_2 = chemical and sediment net exchange with bed, E = longitudinal dispersion and V = segment volume.

The main assumptions of the TOXIWASP model are:

1. All segments are well mixed.
2. Sorption is an instantaneous process within each segment.
3. The chemical properties of the compound can be coupled with the characteristics of the environment to formulate a first order reaction for the degradation processes.
4. All the first order rates can be combined linearly.

The model is based on an explicit, backward difference numerical solution to the conservation of mass equation. Dividing the water body into completely mixed finite segments, the mass balance equation for the one dimensional case can then be reduced to the following form:

$$\frac{\partial M}{\partial t} = \sum_{i+1}^{n} [Q_{ij} C_i + E_{ij} A_{ij} (\frac{1}{\ell})_{ij}] + W_j - KV_j \qquad [3.40]$$

Where M = constituent mass; C = constituent concentration; Q = water flow; E = longitudinal dispersion; A = cross sectional area; ℓ = characteristic mixing length; W = mass loading; K = kinetic transformation rate; V = segment volume; j= segment number; i= adjacent segments and ij = interface between segment j and adjacent segments i.

3.5.1 River Segmentation

Let us now consider a description of the calculations for the concentration dynamics of the contaminants and suspended solids. The first step in the numerical scheme is to divide the river into completely mixed finite cells. Each cell is composed of two horizontal layers called segments, namely a water segment above an active sediment segment. The depth of the water segment represents the actual mean water depth in the river at this location. The depth of the bed segment is based on the sedimentation rates. Since the residence time of the water in a river is usually short, the simulation time step is on the order of hours, while the sedimentation time step is on the order of months to years.

CHAPTER IV

RIVER MODELS CALIBRATION AND VALIDATION

4.1 General

The mathematical aspects of the proposed models have been presented in Chapter III, including the approximations and schematizations relevant to the solution of the flow and transport problems for the specific sites (St.Clair and Detroit Rivers). The models have to be predictive in the sense that it may give an insight into relevant characteristics, such as magnitudes of velocities and concentrations, under conditions which do not exist as yet. "The predictions must be accurate enough to allow a sufficient reliable answer to the engineering questions behind the mathematical model study" (after Saffman, 1977). It is important, then, to calibrate and verify these mathematical models.

Therefore, this Chapter is concerned with the calibration and verification computations of the proposed models for both St.Clair and Detroit Rivers using field measurements. In the following sections calibration is defined as the process of making the output of the model agree with a limited number of known responses of the problem area to known excitations. In a negative sense this process can be referred to as the process of forcing agreement between the model output and the known responses. Verification is defined as the process of checking how well the calibrated mathematical model responds to excitations other than those utilized in the calibration, without changing the model.

4.2 St.Clair River

Model applications for toxic chemicals involve many difficulties. There is the problem of loading estimates. Unfortunately, the models require very accurate inputs which are generally not available, given the limited extent of the historical industry production and quality control records. The distribution and amount of pollutant in sediment cores and sedimentation rates can also introduce an additional source of errors on the sediment-chemical interaction processes. Furthermore, along the shipping channel it is necessary to periodically dredge many sections to keep the channel open. This unnatural movement of the sediment with its associated contaminant movement is a potential source of uncertainty on the long-term simulation results.

Recognizing these complications, each numerical submodel will be calibrated and verified individually in order to minimize the overall error which might be introduced in the simulation process. In addition, the analysis is performed for selected contaminants during selected simulation periods where the mass balance can be performed with more confidence.

4.2.1 The Hydrodynamics For St.Clair River

The hydrodynamic submodel has been applied to St.Clair River in order to predict the velocity distribution from the inlet to the outlet of the river. The surface velocities collected by U.S. Army Corps of Engineers (1983) are used for the calibration of the hydrodynamic submodel. The following assumptions were made in the simulation runs:

1. The mean river flow rate was 5350 m^3s^{-1}, (189000 cfs), during the period of the velocity measurements.
2. Minor variations in the flow rate should not significantly change the results due to the high flow of the river. Therefore, as a simplification, any deviation from this flow, (i.e., 2% flow change), can be assumed to yield a corresponding deviation from the measured velocities, (i.e., 2% velocity change).
3. Wind speeds during the field measurements were less than 15 $km.h^{-1}$ and the wave heights were less than 30 cm. These conditions would not seriously effect the average flow pattern in the river.

4. The surface velocity is used to estimate the vertically average velocity at each sampling station.
5. The total flow splits in two parts around Stag Island. The Channel along the Canadian shore containes 30.3% of the flow.
6. The flow distribution in the St.Clair Delta is: 4.7% of the flow goes to Channel Ecarte, 42.6% of the flow in the South channel, and 52.7% of the flow in the North Channel.
7. Manning's roughness coefficient for the reaches along the St.Clair River varies from 0.020 to 0.029 as recommended by the hydraulic study of Derecki and Kelley (1981).

A series of computer runs were made using the previously described St.Clair River assumptions. The only parameters that were adjusted to fit the simulated results, to the measured data in the river, were the empirical exponent, n_1. The model hydraulic parameters used in this study are listed in Table 4.1. Two arbitrary cross sections were used to establish the best value of the empirical exponent n_1 (Equ. 3.2) in each reach of the river. As shown in Figure 4.1 and Figure 4.2, the computed values from the numerical model showed good agreement with the measured velocity profiles, when n_1 was assumed to be 0.12 in the first reach. As can be seen from the figures, the variations for the dispersion coefficient (δ) vary from 0.4 to 1.0 m^2s^{-1}. Generally, these variations are similar to the patterns of the velocity. The values of the dispersion coefficients are lowest in the shallow parts of the river. The lateral variation of the vertically averaged velocity is shown With regard to the dispersion coefficient (δ), it can be seen that the same overall pattern exists in Figure 4.3 for reach number two. Figure 4.4 and Figure 4.5 show the good agreement between the measured and predicted velocity distribution for reaches number three and four. The values of the calibrated coefficients were proven to be adequate to yield a good overall agreement with the measured velocity fields.

4.2.2 HCB Simulation

During the summers of 1984 and 1985, a sampling and analysis project was undertaken by the Ontario Ministry of the Environment (MOE) to determine the levels and distribution patterns of HCB (Hexa Chloro Benzene) in the water and bed sediments of St.Clair River. The results of this project were synthesized within the pollutant transport (k-δ) model and the dynamic mass balance (TOXIWASP) model. The goal of this simulation is to use the available data in order to validate the proposed models as well as to show an example of the mass transfer characteristics of an organic chemical such as HCB.

4.2.2.1 Pollutant Transport Submodel In St.Clair River

The St.Clair River has variable depths and flow rates in its various reaches so a constant lateral dispersion was not used. The effective lateral dispersion coefficients of the various reaches were established based on the study made by McCorquodale et al., 1983. The lateral dispersion coefficients were expressed as a function of the locally available turbulent energy, k, and the local dissipation rate of turbulent energy, ε, as discussed in Section 3.4. Since the main conclusion of Rodi's (1980) state of the art review indicates that the two-equation k-ε model has a fair degree of universality and can be applied with some confidence to new problems, it was believed that the generated dispersion coefficients are appropriately suitable and do not need excessive calibration. Figure 4.1 to Figure 4.5, also show representative dispersion coefficient distributions in some of the river cross sections.

Thus, in order to validate the hydrodynamic and dispersion submodels, a qualitative comparison between calculated and measured HCB concentrations was used. The model constants are all kept the same as calibrated. The measurement results indicated that there are no major sources of HCB along the entire U.S. shoreline of the St.Clair River. Consequently, the loadings from the U.S. side are assumed to be zero. In contrast, along the

Canadian shoreline, at least 7 outfalls, reported by the MOE, are considered to be responsible for virtually all of the HCB entering into the river system. The HCB loadings from industrial point sources for the simulation period are tabulated in Table 4.2. The non-point loadings were estimated based on the mean flow rates and the actual concentrations of HCB on suspended solids in these tributaries. The total loading rate from each stream was therefore the product of the average HCB concentration on suspended solids and the mean daily suspended solids loads. The concentrations of HCB in stream waters were also included as shown in Table 4.3. A user guide is available in Appendix C for the (k-δ) computer program which describes all of the required input data. The model was then used to perform reach by reach mass balances.

4.2.2.2 Toxic Chemical Model For HCB

The entire St.Clair River is divided into 52 segments, 26 segments for the active sediments which underlie another 26 surface water segments, as shown in Figure 4.6 and Figure 4.7. In this model the river was divided into large segments approximately 3,000 meter (10,000 feet) in length. The reason for this is that the TOXIWASP model cannot handle more than this number of segments. The various parameters and dimensions used in this model can be found in Appendix

B. Figure 4.8 describes the St.Clair River flow and segment interactions for a river flow of 5285 $m^3.s^{-1}$.

The river is divided laterally into four segments of about 60 to 180 meters(200 to 500 feet) in width and 610 meters(2000 feet) in length. The inner St.Clair River segments carry 64% of the total river discharge, while the outer segments carry 18% each in this reach. The lower reach of St.Clair River contains few waste inputs. Therefore, long segments are used in this reach.

As part of the verification process, modified segments were used, because all the available sampling stations are located in the upper region of the river. Therefore, the upper part of St.Clair River was divided into 48 spatial segments, 24 water segments and 24 bed surface segments. The model segments for the upper part of St.Clair River and the position of the main outfalls are represented in Figure 4.9. Figure 4.10 shows the flow pattern for the modified segments in this region. This segmentation scheme was based partly on the location of major industrial outfalls, and partly on a decision to reduce computational complexity. Since, the heavy industrialization area is located in the upper reach of St.Clair River, finer segments are used to model the higher concentration gradients.

Since the HCB loading sources are located along the Canadian shoreline, the total river flow is divided laterally into the following four segments, 5%, 21%, 24% and 50% starting from the Canadian side. The hydrodynamic model as well as U.S. Department of Commerce, National Oceanic and Atmospheric Administration (NOAA), navigation charts (scale 1:15,000) are used to calculate the segment depths, volumes, widths, lengths, cross sectional areas, velocities, flows and dispersion coefficients. Model segment dimensions, flows, volumes and eddy diffusivities are listed in Appendix B.

The kinetic simulation parameters used, relating specifically to HCB are shown in Table 4.4. The possible loading rates from point/nonpoint sources during the simulation time are considered to be discharging continuously. These loads are identical to those used in the steady state (k-δ) simulation model. The input water concentrations of HCB from Lake Huron were estimated from raw water measurements. The model therefore, maintains constant boundary concentrations of 0.1 $ng.l^{-1}$ for the entire simulation period. The HCB concentrations at the start of the simulation within the water and sediments were put to zero as intial condition.

4.2.2.3 Simulation Results For HCB

The predicted and measured longitudinal concentration distributions along the Canadian shorelines for HCB are shown in Figure 4.11. The predicted concentrations are representative of the concentrations after the near field mixing. From the MOE field data at six stations in the upper St.Clair River a detailed sediment contaminant map was plotted in Figure 4.12. The results from the TOXIWASP model for the HCB levels in bed sediment were superimposed on the same map. An analysis of these data revealed that HCB remain near the Canadian shore of the river with the center of the river and the U.S.A. shore remaining relatively clean. The trends of the field data generally support the trend of the computer simulation. For example, the water quality of the river changed significantly below outfall number 5. However, increased concentrations in both the water and the bottom sediment were also found in the region downstream of outfall number 3 and 4, which suggests that the HCB loading used during the simulation from these two outfalls may have been too low to predict the observed values. The other alternative is a possible, although not confirmed, source of HCB leaching from old dump sites directly or indirectly to the St.Clair River.

It is particularly useful to analyze the behaviour of the contaminant in the bed sediment if the inputs are held constant, which the river system is likely to meet. Figure 4.13 shows HCB concentration in bed sediment along the Canadian shoreline segments, extended up to a simulation period of six years. This plot includes results of HCB concentrations in suspended solids. It can be seen from the figure that the increase in the HCB level in bed sediment, for example segment number 18, would converge to an equilibrium state after six to eight years under this loading rate. Further, it can be shown that equilibrium concentrations of the HCB in bed sediment is asymptotically stable and will approach the levels in suspended solids, i.e., 1100 ug.L^{-1} in segment 17. Once segment 18 has reached its saturation state, the HCB loads from the outfalls will be flushed downstream through the water segment directly to segment number 25. This would cause higher concentration levels in the downstream bed segments. Due to this mechanism, the net HCB load released from St.Clair River into Lake St.Clair would increase in the long term even if the present loads are held constant.

Predicted raw water concentrations, concentrations in suspended solids and measured HCB concentrations in bed sediments are plotted in Figure 4.14 at station number SR-33.4. It should be noted that the initial conditions for the HCB concentration in the simulation results was assumed to be zero in both water and bed sediments. The good agreement between the predicted HCB levels in suspended sediment and the measured HCB concentrations in bed sediment would approach the same level as in the suspended solids.

4.3 Detroit River

As has already been indicated, the general proposed models, for the transport of contaminants in St.Clair River, can be applied for Detroit River. Therefore, the approach to the calibration and verification of the models for Detroit River is similar to the previous sections which has been developed for St.Clair River.

4.3.1 Hydrodynamics Of Detroit River

The calibration of the hydrodynamic submodel was performed by comparing model predictions of the vertically average velocities to actual surface velocity measurements made by the Corps of Engineers in 1974 in Detroit River. The mean river flow at the time of the measurement study was 6230 m^3s^{-1}. Therefore, all of the predicted velocities from the model are based on this flow. The constraints related to the field measurements in St.Clair River Study were also applicable for this study including, a preference for calm water. Also, Lake Erie had to be stable with no seiches occurring at flight time, and winds not to exceed 24 $km.h^{-1}$

The hydrodynamic model was run for different values of the empirical exponent, n_1. The model hydraulic parameters used for Detroit River are listed in Table 4.5. Three arbitrary cross-sections will be presented to show the agreement between the trend of the predicted and measured velocities. Figure 4.15 gives the computed lateral variation of the vertically averaged velocity as well as the observed surface velocities in Reach No. 4. In Reach No. 5, the resulting velocities agree with the observed values as shown in Figure 4.16. Similar agreement was observed for the selected section in Reach No. 6 as shown in Figure 4.17.

4.3.2 Cadmium Calibaration In Detroit River

The calibration of the proposed models were performed by comparing the model predictions to the actual cadmium levels in bed sediments. The method and simulation procedure for cadmium are identical to those already outlined in the HCB section for St.Clair River. However, The calibration and verification processes for the analytical submodels for Detroit River are much difficult than those performed for St.Clair River. The reason for this is that there are several outfalls on both sides of the Detroit River discharging unknown contaminant quantities of cadmium. Furthermore, given that there may already be substantial risk from using the actual concentration measurements such as the EPA STORET data in the analysis since these measurements are taken at different time periods.

4.3.2.1 Pollutant Transport Submodel For Detroit River

The analytical (k-δ) model is used to describe the cadmium contaminant transport. The major sources of cadmium loadings from the U.S. shoreline are: The Detroit Treatment Plant which contributes about 100 lbs.day^{-1}. The Rouge River whose loads can be estimated from the average water concentrations and the mean flow at the mouth using the Rouge River STORET data. On the Canadian side the West Windsor Treatment Plant is the only quantified point source on this shoreline. In addition, some contributions come from the small tributaries.

The estimated average cadmium loadings are tabulated in Table 4.6. To provide the model with head water boundary concentrations, the average of river sample station data at the head of the Detroit River was used. The observed headwater concentrations for segments 1 and 3 are 0.4 and 0.2 ug.L^{-1} respectively. Since these observations were taken during storm events, they are about three to four times higher than the mean values. Thus, the boundary concentrations were adjusted several times to bring the predicted concentrations close to the measured values.

4.3.2.2 Toxic Chemical Model For Cadmuim

Detroit River was divided into 46 segments as indicated in Figure 4.18 and Figure 4.19. The model segment flow pattern is shown in Figure 4.20. The river is fairly uniform in the concentration in the upper reach with very few outfalls. Therefore, two large segments are used across the river, each segment was approximately 7,000 meter (20,000 feet) in length. In contrast with the upper reach, there are many industrial and waste outfalls in the lower part of the river. As a result, some segments are much shorter than in the rest of the river segments, to account for the larger concentration gradients in this part of the river. The model segment dimensions, volumes, flows and the hydraulic parameters used to analyze the contaminants in Detroit River are given in Appendix B.

The parameters used relating specifically to cadmium are given in Table 4.7. The advective surface water parameters were obtained from the hydrodynamic model. Then, the dynamic TOXIWASP model is run under the same loads and boundary conditions which were used in the (k-ε) model, in order to compare the output results to each other as well as to the observed values.

4.3.2.3 Calibration Results For Cadmium

The cadmium concentration distribution in the Detroit River water segments are shown in Figure 4.21. The results indicated that, the concentrations near the Canadian shoreline were 0.13 to 0.32 $ug.L^{-1}$ in water and 6.20 to

16.11 $ug.g^{-1}$ in suspended solids. The range for cadmium in the American side was 0.16 to 0.31 $ug.L^{-1}$ in water segments and 7.42 to 14.64 in suspended sediments. The highest level of cadmium in the upper part of the river was observed in segment No. 7. A maximum level of 4.0 $ug.g^{-1}$ in the sediment was estimated in this area. The results suggested two main sources in this area, the municipal sewage treatment plant for the city of Detroit, and the Great Lakes Steel Division of National Steel Corporation.

PART 2

SIMULATION OF LAKE TRANSPORT

CHAPTER V

THEORETICAL DEVELOPMENTS

5.1 General

The overall model will comprise three submodels. In the following sections the mathematical aspects of the numerical models are presented. First, the circulation submodel is developed which establishes the velccity fields. Then, a transport model is developed, which uses the velocity fields to predict the steady state concentration distribution of a conventional pollutant within the lake.

Since sediment is a major carrier of many toxic substances, the process of sediment migration is assessed by treating it as a transport phenomenon. Therefore, the construction of the suspended solid submodel as well as a brief description of the unsteady toxic chemical model are presented.

5.2 Hydrodynamic Submodel

The governing equations of continuity and momentum are simplified to the conditions that prevail in Lake St.Clair. It will be shown that the linear form of the equations presented here are both applicable and mathematically convenient. The finite element method was selected to numerically solve the governing equations. Thus, for given boundary conditions the three dimensional velocity field is established within the lake.

5.2.1 Mathematical Formulation

In order to keep this section from becoming overly long, only a brief outline is presented here. The development of the steady state governing equations for Lake St.Clair is given by Ibrahim and McCorquodale,1985.

The resulting momentum and continuity equations for motion in the Cartesian coordinate become respectively:

$$-fv = -\frac{1}{\rho}\frac{\partial p}{\partial x} + \varepsilon_0 \frac{\partial^2 u}{\partial z^2} \qquad [5.1]$$

$$fu = -\frac{1}{\rho}\frac{\partial p}{\partial y} + \varepsilon_0 \frac{\partial^2 v}{\partial z^2} \qquad [5.2]$$

$$g = -\frac{1}{\rho}\frac{\partial p}{\partial z} \qquad [5.3]$$

$$\frac{\partial u}{\partial x} + \frac{\partial v}{\partial y} + \frac{\partial w}{\partial z} = 0 \qquad [5.4]$$

The boundary conditions are: the normal flux of momentum must equal to the wind stresses at the water surface and equal to the bottom stresses at the bed, as shown in Figure 5.1. Here, the bottom stresses are chosen to be parallel and linearly related to the bottom velocity, i.e.,

(1) At the free surface

$$\varepsilon_o \frac{\partial u}{\partial z} = T_x \quad ; \quad \varepsilon_o \frac{\partial v}{\partial z} = T_y \qquad [5.5]$$

(2) At the bottom

$$s \frac{\partial u}{\partial z} = u_b \quad ; \quad s \frac{\partial v}{\partial z} = v_b \qquad [5.6]$$

in which T_x, T_y = wind stress function in the x and y directions; u_b, v_b = the x and y velocities at the bottom and s = slip coefficient. However, if s is chosen to be zero this will give the full slip condition, but if s = ∞ this gives the no slip condition.

Since lake circulation is mostly driven by wind which induced shear at the surface, an error in estimating wind stress will lead to a similar error in the calculated results. Thus, the problem of estimating over-lake wind stresses has received considerable attention but without a definite resolution. Actually the problem is not simple since the surface stress is dependent on many factors such as the height and type of waves, the fetch and relative temperatures of the air and water. In order to estimate the wind stresses over the lake, Schwab and Morton (1984) reviewed and tested the applicability of three different lake-wind estimation methods for Lake Erie. They found that the method of Phillips and Irbe (1978) gave the best correlation coefficient of 0.69. Therefore, the over-lake wind velocities were obtained from Phillips and Irbe relations, while the surface wind stresses were estimated as:

$$T_s = \frac{C_o \rho_a}{\rho} |V_s| V_s \qquad [5\text{-}7]$$

where V_s = wind velocity at 4 m above water surface; ρ_a and ρ = air and water density respectively; C_o = drag coefficient; and $(C_o \rho_a/\rho) = 3{*}10^{-6}$. The relationships given by Wu (1969) were also used to obtain the wind stresses over the lake; it was found that these agreed within approximately 7% with Phillips relations.

In order to compare the magnitudes of various terms in the equations of motion to establish the validity of the shallow- lake theory, the equations are written in nondimentional form through the introduction of the variables:

$$x_* = x/L, \; y_* = y/L, \; z_* = z/D, \; h_* = h/D \qquad [5.8a]$$

$$u_* = (fL/gD)\,u, \; v_* = (fL/gD)\,v, \; w_* = (fL^2/gD^2)\,w \qquad [5.8b]$$

$$p_* = P/(\rho g D) \qquad [5.8c]$$

Where h = the local depth; L = horizontal reference dimension and D = vertical reference dimension. The following dimensionless numbers appear when these quantities as substituted into the governing equations:

$$R_o = \text{Rossby number} = (gD/f^2L^2) \qquad [5.9]$$

$$E_1 = \text{horizontal Ekman number} = \delta_1/fL^2 \qquad [5.10a]$$

$$E_0 = \text{vertical Ekman number} = \delta_0/fD^2 \qquad [5.10b]$$

For Lake St.Clair, $f=0.0001$ rad s^{-1}. The horizontal length scale, L= 40 km in x-direction and L= 45 km in y-direction. The vertical length scale, D= 12 m in the shipping channel and about 4 m in the eastern basin. Estimates of values for the vertical and horizontal eddy viscosities, δ_0 and δ_1 in Lake St.Clair were 20 $cm^2.s^{-1}$ and 10^5 $cm^2\ s^{-1}$ respectively based on the results of this study as reported in Chapter VI.

Several comments are appropriate on the foregoing nondimensional parameters. Small Rossby number, which is a measure of the ratio of the nonlinear acceleration term to the Coriolis term is often used as justification for linearizing the equation of motion. However, the model was modified in Chapter VI, to include the nonlinear acceleration terms. The computations have shown that there was very little difference in the results from using the linear equations as opposed to the nonlinear equations.

The Ekman number is a measure of the viscous effects (eddy viscosity). It can also be seen, from the scale analysis, that the horizontal Ekman number is very small, of the order of 10^{-5}, which implies that the turbulent stresses due to horizontal shear can be neglected. In fact computations have shown that values of horizontal eddy viscosity as large as 10^{7} $cm^{2}.s^{-1}$ have very little influence on the transport stream functions, Hamblin (1969). The nondimensionalized resulting equations after dropping the asterisks are:

$$-v = -\frac{\partial p}{\partial x} + \frac{\delta_0}{fD^2}\frac{\partial^2 u}{\partial z^2} \qquad [5.11]$$

$$u = -\frac{\partial p}{\partial y} + \frac{\delta_0}{fD^2}\frac{\partial^2 v}{\partial z^2} \qquad [5.12]$$

$$\frac{\partial p}{\partial z} = -1 \qquad [5.13]$$

$$\frac{\partial u}{\partial x} + \frac{\partial v}{\partial y} + \frac{\partial w}{\partial z} = 0 \qquad [5.14]$$

It was found convenient to introduce a complex notation as follows:

$$W = u + iv, \qquad \frac{\partial^2 W}{\partial z^2} = \frac{\partial^2 u}{\partial z^2} + i\,\frac{\partial^2 v}{\partial z^2} \qquad [5.15]$$

Multiply Equ. 5.12 by i and add to Equ. 5.11 to give:

$$iW = -\left(\frac{\partial p}{\partial x} + i\frac{\partial p}{\partial y}\right) + \frac{\delta_0}{fD^2}\frac{\partial^2 W}{\partial z^2} \qquad [5.16]$$

With the same boundary conditions,

$$(1) \quad \frac{\partial W}{\partial z} = R \quad \text{at water surface} \qquad [5.17]$$

$$(2) \quad \frac{\partial W}{\partial z} = sw_b \quad \text{at the bottom} \qquad [5.18]$$

Where $R = R_x + iR_y$ [5.19]

$R_x = (fL/\delta_0 g)T_x$, $R_y = (fL/\delta_0 g)T_y$ [5.20] where R = complex surface wind stress and w_b = complex bottom current.

Since the problem is linear, Ekman theory can be applied in which the solution of the three-dimensional circulation problem is separated into two parts: first find the vertical distribution of the current, then find the horizontal variations. As a result, the problem is reduced into two-dimensional problem. Therefore, if we consider for a moment that the pressure gradients and wind stresses are prescribed, Equ. 5.16 can be solved analytically with the surface and boundary conditions in Eqs. 7.17 to 7.19, the results in complex form are (Jelesnianski, 1967):

$$W = R^* \ R + T^* \left(\frac{\partial p}{\partial x} + i \frac{\partial p}{\partial y} \right) \qquad [5.21]$$

$$R^* = \frac{1}{n} \left[\sinh nz + \frac{\cosh nz}{\sinh nz} (\cosh nh - nN^*) \right] \qquad [5.22]$$

$$T^* = \frac{2m}{(1+i)} \left[N^* \ \cosh nz - \frac{1}{n} \right] \qquad [5.23]$$

$$N^* = (\cosh nh) / \left[\frac{ifD}{s} + n \coth nh \right] \qquad [5.24]$$

$$n = (1+i)m; \quad 2m^2 = fD^2/\delta_0 \qquad [5.25]$$

The solution gives the vertical profile of the horizontal velocities at any horizontal location as a function of two terms: the first term represents the surface drift current, while the second term represents the gradient or the bottom current. Equ. 5.21 has the following real and imaginary parts:

$$u = R^*_r R_x - R^*_i R_y + T^*_r \frac{\partial p}{\partial x} - T^*_i \frac{\partial p}{\partial y} \qquad [5.26]$$

$$v = R^*_r R_y + R^*_i R_x + T^*_r \frac{\partial p}{\partial y} + T^*_i \frac{\partial p}{\partial x} \qquad [5.27]$$

where R^*_r, R^*_i, T^*_r and T^*_i are given in Appendix (A).

Now let us consider the problem of determining the slopes $\partial p/\partial x$ and $\partial p/\partial y$. Welander (1957) has shown that a single second order differential equation in p can be obtained using the integration of the continuity equation, Equ. 5.14, i.e. :

$$w = - \int_{-h}^{o} \left(\frac{\partial u}{\partial x} + \frac{\partial v}{\partial y} \right) dz = 0 \qquad [5.28]$$

$$\text{or} \quad \frac{\partial}{\partial x}(hU) + \frac{\partial}{\partial y}(hV) = 0 \qquad [5.29]$$

In the above equation the rigid-lid approximation has been employed, i.e., the vertical velocity at the undisturbed water surface is assumed to be zero. The significant wave height for normal winds over Lake St.Clair is about 30 cm and the wind set-up is estimated to be 10 cm. Therefore, the expected error due to this approximation should be small for most of the lake.

Though, it is more convenient to formulate the horizontal problem in terms of a stream function, Gedney (1971), because the horizontal boundary conditions are much simpler in this case. The sign convention for the stream function is taken so that it denotes the flow rate from right to left as the observer views the line from A looking toward P as shown in Figure 5.2. The vertically integrated velocities, U and V, can be represented in terms of a stream function as :

$$U = - \frac{1}{h} \frac{\partial \psi}{\partial y} \; ; \quad V = \frac{1}{h} \frac{\partial \psi}{\partial x} \qquad [5.30]$$

The solution proceeds by vertically integrating Equ. 5.21 for z = -h to 0, in order to obtain a relation between the stream function and the pressure derivatives :

$$- \frac{\partial \psi}{\partial y} + i \frac{\partial \psi}{\partial x} = A^* (R_x + iR_y) + B^* (\frac{\partial P}{\partial x} + i \frac{\partial P}{\partial y}) \qquad [5.31]$$

Equ. 5.31 has the following real and imaginary parts:

$$-\frac{\partial\psi}{\partial y} = A^*_r R_x - A^*_i R_y + B^*_r \frac{\partial P}{\partial x} - B^*_i \frac{\partial P}{\partial y} \qquad [5.32]$$

$$\frac{\partial\psi}{\partial x} = A^*_r R_y + A^*_i R_x + B^*_r \frac{\partial P}{\partial y} + B^*_i \frac{\partial P}{\partial x} \qquad [5.33]$$

Solving Equ. 5.32 and Equ. 5.33 for the pressure derivatives produces :

$$\frac{\partial P}{\partial x} = [B^*_i \frac{\partial\psi}{\partial x} - B^*_r \frac{\partial\psi}{\partial y} - (A^*_r B^*_r + A^*_i B^*_i) R_x + (A^*_i B^*_r - A^*_r B^*_i) R_y] / [B^{*2}_r + B^{*2}_i] \qquad [5.34]$$

$$\frac{\partial P}{\partial y} = [B^*_r \frac{\partial\psi}{\partial x} - B^*_i \frac{\partial\psi}{\partial y} - (A^*_i B^*_r - A^*_r B^*_i) R_x + (A^*_r B^*_r - A^*_r B^*_r) R_y] / [B^{*2}_r + B^{*2}_i] \qquad [5.35]$$

where A^*_r, A^*_i, B^*_r and B^*_i are real coefficients related to the complex coefficients A^* and B^* above, and explicitly given in Appendix (A).

The pressure is eliminated from the momentum equations by cross differentiating Equ. 5.34 and Equ. 5.35 . Then, one partial differential equation in the stream function results:

$$\frac{\partial^2\psi}{\partial x^2} + \frac{\partial^2\psi}{\partial y^2} + A(x,y)\frac{\partial\psi}{\partial x} + B(x,y)\frac{\partial\psi}{\partial y} - C(x,y) = 0 \qquad [5.36]$$

The coefficients of Equ. 5.36 are given in Appendix (A). Where A(x,y) and B(x,y) are known functions of local depth, its partial first derivatives and eddy viscosity, while C(x,y) depends on these variables as well as the wind shear stresses. Equ. 5.36 is an inhomogeneous, linear, elliptic, second order partial differential equation for the stream function. For a given depth topography h(x,y) and a prescribed surface stress distribution, T (x,y) and T (x,y), it can be solved by the finite element method, because it has the advantage in the treatment of irregular lake geography and the flexibility in the choice of computational mesh.

5.2.2 Formulation of the Numerical Schemes

Galerkin's method has been discussed by several authors and its applications to some finite element problems is given by Martin and Carey (1973), and Zienkiewicz (1977).

Galerkin's method is a means of obtaining an approximate solution to a differential equation. It does this by requiring that the error between the approximate solution and the true solution be orthogonal to the functions used in the approximation.

The application of Galerkin method (Finlayson 1972, Gallagher et al., 1973, Pinder and Gray, 1977) with the finite element method to Equ. 5.36 yields:

$$\int_A [N]^T \left\{\frac{\partial^2\psi}{\partial x^2} + \frac{\partial^2\psi}{\partial y^2} + A(x,y)\frac{\partial\psi}{\partial x} + B(x,y)\frac{\partial\psi}{\partial y} - C(x,y)\right\} dA = 0 \quad \text{--- [5.37]}$$

The flow domain is divided into a series of elements interconnected at nodal points. Using two-dimensional simplex elements, the linear interpolation polynomial for the stream function in each element is:

$$\psi = \sum_{i=1}^{k} N_i \psi_i \qquad [5.38]$$

where ψ = stream function values at the nodes; N = the corresponding shape function. In the Galerkin formulation, the shape functions are chosen as weighting functions, while simplex elements have an approximating polynomial that consists of the constant term plus the linear terms. The number of coefficients in the polynomial is equal to the dimension of the coordinate space plus one. The two-dimensional simplex element is the triangle shown in Figure 5.3, with the interpolating linear polynomial:

$$\psi = N_i \psi_i + N_j \psi_j + N_k \psi_k \qquad [5.39]$$

The element has three shape functions one for each node

$$N_i = \frac{1}{2A}[a_i + b_i x + c_i y] \qquad [5.40]$$

where: $a_i = x_i y_k - x_k y_j$

$b_i = y_i - y_k$

$c_i = x_k - x_j$

$$N_j = \frac{1}{2A}[a_j + b_j x + c_j y] \qquad [5.41]$$

where: $a_j = x_k y_i - x_i y_k$

$b_j = y_k - y_i$

$c_j = x_i - x_k$

$$N_k = \frac{1}{2A}[a_k + b_k x + c_k y] \qquad [5.42]$$

where: $a_k = x_i y_j - x_j y_i$

$b_k = y_i - y_j$

$c_k = x_j - x_i$

and A is the area of the triangle.

The highest-order derivative that is allowable in Equ. 5.37 is one greater than the order of the continuity in the interpolation equation, which is of order zero (continuity in ψ but not in the first derivative). Therefore, derivatives of the second order should be reduced to the first order using integration by parts as follows:

$$\frac{\partial}{\partial x}\left(\{N\}\frac{\partial\psi}{\partial x}\right) = \{N\}\frac{\partial^2\psi}{\partial x^2} + \frac{\partial\{N\}}{\partial x}\frac{\partial\psi}{\partial x} \qquad [5.43]$$

Then the first term in the volume integral becomes

$$\int_V \{N\}\frac{\partial^2\psi}{\partial x^2}dV = \int_V \frac{\partial}{\partial x}\left(\{N\}\frac{\partial\psi}{\partial x}\right)dV - \int_V \frac{\partial\{N\}}{\partial x}\frac{\partial\psi}{\partial x}dV \qquad [5.44]$$

Applying Gauss divergence theorem to the first integral gives

$$\int_V \frac{\partial}{\partial x} \left(\{N\} \frac{\partial \psi}{\partial x}\right) dV = \int_S \ell_x \{N\} \frac{\partial \psi}{\partial x} dS \qquad [5.45]$$

where ℓ_x is the direction cosine of the normal to the outer surface with respect to x axis. Performing similar operations on the other term in Equ. 5.36 and combining the results and noting that dV = h dA and dS = h dL, the result is:

$$\int_L \{N\} \left\{\frac{\partial \psi}{\partial x} \ell_x + \frac{\partial \psi}{\partial y} \ell_y\right\} dL - \int_A \left\{\frac{\partial \{N\}}{\partial x} \frac{\partial \psi}{\partial x} + \frac{\partial \{N\}}{\partial y} \frac{\partial \psi}{\partial y}\right\} dA$$

$$+ \int_A \left\{A(x,y) \{N\} \frac{\partial \psi}{\partial x} + B(x,y) \{N\} \frac{\partial \psi}{\partial x}\right\} dA - \int_A C(x,y) \{N\} \, dA = 0$$

$$\text{---} \qquad [5.46]$$

where L = the length of the element side. The first integral in Equ. 5.46 is the surface flux term, which at the external boundaries of the lake can be satisfied immediately at the boundary nodes by specification of the appropriate jumps in ψ across each inflow or outflow. The closure integrals along internal (interelement) boundaries would uniformly vanish (Szabo and Lee, 1969). Therefore, the boundary conditions can be introduced by modifying the rows and columns of the global stiffness matrix [R] corresponding to the prescribed variables, and incorporating the prescribed terms in the forcing vector {F}.

Evaluation of Equ. 5.46 yields the system of equations

$$[R^e]\{\psi\} = \{F^e\} \qquad [5.47]$$

where :

$$[R^e] = \int_A \{- \frac{\partial\{N\}}{\partial x} \frac{\partial[N]}{\partial x} - \frac{\partial\{N\}}{\partial y} \frac{\partial[N]}{\partial y}$$

$$+ A(x,y)\{N\} \frac{\partial[N]}{\partial x} + B(x,y)\{N\} \frac{\partial[N]}{\partial x}\} dA \qquad [5.48]$$

$$\{F^e\} = \int_A C(x,y)\ \{N\}\ dA = 0 \qquad [5.49]$$

To simplify the integration of Equ. 5.48 and 5.49, the terms A(x,y), B(x,y) and C(x,y) will be considered as constants for each element. The full set of equations for Lake St.Clair can be constructed by simple addition of all elements, i.e.

$$[R]\{\psi\} = \{F\} \qquad [5.50]$$

$$\text{where } R_{ij} = \sum_{e=1}^{NE} R_{ij}^{e} \qquad [5.51]$$

$$F_{i} = \sum_{e=1}^{NE} F_{i}^{e} \qquad [5.52]$$

and NE = number of elements.

The resulting matrix from Equ. 5.51 is sparse and nonsymmetric. The computer program of Gupta and Tanji (1977) was found to be efficient in solving these large, sparse, unsymmetric systems of linear equations.

The solution of Equ. 5.50 gives the values of stream function at the nodal points, from which the depth averaged velocities can easily be computed for each element. The pressure gradients can be found from Equ. 5.30. By back substitutions into Equ. 5.25 as in the previous work of Gallagher et al. (1973), the distribution of horizontal velocities over depth can be obtained. To avoid computational singularity due to zero depth, a finite small depth of 0.5 m was considered to bound the flow region except at the inlet/outlet streams where the actual depths were used.

5.3 Pollutant Transport Model

The velocity and the circulation patterns established from the hydrodynamic submodel are used as input to predict the concentration profiles of many conventional pollutantsin Lake St.Clair.

5.3.1 Governing Equations

The transport of a conventional pollutant in a lake can be solved by means of the following turbulent diffusion and continuity equations:

$$\frac{\partial C}{\partial t} + u\frac{\partial C}{\partial x} + v\frac{\partial C}{\partial y} + w\frac{\partial C}{\partial z} = \frac{\partial}{\partial x}E_x\frac{\partial C}{\partial x} + \frac{\partial}{\partial y}E_y\frac{\partial C}{\partial y} + \frac{\partial}{\partial z}E_z\frac{\partial C}{\partial z}$$

$$+k'C + G \qquad [5.53]$$

$$\frac{\partial u}{\partial x} + \frac{\partial v}{\partial y} + \frac{\partial w}{\partial z} = 0 \qquad [5.54]$$

In which C = concentration of the contaminant; u, v and w = velocity components in x, y and z directions; G = source or sink term; k'= first order reaction coefficient and t = time. The underlying assumptions of the model for Lake St.Clair include:

1. The contaminant concentration is nearly homogeneous in vertical for shallow lakes.

2. The hydraulic detention time for the freshwater in the lake is relatively short (one week). Therefore, a steady state condition can simplify the model parameters without any serious liability on the analysis.

3. A constant eddy coefficient was used in this study.

Under the foregoing assumptions, Equ. 5.53 is integrated vertically between the bottom and the water surface to give the following form (Salmon et al., 1980).

$$U\frac{\partial C}{\partial x} + V\frac{\partial C}{\partial y} = \frac{1}{h}\frac{\partial}{\partial x}\left(hE_x\frac{\partial C}{\partial x}\right) + \frac{1}{h}\frac{\partial}{\partial y}\left(hE_y\frac{\partial C}{\partial y}\right)$$

$$- \frac{1}{h}\left(E_x\frac{\partial C}{\partial x}\frac{\partial h}{\partial x}\right) - \frac{1}{h}\left(E_y\frac{\partial C}{\partial y}\frac{\partial h}{\partial y}\right) + k'C + G \qquad [5.55]$$

where C = depth averaged concentration; U, V = depth averaged velocities in x and y directions. The boundary conditions on Equ. 5.55 are: (1) prescribed values of concentrations on the S_1 part of the inlet boundary at the rivers as shown in Figure 5.4 (2) no contaminant transfer by flux across the boundary S_2. Source/sink terms acting on the volume are divided into distributed source rate term G (external input), and a decay rate term k'C (internal reaction).

5.3.2 Finite Element Formulations

The numerical model in this study is similar to the two-dimensional finite element model by Salmon et al. (1980), except for the addition of the upwinding finite element scheme and the steady state assumption. However, the application of Galerkin method to Equ. 5.55 is similar to that used in the hydrodynamic model. The linear interpolation polynomial for the concentration of the contaminant is:

$$C = \sum_{i=1}^{k} N_i C_i \qquad [5.56]$$

where N = the same shape functions as employed in the hydrodynamic model. Equation 7.55 is transformed into an equation containing first derivatives in x and y directions. Introducing the boundary terms into the resulting integral gives the following set of equations:

$$[T^e] \{C\} = \{G^e\} \qquad [5.57]$$

where :

$$[T^e] = \int_A \{N\} \{U \frac{\partial [N]}{\partial x} + V \frac{\partial [N]}{\partial y} - \frac{1}{h} \frac{\partial}{\partial x}[hE_x \frac{\partial [N]}{\partial x}] - \frac{1}{h} \frac{\partial}{\partial y}[hE_y \frac{\partial [N]}{\partial y}]$$

$$+ \frac{1}{h}[E_x \frac{\partial h}{\partial x} \frac{\partial [N]}{\partial x} + E_y \frac{\partial h}{\partial y} \frac{\partial [N]}{\partial y} - k']\} \, dA \qquad [5.58]$$

$$\{G^e\} = \int_A \{N\} \, G \, dA \qquad [5.59]$$

The contour integral term has been excluded from Equ. 5.57 by introducing the boundary conditions as in Figure 5.4. The global equations take the form:

$$[T] \{C\} = \{G\} \qquad [5.60]$$

$$\text{where } T_{ij} = \sum_{e=1}^{NE} T_{ij}^e \qquad [5.61]$$

$$G_i = \sum_{e=1}^{NE} G_i^e \qquad [5.62]$$

5.3.3 The Convective Transport Problem

The Galerkin finite element solution of Equ. 5.53 leads to numerical instability especially at very high velocities where the convective terms become relatively more important than the diffusion terms. These difficulities stem from the fact that the formulation of Galerkin finite element method gives a central difference approximation to the convective term. These difficulties have been recognized in the finite element method, and have been overcome by upwind finite element schemes (Christie et al., 1976, Heinrich and Zienkiewicz, 1977 and Hughes, 1978). More recently, Payre et al., 1982, presented another upwinding technique that uses a standard numerical integration scheme so that the relocation of integration nodes gives the optimum upwinding effect without seriously decreasing the accuracy of the solution. Quadrangular isoparametric elements were used in their study.

The application of their work to the simplex two-dimensional elements will be considered here. For the linear system in Equ. 5.57, one can evaluate the integration of the element shape function by numerical formulae defined on each reference element (Kreyszing, 1972):

$$\int_R C(x,y)\,dx\,dy = \int_{R*} C[x(s,t),y(s,t)]\,|J(s,t)|\,ds\,dt$$

$$= \sum_{i=1}^{N} C[x(s_i,t_i),y(s_i,t_i)]\,|J(s_i,t_i)|\,W_i \qquad [5.63]$$

where x,y = the global coordinates; s,t = the local coordinates; W_i = the weight associated with integration node (s_i, t_i); $|J(s,t)|$ = the Jacobian of the transformation (Zienkiewicz, 1977) and N = number of integration points. In the simplex elements it is accurate enough to evaluate the integration at one point, while allowing this node to be dragged along the streamline. The streamline is determined by the velocity components (U,V) at the centroid of the element as shown in Figure 5.5. This displacement can be calculated according to the relocation:

$$o\,o' = a\,H_1 \qquad [5.64]$$

where a = the upwinding coefficient $0 \leq a \leq 1.0$; H_1 = the downstream part of the streamline through the node. Clearly, if a = 1.0 in Equ. 5.64, the expression gives full upwinding which represents the backward difference in the finite difference analog, while a = 0 gives no upwinding, which corresponds to the central difference approximation in finite difference schemes. Thus it is seen that, the upwinding coefficient controls the required degree of upwinding. Christie et al. (1976) give the value of , (a) for the uniform case as:

$$a = \coth(P_e/2) - (2/P_e) \qquad [5.65]$$

where $P_e = |V|H/E$

$$V = (U^2 + V^2)^{1/2}$$

$$E_c = (E_x^2 + E_y^2)^{1/2}$$

where P_e = local Peclet number, the ratio of the diffusion to the convection phenomena, and therefore controls the necessity of upwinding; V = the fluid velocity at the node; H = the curvilinear length of the steamline through the node; E = diffusion coefficient. Once the integration point is located, one can calculate the local coordinate of that point in the reference element R* .

5.4 Suspended Solids Transport

In the next section a description of the suspended sediment model is first given, followed by a brief description of a statistical model based on turbidity and suspended solids data. These are used as tools to understand better the complex phenomena of sediment resuspension.

5.4.1 Model Structure

The governing equation of the vertically averaged, two-dimensional sediment transport is similar to the pollutant transport equation, Equ. 5.55, except in the appearance of the vertical convection terms due to the gravitational settling of the sediment. This turbulent, steady state diffusion equation reads:

$$U\frac{\partial C}{\partial x} + V\frac{\partial C}{\partial y} = \frac{1}{h}\frac{\partial}{\partial x}\left(hE_x\frac{\partial C}{\partial x}\right) + \frac{1}{h}\frac{\partial}{\partial y}\left(hE_y\frac{\partial C}{\partial y}\right)$$

$$-\frac{1}{h}\left(E_x\frac{\partial C}{\partial x}\frac{\partial h}{\partial x}\right) - \frac{1}{h}\left(E_y\frac{\partial C}{\partial y}\frac{\partial h}{\partial y}\right) + \frac{V^*}{h}C + G_o \qquad [5.66]$$

where C = depth average concentration of sediment per unit volume; U, V = depth average velocities in x and y directions; G_o= source term accounts for the resuspension of already settled sediments and V^* = settling velocity. The fluid velocity field (U,V) required for the solution of Equ. 5.66 is determined from the lake circulation submodel.

In general, wind stress has two main effects on the water movements: one effect is the mean circulation which responsible for the transport of the sediment and pollutant, while the other effect is due to the wave generation and the oscillatory motions which are considered to be the main cause of the resuspension of the already settled sediment particles. Therefore, sediment deposition and erosion rates, (V^*/h) and Q_o, are evaluated separately at each element for different wind speeds and directions.

5.4.2 Numerical Solution

The Galerkin finite element representation of Equ. 5.66 is completely analogous to that used in the pollutant transport submodel. At the element level, the prediction equation will be:

$$[T_o^e]\{C\} = \{G_o^e\} \qquad [5.67]$$

where :

$$[T_o^e] = \int_A \{N\}[U\frac{\partial[N]}{\partial x} + V\frac{\partial[N]}{\partial y} - \frac{1}{h}\frac{\partial}{\partial x}[hE_x\frac{\partial[N]}{\partial x}] - \frac{1}{h}\frac{\partial}{\partial y}[hE_y\frac{\partial[N]}{\partial y}]$$

$$+ \frac{1}{h}[E_x\frac{\partial h}{\partial x}\frac{\partial[N]}{\partial x} + E_y\frac{\partial h}{\partial y}\frac{\partial[N]}{\partial y} - V^*)]\,dA \qquad [5.68]$$

$$\{G_o^e\} = \int_A \{N\}\,G_o\,dA \qquad [5.69]$$

The global equations take the form:

$$[T_0]\{C\} = \{G_0\} \qquad [5.70]$$

$$\text{where } T_{0_{ij}} = \sum_{e=1}^{NE} T_{0_{ij}}^{e} \qquad [5.71]$$

$$G_{0_{i}} = \sum_{e=1}^{NE} G_{0_{i}}^{e} \qquad [5.72]$$

The upward flux of the sediments from the bottom due to shear stresses generated by waves and currents is estimated based on the study made by Sheng and Lick, (1979) for the Western Basin of Lake Erie. Briefly, the wave characteristics are hindcast by the shallow water Sverdrup-Munk-Betschneider (SMB) method [U.S. Army Coastal Engineering Research Center, 1977]. Then, the rate of resuspension was empirically related to the bottom stress by:

$$G_0 = C_1 (T_B - 0.5) \qquad T_B \le 2$$

$$G_0 = C_2 (T_B - 1.515) \qquad T_B > 2 \qquad [5.73]$$

where $C_1 = 1.33*10^{-6}$ s cm^{-1}; $C_2 = 4.12*10^{-4}$ s cm^{-1} and T_B= the bottom stress. In their model, they assumed that the currents and the waves are parallel to each other. Therefore, for the steady state condition the current and wave stress are represented by:

$$\tau_c = \rho f_c |v_b| v_b \qquad [5.74]$$

$$\tau_w = \rho f_w |u_m| u_m \qquad [5.75]$$

where u_m = the maximum horizontal velocity at the edge of the bottom caused by the wave; v_b = bottom flow velocity due to the currents; f_c and f_w = 0.004 (Sternberg, 1972) and were assumed to be constants.

5.4.3 Statistical Model

In order to understand the significance of various parameters and the relative importance of various mechanisms of sediment transport, extensive field data have been collected on wind, rainfall, raw water turbidity and suspended sediments. The strategy used for collecting the data for Lake St.Clair was based on fixed station design, to follow the temporal changes at these fixed locations. Statistical techniques are used to summarize the historical information available from Belle River and Windsor Water Treatment Plants, in order to develop an adequate empirical model for the suspended sediment concentrations in Lake St.Clair. Moreover, the collected data have allowed us to re-examine and modify the toxic chemical TOXIWASP model. The following steps were followed to build the model: An initial model to predict the raw water turbidity was fitted to the observed data. The decision was made here to use model of the form

$$TR = e_1 + e_2 (W^2) + e_3 (Rf) + e_4 (TR^*) \qquad [5.76]$$

where TR and TR* = raw water turbidity at day t and t-1, W = wind speed in km h^{-1}, Rf = rain fall intensity per day and e_1,e_2 and e_3 are unknown constants. Since model (5.76) is linear in the parameters e_1,e_2 and e_3, their values can be easily estimated using least squares. Using the available suspended sediments data, a linear relationship between the raw water turbidity and suspended sediments is obtained. Finally, using these two models a direct relation between the suspended sediment concentrations and wind speed can be obtained.

5.5 Toxic Chemical Model

The mass balance model (TOXIWASP) disscused in Sec. 3.5 will be used to calculate the transient concentration distribution for the chemicals in the water column and in the sediment in lake St.Clair. It is understood that the transient values of the physical processes such as the input loading, advection, diffusion and sediment transport have been calculated. TOXIWASP model treats sediments as a single size fraction that is advected and dispersed in the water and that settles (and deposits). Sediment is also returned from the bed to water column through erosion. The net exchange of sediments with the bed, S_2, in Equ. 3-40, is calculated in the model as:

$$S_2 = (Ws \cdot Sb/Lb) - (Wd \cdot Sw/Lw) \qquad [5\text{-}77]$$

where Ws = scour (erosion) velocity of bed sediment, Wb = deposition velocity of suspended sediments, Lb = depth of active bed sediment, Lw = depth of water layer, Sb = concentration of sediment in bed and Sw = concentration of sediment in water.

The approach used by TOXIWASP model for the sediment transport processes is based on constant settling or scour velocity for each segment during the simulation period, which are read in using the parameter Ws(j). Since Lake St.Clair is relatively shallow, the resuspension rate of sediments from the bottom must account for the seasonal variabilities of the wind speed and water currents. However, because Ws(j) are unknown variables, the estimation of these velocities can be obtained only by iteration, which is performed in the following manner. Assume first a steady wind speed from a known direction, then calculate the hydrodynamics in the lake under this wind condition. From the statistical analyses of the sediment model estimate the suspended sediment concentrations under this wind condition. To start the iteration, intial values of Ws(j) are chosen, then the estimated suspended sediment concentrations are compared with the predicted values from the model. The final estimates for Ws(j) should give the same estimated suspended sediment concentrations. Therefore, the subroutine TOXISED in the model was modified to handle the settling or erosion rates as piecewise linear functions in time.

Leach, 1980 characterized Lake St.Clair based on cluster analyses of physical and chemical data as it has two distinct major water masses which shifted according to wind direction and speed. However, the horizontal gradients in water quality parameters in the lake are large, ranging from degraded water quality in the southeastern basin due to input from Ontario tributaries and shoreline urban development, to nearly high quality water flowing from the main channels of the St.Clair River in the northwestern basin. However, in the vertical direction, the lake is generally well-mixed. Therefore, the lake is divided into 24 spatial segments (8 water, 8 surface bed and 8 subsurface bed segments) as shown in Figure 5.6. Each segment is assumed homogeneous and can be represented by average concentration of sediment and chemical.

CHAPTER VI

LAKE MODELS CALIBRATION AND VALIDATION

6.1 General

Just as in river simulation, the basic mathematical equations relevent to a given problem contain a number of empirical constants, which cannot be determined from theory alone but must be tuned by means of a proper field data. In this chapter, the calibration and verification results of the hydrodynamic, pollutant transport, sediment transport and toxic chemical submodels will be presented.

The data collected by the Water Characteristics of the Lake Survey Center and GLERL from nine cruises for the year 1974 are used in this study (Bell, 1980). In addition, levels of PCBs in bed sediment on a grid from lake St.Clair for the year 1970 and 1974 have been reported by Frank, et al., 1977 is used to calibrate the TOXIWASP model. Also, velocity measurements are obtained from Lake St.Clair for the hydrodynamic model. Other sources of data necessary to accurately calibrate and verify the submodels are obtained from the following agencies:

1. Environment Canada,
2. U.S. Geological Survey,

3. U.S. Corps of Engineers,

4. Ontario Ministry of Environment,

5. The International Joint Commission,

6. U.S. Environmental Protection Agency,

7. U.S. National Oceanic and Atmospheric Administration.

The proposed finite element hydrodynamic and transport models were programmed in FORTRAN IV G LEVEL 21. The details of the computer programs are presented in Appendix C. The following sections summarize the various tests that were used to investigate the behaviour of the models.

6.2 Hydrodynamic Submodel

In general, a model which is successfully calibrated by observations is not considered to be automatically verified. Therefore, we will investigate how well the model represents the movements of water in Lake St.Clair using various approaches. The first approach for validation is to check the validity of the assumptions made in the model. Although, the principal assumptions made in the model were discussed earlier in Section 5.2, the effect of the nonlinear inertia terms on the flow pattern will be presented now. The second approach in validation is to test the sensitivity of the chosen unknown parameters of the model. The main parameters for this model are the vertical eddy term and the slip-coefficient at the lake bottom. The reason for this is that the chosen constants must be fairly universal, which means that further data sets can be simulated as well as the original ones. A sensitivity analysis is always very useful, showing how strongly a state quantity, such as current velocities responds to the variation of the model parameters. Finally, a station by station comparison of computed currents and observed data was performed, also a qualitative comparision of the various characteristics between the model output and measured data was obtained.

6.2.1 The Effect of Inertia on Flow Pattern

An order of magnitude analysis, Section 5.2, indicates that the inertia terms are not important in most of the lake. However, one should be cautious in a zone of coastal jets or other rapid flow, such as near the outlets of the St.Clair River and the entrance of the Detroit River. Therefore, the effect of the inertia term on the flow pattern was tested. The standard method of carrying out this test is as follows: consider two models, the first has the particular term under consideration and a second model which is similar to the first except that it does not have the particular term under consideration. Comparison of these two models gives us an idea of whether the particular term is significant for the model or not. By incorporating the nonlinear term as a secondary effect, The equation of motions in nondimensional form become:

$$R[u\frac{\partial u}{\partial x} + v\frac{\partial u}{\partial y}] - v = -\frac{\partial p}{\partial x} + \frac{\delta_0}{fD^2}\frac{\partial^2 u}{\partial z^2} \qquad [6.1]$$

$$R[u\frac{\partial v}{\partial x} + v\frac{\partial v}{\partial y}] + u = -\frac{\partial p}{\partial y} + \frac{\delta_0}{fD^2}\frac{\partial^2 v}{\partial z^2} \qquad [6.2]$$

$$\frac{\partial P}{\partial z} = -1 \qquad [6.3]$$

$$\frac{\partial u}{\partial x} + \frac{\partial v}{\partial y} + \frac{\partial w}{\partial z} = 0 \qquad [6.4]$$

where $R = (v/fL)$ = Rossby number.

The following iterative algorithm was used for solving the nonlinear equations of motion:

1. Consider the inertia terms in Eqs. 6.1 and 6.2 equal to zero and solve the linearized equations to obtain the vertically integrated velocities U and V for each element.
2. Use an interlacing finite element model formulation, as shown in Figure 6.1. to calculate the derivatives of U and V with respect to x and y. Then, the approximate values for the inertia terms are:

$$I = R[u \frac{\partial u}{\partial x} + v \frac{\partial u}{\partial y}] \qquad [6.5]$$

$$J = R[u \frac{\partial v}{\partial x} + v \frac{\partial v}{\partial y}] \qquad [6.6]$$

where:

$$u = [N]\{U\} \qquad , v = [N]\{V\} \qquad [6.7]$$

$$\frac{\partial u}{\partial x} = \frac{\partial [N]}{\partial x}\{U\} \qquad , \frac{\partial v}{\partial x} = \frac{\partial [N]}{\partial x}\{V\} \qquad [6.8]$$

$$\frac{\partial u}{\partial y} = \frac{\partial [N]}{\partial y}\{U\} \qquad , \frac{\partial v}{\partial y} = \frac{\partial [N]}{\partial y}\{V\} \qquad [6.9]$$

3. Solve Eqs. 6.1 and 6.2 considering that the inertia terms are constants and obtain new values for U and V for each element.
4. Repeat step 2 and 3 several times until stable values for U and V are reached.

The results showed that the changes in the values of the velocities U and V are in the range of 3% of the velocities without the inertia terms. This is not surprising since the water mass flux that is transported across the finite element grids at the entrance to the lake has its horizontal momentum arbitrarily diffused along the element side thus reducing the effect of inertia.

6.2.2 Sensitivity Analysis

There is a degree of uncertainity associated with the estimation of model parameters. If a small variation in an input parameter causes a large difference in the model output, the model is, then, said to be sensitive to this parameter. One of the advantages of sensitivity analysis is that, it allows us to concentrate the data abstraction effort on the parameters which will most significantly affect the model results. In this section, we examine the sensitivity of the solution of the constructed hydrodynamic submodel to variation in the following parameters: wind speed and direction, the slip-coefficient for bottom friction and the vertical eddy viscosity.

6.2.2.1 Wind Stresses

Winds constitute a principal force driving Lake St.Clair currents. A variety of results can be obtained from the hydrodynamic model for cases of uniform and steady surface wind stress. The direction and the magnitude of the wind can be chosen to simulate many storms to study their effects on the circulation pattern. The wind speed, for this study, was varied from 0 to 40 km h^{-1}. While 8 wind directions, N, NE, E, SE, S, SW, W and NW, were tested for each wind speed. Detailed results of the hydrodynamic calculations with 8.0m.s^{-1} over-land wind speed from only four directions are presented here for steady state conditions.

Southwest Wind:

The vertically integrated velocities under this wind speed from the southwest direction, as shown in Figure 6.2, indicated that the circulation consists of downwind flow in the shallower water along the shores of the lake parallel to the wind vector and upwind or return flow in the deeper parts of the lake. This would cause two secondary opposite circulations, large anticlockwise circulation in the south and small clockwise one in the north part of the eastern basin. In localized areas, like the shipping channel, the hydraulic flow dominates the circulation, while an appreciable influence is also exerted by inertial forces formed by large outflows to Detroit River.

The highest velocities occur near the surface and are in the downwind direction as shown in Figure 6.3. However, as can be seen from Figure 6.4, the current velocities at 0.2 depth below water surface significantly decreased in the deeper parts of the lake. At 0.6 depth nearly most of the velocities are in the upwind direction, except at the outlet of the lake near the Detroit River as shown in Figure 6.5. Also, an anticlockwise circulation is observed in the north part of the eastern basin.

Northwest Wind:

With a wind from the northwest a large anticlockwise circulation in the southern portion of the eastern basin, forms, while a weak clockwise circulation occurs in the northeast basin, as shown in Figure 6.6. The surface currents are towards the southeast in most of the lake, except in the main shipping channel near the entrance of the Detroit River where the currents deflect 30° to the right of the wind direction as indicated in Figure 6.7. This was due to the strong outflow current components in this area. In Figure 6.8 similar patterns are observed for the velocities at 0.2 depth below water surface. The major difference is the currents near the main shipping channel, where the directions are towared the southwest. However, at 0.6 of the depth the upwind return flow is clearly seen in Figure 6.9.

Northeast Wind:

A northeast wind will produce an anticlockwise circulation in the northeast quadrant of the lake and cause anticlockwise circulation in the western sector in the neighbourkood of the navigation channel as shown in Figure 6.10. The surface current tends to be downwind in all the lake, as observed in Figure 6.11. Similar patterns are observed for the velocities at 0.2 depth below water surface, as given in Figure 6.12. It can be seen from Figure 6.13 that the currents near the bottom are in the upwind direction for the eastern basin, while a large anticlockwise circulation is formed to the west of the shipping channel.

West Wind:

The circulation patterns for the same wind speed from the west include a large anticlockwise rotation in the eastern basin, as shown in Figure 6.14. The surface water layer follows the general direction of the wind stress, thus opposing the near bottom flow in most of the lake. This is strongest in the eastern basin and near the navigation channel as indicated in Figure 6.15, Figure 6.16 and Figure 6.17. These two opposing motions in the vertical direction would tend to increase the mixing in the flow.

6.2.2.2 Vertical Eddy Viscosity

Vertical eddy viscosity arises from the turbulent friction force between water layers. Ekman used the laminar analogy to write these stresses as function of a constant turbulent vertical eddy viscosity coefficient, ε_0. In fact, the actual value of the vertical eddy viscosity in a lake would be nearly zero at the surface and the bottom, as a result of the inhibiting effect of the boundaries, (no breaking waves at the water surface and solid boundary exist at the bottom). A maximum value for the eddy viscosity would be between the bed and surface, where the flow velocity is the largest, Pearce (1981). However, the actual variation of eddy viscosity is not known. Some recent solutions for depth dependent eddy viscosity have been presented by Thomas (1975) and Madsen (1977). Although these modifications for different vertical distributions of eddy viscosity can usually be readily anticipated, they make the numerical calculations rather difficult.

It appears that there is no agreement among researchers on how to treat the vertical eddy viscosity, and thus it will be considered as part of the calibration process. The present discussion, therefore, will be restricted to the case of constant eddy viscosity in the vertical. As indicated by Cheng and Tung (1970), it is possible to calibrate such a model using field measurements. For instance, consider the effect of different eddy coefficient values on the magnitude of the currents with selected slip coefficient. The variation in increasing eddy viscosity values with the horizontal velocity is shown in Table 6.1. Figure 6.18 and Figure 6.19 indicated that, by increasing the vertical eddy coefficient by a factor 5, both the u and v components decreased by a factor of 5 to 10. Therefore, the model is highly sensitive to the eddy coefficient values, especially near the water surface.

6.2.2.3 Bottom Boundary Conditions

It has been observed that the vertical distribution of horizontal velocity with no-slip condition at the bed, exhibits significant changes due to the small changes of the eddy viscosity parameter. However, the introduction of a second dissipating parameter, such as slip coefficient, greatly reduces this sensitivity and also gives more freedom when working with dependent data to better fit computed and observed velocity measurements.

The effect of various values of the slip coefficient is indicated in Table 6.2. Figure 6.20 and Figure 6.21 show the effect of changing the slip coefficient at the bottom. The velocity components u and v were found to be slightly sensitive to the variation of the bottom slip coefficient.

6.2.3 Velocity Measurement

Water current data were collected at 26 stations, to ensure uniform coverage of the lake system, as shown in Figure 6.22. The work was carried out on four days representing different wind conditions. Because of limitations of the measurement equipment and the boat, all the measurements were made when the near surface winds were less than 4m s^{-1} and the surface wave heights were below 30 cm. An electromagnetic water current meter (Marsh-McBirny Model No. 201-D) was used to measure the point velocities, while the current direction was determined using a Brunton Cadet Compass. The current could be measured within ±1.0 cm s^{-1}, while the direction could be estimated to ±10°. A drogue consisting of an X-vane with a nearly submerged float was also used to evaluate near surface currents as shown in Figure 6.23. The survey boat was navigated and stations were established by using an inertial coordinate locator. The boat was secured on station by two anchors.

The water depth, h, was measured at each station. Then, the vertical profile of the horizontal velocity was determind by taking readings at the water surface, 0.2h, 0.5h and 0.8h. The wind speed and direction observations for this study were obtained from the Windsor, City Airport. In the calibration process one set of measured data was used to select a suitable value for the vertical eddy viscosity through an iterative process so that the calculated currents fit those measured, while the rest of the data were used to check the calibrated model. In general, the current magnitudes indicate a fairly good agreement with the measured values as shown in Figure 6.24. The overall correlation coefficient and the root mean square difference between the paired measured and predicted current values were 0.99 and 1.30 cm s^{-1}, respectively, while the direction of the measured and predicted currents gave a correlation coefficient of 0.95 and root square difference of 22.5°. The mean difference between the predicted and measured current magnitudes was -0.25 cm s^{-1} while the mean difference for the directions was +5°.

6.3 Pollutant Submodel

Chloride was used as a conservative ion to calibrate the finite element transport submodel by adjusting the horizontal diffusion coefficient to optimize the agreement between calculated and measured concentrations. Therefore, data for the chloride distribution from cruise no. 5 (Bell, 1980) was selected for the model calibration. The reason for this is the consistency of the conditions for the recorded wind conditions during the two-week cruise, since the simulation will be for steady state conditions. The average chloride concentrations for the inflows to Lake St.Clair were held constant during the simulation. To provide the model with the headwater concentrations, the average of river cruise sample stations data at the head of Thames River, Clinton River and the branches of the Delta of St.Clair River, were used. The model parameters are given in Table 6.3. The calculated concentrations for the same wind and load conditions indicate a fairly good agreement with the measured values as shown in Figure 6.25. After calibration under this wind condition, a diffusion coefficient of 10^5 cm^2 s^{-1} was obtained for Lake St.Clair.

In order to verify the model, the data from cruise no. 6 (Bell, 1980) is selected to be compared with the predicted results. Essentially, the previously specified diffusion coefficient is kept the same as given previously.

Figure 6.26 shows the computed and observed results. Since the agreement is as good as in the other cruise, the model is considered to be verified in application for Lake St.Clair under moderate to high winds.

Thus, the first part of the simulation model has been shown to be reliable in establishing the velocity fields and the dispersion coefficients which are the input to the sediment/toxic chemical (TOXIWASP) model.

6.4 Suspended Solids

Examination of the loading results of fine-grained sediment to Lake St.Clair shows the dominant influence of the St.Clair and Thames Rivers. Much of the river loading occurs during the heavy runoff events following the melting of ice and snow in spring. After ice breakup, wind constitutes a principal force for providing Lake St. Clair with energy which generates currents and waves. As a result, a significant erosion along the shoreline, during high wind storms, can be a significant source of fine-grained sediments in the lake. In general, this large amount of sediment loading and the shallow depth of Lake St.Clair result in high surface water sediment concentrations and fast response to meteorological changes. As indicated previously, wind speed and rainfall data are important in the analyses. Figure 6.27 shows the records of the daily means of wind speed in 1983. The lake has the highest wind speed during spring and fall. Figure 6.28 illustrates the seasonal variabilities of the turbidity records from Windsor Water Treatment Plant, (WTP), for the same year.

Therefore, the purpose of the following analysis is to develop a statistical model for estimating the changes in the turbidity concentrations due to different wind speeds and rainfall conditions. To determine this pattern, the turbidity values from Belle River and Windsor Water Treatment Plants for the years 1983 and 1984 are used in model Equ. 5.76. The results of fitting model Equ. 5.76 to the observed turbidity data can be summarized as follows. The parameters e_1, e_2, e_3 and e_4 for the regression model were -1.1082, 0.0291, 0.2286 and 0.7410 respectively. The model explains very well the pattern of the daily variations as function of the square wind speed, rainfall and turbidity concentrations in the previous day as independent variables. The values of the F-statistic were 70, 6 and 534 respectively, which are highly significant. The corresponding R^2 value for the model was high (0.698). Using the available suspended solids data from Windsor WTP, a linear relationship between the raw water turbidity and suspended solids is obtained in Figure 6.29a. From these two relations, the suspended solids concentrations can be obtained at this location. Similar relationships can be obtained for other locations around Lake St.Clair. The model was found to be appropriate for estimating the suspended solids concentrations at the outlet of Lake St.Clair. This was supported by the observed suspended solids concentrations from Windsor WTP as well as from sampling stations at the head of Detroit River. These values were plotted against the square of wind speed in Figure 6.29b. The Figure shows the strong correlation between these measurements and their corresponding wind speed.

In determining an average estimate for the settling velocity of suspended solids in Lake St.Clair, the data from cruise No.5 and No. 6 (Bell, 1980) were used in the finite element transport model. Since the average daily wind speeds during both cruises were low, the apparent net resuspension rate of the sediment was taken to be zero. Therefore, the calibration for suspended solids was accomplished by only adjusting the settling velocity. Table 6.4 contains the parameter values associated with the suspended solids calibration. However, the sample stations in determining the headwater suspended solids concentrations for Channel Ecarte, Rankin Creek and Boyle Drain were missing. Thus, the boundary concentrations for those streams were assumed to be zero.

Figure 6.30 and Figure 6.31 present the direct comparison of model output to observed data. In general, the estimated suspended solid concentrations matched the observed data. However, in the north part of the eastern basin the observed concentrations were always more than the estimated values. An important source of discrepancy is that there are no external sediments coming into this area.

6.5 PCBs: Calibration, 1970 to 1974

An historical simulation over a period of four years has been implemented for the distribution of PCBs in Lake St.Clair. The observed data on the concentration of PCBs in the sediment used in the calibration were taken from the study by Frank, et al., 1977. The initial condition for the model was set based on the 1970 data as given in Table 6.5. Then, a comparison between the observed concentration of PCBs in sediment for 1974 and the calculated values was used to calibrate the model. It is important to note here that, given the uncertainties surrounding the historical time-series of the loads over the period 1970 to 1974, the simulation results are intended primarily as a preliminary check on the consistency of the loading data and the lake concentration data. The observed distribution of PCBs in bed sediment is given in Figure 6.32.

6.5.1 Loading Estimates

Time-variable forcing functions must be known over the entire period of time, that the model is to simulate. This includes the physical data of the study region, advective flows and bulk dispersions among the different segments, wind speed and direction, temperature values and ice cover information. In addition, the pollutant and suspended solids loading rates from tributaries that flow directly into Lake St.Clair should be known.

6.5.1.1 Suspended Sediments

The loads of suspended solids from St.Clair River are assumed to be associated more with the advective flow and the observed concentrations in the River, while the sediments entering the lake from Clinton and Thames rivers were derived from the tributary drainage areas as given in Table 6.6. The concentrations of sediment for the segments in the beginning of the simulation time were assumed based on the wind conditions. Since a major portion of sediment load transports during storm events which are caused by washoff from land erosion, in addition to the resuspension of bed sediments in rivers and lakes, it is reasonable, for this simulation, to assume that 50% of the total annual sediment load would be generated during the strong storms, 30% during moderate winds and 20% during low wind conditions. The variation of wind stresses over the lake surface has been represented as a periodic time function with period equal to 71 days, as shown in Figure 6.33. The total simulation period per year is 250 days for free water surface, followed by 115 days for complete and partial ice cover.

6.5.1.2 Atmospheric Loads

Reliance was placed on published loads for atmospheric contributions. The average atmospheric loading rate was assumed to be $1.0*10^{-10}$ lbs $m^{-2}day^{-1}$ which is an average of the lakes Erie and Huron values (Thomann and Di Toro, 1982).

6.5.1.3 Tributaries and Point Sources

The actual values of the runoff concentrations and industrial loads were unknown. Therefore, a new approach to define the PCBs is proposed. Briefly, the average point loads were modified several times in the model to reach the best comparison of model predictions of measured values after four years of simulation (1970-1974). Also, because large amounts of PCBs are sorbed to the suspended solids, the PCBs time function loads would be similar to that of the suspended solids. Figure 6.34 explains the piecewise approximation that represents an average unit input load of 1.0 lb day^{-1} for PCBs or suspended solids, while these loads were held constant during the complete ice cover simulation period as given in Table 6.7.

6.5.2 Currents and Wind Stresses

In general, wind speed and direction vary from day to day thus it is highly unlikely that a true steady state balance of forces is ever reached in the lake. However, averaging wind data over suitable lengths of time shows significant prevailing wind speeds and directions. Therefore, in order to interpret the variation of the wind stresses over the lake, the frequency and the intensity of the wind are arranged in terms of three speed classes in four directions as shown in Table 6.8.

Thus, to obtain an unsteady solution for the lake circulation the hydrodynamic submodel is used to generate the typical lake circulation patterns for each wind case to represent the fluctuations in the wind conditions, in addition to the simulation for a complete ice cover. Therefore, at each time step, the TOXIWASP model will read the wind time function and its corresponding current values. This includes the intersegment flows and the mean water segment velocities.

Since the lake is completely covered by ice for almost three months each year, the wind shear on the water surface and the wave generated eddy viscosity are reduced or eliminated. Furthermore, the underside of the ice cover introduces increased frictional resistance to the flow. Due to lower flows in winter and due to the ice thickness, the water depth in the lake is reduced. The case of complete ice cover was simulated by introducing friction at the bed and at the ice cover and by reducing the wind shear on the water body to zero and the vertical eddy viscosity to 0.1 $cm^2 s^{-1}$. The depth averaged circulation pattern under an ice cover is shown in Figure 6.35. Most of the large eddies in the lake have been reduced or eliminated. The currents remain but their speed is much reduced. Also, as the resuspension of bottom sediment was considered to be wind dependent, the ice cover would essentially halt this phenomena. In addition, the atmospheric loading component of PCBs to the water segments was assumed to be zero. The interchange flow rates between water segments for the proposed wind stresses are listed in Table 6.9.

6.5.3 PCBs Simulation Results

The simulation parameters required that relate to the properties of PCBs are given in Table 6.10. The simulation results, for the PCBs and sediment transport in lake St.Clair, revealed that the greatest decline in the PCBs level in bed sediment, between 1970 and 1974, is most likely due to the high transportation capacity of the large flow through of the lake. Saying this does not deny the possibility of a real decline in the input loads. However, since the calculated PCBs concentrations in bed sediments provide a good agreement with the observed 1974 values as shown in Figure 6.36, an annual loading rate can be estimated based on this simulation. The annual total loadings to the lake were estimated to be 850 kgs, (1860 lbs). The highest loadings occur in segment 16 which receives about 560 kgs directly from the St. Clair River. The highest loading on the U.S. side comes from the Clinton River, about 140 kgs.

As can be seen from Figure 6.37, there were significant variations in the PCBs concentrations in the water segments, ranging from 0.1 to 2.0 $ng.L^{-1}$. The higher concentrations during wind storms can be attributed to the fact that the resuspended contaminated sediments from the bed have a major influence on the water segments. This trend was also observed in the EPA STORET data. By observing Figure 6.38, the eastern basin of Lake St. Clair shows similar peaks but with higher overall concentrations. From Figure 6.39 and Figure 6.40, it becomes apparent that the same general pattern exists as well for the concentrations of PCBs on suspended solids. The reason for this is that the partition coefficient for PCBs is relatively large which means that only about 10% of the total contaminant is dissolved in water, while most of it is adsorbed to the sediments. The results of the suspended solids concentrations in water, as shown in Figure 6.41 and Figure 6.42, revealed the strong correlation between suspended solids and the contaminant levels in the water segments.

From the concentrations of PCBs in the bed sediment, as shown in Figure 6.43 and Figure 6.44, it appears that there is an overall decrease in the levels for the entire lake between 1970 and 1974. However, the rate of decline is much higher on the U.S. side of the lake inspite of the fact that Clinton River is one of the major sources. An obvious reason for this is the high flow velocity through this region which minimizes the sedimentation processes specially in segments 2 and 14. As a result most of the input contaminant will be carried away directly to Detroit river. The cumulative amounts of PCBs lost from the different segments are given in Figure 6.45 and Figure 6.46. The eastern basin of the lake appears to contribute more PCBs to the atmosphere than the U.S. side. Most likely the contaminant concentration are responsible for these variations. The total mass of PCBs in bed sediments is shown in Figure 6.47 and Figure 6.48. The rate of decline of PCBs in the Canadain side of the lake is relatively slow compared to the U.S. side.

PART 3

MODEL APPLICATIONS AND CONCLUSIONS

CHAPTER VII

MODEL APPLICATIONS

7.1 General

The methodology proposed in this study is intended to apply to four kinds of contaminants OCS, PCBs, lead and cadmium. The proposed numerical submodels, previously presented, can simulate and predict the distribution and differential accumulation of suspended solids and associated pollutants in Lake St.Clair and the connecting channels.

Since the contaminant loading rates are important parameters in the analysis, emphasis was placed on determining the best estimates for these contaminant loads. Then, the selected toxic chemicals are investigated, to demonstrate and quantify the mass transport processes as measured by mass or concentration on suspended solids and bottom sediments throughout the study area. Therefore, a general computer program for performing the analysis has been developed, in three stages, (the hydrodynamic submodels for steady state conditions, the dispersion and sediment submodels, and the TOXIWASP model which is the unsteady state model). This approach proved to be computationally efficient. At each simulation time step, the required input data for TOXIWASP model are obtained from the hydrodynamic and the transport submodels.

Nevertheless, no matter how well a study is planned originally, many new interesting observations come forth during the course of the analysis. While completing the simulation study for these chemicals, it became quickly apparent that the released amounts of the chemicals as well as the locations of their outfalls had a significant influence on their distribution in the region. Therefore, further investigations were carried out using hypothetical loads released from selected locations to make inferences about the distribution patterns of these contaminants in the study area. In other words, for a finite release of toxic chemical from known outfalls, what is the behaviour of the system including the concentrations in each compartment? Such results furnish good indicator and give an important information regarding the potential harm of a given contaminant so as to enable adequate management action to be taken.

7.2 Simulation Procedure

Having broadly developed the mathematical models for toxic contaminants in the previous Chapters, the following Sections will consider the three basic ingredients of the problem: source, transport and impact. As discussed in the first Chapter, the dynamic TOXIWASP model will be used in this analysis. Therefore, the study domain has been divided into three regions, using three different models, the 52 segment model for the St.Clair River, the 24 segment model for Lake St.Clair and the 46 segment model for the Detroit River. The physical and hydrodynamic data used in these models are summarized in Appendix B.

Before applying the models, an approximate sediment balance is conducted to obtain values for the suspended solids loads and the settling and resuspension velocities. This was accomplished by making the following assumptions:

1. The settling velocities of the suspended sediments are constant but variable from segment to segment;
2. In the connecting channels the resuspension and sedimentation velocities are constant but also variable from segment to segment;
3. The resuspension and sedimentation velocities in Lake St.Clair are variable in time and space, that is they are correlated to the wind stresses.

In all of the following simulations no wind effects were included for the connecting channels. However, the unsteady motions through Lake St.Clair are studied as a succession of steady motions corresponding to a series of steady wind events. The representative wind time function which was used to approximate the wind effects on the lake circulation, with April 1 as day 0, is shown in Figure 7.1. The estimated wind speed function was based on the actual meteorological data in 1982 and 1983 from Windsor Airport. The resulting suspended solids concentrations in response to these wind conditions are given in Figure 7.2 and Figure 7.3. In general, the estimated results are supported again by the raw water data observed at the Belle River and Windsor Water Treatment Plants as plotted in Figure 6.29. When wind speed rises, the suspended solids concentrations rises. However, some nonlinear variation is exhibited in the suspended solids concentrations because of the more complex changes in intersegment transports and internal flows.

7.3 Sediment Balance

The total sediment discharge from stream tributaries, generally, consists of two components, suspended sediment discharge and bed load discharge. Suspended sediments or suspended solids move in suspension in water, either as a colloid or through the influence of the upward component of turbulent currents. Bed load is that material moving in almost continuous contact with the stream bed, being rolled or pushed along the bottom by the current force near the bottom. The bed load movement, however, is more complex and depends upon many factors which often are difficult to evaluate. Within the TOXIWASP model, the chemical or sediment can migrate downward or upward but no lateral migration of the chemical or sediment within the bed segments is allowed. Thus, the simulation in this study only includes the transport of suspended solids, and considers the lateral motion of bed sediments to be of minimal importance. The mean daily concentrations of suspended sediments from the Canadian and the American streams are shown in Table 7.1 and Table 7.2 respectively. These values were estimated on a watershed basis using the runoff factors. Figure 7.4 shows the location and numeration of the drainage basins of the streams which contribute to the Huron-Erie corridor.

7.4 Octachlorostyrene

Substantial levels of OCS have been reported in two areas of the world, Norway (Lunde and Ofstad, 1976) and the lower Great Lakes (Kuehl et al., 1980). In the fifteen years since OCS has been recognized to be of environmental concern (Ten Noever de Brouw et al., 1969), information are very limited on the production and implication of OCS. Little research has been carried out on the toxicity of OCS. It has been determined, however that OCS produces changes in the liver at low levels. Unlike the other toxics in this study, OCS is produced only as an unintended by-product of other processes, and is not distributed commercially. The only documented and recognized source of OCS in the geographical region of the present study is Dow Chemical Ltd in the Sarnia area. The Dow Chemical outfalls contribute significantly to the total loading but no actual figures are available. Moreover, to date there are no measured atmospheric ambient concentrations of OCS in this region.

Consequently, the first important step is to predict how much OCS is released from this source, and identify other unknown sources that could release OCS to the region. An appropriate way of evaluating the suspected sources is to correlate varying amounts of OCS released from these sources against the available field data for the levels and distribution patterns of OCS in surficial sediments throughout this area. The second, equally important, step is to evaluate the efficiency or even the effectiveness, of different policies for the control of OCS. Using the mathematical models we can now provide a general insight on how various combinations of policies may work together.

7.4.1 Simulation Parameters

The simulation parameters required that relate to the properties of OCS, are assumed similar to those observed for PCBs values found in Table 7.3. An n-octanol water partition coefficient of $1.9*10^6$ is given which can be used, according to Karickhoff, et al., 1979, to obtain a sediment/soil sorption constant of 25000 to 49000 for material of 2-4% organic carbon content.

To demonstrate the dynamics of contaminant transport through the three regions (St.Clair River, Lake St.Clair and Detroit River), two simulations are presented in detail for OCS. The first simulation is for one year using the calibrated OCS loading. As an initial condition, it assumes zero OCS concentrations in both water and bed sediments. Although solids input to the system changes on a day to day basis due to meteorological factors, steady state inputs were assumed in the following analysis. This can be a reasonable approximation, since the OCS is discharging continuously from one major source, while no other OCS loads were assumed to be associated with sediments from the small tributaries. The second simulation is also for one year, but uses the estimated equilibrium OCS concentrations in bed segments as an initial condition. It then assumes no input loading to the system. This form of analysis is frequently useful to show how the concentrations would be changed with time if a particular load is changed.

7.4.2 Simulation Results

The concentrations obtained for the OCS in sediments, (Pugsley et al., 1985), as well as the measurements by the MOE for the upper St.Clair River indicated that, along the Canadian shore, there are at least two local sources of OCS in segment number 1 in the St.Clair River (The 52 segment model). A major source near Dow Chemical and a second suspected source is about 2,000 meters upstream of the first one. The input OCS load to segment 1 was then calibrated by direct comparison between the estimated OCS concentrations in bed sediments in both the St.Clair River and Lake St.Clair with the observed values. It was found that at least 910 g.day^{-1} of OCS released continuously over the year to segment 1, gives almost the same OCS distributions as measured in bed sediments.

The direct comparison between the measured and estimated OCS concentrations in bed sediments shows good agreement as given in Figure 7.5 and Figure 7.6. It should be noted that, the measured OCS levels were based on samples from the upper 10 cm of the bottom sediment. However, the depth of the active sediment segments were assumed in the model to be only 2.5 cm, according to the previous studies of Durham and Oliver, 1983, which suggest that most of the contaminants are located in the uppermost sediment layer. Therefore, the predicted concentrations should be 2 to 4 times greater than the measured values, depending on the suspended solids settlement velocity in each water segment. It is apparent that the average OCS concentration measured in segment 20 seems to be much lower than expected. This is due to the fact that most of the contaminanted sediments settle near the outlet of the Channel Ecarte, the Chemalogum channel and the Bassett channel, where no field measurements were taken.

Therefore, greater priority should be given to monitoring the OCS levels at the outlet of these small tributaries.

In order to clarify the effect of the sample collection method on the measured levels of contaminant in bed sediment, the model was modified by changing the depth of the active sediment segments to be 10 cm instead of 2.5 cm. All the previous parameters and the loads are kept the same during the simulation period. The results, as given in Figure 7.7, indicated a close agreement with the measurements given by Pugsley et al., 1985. The foregoing simulation, provides strong evidence on how the deep sediment samples can dilute the contaminant and therefore, under-predict the concentrations which may lead to some misunderstanding.

The simulation results reflect the differing properties of OCS in the rivers and the lake. The results for St.Clair River indicate that the bulk of the loading remains in the water column (in forms of dissolved fraction in water and adsorped to suspended sediments) and only 20% is carried to the bed sediments. This result is due to the fact that flushing is the overwhelming cleaning mechanism for St.Clair River, which leads to a slow bed layer response time and a relatively smooth concentration trend in the bed sediments.

In contrast, OCS displays relatively sharp concentration fluctuations in Lake St.Clair. This is due to the faster response time for the lake bed, because most of the suspended solids settle down in deposition zones near the mouth of the streams. This mechanism leads to a large fraction of the contaminant in the bed sediments. It was found that only 40% of the input loads to the lake, i.e., 33% of the total to St.Clair River, is released into the Detroit River. Most of the lower part of Detroit River is relatively wide and has low velocities due to the flat river slopes and the backwater effect of Lake Erie. Therefore, the transport capacity of Detroit River is expected to be less than that of St.Clair River. Thus, about 50% of the input load to Detroit River leaves the river into Lake Erie. The percentage distribution of the total mass loading of OCS as determined at the end of one year period indicated that about 26% of the OCS mass will be accumulated in Lake St.Clair, while only 16% will be released to Lake Erie.

The model for Lake St.Clair has been developed for shallow lakes, that includes sediment resuspension. During high wind conditions, much of the contaminated sediment deposited on the lake bottom can be resuspended. The results illustrate the importance of the effects of wind induced turbulence on many variables in model segments. The variables which will be presented for this simulation are:

1. The chemical concentration in each water segment,
2. The chemical sorbed onto suspended sediment,
3. The chemical sorbed onto bed sediment,

4. The cumulative mass of chemical lost from the system by volatilization through the surface water,

5. The total mass of chemical in each segment.

The variables were set to zero at the start of the simulation and the model subjected to a constant loading rate. The response time of those variables is quantified more directly in the following figures. From Figure 7.8 and Figure 7.9, the OCS contaminant levels estimated in the water varied from 0.25 to 2.4 $ng.l^{-1}$. For all but segment No. 22, the levels of the OCS are directly proportional to wind shear stresses. The levels in Anchor Bay are more uniform and steady due to its geographical shape and the relatively small wind fetch. The results suggested that,the OCS level in water segment No. 4 can reach more than 1.4 $ng.l^{-1}$. This may deserve consideration, particularly since Windsor water supply system takes its water directly from segment number 4. The OCS concentrations on suspended solids are shown in Figure 7.10 and Figure 7.11. From this computation, the same general pattern is obtained. The total mass of OCS in bed sediments are given in Figure 7.12 and Figure 7.13. The cumulative amounts of CCS lost from the different water segments are given in Figure 7.14 and Figure 7.15. The results of the total OCS mass in the bed sediments are shown in Figure 7.16 and Figure 7.17. An important conclusion can be obtained from these results for the lake. The percentage total accumulated OCS mass in bed sediments was 12% on the United States side, while 88% of that mass deposited in the Canadian waters.

7.4.3 Analysis

Having characterized the transport of OCS in the system, we can now make use of a wide range of the mathematical results on the behaviour of OCS in the system. For instance, the time required for the system to recover following the cessation of contaminant loadings is important information for water management. As has been already indicated, the accumulation of OCS in bed sediment will converge to an equilibrium. Therefore, the results were extrapolated to estimate the equilibrium concentrations in all bed segments. The model was then applied to the study region, using the previously estimated equilibrium concentration values as an initial condition in the system with no external OCS loads. The simulation period was for one year, then the results were extrapolated.

In the St. Clair River, the recovery for the bed sediment would require approximately two years in order to reach 25% of the starting concentrations. The recovery time for the river is unusually short due to the mechanism of flushing of the river, where the contaminant in the sediments are released from the particles and diffused back into the water segments. However, it should be noted that this mechanism reduces the speed with which the system converges to its equilibrium, (6 to 8 years), as shown in Figure 7.18, when the constant OCS load is applied to the system.

In Lake St. Clair, these response time calculations are the reverse of those computed for St. Clair River. For instance, when the model is subjected to a constant loading rate, the results as depicted in Figure 7.19 and Figure 7.20, indicate that a great portion of the contaminant is carried to the lake's sediments by settling particles. Consequently, the OCS level increases markedly up to an equilibrium condition within about three years for most of the bed segments. Following the termination of loadings, the sediments reintroduced the contaminants back to the water but at very slow rate, as shown in Figure 7.21 and Figure 7.22. Thus, if the lake is subjected to spills of toxic chemicals, even for short periods, the resulting health and environmental effects could be of considerable duration.

7.5 Polychlorinated Biphenyls

Researchers for the International Joint Commission estimated that approximately 500 Mkgs (million kilograms) of PCBs were produced in the United States in the years 1930 to 1975, and approximately 340 Mkgs are still in use, with an additional 9 Mkgs in storage (International Joint

Commission, 1980). Significant losses of PBCs to the environment has occurred as a result of spills leakages and atmospheric releases from electrical equipment. Fishbein, 1973 estimated 30 Mkgs have been lost to the air, 60 Mkgs into fresh water and coastal water, and 3 Mkgs into dumps and land fills. Theoretically, there will be no direct discharges to the land, water or atmosphere, because of the strict regulations that keep careful check on materials that are contaminated with PCBs. Therefore, PCBs distribution today is approximately a reflection on the past use. It is possible as evidenced by significant incidents of past exposure that spills and illegal releases of PCBs still occur especially from transformers (Environment Canada, 1983). In these cases it would be extremely difficult to determine the magnitude of spills and leakage from any particular site.

The toxic effects of PCBs on humans are diverse and many. At various times the effects have included abdominal pain, numbness of limbs, swelling of joints and headache. In the longer term exposure to PCBs can lead to liver damage, memory loss and is considered to be cancer causing. The major route of public exposure to PCBs is from contamination of fish consumed by humans, which accumulate PCBs to levels 10^4 to 10^6 times greater than their exposure levels in water.

7.5.1 PCBs Simulation Parameters

The simulation parameters used, relating to PCBs, are given in Table 6.10. The PCBs loading rates were estimated based on the previous calibration study for the long-term simulation of PCBs in Lake St.Clair. It was found that the annual loading rates of PCBs from the main streams during the period between 1970 and 1974 were 140 kgs from Clinton River, 7 kgs from Thames River and about 590 kgs from St.Clair River. The total PCBs released from the lake to Detroit River was estimated to be 360 kgs.yr^{-1}.

Frank et al., 1977, estimated the annual average PCBs loads of 1500 kgs to the Western Basin of Lake Erie. According to the sedimentation rates presented by Kemp et al., 1976, the highest PCBs loadings occur in the Western Basin, particularly, associated with the west bank water masses of the Detroit River. Therefore, it is reasonable to assume that 70% of that loads (about 1050 kgs) came from Detroit River.

In the Detroit River, Thornley and Hamdy, 1984, measured the PCBs concentrations in bed sediments. The stations sampled indicated a mean value of 523 ng.g^{-1} in the American side, whereas only 74 ng.g^{-1} was observed in the Canadian side. Therefore, the total PCBs loadind rate to Detroit River was correlated to the observed PCBs levels in bed sediments, i.e., about 90 and 800 kg.yr^{-1} discharged from the Canadian and the American shorelines respectively.

7.5.2 Simulation Results

The predicted concentrations of PCBs in water and on suspended solids for Lake St.Clair under complete ice cover is given in Figure 7.23. The simulation results for PCBs indicated that 65% of the input loads to the Lake will be released directly to Detroit River, whereas about 35% will be accumulated in its bed sediments. However, there will be no volatilized PCBs due to the ice cover. In addition the biodegradation rate drops significantly.

The simulation results during the free water conditions for PCBs in Lake St.Clair are summarized in the following figures. The PCBs concentrations in the water segments are shown in Figure 7.24 and Figure 7.25. The range of concentrations was from 0.5 to 2.75 $ng.L^{-1}$ for the Canadian side and from less than 1.0 to 4.0 $ng.L^{-1}$ for the American side of the Lake. This variation depends on weather patterns and can be further demonstrated by the estimated suspended solid concentrations in water segments. For example, in Figure 7.26 and Figure 7.27 similar patterns are observed for the sorbed PCBs onto suspended sediments in water segments. Therefore, the PCBs concentrations in water and suspended solids can be drastically altered by meteorological conditions. However, the concentrations of PCBs in bed sediments, as shown in Figure 7.28 and Figure 7.29 are, in general, less than 25.0 $ng.g^{-1}$ in all the lake segments except in segment No. 14 where the PCBs level is 50 $ng.g^{-1}$. This high level of PCBs suggested two sources of significant impairment, the Clinton River and St.Clair River. The total mass of PCBs in bed segments, as given in Figure 7.30 and Figure 7.31, indicated that 50% of the total PCBs in bed segments will be accumulated in the Canadian side. The cumulative mass of PCBs lost by Volatilization is shown in Figure 7.32 and Figure 7.33.

7.5.3 Analysis

The distribution of PCBs concentrations in water segments as well as on suspended solids are shown in Figure 7.34. It was estimated that 14.5% of the input PCBs loads to St.Clair River were accumulated in its bed sediments or lost by volatilization and biodegradation, whereas about 85.5% were released into Lake St.Clair. The accumulated PCBs in Lake St.Clair bed sediments were 16% of the input load, whereas 26% was estimated to be lost by volatilization. It was found also that, about 48% of that input load was transported to Detroit River, while 10% was lost in other processes such as biodegradation and bioaccumulation. In addition to the previously estimated loading rates into Detroit River, 20 $lbs.day^{-1}$ of PCBs were assumed to be released from Detroit WWTP. The purpose for this simulation is to predict the effect of this particular source on the distribution pattern in the River. The estimated PCBs concentrations in water segments as well as on suspended solids are shown in Figure 7.35. The simulation results indicated that the high concentration levels of PCBs remain near the American shore of the river. It was found that 72% of the input loads were released to Lake Erie.

7.6 Lead

For at least 3000 years, lead has been one of the most widely used metals. Its physical and chemical properties ensure that it will continue to be a key material in a variety of uses, such as gasoline additive to prevent knocking, lead storage batteries and paint. However, most studies have indicated that lead, like cadmium, plays no beneficial or essential role in the health of man or animals, and is toxic at any concentration. In human beings, it is taken up primarily in the blood, where it has a mean residence time of 23 days, and in bones where its residence time is about 20 years. In Canada, the average human exposure has been estimated to be 12-16 ug.day^{-1} from the atmosphere, 3-6 ug.day^{-1} from water and about 16 ug.day^{-1} from food (Jaworski, 1978).

The major sources of environmental contamination by lead are direct emissions into the atmosphere from motor vehicle exhaust, lead mining and production, and industrial smelting operations. Although the quantification of these releases is difficult on a watershed basis, a national total of 8,000 tonnes of lead emitted into the atmosphere has been accepted as reasonable figure during the year 1983, (Environment Canada, 1983). Wet/dry fall phenomena remove the lead from the atmosphere through deposition onto the land or water areas. Some of the lead deposited on land will be carried into rivers by runoff water. It can therefore be said that a large portion of the lead released to the atmosphere is eventually deposited in rivers and lakes.

7.6.1 Simulation Parameters

The simulation parameters used, relating specifically to lead, are shown in Table 7.4. The partitioning coefficient in water was taken as 464 $L.g^{-1}$ (Dolan and Biormann, 1982) for all water segments. One major industrial source which may contribute significant amounts of lead is the Ethyl Canada operation in Moore Township, which emits 100 $kg.day^{-1}$. Although no figures are presented on a watershed basis regarding atmospheric loading rates, it is reasonable to link these input rates directly to the population in each watershed. The estimated average atmospheric loading rates due to auto emissions and from selected manufacturing activities in the Essex Region are 3.763 and 0.075 $g.day^{-1}$ per person. The atmospheric release rate from each watershed was therefore the product of the total population in this area and the total atmospheric rate per person.

However, it is difficult to determine precisely how much of the lead released to the atmosphere of a particular watershed will travel into the main streams. It has been suggested that most of that lead will settle out within a short distance of their source. Therefore, it is assumed that all the released lead from a particular watershed will eventually deposit in that watershed. It should be noticed that some of the cumulative lead in the soil will be washed out by the rain. Thus, based on the partition coefficient of lead, it was estimated that about 25% of that lead would be carried away with the rain water. However, based on the runoff/rainfall ratio for these watersheds, it was estimated that only 30% of the total rain will travel into the small streams, i.e, 7.5% of the total lead loadings. The results from the river simulation study indicated that around 30% of the input loads into these streams would be accumulated inside them. Correspondingly, only 5% of the total lead will reach the main streams. The total loading rates used in the simulation study are given in Table 7.5.

7.6.2 Simulation Results

It was estimated that, the average lead loading rates are 640 $lb.day^{-1}$ enter into the study region from the Canadian shoreline and about 1750 $lb.day^{-1}$ released from the U.S. shoreline. At this rate of input a quantitative agreement has been obtained between the predicted concentrations of lead in bed sediment and the measured values. For instance, Figure 7.36 shows the estimated lead levels in bed sediment of Lake St.Clair and the measured values. It should be noticed that the measured concentrations of lead were based on samples from the upper 10 cm. Therefore, these values were adjusted based on the previous OCS studies in Lake St.Clair. Almost the entire American side of the study area indicated a general agreement between the predicted and measured values. However, the distribution of lead levels in bed sediments suggested that the assumed industrial loads from Sarnia area must be much greater than 100 $kg.day^{-1}$.

The variation of lead levels from the simulation results in Lake St.Clair is shown in the following plots. The total dissolved lead in the water segments of Lake St.Clair, shown in Figure 7.37 and Figure 7.38, indicated that the range of lead concentrations in the U.S. waters was 0.30 to 1.70 $ug.L^{-1}$ with a mean of 0.6 $ug.L^{-1}$, whereas the range in the Canadian side was 0.15 to 1.40 $ug.L^{-1}$ with a mean of 0.36 $ug.L^{-1}$. The variations of the sorbed lead onto suspended sediments are given in Figure 7.39 and Figure 7.40. The greatest variability in the concentrations of lead is at the period of maximum wind speeds. The concentration of lead in bed sediments in Lake St.Clair indicated that almost all the levels in the lake are below the Ontario guideline for open-water disposal of dredged materials (50 $ug.L^{-1}$) as shown in Figure 7.41 and Figure 7.42. The total mass of lead deposited in the Canadian side of the lake is about 60% of the total mass in the bed sediments, as given in Figure 7.43 and Figure 7.44.

The distribution of lead levels in St.Clair River is shown in Figure 7.45. The simulation results exhibited high dissolved lead concentrations along the Canadian shoreline. Some high values were observed in the American shoreline, specifically downstream of Stag Island. However, the shipping channel and most of the center of the River have relatively low concentrations. It was found that 85% of the lead input to the St.Clair River was released to Lake St.Clair, while 15% accumulated in its bed sediments. However, the accumulated lead in Lake St.Clair was 80% of the input loads, whereas 20% was released to Detroit River. The Detroit River released about 65% of its lead loads to Lake Erie, while 35% was accumulated in its bed sediment.

7.6.3 Analysis

The preceding analysis has indicated that lead from gasoline additives had contributed 75% to the contamination of sediment in the study area. Therefore, in order to evaluate the benefit from reductions in lead additives, we performed the simulation of the previous section for Lake St.Clair, but using only 10% of the lead released from gasoline. Moreover, the initial concentrations of lead in the bed sediments of Lake St.Clair were chosen to be equal to the measured values by the GLI in 1983. The distribution of lead levels in Lake St.Clair is shown in Figure 7.46. This simulation showed that, the concentrations of lead in bed sediments can drop to 30% of the present condition after only one year in the top 2.5 cm of the bed.

7.7 Cadmium

Cadmium is produced as a by-product of zinc production, but also remains as a contaminant in finished zinc product. It also appears in significant concentrations in the phosphate and sewage sludge fertilizers. Cadmium is used primarily to plate other metals, but also has important uses in pigments, plastics (particularly PVC) as a stabilizer, batteries and fungicides. From all these uses, cadmium seems to be widely dispersed into the environment, whether by welding, cutting or resmelting of cadmium-plated metals, by direct application to the land in the case of fertilizers and fungicides, or by incineration and landfill disposal of these and other products.

As with lead, cadmium is not only highly toxic but also its toxicity is cumulative. Furthermore, since they are persistent toxic contaminants, they cannot be destroyed and therefore remain available and reactive in the environment. They can eventually find their way into the human system.

Cadmium tends to accumulate in human tissues, particularly in the liver and kidney where it is estimated to have a biological half-life of 19 to 38 years. In addition to its human health effects, cadmium has toxic effects on other forms of life, particularly some crops and aquatic animals.

7.7.1 Simulation Parameters

To date, there are very little quantitative data available on local sources. However, it is apparent that it is the cadmium emissions into the air and directly to the soil, which are the most critical. Unfortunately, there is a considerable discrepancy in published data on atmospheric emissions. An inventory of cadmium emissions in Canada during 1972, (Nriagu, 1980), includes large emission figures from mining and smelting operations, remote from the Essex Region. On the other hand, the emission estimates for the United States, list only anthropogenic sources. Such data must be assessed with great caution, because it is generally produced from rough estimates of (emission factors) related to various cadmium emitting activities.

Recent results about the atmospheric transport in the Essex region indicated that the amount of cadmium generated locally from the Wayne County industrial complex and possibly Windsor establishments are higher than the amounts which might be carried into the region by long range transport from beyond Michigan and Ontario boundaries. From a survey of the literature the average concentration of cadmium in bulk precipitation samples in the Great Lakes basin is 1.2 $ug.L^{-1}$ (Allen and Halley 1980). However, from the number of precipitation samples analyzed for cadmium to date, the annual atmospheric loading of cadmium from all sources is approximately 7.0 $g.ha^{-1}$ in the urban area and 4.0 $g.ha^{-1}$ in the rural area for the Essex County.

In addition to the atmospheric emissions, phosphate fertilizer and sludge fertilizer are major sources of cadmium to the surface of the earth. Phosphate fertilizers from the United States contain 15 to 100$mgkg^{-1}$ (USEPA, 1978, Webber, 1979). Phosphates from other contries have even higher cadmium contents, ranging up to 255$mg.kg^{-1}$ (Hutton, 1982). The recommended additions of fertilizer to soil are in the range of 20 to 100 $kg.ha^{-1}yr^{-1}$. However, it is generally the practice to add two to three times the recommended application of phosphate fertilizer. In this case, cadmium additions of up to 4.5$gha^{-1}yr^{-1}$ would result.

7.7.2 Simulation Results

The concentration used for cadmium in bed sediment was assumed to be zero at the beginning of the simulation time. In general, the predicted concentrations of cadmium in bed sediment agree well with the pattern of observed data, except for the eastern basin of Lake St.Clair, as shown in Figure 7.47. A possible reason for such discrepancies is the problem discussed earlier, of the lack of sediment samples data in this area. Recall that, the field sediment samples were taken from the upper 10 cm of the surface bed, the model results for cadmium concentration in bed sediment were, in general, 3 to 6 times higher than the measured values by Pugsley, 1985. This is consistent with what would be expected from these measurements.

It was estimated that, the total loading inputs of cadmium are 250 $lbs.day^{-1}$ from the U.S. shoreline and 75 $lbs.day^{-1}$ from the Canadian side. On further analyzing the transport of cadmium along the waterway, one interesting observation is made. It appears that 60% of the loading rates of cadmium to St.Clair River will be released to Lake St.Clair, while only 40% of the total loading rates to Lake St.Clair will be released to Detroit River. In Detroit River, most of the cadmium which enters the river will be accumulated in the bed sediments, about 60%, specially in the American side of the River. The accumulation percentage of cadmium in bed sediment, in general, is higher than that observed for the organic chemicals earlier.

The variation of cadmium levels from the simulation results in Lake St.Clair, indicated that the sediment resuspension also seems to be critical to the dynamics of the pollutant in the lake. For example the concentration of dissolved cadmium in water segments as shown in Figure 7.48

and Figure 7.49 are strongly influenced by wind shear stresses. Similarly, the cadmium sorbed onto suspended solids agree with this fact, as shown in Figure 7.50 and Figure 7.51. The predicted distribution of cadmium in bed sediment for Lake St.Clair shows levels in excess of the dredging guidline for open water disposal in most of the lake as shown in Figure 7.52 and Figure 7.53. The total mass of cadmium in bed sediments of the lake shows high accumulation rates in segments No. 8, near Belle River and segment No. 14 downstream of Clinton River as given in Figure 7.54 and Figure 7.55.

The predicted distribution of cadmium in water segments in the St.Clair River is shown in Figure 7.56. The estimated cadmium levels in water segments, as well as on suspended solids in Detroit River, are given in Figure 7.57.

7.8 Evaluations of Model Performance

Field measurements from different sources were used to evaluate the overall performance of the TOXIWASP model. Table 7.6 presents the corresponding comparison for the selected contaminants along the Canadian shoreline of the St.Clair and the Detroit Rivers. The computed lead concentrations on suspended solids show good agreement with the observations. The overall mean predicted concentrations of lead are 60.4 and 35.5 $ug.g^{-1}$ in St.Clair and Detroit

River respectively, while the observed values are 45.7, 62.7 and 68.0 $ug.g^{-1}$ in St.Clair River and 28.0, 31.0 and 48.1 $ug.g^{-1}$ in Detroit River as reported in references 1, 2 and 3 respectively. The results for the cadmium indicated that the predicted concentrations on suspended solids are consistently higher than the measured levels in bed sediments. This suggested that cadmium levels may still be increasing in bed sediments (Nriagu, 1980).

The predicted OCS concentrations on suspended solids seem to be higher than the observed values by Pugsley, 1985. However, they appear to compare well with the MOE observations. The same behaviour was observed for the PCBs. One important source of this discrepancy is the sample collection method. The bed sediment layer was assumed to be 2.5 cm in the TOXIWASP model, while Pugsley et al., 1985, collected samples from the upper 10 cm of the bed sediments. This in fact may have diluted the contaminant. Other reasons may be considered such as the differences in the analytical procedure and the location of sampling sites. Also the bed contaminant transport is affected by the bedform movement, which could cause large variations in the near surface contaminants.

CHAPTER VIII

CONCLUSIONS AND RECOMMENDATIONS

8.1 General

A mathematical modelling framework for simulating the transport of toxic and conventional substances in the Huron-Erie waterway has been presented. The primary distinctions between the proposed framework and the previous work are the explicit consideration of sediment/contaminant interaction and the prediction of both the velocity field and the dispersion coefficients which are important for the transport models.

Chapter II was devoted to a literature review of pollutant transport models in rivers and the lake circulation models. A brief discussion, about the main processes which take place in rivers and lakes, for toxic organic chemicals, was also presented. Some of these processes act on metals as well, but the complexity of the environmental chemistry of metals makes them more difficult to handle. Therefore, in this study it is assumed that the heavy metals have zero decay rate. This approach yields the highest possible levels since metal decay is neglected.

Chapter III and IV were devoted to the theoretical developments and the calibration results for the simulation of river transport. The hydrodynamic and dispersion submodel was restricted to those mean steady flows which are of constant density and nearly two-dimensional. However, in the main rivers such as St.Clair and Detroit Rivers, those restrictions are usually very close to reality during a considerable interval of time. A general description of the EPA (TOXIWASP) model is also given in Chapter III. This model accounts for various processes such as the transport, the transformation and the volatilization of toxic substances. Together with the hydrodynamic and dispersion submodel, the TOXIWASP model was verified by field data of an organic chemical (HCB) in the St.Clair River and a heavy metal (cadmium) in the Detroit River. A good agreement was obtained between the theory and the observations.

Chapter V and VI were devoted to the theoretical development, calibration and verification results for the simulation of lake transport. A steady state finite element circulation model was developed and verified with field data. The model successfully predicted the circulation patterns under various wind conditions. However, the unsteady motions through the lake were studied as a succession of steady motions. The model was applied to study the effect of vertical eddy viscosity, wind speed and direction, bottom friction and the inertia on flow pattern.

The finite element model was further expanded by incorporating the transport equations for convectional pollutants and suspended solids. The model was found to give a satisfactory prediction of conservative pollutants such as chloride ion as well as suspended solids in Lake St.Clair. In simulating the sediment/contaminant interaction the EPA (TOXIWASP) model was modified in order to more effectively account for the vertical entrainment and wind-wave resuspension in Lake St.Clair. The models were used to simulate the levels of PCBs in Lake St.Clair over the period from 1970 to 1974. However, even with the inclusion of the averaged weather conditions, the simulation results give, at best, only a rough estimate for the PCBs loading during this period. Better sediment and water measurements are required to simulate those loads more accurately.

In Chapter VII, the proposed models were applied to simulate the transport of four toxic chemicals (OCS, PCBs, Pd and Cd) in the waterway between Lakes Huron and Erie. The models proved to be able to simulate the transport of these chemicals in rivers and shallow lakes. They can be used to estimate the loadings from several sources. In summary, the models developed and tested provide a simple framework for simulating the levels and response characteristics of water system contamination. They are designed to provide estimates of toxic substances in the sediments and water. As such, they are very useful in evaluating most of the policy alternatives (options) for regulating the toxic contaminant levels in the ecosystem.

8.2 Specific Conclusions

The simulation results from the preceding study indicated that bed sediment resuspension is critical to the dynamics of toxic substances. For instance, Lake St.Clair has high transportation capacity, especially during stormy conditions. Wind stresses have the capability of resuspending the already settled contaminated sediments, as such, the fraction of contaminants in suspension or dissolved in water segments would increase significantly, while, the large flow through of the lake will carry away a lot of the solids with the contaminants before they can settle down again. This behaviour is very important since there are many water treatment plants taking their drinking water from this system. Therefore, appropriate precautions should be considered for treating the drinking water, particularly during and immediately after wind-storms. Furthermore, an environmental monitoring program aimed at spill detection would be very useful in this region.

The proposed models were used to study the distribution of OCS in the region, using bed sediment data collected by the GLI (University of Windsor) during the period 1983 to 1984. It is concluded that two major sources near Sarnia in the upper part of St.Clair River are discharging at least 910 g.day^{-1} of OCS continuously into the water segments. It was found at the end of one year simulation period that only 20% of that loading rate is carried to the bed sediments or lost by volatilization, biodegradation and other processes in St.Clair River, whereas 80% goes to Lake St.Clair. However, 32% of that OCS input loads to the lake will be accumulated in its bed sediments, about 25% volatilized and 2% lost by other processes. The remaining 40% is released to Detroit River. In Detroit River 50% of its input OCS loads leaves the river into Lake Erie. The simulation results under the estimated load indicated that, the concentrations of OCS in the bed sediments take about two years for the St. Clair River to reach to equilibrium values, and about three years in Lake St.Clair. It was estimated that if OCS loads were then terminated, the recovery time, time to reduce the equilibrium concentrations by 75%, in St.Clair River is short, about one year. The recovery time in Lake St.Clair can be of considerable duration, about three years.

Although the PCBs levels in bed sediments indicated a general declination in most of St.Clair River and Lake St.Clair, there is still high levels observed near Clinton

River and on the American side of Detroit River. It was estimated that the annual loading rates of PCBs into Lake St.Clair are 140 kgs from Clinton River, 7 kgs from Thames River, 590 kgs from St.Clair River and 11.6 kgs from the atmosphere. However, only 360 kgs of PCBs are released from the Lake to Detroit River. An additional 800 kgs of PCBs may be discharged from the American side of Detroit River and about 90 kgs from the Canadian side of the river. It was found that, St.Clair River releases about 85.5% of its input PCBs loads into Lake St.Clair, while Detroit River releases about 72% of its input loads to Lake Erie. On the other hand Lake St.Clair releases only 48% of its input loads, while 26% were volatilized, 16% accumulated on bed sediments and 10% lost by other processes.

It was concluded also that, leaded gasoline accounts for 70 to 75% of total airborne lead. It became apparent that significant amounts of lead are discharged into St.Clair River from those industries near Sarnia. It was estimated that, the total lead loading rates to the system are 640 $lb.day^{-1}$ from the Canadian shoreline and 1750 $lb.day^{-1}$ from the American shoreline. The simulation results for the transport of lead indicated that only 15% of the input lead loads to St.Clair River is accumulating in its bed sediments. The remaining 85% is released to Lake St.Clair. However, 80% of the lead input loads to Lake St.Clair will be accumulated in its sediment, while 20% is released to Detroit River. It was pointed out that, reducing emissions from lead additives in gasoline would in fact considerably reduce lead levels in both water and bed segments.

The simulation results for cadmium indicated high levels in most of the bed segments in Lake St.Clair and Detroit River. The measurements also indicated little increase in cadmium levels recently, (Nriagu, 1980). It was estimated that, the total system loading inputs of cadmium were 250 $lb.day^{-1}$ and 75 $lb.day^{-1}$ from the American and the Canadian sides respectively. The large cadmium contained in fertilizers applied to agricultural soil are believed to be responsible for most of the nonpoint loadings.

8.3 Recommendations

The major objective of this dissertation has been to develop a framework in order to simulate the transport of conventional and toxic pollutants in Lake St.Clair and the connecting channels. Because of the study's comprehensive nature, it can serve to delineate areas of future research. These include:

8.3.1 Measurements

A number of measurements related to the pollutant model application were not available. In particular, detailed water and suspended solid samples for the levels of lead, cadmium, PCBs and OCS at four controlling locations, i.e, the inlet of St.Clair River, the outlet of St.Clair Delta Channels or the inlet to the Delta, the inlet of Detroit River and the outlet of Detroit River are very important. These data should be collected during various weather conditions. Further research on monitoring the wet and dry deposition of the contaminants should be conducted, particularly around stationary point sources. In addition, better water quality data for all tributaries and streams which contribute to the study area, are needed. Detailed data on atmospheric sources and emission rates as well as the magnitude of direct discharge rates into the streams are required in order to improve the simulation results.

8.3.2 Parameter Estimation

Another area that requires further study is the development of simple techniques to predict the partition coefficients within the water and bed segments as a function of sediment concentrations and characteristics. Greater research priority should be given to estimating the partitioning coefficient within the top layer of the land and the pH effects on the biodegradation rates, to determine the contaminant mass which transfer to the storm water runoff or infiltrated with the downward movement of water to the ground. In addition, quantification of resuspension (scour) of bed sediments and runoff-erosion of suspended solids from land has to be done prior to any simulation.

8.3.3 Theoretical Developments

Several additional research topics in this area need to be conducted before the proposed framework can be considered complete. Unsteady circulation model for Lake St.Clair which may be directly linked to the EPA (TOXIWASP) model can improve the short-term simulation. More investigation and information concerning the relationship between wind-wave effects on bottom shear stresses and the settling velocity of suspended solids are required. The EPA (TOXIWASP) model should be modified to incorporate buoyancy effects and density differences in inflow or spilled pollutants temperatures. In this way it could simulate immissible fluids such as spilled oil on water surfaces or on bed sediments.

Although the pollutant transport (k-ε) model used in this study yielded satisfactory results, the model needs to be extended to include unsteady state simulations. One compromise to achieve reasonable computational time is to decouple the convection diffusion equations from the hydrodynamic and (k-ε) turbulence equations.

APPENDIX A

COEFFICIENTS OF THE LAKE CIRCULATION EQUATIONS

Coefficents for the Hydrodynamic Submodel

(1) The coefficients of Eqs. 5.26 and 5.27.

$$R_r^* = \frac{1}{2m}\{(C_6+C_5) + \frac{1}{2G}[E(C_8+C_7)-F(C_8-C_7)]\} \quad [A.1]$$

$$R_i^* = \frac{-1}{2m}\{(C_6-C_5) + \frac{1}{2G}[E(C_8-C_7)-F(C_8+C_7)]\} \quad [A.2]$$

$$T_r^* = \frac{m}{V_0}[C_8(a-b) + C_7(a+b)] \quad [A.3]$$

$$T_i^* = \frac{-m}{V_0}[C_8(a+b) - C_7(a+b)] + 1 \quad [A.4]$$

C_1 = sin mh . cosh mh

C_2 = cos mh . sinh mh

C_3 = -2 (sin mh . sinh mh)

C_4 = 2 (cos mh . cosh mh)

C_5 = sin mz . cosh mz

C_6 = cos mz . sinh mz

C_7 = (sin mz . sinh mz)

C_8 = (cos mz . cosh mz)

$W_0 = fD/s$

$a = [m(C_4+C_3)/2.] - W_0C_1$

$b = [m(C_4-C_3)/2.] + W_0C_2$

$V_0 = a^2 + b^2$

$C_{12} = (C_1)^2 + (C_2)^2$

$G = V_0 \cdot C_{12}$

$E = V_0[C_4C_2 - C_3C_1] - 2m[C_2(a+b) + C_1(a-b)]$

$F = V_0[C_3C_2 + C_4C_1] + 2m[C_2(a-b) - C_1(a+b)]$

(2) <u>The coefficients of Eqs. 5.31 to 5.35.</u>

$$A^* = \int_{-h}^{0} R^* \, dz \; ; \; B^* = \int_{-h}^{0} T^* \, dz \qquad [A.5]$$

$$A^* = \frac{1}{n} \{\frac{1}{n} - (\text{csch } nh) / [\, iW_0 + n \coth nh] \qquad [A.6]$$

$$B^* = i\,[h - 1/[iW_0 + n \coth nh\;] \qquad [A.7]$$

$$A^{*} = A^{*}_{r} + iA^{*}_{i} \qquad [A.8]$$

$$B^{*} = B^{*}_{r} + iB^{*}_{i} \qquad [A.9]$$

$$A^{*}_{r} = \frac{-1}{2m^{2}} \left\{ \frac{m(a+b)}{V_0} \right\} \qquad [A.10]$$

$$A^{*}_{i} = \frac{1}{2m^{2}} \left\{ \frac{m(a+b)}{V_0} - 1 \right\} \qquad [A.11]$$

$$B^{*}_{r} = (aC_1 - bC_2) / V_0 \qquad [A.12]$$

$$B^{*}_{i} = [\, -(aC_2 + bC_1) / V_0 \,] + h \qquad [A.13]$$

(3) The coefficients of Equ. 5.36.

$$A(x,y) = \frac{1}{N_1} \left[\frac{\partial N_1}{\partial x} + \frac{\partial N_2}{\partial y} \right] \qquad [A.14]$$

$$A(x,y) = \frac{1}{N_1} \left[\frac{\partial N_1}{\partial x} - \frac{\partial N_2}{\partial y} \right] \qquad [A.15]$$

$$C(x,y) = \frac{1}{N_1} \left[\frac{\partial}{\partial x} (N_3 R_y + N_4 R_x) + \frac{\partial}{\partial y} (N_4 R_y - N_3 R_x) \right] \qquad [A.16]$$

Where:

$$N_1 = B^*_r / [B^{*2}_r + B^{*2}_i] \qquad [A\text{-}17]$$

$$N_2 = -B^*_i / [B^{*2}_r + B^{*2}_i] \qquad [A\text{-}18]$$

$$N_3 = [A^*_r B^*_r + A^*_i B^*_i] / [B^{*2}_r + B^{*2}_i] \qquad [A\text{-}19]$$

$$N_4 = [A^*_i B^*_r - A^*_r B^*_i] / [B^{*2}_r + B^{*2}_i] \qquad [A\text{-}19]$$

APPENDIX B

TOXIWASP MODEL SEGMENT PARAMETERS

B.1 General

The segment interaction data for four different models is listed in the following pages. The different models are identified by the number of segments in each:

1. The 48 Segment Model for the upper part of St.Clair River,
2. The 52 Segment Model for the entire St.Clair River,
3. The 24 Segment Model for Lake St.Clair,
4. The 46 Segment Model for the Detroit River.

Table B.1: Segment Data for 48 SEGMENT MODEL

IR	JR	A	IL	JL	E
0	1	0.220E 05	0.220E 05	0.500E 04	0.550E 01
0	3	0.220E 05	0.220E 05	0.800E 04	0.550E 01
0	5	0.220E 05	0.220E 05	0.800E 04	0.550E 01
0	7	0.220E 05	0.220E 05	0.280E 05	0.550E 01
1	2	0.260E 02	0.820E-01	0.672E 07	0.300E-04
1	3	0.180E 03	0.270E 03	0.840E 06	0.400E-01
1	9	0.220E 05	0.200E 04	0.500E 04	0.550E 01
3	4	0.300E 02	0.820E-01	0.288E 07	0.300E-04
3	5	0.270E 03	0.300E 03	0.840E 06	0.400E-01
3	11	0.220E 05	0.200E 04	0.800E 04	0.550E 01
5	6	0.360E 02	0.820E-01	0.233E 07	0.300E-04
5	7	0.300E 03	0.850E 03	0.927E 06	0.400E-01
5	13	0.220E 05	0.200E 04	0.800E 04	0.550E 01
7	8	0.330E 02	0.820E-01	0.206E 08	0.300E-04
7	15	0.220E 05	0.200E 04	0.280E 05	0.550E 01
9	10	0.250E 02	0.820E-01	0.360E 06	0.300E-04
9	11	0.180E 03	0.280E 03	0.560E 05	0.400E-01
9	17	0.200E 04	0.200E 04	0.500E 04	0.550E 01
11	12	0.300E 02	0.820E-01	0.560E 06	0.300E-04
11	13	0.280E 03	0.220E 03	0.640E 05	0.400E-01
11	19	0.200E 04	0.200E 04	0.900E 04	0.550E 01
13	14	0.360E 02	0.820E-01	0.440E 06	0.300E-04
13	15	0.220E 03	0.540E 03	0.700E 05	0.400E-01
13	21	0.200E 04	0.200E 04	0.500E 04	0.550E 01
15	16	0.300E 02	0.820E-01	0.188E 07	0.300E-04
15	23	0.200E 04	0.200E 04	0.160E 05	0.550E 01
17	18	0.250E 02	0.820E-01	0.360E 06	0.300E-04
21	22	0.360E 02	0.820E-01	0.440E 06	0.300E-04
17	19	0.180E 03	0.280E 03	0.580E 05	0.400E-01
17	25	0.200E 04	0.200E 04	0.500E 04	0.550E 01
19	20	0.300E 02	0.820E-01	0.560E 06	0.300E-04
19	27	0.200E 04	0.200E 04	0.900E 04	0.550E 01
21	23	0.220E 03	0.540E 03	0.700E 05	0.400E-01
21	29	0.200E 04	0.200E 04	0.800E 04	0.550E 01
23	24	0.300E 02	0.820E-01	0.188E 07	0.300E-04
23	31	0.200E 04	0.200E 04	0.160E 05	0.550E 01
25	26	0.250E 02	0.820E-01	0.360E 06	0.300E-04
25	27	0.180E 03	0.280E 03	0.580E 05	0.400E-01
25	33	0.200E 04	0.200E 04	0.500E 04	0.550E 01
27	28	0.300E 02	0.820E-01	0.560E 06	0.300E-04

Table B.2: Segment Data for 48 SEGMENT MODEL (CONT.)

IR	JR	A	IL	JL	E
27	29	0.280E 03	0.220E 03	0.640E 05	0.400E-01
27	35	0.200E 04	0.800E 04	0.900E 04	0.550E 01
29	30	0.360E 02	0.820E-01	0.440E 06	0.300E-04
29	31	0.220E 03	0.540E 03	0.700E 05	0.400E-01
29	37	0.200E 04	0.800E 04	0.800E 04	0.550E 01
31	32	0.300E 02	0.820E-01	0.188E 07	0.300E-04
31	39	0.200E 04	0.800E 04	0.160E 05	0.550E 01
33	34	0.250E 02	0.820E-01	0.144E 07	0.300E-04
33	35	0.180E 03	0.280E 03	0.232E 06	0.400E-01
33	41	0.800E 04	0.800E 04	0.500E 04	0.550E 01
35	36	0.300E 02	0.820E-01	0.224E 07	0.300E-04
35	37	0.280E 03	0.220E 03	0.256E 06	0.400E-01
35	43	0.800E 04	0.800E 04	0.900E 04	0.550E 01
37	38	0.360E 02	0.820E-01	0.176E 07	0.300E-04
37	39	0.220E 03	0.540E 03	0.280E 06	0.400E-01
37	45	0.800E 04	0.800E 04	0.800E 04	0.550E 01
39	40	0.300E 02	0.820E-01	0.752E 07	0.300E-04
39	47	0.800E 04	0.800E 04	0.160E 05	0.550E 01
41	42	0.250E 02	0.820E-01	0.144E 07	0.300E-04
41	43	0.180E 03	0.280E 03	0.232E 06	0.400E-01
41	0	0.800E 04	0.800E 04	0.500E 04	0.550E 01
43	44	0.300E 02	0.820E-01	0.224E 07	0.300E-04
43	45	0.280E 03	0.220E 03	0.256E 06	0.400E-01
43	0	0.800E 04	0.800E 04	0.900E 04	0.550E 01
45	46	0.360E 02	0.820E-01	0.176E 07	0.300E-04
45	47	0.220E 03	0.540E 03	0.280E 06	0.400E-01
45	0	0.800E 04	0.800E 04	0.800E 04	0.550E 01
47	48	0.300E 02	0.820E-01	0.752E 07	0.300E-04
47	0	0.800E 04	0.800E 04	0.160E 05	0.550E 01
19	21	0.280E 03	0.220E 03	0.640E 05	0.400E-01

Table B.3: Segment Volumes (MCF) for 48 SEGMENT MODEL

SEG	VOL	SEG	VOL	SEG	VOL
1	0.175E 03	2	0.560E 00	3	0.864E 02
4	0.240E 00	5	0.839E 02	6	0.193E 00
7	0.680E 03	8	0.171E 01	9	0.900E 01
10	0.300E-01	11	0.168E 02	12	0.460E-01
13	0.158E 02	14	0.360E-01	15	0.564E 02
16	0.156E 00	17	0.900E 01	18	0.300E-01
19	0.168E 02	20	0.460E-01	21	0.158E 02
22	0.360E-01	23	0.564E 02	24	0.156E 00
25	0.900E 01	26	0.300E-01	27	0.168E 02
28	0.460E-01	29	0.158E 02	30	0.360E-01
31	0.564E 02	32	0.156E 00	33	0.360E 02
34	0.119E 00	35	0.672E 02	36	0.186E 00
37	0.634E 02	38	0.146E 00	39	0.226E 03
40	0.624E 00	41	0.360E 02	42	0.119E 00
43	0.672E 02	44	0.186E 00	45	0.634E 02
46	0.146E 00	47	0.226E 03	48	0.624E 00

Table B.4: Segment Flow Rates (CFS) for 48 SEGMENT MODEL

JQ	IQ	BQ	JQ	IQ	BQ	JQ	IQ	BQ
0	1	0.94E 04	0	3	0.39E 05	0	5	0.45E 05
0	7	0.94E 05	1	9	0.94E 04	1	3	0.20E 02
3	11	0.39E 05	3	5	0.20E 02	5	13	0.45E 05
5	7	0.20E 02	7	15	0.94E 05	9	17	0.94E 04
9	11	0.00E 00	13	21	0.45E 05	11	13	0.20E 02
17	19	0.20E 02	11	19	0.39E 05	13	15	0.20E 02
15	23	0.94E 05	17	25	0.94E 04	21	23	0.20E 02
23	31	0.94E 05	25	33	0.94E 04	25	27	0.20E 02
27	35	0.39E 05	27	29	0.20E 02	29	37	0.45E 05
29	31	0.20E 02	31	39	0.94E 05	33	41	0.94E 04
33	35	0.20E 02	35	43	0.39E 05	35	37	0.20E 02
37	45	0.45E 05	37	39	0.20E 02	39	47	0.94E 05
41	0	0.94E 04	41	43	0.20E 02	43	0	0.39E 05
43	45	0.20E 02	45	0	0.45E 05	45	47	0.20E 02
47	0	0.94E 05	21	29	0.45E 05	19	27	0.39E 05
19	21	0.00E 00						

Table B.5: Segment Data for 52 SEGMENT MODEL

IR	JR	A	IL	JL	E
0	1	0.200E 05	0.200E 05	0.115E 05	0.550E 01
0	3	0.200E 05	0.200E 05	0.214E 05	0.550E 01
0	5	0.200E 05	0.200E 05	0.180E 05	0.550E 01
0	7	0.200E 05	0.200E 05	0.123E 05	0.550E 01
1	3	0.502E 03	0.584E 03	0.630E 06	0.400E-01
1	9	0.200E 05	0.100E 05	0.206E 05	0.550E 01
3	4	0.335E 02	0.820E-01	0.117E 08	0.300E-04
3	5	0.584E 03	0.579E 03	0.717E 06	0.400E-01
3	11	0.200E 05	0.100E 05	0.360E 05	0.550E 01
5	6	0.330E 02	0.820E-01	0.116E 08	0.300E-04
5	7	0.579E 03	0.550E 03	0.600E 06	0.400E-01
5	13	0.200E 05	0.100E 05	0.250E 05	0.550E 01
7	8	0.210E 02	0.820E-01	0.110E 08	0.300E-04
7	15	0.200E 05	0.100E 05	0.230E 05	0.550E 01
3	13	0.200E 05	0.100E 05	0.240E 05	0.550E 01
9	10	0.200E 02	0.820E-01	0.650E 07	0.300E-04
9	11	0.650E 03	0.600E 03	0.295E 06	0.400E-01
9	17	0.100E 05	0.240E 05	0.180E 05	0.550E 01
11	12	0.240E 02	0.820E-01	0.600E 07	0.300E-04
11	19	0.100E 05	0.240E 05	0.220E 05	0.550E 01
13	19	0.100E 05	0.240E 05	0.700E 04	0.550E 01
13	14	0.206E 02	0.820E-01	0.109E 08	0.300E-04
13	15	0.143E 04	0.495E 03	0.295E 06	0.400E-01
13	21	0.100E 05	0.240E 05	0.120E 05	0.550E 01
15	16	0.180E 02	0.820E-01	0.846E 07	0.300E-04
15	23	0.100E 05	0.240E 05	0.140E 05	0.550E 01
17	18	0.197E 02	0.820E-01	0.155E 08	0.300E-04
17	19	0.644E 03	0.698E 03	0.765E 06	0.400E-01
17	25	0.240E 05	0.240E 05	0.110E 05	0.550E 01
19	20	0.315E 02	0.820E-01	0.167E 08	0.300E-04
19	21	0.698E 03	0.851E 03	0.737E 06	0.400E-01
19	27	0.240E 05	0.240E 05	0.200E 05	0.550E 01
21	22	0.308E 02	0.820E-01	0.204E 08	0.300E-04
21	23	0.851E 03	0.574E 03	0.714E 06	0.400E-01
21	29	0.240E 05	0.240E 05	0.150E 05	0.550E 01
23	24	0.252E 02	0.820E-01	0.138E 08	0.300E-04
23	31	0.240E 05	0.240E 05	0.120E 05	0.550E 01
25	26	0.244E 02	0.820E-01	0.142E 08	0.300E-04
25	27	0.592E 03	0.489E 03	0.812E 06	0.400E-01
25	33	0.240E 05	0.240E 05	0.190E 05	0.550E 01

Table B.6: Segment Data for 52 SEGMENT MODEL (CONT.)

IR	JR	A	IL	JL	E
27	28	0.375E 02	0.820E-01	0.117E 08	0.300E-04
27	29	0.489E 03	0.461E 03	0.101E 07	0.400E-01
27	35	0.240E 05	0.240E 05	0.240E 05	0.550E 01
29	30	0.389E 02	0.820E-01	0.111E 08	0.300E-04
29	31	0.461E 03	0.487E 03	0.883E 06	0.400E-01
29	37	0.240E 05	0.240E 05	0.240E 05	0.550E 01
31	32	0.241E 02	0.820E-01	0.117E 08	0.300E-04
31	39	0.240E 05	0.240E 05	0.160E 05	0.550E 01
33	34	0.185E 02	0.820E-01	0.207E 08	0.300E-04
33	35	0.860E 03	0.107E 04	0.669E 06	0.400E-01
33	41	0.240E 05	0.240E 05	0.190E 05	0.550E 01
35	36	0.311E 02	0.820E-01	0.256E 08	0.300E-04
35	37	0.107E 04	0.742E 03	0.767E 06	0.400E-01
35	43	0.240E 05	0.240E 05	0.200E 05	0.550E 01
37	38	0.390E 02	0.820E-01	0.178E 08	0.300E-04
37	39	0.742E 03	0.600E 03	0.745E 06	0.400E-01
37	45	0.240E 05	0.240E 05	0.260E 05	0.550E 01
39	40	0.216E 02	0.820E-01	0.144E 08	0.300E-04
39	45	0.240E 05	0.240E 05	0.160E 05	0.550E 01
47	0	0.300E 05	0.300E 05	0.200E 05	0.550E 01
41	42	0.287E 02	0.820E-01	0.141E 08	0.300E-04
41	43	0.586E 03	0.509E 03	0.106E 07	0.300E 01
41	47	0.240E 05	0.300E 05	0.320E 05	0.550E 01
43	44	0.375E 02	0.820E-01	0.122E 08	0.300E-04
43	45	0.509E 03	0.136E 04	0.727E 06	0.400E-01
43	49	0.240E 05	0.300E 05	0.380E 05	0.550E 01
45	46	0.280E 02	0.820E-01	0.326E 08	0.300E-04
45	51	0.240E 05	0.200E 05	0.560E 05	0.550E 01
47	48	0.231E 02	0.820E-01	0.209E 08	0.300E-04
47	49	0.104E 04	0.157E 04	0.106E 07	0.400E-01
49	0	0.300E 05	0.300E 05	0.215E 05	0.550E 01
1	2	0.210E 02	0.820E-01	0.100E 08	0.300E-04
49	50	0.219E 02	0.820E-01	0.307E 08	0.300E-04
51	0	0.200E 05	0.200E 05	0.600E 05	0.550E 01
51	52	0.240E 02	0.820E-01	0.405E 08	0.300E-04

Table B.7: Segment Volumes (MCF) for 52 SEGMENT MODEL

SEG	VOL	SEG	VOL	SEG	VOL
1	0.211E 03	2	0.823E 00	3	0.391E 03
4	0.958E 00	5	0.382E 03	6	0.949E 00
7	0.231E 03	8	0.902E 00	9	0.955E 02
10	0.392E 00	11	0.186E 03	12	0.634E 00
13	0.224E 03	14	0.893E 00	15	0.152E 03
16	0.693E 00	17	0.304E 03	18	0.127E 01
19	0.528E 03	20	0.137E 01	21	0.630E 03
22	0.168E 01	23	0.345E 03	24	0.113E 01
25	0.346E 03	26	0.117E 01	27	0.440E 03
28	0.962E 00	29	0.431E 03	30	0.907E 00
31	0.281E 03	32	0.957E 00	33	0.383E 03
34	0.169E 01	35	0.796E 03	36	0.210E 01
37	0.694E 03	38	0.146E 01	39	0.311E 03
40	0.118E 01	41	0.403E 03	42	0.115E 01
43	0.458E 03	44	0.100E 01	45	0.926E 03
46	0.268E 01	47	0.576E 03	48	0.204E 01
49	0.822E 03	50	0.309E 01	51	0.688E 03
52	0.235E 01				

Table B.8: Segment Flow Rates (CFS) for 52 SEGMENT MODEL

JQ	IQ	BQ	JQ	IQ	BQ	JQ	IQ	BQ
0	1	0.34E 05	0	3	0.60E 05	0	5	0.60E 05
0	7	0.34E 05	1	9	0.34E 05	1	3	0.20E 02
3	11	0.22E 05	3	5	0.20E 02	5	13	0.60E 05
5	7	0.20E 02	7	15	0.34E 05	9	17	0.34E 05
9	11	0.00E 00	13	21	0.60E 05	13	15	0.20E 02
3	13	0.37E 05	11	19	0.22E 05	19	21	0.20E 02
15	23	0.34E 05	17	25	0.34E 05	17	19	0.20E 02
21	29	0.60E 05	13	19	0.37E 05	19	27	0.60E 05
21	23	0.20E 02	23	31	0.34E 05	25	33	0.34E 05
25	27	0.20E 02	27	35	0.60E 05	27	29	0.20E 02
29	37	0.60E 05	29	31	0.20E 02	31	39	0.34E 05
33	41	0.34E 05	33	35	0.20E 02	35	43	0.60E 05
35	37	0.20E 02	37	45	0.60E 05	37	39	0.20E 02
39	45	0.34E 05	41	47	0.47E 05	43	41	0.13E 05
43	49	0.41E 05	43	45	0.56E 04	45	51	0.99E 05
47	49	0.00E 00	47	0	0.47E 05	49	0	0.41E 05
51	0	0.99E 05						

Table B.9: Segment Data for 24 SEGMENT MODEL

IR	JR	A	IL	JL	E
1	2	0.181E 02	0.820E-01	0.304E 09	0.000E 00
2	3	0.820E-01	0.820E-01	0.304E 09	0.000E 00
1	0	0.264E 05	0.264E 05	0.147E 06	0.400E 00
1	4	0.106E 05	0.158E 05	0.489E 06	0.400E 00
1	13	0.264E 05	0.422E 05	0.318E 06	0.334E 00
4	5	0.113E 02	0.820E-01	0.454E 09	0.000E 00
5	6	0.820E-01	0.820E-01	0.454E 09	0.000E 00
4	0	0.290E 05	0.290E 05	0.111E 06	0.400E 00
4	7	0.290E 05	0.607E 05	0.459E 06	0.334E 00
7	8	0.141E 02	0.820E-01	0.241E 10	0.000E 00
8	9	0.820E-01	0.820E-01	0.241E 10	0.000E 00
7	10	0.607E 05	0.448E 05	0.443E 06	0.100E 00
7	16	0.396E 05	0.369E 05	0.199E 07	0.220E 00
10	11	0.121E 02	0.820E-01	0.143E 10	0.000E 00
11	12	0.820E-01	0.820E-01	0.143E 10	0.000E 00
10	19	0.317E 05	0.237E 05	0.554E 06	0.100E 00
13	14	0.159E 02	0.820E-01	0.150E 10	0.000E 00
14	15	0.820E-01	0.820E-01	0.150E 10	0.000E 00
13	16	0.211E 05	0.317E 05	0.162E 07	0.334E 00
13	22	0.422E 05	0.475E 05	0.732E 06	0.334E 00
16	17	0.171E 02	0.820E-01	0.164E 10	0.000E 00
17	18	0.820E-01	0.820E-01	0.164E 10	0.000E 00
0	16	0.369E 05	0.369E 05	0.342E 06	0.250E 00
16	19	0.422E 05	0.396E 05	0.310E 06	0.150E 00
19	20	0.740E 01	0.820E-01	0.112E 10	0.000E 00
20	21	0.820E-01	0.820E-01	0.112E 10	0.000E 00
0	19	0.237E 05	0.237E 05	0.145E 06	0.250E 00
22	23	0.810E 01	0.820E-01	0.215E 10	0.000E 00
23	24	0.820E-01	0.820E-01	0.215E 10	0.000E 00
0	22	0.237E 05	0.237E 05	0.885E 05	0.250E 00
0	1	0.256E 05	0.256E 05	0.203E 05	0.550E 01
0	3	0.256E 05	0.256E 05	0.612E 05	0.550E 01
1	2	0.323E 02	0.820E-01	0.538E 08	0.300E-04
1	3	0.188E 04	0.250E 04	0.762E 05	0.400E-01
1	5	0.256E 05	0.256E 05	0.544E 05	0.550E 01
3	4	0.205E 02	0.820E-01	0.643E 08	0.300E-04
5	6	0.355E 02	0.820E-01	0.306E 08	0.300E-04
5	7	0.111E 04	0.111E 04	0.978E 06	0.400E-01
5	9	0.275E 05	0.105E 05	0.346E 05	0.550E 01
7	8	0.354E 02	0.820E-01	0.306E 08	0.300E-04

Table B.10: Segment Volumes (MCF) for 24 SEGMENT MODEL

SEG	VOL	SEG	VOL	SEG	VOL
1	0.553E 04	2	0.254E 02	3	0.254E 02
4	0.514E 04	5	0.379E 02	6	0.379E 02
7	0.341E 05	8	0.201E 03	9	0.201E 03
10	0.174E 05	11	0.120E 03	12	0.120E 03
13	0.239E 05	14	0.125E 03	15	0.125E 03
16	0.281E 05	17	0.136E 03	18	0.136E 03
19	0.829E 04	20	0.931E 02	21	0.931E 02
22	0.174E 05	23	0.180E 03	24	0.570E 04

Table B.11: Segment Flow (CFS) - Time (DAYS) Functions for 24 SEGMENT MODEL

16 13 50

-20034.0	0.0	1137.0	8.6	-10922.0	11.4
-40808.0	19.3	-30736.0	23.5	-19638.0	28.2
57064.0	37.4	-22809.0	39.0	-8936.0	43.6
-96736.0	46.1	-21234.0	50.0	-16863.0	57.2
-8936.0	61.0	-19638.0	62.1	-40808.0	73.6
-30736.0	76.3	-20034.0	78.6	57064.0	91.9
-16863.0	92.7	-96736.0	95.5	1137.0	97.0
-10922.0	99.5	-21234.0	110.7	-22809.0	117.8
57064.0	122.0	-22809.0	122.4	-21234.0	127.9
-8936.0	140.0	-20034.0	140.5	-16863.0	164.2
-40808.0	166.7	-30736.0	170.0	-10922.0	171.5
-96736.0	187.3	-19638.0	188.4	1137.0	203.9
-13176.0	205.9	-20034.0	214.0	-22809.0	229.0
-96736.0	234.9	-40808.0	237.2	-8936.0	240.8
-19638.0	241.4	1137.0	248.5	-30736.0	250.5
-10922.0	254.2	57064.0	264.1	-21234.0	265.2
-16863.0	273.4	-16863.0	275.0		

Table B.12: Segment Flow (CFS) - Time (DAYS) Functions for 24 SEGMENT MODEL

1	0	50			
125457.0	0.0	125457.0	8.6	125457.0	11.4
125457.0	19.3	125457.0	23.5	125457.0	28.2
125457.0	37.4	125457.0	39.0	125457.0	43.6
125457.0	46.1	125457.0	50.0	125457.0	57.2
125457.0	61.0	125457.0	62.1	125457.0	73.6
125457.0	76.3	125457.0	78.6	125457.0	91.9
125457.0	92.7	125457.0	95.5	125457.0	97.0
125457.0	99.5	125457.0	110.7	125457.0	117.8
125457.0	122.0	125457.0	122.4	125457.0	127.9
125457.0	140.0	125457.0	140.5	125457.0	164.2
125457.0	166.7	125457.0	170.0	125457.0	171.5
125457.0	187.3	125457.0	188.4	125457.0	203.9
125457.0	205.9	125457.0	214.0	125457.0	229.0
125457.0	234.9	125457.0	237.2	125457.0	240.8
125457.0	241.4	125457.0	248.5	125457.0	250.5
125457.0	254.2	125457.0	264.1	125457.0	265.2
125457.0	273.4	125457.0	275.0		
4	0	50			
61793.0	0.0	61793.0	8.6	61793.0	11.4
61793.0	19.3	61793.0	23.5	61793.0	28.2
61793.0	37.4	61793.0	39.0	61793.0	43.6
61793.0	46.1	61793.0	50.0	61793.0	57.2
61793.0	61.0	61793.0	62.1	61793.0	73.6
61793.0	76.3	61793.0	78.6	61793.0	91.9
61793.0	92.7	61793.0	95.5	61793.0	97.0
61793.0	99.5	61793.0	110.7	61793.0	117.8
61793.0	122.0	61793.0	122.4	61793.0	127.9
61793.0	140.0	61793.0	140.5	61793.0	164.2
61793.0	166.7	61793.0	170.0	61793.0	171.5
61793.0	187.3	61793.0	188.4	61793.0	203.9
61793.0	205.9	61793.0	214.0	61793.0	229.0
61793.0	234.9	61793.0	237.2	61793.0	240.8
61793.0	241.4	61793.0	248.5	61793.0	250.5
61793.0	254.2	61793.0	264.1	61793.0	265.2
61793.0	273.4	61793.0	275.0		

Table B.13: Segment Flow (CFS) - Time (DAYS) Functions for 24 SEGMENT MODEL

4 1 50

46249.0	0.0	25077.0	8.6	37136.0	11.4
67023.0	19.3	56950.0	23.5	45852.0	28.2
-30850.0	37.4	49024.0	39.0	35150.0	43.6
122950.0	46.1	47448.0	50.0	43077.0	57.2
35150.0	61.0	45852.0	62.1	67023.0	73.6
56950.0	76.3	46249.0	78.6	-30850.0	91.9
43077.0	92.7	122950.0	95.5	25077.0	97.0
37136.0	99.5	47448.0	110.7	49024.0	117.8
-30850.0	122.0	49024.0	122.4	47448.0	127.9
35150.0	140.0	46249.0	140.5	43077.0	164.2
67023.0	166.7	56950.0	170.0	37136.0	171.5
122950.0	187.3	45852.0	188.4	25077.0	203.9
39390.0	205.9	46249.0	214.0	49024.0	229.0
122950.0	234.9	67023.0	237.2	35150.0	240.8
45852.0	241.4	25077.0	248.5	56950.0	250.5
37136.0	254.2	-30850.0	264.1	47448.0	265.2
43077.0	273.4	43077.0	275.0		

13 1 50

79209.0	0.0	100380.0	8.6	88321.0	11.4
58434.0	19.3	68507.0	23.5	79605.0	28.2
156307.0	37.4	76434.0	39.0	90307.0	43.6
2507.0	46.1	78009.0	50.0	82380.0	57.2
90307.0	61.0	79605.0	62.1	58434.0	73.6
68507.0	76.3	79209.0	78.6	156307.0	91.9
82380.0	92.7	2507.0	95.5	100380.0	97.0
88321.0	99.5	78009.0	110.7	76434.0	117.8
156307.0	122.0	76434.0	122.4	78009.0	127.9
90307.0	140.0	79209.0	140.5	82380.0	164.2
58434.0	166.7	68507.0	170.0	88321.0	171.5
2507.0	187.3	79605.0	188.4	100380.0	203.9
86067.0	205.9	79209.0	214.0	76434.0	229.0
2507.0	234.9	58434.0	237.2	90307.0	240.8
79605.0	241.4	100380.0	248.5	68507.0	250.5
88321.0	254.2	156307.0	264.1	78009.0	265.2
82380.0	273.4	82380.0	275.0		

Table B.14: Segment Flow (CFS) - Time (DAYS) Functions for 24 SEGMENT MODEL

7 4 50

108041.0	0.0	86870.0	8.6	98929.0	11.4
128815.0	19.3	118743.0	23.5	107645.0	28.2
30943.0	37.4	110817.0	39.0	96943.0	43.6
184743.0	46.1	109241.0	50.0	104870.0	57.2
96943.0	61.0	107645.0	62.1	128815.0	73.6
118743.0	76.3	108041.0	78.6	30943.0	91.9
104870.0	92.7	184743.0	95.5	86870.0	97.0
98929.0	99.5	109241.0	110.7	110817.0	117.8
30943.0	122.0	110817.0	122.4	109241.0	127.9
96943.0	140.0	108041.0	140.5	104870.0	164.2
128815.0	166.7	118743.0	170.0	98929.0	171.5
184743.0	187.3	107645.0	188.4	86870.0	203.9
101183.0	205.9	108041.0	214.0	110817.0	229.0
184743.0	234.9	128815.0	237.2	96943.0	240.8
107645.0	241.4	86870.0	248.5	118743.0	250.5
98929.0	254.2	30943.0	264.1	109241.0	265.2
104870.0	273.4	104870.0	275.0		

10 7 50

11632.0	0.0	15042.0	8.6	11060.0	11.4
6971.0	19.3	45420.0	23.5	10381.0	28.2
25802.0	37.4	20392.0	39.0	23408.0	43.6
3788.0	46.1	10737.0	50.0	1621.0	57.2
23408.0	61.0	10381.0	62.1	6971.0	73.6
45420.0	76.3	11632.0	78.6	25802.0	91.9
1621.0	92.7	3788.0	95.5	15042.0	97.0
11060.0	99.5	10737.0	110.7	20392.0	117.8
25802.0	122.0	20392.0	122.4	10737.0	127.9
23408.0	140.0	11632.0	140.5	1621.0	164.2
6971.0	166.7	45420.0	170.0	11060.0	171.5
3788.0	187.3	10381.0	188.4	15042.0	203.9
10795.0	205.9	11632.0	214.0	20392.0	229.0
3788.0	234.9	6971.0	237.2	23408.0	240.8
10381.0	241.4	15042.0	248.5	45420.0	250.5
11060.0	254.2	25802.0	264.1	10737.0	265.2
1621.0	273.4	1621.0	275.0		

<u>Table B.15</u>: Segment Flow (CFS) - Time (DAYS) Functions for 24 SEGMENT MODEL

16	7	50			
96408.0	0.0	71828.0	8.6	87868.0	11.4
121844.0	19.3	73322.0	23.5	97263.0	28.2
5141.0	37.4	90424.0	39.0	73534.0	43.6
180954.0	46.1	98503.0	50.0	103248.0	57.2
73534.0	61.0	97263.0	62.1	121844.0	73.6
73322.0	76.3	96408.0	78.6	5141.0	91.9
103248.0	92.7	180954.0	95.5	71828.0	97.0
87868.0	99.5	98503.0	110.7	90424.0	117.8
5141.0	122.0	90424.0	122.4	98503.0	127.9
73534.0	140.0	96408.0	140.5	103248.0	164.2
121844.0	166.7	73322.0	170.0	87868.0	171.5
180954.0	187.3	97263.0	188.4	71828.0	203.9
90388.0	205.9	96408.0	214.0	90424.0	229.0
180954.0	234.9	121844.0	237.2	73534.0	240.8
97263.0	241.4	71828.0	248.5	73322.0	250.5
87868.0	254.2	5141.0	264.1	98503.0	265.2
103248.0	273.4	103248.0	275.0		

0	10	50			
1872.0	0.0	1872.0	8.6	1872.0	11.4
1872.0	19.3	1872.0	23.5	1872.0	28.2
1872.0	37.4	1872.0	39.0	1872.0	43.6
1872.0	46.1	1872.0	50.0	1872.0	57.2
1872.0	61.0	1872.0	62.1	1872.0	73.6
1872.0	76.3	1872.0	78.6	1872.0	91.9
1872.0	92.7	1872.0	95.5	1872.0	97.0
1872.0	99.5	1872.0	110.7	1872.0	117.8
1872.0	122.0	1872.0	122.4	1872.0	127.9
1872.0	140.0	1872.0	140.5	1872.0	164.2
1872.0	166.7	1872.0	170.0	1872.0	171.5
1872.0	187.3	1872.0	188.4	1872.0	203.9
1872.0	205.9	1872.0	214.0	1872.0	229.0
1872.0	234.9	1872.0	237.2	1872.0	240.8
1872.0	241.4	1872.0	248.5	1872.0	250.5
1872.0	254.2	1872.0	264.1	1872.0	265.2
1872.0	273.4	1872.0	275.0		

Table B.16: Segment Flow (CFS) - Time (DAYS) Functions for 24 SEGMENT MODEL

0 19 50

16852.0	0.0	16852.0	8.6	16852.0	11.4
16852.0	19.3	16852.0	23.5	16852.0	28.2
16852.0	37.4	16852.0	39.0	16852.0	43.6
16852.0	46.1	16852.0	50.0	16852.0	57.2
16852.0	61.0	16852.0	62.1	16852.0	73.6
16852.0	76.3	16852.0	78.6	16852.0	91.9
16852.0	92.7	16852.0	95.5	16852.0	97.0
16852.0	99.5	16852.0	110.7	16852.0	117.8
16852.0	122.0	16852.0	122.4	16852.0	127.9
16852.0	140.0	16852.0	140.5	16852.0	164.2
16852.0	166.7	16852.0	170.0	16852.0	171.5
16852.0	187.3	16852.0	188.4	16852.0	203.9
16852.0	205.9	16852.0	214.0	16852.0	229.0
16852.0	234.9	16852.0	237.2	16852.0	240.8
16852.0	241.4	16852.0	248.5	16852.0	250.5
16852.0	254.2	16852.0	264.1	16852.0	265.2
16852.0	273.4	16852.0	275.0		

0 16 50

69282.0	0.0	69282.0	8.6	69282.0	11.4
69282.0	19.3	69282.0	23.5	69282.0	28.2
69282.0	37.4	69282.0	39.0	69282.0	43.6
69282.0	46.1	69282.0	50.0	69282.0	57.2
69282.0	61.0	69282.0	62.1	69282.0	73.6
69282.0	76.3	69282.0	78.6	69282.0	91.9
69282.0	92.7	69282.0	95.5	69282.0	97.0
69282.0	99.5	69282.0	110.7	69282.0	117.8
69282.0	122.0	69282.0	122.4	69282.0	127.9
69282.0	140.0	69282.0	140.5	69282.0	164.2
69282.0	166.7	69282.0	170.0	69282.0	171.5
69282.0	187.3	69282.0	188.4	69282.0	203.9
69282.0	205.9	69282.0	214.0	69282.0	229.0
69282.0	234.9	69282.0	237.2	69282.0	240.8
69282.0	241.4	69282.0	248.5	69282.0	250.5
69282.0	254.2	69282.0	264.1	69282.0	265.2
69282.0	273.4	69282.0	275.0		

Table B.17: Segment Flow (CFS) - Time (DAYS) Functions for 24 SEGMENT MODEL

0	22	50			
99243.0	0.0	99243.0	8.6	99243.0	11.4
99243.0	19.3	99243.0	23.5	99243.0	28.2
99243.0	37.4	99243.0	39.0	99243.0	43.6
99243.0	46.1	99243.0	50.0	99243.0	57.2
99243.0	61.0	99243.0	62.1	99243.0	73.6
99243.0	76.3	99243.0	78.6	99243.0	91.9
99243.0	92.7	99243.0	95.5	99243.0	97.0
99243.0	99.5	99243.0	110.7	99243.0	117.8
99243.0	122.0	99243.0	122.4	99243.0	127.9
99243.0	140.0	99243.0	140.5	99243.0	164.2
99243.0	166.7	99243.0	170.0	99243.0	171.5
99243.0	187.3	99243.0	188.4	99243.0	203.9
99243.0	205.9	99243.0	214.0	99243.0	229.0
99243.0	234.9	99243.0	237.2	99243.0	240.8
99243.0	241.4	99243.0	248.5	99243.0	250.5
99243.0	254.2	99243.0	264.1	99243.0	265.2
99243.0	273.4	99243.0	275.0		
19	10	50			
9760.0	0.0	13170.0	8.6	9188.0	11.4
5099.0	19.3	43548.0	23.5	8509.0	28.2
23930.0	37.4	18520.0	39.0	21536.0	43.6
1916.0	46.1	8865.0	50.0	-251.0	57.2
21536.0	61.0	8509.0	62.1	5099.0	73.6
43548.0	76.3	9760.0	78.6	23930.0	91.9
-251.0	92.7	1916.0	95.5	13170.0	97.0
9188.0	99.5	8865.0	110.7	18520.0	117.8
23930.0	122.0	18520.0	122.4	8865.0	127.9
21536.0	140.0	9760.0	140.5	-251.0	164.2
5099.0	166.7	43548.0	170.0	9188.0	171.5
1916.0	187.3	8509.0	188.4	13170.0	203.9
8923.0	205.9	9760.0	214.0	18520.0	229.0
1916.0	234.9	5099.0	237.2	21536.0	240.8
8509.0	241.4	13170.0	248.5	43548.0	250.5
9188.0	254.2	23930.0	264.1	8865.0	265.2
-251.0	273.4	-251.0	275.0		

Table B.18: Segment Flow (CFS) - Time (DAYS) Functions for 24 SEGMENT MODEL

19 16 50

7092.0	0.0	3682.0	8.6	7664.0	11.4
11754.0	19.3	-26696.0	23.5	8343.0	28.2
-7077.0	37.4	-1667.0	39.0	-4684.0	43.6
14936.0	46.1	7987.0	50.0	17103.0	57.2
-4684.0	61.0	8343.0	62.1	11754.0	73.6
-26696.0	76.3	7092.0	78.6	-7077.0	91.9
17103.0	92.7	14936.0	95.5	3682.0	97.0
7664.0	99.5	7987.0	110.7	-1667.0	117.8
-7077.0	122.0	-1667.0	122.4	7987.0	127.9
-4684.0	140.0	7092.0	140.5	17103.0	164.2
11754.0	166.7	-26696.0	170.0	7664.0	171.5
14936.0	187.3	8343.0	188.4	3682.0	203.9
7930.0	205.9	7092.0	214.0	-1667.0	229.0
14936.0	234.9	11754.0	237.2	-4684.0	240.8
8343.0	241.4	3682.0	248.5	-26696.0	250.5
7664.0	254.2	-7077.0	264.1	7987.0	265.2
17103.0	273.4	17103.0	275.0		

22 13 50

99243.0	0.0	99243.0	8.6	99243.0	11.4
99243.0	19.3	99243.0	23.5	99243.0	28.2
99243.0	37.4	99243.0	39.0	99243.0	43.6
99243.0	46.1	99243.0	50.0	99243.0	57.2
99243.0	61.0	99243.0	62.1	99243.0	73.6
99243.0	76.3	99243.0	78.6	99243.0	91.9
99243.0	92.7	99243.0	95.5	99243.0	97.0
99243.0	99.5	99243.0	110.7	99243.0	117.8
99243.0	122.0	99243.0	122.4	99243.0	127.9
99243.0	140.0	99243.0	140.5	99243.0	164.2
99243.0	166.7	99243.0	170.0	99243.0	171.5
99243.0	187.3	99243.0	188.4	99243.0	203.9
99243.0	205.9	99243.0	214.0	99243.0	229.0
99243.0	234.9	99243.0	237.2	99243.0	240.8
99243.0	241.4	99243.0	248.5	99243.0	250.5
99243.0	254.2	99243.0	264.1	99243.0	265.2
99243.0	273.4	99243.0	275.0		

Table B.19: Segment Data for 46 SEGMENT MODEL

IR	JR	A	IL	JL	E
7	11	0.275E 05	0.105E 05	0.174E 05	0.550E 01
7	13	0.275E 05	0.105E 05	0.174E 05	0.550E 01
3	7	0.256E 05	0.275E 05	0.525E 05	0.550E 01
9	10	0.338E 02	0.820E-01	0.131E 08	0.300E-04
9	11	0.125E 04	0.625E 03	0.347E 06	0.400E-01
9	15	0.105E 05	0.875E 04	0.462E 05	0.550E 01
11	12	0.355E 02	0.820E-01	0.656E 07	0.300E-04
11	13	0.625E 03	0.625E 03	0.378E 06	0.400E-01
11	17	0.105E 05	0.875E 04	0.241E 05	0.550E 01
13	14	0.394E 02	0.820E-01	0.683E 07	0.300E-04
15	16	0.194E 02	0.820E-01	0.160E 08	0.300E-04
13	19	0.105E 05	0.875E 04	0.260E 05	0.550E 01
15	17	0.170E 04	0.700E 03	0.284E 06	0.250E 01
15	21	0.875E 04	0.273E 05	0.318E 05	0.550E 01
17	19	0.700E 03	0.700E 03	0.325E 06	0.400E-01
17	23	0.875E 04	0.273E 05	0.272E 05	0.550E 01
19	20	0.362E 02	0.820E-01	0.613E 07	0.300E-04
19	25	0.875E 04	0.273E 05	0.297E 05	0.550E 01
21	27	0.273E 05	0.288E 05	0.560E 05	0.550E 01
21	22	0.128E 02	0.820E-01	0.900E 08	0.300E-04
23	24	0.221E 02	0.820E-01	0.932E 08	0.300E-04
23	25	0.330E 04	0.750E 03	0.202E 06	0.400E-01
23	29	0.273E 05	0.288E 05	0.608E 05	0.550E 01
25	26	0.170E 02	0.820E-01	0.280E 08	0.300E-04
17	18	0.301E 02	0.820E-01	0.613E 07	0.300E-04
25	31	0.273E 05	0.150E 05	0.900E 04	0.550E 01
21	23	0.300E 04	0.390E 04	0.235E 06	0.400E-01
25	33	0.273E 05	0.150E 05	0.170E 05	0.550E 01
27	28	0.122E 02	0.820E-01	0.924E 08	0.300E-04
27	29	0.330E 04	0.400E 04	0.500E 05	0.225E 01
27	39	0.288E 05	0.156E 05	0.560E 05	0.550E 01
29	30	0.750E 01	0.820E-01	0.113E 09	0.300E-04
29	41	0.288E 05	0.156E 05	0.188E 05	0.550E 01
31	32	0.164E 02	0.820E-01	0.938E 07	0.300E-04
31	33	0.625E 03	0.625E 03	0.353E 06	0.225E 01
31	35	0.150E 05	0.170E 05	0.139E 05	0.550E 01
33	37	0.150E 05	0.170E 05	0.139E 05	0.550E 01
33	34	0.192E 02	0.820E-01	0.938E 07	0.300E-04
35	36	0.306E 01	0.820E-01	0.212E 08	0.300E-04
35	37	0.120E 04	0.120E 04	0.242E 06	0.400E-01

Table B.20: Segment Data for 46 SEGMENT MODEL (CONT.)

IR	JR	A	IL	JL	E
35	43	0.170E 05	0.156E 05	0.128E 05	0.550E 01
37	38	0.963E 01	0.820E-01	0.212E 08	0.300E-04
39	40	0.944E 01	0.820E-01	0.819E 08	0.300E-04
37	45	0.170E 05	0.156E 05	0.160E 05	0.550E 01
41	42	0.427E 01	0.820E-01	0.683E 08	0.300E-04
39	41	0.525E 04	0.438E 04	0.125E 06	0.400E-01
41	43	0.438E 04	0.465E 04	0.125E 06	0.225E 01
39	0	0.156E 05	0.156E 05	0.816E 05	0.550E 01
41	0	0.156E 05	0.156E 05	0.262E 05	0.550E 01
43	44	0.763E 01	0.820E-01	0.698E 08	0.300E-04
43	45	0.465E 04	0.450E 04	0.700E 05	0.400E-01
43	0	0.156E 05	0.156E 05	0.477E 05	0.550E 01
45	0	0.156E 05	0.156E 05	0.270E 05	0.550E 01
45	46	0.483E 01	0.820E-01	0.675E 08	0.300E-04

Table B.21: Segment Volumes (MCP) for 46 SEGMENT MODEL

SEG	VOL	SEG	VOL	SEG	VOL
1	0.173E 04	2	0.441E 01	3	0.132E 04
4	0.527E 01	5	0.108E 04	6	0.251E 01
7	0.108E 04	8	0.251E 01	9	0.443E 03
10	0.108E 01	11	0.233E 03	12	0.538E 00
13	0.269E 03	14	0.559E 00	15	0.309E 03
16	0.131E 01	17	0.185E 03	18	0.502E 00
19	0.221E 03	20	0.502E 00	21	0.116E 04
22	0.738E 01	23	0.206E 04	24	0.764E 01
25	0.476E 03	26	0.229E 01	27	0.113E 04
28	0.757E 01	29	0.852E 03	30	0.930E 01
31	0.154E 03	32	0.770E 00	33	0.180E 03
34	0.760E 00	35	0.171E 03	36	0.174E 01
37	0.205E 03	38	0.174E 01	39	0.773E 03
40	0.672E 01	41	0.312E 03	42	0.557E 01
43	0.532E 03	44	0.572E 01	45	0.326E 03
46	0.553E 01				

Table B.22: Segment Flow Rates (CFS) for 46 SEGMENT MODEL

JQ	IQ	BQ	JQ	IQ	BQ	JQ	IQ	BQ
0	1	0.47E 05	0	3	0.14E 06	3	1	0.47E 05
1	5	0.94E 05	3	7	0.94E 05	5	7	0.10E 02
5	9	0.94E 05	7	11	0.47E 05	7	13	0.47E 05
9	11	0.00E 00	11	13	0.00E 00	9	15	0.94E 05
11	17	0.47E 05	13	19	0.47E 05	15	17	0.37E 05
17	19	0.00E 00	15	21	0.56E 05	17	23	0.84E 05
19	25	0.47E 05	21	23	0.00E 00	23	25	0.00E 00
21	27	0.56E 05	23	29	0.84E 05	25	31	0.15E 05
25	33	0.32E 05	29	27	0.51E 05	33	31	0.11E 05
31	35	0.26E 05	33	37	0.21E 05	35	37	0.00E 00
27	39	0.11E 06	29	41	0.34E 05	35	43	0.26E 05
37	45	0.21E 05	39	0	0.11E 06	41	0	0.21E 05
43	0	0.43E 05	45	0	0.17E 05	39	41	0.00E 00
41	43	0.13E 05	45	43	0.37E 04			

APPENDIX C

FLOW CHARTS AND LISTING OF THE COMPUTER PROGRAMS

C.1 Users Guide for River Pollutant Transport Model

The program consists of main directory and short subroutines. The detailed USERS GUIDE is given by McCorquodale, 1983. However, the main subroutines in the program are:

1. HYD, which is the simplified flow distribution subroutine. It reads the width and radius of curvature followed by 40 equally spaced water depths across each section in the channel. Then, it computes the flow distribution including the secondary flow near the water surface and the bed at the centre line of the reach.
2. DISPX, which can be applied to any simple river reach in order to obtain the far field dispersion calculation. The subroutine may use a constant dispersion coefficient or call the (k-ε) turbulence subroutine to obtain the dispersion coefficient.
3. SPLIT, this subroutine divides the nodal concentrations between two channels with new nodal concentrations.
4. COMB, the subbroutine combines and mixes the loads from two channels at their confluence.

C.2 Listing of the (k-ε) Computer Program

```
CCCCCCCCCCCCCCCCCCCCCCCCCCCCCCCCCCCCCCCCCCCCCCCCCCCCCCCCCCCCCCCCCCCCC
C*******                                                           **C
C*        PROGRAM TO SOLVE TWO DIMENSIONAL RIVER DISPERSION          *C
C*                   OF CONTAMINANTS IN R.ST.CLAIR                   *C
C* UNIV OF WINDSOR/CCIW    FEB.10,1985  FINITE DIFF. MOD.            *C
C*                 ---------------------------------                 *C
C*    NOD:NUMBER OF NODES/CROSS SECTION                              *C
C*   C(-):CONCENTRATIONS AT LATERAL NODES IN REACH(-)                *C
C*    UPR:ACCUMULATED PERCENT OF FLOW FROM BASE SHORE                *C
C* DECAY:DECAY CONSTANT                                              *C
C*    QDZ:FRACTION OF THE FLOW BETWEEN TWO SUCSSISIVE NODES          *C
C*     NS:NUM. OF CROSS SEC. IN A REACH                              *C
C*     NC:NUM. OF SUBDIVISIONS BETWEEN THE CROSS SEC                 *C
C*     DX:DISTANCE BETWEEN THE CROSS SECTIONS                        *C
C*     QH:AVERAGE FLOW IN A REACH                                    *C
C*   DDXX:DISTANCE BETWEEN SUBDIVISIONS                              *C
C*    DXK:+DX FOR K-E MODEL CALCULATIONS                             *C
C*        -DX BYPASSES THE K-E MODEL                                 *C
C*   FACT:FACTOR TO ADJUST DEFAULT DISPERSION COEFFICIENT            *C
C*        WHICH IS 15.0 SFPS                                         *C
C*NUMBER:IDENTIFICATION FOR REACH NUM.                               *C
C* NHALF:NODE AT WHICH TRANSBOUNDARY ESTIMATE IT TO NODE             *C
C*******                                                             *C
CCCCCCCCCCCCCCCCCCCCCCCCCCCCCCCCCCCCCCCCCCCCCCCCCCCCCCCCCCCCCCCCCCCCCCC
      COMMON/KKK/APR(20),UPR(14),QDZ(14)
      COMMON/AREA1/DECAY,SFR(50)
      DIMENSION C(15),C1(15),C2(15),C3(15),C4(15),C5(15),
     *C6(15),C7(15)
      READ,NOD,DX
      NO=NOD-1
      READ,C
      READ,UPR
      APR(1)=0.0
      DO 10 LI=2,NOD
      APR(LI)=UPR(LI-1)
   10 CONTINUE
      DO 20 IR=1,NO
   20 QDZ(IR)=(APR(IR+1)-APR(IR))/100.
      PRINT,QDZ
      READ,DECAY
      WRITE(6,400) (C(J),J=1,NOD)
      PRINT,UPR
      WRITE(6,200) DECAY
  200 FORMAT(2X,'DECAY CONSTANT = ',F12.9,'1/S')
      WRITE(6,300) (APR(J),J=1,NOD)
  300 FORMAT(2X,'NQ',15F8.1)
  400 FORMAT(2X,'C ',15F8.1)
```

```
C*****************************************************************
C***************** D I R E C T O R Y *****************************
C****** CALL STATEMENTS TO BE INSERTED BY THE.MODELLER ******
C*****************************************************************
      NS=23
      NC=4
      CALL DISPX(1,NS,186600.0,DX,NC,-500.,15,C,1.0,1,8)
      CALL SPLIT(60.0,40.,15,C,C1,C2)
      NS=6
      CALL DISPX(1,NS,111960.,DX,NC,50.0,.15,C1,1.0,2,8)
      NS=6
      CALL DISPX(1,NS,74640.0,DX,NC,-500.,15,C2,1.0,3,8)
      NS=2
      CALL COMB(30.0,1,DX,NC,25.0,NS,.60,.40,C1,C2,15,41,C)
      NS=49
      CALL DISPX(1,NS,186600.0,DX,NC,-500.0,15,C,1.0,4,8)
      CALL SPLIT(60.,40.,15,C,C2,C1)
      NS=15
      CALL DISPX(1,NS,74640.00,DX,NC,-500.,15,C1,1.0,5,8)
      NS=19
      CALL DISPX(1,NS,111960.0,DX,NC,-500.,15,C2,1.0,6,8)
      STOP
      END
C*****************************************************************
C                                                                *
C               PROGRAMME VELOCITY DISTRIBUTION                  *
C           F.D.M        APR.12,1983                             *
C                        -----------                             *
C    THIS PROG. CALCULATE THE VEL. DIST. ALONG  THE              *
C    CROSS SEC. OF A RIVER .                                     *
C    M : NO. OF CROSS SECTIONS / RIVER                           *
C    NO: NO. OF SUBDIVISIONS / CROSS SECTION                     *
C    W : WIDTH OF THE CROSS SECTION                              *
C    Q : WATER DISCHARGES AT CROSS SEC. N                        *
C    DY: WIDTH OF SUBDIVISION FOR SEC. N                         *
C    D : WATER DEPTHS                                            *
C    U : MEAN VEL. / EACH DIVISION                               *
C  DX: DISTANCE BETWEEN CROSS SECTIONS                           *
C   RC :RADIUS OF CURVATURE TO MIDEL OF THE CHANNEL              *
C*****************************************************************
      SUBROUTINE HYD(QT,DX,NC,MPL,M,NO,XM,HM,UM,EPSI,DZ,VZ,
     @DXK,PZ,SV)
      COMMON/KKK/APR(20),UPR(14),QDZ(14)
      COMMON/AREA1/DECAY,SFR(50)
      DIMENSION D(118),B(118),U(118),DQ(118),UM(750),DZ(750)
     *,VZ(750),EPSI(750),XM(750),YM(750),HM(750),QT(200),
     @PZ(750),SV(750)
      NOD=NO+1
```

```
      DO 1 I=1,MPL
      PZ(I)=0.0
      SV(I)=0.0
      DZ(I)=0.0
      VZ(I)=0.0
    1 UM(I)=0.0
      EZTA=15.0
      C=0.12
      N=117
      EP=0.0
      DO 40 K=1,M
      Q=QT(M)
      YOR=DX*(K-1)
      KM=(K-1)*NOD+1
      KMI=KM+1
      KMP=KM+NOD-1
      READ,W,RC
      DY=W/117.
      XOR=3500.0-W/2.0
      XM(KMI-1)=XOR
      YM(KMI-1)=YOR
      EPSI(KMI-1)=EP
      NN=N+1
      DO 5 ND=1,NN,60
      NI=ND
      NF=ND+57
      IF(NF.GE.NN) NF=NN
      READ,(D(I),I=NI,NF,3)
      DO 3 J=NI,NF,3
      IF(J.GE.NF)GO TO 3
      DD=D(J+3)-D(J)
      D(J+1)=D(J+3)-2.0*DD/3.0
      D(J+2)=D(J+3)-DD/3.0
    3 CONTINUE
    5 CONTINUE
      DD=D(61)-D(58)
      D(59)=D(61)-2.0*DD/3.0
      D(60)=D(61)-DD/3.0
      DO 6 KK=1,118
    6 D(KK)=D(KK)+2.5
      SQ=0.0
      Y=-DY/2.0
      DO 10 J=1,N
      H=(D(J)+D(J+1))/2.0
      Y=Y+DY
      B(J)=((0.25-((Y/W)-0.50)**2)**C)*SQRT(RC/(RC-W/2+Y))
```

```
10 SQ=SQ+B(J)*(H**1.6667)*DY
   A=Q/SQ
   DC=D(N/2)
   SPR(K)=ABS(W*(DC**0.166667)/RC/0.136)
   CALL SYFLOW(DC,0.95,RC)
   CALL SYFLOW(DC,0.05,RC)
   DQ(1)=0.0
   IC=1
   X=0.0
   SAREA=0.0
   SDIS=0.0
   XM(KM)=0.0
   HM(KM)=D(1)
   UM(KM)=((.25-((DY/W)-.5)**2)**C)*(D(1)**.6667)*A*
  @SQRT(RC/(RC-W/2+Y))
   PZ(KM)=EZTA*(D(1)**2)*UM(KM)
   DO 20 J=1,N
   COMP=UPR(IC)*Q/100.0
   JJ=J
   IF(JJ.EQ.1)JJ=2
   H=(D(J)+D(J+1))/2.0
   U(J)=B(J)*(H**0.6667)*A
   SUM=U(J)*H*DY
   SDIS=SDIS+SUM
   AREA=H*DY
   SAREA=SAREA+AREA
   X=X+DY
   DQ(J)=SUM+DQ(JJ-1)
   P=DQ(J)*100.0/Q
   TEST=COMP-DQ(J)
   IF(J.EQ.N)TEST=0.0
   IF(J.EQ.N) X=W-DY/2.
   IF(TEST)15,15,20
15 BB=(0.25-((X/W)-0.5)**2)**C
```

```
      UM(IC+KM)=BB*(D(J+1)**0.6667)*A*SQRT(RC/(RC-W/2.+X))
      PZ(IC+KM)=UM(IC+KM)*EZTA*(D(J+1)**2)
      EPSI(IC+KM)=DQ(J)*100.0/Q
      HM(IC+KM)=D(J+1)
      IF(J.EQ.N)X=W
      XM(IC+KM)=X+TEST*DY/SUM
      IC=IC+1
      SAREA=0.0
      SDIS=0.0
   20 CONTINUE
   40.CONTINUE
      L=0
      LLL=MPL-2*NOD+1
      DO 80 I=1,LLL,NOD
      II=I+1
      N=I+NOD-2
      IC=1
      DO 70 M=II,N
      IC=IC+1
      D1=((PZ(M-1)+PZ(M+NO)-PZ(M)-PZ(M+NOD))*QDZ(IC))/(QDZ(IC-1)*
     *(QDZ(IC)+QDZ(IC-1)))
      D2=((PZ(M)+PZ(M+NOD)-PZ(M+1)-PZ(M+NOD+1))*QDZ(IC-1))/(QDZ(IC)
     **(QDZ(IC)+QDZ(IC-1)))
   70 SV(M)=(D1+D2)/(2.0*Q**2)
   80 CONTINUE
      DO 85 I=1,MPL
   85 PZ(I)=(PZ(I))/(Q**2)
      RETURN
      END
      SUBROUTINE DISPX(IC,NS,QH,DDXX,NC,DXK,NOD,C,FACT,NUMBER,NHALF)
CCCCCCCCCCCCCCCCCCCCCCCCCCCCCCCCCCCCCCCCCCCCCCCCCCCCCCCCCCCCCCCCCCCCCCC
C*******                                                        *******C
C*    SUBROUTINE TO SOLVE TWO DIMENSIONAL RIVER DISPERSION            *C
C*   IT MAY CALL SUBROUTINE HYD OR READ THE HYDRODYNAMIC DATA         *C
C*             FINITE DIFF. MODEL   MAY 10,1983                       *C
C*             -------------------------------                        *C
C* CONTROL PARAMETERS                                                 *C
C*   IC .INDEX =1 TO CALL SUB. HYD  & =0 TO READ THE DATA             *C
C*NB READ OPTION CANCELLED IN THIS VERSION ; IC=1                     *C
C*   NS .NO. OF CROSS SECTIONS                                        *C
C*   QH .AVERAGE FLOW RATE IN THE REACH                               *C
C*   DX .DISTANCE BETWEEN CROSS SECTIONS                              *C
C*******                                                        *******C
CCCCCCCCCCCCCCCCCCCCCCCCCCCCCCCCCCCCCCCCCCCCCCCCCCCCCCCCCCCCCCCCCCCCCCC
      COMMON/KKK/APR(20),UPR(14),QDZ(14)
      COMMON/AREA1/DECAY,SPR(50)
      DIMENSION C(15),F(15),S(3,15),Q(15),P(15),R(15),D(15)
     *,V(15),NR(15),AINPUT(200),CX(200),QX(200),QT(200),JT(200)
     *,XM(750),HM(750),UM(750),EPSI(750),DZ(750),VZ(750),Y(30)
     *,XN(15),YN(15),UN(15),EN(15),UI(2,15),H(2,15),EPS(2,15),
```

```
     @PZ(750),SV(750)
      NO=NOD-1
      DX=DDXX
      NT=NO+1
      NFL=NS*NOD
       DXC=DX/NC
      G=2.0/3.
      B=1.0/3
      MM=(NS-1)*NC
      MMH=NS-1
      TTBQ=0.0
      WRITE(6,555) NUMBER
      WRITE(6,666)
 555  FORMAT(///,20X,'REACH NO. =',I3,'      SUBROUTINE DISPX ',/)
 666  FORMAT(15X,40('*'),/)
       READ,QREACH,NFALL

       DO 1001 N=1,MM
       NXX=N
       JT(NXX)=2
       QX(NXX)=0.0
       CX(NXX)=0.0
       QT(NXX)=QREACH
       AINPUT(NXX)=0.0
1001  CONTINUE
      DO 101 N=1,NFALL
       NXX=N
       READ, XFALL,JFALL,CFALL,QFALL,QREACH
      NXX=XFALL/DXC+1
      JT(NXX)=JFALL
      CX(NXX)=CFALL
      QT(NXX)=QREACH
      QX(NXX)=QFALL
      AINPUT(NXX)=CX(NXX)*QX(NXX)
      AMKD=AINPUT(NXX)*2.447/1000000.
      WRITE(6,906) XFALL,JFALL,CFALL,QFALL,AMKD
 906  FORMAT(2X,'LX= ',F10.1,' J=',I3,' CO= ',F9.3,' QO= ',F8.3,
     @' MASS RATE= ',F10.4)
 101  CONTINUE
      NH2=NHALF+1
      NH1=NHALF-1
      HM1=C(1)*QDZ(1)/2.
      DO 793 I=2,NH1
 793  HM1=HM1+C(I)*QDZ(I-1)/2.+C(I)*QDZ(I)/2.
      HM1=HM1+C(NHALF)*QDZ(NH1)/2.
      UM1=C(NHALF)*QDZ(NHALF-1)/2.
      DO 493 I=NHALF,NO
 493  UM1=UM1+C(I)*QDZ(I-1)/2.+C(I)*QDZ(I)/2.
      UM1=UM1+C(NOD)*QDZ(NO)/2.
      QT(NS)=QT(MMH)
```

```
      WRITE(6,777)
  777 FORMAT(//)
      XX=000000.
      IF(IC.EQ.0)GO TO 5
      CALL HYD(QT,DX,NC,NPL,NS,NO,XM,HM,UM,EPSI,DZ,VZ,DXK,PZ,SV)
    5 CONTINUE
      DO 100 N=1,NN
      JJ=((N-1)/NC)*NOD
      XX=XX+DXC
      LP=(XX-1.)/DX
      NPP=(XX-(LP*DX))/DXC
      IF(DXK.GT.9.9)GOTO 6667
      DO 8 J=1,NOD
      DZ(J)=PZ(J+JJ)
      DZ(J+NOD)=PZ(J+JJ+NOD)
      VZ(J)=SV(J+JJ)
      UI(1,J)=UM(J+JJ)
      UI(2,J)=UM(J+NOD+JJ)
      H(1,J)=HM(J+JJ)
    8 H(2,J)=HM(J+NOD+JJ)
      GOTO 6666
 6667 CALL KE(QH,NO,N,DX,NC,DXC,UM,HM,UI,H,DZ,VZ,EPS,ICT,DXK,PZ,SV)
 6666 CONTINUE
      DO 1 J=1,NOD
      Y1=XM(J+JJ)
      Y2=XM(J+NOD+JJ)
      DYDX=(Y2-Y1)/DX
    1 Y(J)=Y1+DYDX*DXC*(NPP)
      CMAX=C(1)
      CMIN=C(1)
      DO 91 I=1,NOD
      IF(C(I).GT.CMAX)CMAX=C(I)
      IF(C(I).LT.CMIN)CMIN=C(I)
   91 CONTINUE
      I=(N/NC-1)*NOD
      IF(I.LE.0) I=0
      DO 103 J=1,NOD
      EPSI(J)=EPSI(J+I)
  103 XM(J)=XM(J+I)
       NXX=N
      JTT=JT(NXX)
      DO 10 I=1,NOD
      F(I)=0.0
      Q(I)=0.0
      P(I)=0.0
      R(I)=0.0
      S(1,I)=0.0
      S(2,I)=0.0
   10 S(3,I)=0.0
```

```
700 FORMAT(2X,'C ',15F8.1)
701 FORMAT(2X,'Y ',15F8.1)
702 FORMAT(2X,'H ',15F8.1)
703 FORMAT(2X,'U ',15F8.1)
704 FORMAT(2X,'EM',15F8.1)
800 FORMAT((2X,'LX=',F10.1,I3,7F10.2),//)
    VZ(2)= VZ(2)*0.85
    VZ(NO)= VZ(NO)*0.85
    DO 53 I=1,NOD
    VZ(I)=VZ(I)*FACT*SQRT((1.+SFR(N/NC+1)/2.))
 53 DZ(I)=(DZ(I)+DZ(I+NOD))*FACT*SQRT((1.+SFR(N/NC+1)/2.))/2.
    DO 40 I=2,NO
    II=I-1
    DE=QDZ(II)
    DW=QDZ(I)
    DT=DE+DW
    BX=DT/DE
    CN=VZ(I)*DXC/DE
    B1=1.-0.5*BX*CN-(0.5*BX+1)*CN**2
    IF(B1.GT.BX) B1=BX
    B2=DT/DW*(1-B1/BX)
    IF(B2.GT.(DT/DW))B2=DT/DW
    S(1,I)=1./(6.*DXC)+DZ(I)/(DE*DT)+B2*VZ(I)*DW/(2.*DE*(DT))
    S(2,I)=2./(3.*DXC)-DZ(I)/(DE*DW)+VZ(I)/(2*DT)*(B1*DE/DW-B2*DW/DE)
    S(3,I)=1./(6.*DXC)+DZ(I)/(DW*DT)-VZ(I)*B1*DE/(2.*DW*DT)
    Q(I)=2./(3.*DXC)+VZ(I)/(2*DT)*(B2*DW/DE-B1*DE/DW)+DZ(I)/
   *     (DE*DW)
    R(I)=1./(6.*DXC)+B1*VZ(I)*DE/(2.*DW*DT)-DZ(I)/(DW*DT)
    P(I)=1./(6.*DXC)-VZ(I)*B2*DW/(2*DE*DT)-DZ(I)/(DE*DT)
 40 CONTINUE
    DO 50 I=2,NO
 50 F(I)=S(1,I)*C(I-1)+S(2,I)*C(I)+S(3,I)*C(I+1)
    Q(1)=G/DXC+DZ(2)/QDZ(1)/QDZ(1)/6.
    R(1)=B/DXC-DZ(2)/QDZ(1)/QDZ(1)/6.
    Q(NOD)=G/DXC+DZ(NO)/QDZ(NO)/QDZ(NO)/6.
    P(NOD)=B/DXC-DZ(NO)/QDZ(NO)/QDZ(NO)/6.
    F(1)=(G*C(1)+B*C(2))/DXC+DZ(2)*(C(2)-C(1))/QDZ(1)/QDZ(1)/6.
    F(NOD)=(B*C(NO)+G*C(NOD))/DXC+DZ(NO)*(C(NO)-C(NOD))/QDZ(NO)
   */QDZ(NO)/6.
```

```
      CALL RELAX(NOD,P,Q,R,F,C)
      DO 92 I=1,NOD
      IF(C(I).GT.CMAX)C(I)=CMAX
   92 IF(C(I).LT.CMIN)C(I)=CMIN
      SUM=C(1)*QDZ(1)/2.
      UAV=(UI(1,1)+UI(2,1))/2.
      SDM=C(1)*(1.-EXP(-DECAY*DXC /(UAV+.1)))*QDZ(1)/2.
      DO 79 I=2,NO
      UAV=(UI(1,I)+UI(2,I))/2.
      SUM=SUM+C(I)*QDZ(I-1)/2.+C(I)*QDZ(I)/2.
      IF(I.EQ.NHALF)SDMC=SDM+C(I)*(1.-EXP(-DECAY*DXC /(UAV+.1)))*
     *(QDZ(I-1))/2.
   79 SDM=SDM+C(I)*(1.-EXP(-DECAY*DXC/(UAV+.1)))*(QDZ(I-1)+QDZ(I))/2.
      SUM=SUM+C(NOD)*QDZ(NO)/2.
      UAV=(UI(1,NOD)+UI(2,NOD))/2.
      SDM=SDM+C(NOD)*(1.-EXP(-DECAY*DXC/(UAV+.1)))*QDZ(NO)/2.
      IF(N.LE.1)AMASS=SUM
      FM=AMASS/SUM
      DMASS = SUM*(1.-FM)/100.
      AINP=AINPUT(NXX)-SDM*QT(NXX)
      AMASS=AMASS+AINP/QT(NXX)
      DO 71 I=1,NOD
      IF(FM.GT.1..AND.C(I).GT.(CMAX/FM))GOTO 71
      IF(FM.LT.1..AND.C(I).LT.(CMIN/FM))GOTO 71
      C(I)=C(I)*FM
   71 CONTINUE
   73 CONTINUE
      DO 61 I=1,NOD
      UAV=(UI(1,I)+UI(2,I))/2.
   61 C(I)=C(I)*EXP(-DECAY*DXC /(UAV+.1))
      IF(JT(NXX).LE.1.OR.JT(NXX).EQ.15)GOTO 1058
      MT=JT(NXX)
      IF(MT.GT.NOD/2)GOTO 1059
      SQD=-QDZ(MT)/2.
      DO 64 MS=1,MT
   64 SQD=SQD+QDZ(MS)
      DO 65 MS=1,MT
   65 C(MS)=C(MS)+AINPUT(NXX)/(QT(NXX)*SQD)
      GOTO 1053
 1059 SQD=QDZ(MT -1)/2.
      DO 66 MS=MT,NO
   66 SQD=SQD+QDZ(MS)
      DO 67 MS=MT,NOD
   67 C(MS)=C(MS)+AINPUT(NXX)/(SQD*QT(NXX))
      GOTO 1053
 1058 CONTINUE
      IF(JT(NXX).LT.1)GOTO 105
      IF(JT(NXX).NE.1)GOTO 1051
      C(1)=2.*AINPUT(NXX)/QT(NXX)/((2.*QDZ(1))+QDZ(2))+C(1)
      C(2)=2.*AINPUT(NXX)/QT(NXX)/((2.*QDZ(1))+QDZ(2))+C(2)
      GOTO 1053
```

```
1051 IF(JT(NXX).NE.NOD)GOTO 105
     C(NO)=2.*AINPUT(NXX)/QT(NXX)/((2.*QDZ(NO))+QDZ(NO-1))+C(NO)
     C(NOD)=2.*AINPUT(NXX)/QT(NXX)/((2.*QDZ(NO))+QDZ(NO-1))+C(NOD)
     GOTO 1053
 105 JTT=-JT(NXX)
     C(JTT)=2.*AINPUT(NXX)/QT(NXX)/(QDZ(JTT-1)+QDZ(JTT))+C(JTT)
1053 CONTINUE
     HM2=C(1)*QDZ(1)/2.
     DO 379 I=2,NH1
 379 HM2=HM2+C(I)*QDZ(I-1)/2.+C(I)*QDZ(I)/2.
     HM2=HM2+C(NHALF)*QDZ(NH1)/2.
     UM2=C(NHALF)*QDZ(NHALF-1)/2.
     DO 393 I=NHALF,NO
 393 UM2=UM2+C(I)*QDZ(I-1)/2.+C(I)*QDZ(I)/2.
     UM2=UM2+C(NOD)*QDZ(NO )/2.
      CANIN=0.0
     IF(JTT.LT.NHALF)CANIN=AINPUT(NXX)
      USIN =0.0
     IF(JTT.GE.NHALF)USIN =AINPUT(NXX)
      TBQ=((HM2-HM1+UM1-UM2+SDM-2.*SDMC+DMASS)*QT(NXX)-CANIN+USIN)*
    *      2.447/1000000./2.
      IF(TBQ.LT.0.0.AND.C(NHALF).GE.C(NHALF-1))TBQ=-TBQ/2.
     TTBQ=TTBQ+TBQ
     AMT=AMASS*QT(NXX)*2.447/1000000.
      HM1=HM2
     UM1=UM2
     WRITE(6,800) XX,JT(NXX),CX(NXX),QX(NXX),AMT,FM,QT(NXX),TBQ,TTBQ
     WRITE(6,700) (C(J),J=1,NOD)
     WRITE(6,701) (Y(J),J=1,NOD)
     WRITE(6,702) (H(2,J),J=1,NT)
     WRITE(6,703) (UI(2,J),J=1,NT)
      IF(DXK.LT.9.9) GOTO 21
     WRITE(6,704)  (EPS(2,J),J=1,NT)
  21 CONTINUE
 100 CONTINUE
     RETURN
     END
     SUBROUTINE RELAX(NOD,P,Q,R,F,C)
     DIMENSION Q(NOD),R(NOD),P(NOD),F(NOD),C(NOD)
     NO=NOD-1
     DO 99 IX=1,3
     C(1)=(F(1)-R(1)*C(2))/Q(1)
     DO 98 I=2,NO
  98 C(I)=(F(I)-P(I)*C(I-1)-R(I)*C(I+1))/Q(I)
  99 C(NOD)=(F(NOD)-P(NOD)*C(NO))/Q(NOD)
     RETURN
     END
```

```
CCCCCCCCCCCCCCCCCCCCCCCCCCCCCCCCCCCCCCCCCCCCCCCCCCCCCCCCCCCCCCCCCCCCCCC
C      SUBROUTINE SPLIT                                                C
C      TO CALCULATE THE CONC. ACROSS ANY WATER DIVERSION               C
C      CONTROL PARAMETERS :                                            C
C      C  :CONC. IN THE MAIN CHANNEL                                   C
C      C1 :CONC. IN THE LEFT-HAND DIVERSION                            C
C      C2 :CONC. IN THE RIGHT-HAND DIVERSION                           C
CCCCCCCCCCCCCCCCCCCCCCCCCCCCCCCCCCCCCCCCCCCCCCCCCCCCCCCCCCCCCCCCCCCCCCC
      SUBROUTINE SPLIT(PR1,PR2,NOD,C,C1,C2)
      COMMON/KKK/APR(20),UPR(14),QDZ(14)
      COMMON/AREA1/DECAY,SPR(50)
      DIMENSION C(15),C1(15),C2(15),CS(15),CN(15),S1(15),S2(15)
      NO=NOD-1
      PR=PR1
      C1(1)=C(1)
      C2(NOD)=C(NOD)
      N=NO-1
      DO 10 I=1,N
   10 IF(PR.GE.UPR(I).AND.PR.LE.UPR(I+1)) J=I
      C1(NOD)=C(J+1)+(PR-UPR(J))*(C(J+2)-C(J+1))/(UPR(J+1)-UPR(J))
      C2(1)=C1(NOD)
      CS(1)=C1(1)
      S1(1)=0.0
      DO 20 I=1,J
      CS(I+1)=C(I+1)
   20 S1(I+1)=UPR(I)*100./PR
      CS(J+2)=C1(NOD)
      S1(J+2)=100.0
      NL=J+1
      LN=1
      DO 40 L=1,NL
      M=LN
      DO 30 I=M,NO
      IF(S1(L).EQ.S1(L+1))GOTO 30
      IF(UPR(I).GE.S1(L).AND.UPR(I).LE.S1(L+1)) GO TO 25
      GO TO 30
   25 C1(I+1)=CS(L)+(CS(L+1)-CS(L))*(UPR(I)-S1(L))/(S1(L+1)-S1(L))
      LN=LN+1
   30 CONTINUE
   40 CONTINUE
      PR=PR2
      CN(1)=C2(1)
      S2(1)=0.0
      L=NO-J-1
      DO 50 I=1,L
      CN(I+1)=C(J+I+1)
   50 S2(I+1)=(UPR(J+I)-PR1)*100./PR
      CN(L+2)=C2(NOD)
      S2(L+2)=100.0
      ML=L+1
      LN=1
```

```
      DO 70 N=1,ML
      M=LN
      DO 60 I=M,NO
      IF(S2(N).EQ.S2(N+1))GOTO 60
      IF(UPR(I).GE.S2(N).AND.UPR(I).LE.S2(N+1)) GO TO 65
      GO TO 60
   65 C2(I+1)=CN(N)+(CN(N+1)-CN(N))*(UPR(I)-S2(N))/(S2(N+1)-S2(N))
      LN=LN+1
   60 CONTINUE
   70 CONTINUE
      WRITE(6,1134)
 1134 FORMAT(4X,'SPLIT PERCENTAGES  ')
      PRINT,PR1,PR2
      RETURN
      END


CCCCCCCCCCCCCCCCCCCCCCCCCCCCCCCCCCCCCCCCCCCCCCCCCCCCCCCCCCCCCCCCCCCCCCCCC
C     SUBROUTINE COMB                                                   C
C     ****************                                                  C
C     TO COMB. TWO STREAM FLOWS INTO ONE MAIN CHANNEL                   C
C     CONTROL PARAMETERS                                                C
C     FR :FRACTION OF FLOW IN EACH DIVERSION                            C
C     C1 :CONC. IN DIVERSION NO. 1                                      C
C     C2 :CONC. IN DIVERSION NO. 2                                      C
C     DM :DIF. COFF. IN THE MAIN CROSS SECTION                          C
C     C  :CONC. IN THE MAIN CHANNEL                                     C
CCCCCCCCCCCCCCCCCCCCCCCCCCCCCCCCCCCCCCCCCCCCCCCCCCCCCCCCCCCCCCCCCCCCCCCCC
      SUBROUTINE COMB(FDX,IC,DX,NC,DXK,NS,PR1,PR2,C1,C2,NOD,NUMBER,C)
      COMMON/KKK/APR(20),UPR(14),QDZ(14)
      COMMON/AREA1/DECAY,SFR(50)
      DIMENSION C1(15),C2(15),C(15),CT(30),DT(30),ST(30),QT(200)
     *,XN(15),YN(15),UN(15),EN(15),NR(15),D(15),V(15),JT(2),CX(2),QX(2)
     *,XM(750),HM(750),UM(750),EPSI(750),DZ(750),VZ(750)
     a,AINPUT(200),PZ(750),SV(750)
      WRITE(6,555)NUMBER
      WRITE(6,666)
  555 FORMAT(///,20X,'REACH NO. =',I3,'      SUBROUTINE COMB ',/)
  666 FORMAT(15X,50('*'),/)
      NO=NOD-1
      NXX=1
      DXC=DX/NC
       MFL=NS*NOD
       READ, XFALL,JFALL,CFALL,QFALL,QREACH
```

```
      NXX=XFALL/DXC+1
      JT(NXX)=JFALL
      CX(NXX)=CFALL
      QT(NXX)=QREACH
      QX(NXX)=QFALL
      PRINT,XFALL,JT(NXX),CX(NXX),QX(NXX)
      AINPUT(NXX)=CX(NXX)*QX(NXX)
      QT(2)=QREACH
      QT(1)=QREACH
      QTL=QREACH
      WRITE(6,777)
  777 FORMAT(//)
      CALL HYD(QT,DX,NC,NFL,NS,NO,XN,HN,UN,EPSI,DZ,VZ,DXK,PZ,SV)
      IZ=(NOD+1)/2
      DN=PZ(IZ+NOD)*FDX
      DO 10 I=1,NOD
      DT(I)=C1(I)-C1(NOD)
   10 DT(I+NOD)=C2(I)-C2(1)
      CO=C2(1)-C1(NOD)
      ST(1)=0.0
      DO 20 I=2,NOD
      ST(I)=UPR(I-1)*PR1/100.
   20 ST(I+NOD)=UPR(I-1)*PR2/100.+PR1
      ST(NOD+1)=PR1
      NN=2*NOD
      DO 30 I=1,NN
      CALL MIX(ST(I),PR1,CO,5,DM,4000.,CM)
   30 CT(I)=C1(NOD)+DT(I)+CM
      DO 40 I=1,NN
   40 ST(I)=ST(I)*100.0
      C(1)=CT(1)
      C(NOD)=CT(NN)
      NL=NN-1
      LN=1
      DO 60 L=1,NL
      LL=LN
      DO 50 I=LL,NO
      IF(UPR(I).GE.ST(L).AND.UPR(I).LE.ST(L+1)) GO TO 55
      GO TO 50
   55 C(I+1)=CT(L)+(CT(L+1)-CT(L))*(UPR(I)-ST(L))/(ST(L+1)-ST(L))
      LN=LN+1
   50 CONTINUE
   60 CONTINUE
```

```
       NO=NOD-1
       C(2)=(C(2)+.8*(C1(2)-C(2))*QDZ(1)/(QDZ(1)+QDZ(2)))
       C(NO)=(C(NO)+.8*(C2(NO)-C(NO))*QDZ(1)/(QDZ(NO-1)+QDZ(NO)))
   70 CONTINUE
      WRITE(6,700) (C(J),J=1,NOD)
      LL=NOD+1
      LD=2*NOD
      WRITE(6,701) (XM(J),J=LL,LD)
      WRITE(6,702) (HM(J),J=LL,LD)
      WRITE(6,703) (UM(J),J=LL,LD)
      WRITE(6,704) (EPSI(J),J=LL,LD)
   80 CONTINUE
      SUM=0.0
      DO 86 I=1,NO
   86 SUM=SUM+QDZ(I)*(C(I)+C(I+1))/2.0
      AMT1=SUM*QTL*2.447/1000000.
      SUM=0.0
      DO 84 I=1,7
   84 SUM=SUM+QDZ(I)*(C(I)+C(I+1))/2.0
      AMT2=SUM*QTL*2.447/1000000.
      PRINT,AMT2,AMT1,QREACH
  700 FORMAT(2X,'C ',15F8.1)
  701 FORMAT(2X,'Y ',15F8.1)
  702 FORMAT(2X,'H ',15F8.1)
  703 FORMAT(2X,'U ',15F8.1)
  704 FORMAT(2X,'ES',15F8.1)
      RETURN
      END


CCCCCCCCCCCCCCCCCCCCCCCCCCCCCCCCCCCCCCCCCCCCCCCCCCCCCCCCCCCCCCCCCCCCCCCC
C     SUBROUTINE MIX                                                   C
C     TO DISTRIBUTE THE CONC. OF THE TWO CHANNELS                      C
CCCCCCCCCCCCCCCCCCCCCCCCCCCCCCCCCCCCCCCCCCCCCCCCCCCCCCCCCCCCCCCCCCCCCCCC
      SUBROUTINE MIX(S,Y1,CO,MO,DM,XM,CM)
      SM=SQRT(4*DM*XM)
      NI=2*MO+1
      F=0.0
      DO 10 I=1,NI
      MR=-MO-1+I
   10 F=F+ABS(ERF((.5-S-MR-((-1)**MR)*(.5-Y1))/SM)
     *-ERF((.5-S-MR-((-1)**MR)*(-.5))/SM))
      CM=CO*.5*F
      RETURN
      END
```

```
CCCCCCCCCCCCCCCCCCCCCCCCCCCCCCCCCCCCCCCCCCCCCCCCCCCCCCCCCCCCCCCCCCCCCCCC
C     SUBROUTIN UNIFORM                                                 C
C     TO CALCULATE THE CONC. AFTER COMPLETELY FLOW MIX                  C
CCCCCCCCCCCCCCCCCCCCCCCCCCCCCCCCCCCCCCCCCCCCCCCCCCCCCCCCCCCCCCCCCCCCCCCC
      SUBROUTINE UNFRM(NOD,C,NUMBER,CO,QO,QTL)
      COMMON/KKK/APR(20),UPR(14),QDZ(14)
      COMMON/AREA1/DECAY,SPR(50)
      DIMENSION C(NOD)
      WRITE(6,555) NUMBER
      WRITE(6,666)
  555 FORMAT(///,20X,'OUTPUT CONC. BEFORE AND AFTER  COMP. MIX FOR C'
     *,I1,/)
  666 FORMAT(15X,60('*'),/)
      WRITE(6,700) (C(J),J=1,NOD)
      NO=NOD-1
      SUM=0.0
      DO 10 I=1,NO
   10 SUM=SUM+QDZ(I)*(C(I)+C(I+1))/2.0
      AMT1=SUM*QTL*2.447/1000000.
      SUM=SUM+CO*QO/(QTL+QO)
      AMT2=SUM*QTL*2.447/1000000.
      PRINT,AMT1,AMT2
      DO 20 I=1,NOD
   20 C(I)=SUM
      WRITE(6,700) (C(J),J=1,NOD)
  700 FORMAT(2X,'C-',15F8.1)
      RETURN
      END
      SUBROUTINE KE(QHD,NO,ISEC,DXH,NC,DXC,UM,HM,UI,H,DZ,VZ,EPS,ICT,
     @DXK,PZ,SV)


CCCCCCCCCCCCCCCCCCCCCCCCCCCCCCCCCCCCCCCCCCCCCCCCCCCCCCCCCCCCCCCCCCCCCCCC
C      SUBROUTINE KE TO CALCULATE THE EDDY VISCOSITY BASED ON THE       C
C      THE TRANSPORT OF THE K.E. AND ITS DISSIPATION.                   C
C      CONTROL PARAMETERS:                                              C
C      UM   : VELOCITY AT EACH NODE OF THE HYDR. SECTIONS               C
C      HM   : DEPTH AT EACH NODE OF THE HYDR. SECTONS.                  C
C      UI   : INTERPOLATED VELOCITY AT EACH NODE OF THE KE SECS.        C
C      H    : INTERPOLATED DEPTH AT EACH NODE OF THE KE SECTIONS        C
C      EPS  : THE CALCULATED EDDY VISCOSITY BASED ON K.E. AND ITS       C
C             RATE OF DISSIPATION (K-EPS).                              C
C      DXC  : X-DISTANCE BETWEEN THE SECTIONS WHERE C IS CALCULATED C
C      DXK  : X-DISTANCE BETWEEN THE SECTIONS WHERS EPS IA CALC.        C
CCCCCCCCCCCCCCCCCCCCCCCCCCCCCCCCCCCCCCCCCCCCCCCCCCCCCCCCCCCCCCCCCCCCCCCC
      DIMENSION H(2,15),UI(2,15),DZ(750),VZ(750),EPS(2,15),DIS(15),
     #    XM(750),EPSI(750),AK(15),UST(15),Q(15),P(15),R(15),UN(15),
     #     D(118),B(118),U(118),YN(15),EN(15),UM(750),HM(750),F(15)
     @,PZ(750),SV(750)
```

```
      COMMON /A1/DX,QH,XM,YM,N,NJ,KK
      COMMON /A3/ P,Q,R,F
      COMMON /A4/ C1,C2,CU,ST,SK,SE,CE3,VON
      COMMON /KKK/ APR(20),UPR(14),QDZ(14)
      DATA C1,C2,CU,ST,SK,SE,CE3,VON,ANEW,EZTA /1.43,1.92,0.09,.5,1.
     #          ,1.4,1.0,0.42,0.00001,15.0/
      AN=.024
      G=32.2
      DX=DXH
      NJ=NO
      NOD=NO+1
      QH=QHD
      IF(ISEC.GT.1) GO TO 9
      NDIV=DX/DXK
      NNC=DXC/DXK
      N=NJ+1
      X=0.00
      XX=0.0
      JJ=0
      ICT=0
C     SET INITIAL CONDITIONS
C     ----------------------
      DO 5 J=2,NJ
      UST(J)=0.136*UM(J)/HM(J)**0.1666
      DIS(J)=UST(J)**2*UM(J)/HM(J)
      EPS(1,J)=EZTA*ST
    5 AK(J)=SQRT(EPS(1,J)*DIS(J)/CU)
C     PUT B.C. AT THE INITIAL SECTION
C     -------------------------------
      YWALL1=100.0
      UST(1)=VON*UM(1)/ALOG(30.*YWALL1)
      UST(N)=VON*UM(N)/ALOG(30.*YWALL1)
      AK(1)=UST(1)**2/SQRT(CU)
      AK(N)=UST(N)**2/SQRT(CU)
      YWALL=YWALL1*ANEW
      DIS(1)=UST(1)**4/(VON*YWALL)
      DIS(N)=UST(N)**4/(VON*YWALL)
      EPS(1,1)=CU*AK(1)**2/DIS(1)
      EPS(1,N)=CU*AK(N)**2/DIS(N)
      DO 7 I=1,N
      DZ(I)=DZ(I)*EPS(1,I)/ST/EZTA
      VZ(I)=VZ(I)/EZTA*EPS(1,I)/ST
      UN(I)=VZ(I)
      D(I)=UM(I)
      B(I)=HM(I)
    7 U(I)=EPS(1,I)
C     CALCULATE VALUES OF F TO CALCULATE(V)
C     -------------------------------------
    9 X=X+DXC
      IF(ICT.GE.NDIV) JJ=JJ+N
      IF(ICT.GE.NDIV) ICT=0
```

```
      IF(ICT.NE.0) GO TO 6
      DO 8 J=1,N
      UI(1,J)=UM(J+JJ)
      UI(2,J)=UM(J+N+JJ)
      H(1,J)=HM(J+JJ)
      H(2,J)=HM(J+N+JJ)
      XM(J)=(H(2,J)-H(1,J))/NDIV
    8 EPSI(J)=(UI(1,J)/UI(2,J)-1.)/NDIV
      GO TO 12
    6 DO 11 I=1,N
      H(1,I)=H(2,I)
      UI(1,I)=UI(2,I)
   11 EPS(1,I)=EPS(2,I)
   12 CONTINUE
      DO 99 IJJ=1,NNC
      ICT=ICT+1
      XX=XX+DXK
      DO 10 J=1,N
      H(2,J)=H(1,J)+XM(J)
   10 UI(2,J)=UI(1,J)/(1.+EPSI(J))
      EK1=AK(1)*QDZ(1)/2.
      EDF1=DIS(1)*QDZ(1)/2.
      DO 91 I=2,NJ
      EDF1=EDF1+DIS(I)*QDZ(I-1)/2.+DIS(I)*QDZ(I)/2.
   91 EK1=EK1+AK(I)*QDZ(I-1)/2.+AK(I)*QDZ(I)/2.
      EK1=EK1+AK(N)*QDZ(NJ)/2.
      EDF1=EDF1+DIS(N)*QDZ(NJ)/2.
      DO 20 J=1,N
      DZ(J)=EPS(1,J)*H(1,J)**2*UI(1,J)/SK
   20 DZ(J+N)=EPS(1,J)*H(2,J)**2*UI(2,J)/SK
      IC=1
      DO 70 M=2,NJ
      IC=IC+1
      D1=((DZ(M-1)+DZ(M+NJ)-DZ(M)-DZ(M+N))*QDZ(IC))/(QDZ(IC-1)*(QDZ(IC)
     *+QDZ(IC-1)))
      D2=((DZ(M)+DZ(M+N)-DZ(M+1)-DZ(M+N+1))*QDZ(IC-1))/(QDZ(IC)*(QDZ(IC)
     *+QDZ(IC-1)))
   70 VZ(M)=(D1+D2)/(2.0*QH**2)
      DO 85 I=1,N
   85 DZ(I)=DZ(I+N)/(QH**2)
      CALL TRIDG(VZ,DZ,AK,DXK)
C     SET B.C AT STEP I+1
C     ----------------------
      UST(1)=VON*UI(2,1)/ALOG(30.*YWALL1)
      UST(N)=VON*UI(2,N)/ALOG(30.*YWALL1)
      AK(1)=UST(1)**2/SQRT(CU)
      AK(N)=UST(N)**2/SQRT(CU)
      DIS(1)=UST(1)**4/(VON*YWALL)
      DIS(N)=UST(N)**4/(VON*YWALL)
```

```
      EPS(2,1)=CU*AK(1)**2/DIS(1)
      EPS(2,N)=CU*AK(N)**2/DIS(N)
      CALL SOLVE(AK,NOD,DXK)
      EK2=AK(1)*QDZ(1)/2.
      DO 92 I=2,NJ
   92 EK2=EK2+AK(I)*QDZ(I-1)/2.+AK(I)*QDZ(I)/2.
      EK2=EK2+AK(N)*QDZ(NJ)/2.
      RK=EK2/EK1
      CALL ANALYT(1,UI,H,AK,DIS,AN,G,EPS,DXK)
C     SOLVE FOR DISSIPATION (DIS)
C     ------------------------------
      DO 30 J=1,N
      YN(J)=DIS(J)
      VZ(J)=VZ(J)*SK/SE
   30 DZ(J)=DZ(J)*SK/SE
      CALL TRIDG(VZ,DZ,DIS,DXK)
      CALL SOLVE(DIS,NOD,DXK)
      EDF2=DIS(1)*QDZ(1)/2.
      DO 93 I=2,NJ
   93 EDF2=EDF2+DIS(I)*QDZ(I-1)/2.+DIS(I)*QDZ(I)/2.
      EDF2=EDF2+DIS(N)*QDZ(NJ)/2.
      RDIS=EDF2/EDF1
      CALL ANALYT(2,UI,H,DIS,AK,AN,G,EPS,DXK)
C      CALCULATE NEW VALUES FOR EDDY VISCOSITY
C     ------------------------------------------
       DO 36 J=2,NJ
   36  EPS(2,J)=CU*AK(J)**2/DIS(J)
      DO 40 J=1,N
      EPS(1,J)=EPS(2,J)
      H(1,J)=H(2,J)
   40 UI(1,J)=UI(2,J)
   99 CONTINUE
      DO 95 J=1,N
      UI(1,J)=D(J)
      H(1,J)=B(J)
   95 EPS(1,J)=U(J)
      DO 21 J=1,N
      DZ(J)=EPS(1,J)*H(1,J)**2*UI(1,J)/ST
   21 DZ(J+N)=EPS(2,J)*H(2,J)**2*UI(2,J)/ST
      DO 72 M=2,NJ
      D1=((DZ(M-1)+DZ(M+NJ)-DZ(M)-DZ(M+N))*QDZ(M))/(QDZ(M-1)*(QDZ(M)
     *+QDZ(M-1)))
      D2=((DZ(M)+DZ(M+N)-DZ(M+1)-DZ(M+N+1))*QDZ(M-1))/(QDZ(M)*(QDZ(M)
     *+QDZ(M-1)))
   72 VZ(M)=(D1+D2)/(2.0*QH**2)
      VZ(N+1)=VZ(N+N)=0.0
      DO 86 I=1,N
      DZ(I)=DZ(I)/(QH**2)
   86 DZ(I+N)=DZ(I+N)/(QH**2)
      RETURN
      END
```

```
C     ..........................................................
      SUBROUTINE ANALYT(INDEX,UI,H,DEL,EN,AN,G,EPS,DXK)
      DIMENSION UI(2,15),H(2,15),DEL(15),UST(15),EN(15),EPS(2,15)
     #    ,XM(750),YN(15),D(118)
      COMMON /A1/DX,QH,XM,YN,N,NJ,KK
      COMMON /A4/ C1,C2,CU,ST,SK,SE,CE3,VON
      COMMON /KKK/ APR(20),UPR(14),QDZ(14)
      IC=1
      NJ=N-1
      DO 70 M=2,NJ
      IC=IC+1
      D1=((UI(1,M-1)+UI(2,M-1)-UI(1,M)-UI(2,M))*QDZ(IC))/(QDZ(IC-1)
     #  *(QDZ(IC)+QDZ(IC-1)))
      D2=((UI(1,M)+UI(2,M)-UI(1,M+1)-UI(2,M+1))*QDZ(IC-1))/(QDZ(IC)
     #    *(QDZ(IC)+QDZ(IC-1)))
   70 D(M)=-(D1+D2)/(2.0)
      IF(INDEX.EQ.2)  GO TO 20
      DO 10 J=2,NJ
      UST(J)=0.136*UI(2,J)/H(2,J)**0.166666
      CF=AN**2*(G)/H(2,J)**0.333
      AA=H(2,J )**2*UI(2,J )*EPS(1,J)*(D(J)/QH)**2
      BB=1./UI(2,J)*(UST(J)**3/H(2,J)/SQRT(CF)-EN(J))
   10 DEL(J)=(AA+BB)*DXK+DEL(J)
      GO TO 100
   20 DO 30 J=2,NJ
      CF=AN**2*(G)/H(2,J)**0.333
      C3=CE3*C2*SQRT(CU)/CF**(0.75)
      PE=C3*UST(J)**4/H(2,J )**2
      AA=-C2/UI(2,J )/EN(J)
      BB=H(2,J)**2*EPS(1,J)*UI(2,J)*C1*(D(J)/QH)**2/EN(J)
      CC=PE/UI(2,J )
      DISC= (BB**2-4*AA*CC)
       IF(DISC.LT..000000001)DISC=ABS(DISC/2.)
       SQ=SQRT(DISC)
      CO=(2*AA*YN(J)+BB+SQ)/(2*AA*YN(J)+BB-SQ)
      SAVE=DEL(J)
      DEL(J)=(BB-SQ-(BB+SQ)*EXP(DXK*SQ)/CO)/(2*AA*(EXP(DXK*SQ)/CO-1))
     #   +DEL(J)-YN(J)
   30 CONTINUE
  100 RETURN
      END
```

```
      SUBROUTINE TRIDG(VZ,DZ,C,DXK)
      DIMENSION DZ(750),VZ(750),C(15),P(15),Q(15),R(15),
     #        .  F(15),EPS(2,15),XM(750),YN(15),PZ(750),SV(750)
      COMMON /A1/DX,QH,XM,YN,N,NJ,KK
      COMMON /A3/ P,Q,R,F
      COMMON /KKK/ APR(20),UPR(14),QDZ(14)
      NJ=N-1
      NT=N
      DO 40 J=2,NJ
      II=J-1
      DE=QDZ(II)
      DW=QDZ(J)
      DT=DW+DE
      BX=DT/DE
      CN=0.5*(VZ(J)+VZ(J))*DXK/DE
      B1=1.-0.5*BX*CN-(0.5*BX+1)*CN**2
      IF(B1.GT.BX) B1=BX
      B2=DT/DW*(1-B1/BX)
      IF(B2.GT.(DT/DW))B2=DT/DW
      S1=1./(6.*DXK)+DZ(J)/(DE*DT)+B2*VZ(J)*DW/(2.*DE*DT)
      S2=2./3./DXK-DZ(J)/DE/DW+(VZ(J)/2./DT)*(B1*DE/DW- B2*DW/DE)
      S3=1./6/DXK+DZ(J)/DW/DT-VZ(J)*DE/(2.*DW*DT)*B1
      F(J)=S1*C(J-1)+S2*C(J)+S3*C(J+1)
      Q(J)=2./3/DXK+VZ(J)/2.*(B2*DW/DE-B1*DE/DW)/DT+DZ(J)/(DE*DW)
      R(J)=1./6./DXK+B1*VZ(J)*DE/(2*DW*DT)-DZ(J)/DW/DT
      P(J)=1./6./DXK- B2*VZ(J)*DW/(2*DE*DT)-DZ(J)/DE/DT
   40 CONTINUE
      RETURN
      END

      SUBROUTINE SOLVE (C,NOD,DXK)
      DIMENSION C(15),P(15),Q(15),R(15),F(15)
      COMMON /A3/ P,Q,R,F
       NO=NOD-1
      DO 99 IX=1,3
      DO 98 I=2,NO
   98 C(I)=(F(I)-P(I)*C(I-1)-R(I)*C(I+1))/Q(I)
   99 CONTINUE
       RETURN
       END

      SUBROUTINE SYFLOW(D,Z,R)
      F1=-15.*((Z**2)*ALOG(Z)-.5*(Z**2)+15./54.)
      F2=7.5*((Z*ALOG(Z))**2-(Z**2)*ALOG(Z)+.5*(Z**2)-19./54.)
      VR=(D/R/.4)*(F1-F2*0.136/(.4*(D**0.166667)))
      WRITE(6,599) VR,Z
  599 FORMAT(2X,'SECONDARY VECTOR =',F10.6,'AT Z=',F8.4)
      RETURN
      END
```

C.3 The Computer Flow Chart for the Finite Element Model

The following figure diagrams the sequence of the computer program which used for the hydrodynamic and the transport submodel in Lake St.Clair.

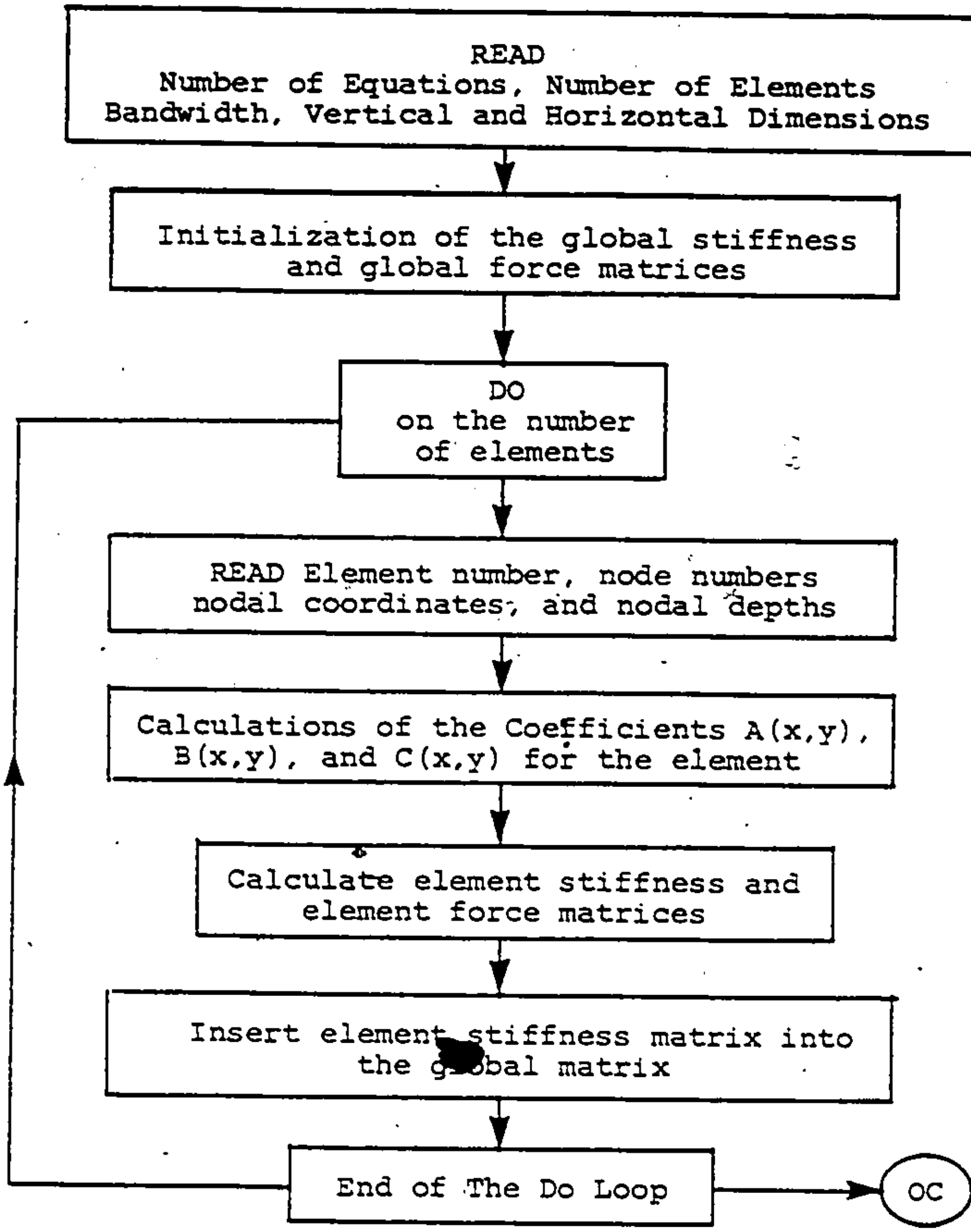
READ
Number of Equations, Number of Elements
Bandwidth, Vertical and Horizontal Dimensions
Initialization of the global stiffness
and global force matrices
DO
on the number
of elements
READ Element number, node numbers
nodal coordinates, and nodal depths
Calculations of the Coefficients A(x,y),
B(x,y), and C(x,y) for the element
Calculate element stiffness and
element force matrices
Insert element stiffness matrix into
the global matrix
End of The Do Loop
OC

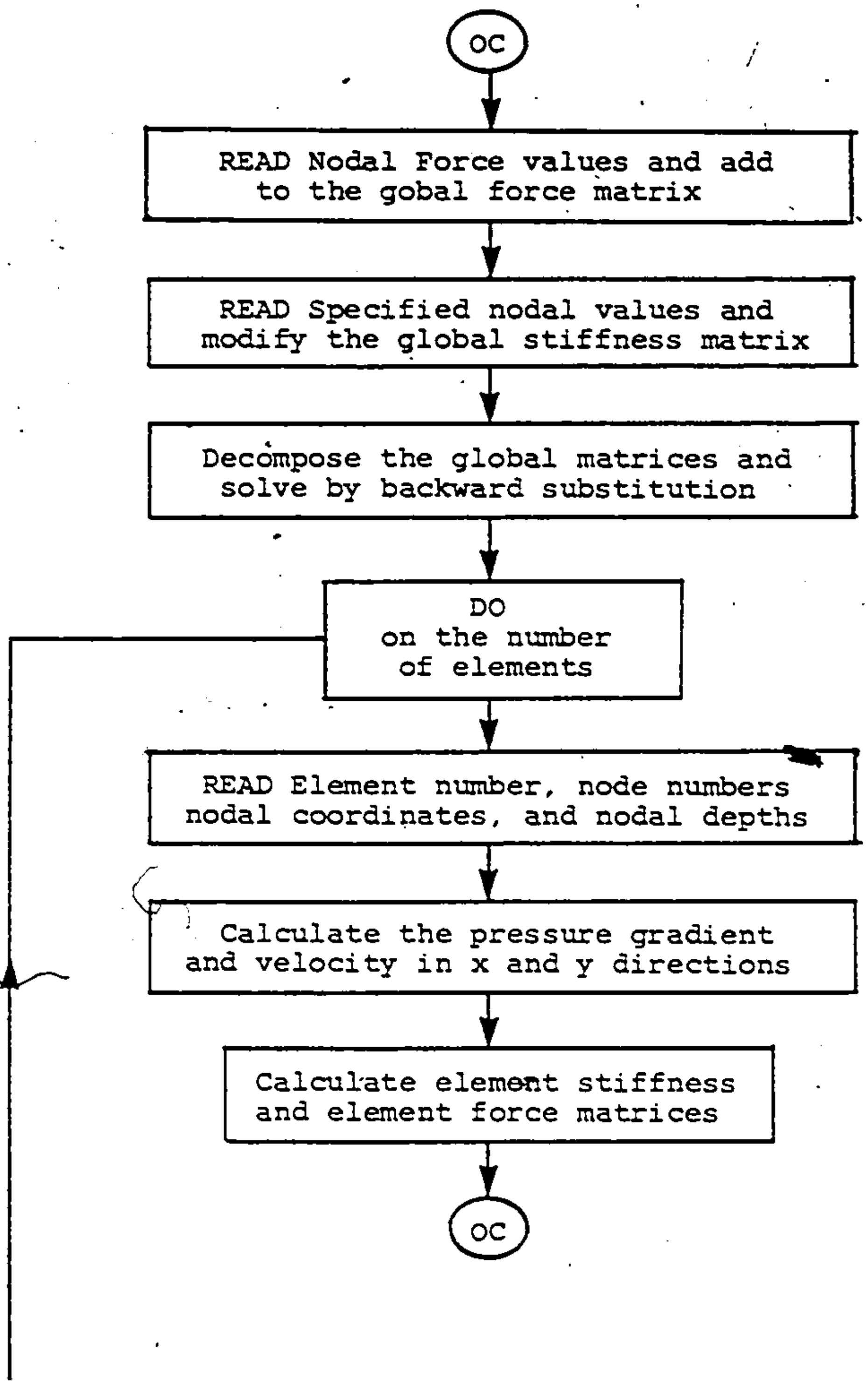

OC
READ Nodal Force values and add to the gobal force matrix
READ Specified nodal values and modify the global stiffness matrix
Decompose the global matrices and solve by backward substitution
DO on the number of elements
READ Element number, node numbers nodal coordinates, and nodal depths
Calculate the pressure gradient and velocity in x and y directions
Calculate element stiffness and element force matrices
OC

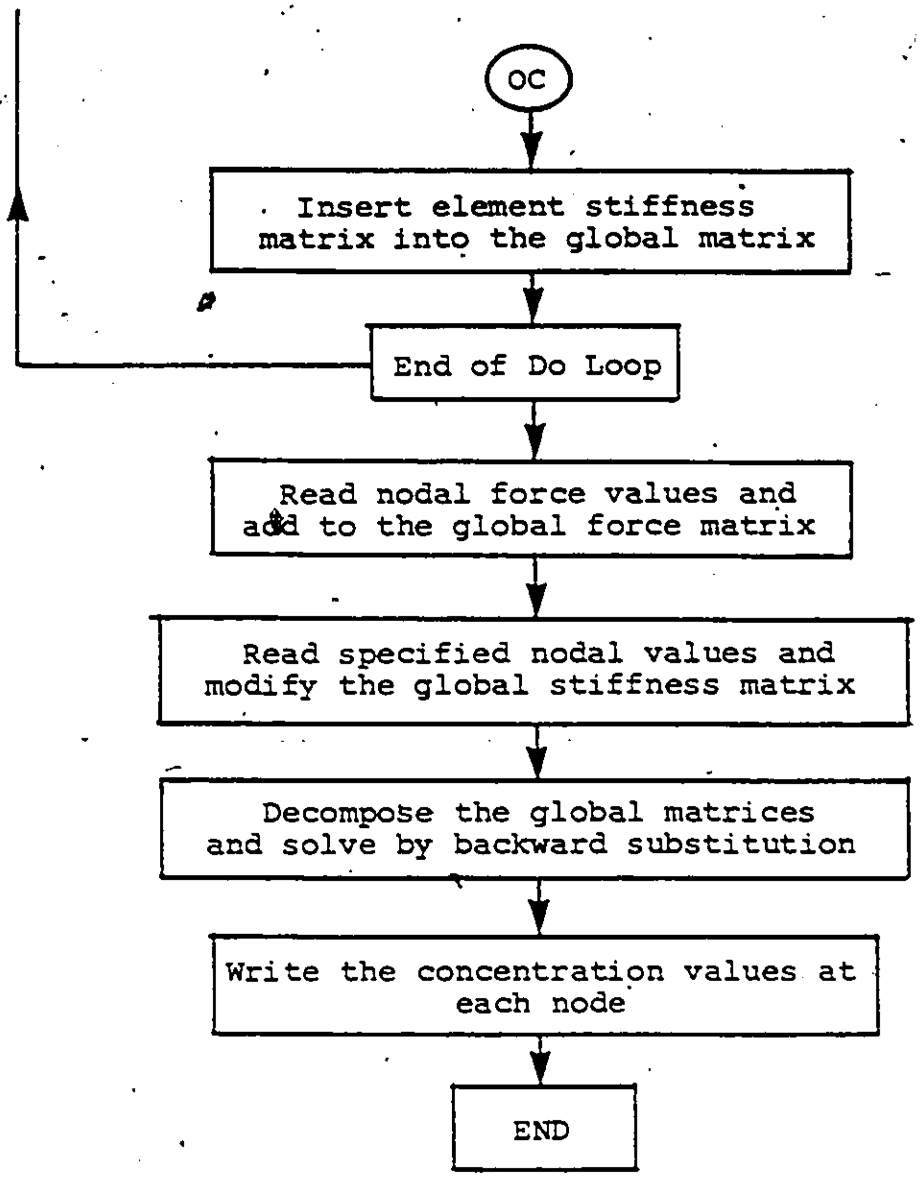
OC
Insert element stiffness matrix into the global matrix
End of Do Loop
Read nodal force values and add to the global force matrix
Read specified nodal values and modify the global stiffness matrix
Decompose the global matrices and solve by backward substitution
Write the concentration values at each node
END

C.4 Listing of the Finite Element Subroutines

```
CCCCCCCCCCCCCCCCCCCCCCCCCCCCCCCCCCCCCCCCCCCCCCCCCCCCCCCCCCCCCCCCCCCCCCC
CCCCCCCCCCCCCCCCCCCCCCCCCCCCCCCCCCCCCCCCCCCCCCCCCCCCCCCCCCCCCCCCCCCCCCC
C*******                                                        *******C
C*       PROGRAM TO SOLVE TWO DIMENSIONAL CIRCULATION MODEL           *C
C*                 WITH INFLOW 'DISPERSION'                           *C
C*               IBRAHIM   JAN.10,1984 PLOT                           *C
C*              ---------------------------------                     *C
C* CONTROL PARAMETERS                                                 *C
C*  NP  : NUMBER OF GLOBAL POTENTIALS                                 *C
C*  NE  : NUMBER OF ELEMENTS                                          *C
C*  NBW : BANDWIDTH                                                   *C
C*  NS  : ELEMENT NODE NUMBERS                                        *C
C*  ESM : ELEMENT STIFFNESS MATRIX                                    *C
C*  EF  : ELEMENT FORCE VECTOR                                        *C
C*  NEL : NUMBER OF AN INDIVIDUAL ELEMENT                             *C
C*  JGF : LAST STORAGE LOCATION FOR {U} IN THE COLUMN ARRAY {A}       *C
C*  JGSM: LAST STORAGE LOCATION FOR {F} IN THE COLUMN ARRAY {A}       *C
C*  JEND: LAST STORAGE LOCATION FOR [K] IN THE COLUMN ARRAY {A}       *C
C*******                                                        *******C
CCCCCCCCCCCCCCCCCCCCCCCCCCCCCCCCCCCCCCCCCCCCCCCCCCCCCCCCCCCCCCCCCCCCCCC
      DOUBLE PRECISION GF,A
      DIMENSION NS(3),ESM(3,3),B(3),C(3),NPIV(173),NNCOL(173),
     *PHI(3),ISIDE(2),STR(173),X(3),Y(3),XL(3),NOZ(18)
      COMMON WFC(200)
      COMMON/KKK/AUP(173,28),ALO(173,28)
      COMMON/HHH/GF(173),A(173,48),ICOL(173,48),IBANDW(173),KNUMR
      COMMON/EEE/TXZ,TYZ,ED,PCP,EM,DISTD,WO,DIMN
      COMMON/TLE/TITLE(20)
      COMMON/CCC/XM(284),YM(284),DIRXON(284,6),UG(284,6),VG(284,6)
      COMMON/AAA/XAR(175),YAR(175),NUMR
      COMMON/BBB/XARB(62),YARB(62)
      CALL PLOTS(53,0,-9)
      CALL NEWPEN(1)
      CALL FACTOR(1.23)
C
      IPLOTV=1
      NCL=1
      IO1=0
      IO=2
      KNUMR=0
      NUMR=KNUMR
      READ(5,301) (NOZ(I),I=1,18)
  301 FORMAT(18I3)
```

```
C     INPUT OF THE TITLE AND THE CONTROL PARAMETERS
C     ---------------------------------------------
      READ(5,100)TITLE
      READ(5,200)NP,NE,NBW,D,DISTD,DL
      DIMN=D
      WRITE(6,300)TITLE,D,DL
      DISTL=DL*160934
      FCP=0.0001
      TXZ=-0.80
      TYZ=0.00
      SLIP=0.3
      WO=0.00
C     WO=(FCP*DISTD)/SLIP
C
C
      ETA=1.00
      EX=100000./(FCP*DISTL**2)
      EY=100000./(FCP*DISTL**2)
C     VS IS THE SETLLING VELOCITY OF SUSPENDED SOLIDS IN FT/SEC
      VS=-2.2/(10**4)
      RK=VS/(FCP*DISTD)
C     CO=  IN ' MG/L '
      Q=00.0/(FCP)
      COV=0.0/FCP
      URF=(980.*DISTD)/(FCP*DISTL)
      Z11=-9.0
      Z22=2.50
C
C
C     INTIALIZATION OF GLOBAL STIFFNESS AND GLOBAL FORCE MATRICES
C     -----------------------------------------------------------
    1 DO 10 I=1,NP
      GF(I)=0.0
      DO 5 KE=1,48
    5 A(I,KE)=0.0
      DO 10 J=1,NBW
      AUP(I,J)=0.0
   10 ALO(I,J)=0.0
      DO 15 I=1,200
   15 WFC(I)=0.0
```

```
C      ASSEMBLYING OF THE GLOBAL STIFFNESS MATRIX AND FORCE MATRIX
C      ************************************************************
C
C      INPUT OF ELEMENT DATA
C      ---------------------
       DO 60 KK=1,NE
       READ(5,110) NEL,NS,X1,Y1,X2,Y2,X3,Y3,H11,H22,H33,ISIDE,ICASE
       IF(NS(1).GT.144)  Y1=Y1+1.0
       IF(NS(2).GT.144)  Y2=Y2+1.0
       IF(NS(3).GT.144)  Y3=Y3+1.0
C
       H11=H11-1.0
       H22=H22-1.0
       H33=H33-1.0
C
       WRITE(6,500) NEL,NS,X1,Y1,X2,Y2,X3,Y3,H11,H22,H33
       XAR(NS(1))=X1
       XAR(NS(2))=X2
       XAR(NS(3))=X3
       YAR(NS(1))=Y1
       YAR(NS(2))=Y2
       YAR(NS(3))=Y3
       XM(NEL)=(X1+X2+X3)/3.0
       YM(NEL)=(Y1+Y2+Y3)/3.0
C
       X1=(X1)/DL
       X2=(X2)/DL
       X3=(X3)/DL
       Y1=(Y1)/DL
       Y2=(Y2)/DL
       Y3=(Y3)/DL
       X(1)=X1
       X(2)=X2
       X(3)=X3
       Y(1)=Y1
       Y(2)=Y2
       Y(3)=Y3
       H11=H11/D
       H22=H22/D
       H33=H33/D
       H=(H11+H22+H33)/3.0
       ED=10.0
       EM=SQRT((FCP*DISTD**2)/(2.0*ED))
```

```
C     ESTIMATION OF THE COEFFICIENTS A(X,Y),B(X,Y)&C(X,Y)
C     ------------------------------------------------
      EMH=EM*H
      B(1)=Y2-Y3
      B(2)=Y3-Y1
      B(3)=Y1-Y2
      C(1)=X3-X2
      C(2)=X1-X3
      C(3)=X2-X1
      AR4=(X2*Y3+X3*Y1+X1*Y2-X2*Y1-X3*Y2-X1*Y3)*2.
      AR2=(X2*Y3+X3*Y1+X1*Y2-X2*Y1-X3*Y2-X1*Y3)
      DHX=(B(1)*H11+B(2)*H22+B(3)*H33)*2.0/AR4
      DHY=(C(1)*H11+C(2)*H22+C(3)*H33)*2.0/AR4
C
      IF(KNUMR.EQ.1) GO TO 65
C
      CALL CONSTA(H,DHX,DHY,AXY,BXY,CXY )
      CALL UPWIND(X,Y,-AXY,-BXY,NEL,ICASE,1.0,AR2,B,C,XL)
C
C     ELEMENT STIFFNESS AND ELEMENT FORCE MATRICES
C     ------------------------------------------
      DO 17 KI=1,3
      ICC=NS(KI)
   17 WPC(ICC)=WPC(ICC)+CXY*AR4/12.0
      DO 20 I=1,3
      DO 20 J=1,3
   20 ESM(I,J)=-(1./AR4)*(B(I)*B(J)+C(I)*C(J))+(XL(I)/2.0)*(AXY*B(J)
     *+BXY*C(J))
C
C
   65 IF(KNUMR.EQ.0) GO TO 16
C
      DO 70 I=1,3
      II=NS(I)
   70 PHI(I)=STR(II)
   72 GRADX=0.0
      GRADY=0.0
      DO 75 I=1,3
      GRADX=GRADX+B(I)*PHI(I)/AR2
   75 GRADY=GRADY+C(I)*PHI(I)/AR2
      UM=-GRADY/H
      VM=GRADX/H
      CALL VELOCI(H,DHX,DHY,UM,VM,NEL,URF)
      UMD=UM*URF
      VMD=VM*URF
```

```
      U=(980.0*DISTD*UM)/(FCP**2*DISTL**2)
      V=(980.0*DISTD*VM)/(FCP**2*DISTL**2)
      DO 117 KI=1,3
      ICC=NS(KI)
  117 WPC(ICC)=WPC(ICC)+Q*AR4/12.0
      EEX=ETA*EX*DHX/H
      EEY=ETA*EY*DHY/H
      UT=U+EEX
      VT=V+EEY
      VSET=RK/H
      CALL UPWIND(X,Y,UT,VT,NEL,ICASE,EX,AR2,B,C,XL)
C
C
      DO 120 I=1,3
      DO 120 J=1,3
      IJI=1
      IF(I.EQ.J) IJI=2
  120 ESM(I,J)=(UT*B(J)+VT*C(J))*XL(I)/2.0+(EX*B(I)*B(J)
     *+EY*C(I)*C(J))/AR4-(VSET*IJI*AR4/48.0)
C
C     CALCULATION OF THE CONVECTION RELATED QUANTITIES
C     ------------------------------------------------
      DO 111 I=1,2
      IF(ISIDE(I).LE.0) GO TO 16
      J=ISIDE(I)
      K=J+1
      IF(J.EQ.3) K=1
      XKJ=(X(K)-X(J))**2
      YKJ=(Y(K)-Y(J))**2
      GL=SQRT(XKJ-YKJ)
      CL=COV*GL
      ESM(J,J)=ESM(J,J)+CL/3.
      ESM(J,K)=ESM(J,K)+CL/6.
      ESM(K,J)=ESM(K,J)+CL/6.
      ESM(K,K)=ESM(K,K)+CL/3.
  111 CONTINUE
   16 CONTINUE
```

```
C     INSERT E.S.M.INTO THE GLOBAL MATRIX
C     ----------------------------------
      DO 50 I=1,3
      II=NS(I)
      DO 40 J=1,3
      JJ=NS(J)
      JJ=JJ-II+1
      IF(JJ)40,40,30
   30 AUP(II,JJ)=AUP(II,JJ)+ESM(I,J)
   40 CONTINUE
   50 CONTINUE
      DO 51 J=1,3
      JJ=NS(J)
      DO 41 I=1,3
      II=NS(I)
      II=II-JJ+1
      IF(II)41,41,31
   31 ALO(JJ,II)=ALO(JJ,II)+ESM(I,J)
   41 CONTINUE
   51 CONTINUE
   60 CONTINUE
C
C     MODIFICATION AND SOLUTION OF THE SYSTEM OF EQUATIONS
C     ----------------------------------------------------
      CALL BDYVAL(NP,NBW,NCL)
      CALL DCMPBO(NP,NBW)
      CALL EQSOLV(173,48,NPIV,NNCOL)
C
C
      IF(KNUMR.GT.0)  GO TO 81
      DO 80 K=1,NP
   80 STR(K)=GF(K)
   81 KNUMR=KNUMR+1
      NUMR=KNUMR
      IF(KNUMR.LE.1)  GO TO 1
      IF(IPLOTV.EQ.0)  GO TO 777
C
C...PLOT OF VELOCITY DISTRIBUTION IN THE Z-DIRECTION
C---------------------------------------------------
C
      DO 777 I=1,6
      Z11=Z11+10.0
      CALL SHORE(Z11,Z22)
      BEL=1.0/XARB(62)
      DO 777 J=1,NE
      XMF=XM(J)*BEL
      YMF=YM(J)*BEL
      UAR=XMF+UG(J,I)*BEL/16.0
      VAR=YMF+VG(J,I)*BEL/16.0
      IF(UG(J,I).EQ.0.000.AND.VG(J,I).EQ.0.000)GO TO 777
      CALL SHADE(6,1.0)
```

```
      CALL PLOT(XMF,YMF,3)
      CALL SHADE(6,1.0)
      CALL SYMBOL(UAR,VAR,0.05,6,DIRXON(J,I),-2)
  777 CONTINUE
C
C...PLOT OF THE AVERAGE CONCENTRATIONS AT THE NODAL POINTS
C---------------------------------------------------------
C
      DO 91 I=1,2
      Z11=Z11+10.0
      CALL SHORE(Z11,Z22)
      DELTA=1.0/XARB(62)
      DO 91 K=1,NP
      GFPRC=GF(K)
      G=STR(K)*100.0
      IF(I.EQ.2) GFPRC=G
      XA=XAR(K)*DELTA
      YA=YAR(K)*DELTA
      NIP=0
C     THIS DO LOOP WAS SPECIFIED FOR GOOD LOOKING PLOTS ONLY
C     ---------------------------------------------------
      DO 90 LN=1,18
      MOZ=NOZ(LN)
   90 IF(MOZ.EQ.K) NIP=1
      IF(NIP.EQ.1) GO TO 91
      CALL SHADE(6,1.0)
      CALL NUMBER(XA,YA,0.07,GFPRC,0.0,1)
   91 CONTINUE
C
      CALL PLOT(50.0,0.0,999)
      END FILE 9
C
  100 FORMAT(20A4)
  110 FORMAT(I3,3I3,9F5.2,3I1)
  200 FORMAT(3I3,1X,3F10.3)
  300 FORMAT(1H1////1X,20A4//1X,6HDEPTH=,F9.1,'FEETS'/1X,7HLENGTH=,
     *F9.2,'MILES'//1X,111HNEL     NODE NUMBER       X(1)        Y(1)
     1X(2)        Y(2)        X(3)        Y(3)        H(1)        H(2)        H(3)
     2    ,/)
C 400 FORMAT(4I3,6F10.4)
  500 FORMAT(1X,I3,2X,3I4,1X,9(2X,F8.1))
  600 FORMAT(1H1////1X,20A4//1X,27HELEMENT VELOCITY COMPONENTS//1X,
     197HELEMENT                         VEL(X)
     *                              VEL(Y),/)
  700 FORMAT(1X,I3,2X,2E12.3)
  800 FORMAT(11X,'0.0',9X,'0.2',9X,'0.4',9X,'0.6',9X,'0.8',10X,'0.0',
     *9X,'0.2',9X,'0.4',9X,'0.6',9X,'0.8')
      STOP
      END
```

```
C.....................................................................
C
C     SUBROUTINE CONST TO CALCULAT A(X,Y)&B(X,Y)&C(X,Y)  FOR EACH ELE.
C     ----------------------------------------------------------------  .
C     D=DISTD=VERTICAL REFRENCE DIMENSION               = 25.0   FT      .
C     L=DISTL=HORIZONTAL REFRENCE DIMENSION             = 29.2   MILE    .
C     FCP= CORIOLIS PARAMETER                           = 0.0005 RAD/SEC.
C     ED=AN EDDY VISCOSITY                              = 10.0 CM**2/SEC.
C     TXZ,TYZ =SURFACE WIND STRESS IN X,Y DIRECTIONS                     .
C     GR=ACCELARATION OF GRAVITY                        = 980 CM/SEC**2 .
C     EM=EKMAN NUMBER                                                    .
C.....................................................................
      SUBROUTINE CONST(H,DHX,DHY,AXY,BXY,CXY)
      COMMON/EEE/TXZ,TYZ,ED,FCP,EM,DISTD,WO,DIMN
      DISTL=29.2*160934
      GR=980.0
      BIGD=(FCP*DISTL*TXZ)/(ED*GR)
      BIGG=(FCP*DISTL*TYZ)/(ED*GR)
      HM=EM*H
      CMH=(EXP(-HM)+EXP(HM))**2
      SMH=(EXP(-HM)-EXP(HM))**2
      ALFA=CMH*(COS(HM))**2+SMH*(SIN(HM))**2
      BETA=(1/(2*EM))*(EXP(-HM)*(SIN(HM)-COS(HM)))
      GAMA=SIN(HM)*(EXP(-HM)-EXP(HM))
      DELTA=(EXP(-HM)/(2.0*EM))*(SIN(HM)+COS(HM))
      EPSI=COS(HM)*(EXP(-HM)+EXP(HM))
      CAPA=(EXP(HM)/(2.0*EM))*(SIN(HM)+COS(HM))
      DNLA=(EXP(HM)/(2.0*EM))*(SIN(HM)-COS(HM))
C-------------------------------------------------
      H1=(GAMA*(BETA+CAPA)+EPSI*(DELTA+DNLA))/(ALFA*H)
      H2=(ALFA*(BETA-DELTA)/(2.0*EM)-(BETA*GAMA+DELTA*EPSI)*(BETA+CAPA)
     *-(BETA*EPSI-DELTA*GAMA)*(DELTA+DNLA))/(ALFA*H)+1.0/(2.*H*EM**2)
      H3=(ALFA*(BETA+DELTA)/(2.0*EM)+(BETA*EPSI-DELTA*GAMA)*(BETA+
     *CAPA)-(BETA*GAMA+DELTA*EPSI)*(DELTA+DNLA))/(ALFA*H)
      H4=((-ALFA*H)+EPSI*(BETA+CAPA)-GAMA*(DELTA+DNLA))/(ALFA*H)
C
C
      DAH=(-4.0*EM**2)*ALFA*H1*H
      DBH=EM*(DELTA-BETA)
      DGH=(-2.0*EM**2)*(BETA+CAPA)
      DDH=-EM*(BETA+DELTA)
      DIH=(-2.0*EM**2)*(DELTA+DNLA)
      DKH=EM*(CAPA-DNLA)
      DLH=EM*(CAPA+DNLA)
```

```
      DH1H=(DGH*(BETA+CAPA)+GAMA*(DBH+DKH)+EPSI*(DDH+DLH)+DIH*(DELTA
     1+DNLA)-(ALFA+H*DAH)*H1)/(ALFA*H)
      DH2H=((DAH*(1./EM+BETA-DELTA)+ALFA*(DBH-DDH))/(2.0*EM)-(BETA*GAMA
     1+DELTA*EPSI)*(DBH+DKH)-(BETA+CAPA)*(DGH*BETA+GAMA*DBH+DELTA*DIH
     2+EPSI*DDH)-(BETA*EPSI-DELTA*GAMA)*(DDH+DLH)-(DELTA+DNLA)*(DIH
     3*BETA+EPSI*DBH-DELTA*DGH-GAMA*DDH)-H2*(ALFA+H*DAH))/(ALFA*H)
      DH3H=((DAH*(BETA+DELTA)+ALFA*(DBH+DDH))/(2.0*EM)+((BETA*EPSI
     1-DELTA*GAMA)*(DBH+DKH)+(BETA+CAPA)*(DIH*BETA+EPSI*DBH-DELTA*
     2DGH-GAMA*DDH))-((BETA*GAMA+DELTA*EPSI)*(DDH+DLH)+(DELTA+DNLA)
     3*(BETA*DGH+GAMA*DBH+DELTA*DIH+EPSI*DDH))-H3*(ALFA+H*DAH))/(ALFA*H)
C
      DH4H=(-(ALFA+DAH*H)+(EPSI*(DBH+DKH)+DIH*(BETA+CAPA))-(GAMA*(DDH
     1+DLH)+DGH*(DELTA+DNLA))-H4*(ALFA+DAH*H))/(ALFA*H)
C
C-----------------------------------------------------------------
      R1=(H1/H)/(H1**2+H4**2)
      S1=(H4/H)/(H1**2+H4**2)
      Q1=(H1*H3+H2*H4)/(H1**2+H4**2)
      T1=(H3*H4-H1*H2)/(H1**2+H4**2)
C-----------------------------------
      DH14H=-(2.0*H1*DH1H+2.0*H4*DH4H)/(H1**2+H4**2)**2
C
      DR1H=H1*DH14H/H+(H*DH1H-H1)/((H1**2+H4**2)*H**2)
C
      DS1H=H4*DH14H/H+(H*DH4H-H4)/((H1**2+H4**2)*H**2)
C
      DQ1H=(H1*H3+H2*H4)*DH14H+(H1*DH3H+H3*DH1H+H2*DH4H+H4*DH2H)/(H1*
     1*2+H4**2)
C
      DT1H=(H3*H4-H1*H2)*DH14H+(H3*DH4H+H4*DH3H-H1*DH2H-H2*DH1H)/
     1(H1**2+H4**2)
C
C--------------------------------------------------------------------
      DRX=DR1H*DHX
      DRY=DR1H*DHY
      DSX=DS1H*DHX
      DSY=DS1H*DHY
      DQX=DQ1H*DHX
      DQY=DQ1H*DHY
      DTX=DT1H*DHX
      DTY=DT1H*DHY
C--------------------------------------------------------------------
      H14=(H/H1)*(H1**2+H4**2)
      AXY=H14*(DRX+DSY)
      BXY=H14*(DRY-DSX)
      CXY=H14*(DQX*BIGG-DQY*BIGD+DTY*BIGG+BIGD*DTX)
C     WRITE(6,100)H,H1,H2,H3,H4,AXY,BXY,CXY
C 100 FORMAT(5X,8E12.4,/)
C
C
      RETURN
```

```
      END

      SUBROUTINE CONSTA(H,DHX,DHY,AXY,BXY,CXY)
      COMMON/EEE/TXZ,TYZ,ED,FCP,EM,DISTD,WO,DIMN
      DISTL=29.2*160934
      GR=980.0
      BIGD=(FCP*DISTL*TXZ)/(ED*GR)
      BIGG=(FCP*DISTL*TYZ)/(ED*GR)
      HM=EM*H
      GAMA=(-2.0*SIN(HM))*SINH(HM)
      EPSI=(2.0*COS(HM))*COSH(HM)
      C1=(SIN(HM))*COSH(HM)
      C2=(COS(HM))*SINH(HM)
      SA=(EM*(EPSI+GAMA)/2.0)-WO*C1
      SB=(EM*(EPSI-GAMA)/2.0)+WO*C2

C-----------------------------------------
      V=(SA**2)+(SB**2)
      AR=-(SA-SB)/(V*2.0*EM)
      AI=((EM*(SA+SB)/V)-1.0)/(2.0*EM**2)
      BR=(SA*C1-SB*C2)/V
      BI=-((SA*C2+SB*C1)/V)+H
      Z2=(BR**2)+(BI**2)
      R1=BR/Z2
      S1=-BI/Z2
      Q1=(AR*BR+AI*BI)/Z2
      T1=(AI*BR-AR*BI)/Z2


C--------------------------------------------------------------
      DGH=-2.0*EM*(C1+C2)
      DEH=-2.0*EM*(C1-C2)
      DC1H=EM*(EPSI-GAMA)/2.0
      DC2H=EM*(EPSI+GAMA)/2.0
      DSAH=(EM*(DEH+DGH)/2.0)-WO*DC1H
      DSBH=(EM*(DEH-DGH)/2.0)+WO*DC2H


C--------------------------------------------------------------
      DVH=2.0*(SA*DSAH+SB*DSBH)
      DARH=((DVH*(SA-SB)/V)-DSAH+DSBH)/(2.0*EM*V)
      DAIH=((DSAH+DSBH-DVH*(SA+SB)/V)/(2.0*EM*V))
      DBRH=(SA*DC1H+C1*DSAH-SB*DC2H-C2*DSBH)/V-DVH*(SA*C1-SB*C2)/(V**2)
      DBIH=-(SA*DC2H+C2*DSAH+SB*DC1H+C1*DSBH)/V+DVH*(SA*C2+
     *SB*C1)/(V**2)+1.0
C-------------------------------------------------------------------
```

```
      DZH=2.0*(BR*DBRH+BI*DBIH)
      DR1H=DBRH/Z2-DZH*BR/(Z2**2)
      DS1H=-DBIH/Z2+DZH*BI/(Z2**2)
      DQ1H=(AR*DBRH+BR*DARH+AI*DBIH+BI*DAIH)/Z2-DZH*(AR*BR+AI*BI)/Z2**2
      DT1H=(AI*DBRH+BR*DAIH-AR*DBIH-BI*DARH)/Z2-DZH*(AI*BR-AR*BI)/Z2**2
C-----------------------------------------------------------------------
      DRX=DR1H*DHX
      DRY=DR1H*DHY
      DSX=DS1H*DHX
      DSY=DS1H*DHY
      DQX=DQ1H*DHX
      DQY=DQ1H*DHY
      DTX=DT1H*DHX
      DTY=DT1H*DHY
C-----------------------------------------------------------------------
      AXY=(DRX+DSY)/R1
      BXY=(DRY-DSX)/R1
      CXY=((DQX+DTY)*BIGG+(DTX-DQY)*BIGD)/R1
C     WRITE(6,100)H,H1,H2,H3,H4,AXY,BXY,CXY
C 100 FORMAT(5X,8E12.4,/)
      RETURN
      END
      SUBROUTINE VELZ(H,DHX,DHY,UM,VM,NEL,URF)
C.......................................................................
C
      COMMON/EEE/TXZ,TYZ,ED,FCP,EM,DISTD,WO,DIMN
      COMMON/CCC/XM(284),YM(284),DIRXON(284,6),UG(284,6),VG(284,6)
      DIMENSION UZ(5),VZ(5),UV(5)
      DISTL=29.2*160934
      GR=980.0
      BIGD=(FCP*DISTL*TXZ)/(ED*GR)
      BIGG=(FCP*DISTL*TYZ)/(ED*GR)
      HM=EM*H
      CMH=(EXP(-HM)+EXP(HM))**2
      SMH=(EXP(-HM)-EXP(HM))**2
      ALFA=CMH*(COS(HM))**2+SMH*(SIN(HM))**2
      BETA=(1/(2*EM))*(EXP(-HM)*(SIN(HM)-COS(HM)))
      GAMA=SIN(HM)*(EXP(-HM)-EXP(HM))
      DELTA=(EXP(-HM)/(2.0*EM))*(SIN(HM)+COS(HM))
      EPSI=COS(HM)*(EXP(-HM)+EXP(HM))
      CAPA=(EXP(HM)/(2.0*EM))*(SIN(HM)+COS(HM))
      DNLA=(EXP(HM)/(2.0*EM))*(SIN(HM)-COS(HM))
C-----------------------------------------
      H1=(GAMA*(BETA+CAPA)+EPSI*(DELTA+DNLA))/(ALFA*H)
      H2=(ALFA*(BETA-DELTA)/(2.0*EM)-(BETA*GAMA+DELTA*EPSI)*(BETA+CAPA)
     *-(BETA*EPSI-DELTA*GAMA)*(DELTA+DNLA))/(ALFA*H)+1.0/(2.*H*EM**2)
      H3=(ALFA*(BETA+DELTA)/(2.0*EM)+(BETA*EPSI-DELTA*GAMA)*(BETA+
     *CAPA)-(BETA*GAMA+DELTA*EPSI)*(DELTA+DNLA))/(ALFA*H)
      H4=((-ALFA*H)+EPSI*(BETA+CAPA)-GAMA*(DELTA+DNLA))/(ALFA*H)
```

```
      UMD=UM*URF
      VMD=VM*URF
      UVMD=SQRT(UMD**2+VMD**2)
      CALL ANGEL(UM,VM,ANG)
      DIRXON(NEL,6)=ANG
      UG(NEL,6)=UMD
      VG(NEL,6)=VMD
C-----------------------------------------------------------
      DPX=(UM*H1-VM*H4-BIGG*(H1*H2-H3*H4)-BIGD*(H1*H3+H2*H4))/
     *(H1**2+H4**2)
C
      DPY=(UM*H4+VM*H1-BIGG*(H1*H3+H2*H4)+BIGD*(H1*H2-H3*H4))/
     *(H1**2+H4**2)
C-----------------------------------------------------------------------------
      C3=(-EPSI*DPX+GAMA*DPY+BIGG*(BETA*EPSI-DELTA*GAMA)+
     *BIGD*(BETA*GAMA+DELTA*EPSI))/ALFA
C
      C4=(-GAMA*DPX-EPSI*DPY+BIGG*(BETA*GAMA+DELTA*EPSI)-
     *BIGD*(BETA*EPSI-DELTA*GAMA))/ALFA
C
      C1=C3+(BIGG-BIGD)/(2.0*EM)
      C2=-C4+(BIGG+BIGD)/(2.0*EM)
C-----------------------------------------------------------------------------
      WRITE(6,100) NEL,UMD,VMD,UVMD
  100 FORMAT(5X,I5,3E12.2,/)
C-----------------------------------------------------------------------------
      DO 10 I=1,5
      Z=0.2
      Z=(Z-0.2*I)*H
      ZM=Z*EM
      ENZ=EXP(-ZM)
      EPZ=EXP(ZM)
      UZ(I)=(-DPY+COS(ZM)*(C2*EPZ-C4*ENZ)-SIN(ZM)*(C1*EPZ-C3*ENZ))*
     *URF
      VZ(I)=(DPX+COS(ZM)*(C1*EPZ+C3*ENZ)+SIN(ZM)*(C2*EPZ+C4*ENZ))*
     *URF
      UV(I)=SQRT(UZ(I)**2+VZ(I)**2)
      CALL ANGEL(UZ(I),VZ(I),ANG)
      DIRXON(NEL,I)=ANG
      UG(NEL,I)=UZ(I)
      VG(NEL,I)=VZ(I)
C
   10 WRITE(6,200) Z,UZ(I),VZ(I),UV(I)
  200 FORMAT(5X,4E12.2)
      RETURN
      END
```

```
      SUBROUTINE VELOCI(H,DHX,DHY,UM,VM,NEL,URF)
C------------------------------------------------------------------
C
      COMMON/EEE/TXZ,TYZ,ED,FCP,EM,DISTD,WO,DIMN
      COMMON/CCC/XM(284),YM(284),DIRXON(284,6),UG(284,6),VG(284,6)
      DIMENSION UZ(5),VZ(5),UV(5)
      DISTL=29.2*160934
      GR=980.0
      BIGD=(FCP*DISTL*TXZ)/(ED*GR)
      BIGG=(FCP*DISTL*TYZ)/(ED*GR)
      HM=EM*H
      GAMA=(-2.0*SIN(HM))*SINH(HM)
      EPSI=(2.0*COS(HM))*COSH(HM)
      C1=(SIN(HM))*COSH(HM)
      C2=(COS(HM))*SINH(HM)
      SA=(EM*(EPSI+GAMA)/2.0)-WO*C1
      SB=(EM*(EPSI-GAMA)/2.0)+WO*C2
C-------------------------------------------
      V=(SA**2)+(SB**2)
      AR=-(SA-SB)/(V*2.0*EM)
      AI=((EM*(SA+SB)/V)-1.0)/(2.0*EM**2)
      BR=(SA*C1-SB*C2)/V
      BI=-((SA*C2+SB*C1)/V)+H
C------------------------------------------------------------
      Z2=(BR**2)+(BI**2)
      R1=BR/Z2
      S1=-BI/Z2
      Q1=(AR*BR+AI*BI)/Z2
      T1=(AI*BR-AR*BI)/Z2
      UMD=UM*URF
      VMD=VM*URF
      UVMD=SQRT(UMD**2+VMD**2)
      CALL ANGEL(UM,VM,ANG)
      DIRXON(NEL,6)=ANG
      UG(NEL,6)=UMD
      VG(NEL,6)=VMD
C-----------------------------------------------
      C12=C1**2+C2**2
      D=C12*V
      E=V*(EPSI*C2-GAMA*C1)-2.0*EM*(C2*(SA+SB)+C1*(SA-SB))
      F=V*(GAMA*C2+EPSI*C1)+2.0*EM*(C2*(SA-SB)-C1*(SA+SB))
C-----------------------------------------------------------
      DPX=-VM*H*S1+UM*H*R1-Q1*BIGD+T1*BIGG
      DPY=VM*H*R1+UM*H*S1-T1*BIGD-Q1*BIGG
C-----------------------------------------------------------
      WRITE(6,100) NEL,UMD,VMD,UVMD
  100 FORMAT(5X,I5,3E12.2,/)
C-----------------------------------------------------------------
```

```
      DO 10 I=1,5
      Z=0.2
      Z=(Z-0.2*I)*H
      ZM=Z*EM
      C1Z=SIN(ZM)*COSH(ZM)
      C2Z=COS(ZM)*SINH(ZM)
      GZ=SIN(ZM)*SINH(ZM)
      EZ=COS(ZM)*COSH(ZM)
C-------------------------------------------------------------
      RR=(1./(2.*EM))*(C2Z+C1Z+(E*(EZ+GZ)-F*(EZ-GZ))/(2.*D))
      RI=(-1./(2.*EM))*(C2Z-C1Z+(E*(EZ-GZ)+F*(EZ+GZ))/(2.*D))
      TR=EM*(EZ*(SA-SB)+GZ*(SA+SB))/V
      TI=(-EM*(EZ*(SA+SB)-GZ*(SA-SB))/V)+1.0
      UZ(I)=(RR*BIGD-RI*BIGG+TR*DPX-TI*DPY)*URF
      VZ(I)=(RR*BIGG+RI*BIGD+TR*DPY+TI*DPX)*URF
C-------------------------------------------------------------
      CALL ANGEL(UZ(I),VZ(I),ANG)
      DIRXON(NEL,I)=ANG
      UG(NEL,I)=UZ(I)
      VG(NEL,I)=VZ(I)
      UV(I)=SQRT(UZ(I)**2+VZ(I)**2)
      Z=Z*DIMN
C
   10 WRITE(6,200) Z,UZ(I),VZ(I),UV(I)
  200 FORMAT(5X,4E12.2)
      RETURN
      END
C.............................................................
C     SUBROUTINE BDYVAL
C     READS THE SPECIFIED VALUES OF {F} AND {U} AND MODIFIES [K].
C.............................................................
C.............................................................
      SUBROUTINE BDYVAL(NP,NBW,NCL)
      DOUBLE PRECISION GF,A
      COMMON/KKK/AUP(173,28),ALO(173,28)
      COMMON/HHH/GF(173),A(173,48),ICOL(173,48),IBANDW(173),KNUMR
      COMMON/AAA/XAR(175),YAR(175),NUMR
      COMMON/BBB/XARB(62),YARB(62)
C
      DIMENSION IB(6),BV(6)
      COMMON /TLE/TITLE(20)
      COMMON WFC(200)
C     WRITE(6,100) TITLE
```

```
C       INPUT OF THE NODAL FORCE VALUES
C       ----------------------------
C       WRITE(6,200)
        DO 30 JM=1,NCL
        ID1=0
        INK=0
        KAM=0
     5  DO 7 I=1,6
        IB(I)=I+KAM
     7  BV(I)=WFC(I+KAM)
        KAM=KAM+6
        ID=0
        DO 10 L=1,6
        IF(IB(L).GE.NP) GO TO 15
        ID=ID+1
        I=IB(L)
    10  GF(I)=BV(L)+GF(I)
        GO TO 20
    15  INK=1
        IF(ID.EQ.0)GO TO 30
    20  IF(ID1.EQ.1)GO TO 25
C       WRITE(6,400)JM
C   25  WRITE(6,500)(IB(L),BV(L),L=1,6 )
    25  IF(INK.EQ.1)GO TO 30
        ID1=1
        GO TO 5
    30  CONTINUE
C       INPUT OF THE PRESCRIBED NODAL VALUES
C       -----------------------------------
C       WRITE(6,600)
        INK=0
        IZ=0
    35  READ(5,110)IB,BV
        ID=0
        DO 75 L=1,6
        IF(IB(L).LE.0)GO TO 80
        ID=ID+1
        I=IB(L)
        IF(NUMR.EQ.1)  GO TO 37
        IZ=IZ+1
        XARB(IZ)=XAR(I)
        YARB(IZ)=YAR(I)
    37  BC=BV(L)
        K=I-1
```

```
C     MODIFICATION OF THE GLOBAL STIFFNESS AND FORCE MATR.
C     ------------------------------------------------------
      DO 60 J=2,NBW
      M=I+J-1
      IF(M.GT.NP)GO TO 45
      DO 40 JM=1,NCL
   40 GF(M)=GF(M)-ALO(I,J)*BC
      AUP(I,J)=0.0
      ALO(I,J)=0.0
   45 IF(K.LE.0)GO TO 60
      DO 50 JM=1,NCL
   50 GF(K)=GF(K)-AUP(K,J)*BC
      AUP(K,J)=0.0
      ALO(K,J)=0.0
      K=K-1
   60 CONTINUE
C  65 IF(AUP(I,1).LT.0.05)AUP(I,1)=500000.
      DO 70 JM=1,NCL
   70 GF(I)=AUP(I,1)*BC
   75 CONTINUE
      GO TO 85
   80 INK=1
      IF(ID.EQ.0)RETURN
C  85 WRITE(6,500)(IB(L),BV(L),L=1,ID)
   85 IF(INK.EQ.1)RETURN
      GO TO 35
  100 FORMAT(1H1,///////,1X,20A4)
  110 FORMAT(6I4,6F6.2)
  200 FORMAT(/1X,15HBOUNDARY VALUES//1X,12HNODAL FORCES)
C 300 FORMAT(6I3,2X,6F10.2)
  400 FORMAT(1X,12HLOADING CASE,I2)
  500 FORMAT(3(5X,I3,E14.5))
  600 FORMAT(////,1X,'PRESCRIBED NODAL VALUES')
      END
```

```
C.................................................................
C      SUBROUTINE DCMPBC                                          .
C      SUBROUTINE SLVBD                                           .
C      TO DECOMPOSE THE BAND MATRIX [K] AND SOLVE THE LINEAR      .
C      EQUATIONS USING GAUSS ELEMINATION METHOD                   .
C.................................................................
      SUBROUTINE DCMPBO(NP,NBW)
      DOUBLE PRECISION GP,A,AAA
      DIMENSION AAA(173)
      COMMON/KKK/AUP(173,28),ALO(173,28)
      COMMON/HHH/GP(173),A(173,48),ICOL(173,48),IBANDW(173),KNUMB
      DO 70 I=1,NP
      DO 10 K=1,48
   10 ICOL(I,K)=0
      DO 20 JI=1,NP
   20 AAA(JI)=0.000
      DO 30 K=1,NBW
      M=I+K-1
      IF(M.GT.NP)GO TO 40
   30 AAA(M)=AUP(I,K)
   40 IF(I.EQ.1)GO TO 55
      DO 45 L=2,NBW
      N=I-L+1
      IF(I.LT.L)GO TO 55
   45 AAA(N)=ALO(N,L)
C-------------------------------
   55 JC=0
      KH=0
      DO 60 IG=1,NP
      KH=KH+1
      IF(AAA(IG).EQ.0.0000000000)GO TO 60
   50 JC=JC+1
      A(I,JC)=AAA(IG)
      ICOL(I,JC)=KH
   60 IBANDW(I)=JC
   70 CONTINUE
      DO 80 I=1,NP
   80 AAA(I)=0.00
      RETURN
      END
```

```
      SUBROUTINE EQSOLV(NPT,NNN,NPIV,NNCOL)
C-----------------------------------------------------------------------C
C                         SOLVES: [A]{X}={B}                             C
C WHERE:                                                                 C
C   A    =MATRIX CONTAINING NONZERO COEFFICIENTS OF THE SYSTEM           C
C  AA    =SINGLE DIMENSIONED ARRAY USED FOR PIVOTAL ROW ELEMENTS         C
C   B    =CONSTANT VECTOR OF EQUATIONS TO BE SOLVED                      C
C        =ALSO USED FOR RETURNING THE SOLUTION                           C
C IBANDW=NUMBER OF NONZERO COEFF. IN EACH ROW                            C
C NCOL   =MATRIX CONTANING INDICES OF NONZERO COEFF. OF [A]              C
C NNCOL  =SINGLE DIMENSIONED ARRAY FOR PIVOTAL ROW INDICES               C
C NNN    =COLUMN DIMENSION IN MAIN PROGRAM FOR [A] & NCOL                C
C NPIV   =SINGLE DIMENSIONED ARRAY TO STORE PIVOTAL COLUMN               C
C NPT    =MAX. NUMBER OF ROWS                                            C
C                                                                        C
C-----------------------------------------------------------------------C
      DOUBLE PRECISION A,AA,B,X,C,AAA,A1,SAVE,ZTEST,BBB
      DIMENSION NNCOL(NPT),NPIV(NPT),AA(173),BBB(173)
      COMMON/TLE/TITLE(20)
      COMMON/HHH/B(173),A(173,48),NCOL(173,48),IBANDW(173),KNUMR
C     INITIALIZE THE BANDWIDTH COUNTER
C     -----------------------------
      ZTEST=0.001
      IF(DABS(ZTEST).GT.0.0001)ZTEST=0.0
      NSTOP=0
      MAXWID=0
      DO 1 I=1,NPT
      IBANDW(I)=0
    1 CONTINUE
      DO 5 I=1,NPT
      DO 2 J=1,NNN
      NC=NCOL(I,J)
      IF(NC.EQ.0)GO TO 3
      IBANDW(I)=J
    2 CONTINUE
    3 IF(MAXWID.LT.J) MAXWID=J
      IF(J.NE.1)GO TO 5
      PRINT 4,I
    4 FORMAT(' ALL ELEMENTS IN ROW ',I5,' ARE =0.0 & PROGRAM IS
     * STOPED TO AVOID SINGULARITY ')
      NSTOP=1
    5 CONTINUE
      IF(NSTOP.EQ.1)STOP
      NPT1=NPT-1
      DO 23 LL=1,NPT1
```

```
C     FINDING THE ROW WITH MINIMUM BANDWIDTH
C     --------------------------------------
      KK=100000
      DO 6 I=LL,NPT
      IC=IBANDW(I)
      IF(IC.LE.0) GO TO 6
      IF(IC.GE.KK) GO TO 6
      MINROW=I
      KK=IC
    6 CONTINUE
C     INTER CHANGE ROWS  MINROW WITH LL
C     ---------------------------------
      LM=IBANDW(LL)
      M=MINROW
      DO 7 I=1,LM
      NNCOL(I)=NCOL(M,I)
      NCOL(M,I)=NCOL(LL,I)
      AA(I)=A(M,I)
      A(M,I)=A(LL,I)
    7 CONTINUE
      SAVE=B(LL)
      B(LL)=B(M)
      B(M)=SAVE
      IBANDW(LL)=IBANDW(M)
      IBANDW(M)=LM
C     FINDING BIG A IN MINROW
C     -----------------------
      NC=IBANDW(LL)
      NNCOL(NC+1)=0
      MINROW=LL
      A1=0.0
      I=MINROW
      DO 8 J=1,NC
      AAA=DABS(AA(J))
      IF(AAA.LT.A1) GO TO 8
      A1=AAA
      IY=J
    8 CONTINUE
      MAXCOL=NNCOL(IY)
      NPIV(LL)=MAXCOL
C     NORMALIZE THE MINROW
C     --------------------
      X=AA(IY)
      DO 9 J=1,NC
      AA(J)=AA(J)/X
      NCOL(MINROW,J)=NNCOL(J)
    9 A(MINROW,J)=AA(J)
      B(MINROW)=B(MINROW)/X
      A(MINROW,IY)=1.0
      AA(IY)=1.0
```

```
C     FINDING THE ROWS WHICH CONTAIN MAXCOL
C     ----------------------------------
      LL1=LL+1
      DO 22 I=LL1,NPT
      IF(IBANDW(I).EQ.0)GO TO 22
      NC=IBANDW(I)
      DO 21 J=1,NC
      IF(NCOL(I,J)-MAXCOL)21,10,22
C     IF NCOL(I,J)=MAXCOL *ROW CONTAINS THE VARIABLE NOPROW
C     ----------------------------------------------------
   10 NOPROW=I
      JKOP=1
      JKPI=1
      C=-A(NOPROW,J)
      B(NOPROW)=B(MINROW)*C+B(NOPROW)
   11 CONTINUE
      IF(NNCOL(JKPI).EQ.0)GO TO 22
      IF(NCOL(NOPROW,JKOP).EQ.0)GO TO 12
      IF(NNCOL(JKPI)-NCOL(NOPROW,JKOP))12,14,20
   12 IBANDW(I)=IBANDW(I)+1
      IF(MAXWID.LT.IBANDW(I))MAXWID=IBANDW(I)
      IF(MAXWID.GT.NNN)GO TO 31
      II=IBANDW(I)
      JKL=JKOP+1
   13 IX=II-1
      A(NOPROW,II)=A(NOPROW,IX)
      NCOL(NOPROW,II)=NCOL(NOPROW,IX)
      II=IX
      IF(IX.GE.JKL)GO TO 13
      A(NOPROW,JKOP)=AA(JKPI)*C
      NCOL(NOPROW,JKOP)=NNCOL(JKPI)
      IX=NCOL(NOPROW,JKOP)
      GO TO 19
C
C
   14 IX=NCOL(NOPROW,JKOP)
      IF(IX.EQ.MAXCOL)GO TO 15
      X=AA(JKPI)*C+A(NOPROW,JKOP)
      A(NOPROW,JKOP)=X
C
C     TESTING TO SEE IF ANY OTHER ELEMENTS WERE ELEMINATED OTHER    C
C     THAN MAXCOL IN THE NOPROW
C     ------------------------------------------------------------
      ATEST=DABS(X)-ZTEST
      IF(ATEST.GT.0.0)GO TO 19
   15 IBANDW(NOPROW)=IBANDW(NOPROW)-1
      IF(IBANDW(NOPROW))16,16,17
   16 PRINT 29,MINROW,MAXROW,NOPROW
      STOP
   17 IX=IBANDW(NOPROW)
      DO 18 NK=JKOP,IX
```

```
      A(I,NK)=A(I,NK+1)
   18 NCOL(I,NK)=NCOL(I,NK+1)
      IX=IX+1
      NCOL(I,IX)=0
      A(I,IX)=0.0
      JKPI=JKPI+1
      GO TO 11
   19 JKPI=JKPI+1
```

```
C     MINROW DOES NOT CONTAIN THIS ELEMENT-SHIFT NOPROW AND CONTINUE
C     -------------------------------------------------------------
   20 JKOP=JKOP+1
      GO TO 11
   21 CONTINUE
   22 CONTINUE
   23 CONTINUE
      NPIV(NPT)=NCOL(NPT,1)
      PRINT 35,MAXWID
C
C     BACK SUBSTITUTION
C     -----------------
      DO 24 I=1,NPT
   24 AA(I)=0.0
      DO 27 I=1,NPT
      II=NPT-I+1
      LM=IBANDW(II)
      NP=NPIV(II)
      IF(NP.EQ.0)GO TO 27
      DO 26 J=1,LM
      NN=NCOL(II,J)
      IF(NN.EQ.NP)GO TO 25
      B(II)=B(II)-AA(NN)*A(II,J)
      GO TO 26
   25 IJ=J
   26 CONTINUE
      AA(NP)=B(II)/A(II,IJ)
   27 CONTINUE
C     STORE THE SOLUTION IN {B} VECTOR
C     --------------------------------
      DO 28 I=1,NPT
      B(I)=AA(I)
      ZT=1.0
      IF(KNUMR.EQ.0)  ZT=187250.0
      BBB(I)=B(I)*ZT
   28 CONTINUE
      WRITE(6,111)TITLE
      WRITE(6,222) (I,BBB(I),I=1,NPT)
  111 FORMAT(1H1,////1X,20A4//1X,26HNODAL VALUES LODING CASE  )
  222 FORMAT(3(I3,E18.9,2X))
      GO TO 33
   29 FORMAT(//'MATRIX IS SINGULAR',/,'   MINROW =',I5,' MAXCOL',
     *I5,' ROW OPERATED',I5//)
   31 PRINT 32,I,LL
      STOP
   32 FORMAT('COLUMN DIMENSIONS OF NCOL AND A EXCEEDED IN ROW ',I5,
     *'WHILE THE NUMBER OF ROWS OPERATED WERE',I5)
   33 RETURN
   35 FORMAT('************ MAXWID=',I6,'**** THIS IS FOR INFORMAT
     *ION FOR SECOND DIMENSION OF NCOL AND A MATRIX')
      END
```

```
      SUBROUTINE UPWIND(X,Y,U,V,NEL,ICASE,EX,AR2,B,C,XL)
      DOUBLE PRECISION VT,SM,BM,S,A,YI,XI,XN,YN,H,XD,YD,HD,VV,UU
      DIMENSION B(3),C(3),XL(3),X(3),Y(3),S(3),A(3),XN(3),YN(3),
     *H(2),XX(2),YY(2)
      FRXN=1.00
      IF(ICASE.EQ.1) FRXN=0.95
      IF(ICASE.EQ.2) FRXN=0.75
      IF(ICASE.EQ.3) FRXN=0.00
C
      XM=0.0
      YM=0.0
      UU=U
      VV=V
      VT=DSQRT(UU**2+VV**2)
      DO 10 I=1,3
      XM=XM+X(I)/3.0
   10 YM=YM+Y(I)/3.0
      IF(U.EQ.0.0.AND.V.EQ.0.0)GO TO 90
      IF(U.EQ.0.0)GO TO 15
      SM=V/U
      BM=(YM-SM*XM)
   15 IAC=1
      XCN=20.0
      YCN=20.0
      XCM=0.0
      YCM=0.0
      DO 20 I=1,3
      IF(XCN.GE.X(I))  XCN=X(I)
      IF(XCM.LE.X(I))  XCM=X(I)
      IF(YCN.GE.Y(I))  YCN=Y(I)
   20 IF(YCM.LE.Y(I))  YCM=Y(I)
      DO 80 I=1,3
      K=I+1
      IF(I.EQ.3)K=1
      IF(X(K).EQ.X(I))  GO TO 30
      S(I)=(Y(K)-Y(I))/(X(K)-X(I))
      IF(S(I).EQ.SM)  GO TO 80
      A(I)=Y(I)-S(I)*X(I)
      IF(U.EQ.0.0)GO TO 45
      XN(I)=(A(I)-BM)/(SM-S(I))
```

```
      GO TO 40
   30 XN(I)=X(I)
      IF(U.EQ.0.0) GO TO 80
   40 YN(I)=SM*XN(I)+BM
      GO TO 48
   45 XN(I)=XM
      YN(I)=S(I)*XN(I)+A(I)
   48 IF(XN(I).GE.XCN.AND.XN(I).LE.XCM) GO TO 50
      GO TO 80
   50 IF(YN(I).GE.YCN.AND.YN(I).LE.YCM) GO TO 60
      GO TO 80
   60 IF(IAC.GT.2) GO TO 80
      H(IAC)=DSQRT((XM-XN(I))**2+(YM-YN(I))**2)
      XX(IAC)=XN(I)
      YY(IAC)=YN(I)
      IAC=IAC+1
   80 CONTINUE
      HT=H(1)+H(2)
      HX=H(1)
      XD=(H(1)*U)/(2.0*VT)+XM
      YD=(H(1)*V)/(2.0*VT)+YM
      HD=DSQRT((XD-XX(1))**2+(YD-YY(1))**2)
      IF(HD.GT.H(1)) HX=H(2)
      PE=(VT*HT)/(EX*2.0)
      IF(PE.LE.0.0)PE=0.005
      ALPA=((1.0/TANH(PE))-(1.0/PE))*FRXN
      IF(PE.LE.0.5)ALPA=0.0
      XI=(ALPA*HX/VT)*U+XM
      YI=(ALPA*HX/VT)*V+YM
      XL(1)=(B(1)*XI+C(1)*YI+(X(2)*Y(3)-X(3)*Y(2)))/AR2
      XL(2)=(B(2)*XI+C(2)*YI-(X(1)*Y(3)-X(3)*Y(1)))/AR2
      XL(3)=1.0-(XL(1)+XL(2))
C     WRITE(6,700) NEL,U,V,H(1),H(2),PE,ALPA,XL(1),XL(2),XM,YM
  700 FORMAT(2X,I3,10E12.3)
      GO TO 100
   90 XL(1)=0.33333
      XL(2)=0.33333
      XL(3)=0.33333
  100 RETURN
      END
```

```
      SUBROUTINE SHORE(Z11,Z22)
      DIMENSION IBUF(1000)
      COMMON/BBB/XARB(62),YARB(62)
      CALL ORIGIN(Z11,Z22,0)
      CALL SCALE(XARB,6.0,60,1)
      CALL SCALE(YARB,6.0,60,1)
C     CALL AXIS(0.0,0.0,19HXDISTANCES IN MILES,-19,6.0,0.0,YARB(61),
C    *YARB(62))
C     CALL AXIS(0.0,0.0,19HYDISTANCES IN MILES,19,6.0,90.0,YARB(61),
C    *YARB(62))
      XARB(61)=YARB(61)
      XARB(62)=YARB(62)
C     WRITE(6,2) Z11,Z22
    2 FORMAT(1H ,2F10.2)
C     DO 1 J=1,62
C     WRITE(6,2) XARB(J),YARB(J)
C   1 CONTINUE
C     CALL LINE(XARB,YARB,60,1,0,2)
      RETURN
      END
C
C*********************************************************************
      SUBROUTINE ANGEL(U,V,ANG)
      X=V/SQRT(U**2+V**2)
      RAD=ARSIN(X)
      IF(U)10,20,30
   10 IF(V)40,40,40
   20 IF(V)50,50,80
   30 IF(V)50,80,80
   40 RAD=3.1416-RAD
      GO TO 80
   50 RAD=2.0*3.1416+RAD
   80 ANG=(180.0*RAD)/3.1416
      ANG=ANG-90.0
      RETURN
      END
```

APPENDIX D

FIGURES

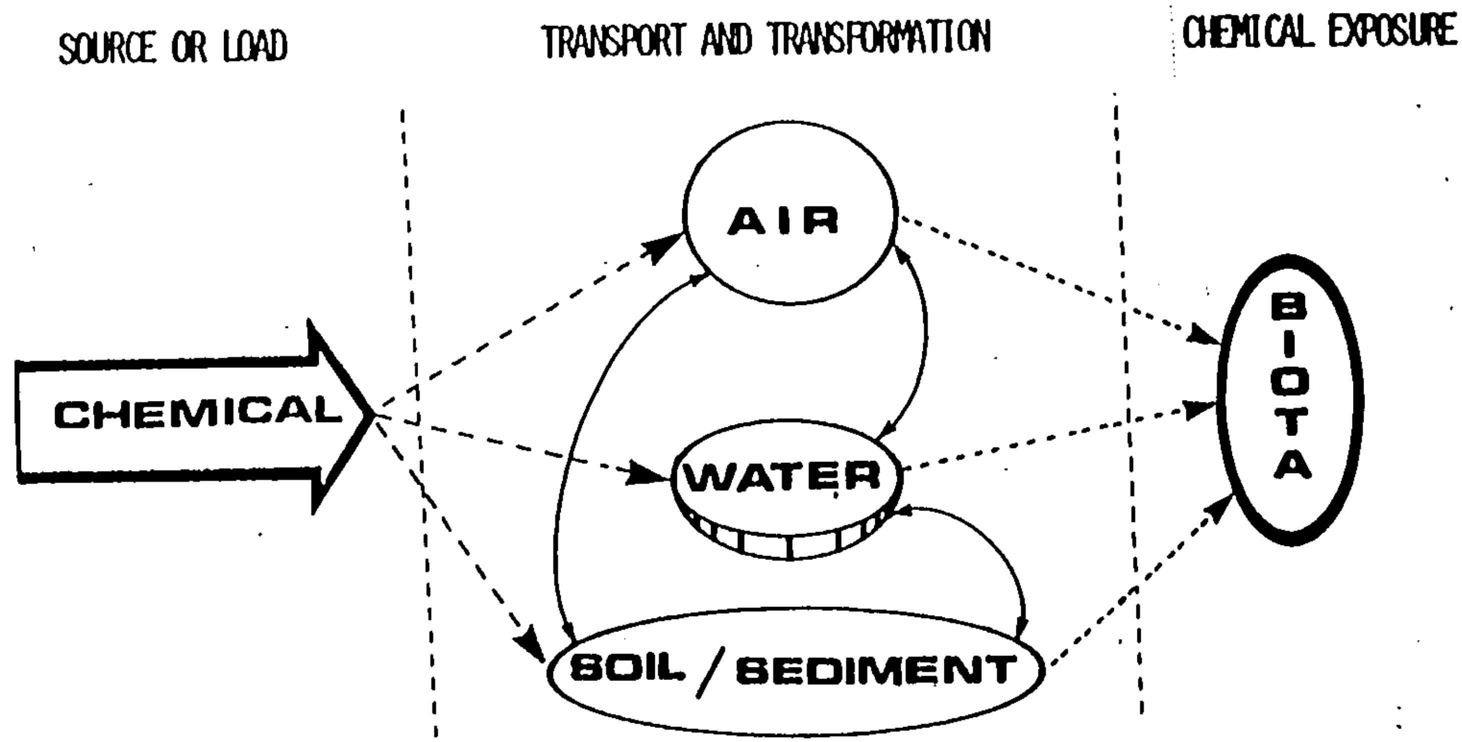

Figure 1.1 Environmental Fate of a Toxic Pollutant (After Haque, 1980)

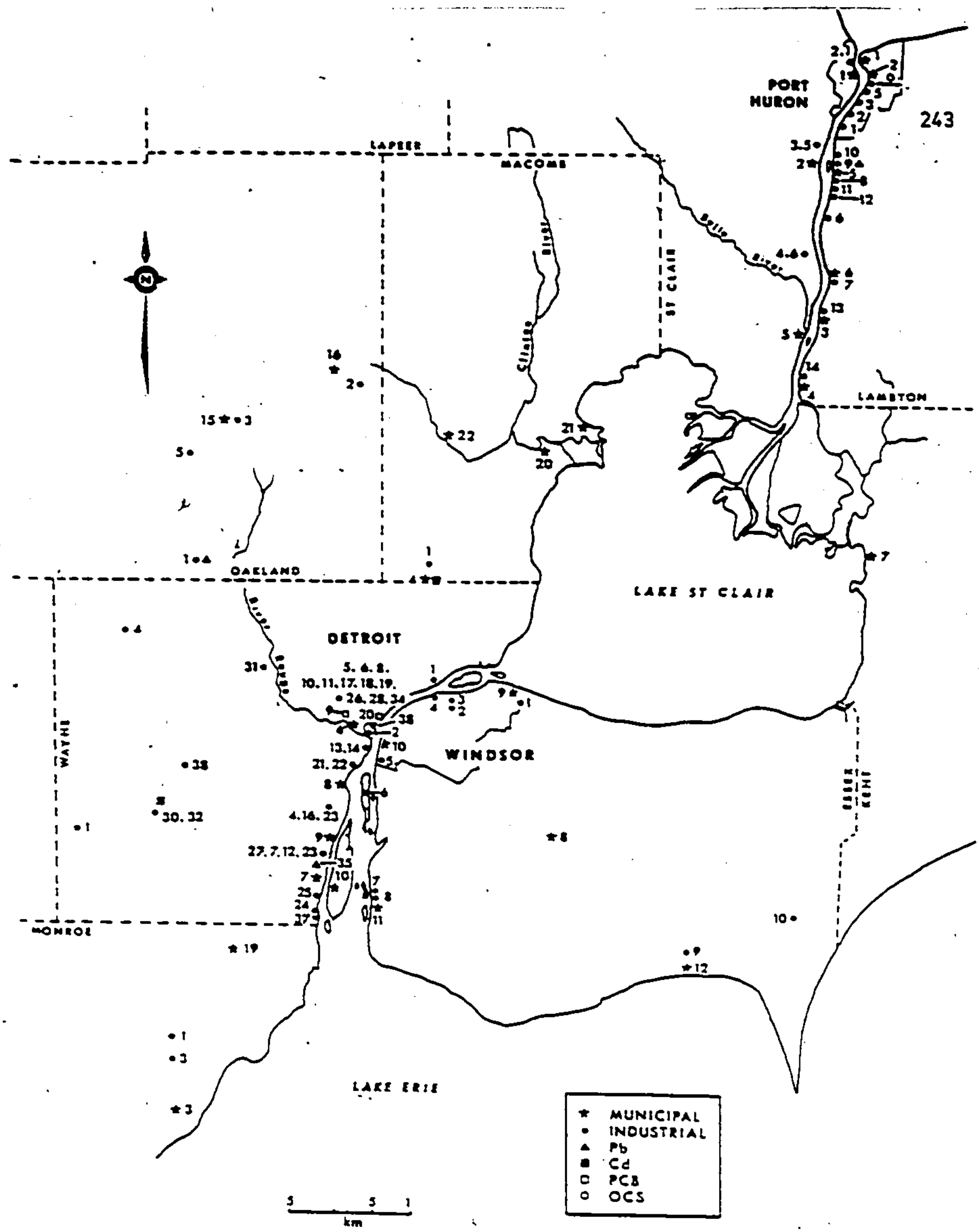

Figure 1.2 The Study Region, Including Surface Water Outfalls and Disposal Sites (Source: GLI, March, 1984, Annual Report)

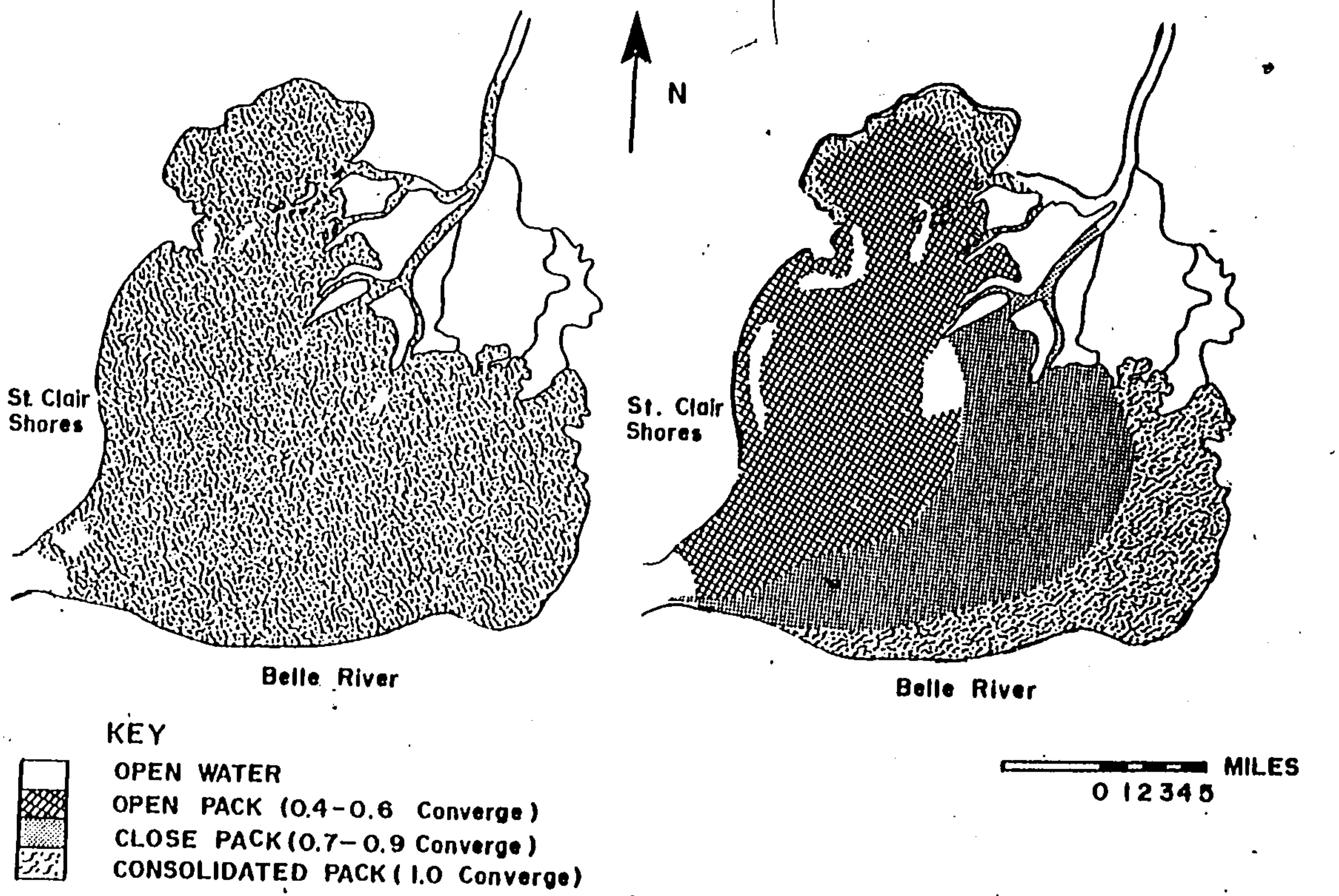

Figure 1.3 Typical Ice Conditions in January, February and March in Lake St. Clair (Source: Great Lakes Atlas, 1971)

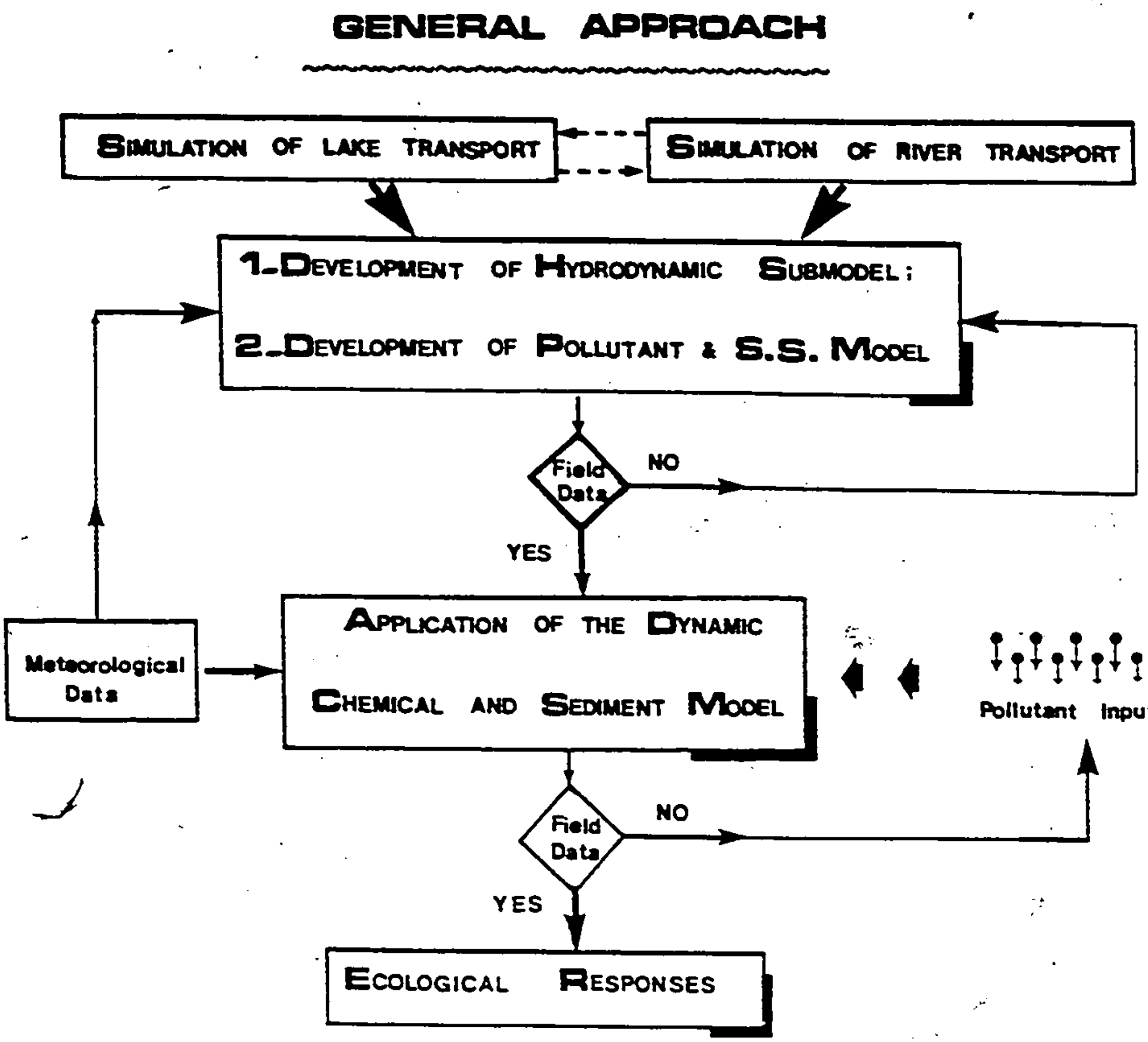

Figure 1.4 The Proposed Structure of The Overall Water Quality Modelling for Lake Huron-Erie Corridor

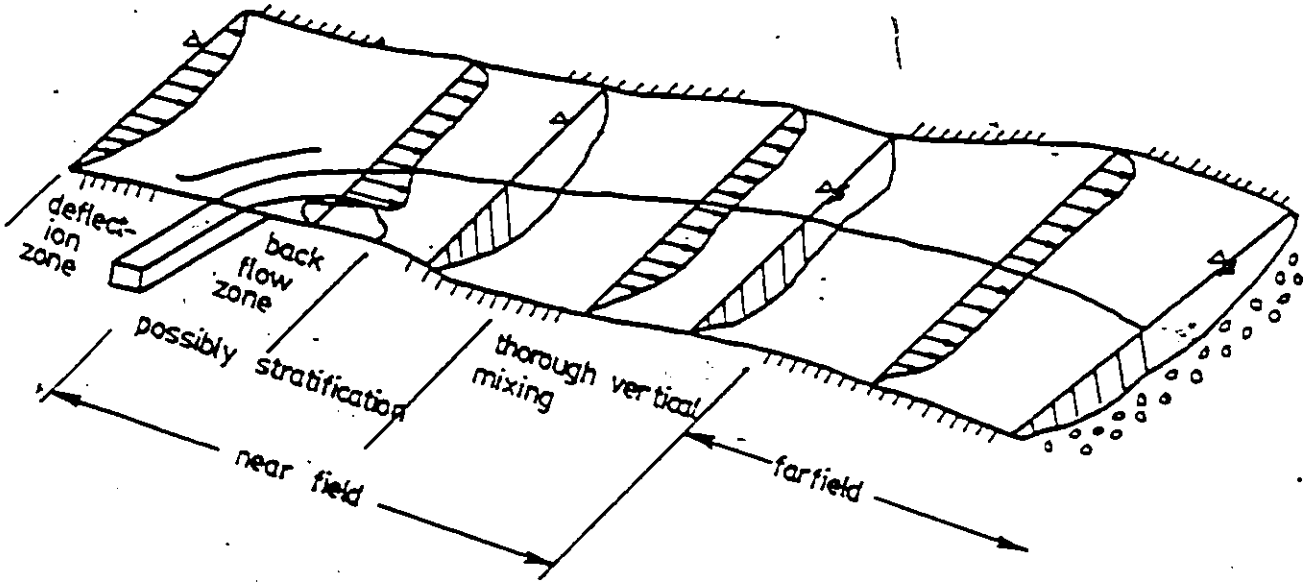

Figure 2.1 Typical Discharge Into a River Indicating
Near and Far Fields

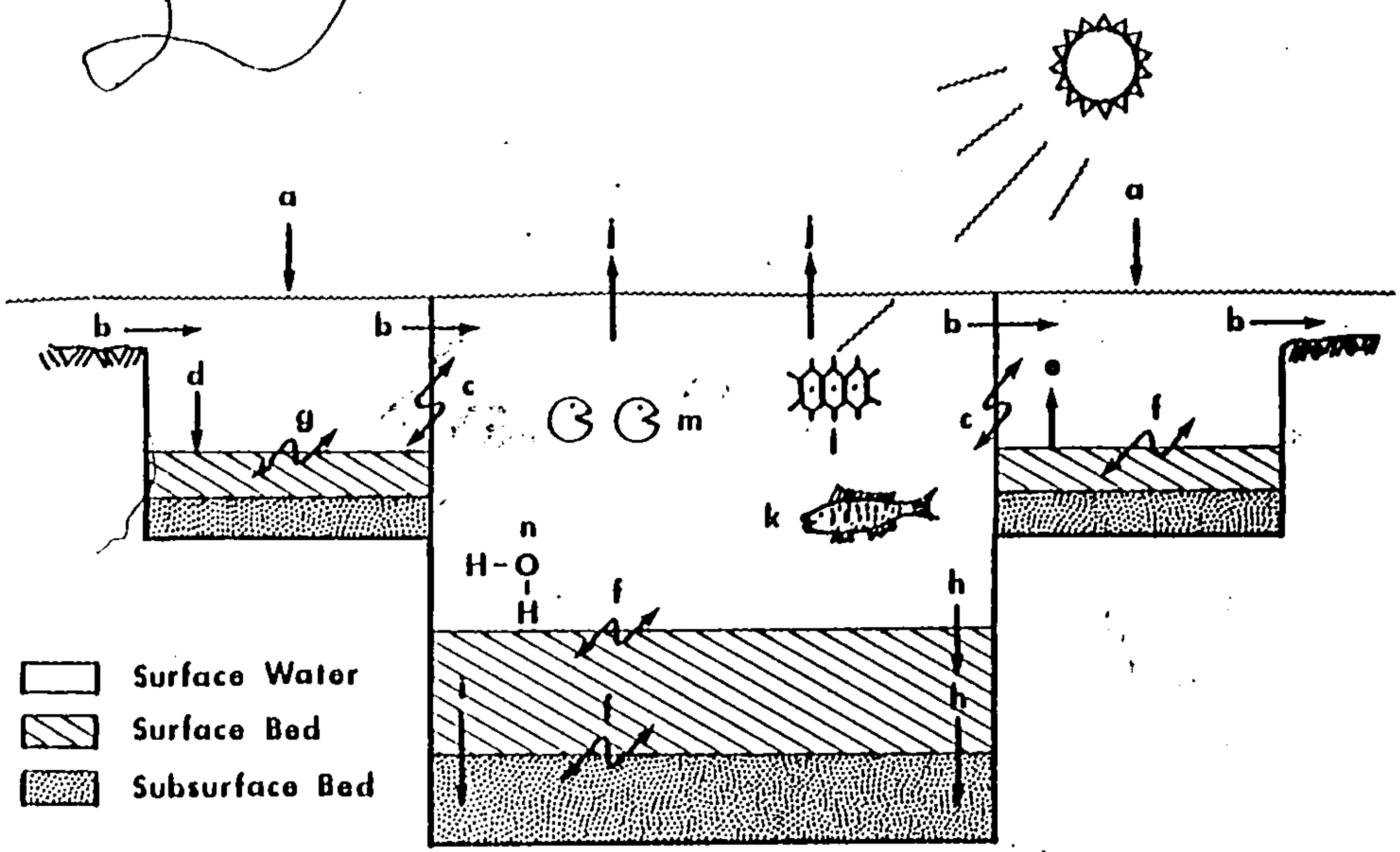

(1) TRANSPORT PROCESSES

A) MASS LOADING
B) ADVECTION
C) DISPERSION
D) SETTLING
E) EROSION
F) PORE WATER DIFFUSION
G) SEDIMENT TURNOVER
H) PERCOLATION
I) SEDIMENTATION
J) VOLATILIZATION

(2) TRANSFORMATION PROCESSES

K) BIOCONCENTRATION
L) PHOTOLYSIS
M) BIODEGRADATION
N) HYDROLYSIS
O) REDUCTION - OXIDATION

Figure 2.2 The Transport and Transformation Processes of TOXIWASP Model

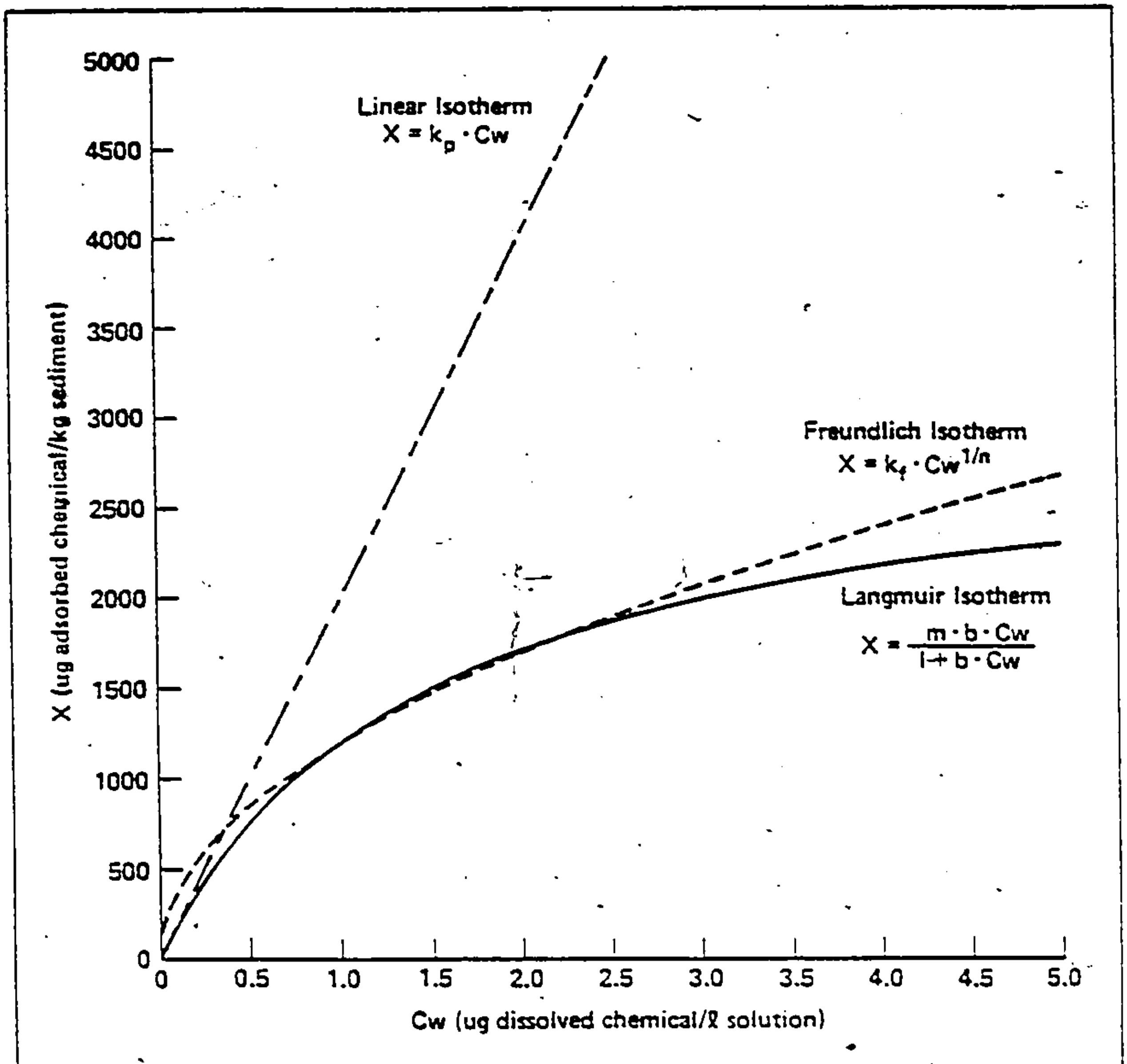

Figure 2.3 Isotherms For Adsorption of a Hydrophobic Pollutant on Sediments. (After: Mills *et al*. 1982)

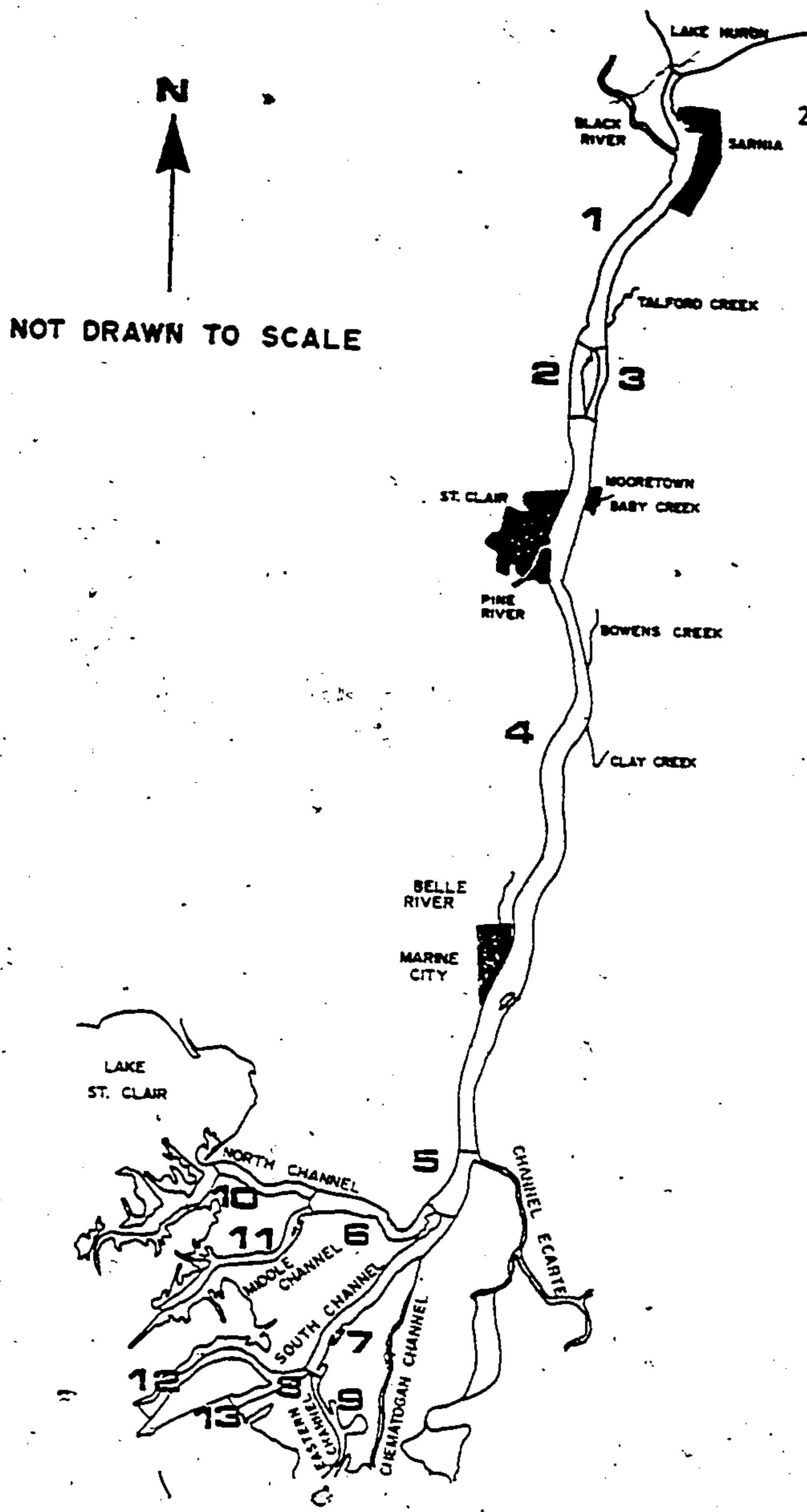

Figure 3.1 Discretization of St. Clair River

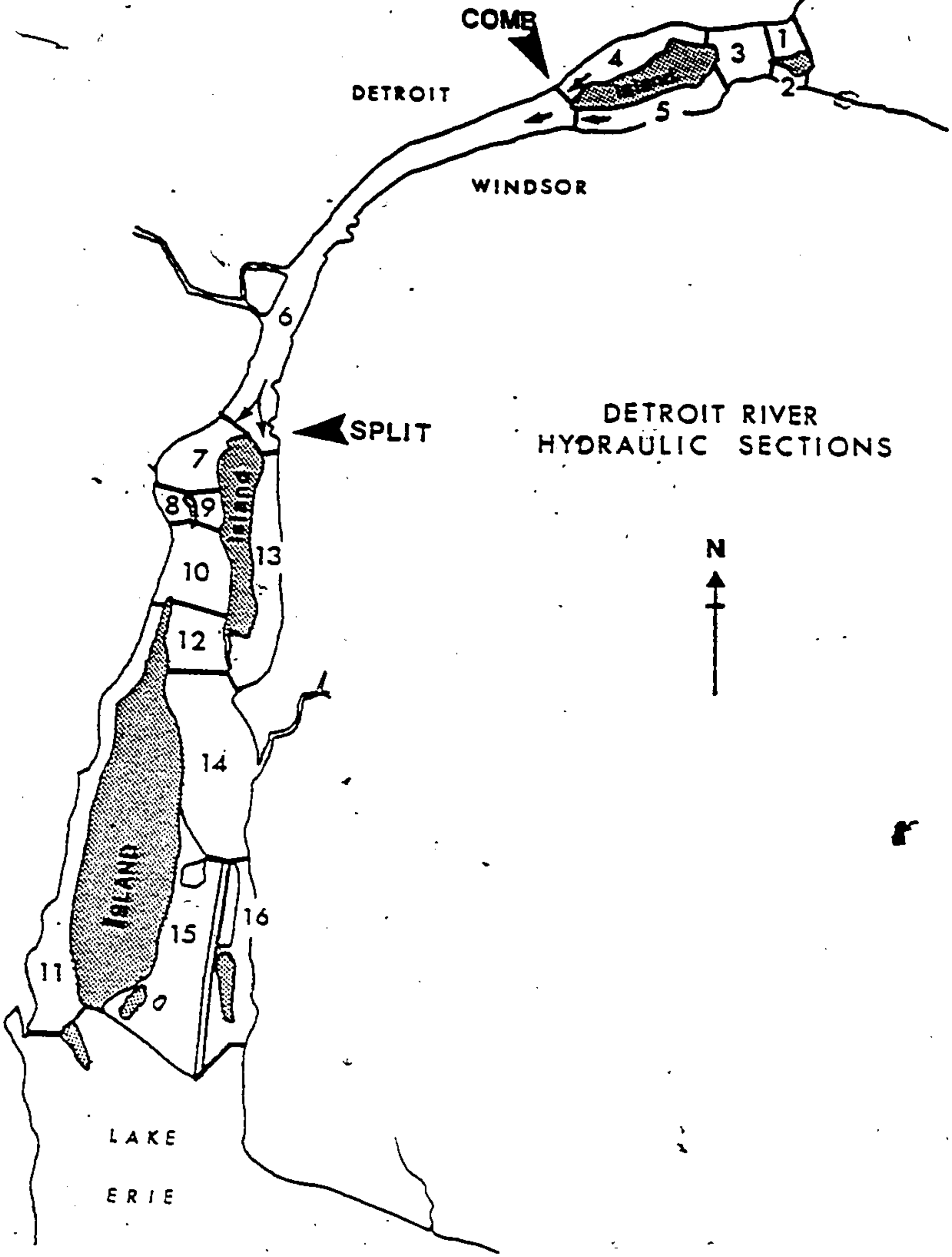

Figure 3:2 Discretization of Detroit River

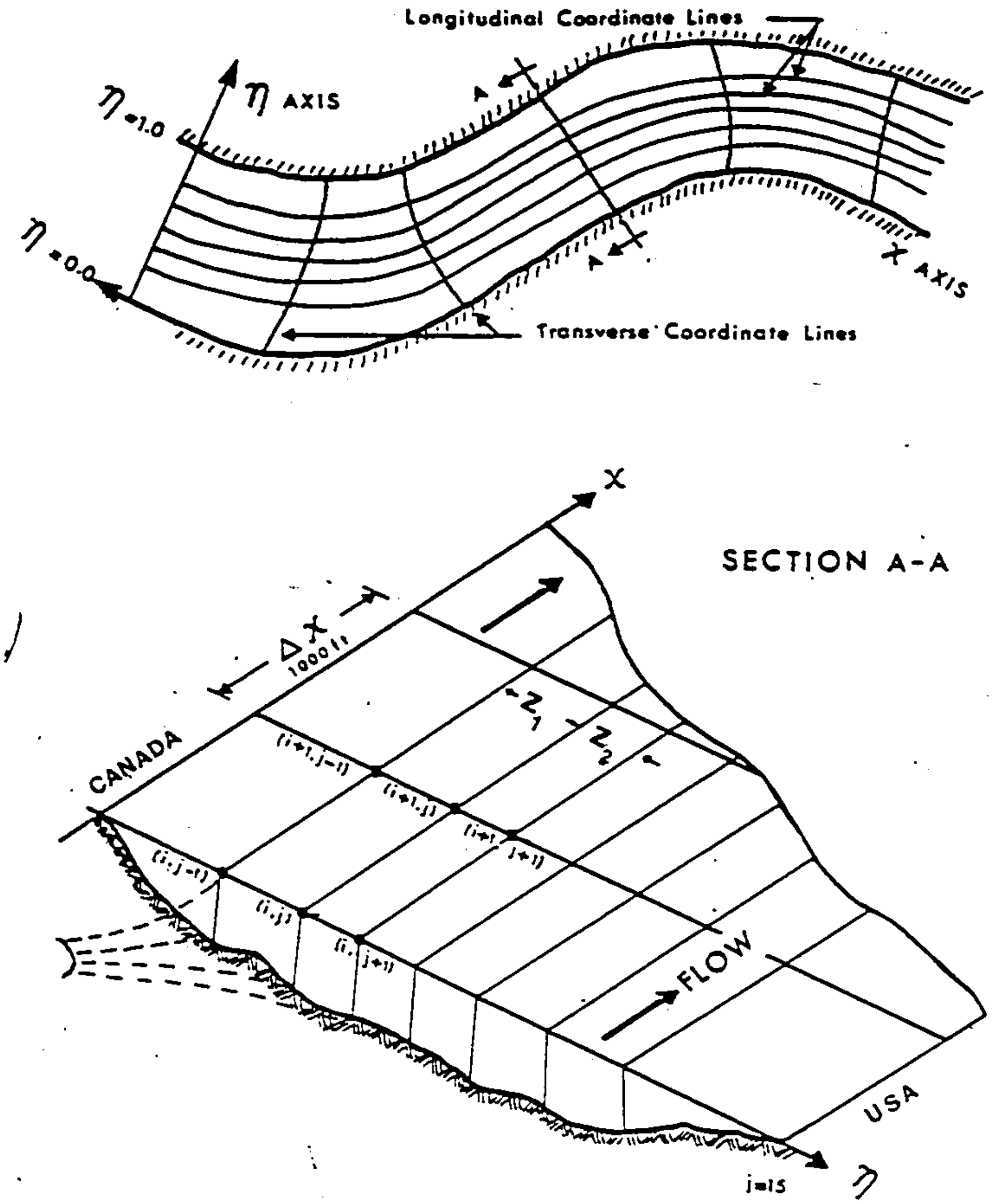

Figure 3.3 Orthogonal Curvilinear Coordinate System For Natural Channels

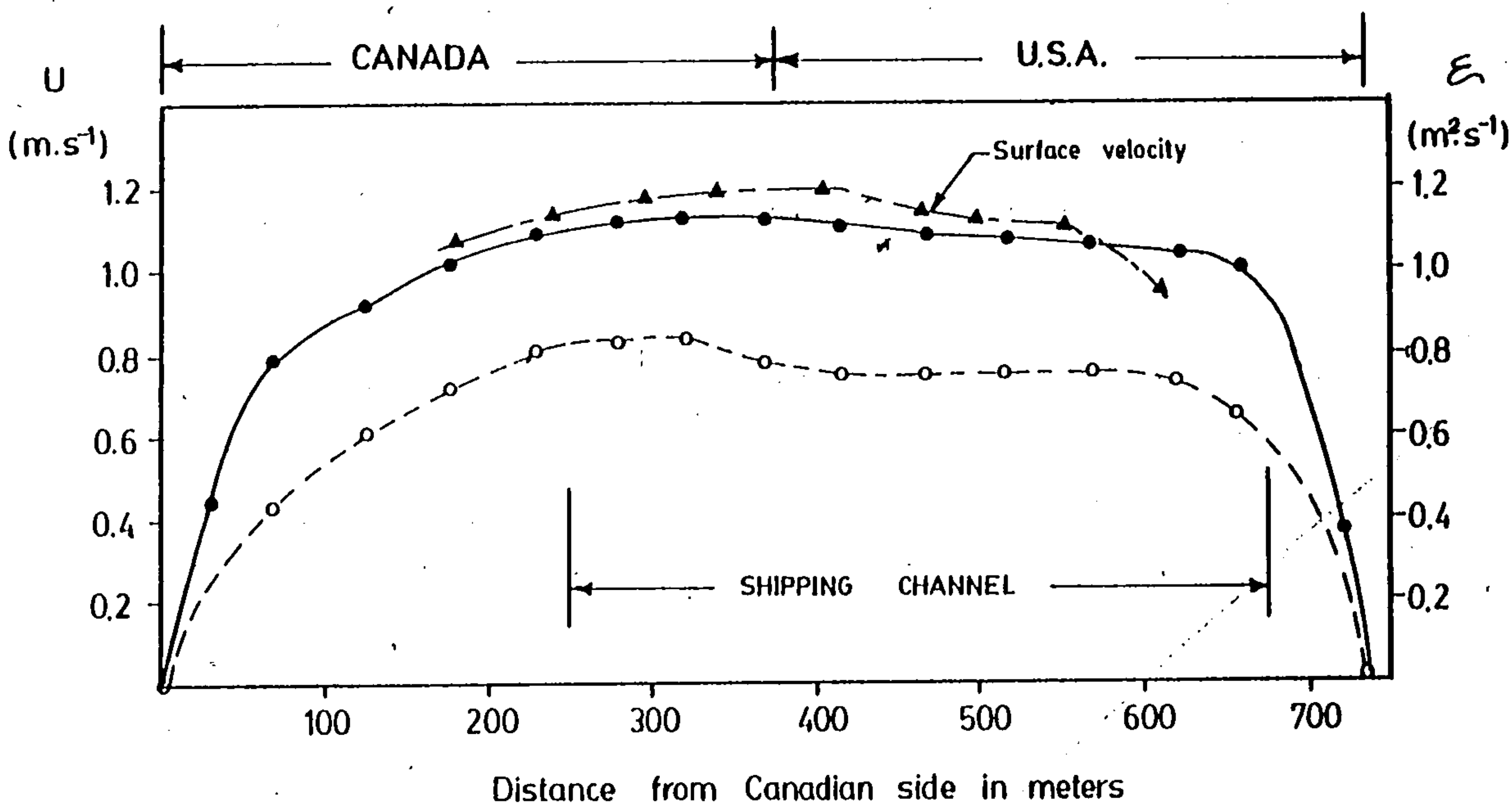

Figure 4.1 Predicted Distribution of Velocity (U) and Dispersion Coefficient (ε_r) at 5,000 m from the Inlet of the St. Clair River, and the Measured Surface Velocities by Corps of Engineers, For Reach No. 1.

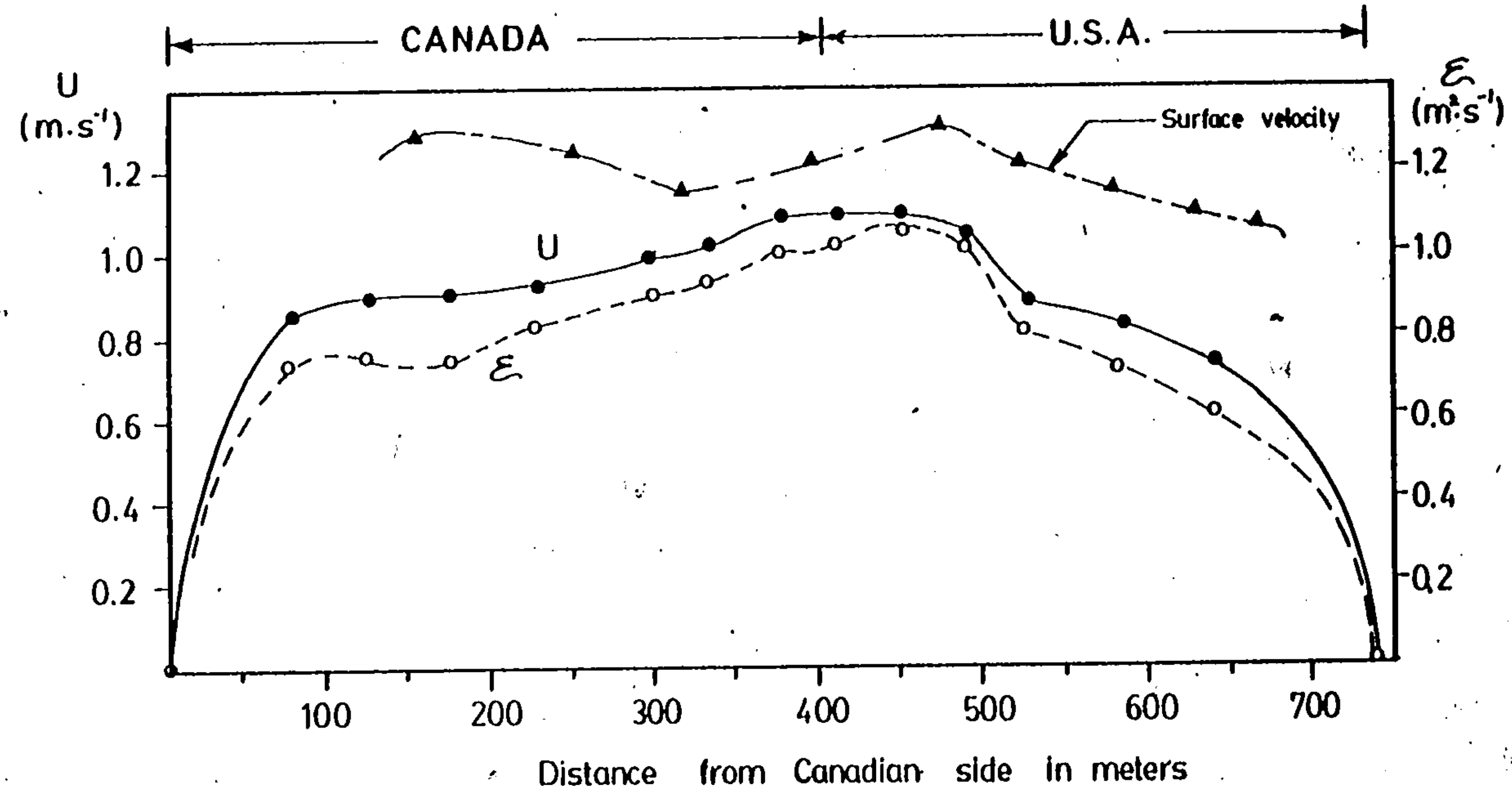

Figure 4.2 Predicted Distribution of Velocity (U) and Dispersion Coefficient ($\mathcal{E}$,) at 10,000 m From The Inlet of The St. Clair River With The Measured Surface Velocities by Corps of Engineers For Reach No. 1.

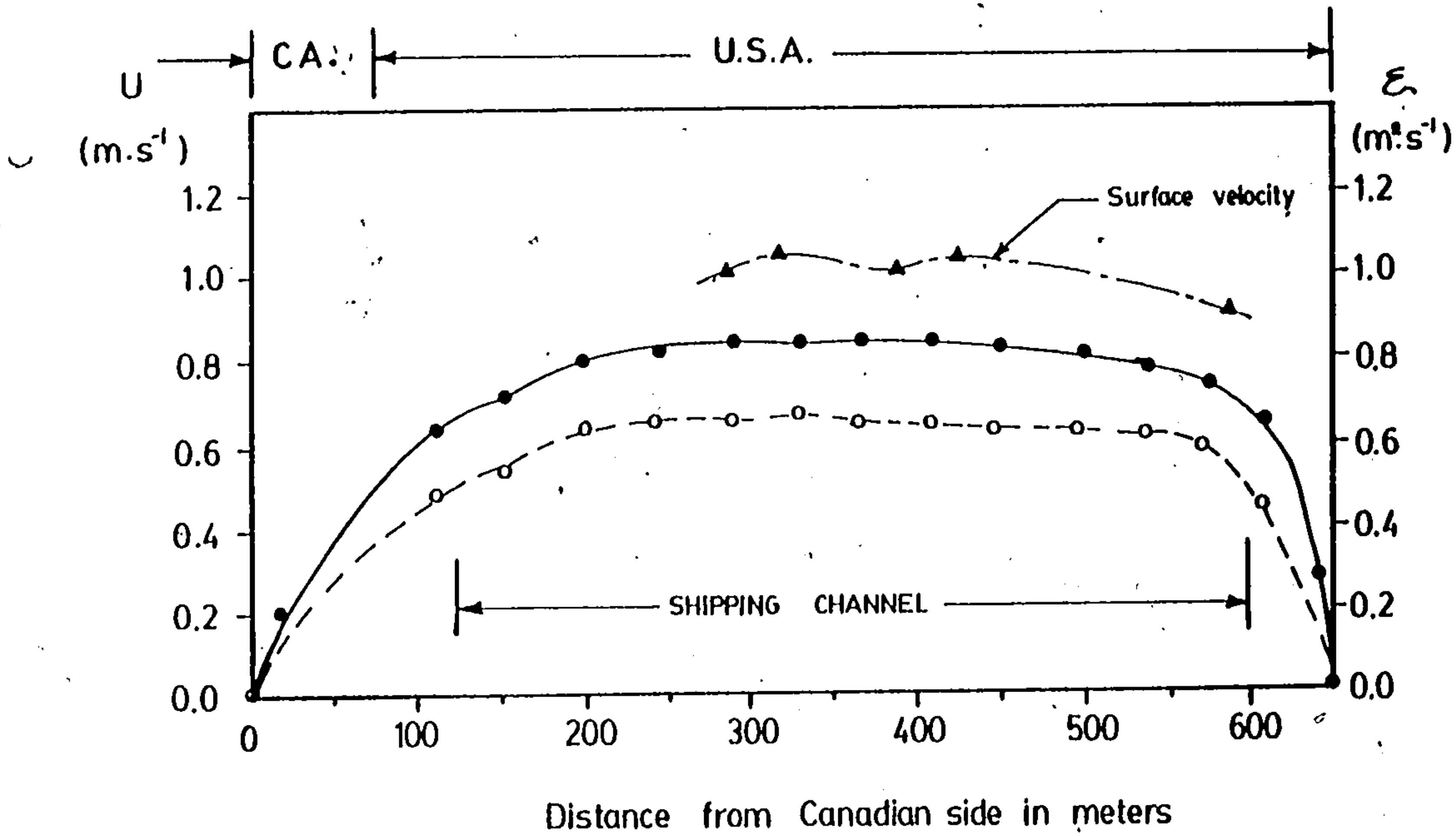

Figure 4.3 Predicted Distribution of Velocity (U), The Dispersion Coefficient ($\mathcal{E}$) and The Measured Surface Velocities by Corps of Engineers, For Reach No. 2 (in St. Clair River)

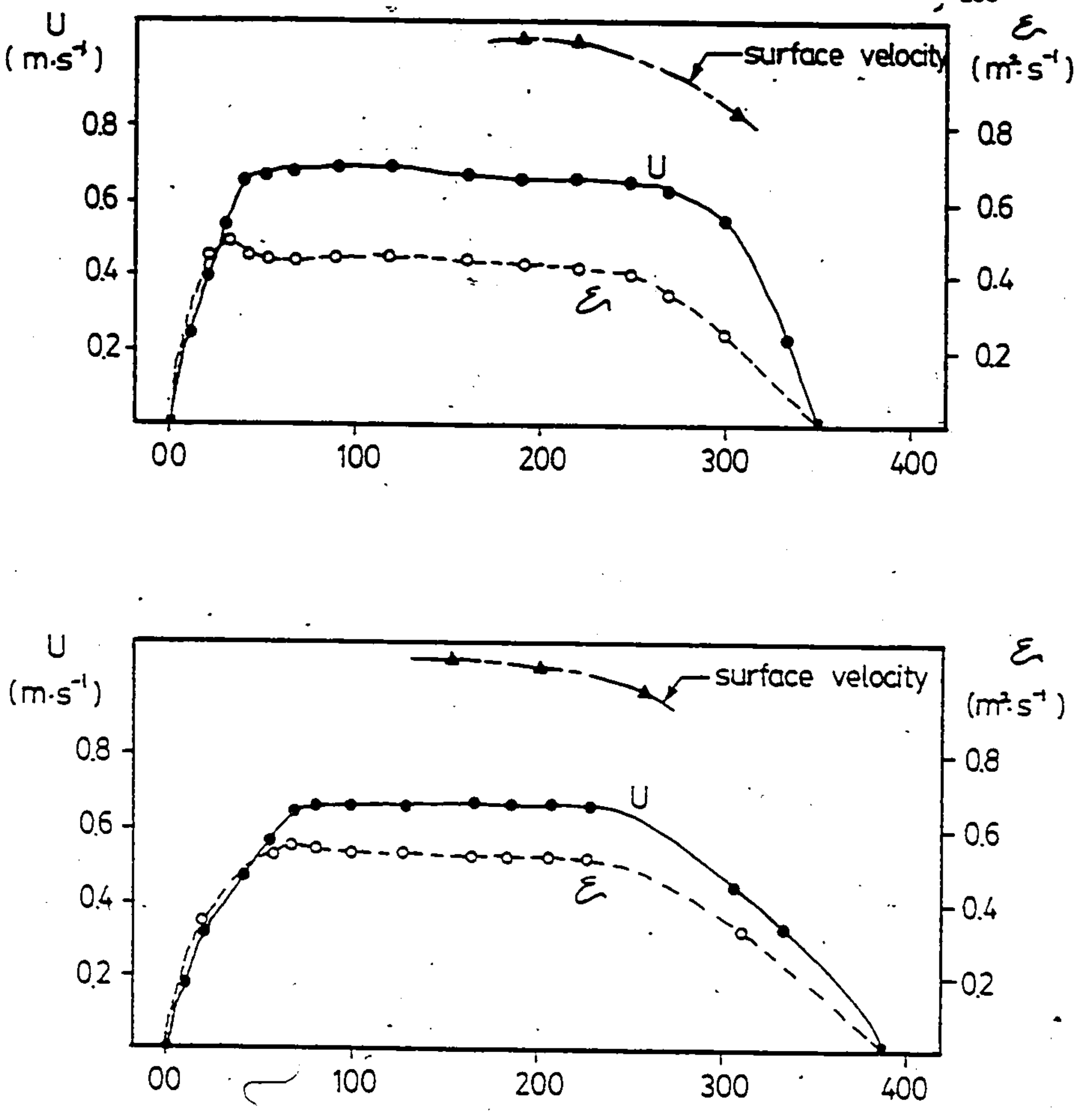

Figure 4.4 Predicted Distribution of Velocity (U), The Dispersion Coefficient ($\mathcal{E}$) and The Measured Surface Velocities by Corps of Engineers, For Reach No. 3 in St. Clair River

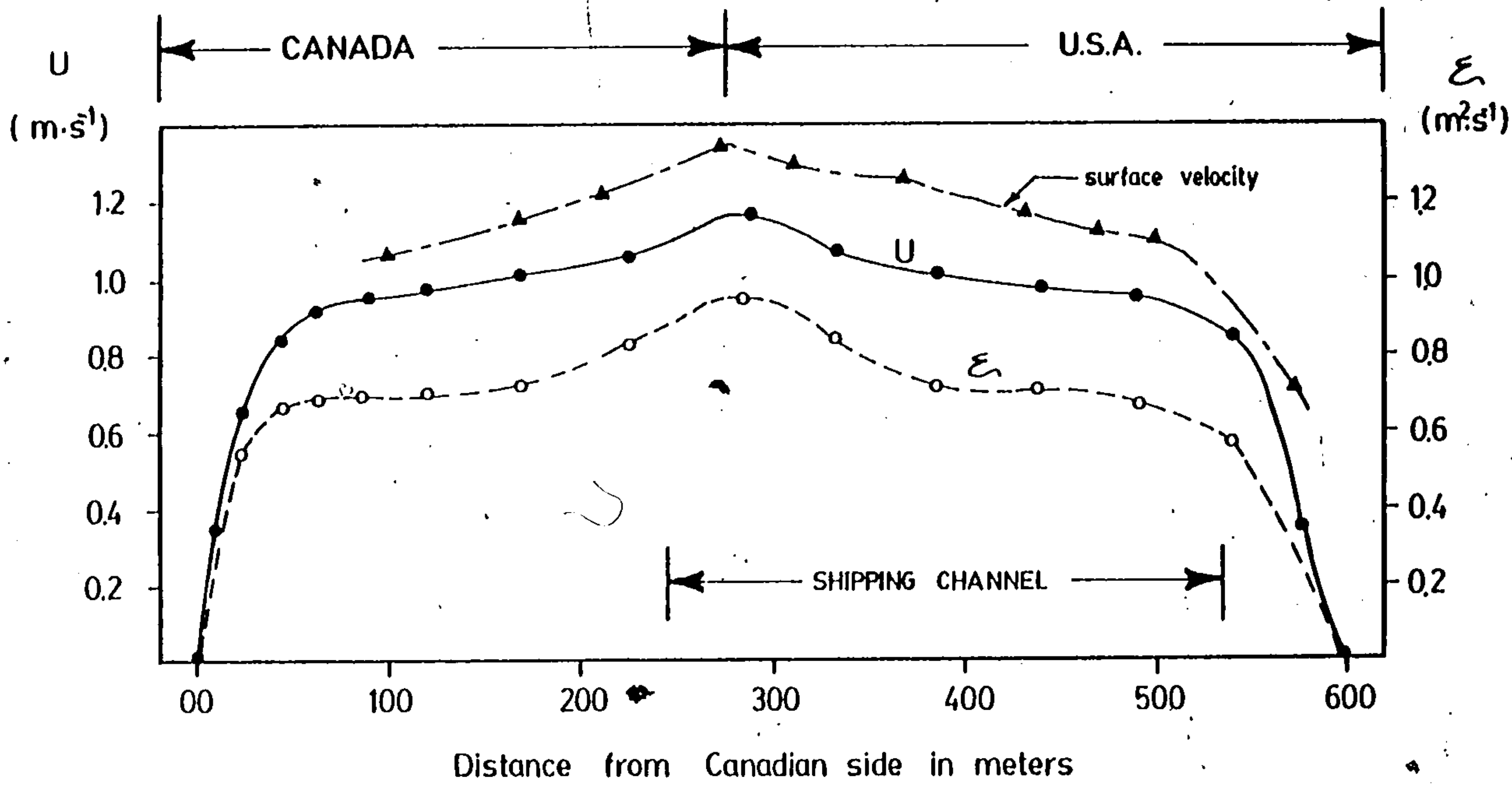

Figure 4.5 Predicted Distribution of Velocity (U), the Dispersion Coefficient ($\mathcal{E}$) and the Measured Surface Velocities by Corps of Engineers, for Reach No. 4 (St. Clair River)

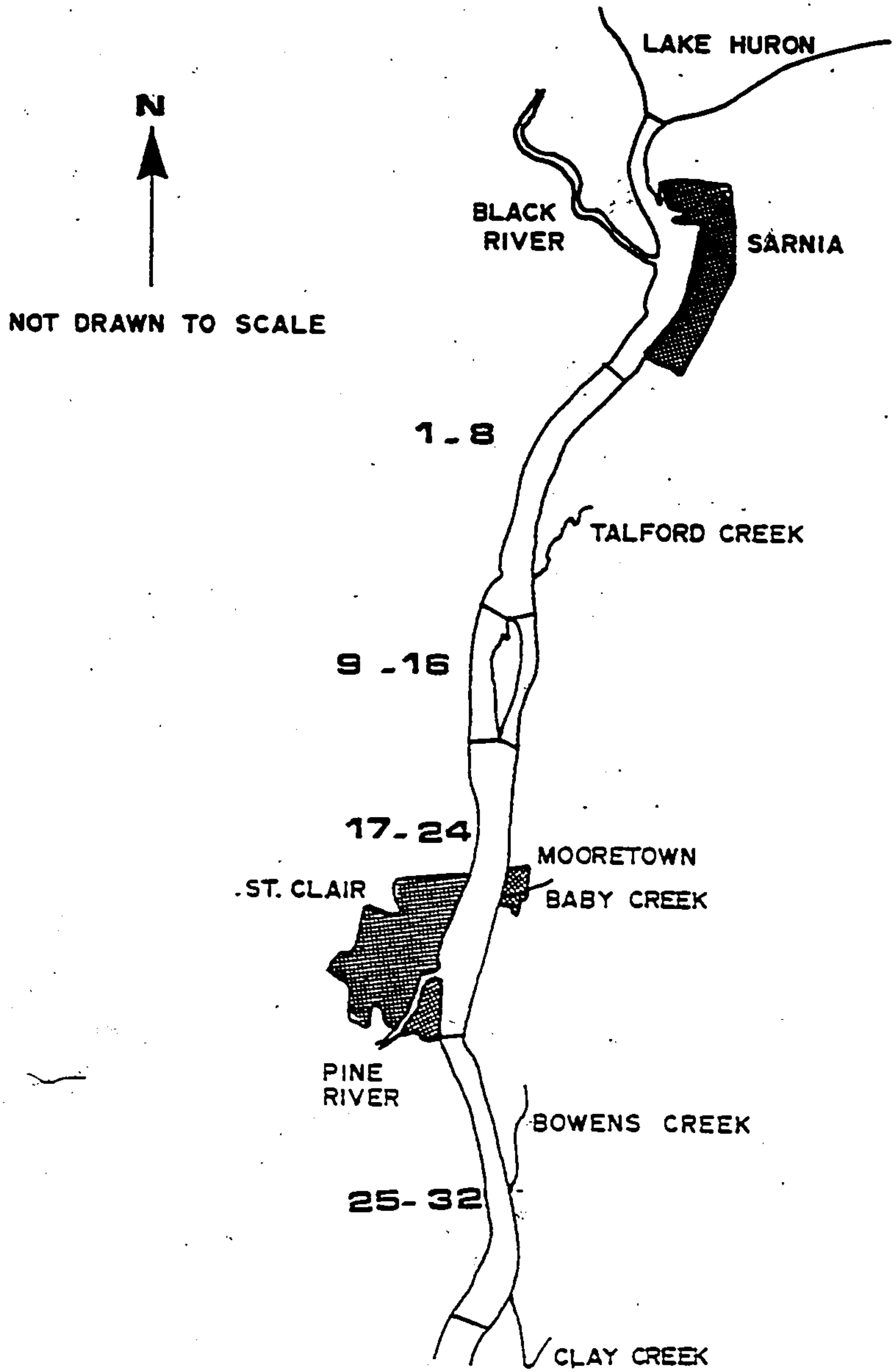

Figure 4.6 Segmentation For The Upper St. Clair River For the 48 Segments Model

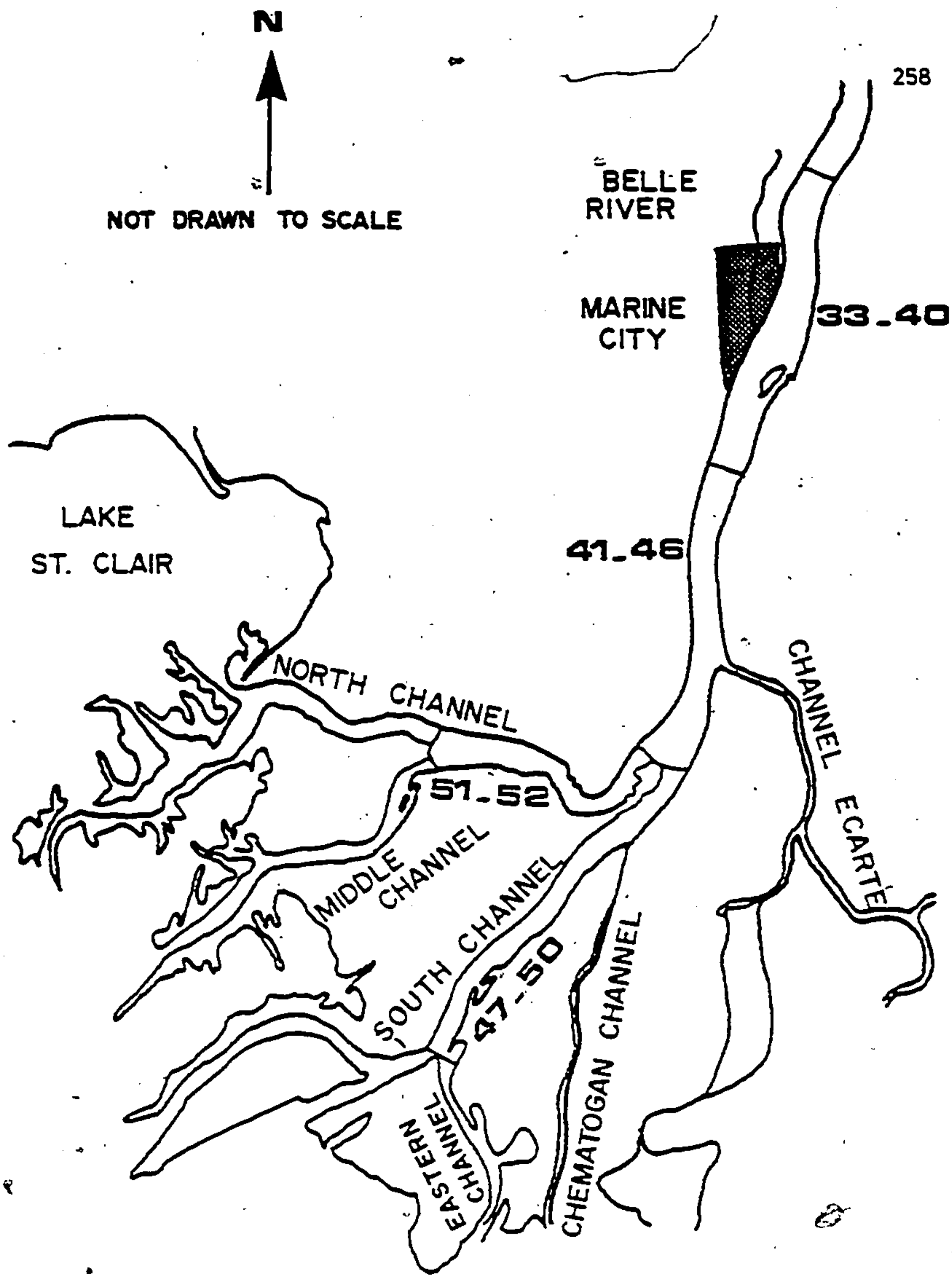

Figure 4.7 Segmentation For the Lower St. Clair River

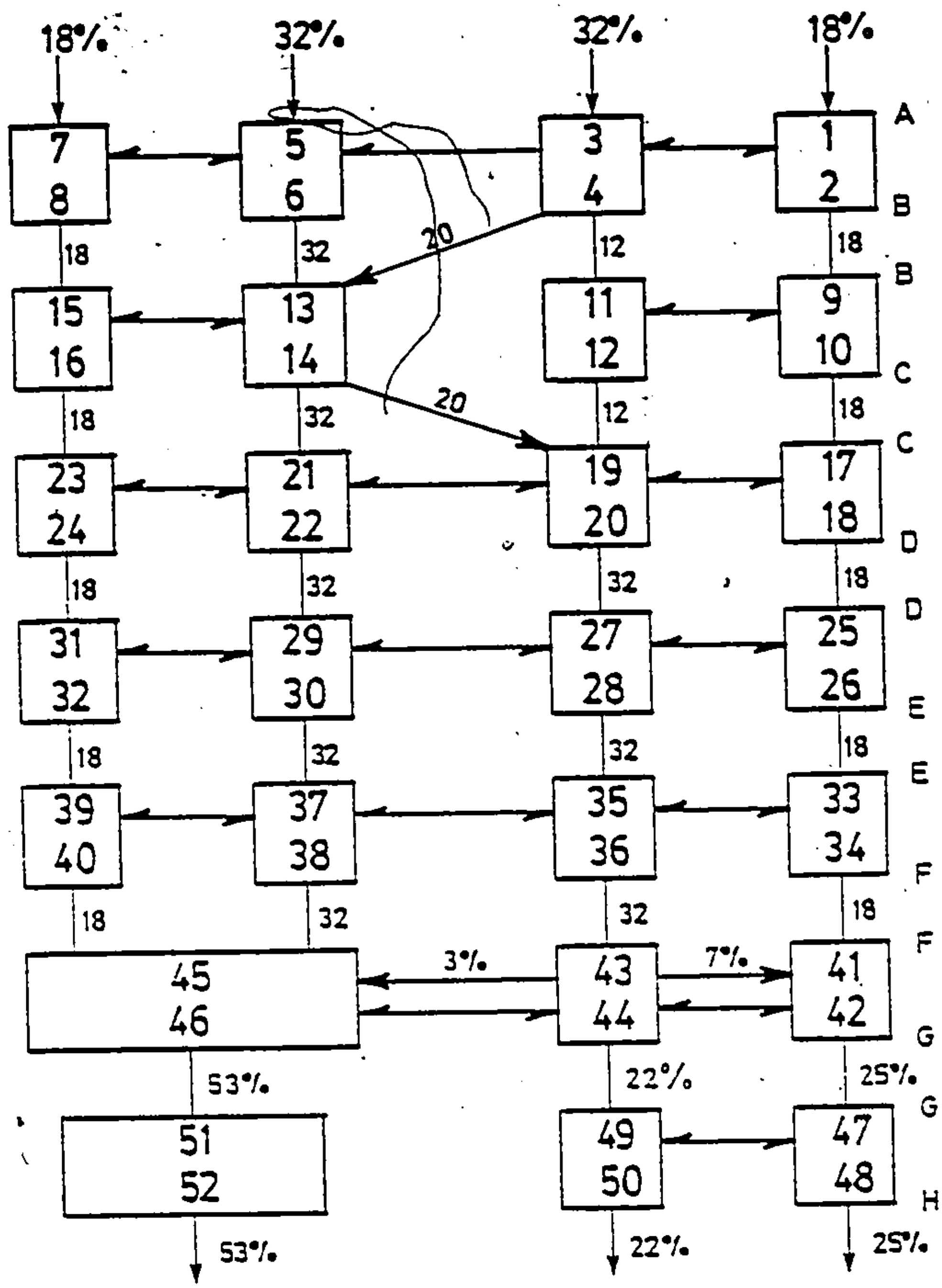

Figure 4.8 St. Clair River Model Segment Flow Pattern (all flows are percent of total flow)

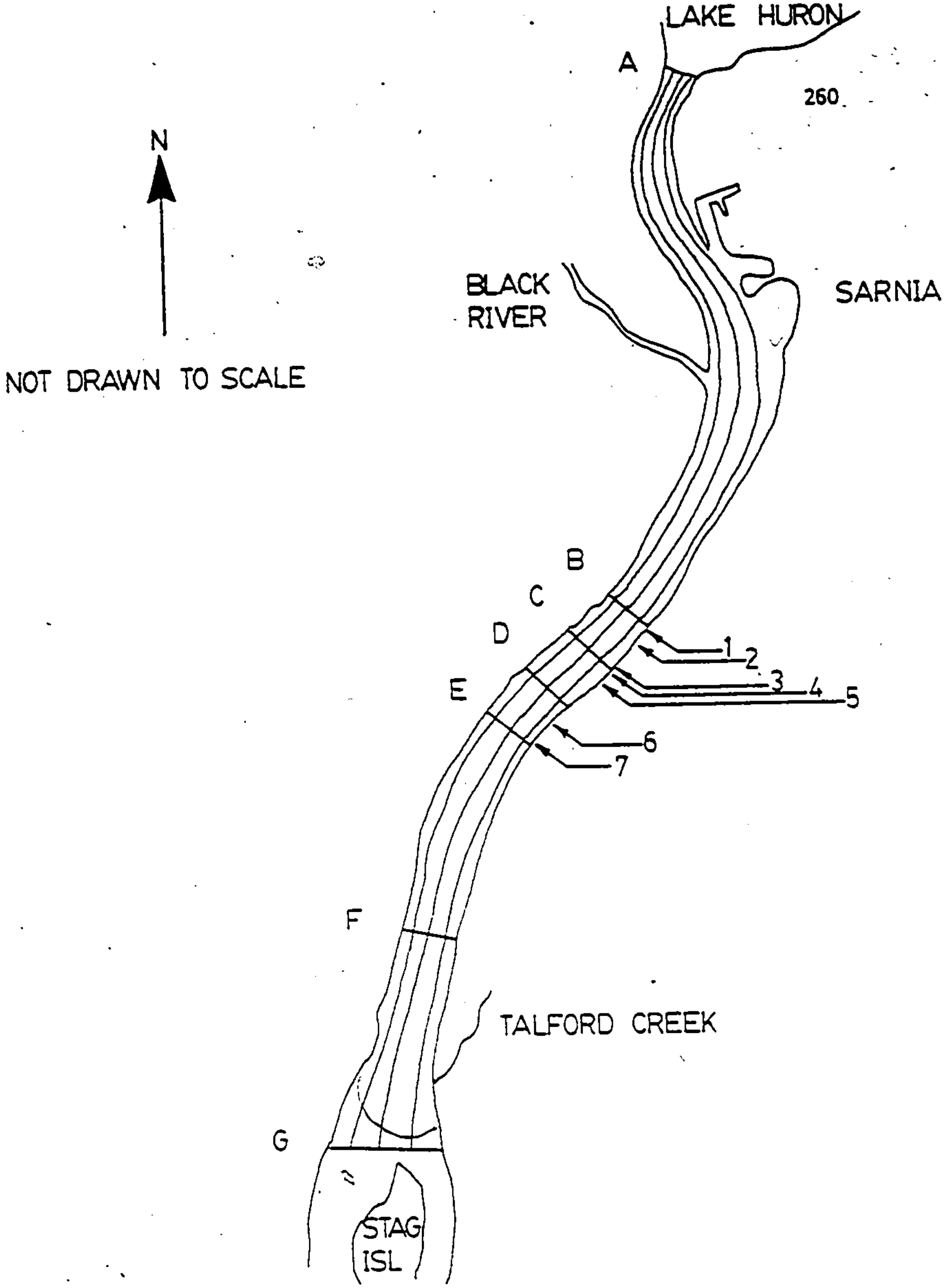

Figure 4.9 Segmentation Grid For the Upper St. Clair River Showing the Locations of HCB Point Sources.

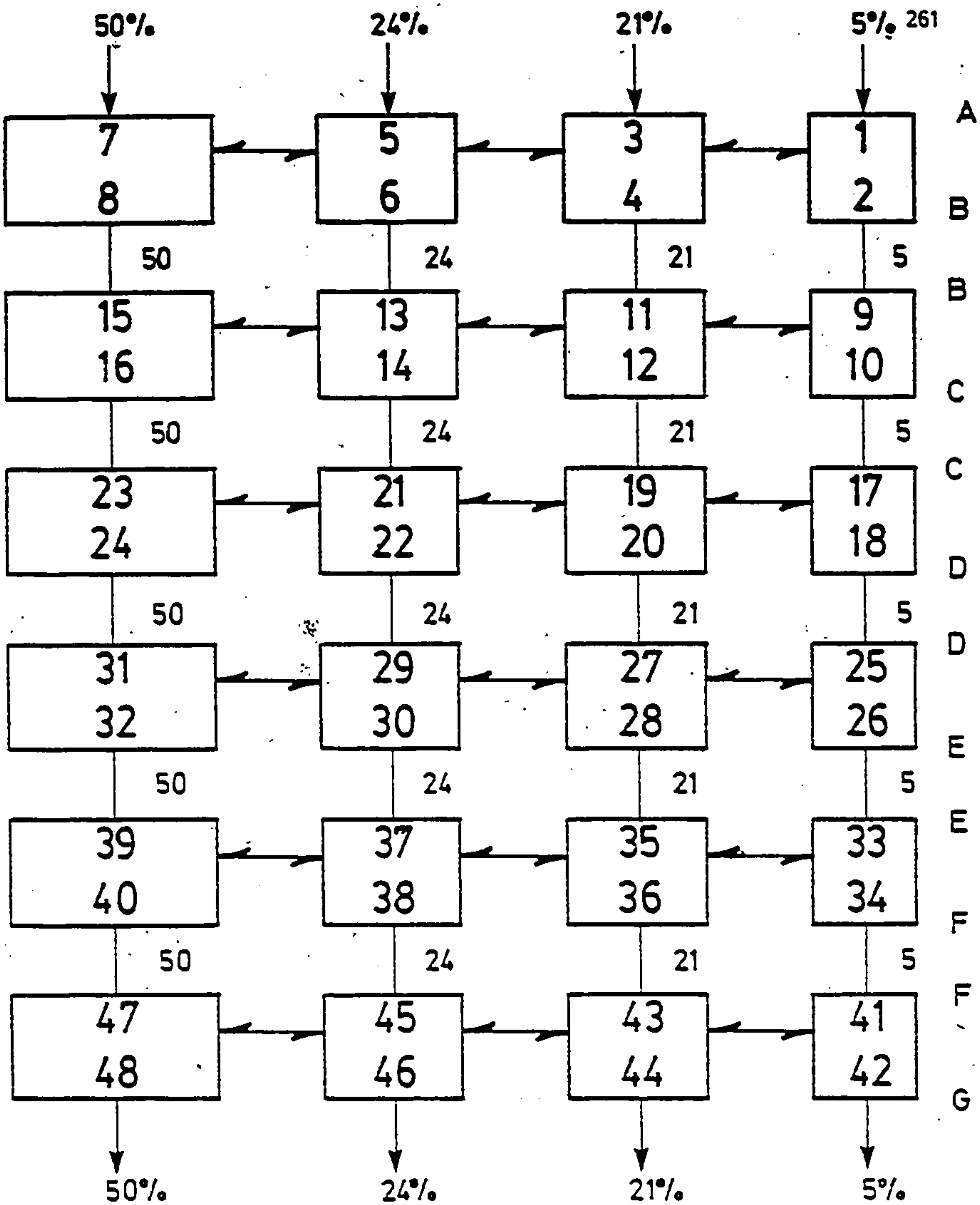

Figure 4.10 Upper St. Clair River Model Segment Flow Pattern
(all flows are percent of total flow)

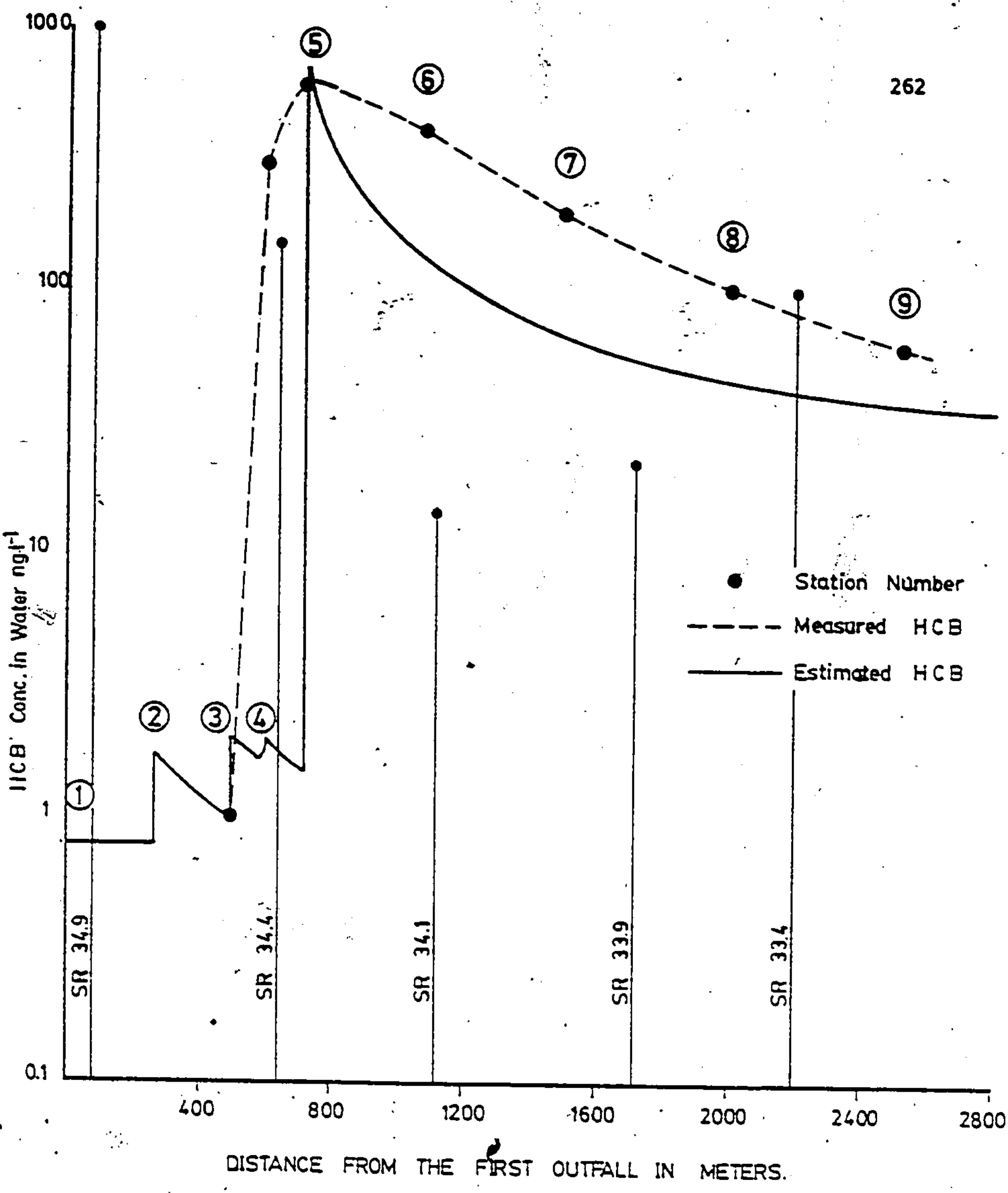

Figure 4.11 HCB levels in Water Along The Canadian Shoreline As Measured by MOE And Predicted From the K-ε Model.

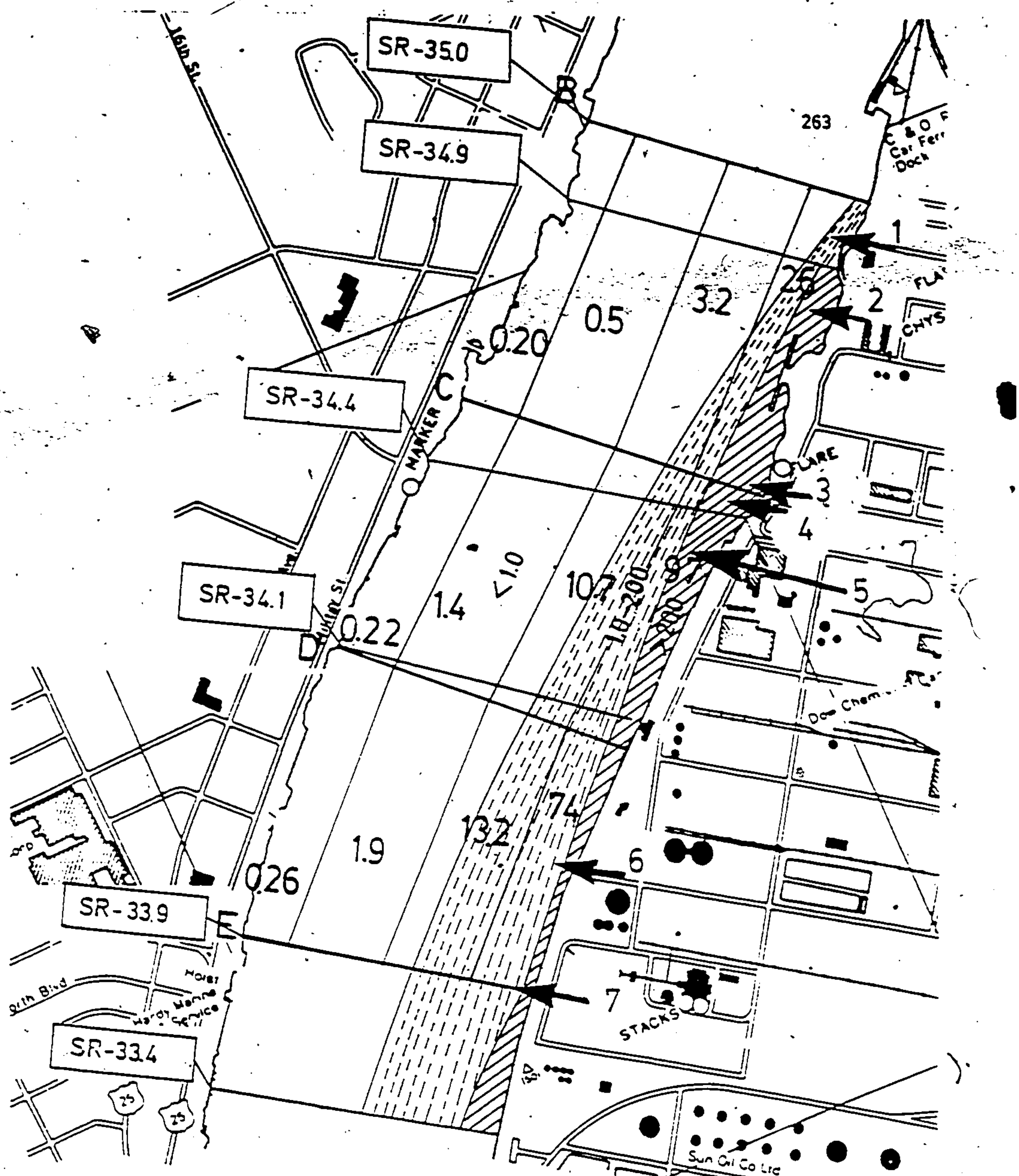

Figure 4.12 Comparison of Predicted and Measured HCB Concentrations in Bed Sediments in the Upper Part of St. Clair River

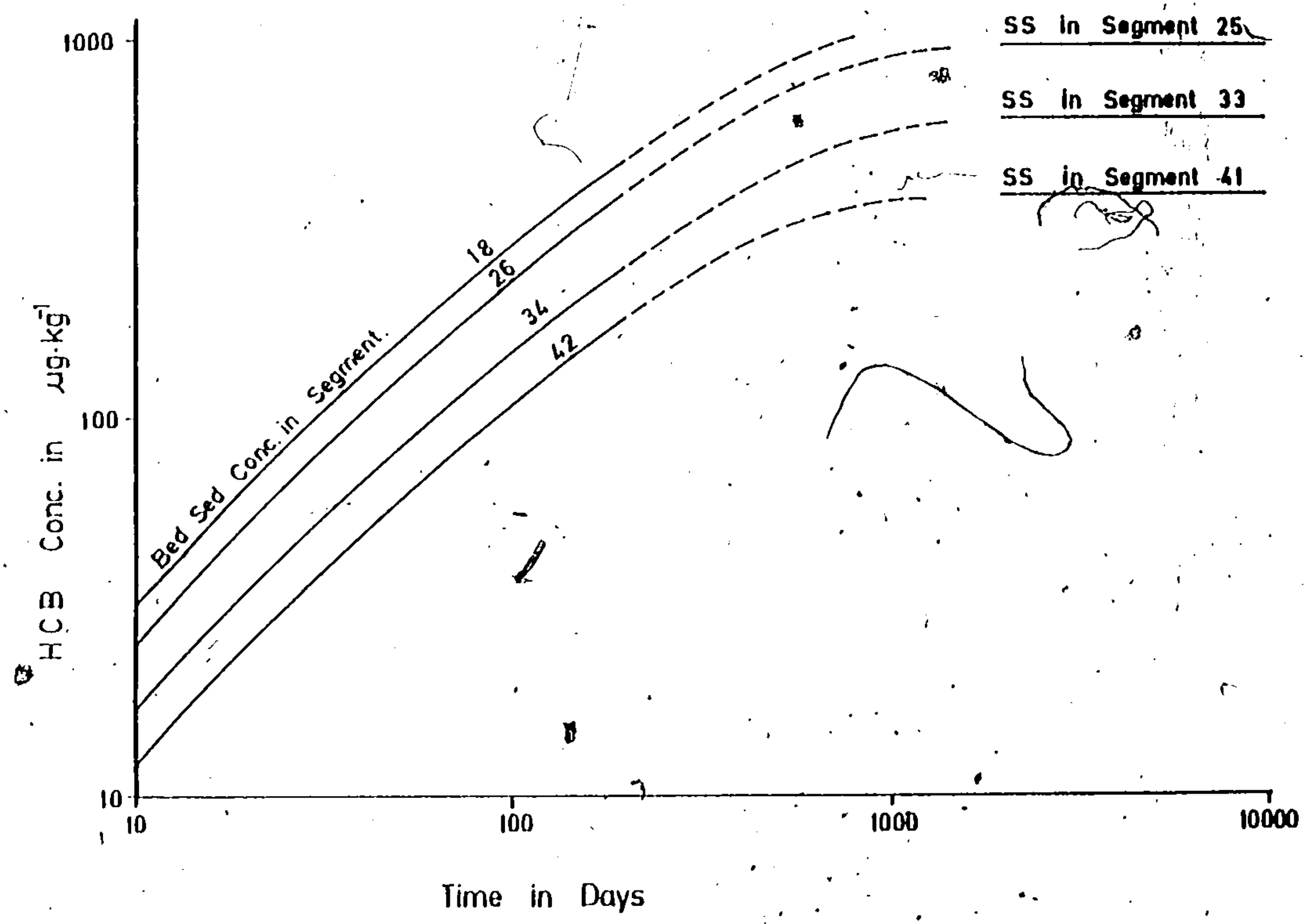

Figure 4.13 Predicted HCB Concentrations in Bed Sediment Along The Canadian Shoreline Segments, extrapolated results up to six years.

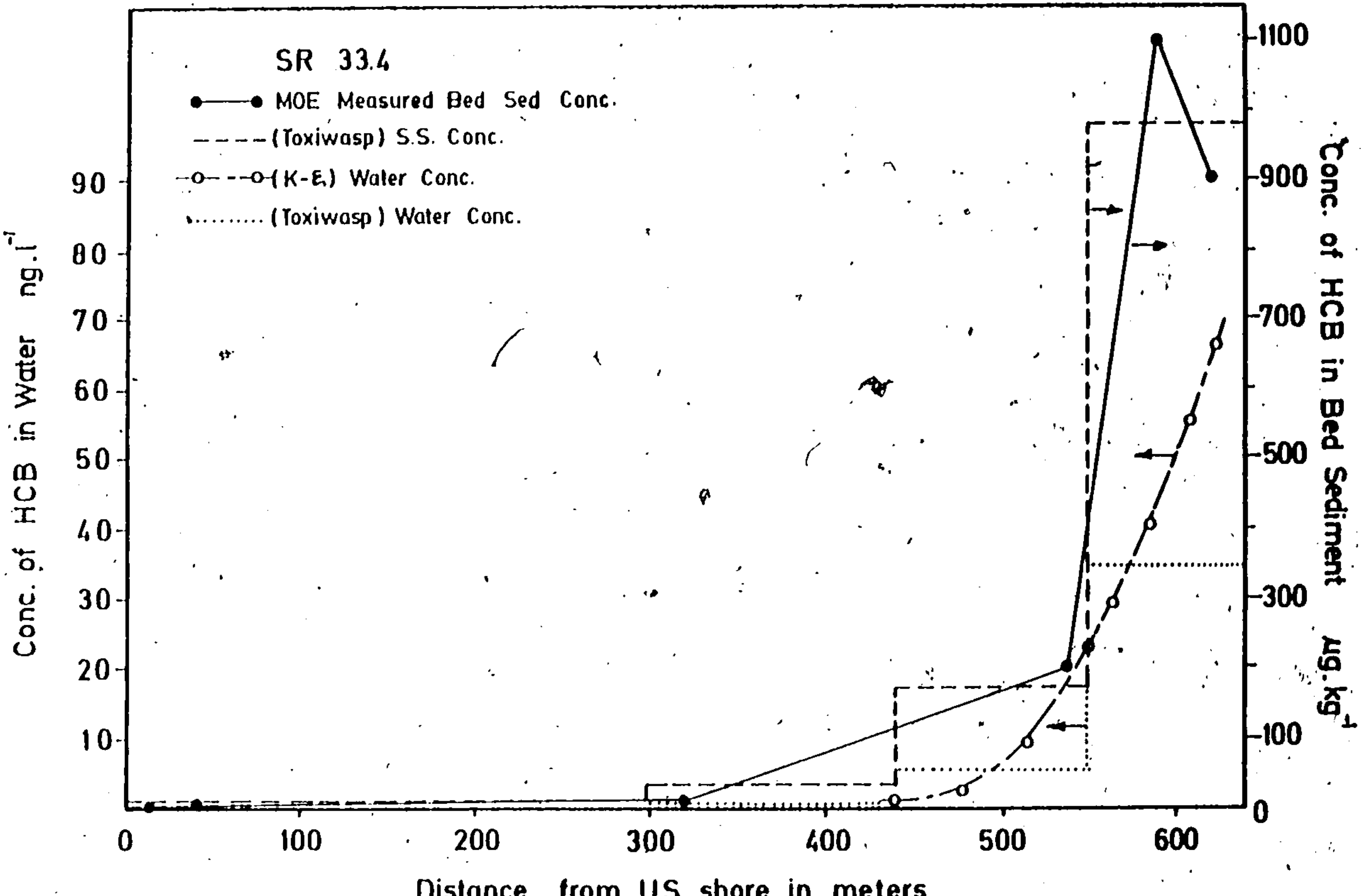

Figure 4.14 Predicted Concentrations of HCB in Water and Bed Sediments Along With Measured Concentrations at Station No. SR 33.4 in The Upper Part of St. Clair River.

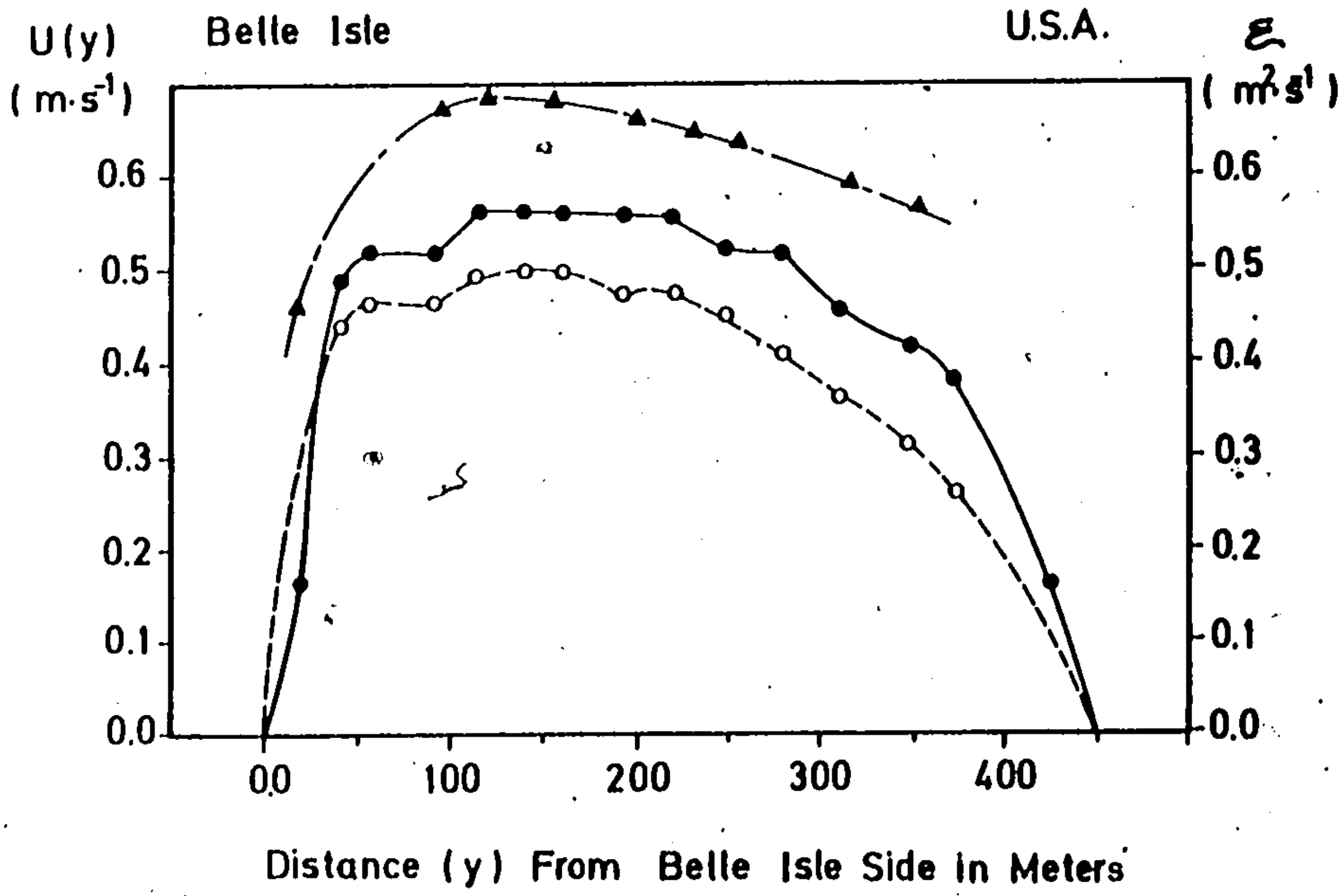

Figure 4.15 Predicted Distribution of Velocity (V), Dispersion Coefficent (ℰ) and The Measured Surface Velocity by Corps of Engineers for Reach No. 4 in the Detroit River

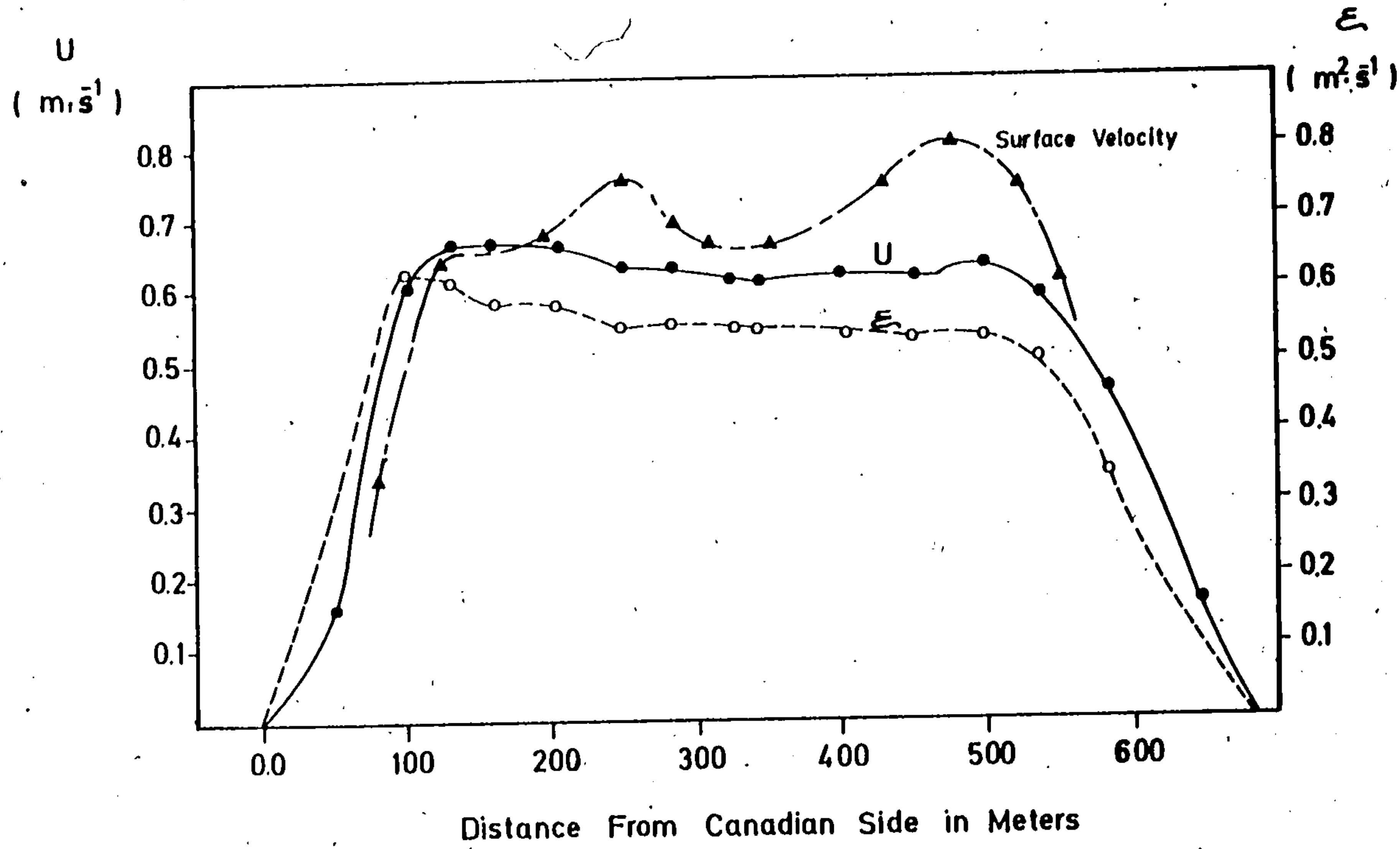

Figure 4.16 Predicted Distribution of Velocity (V), Dispersion Coefficient and Measured Surface Velocity for Reach No. 5 in Detroit River

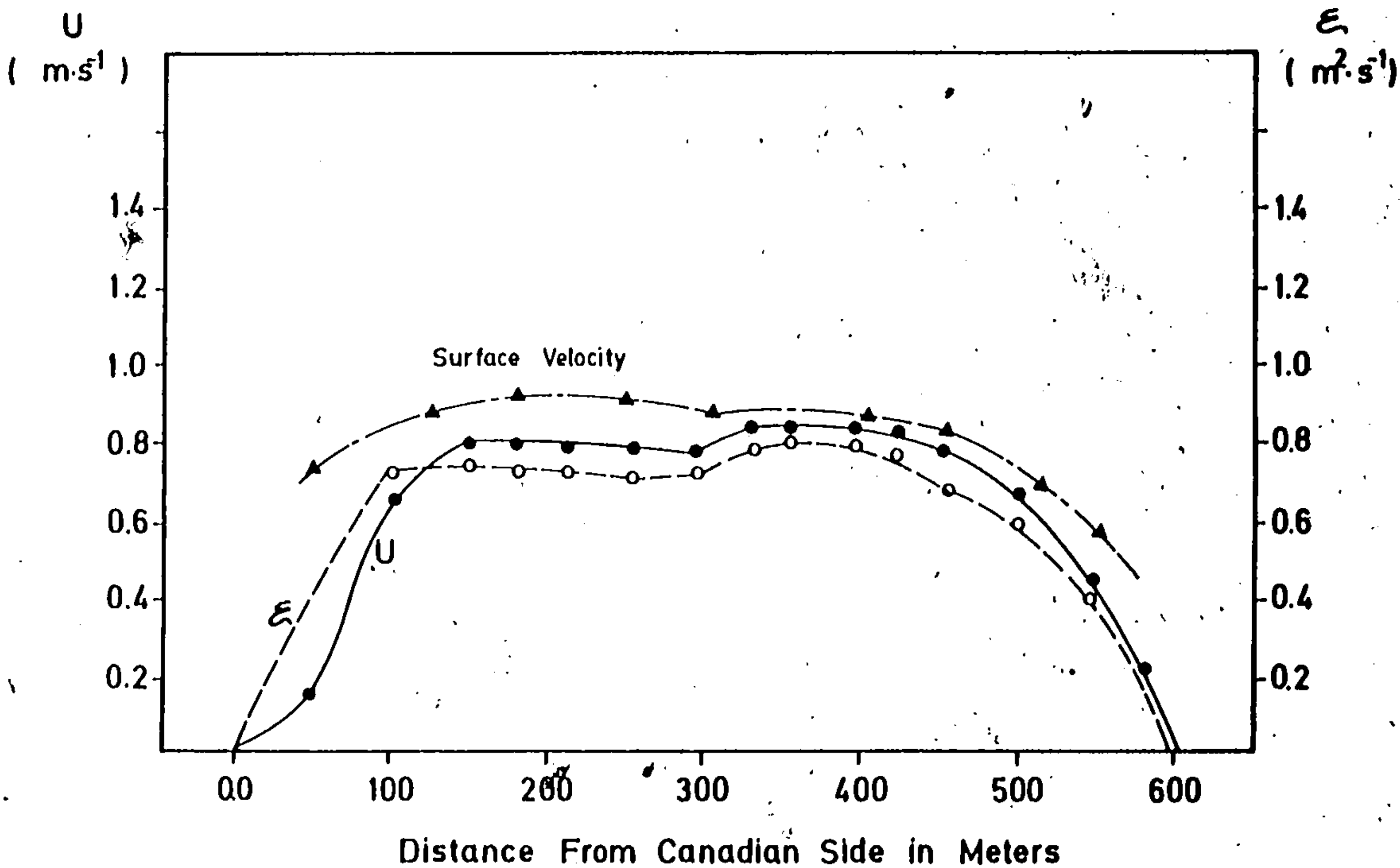

Figure 4.17 Predicted Distribution of Velocity (V), Dispersion Coefficient and Measured Surface Velocity Reach No. 6 in the Detroit River

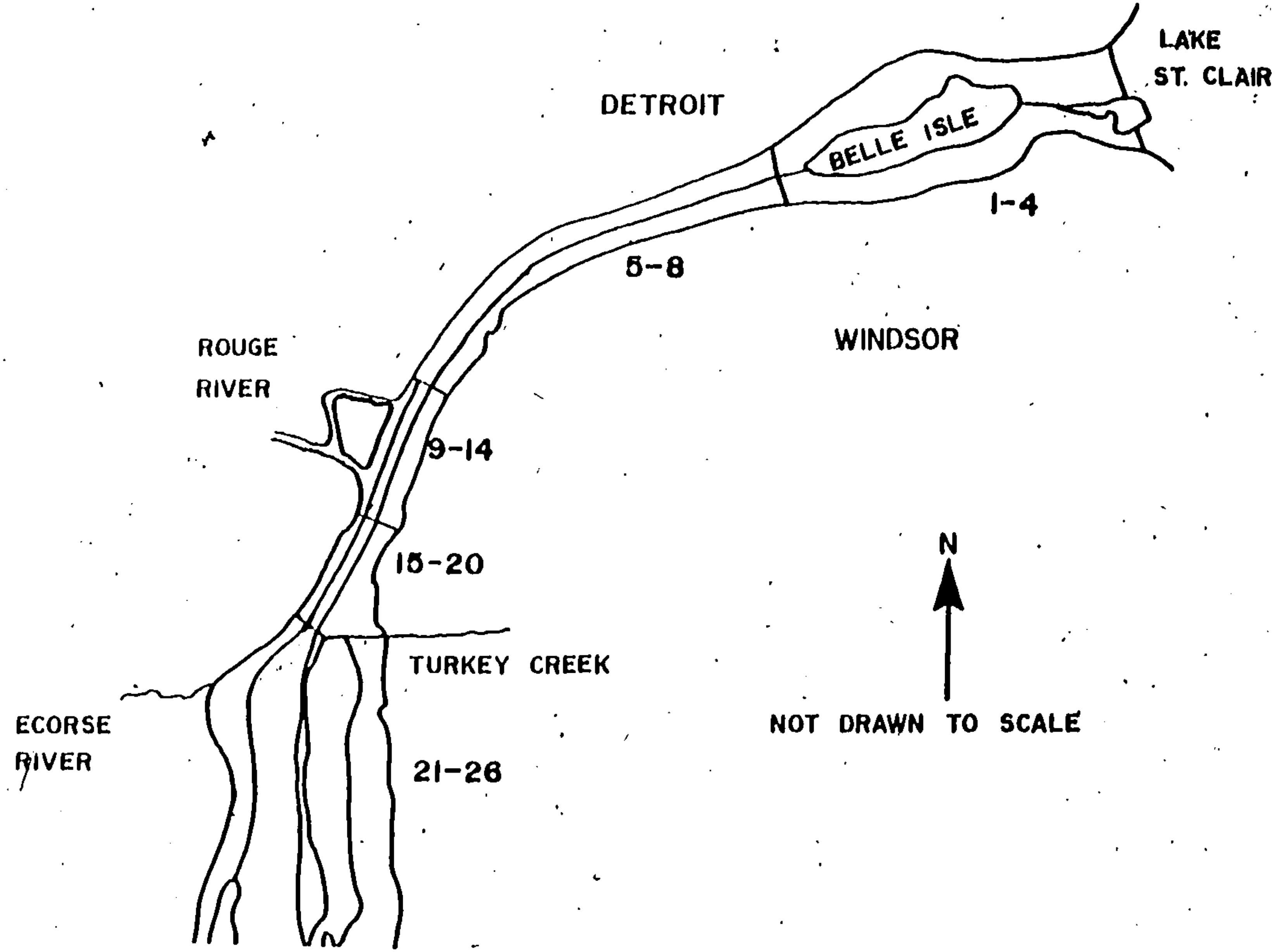

Figure 4.18 Segmentation for the Upper Detroit River

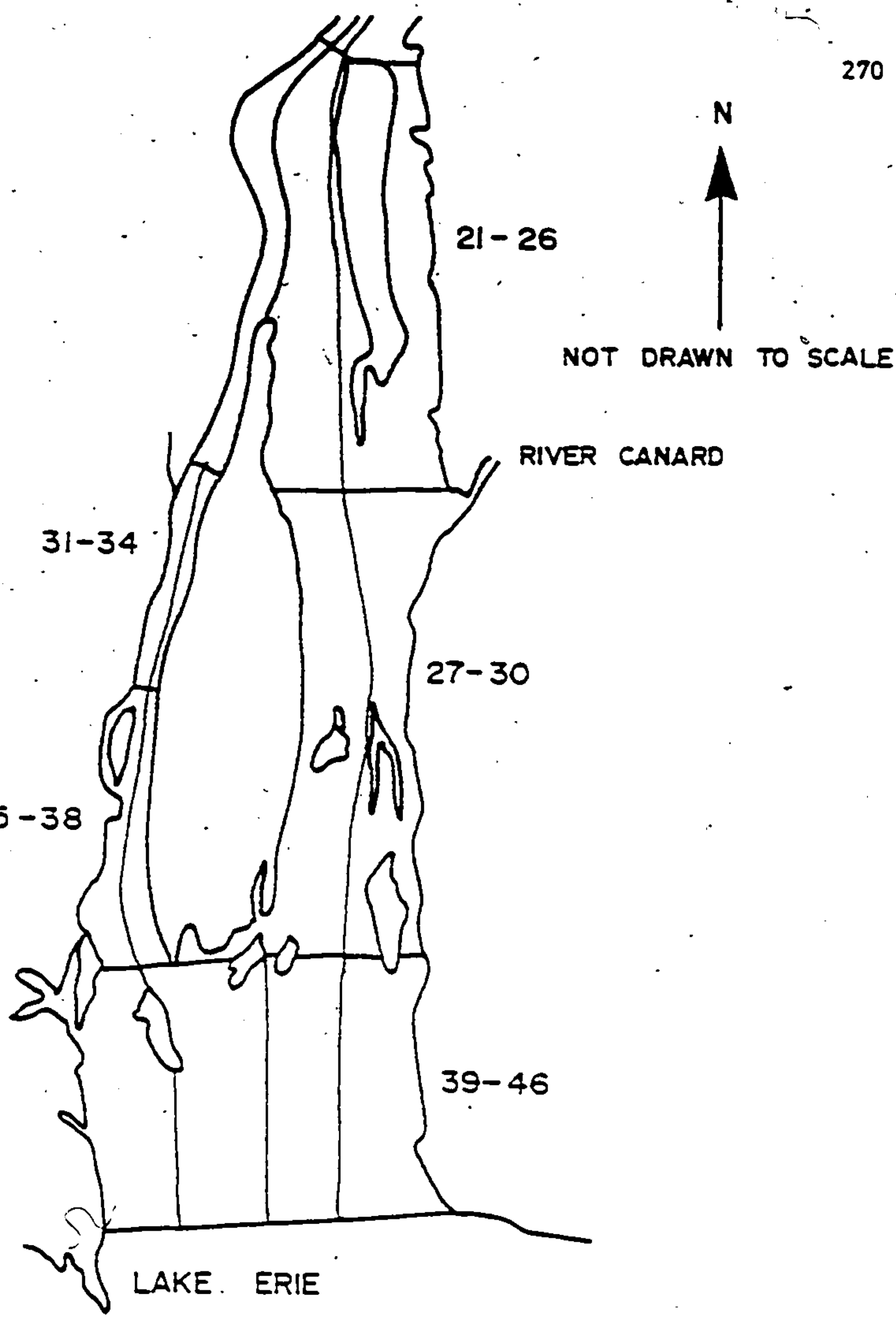

Figure 4.19 Segmentation for the Lower Detroit River

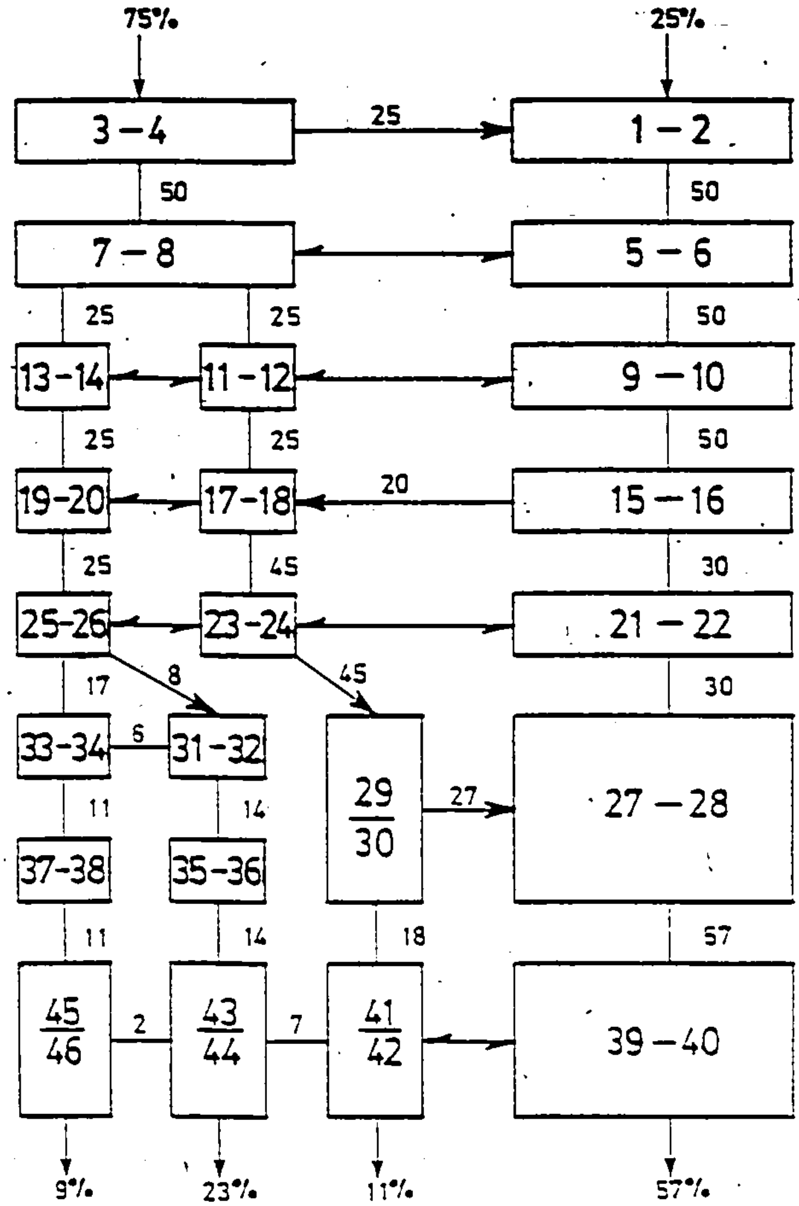

Figure 4.20 Detroit River Model Segment Flow Pattern (all flows are percent of total flow).

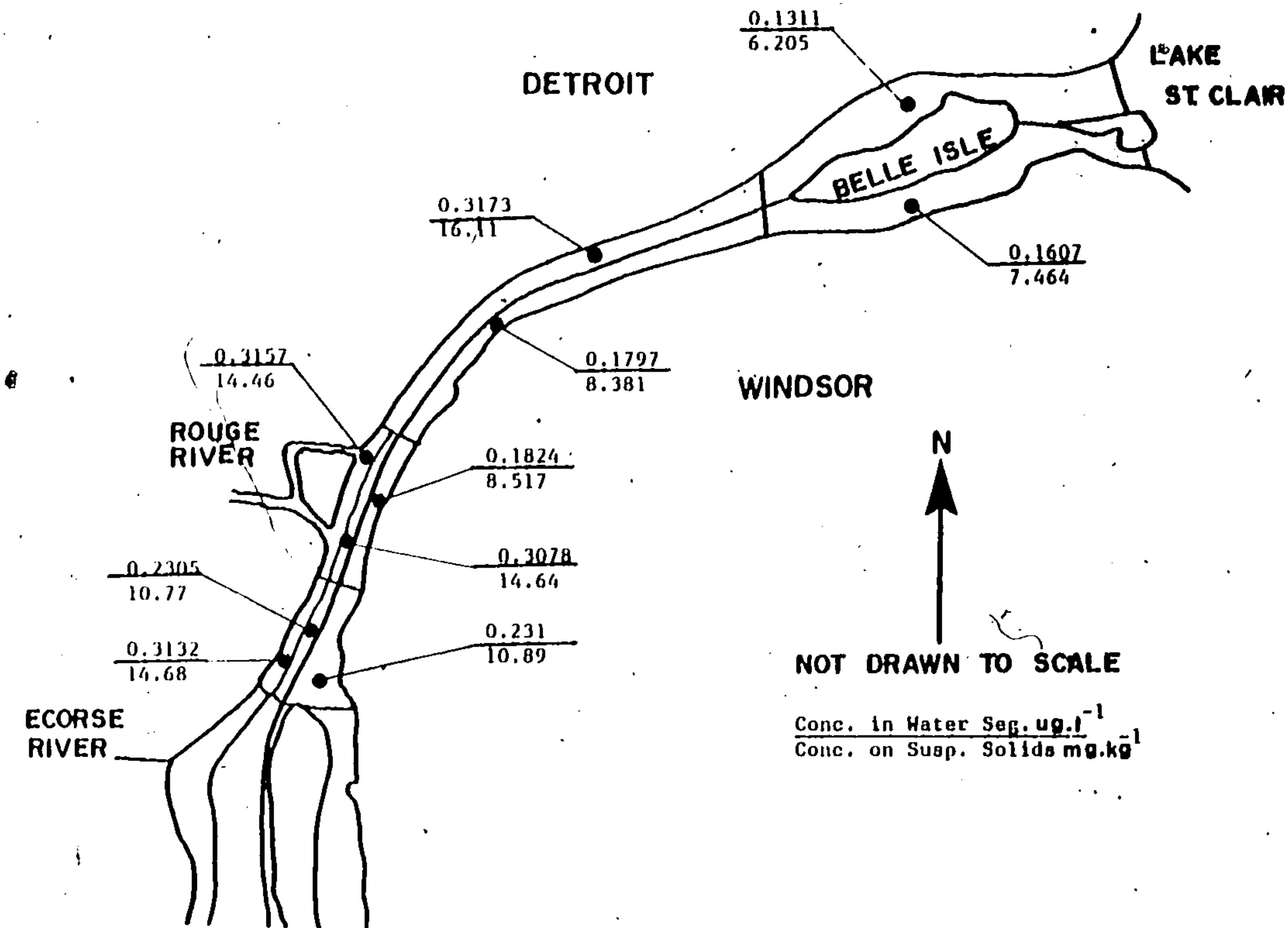

Figure 4.21 The Distribution of Cadmium Concentrations in Water Segments and on Suspended Solids in the Detroit River

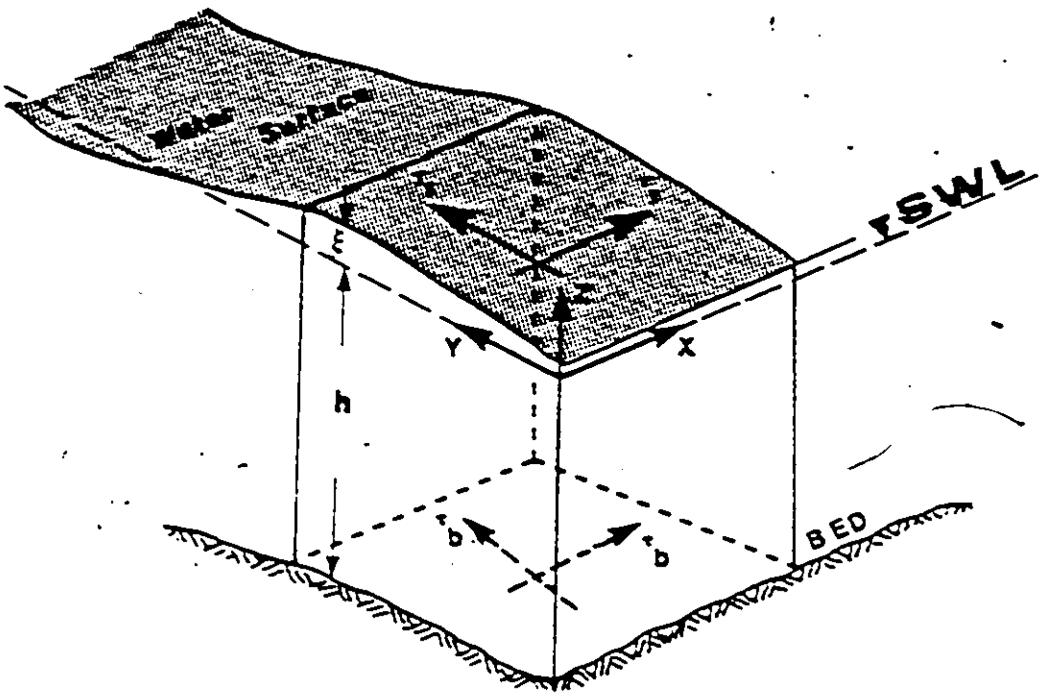

Figure 5.1 Boundary Conditions and Definitions For Shallow Water Flow

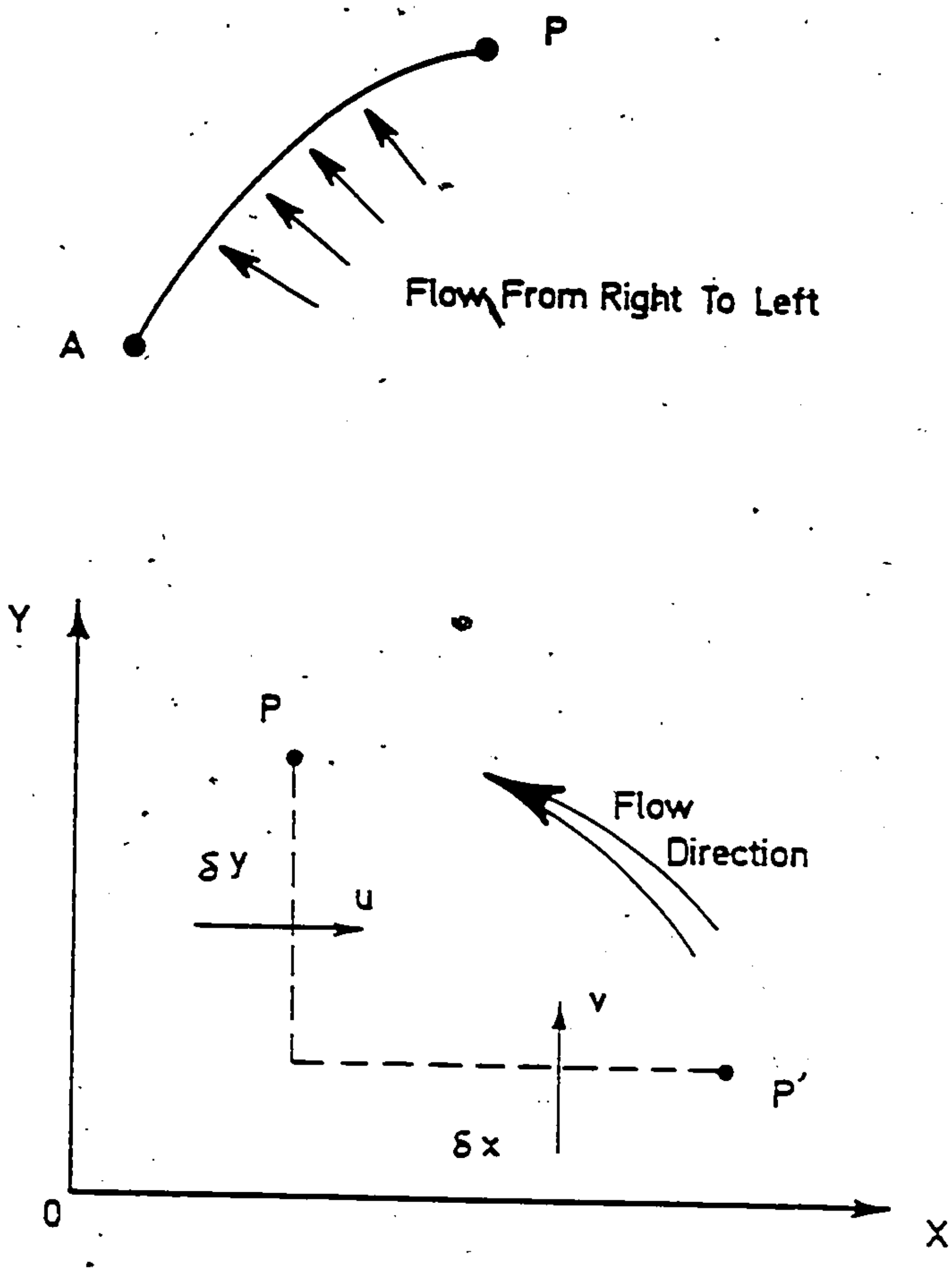

Figure 5.2 Instantaneous Streamlines in a Two Dimensional Flow.

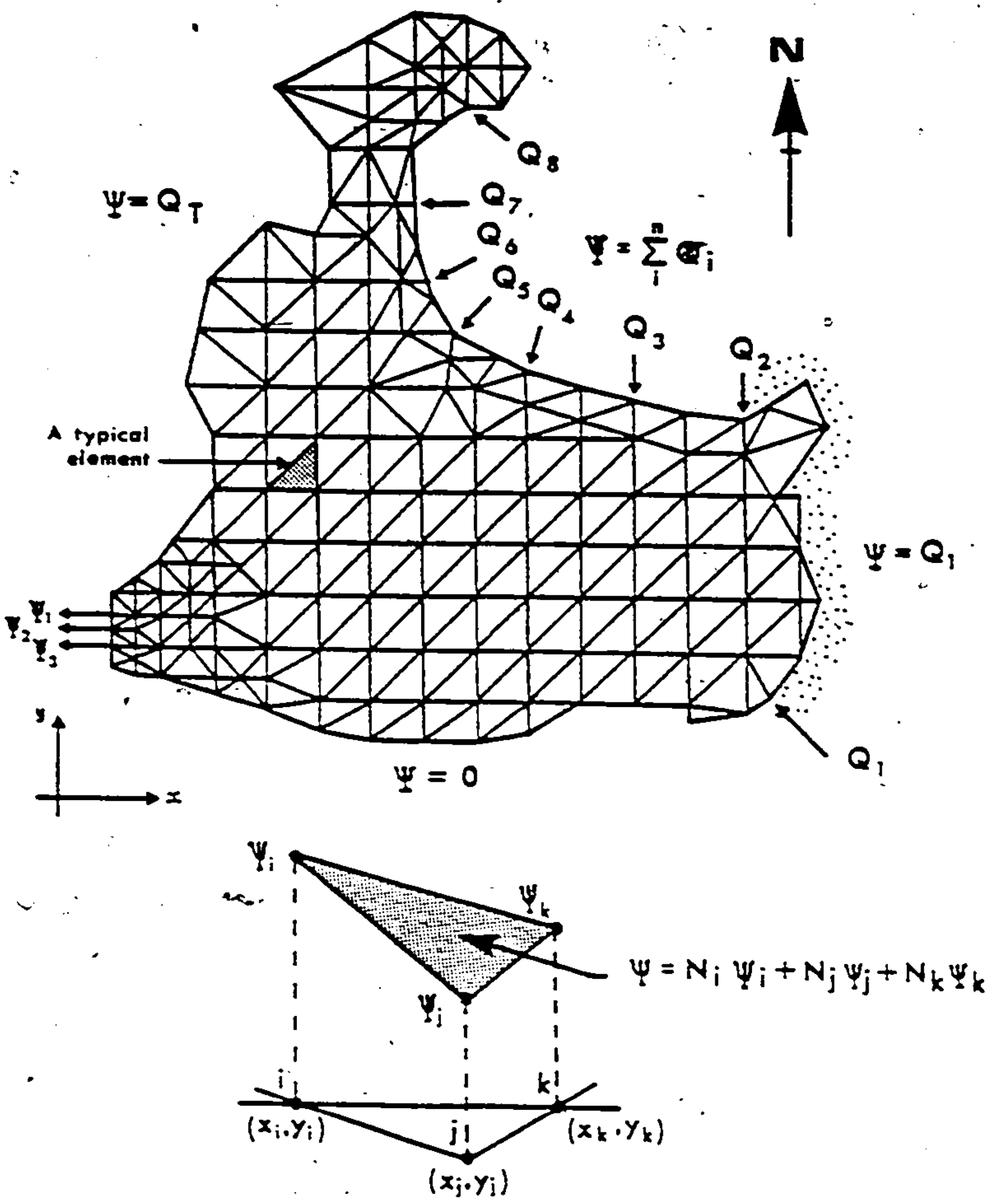

Figure 5.3 The Finite Element Model for Lake St. Clair

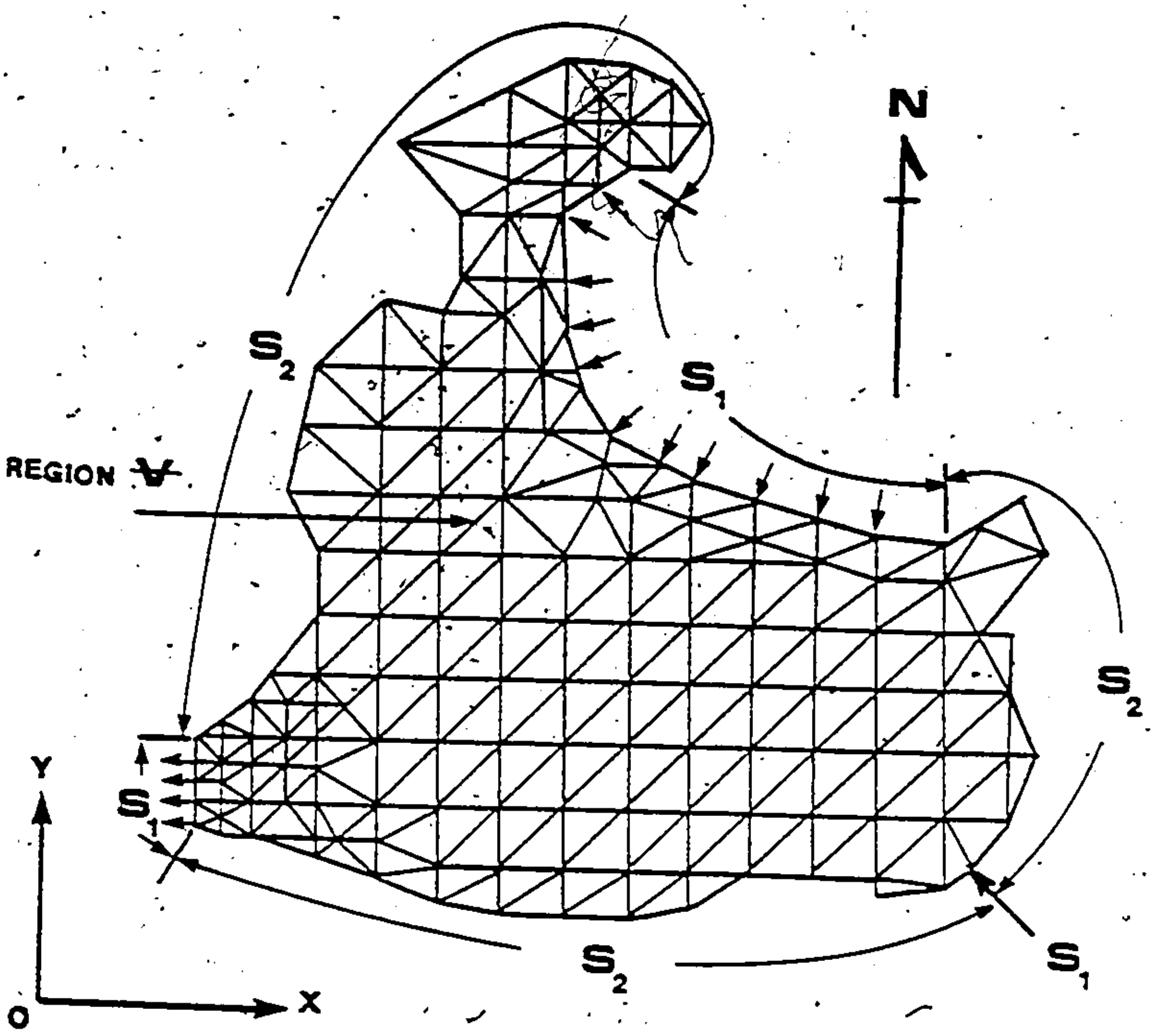

S_1 : Concentration prescribed boundary condition

S_2 : No flux boundary condition

Figure 5.4 Types of Boundary Conditions for the Finite Element Pollutant Model

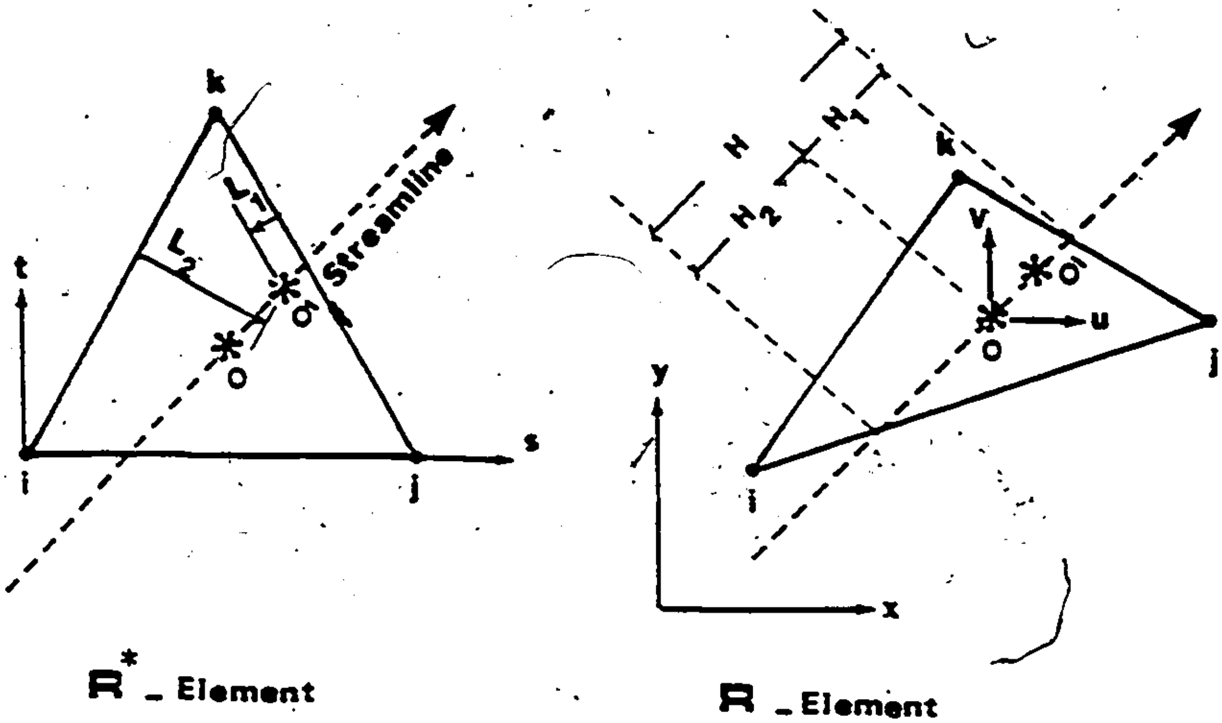

Local co-ordinates (s,t)

Global co-ordinates (x,y)

O Ò : The displacement distance
H_1 : The downstream part
H_2 : The upstream part

Figure 5.5 The Displacement Distance Along The Streamline in R* and R Elements

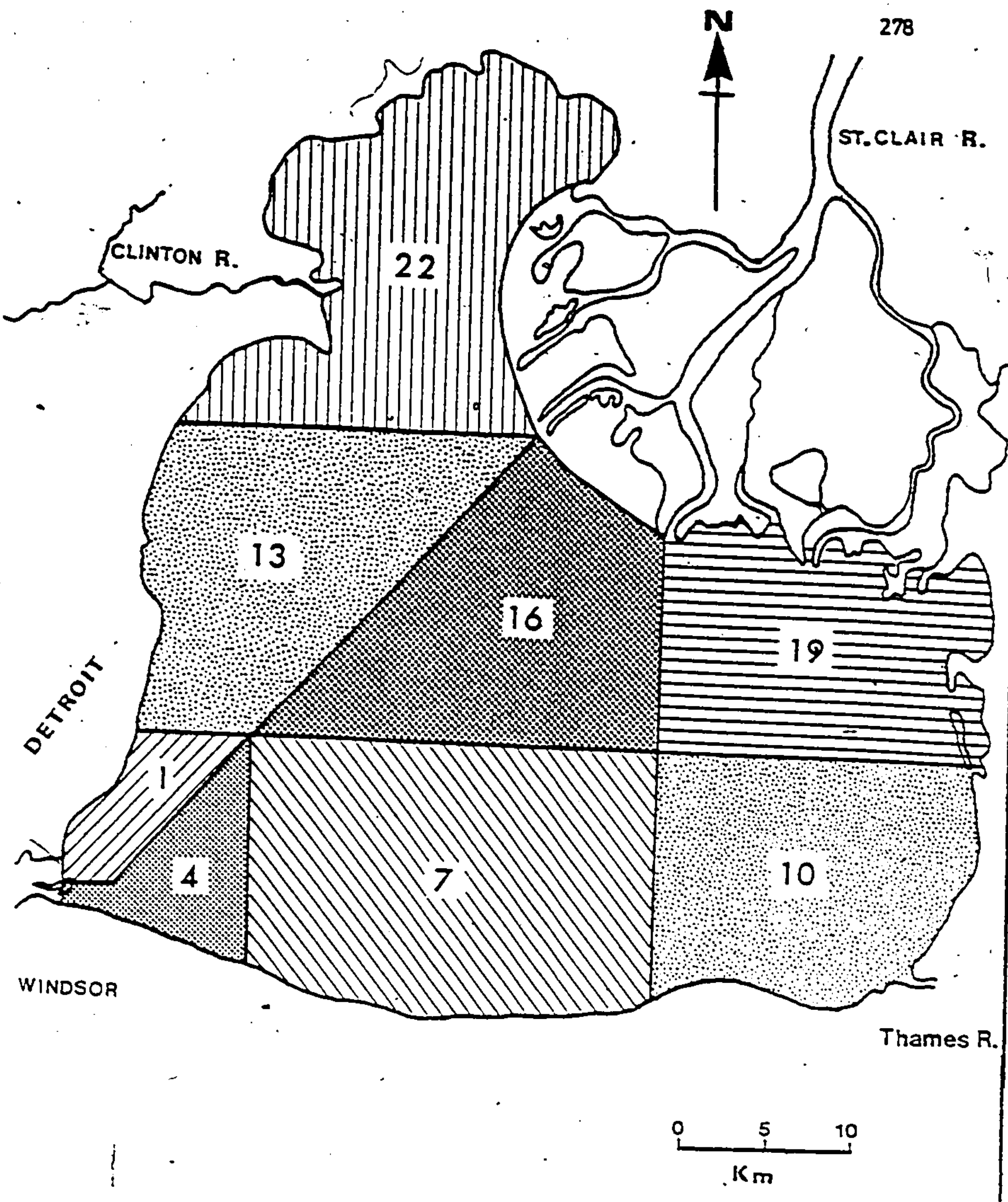

Figure 5.6 Cell Layout for TOXIWASP Model for Lake St. Clair

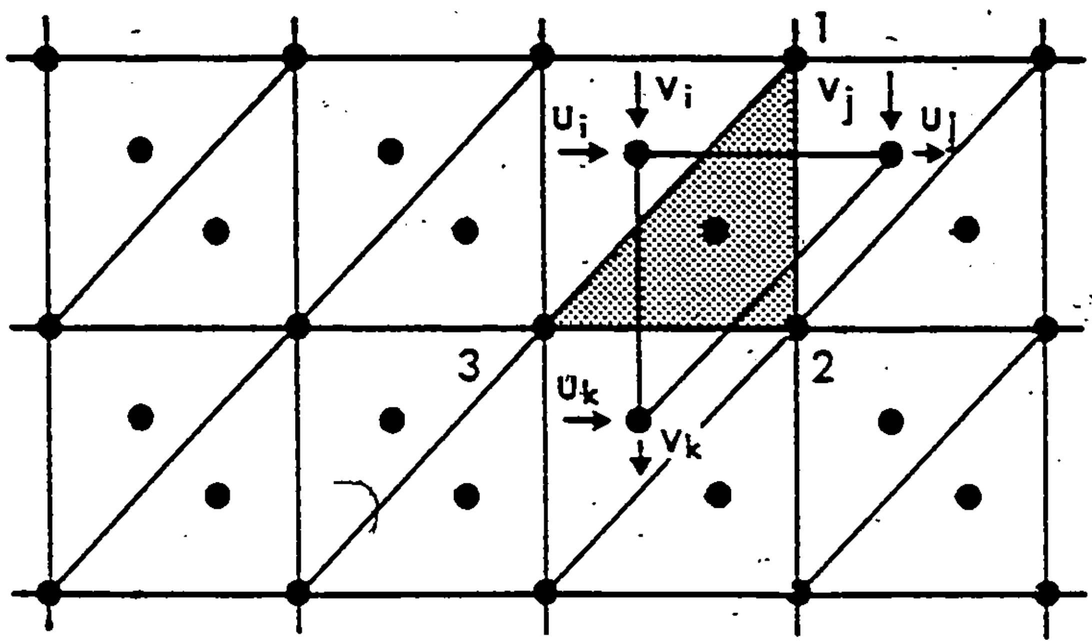

Figure 6.1 Finite Element Scheme with Interlacing Elements

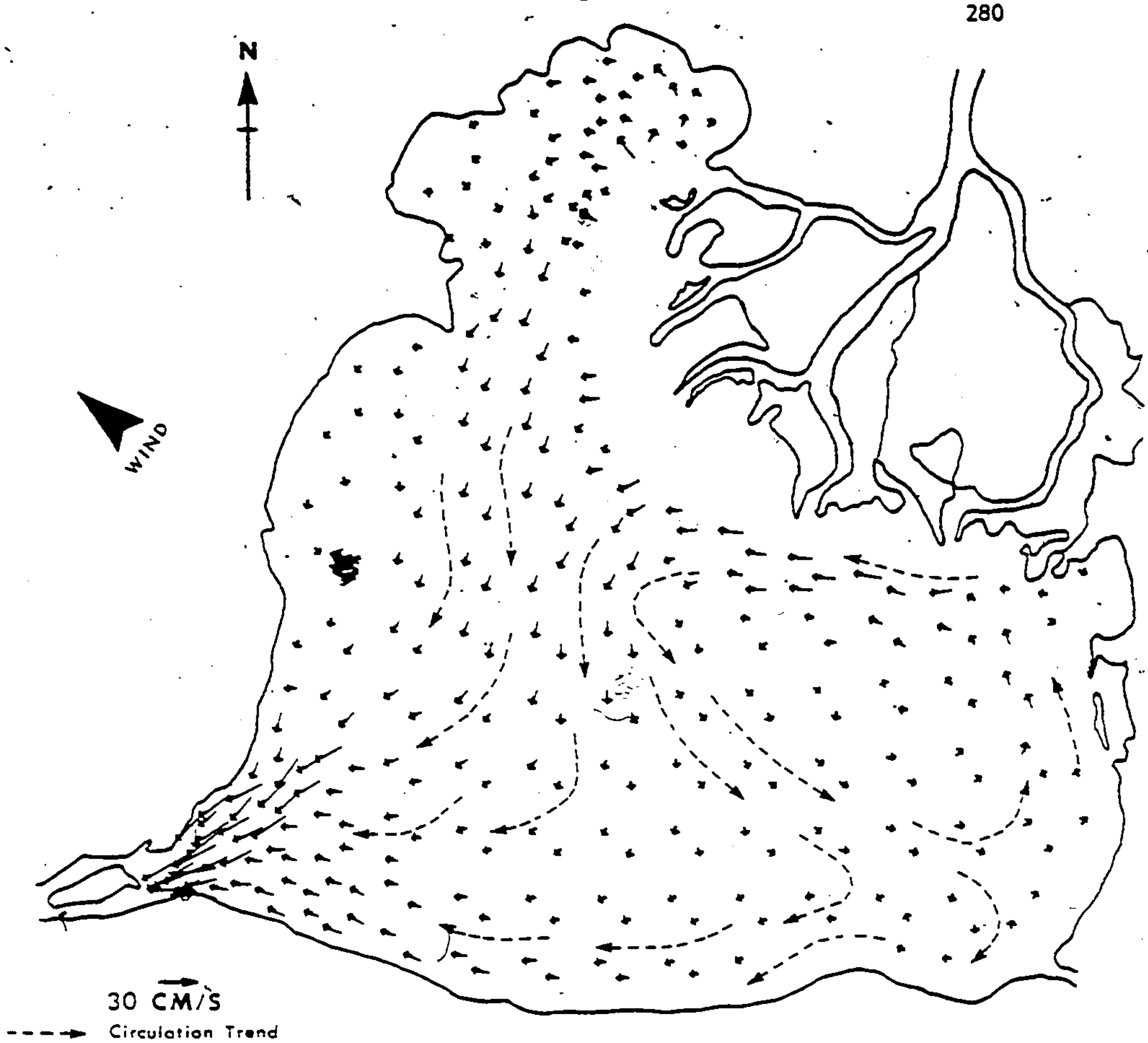

Figure 6.2 Vertically Integrated Velocities for 8 $m \cdot s^{-1}$ Wind Speed From Southwest Direction.

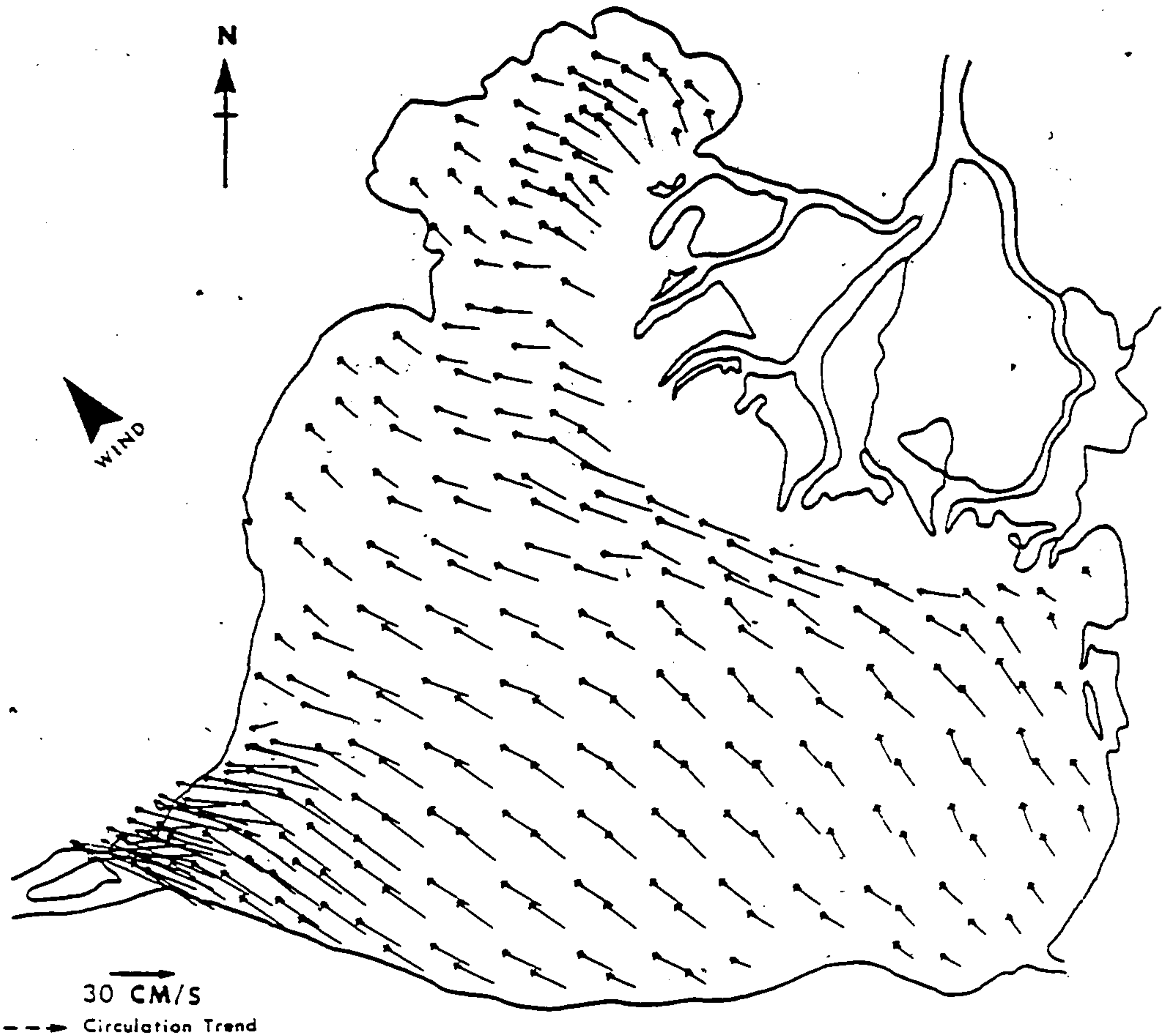

Figure 6.3 Surface Velocities For 8 $m \cdot s^{-1}$ Wind Speed from Southwest Direction

Figure 6.4 Velocities 0.2 Depth Below Water Surface for
8 $m \cdot s^{-1}$ Wind Speed from Southwest Direction

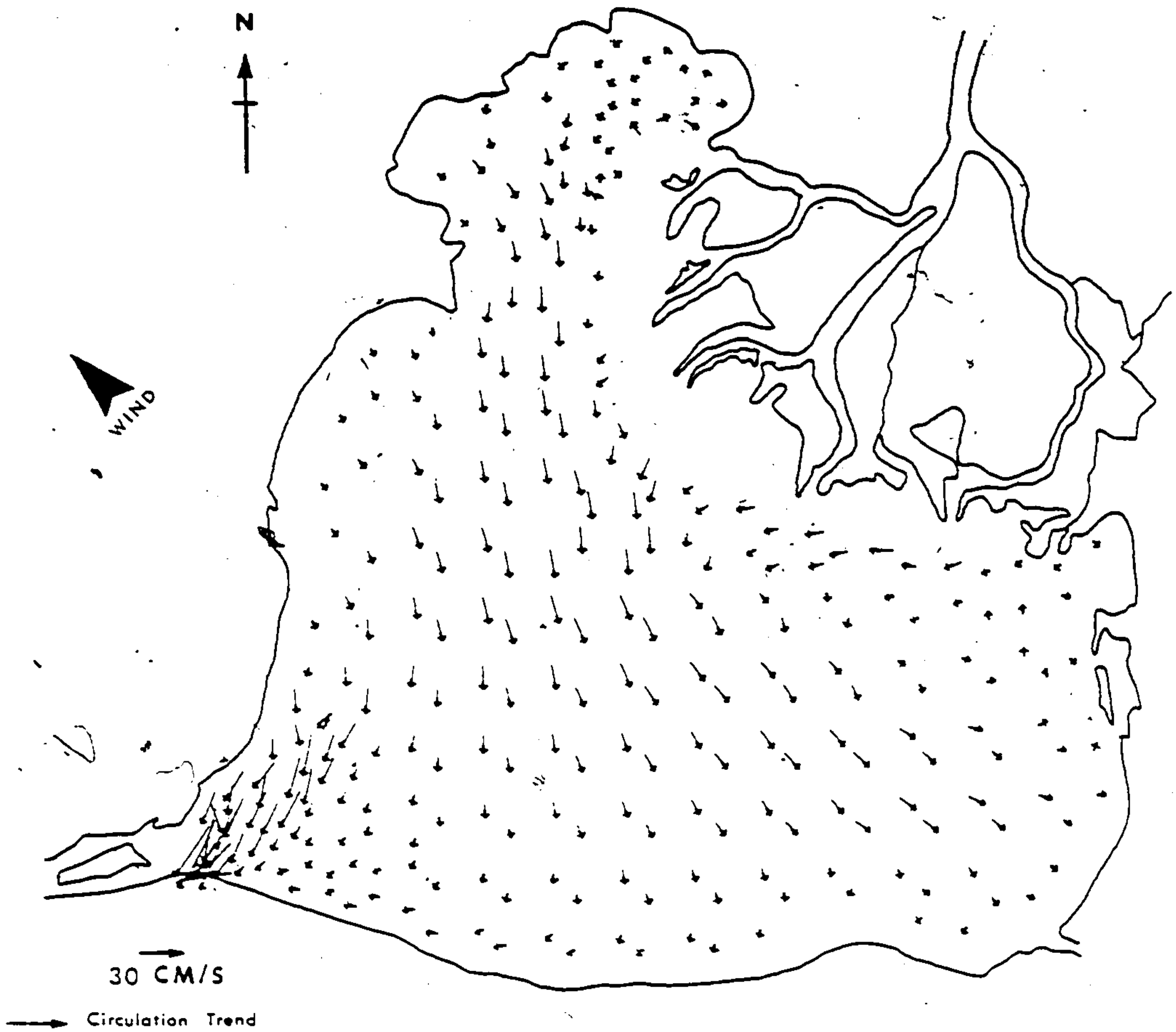

Figure 6.5 Velocities 0.6 Depth Below Water Surface for 8 $m \cdot s^{-1}$ Wind Speed from Southwest Direction

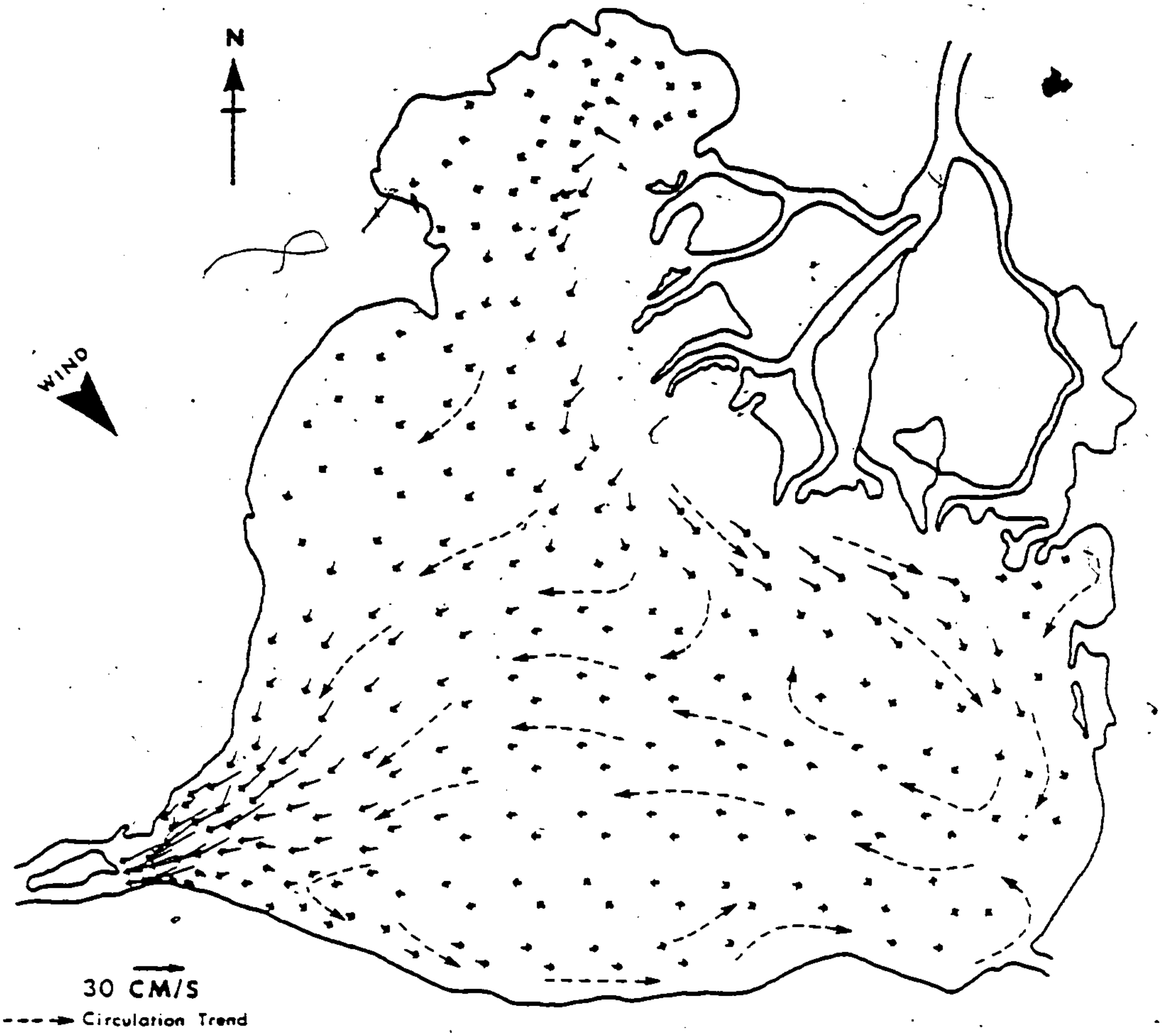

Figure 6.6 Vertically Integrated Velocities for 8 $m \cdot s^{-1}$ Wind Speed from Northwest Direction

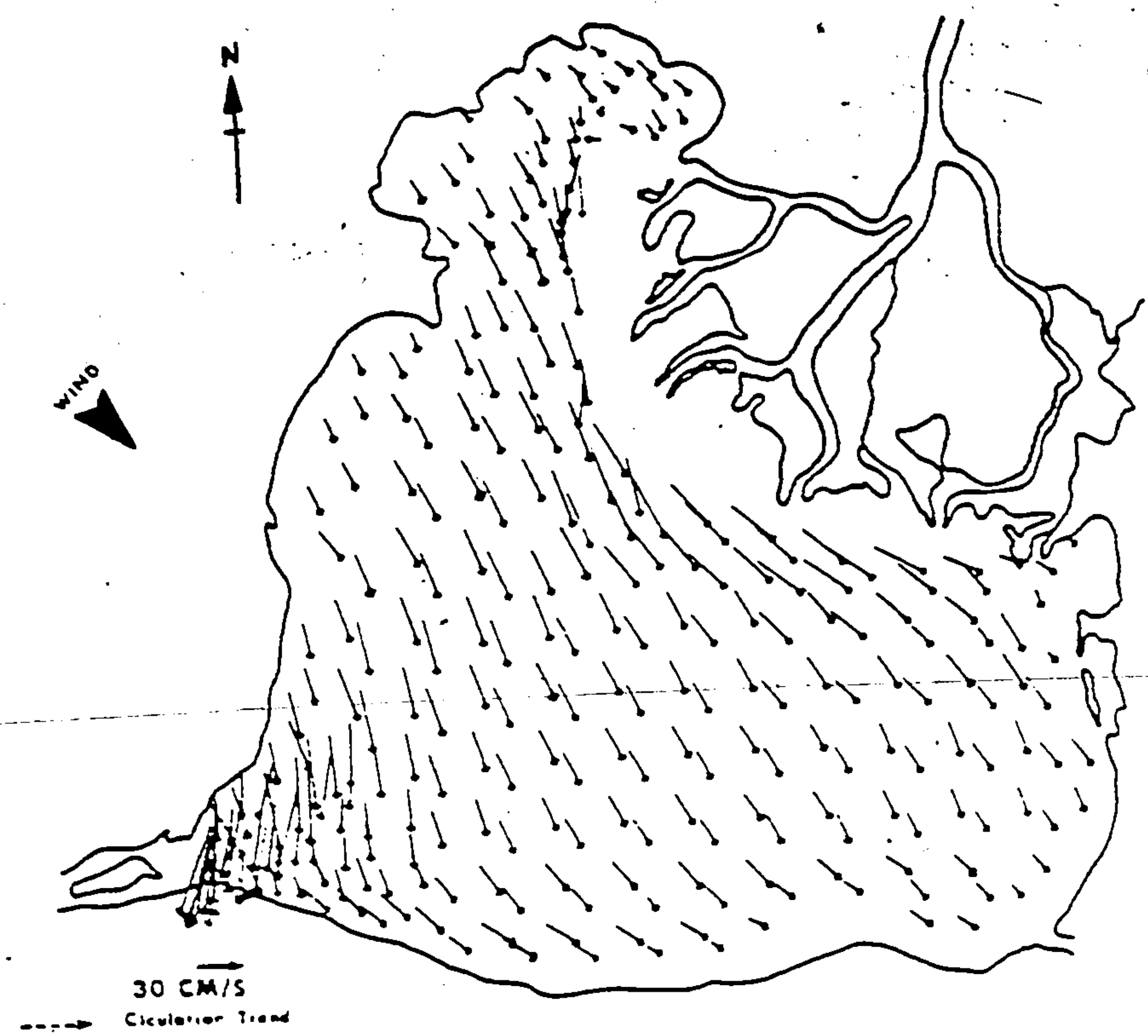

Figure 6.7 Surface Velocities for 8 m s^{-1} Wind Speed from Northwest Direction

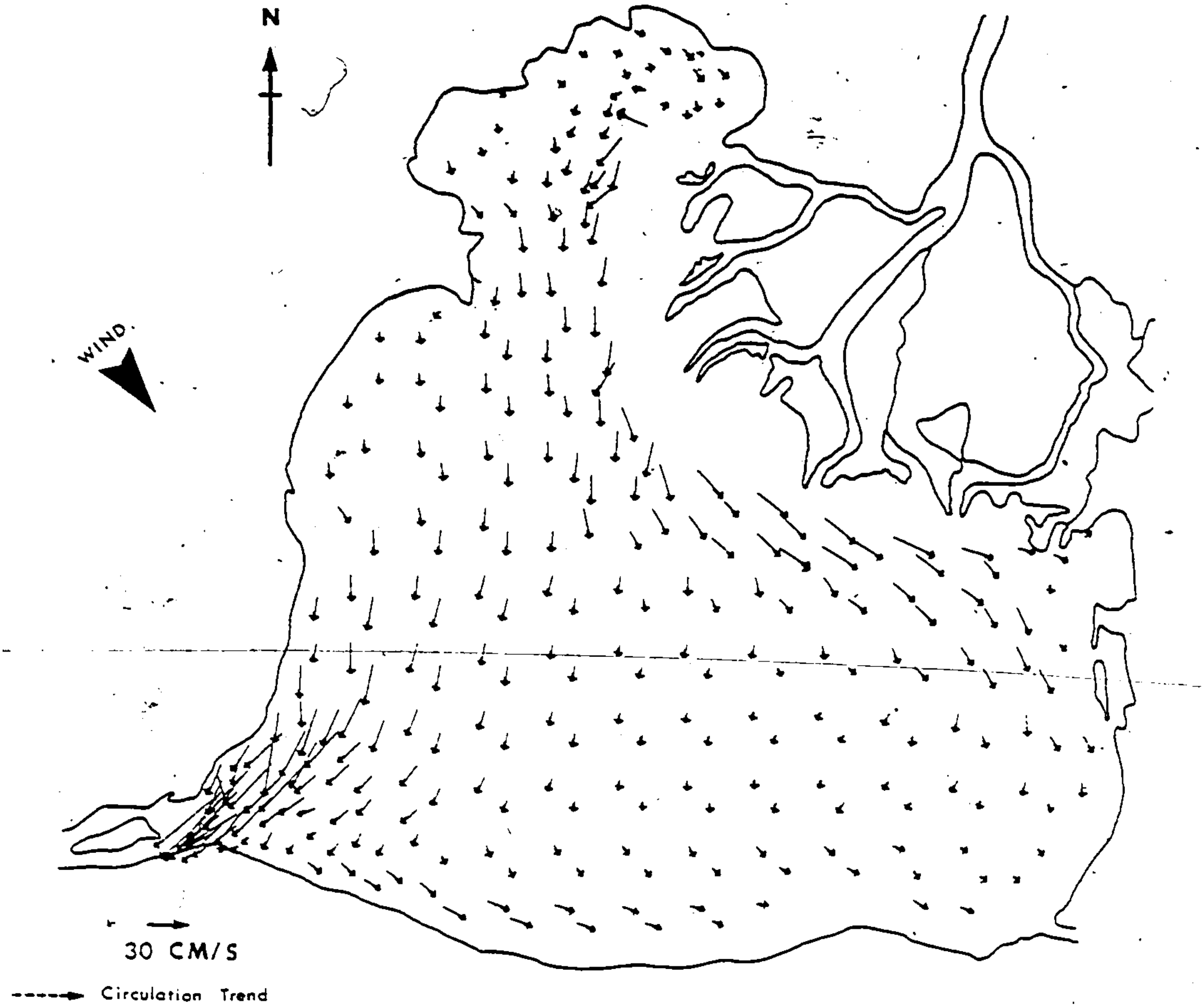

Figure 6.8 Velocities 0.2 Depth Below Water Surface for 8 $m \cdot s^{-1}$ Wind Speed from Northwest Direction

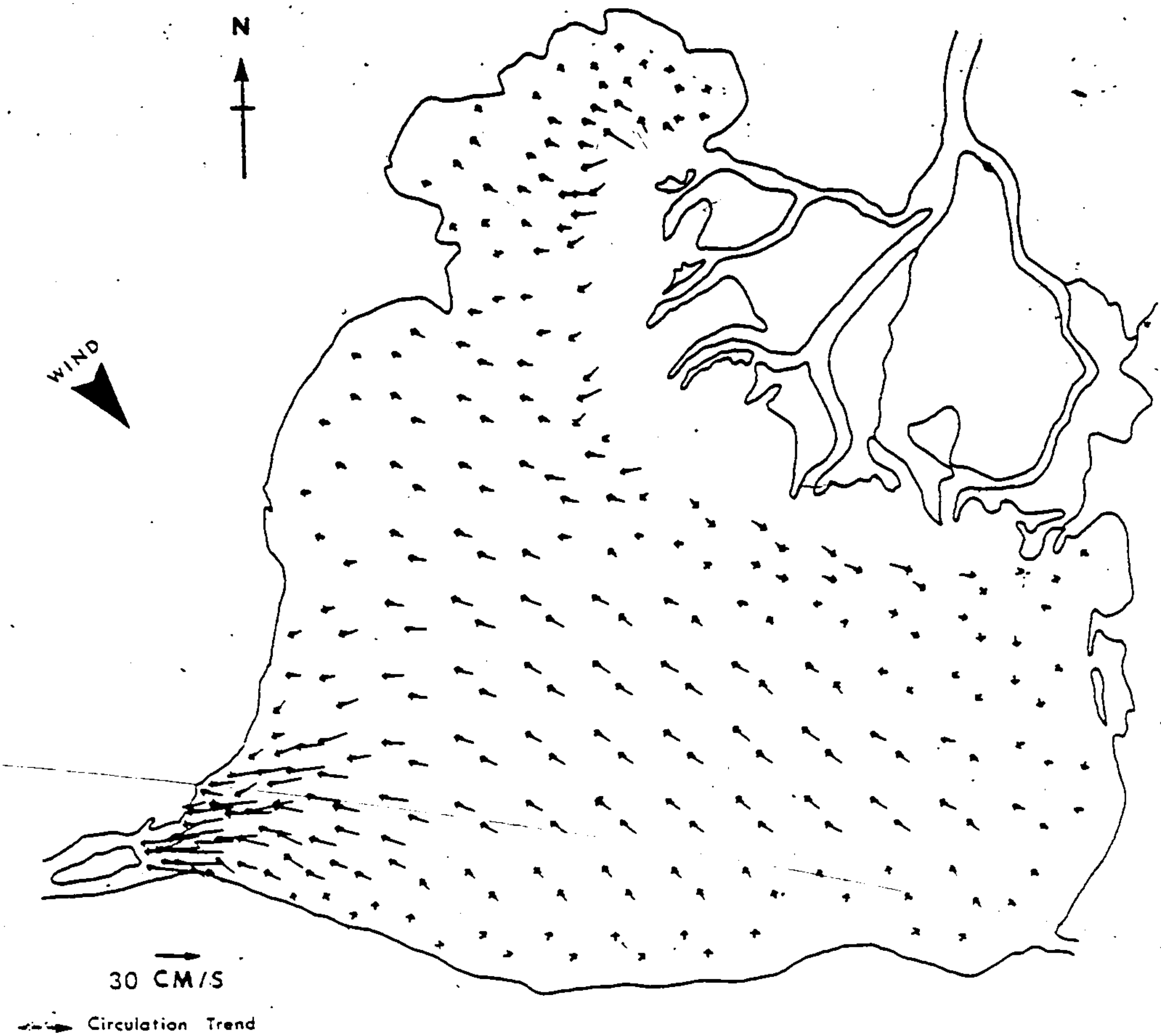

Figure 6.9 Velocities 0.6 Depth Below Water Surface for 8 $m \cdot s^{-1}$ Winds Speed from Northwest Direction

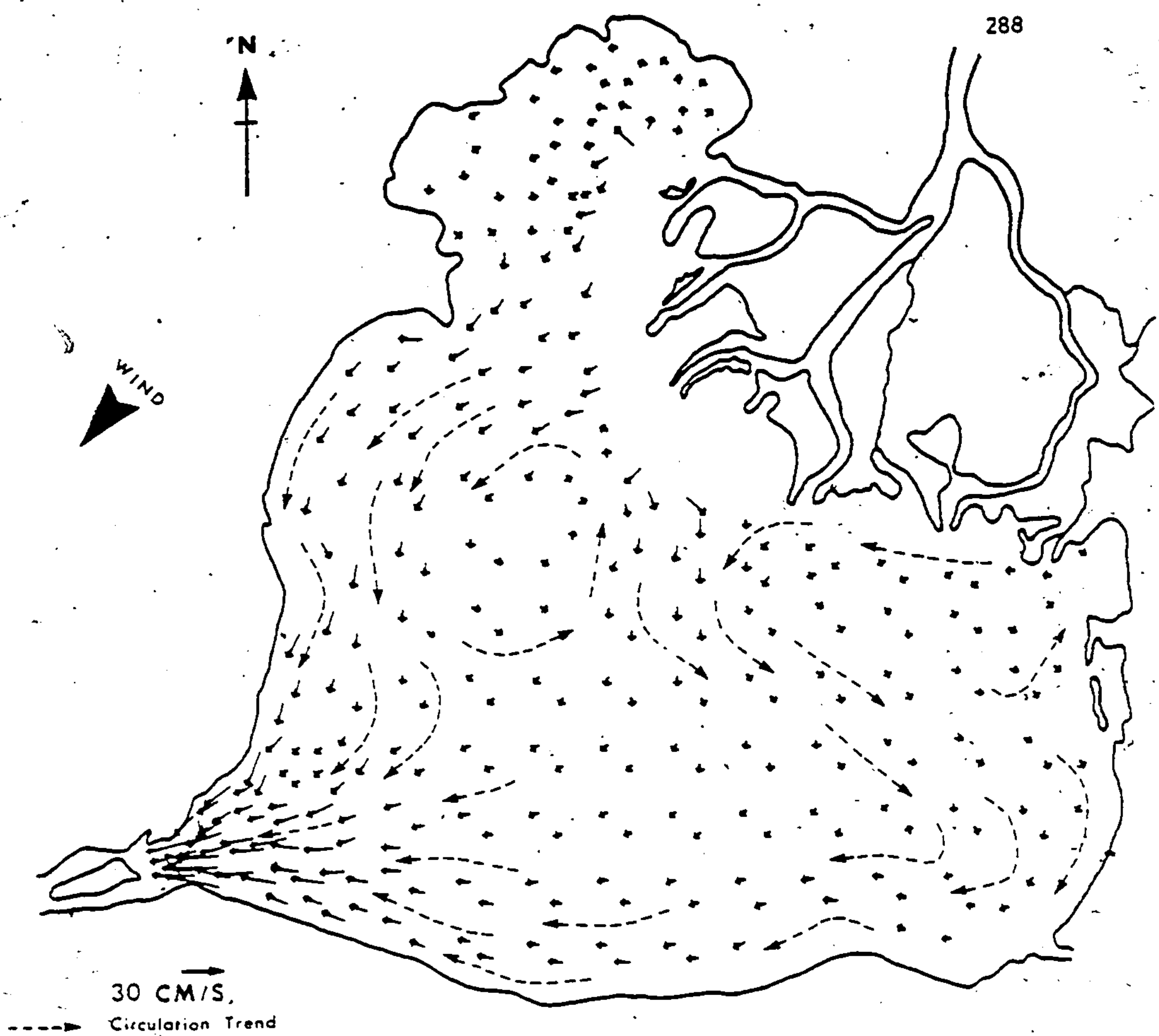

Figure 6.10 Vertically Integrated Velocities for 8 $m \cdot s^{-1}$ Wind Speed from Northeast Direction

Figure 6.11 Surface Velocities for 8 m·s^{-1} Wind Speed from Northeast Direction

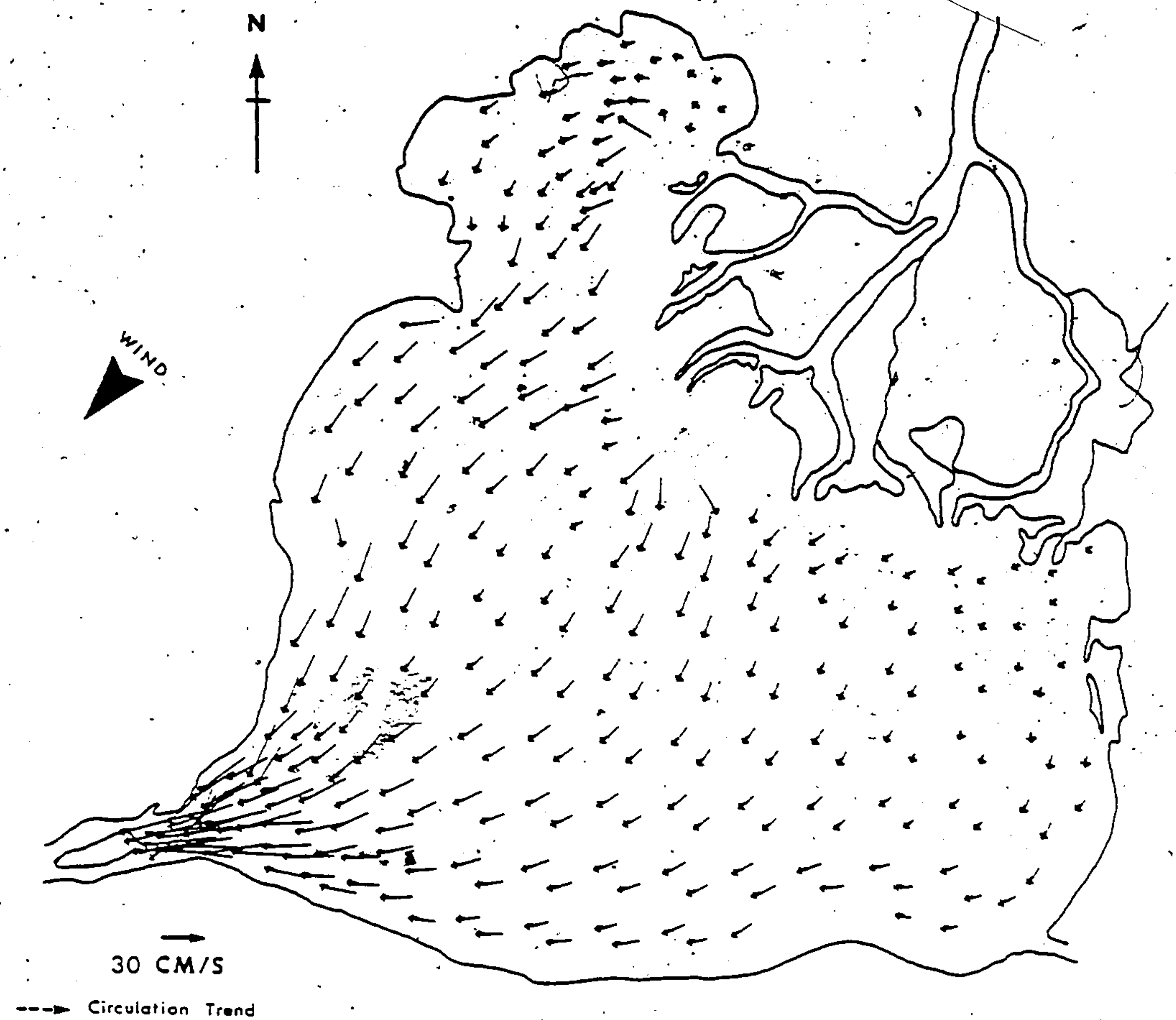

Figure 6.12 Velocities 0.2 Depth Below Water Surface from 8 $m \cdot s^{-1}$ Wind Speed from Northeast Direction

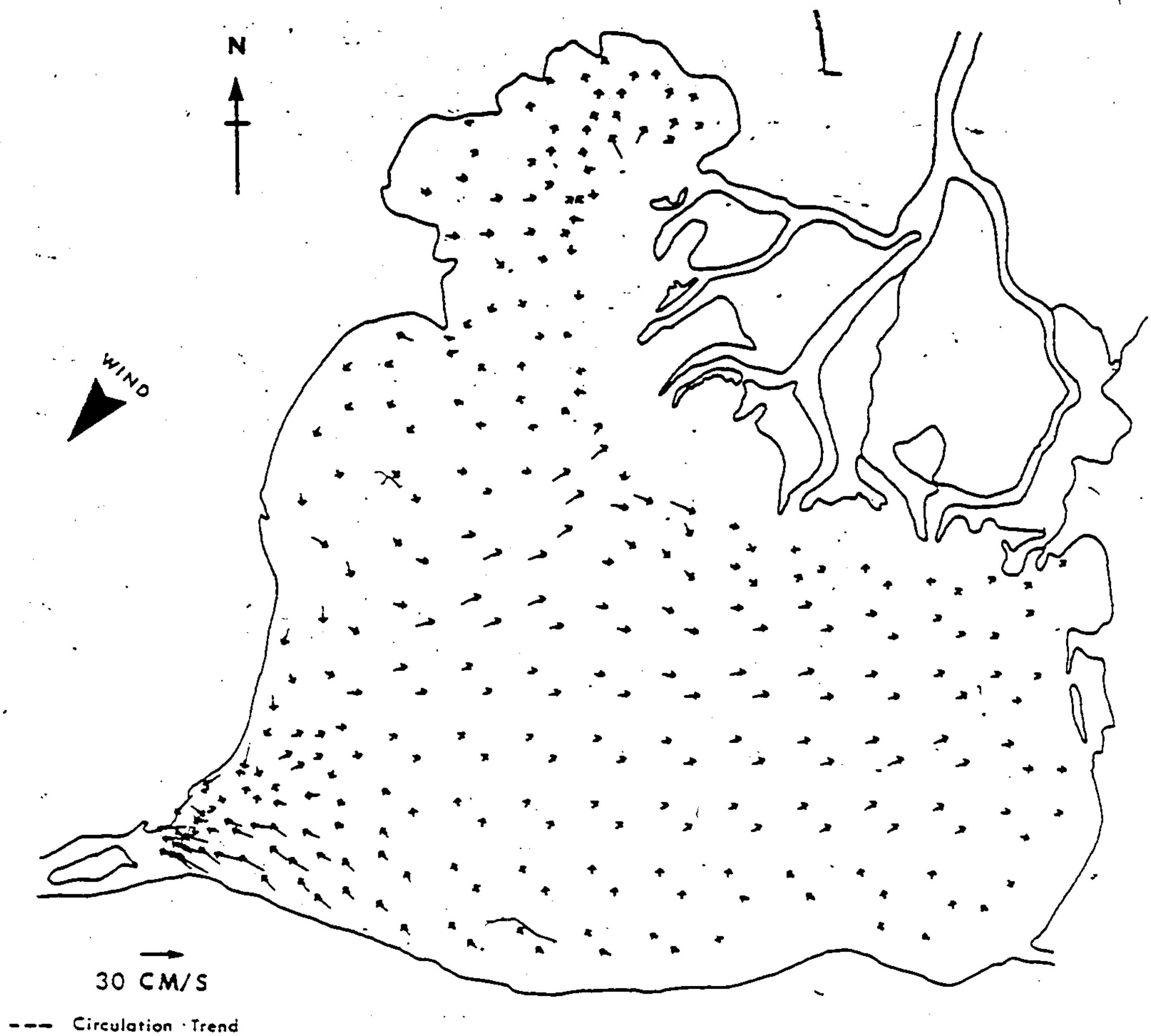

Figure 6.13 Velocities 0.6 Depth Below Water Surface for 8 $m \cdot s^{-1}$ Wind Speed from Northeast Direction

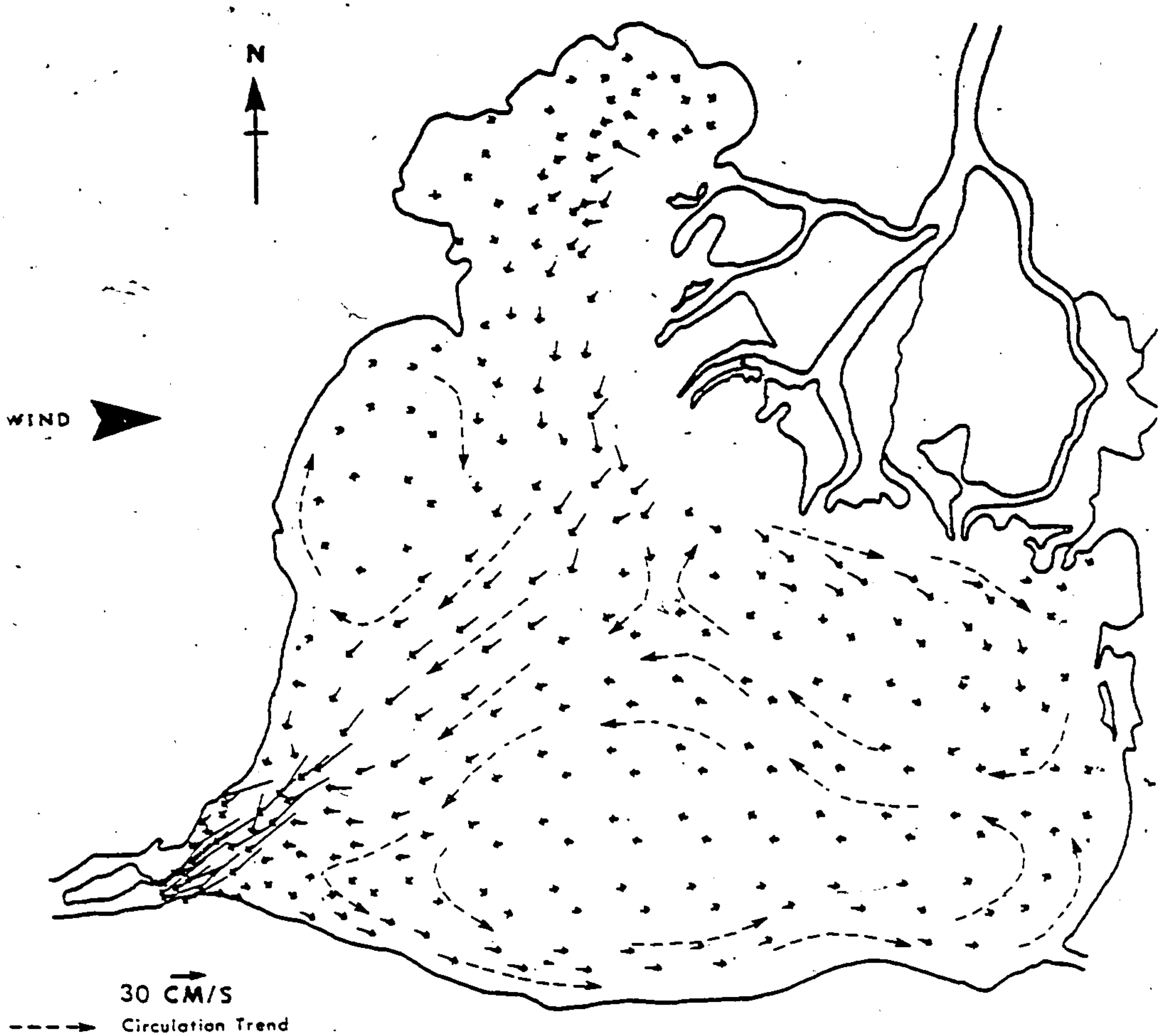

Figure 6.14 Vertically Integrated Velocities for 8 $m \cdot s^{-1}$ Wind Speed from West Direction

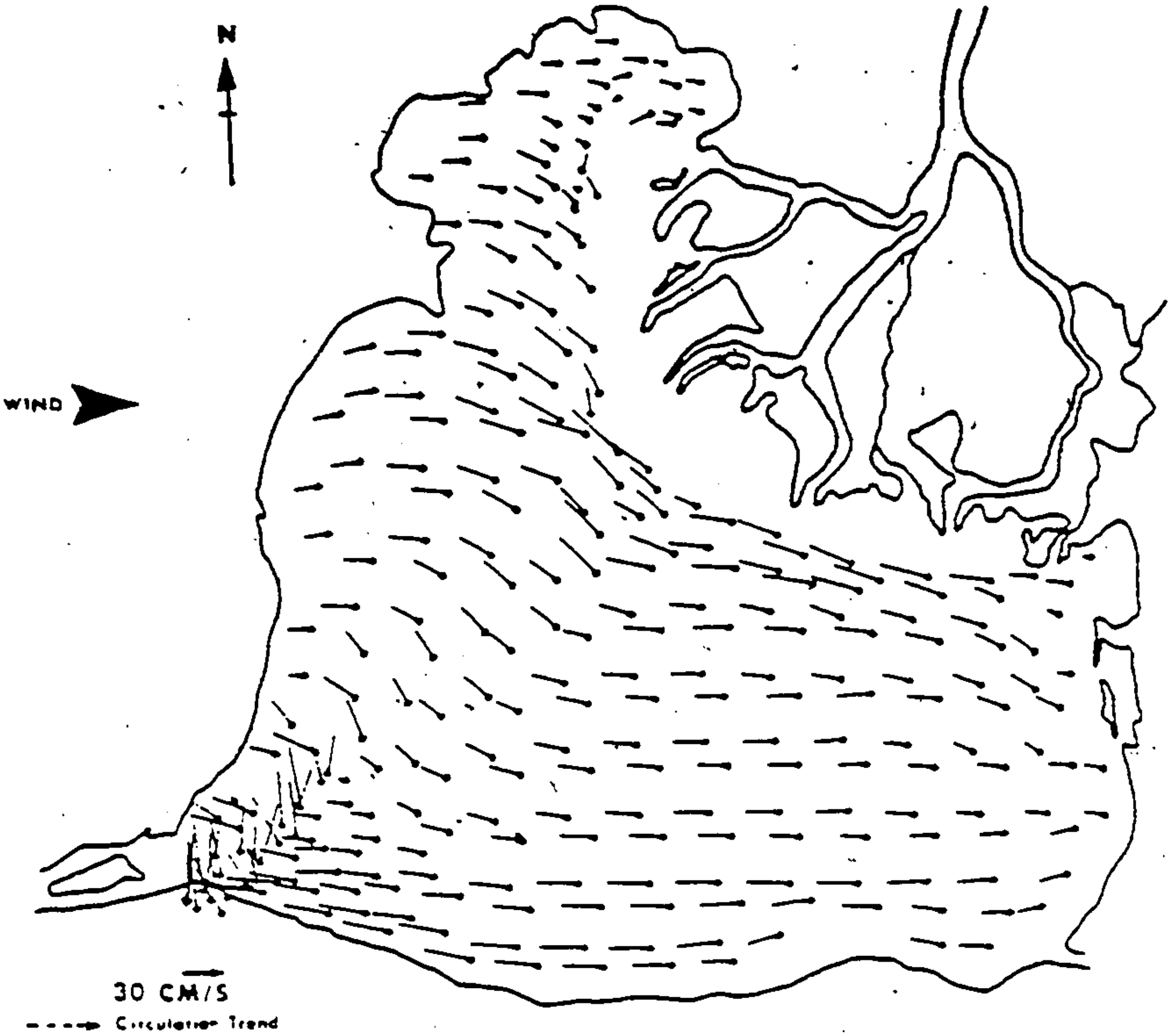

Figure 6.15 Surface Water Velocities for 8 $m \cdot s^{-1}$
Wind Speed from West Direction

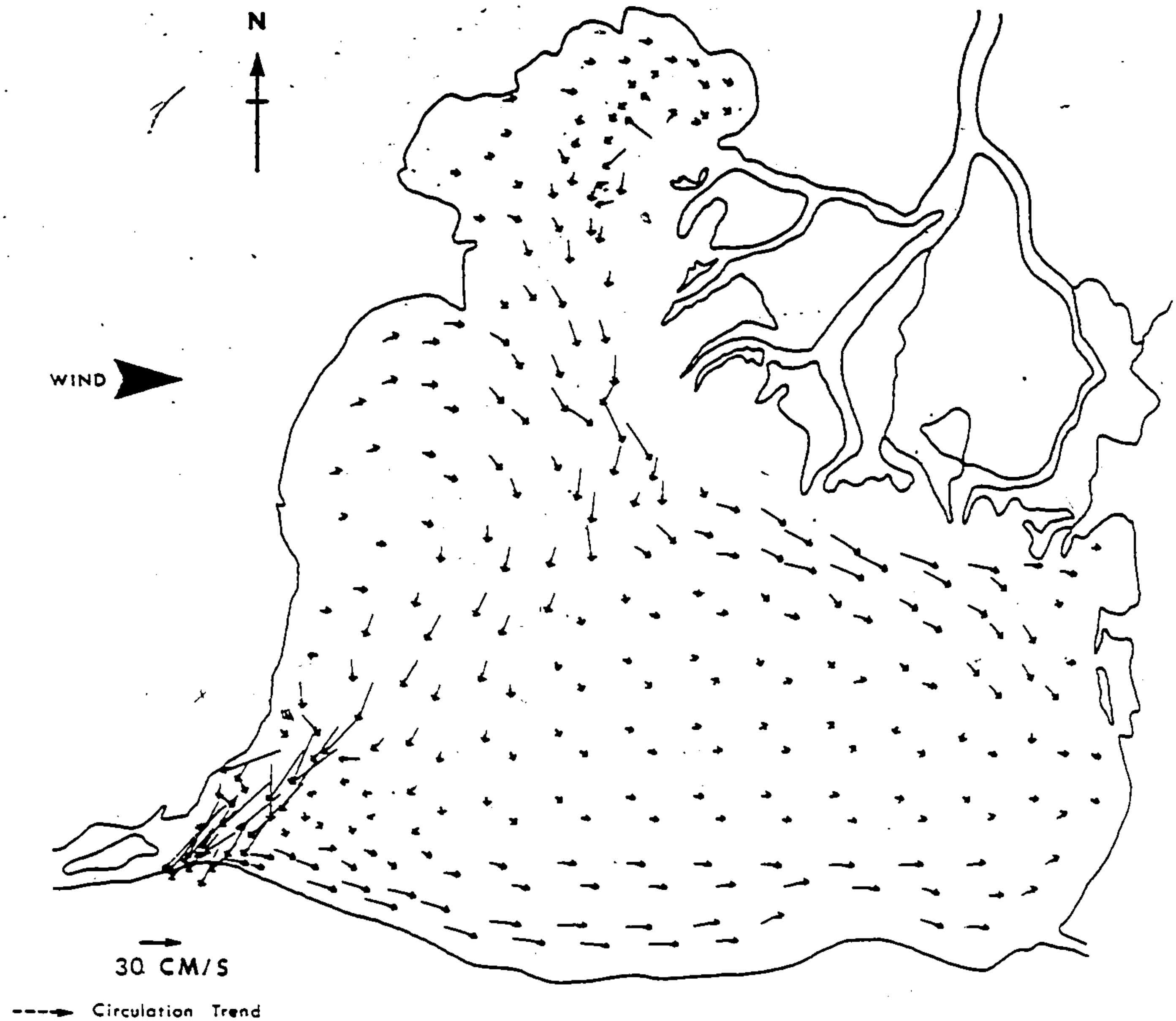

Figure 6.16 Velocities 0.2 Depth below Water Surface for $8\ m \cdot s^{-1}$ Wind Speed from West Direction

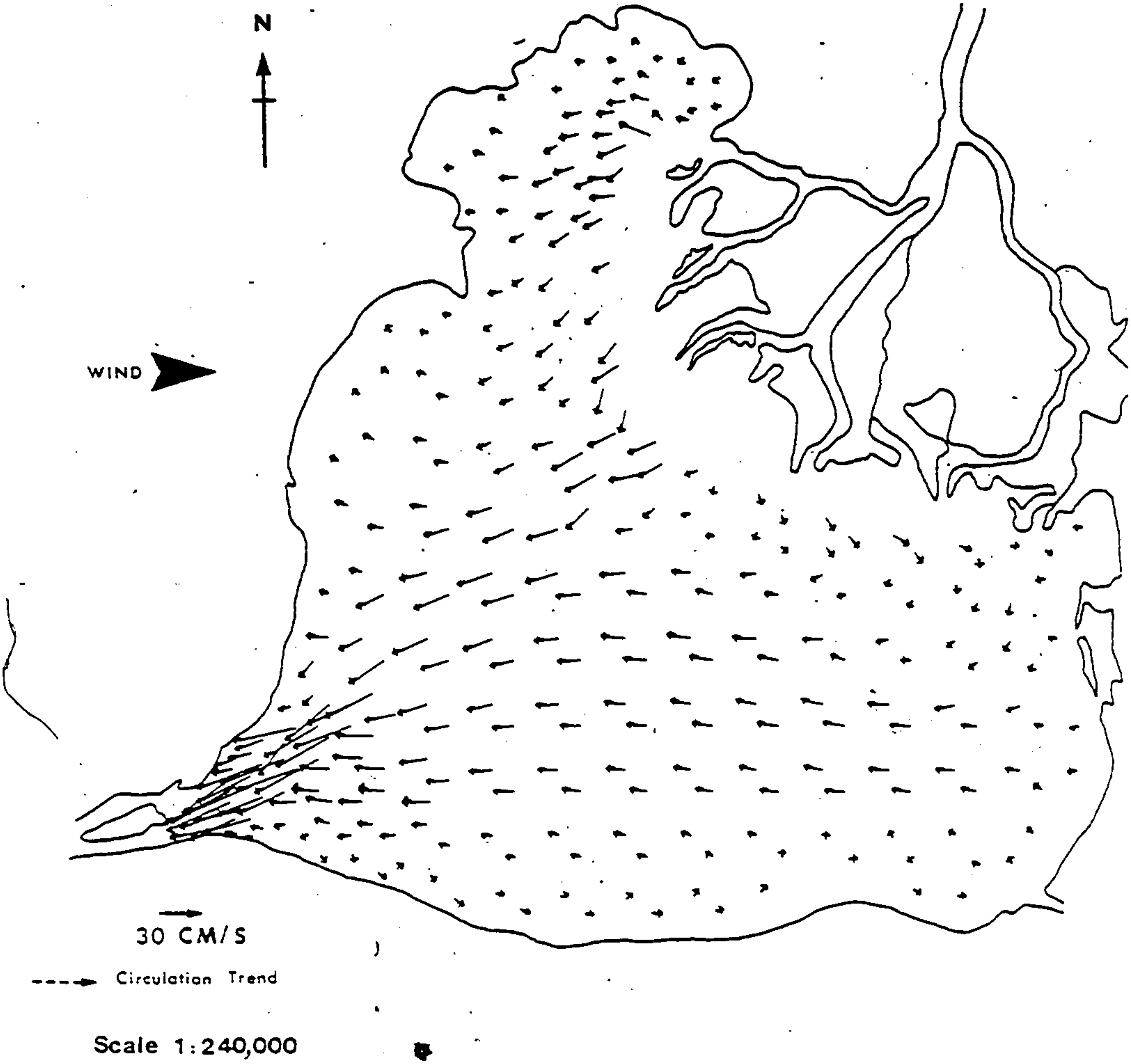

Figure 6.17 Velocities 0.6 Depth Below Water Surface for $8\ m\cdot s^{-1}$ Wind Speed from West Direction

Element 36   s = 0.3, τ_x = 3.5, τ_y = 0.0,   H = 6.7 m

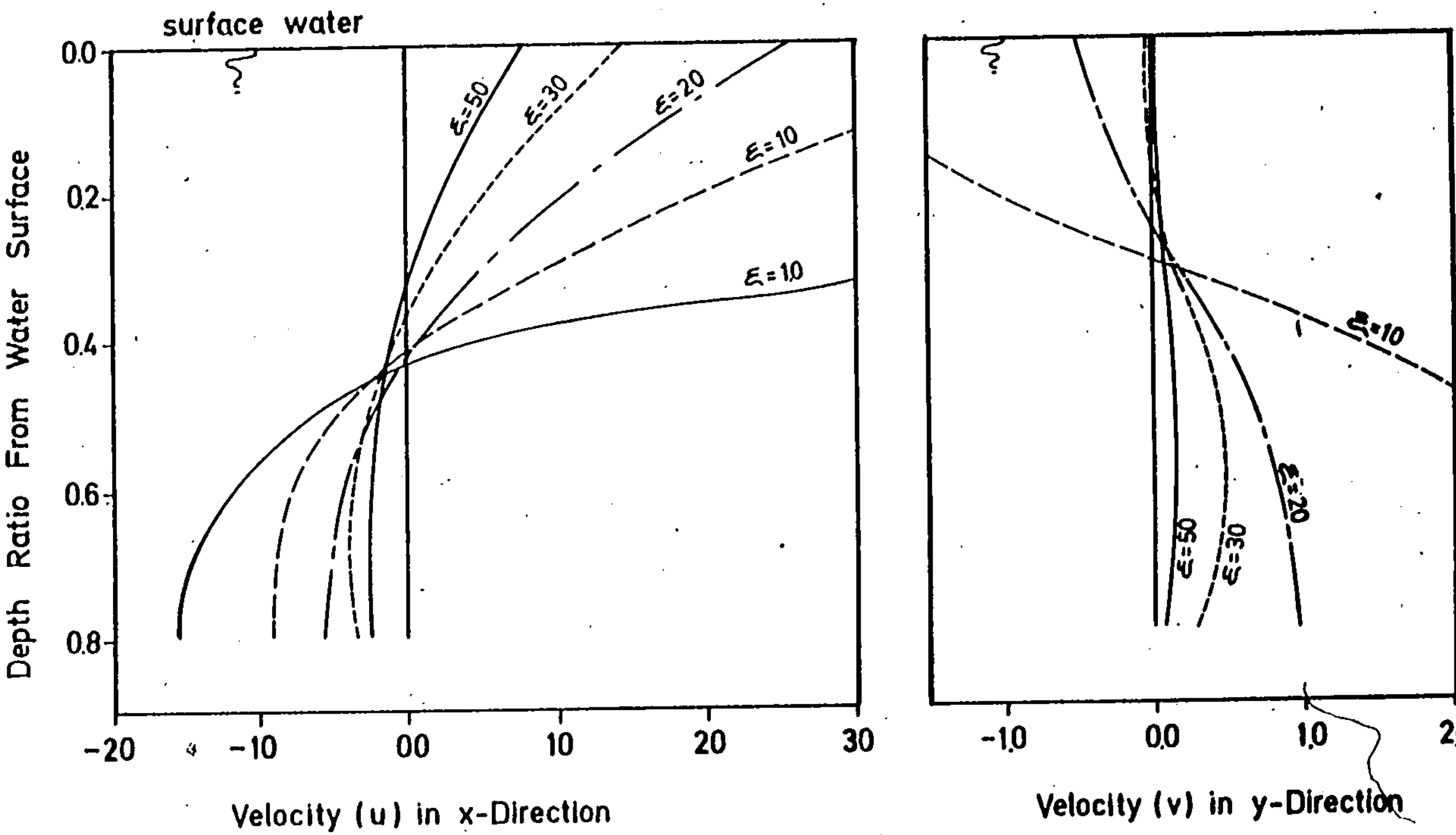

Figure 6.18 The Effect of Vertical Eddy Viscosity on the Velocity Profile in Element No. 36 in Lake St. Clair

Element # 145

$s = 0.3, \quad \tau_x = 3.5, \quad \tau_y = 0.0, \quad H = 6.0$ m

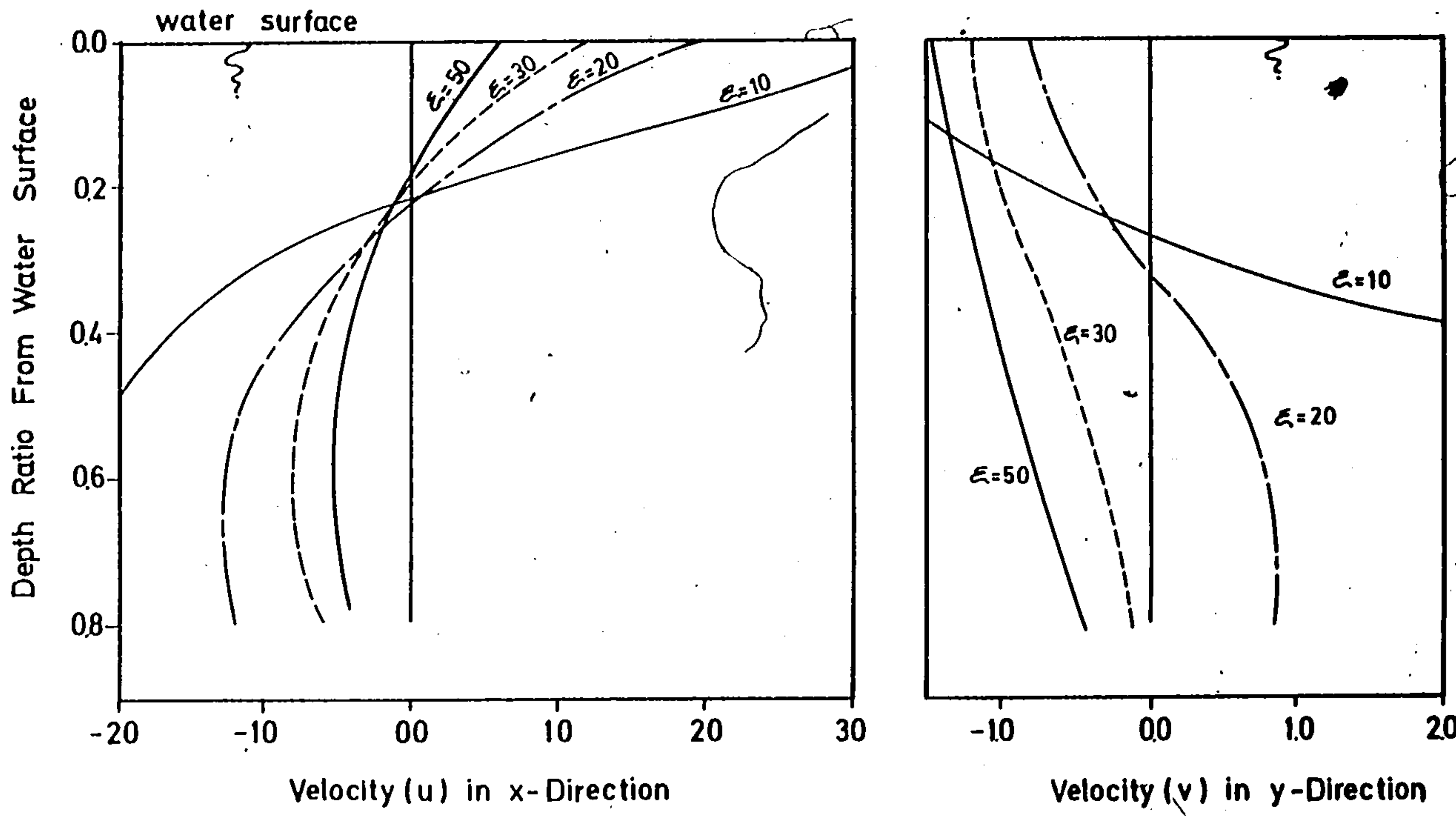

Figure 6.19 The Effect of Vertical Eddy Viscosity on the Velocity Profile in Element No. 145 in Lake St. Clair

Element # 36

$\xi = 20$, $\tau_x = 3.5$, $\tau_y = 0.0$, $H = 6.7$ m

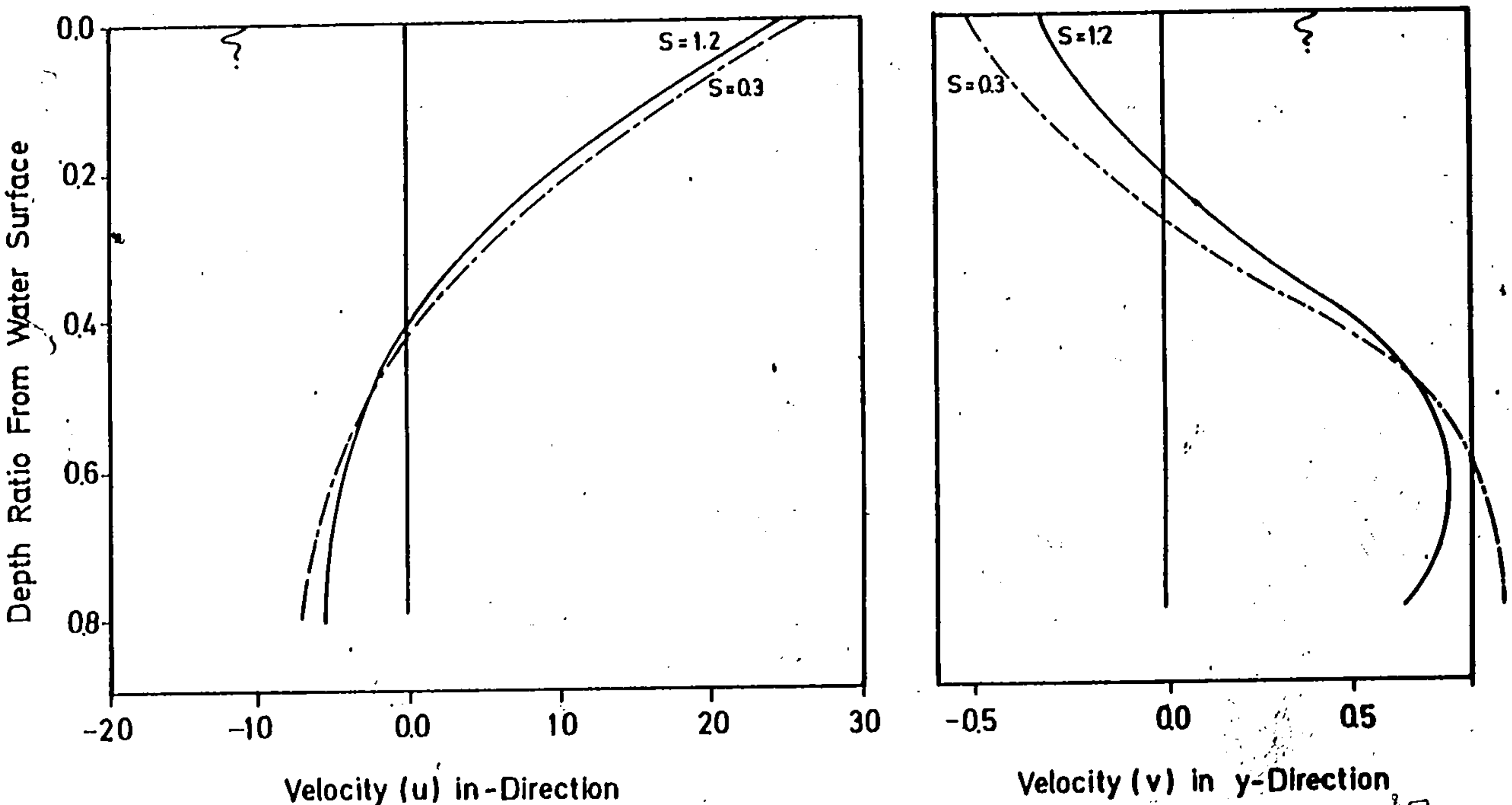

Figure 6.20 The Effect of Bottom Boundary Condition on the Velocity Profile in Element No. 36 in Lake St. Clair

Element # 145

$\xi = 20, \quad \tau_x = 3.5, \quad \tau_y = 0.0, \quad H = 6.0$

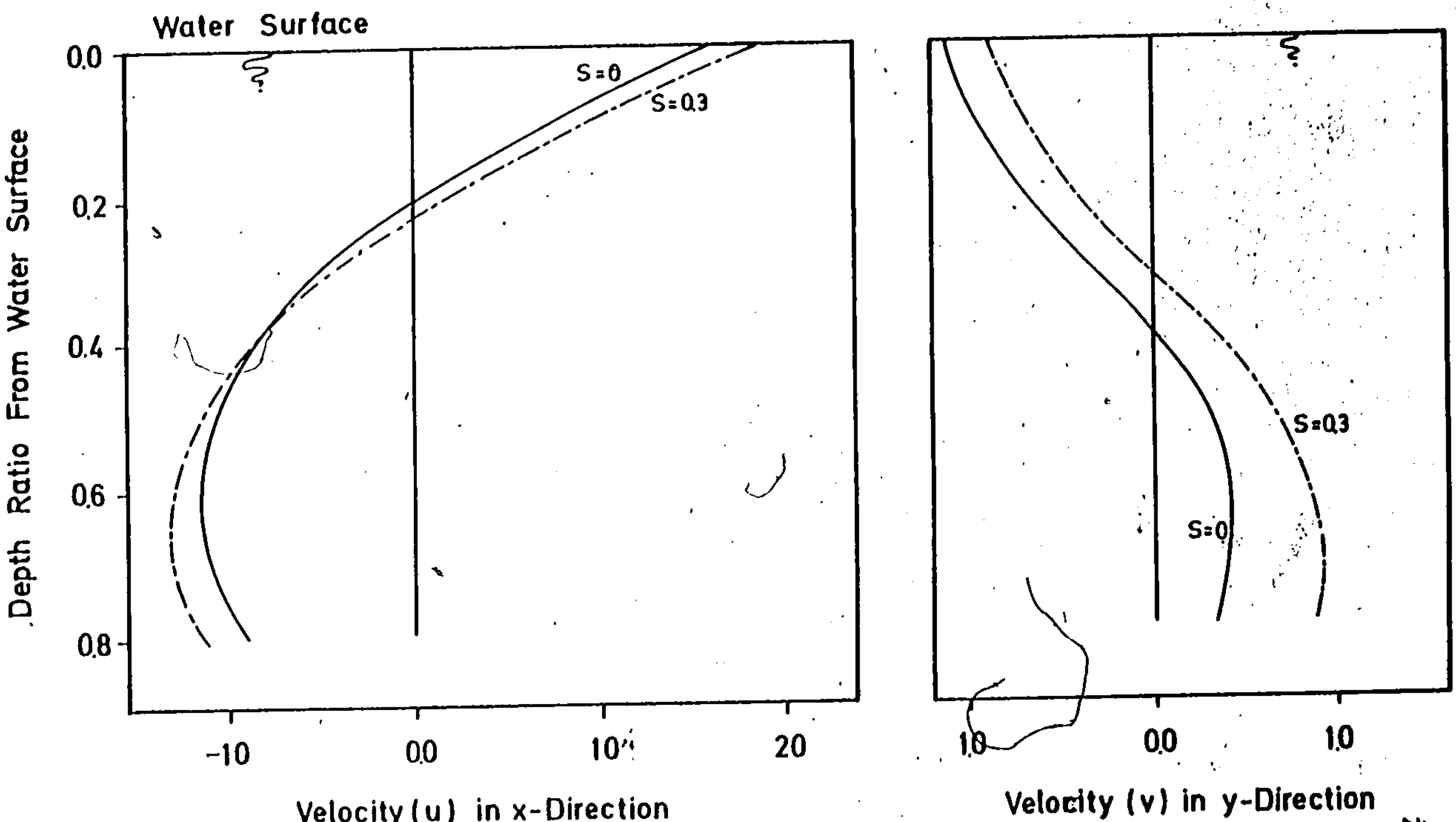

Figure 6.21 The Effect of Bottom Boundary Condition on the Velocity Profile in Element No. 145 in Lake St. Clair

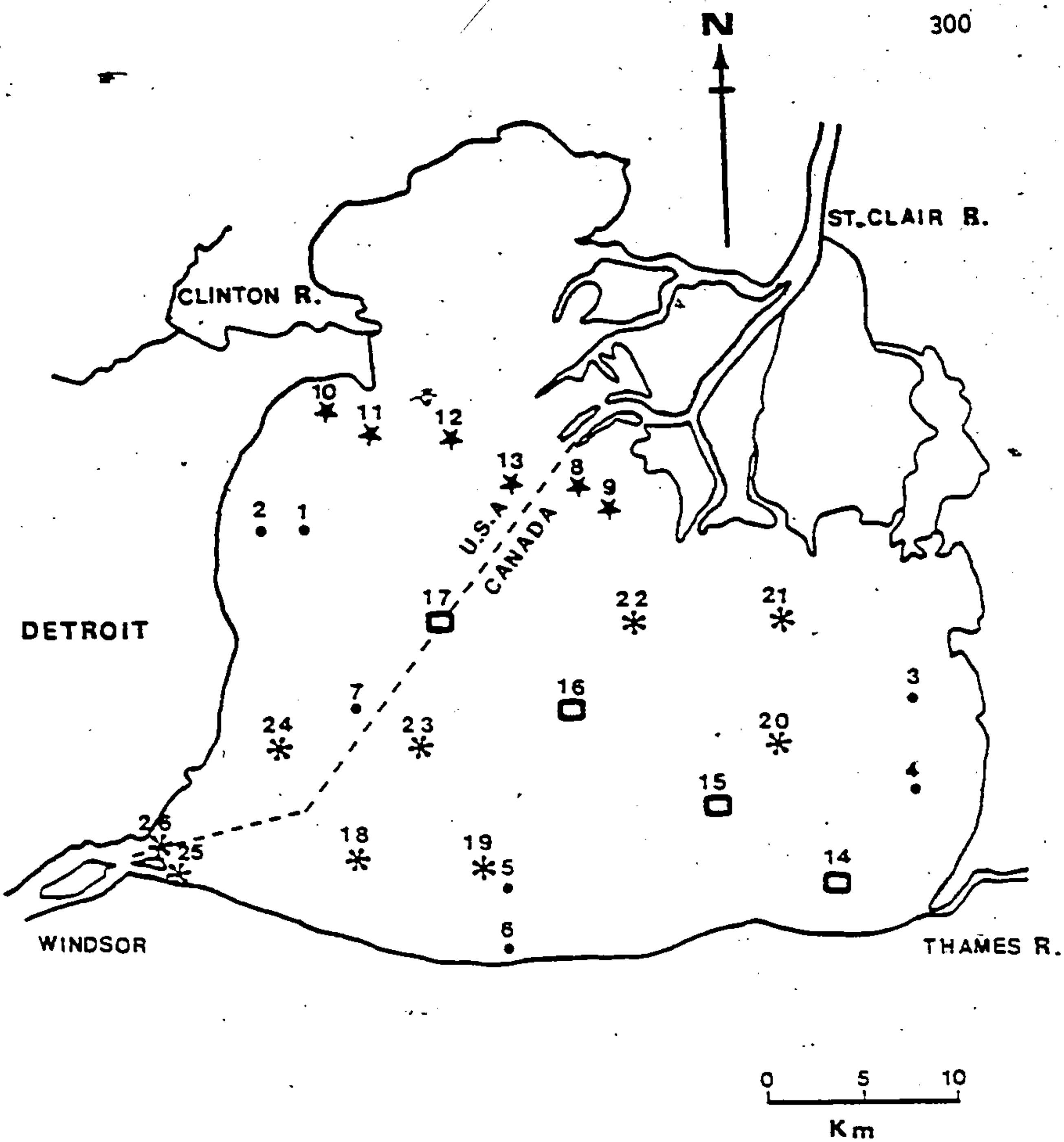

★ Data collected on June 23, 1983 (wind speed 8 km h^{-1} SSW)
• Data collected on Sept. 29, 1983 (wind speed 4.8 km h^{-1} ENE)
▢ Data collected on July 26, 1984 (wind speed 10 km h^{-1} NE)
✳ Data collected on July 31, 1984 (wind speed 13 km h^{-1} SW)

Figure 6.22 Location of Measuring Sites in Lake St. Clair

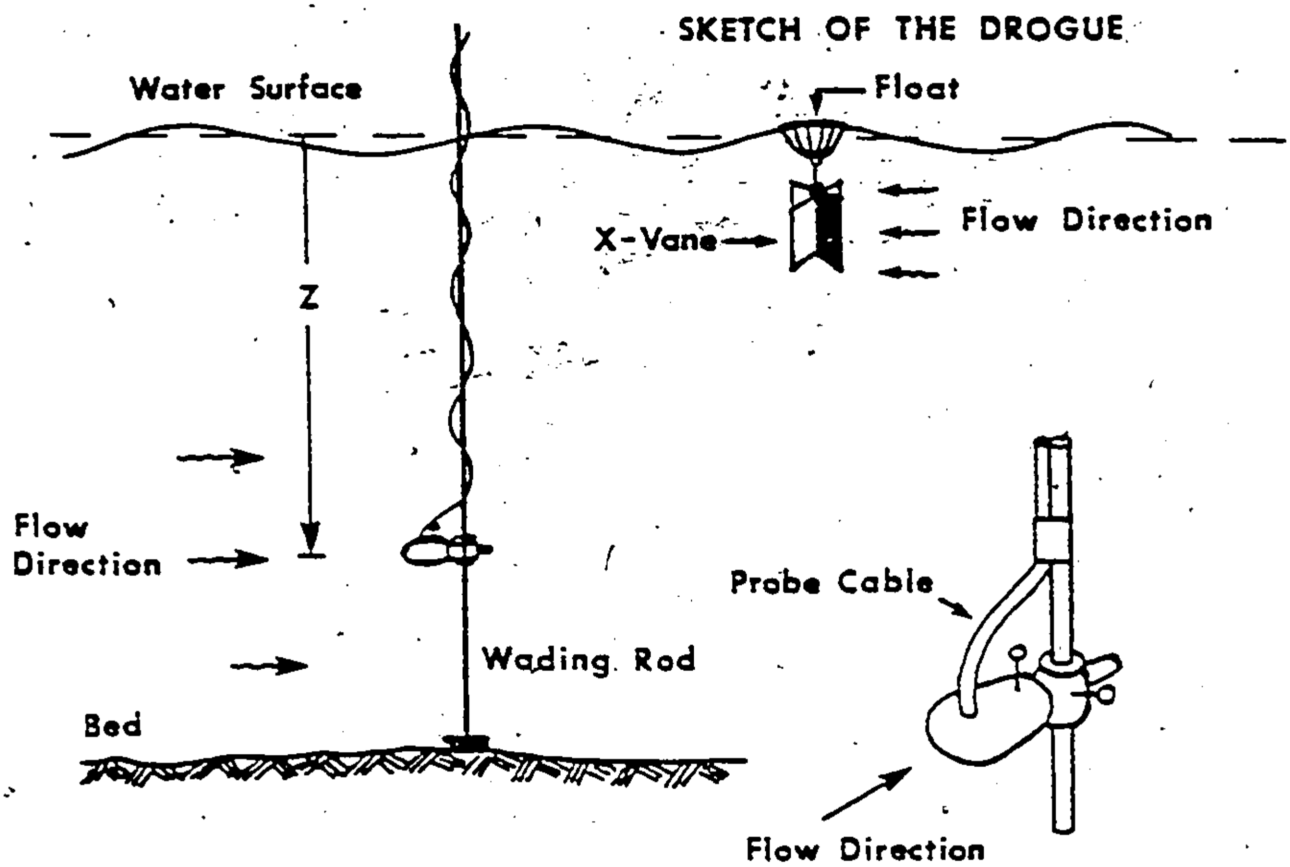

PROBE ORIENTATION TO FLOW DIRECTION

Figure 6.23 Flow Measurement Techniques

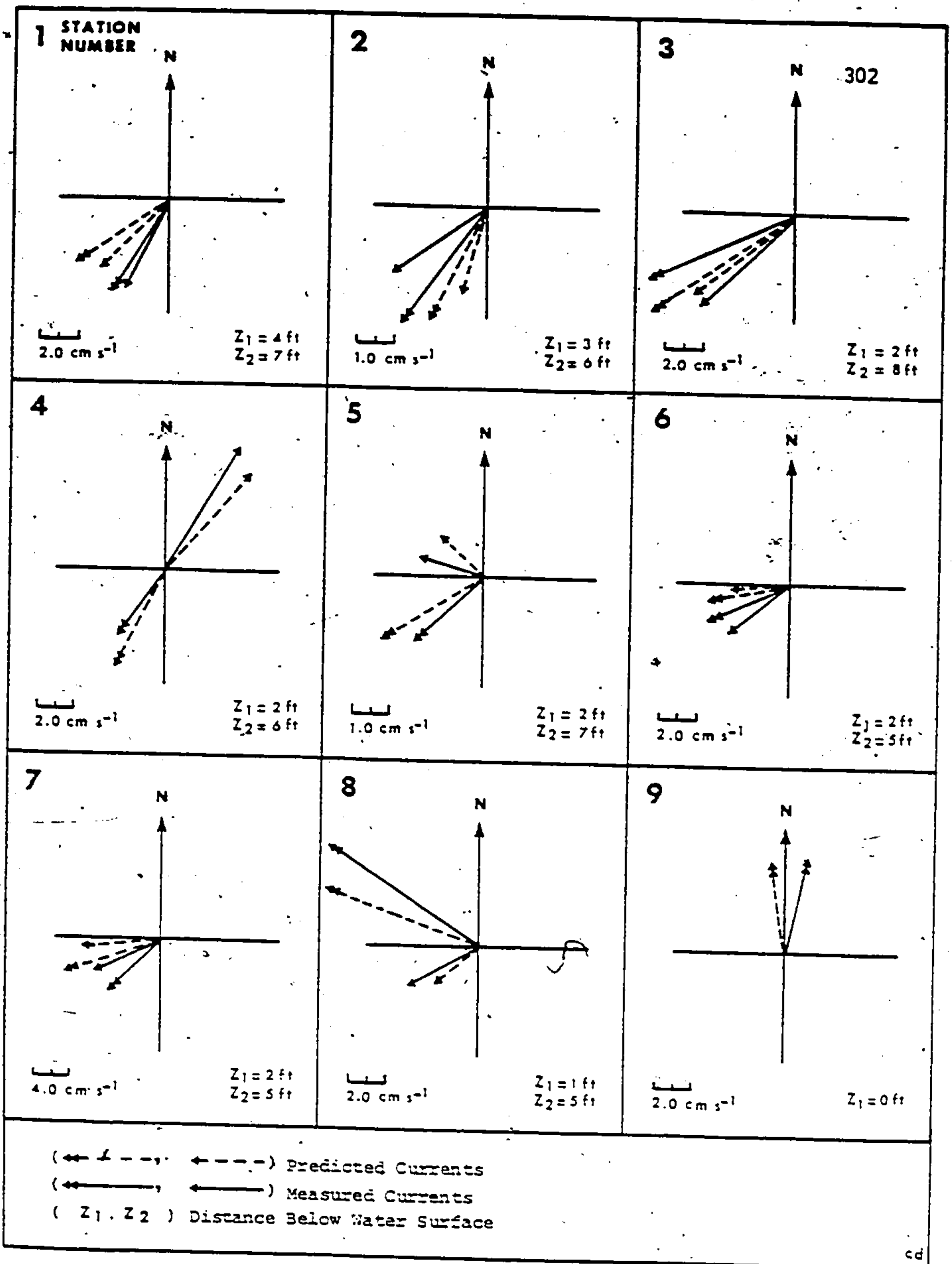

Figure 6.24 Comparison of the Observed and Calculated Currents in Lake St. Clair

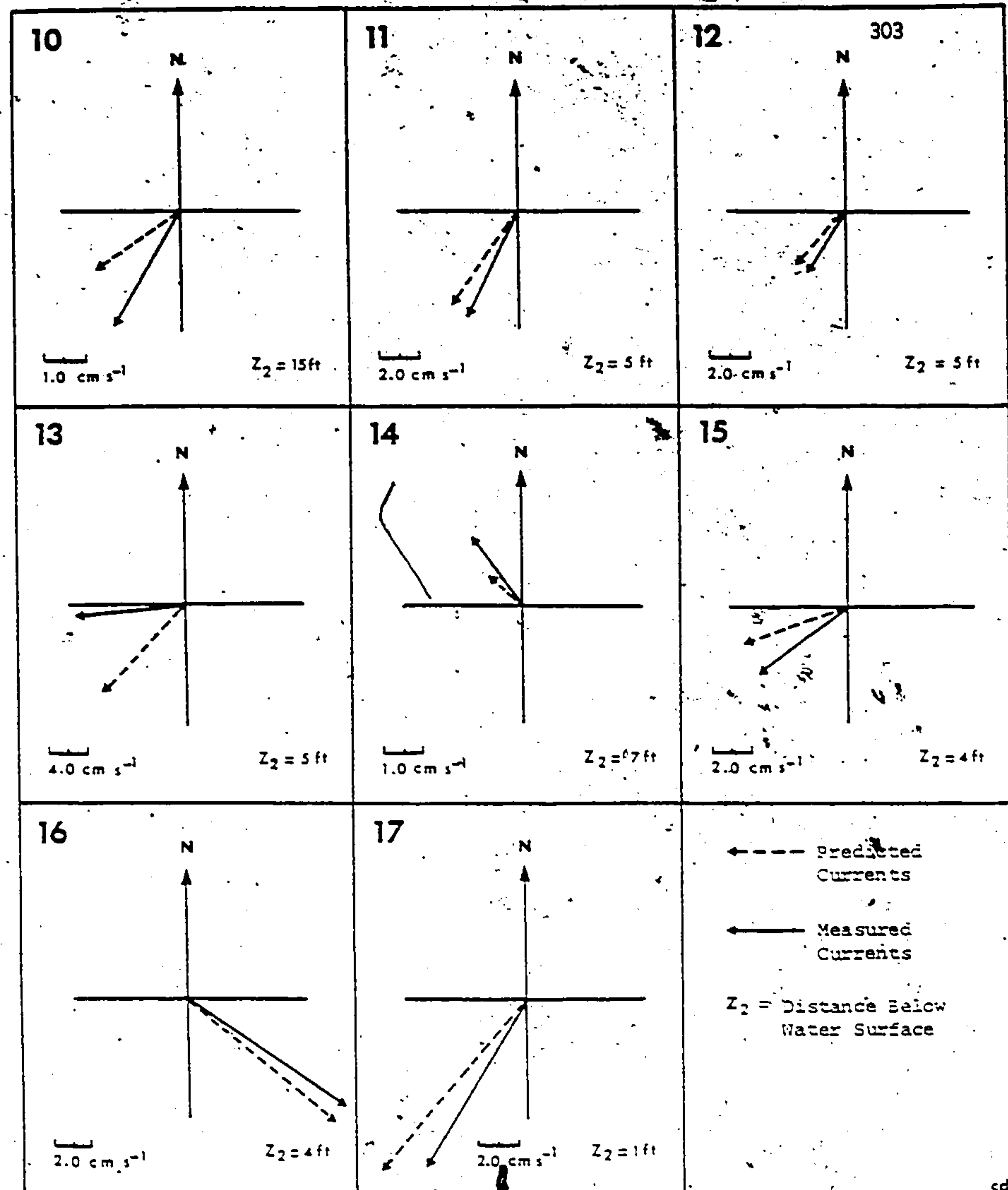

Figure 6.24 Cont.

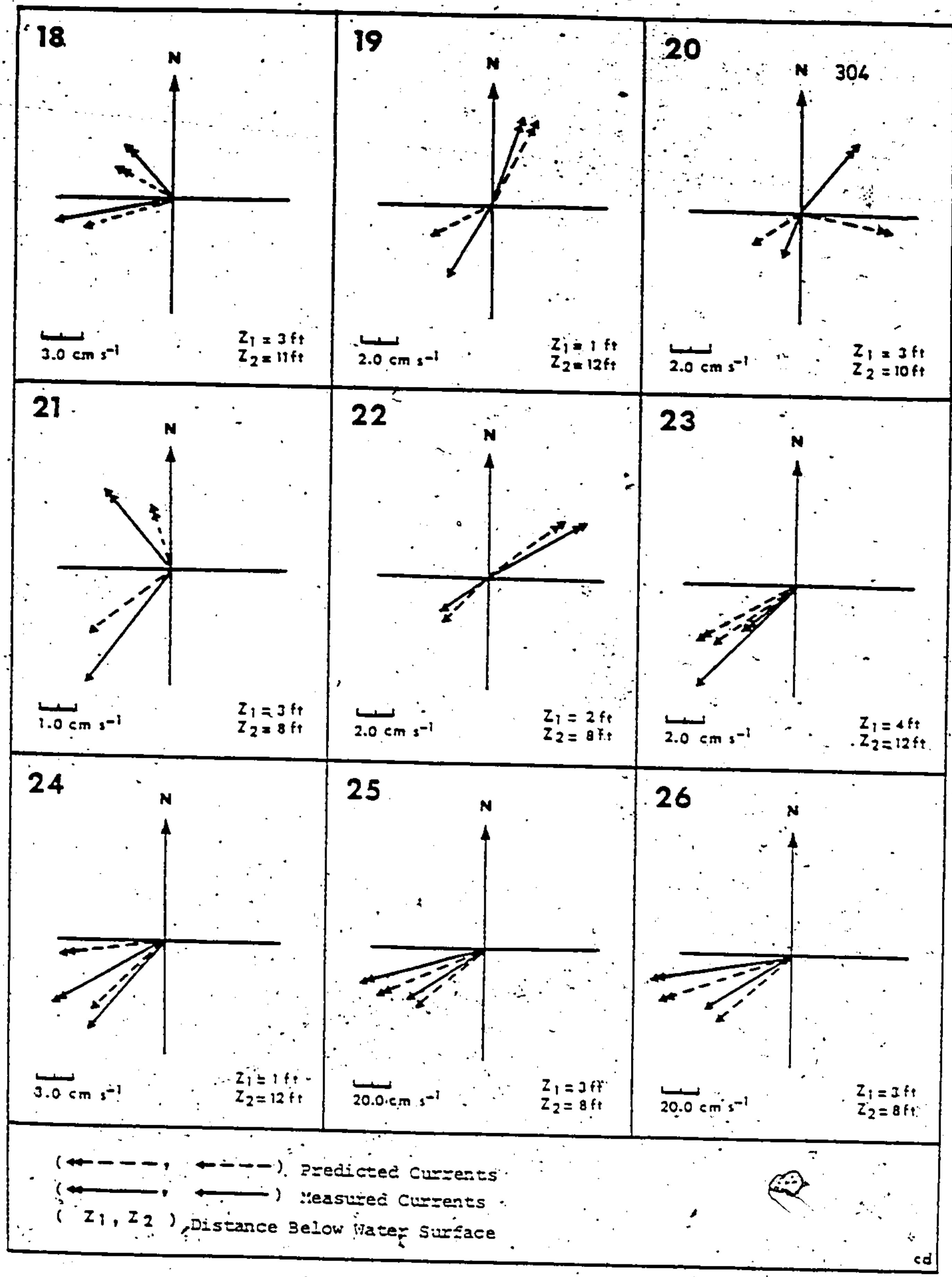

Figure 6.24 Cont.

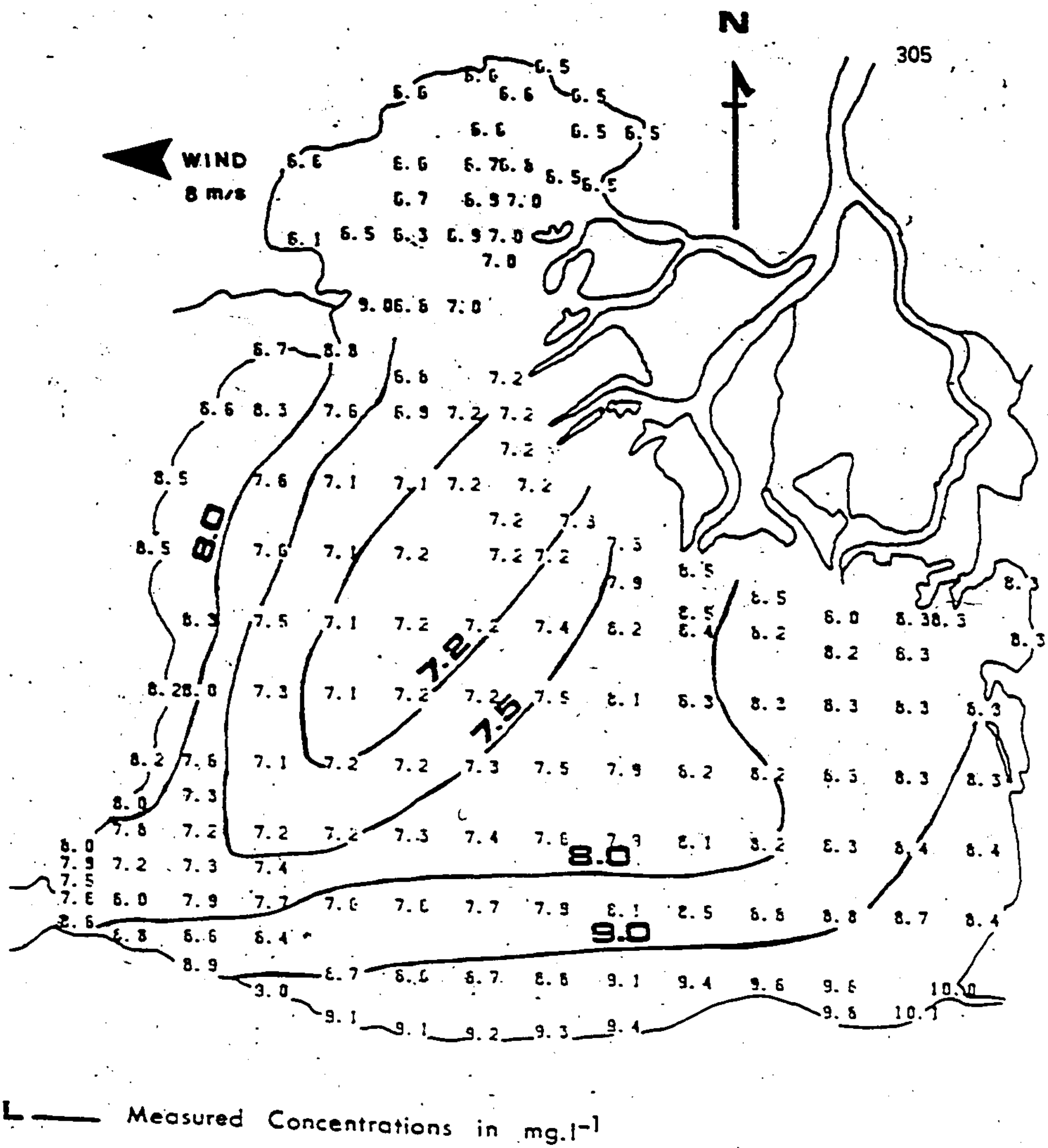

Figure 6.25 The measured and simulated horizontal distribution of the mean chloride concentration in Lake St. Clair

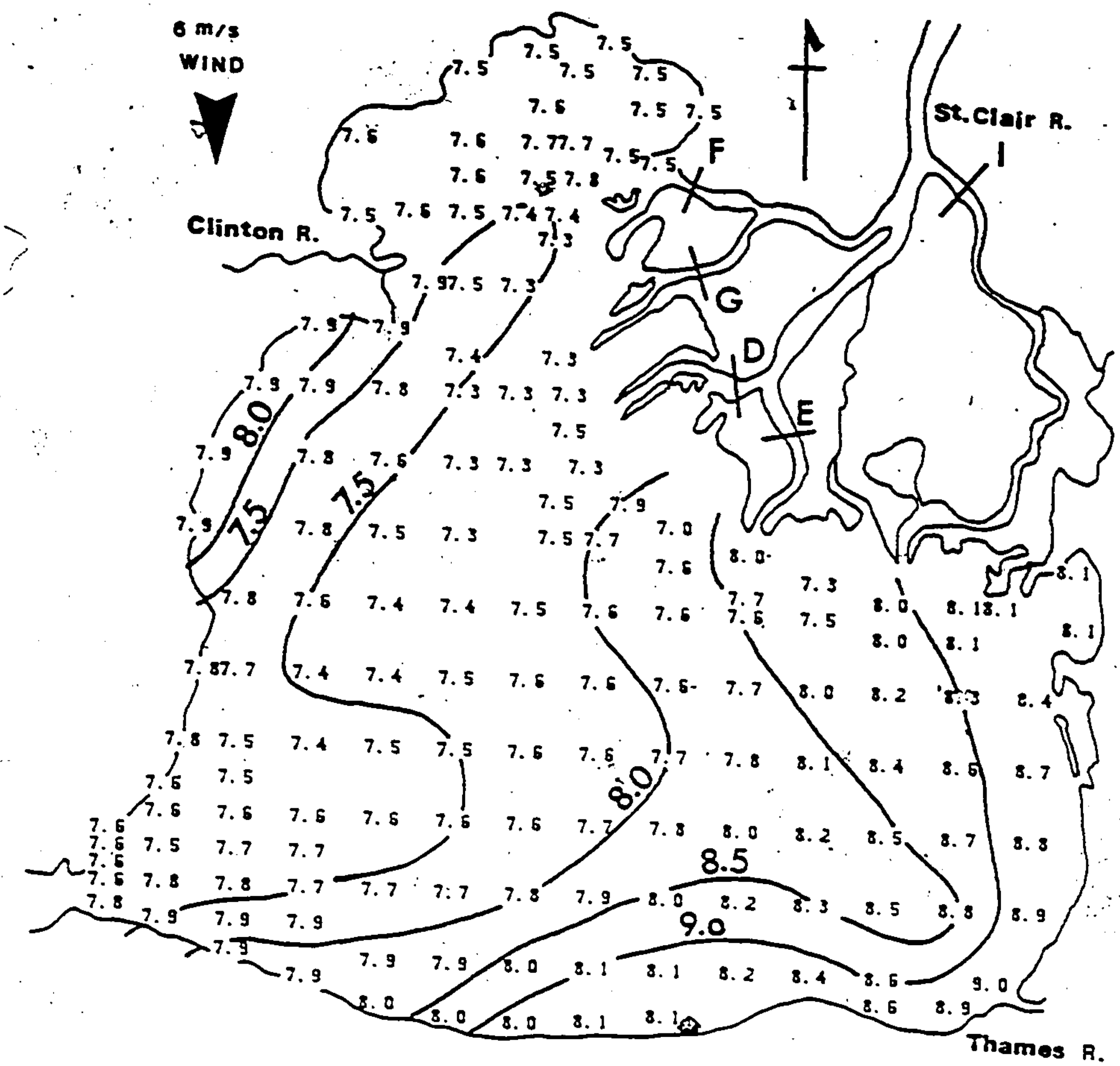

CL —— Measured Concentrations in $mg.l^{-1}$

Figure 6.26 The Measured and Simulated Horizontal Distribution of the Mean Chloride Concentration in Lake St. Clair.

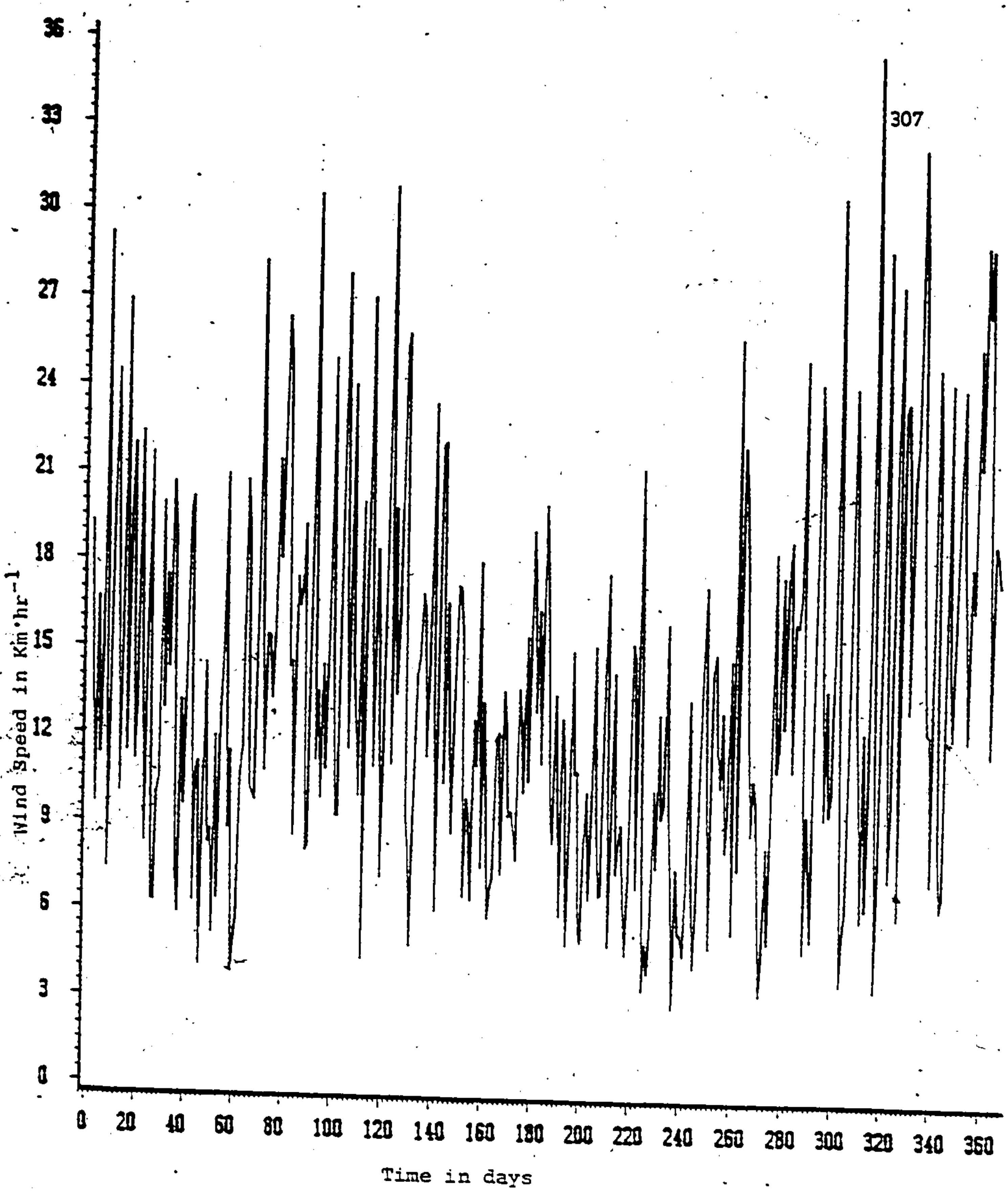

Figure 6.27. Wind Speed Variations from Windsor Airport in 1983

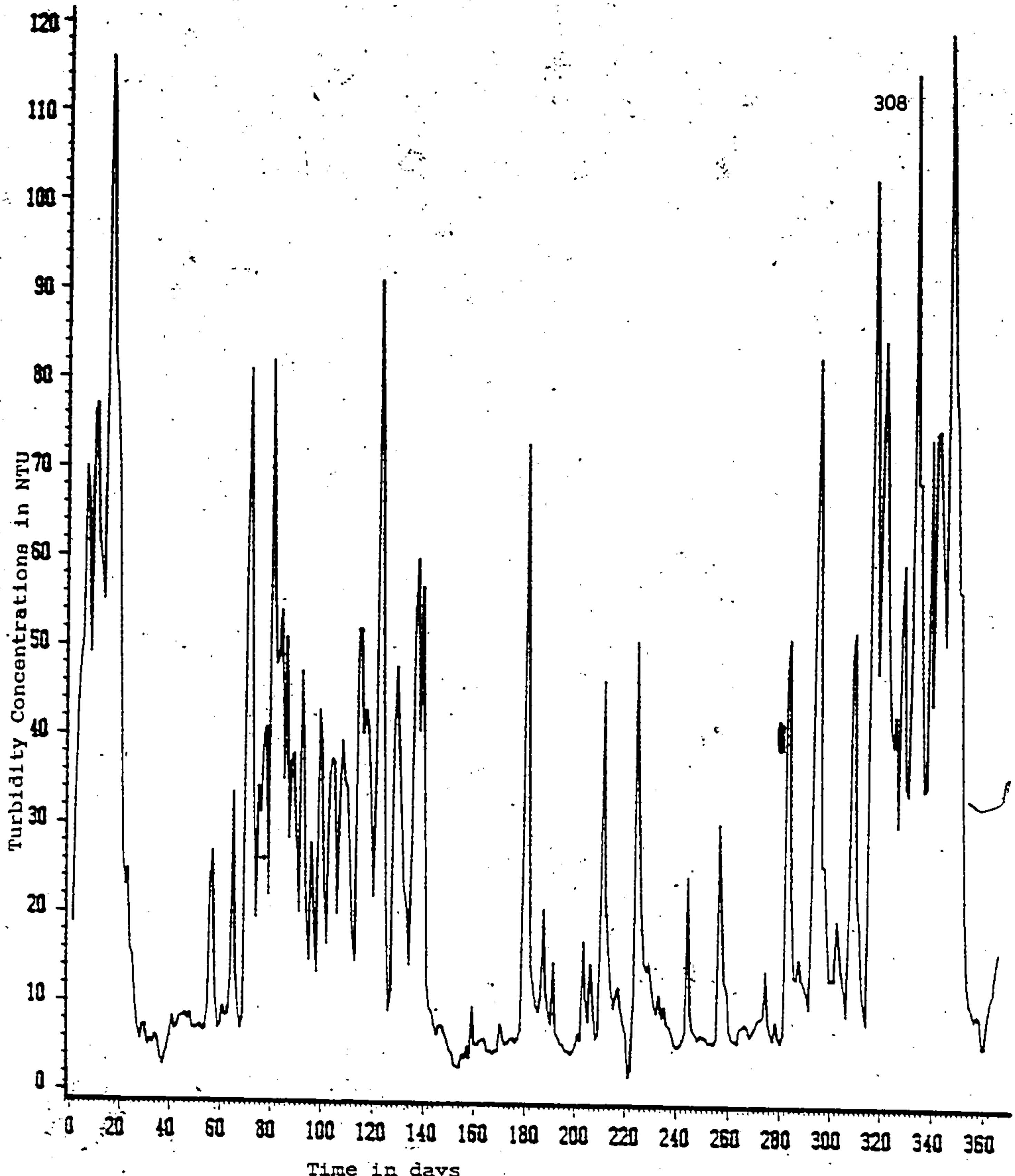

Figure 6.28. Turbidity Data From Windsor Water Treatment Plant in 1983.

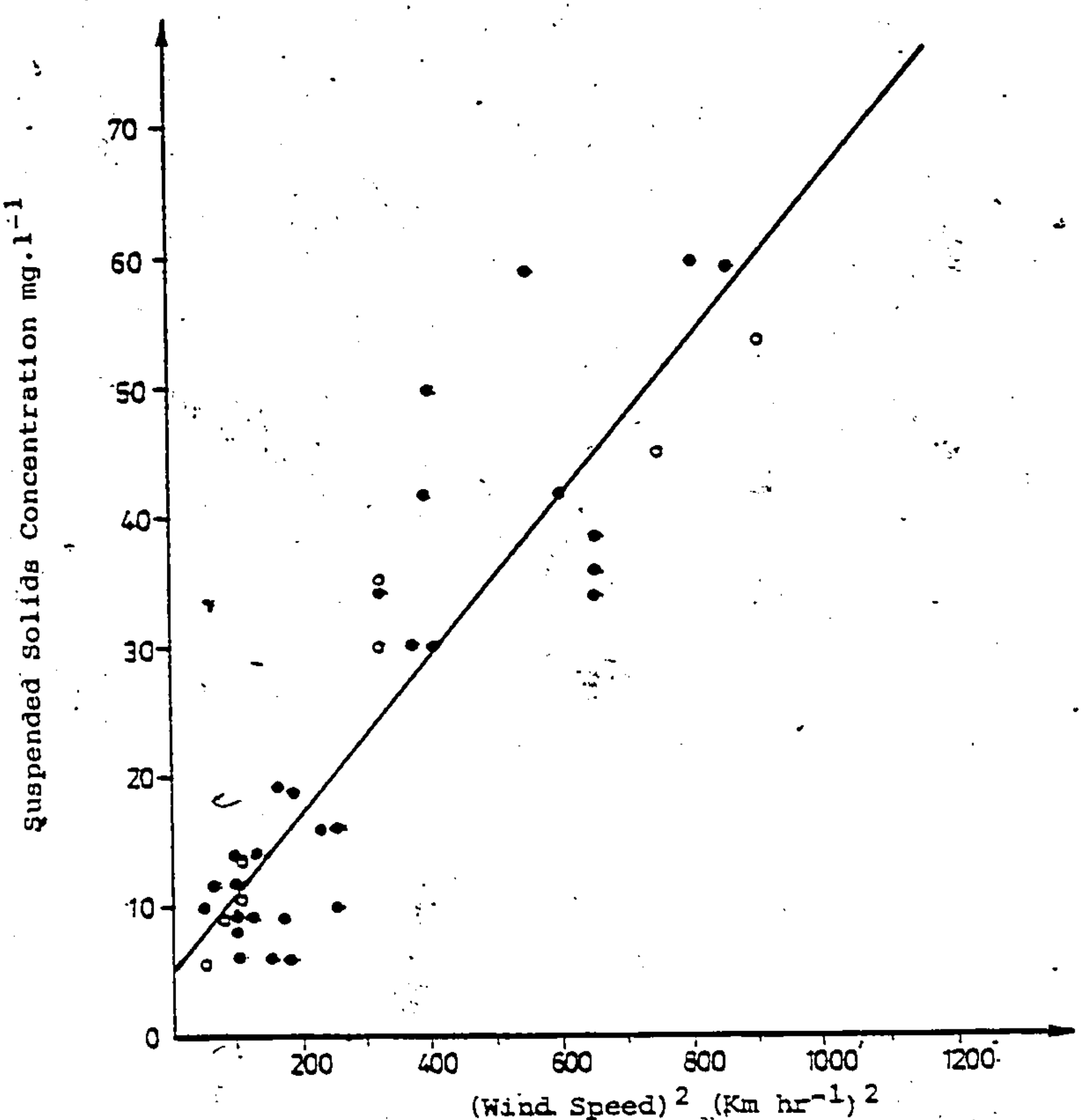

Figure 6.29a Correlation of Suspended Solids and Wind Speed in Lake St. Clair.

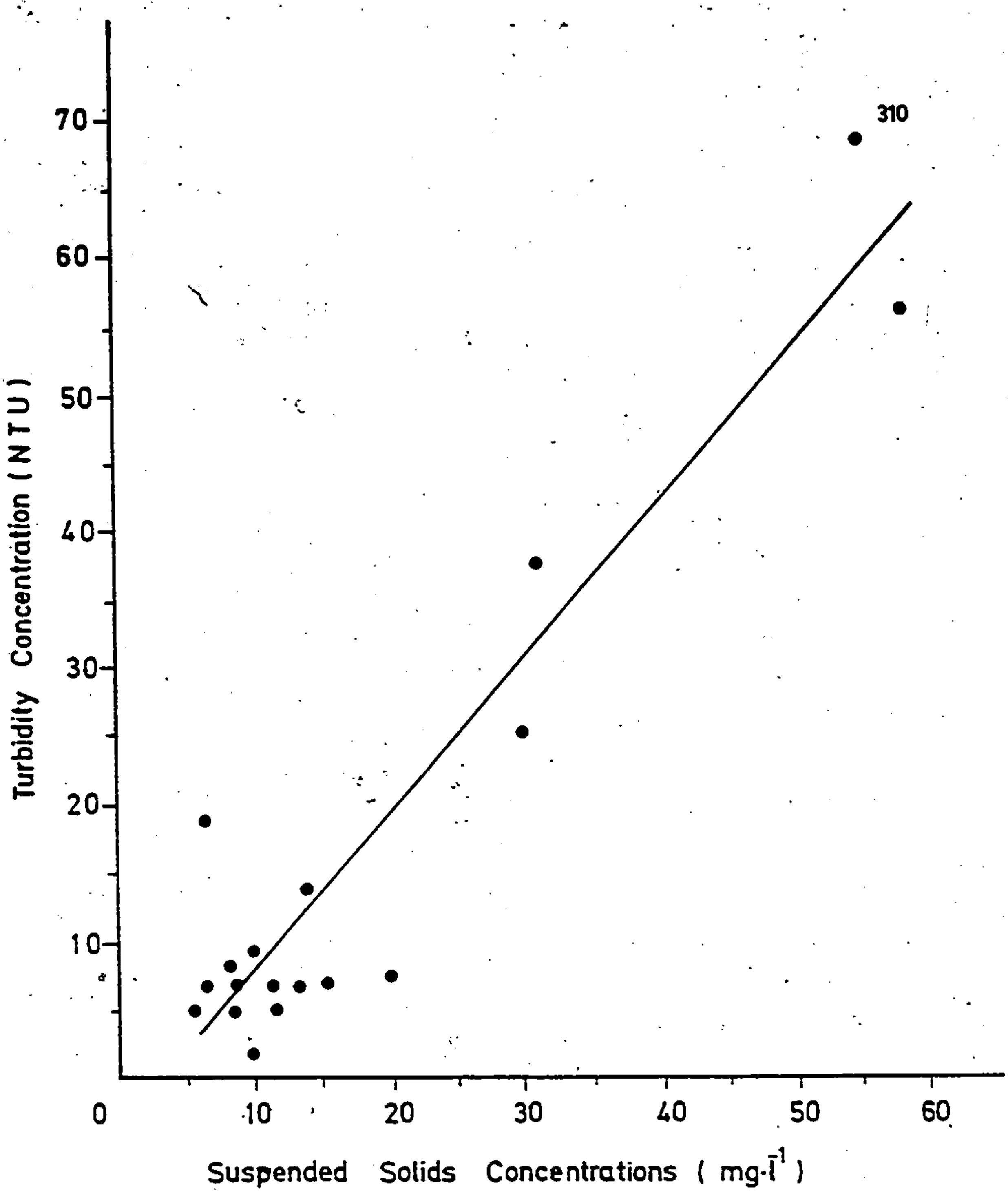

Figure 6.29b: Correlation of Suspended Solids and Turbidity Data in Lake St. Clair.

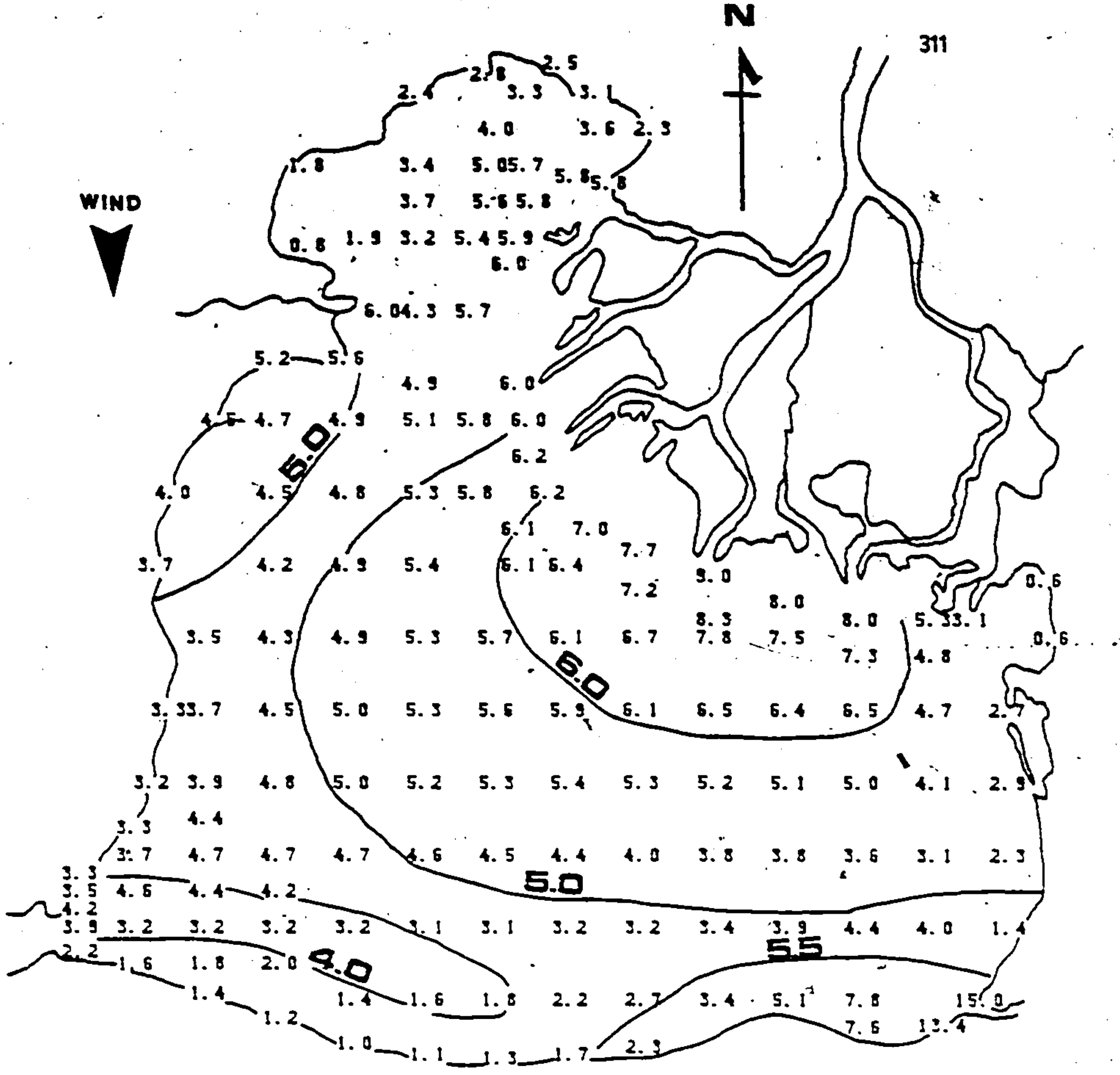

S.S. ____ Measured Concentrations in mg.l^{-1}

Figure 6.30 Measured and Simulated Horizontal Distribution of the Mean Suspended Solids Concentration in Lake St. Clair.

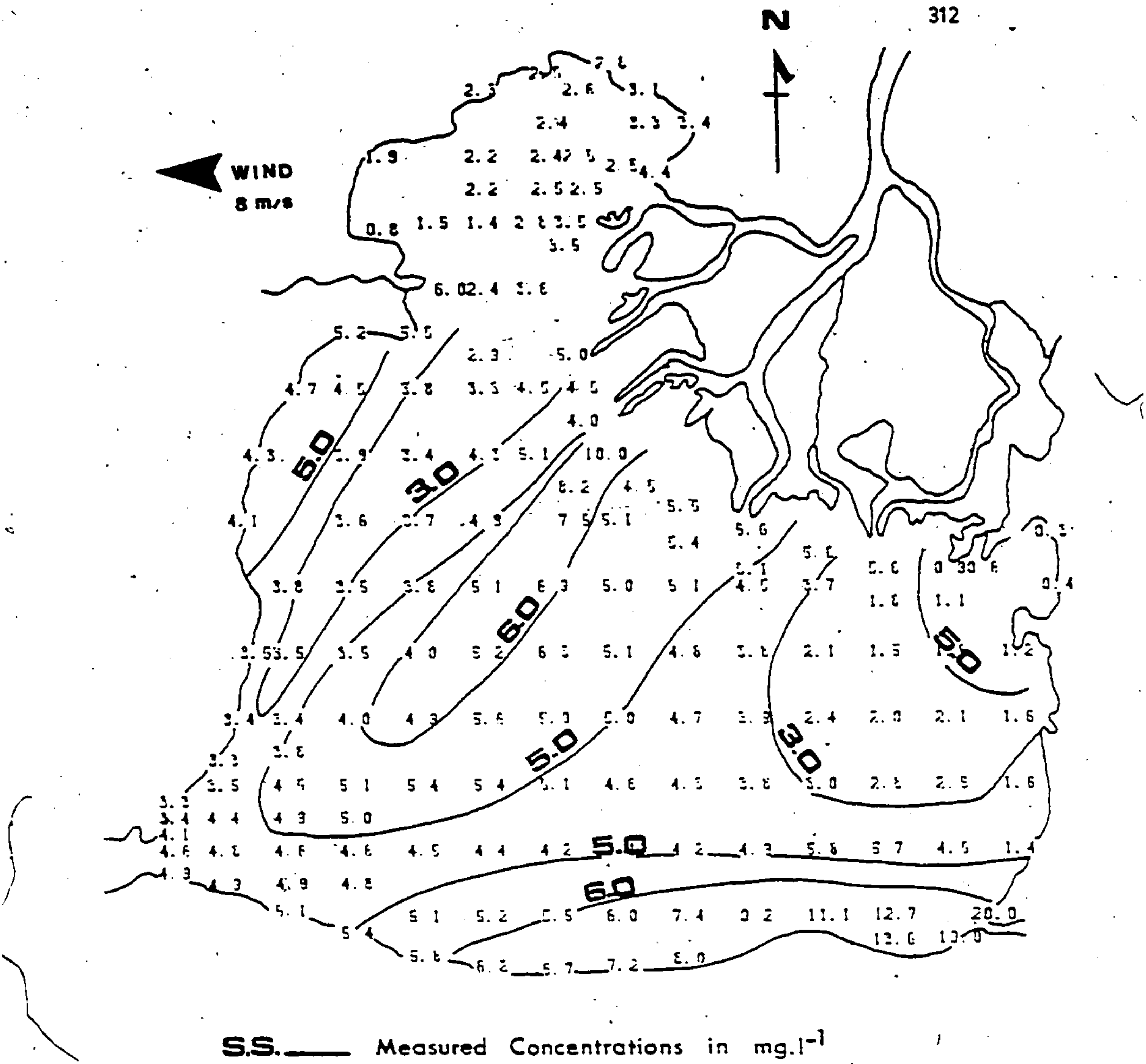

Figure 6.31 Measured and Simulated Horizontal Distribution of the Mean Suspended Solids Concentration in Lake St. Clair.

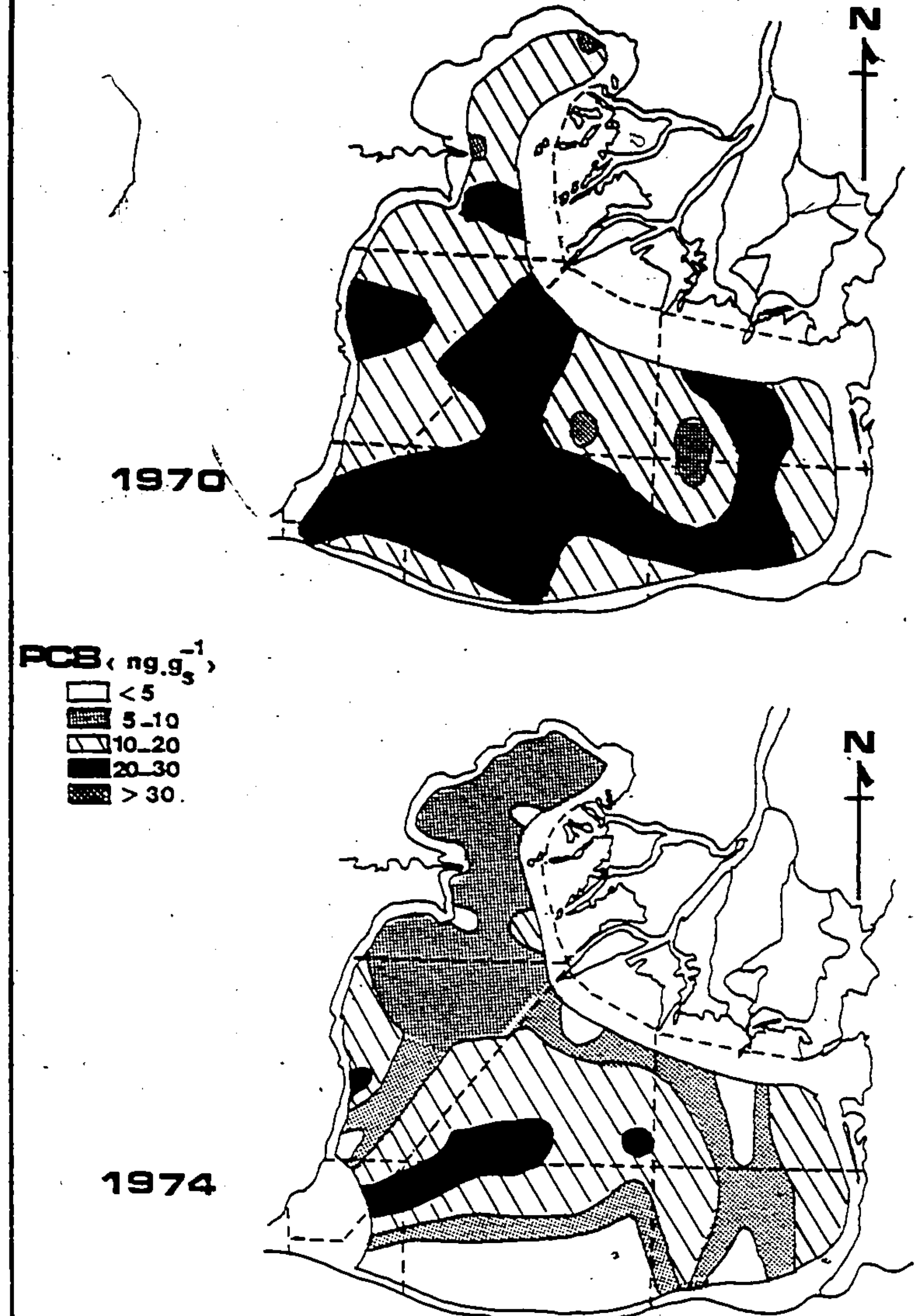

Figure 6.32. Distributed PCBs in Bed Sediment in 1970 and 1974 (After Frank et al., 1977).

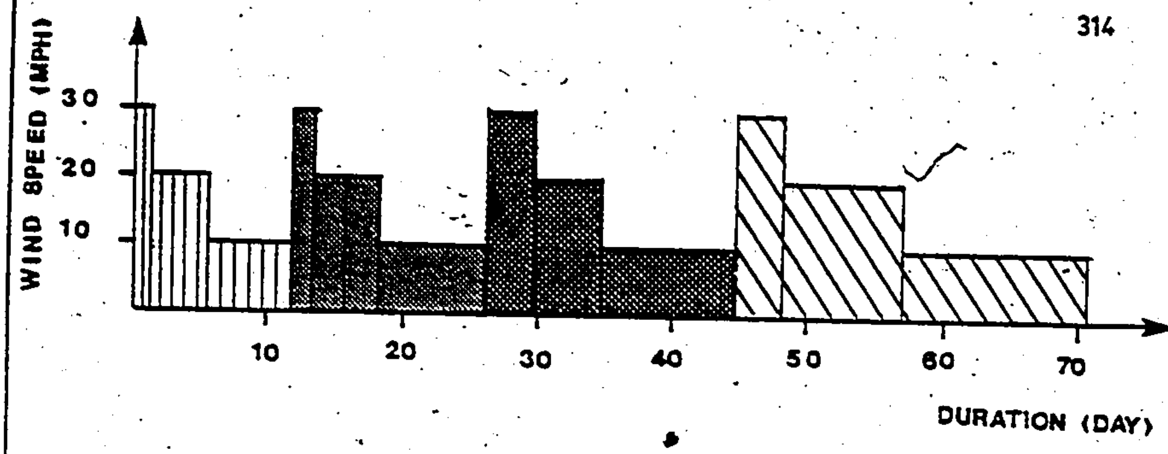

Figure 6.33 Piecewise Approximation for Wind Speed And Direction.

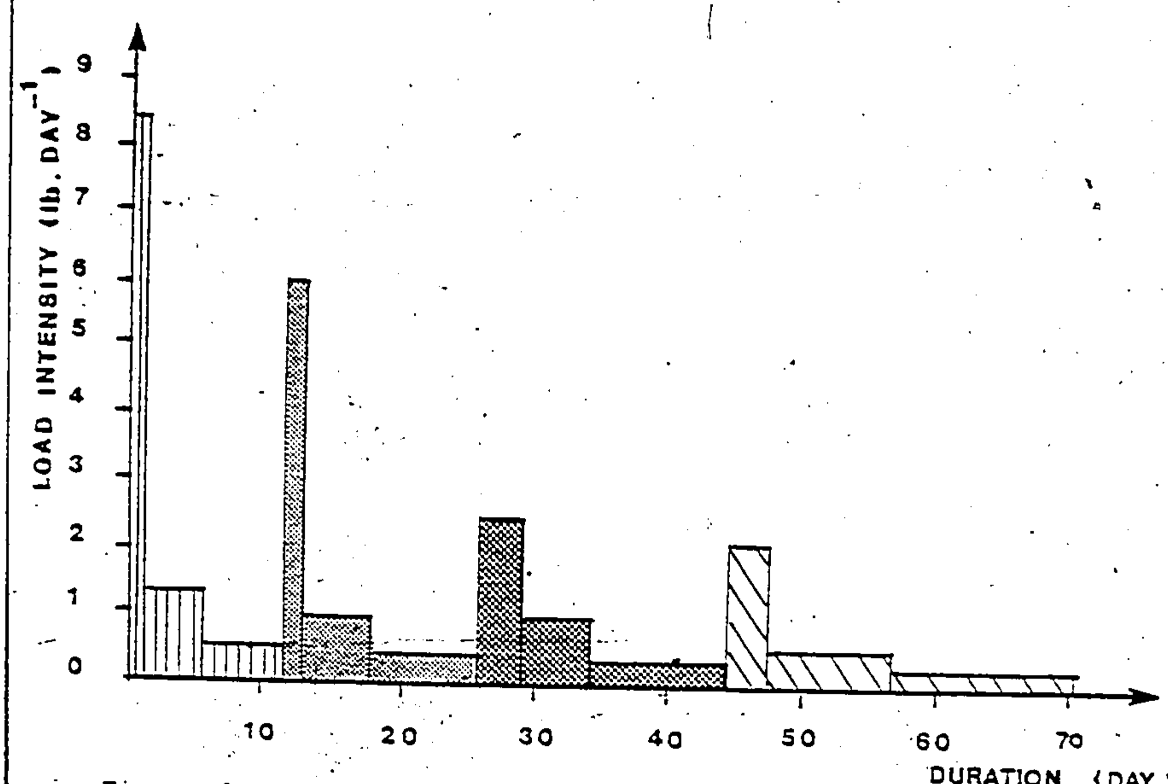

Figure 6.34 Piecewise Approximation for Sediment and PCBs loads

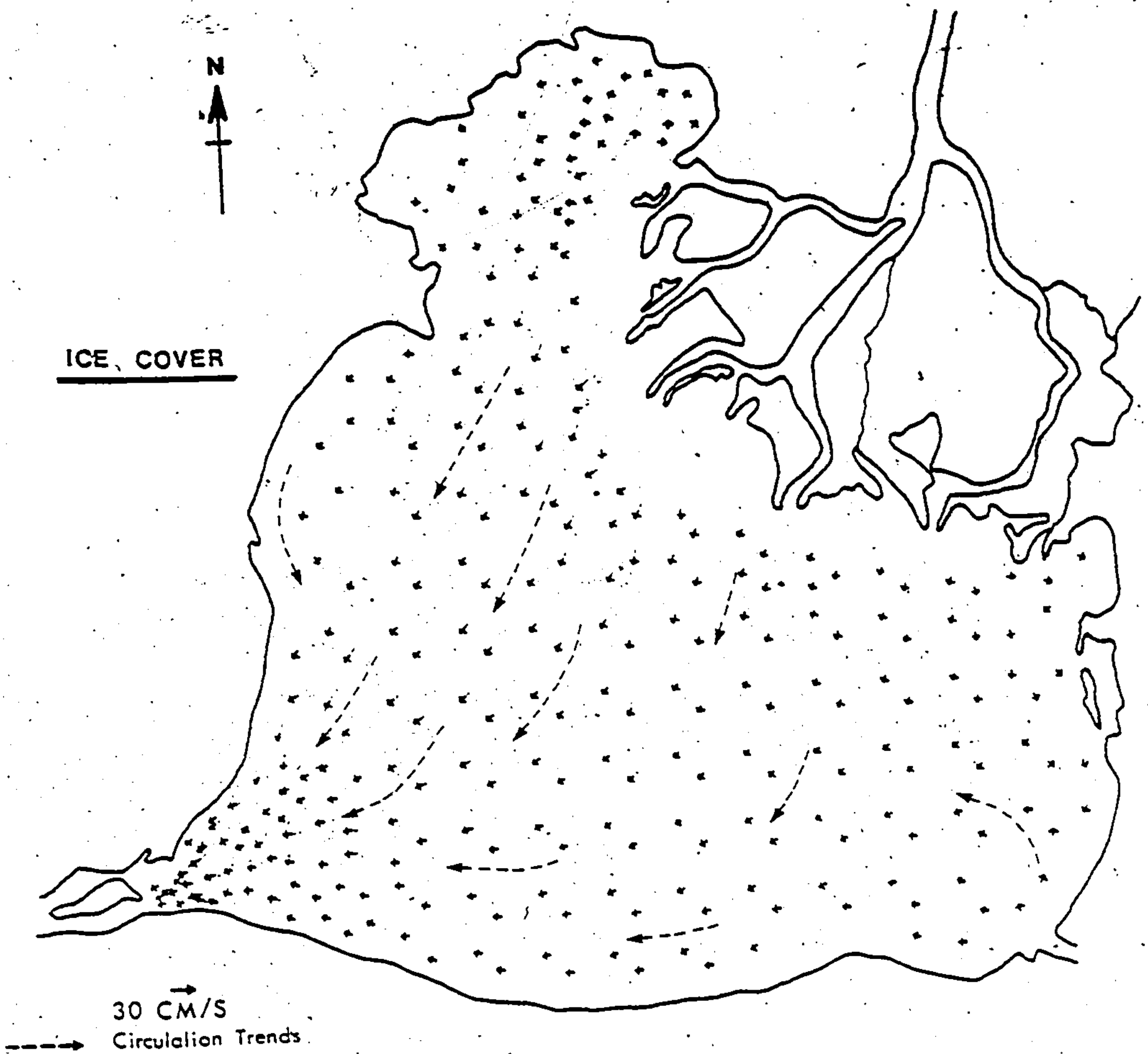

Figure 6.35 Vertically Integrated Velocities Under Complete Ice Cover

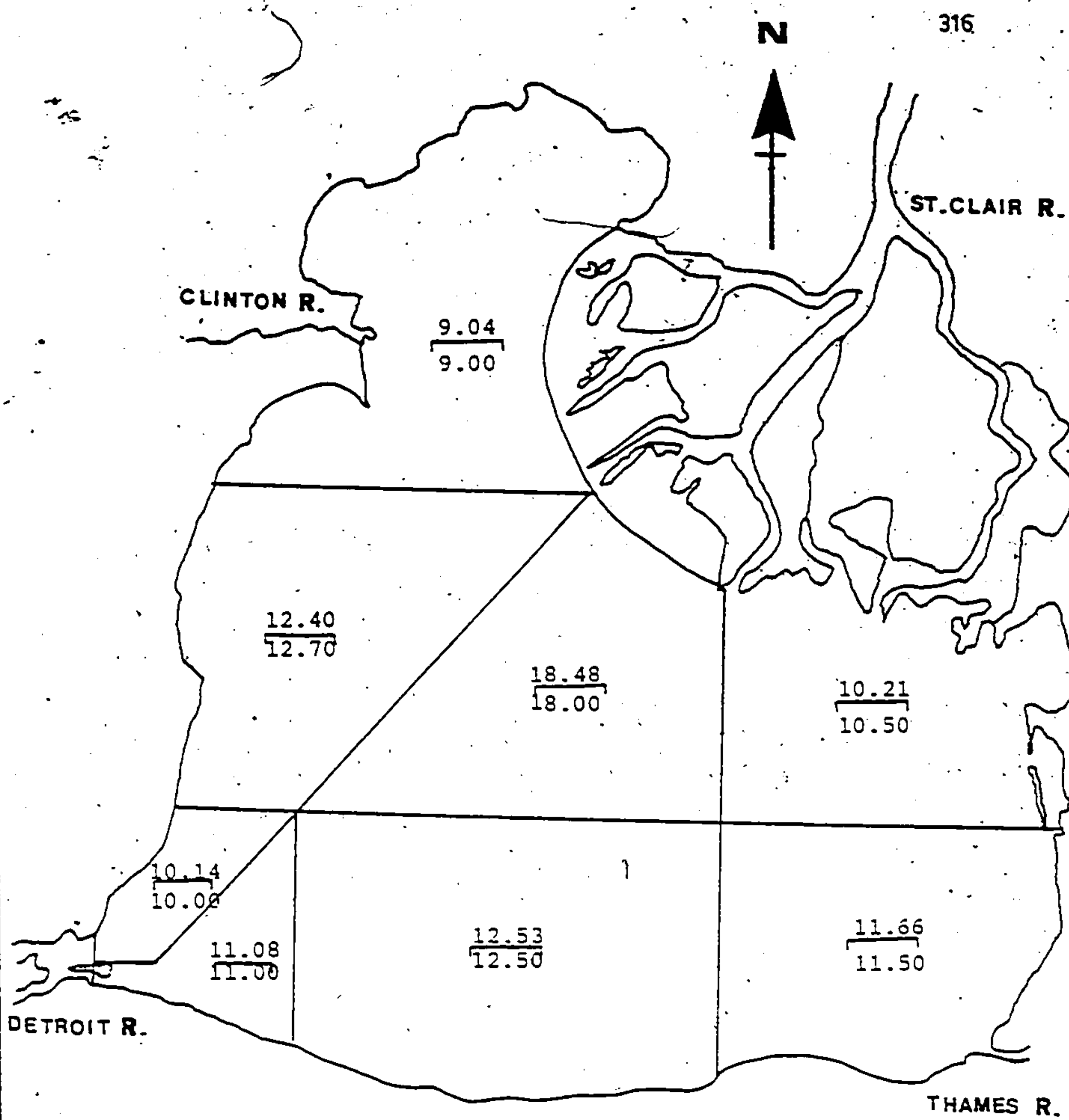

Figure 6.36 Predicted and Measured Concentrations of PCBs in Bed Sediments ($ng \cdot g^{-1}$).

Predicted 1974
Measured 1974

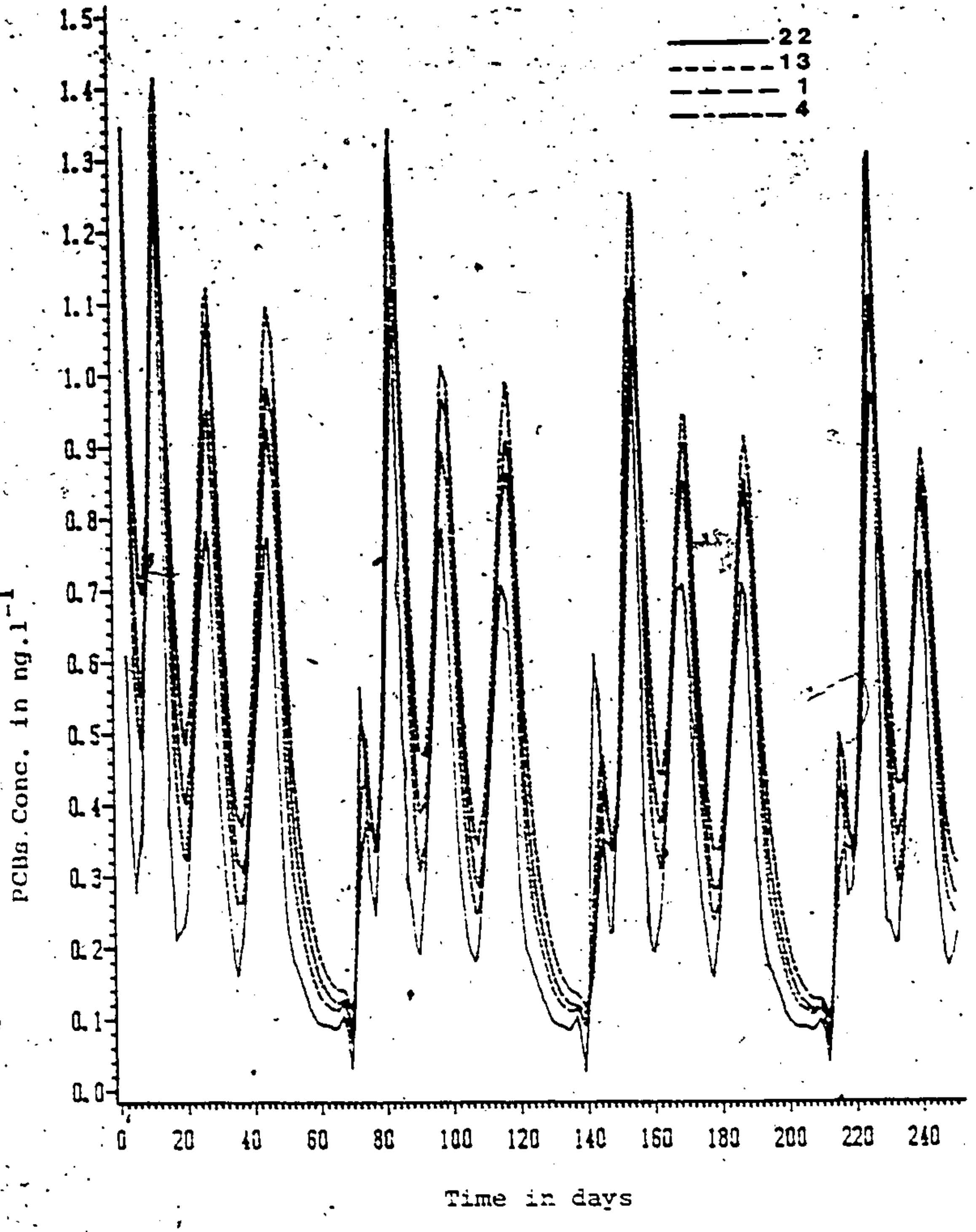

Figure 6.37 Total PCBs Concentration in Water Segments in Lake St. Clair

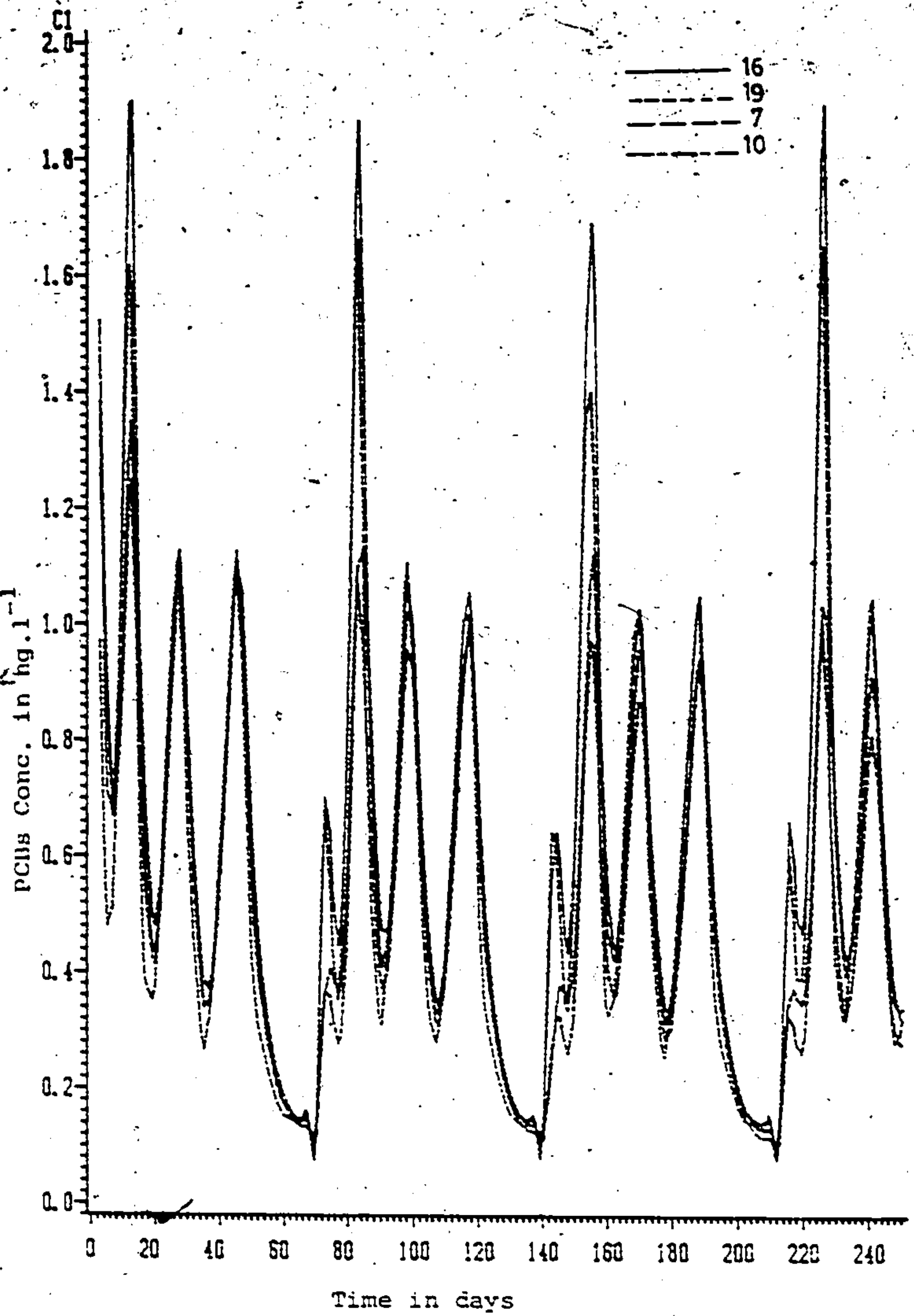

Figure 6.38 Total PCBs in Water Segments in Lake St. Clair

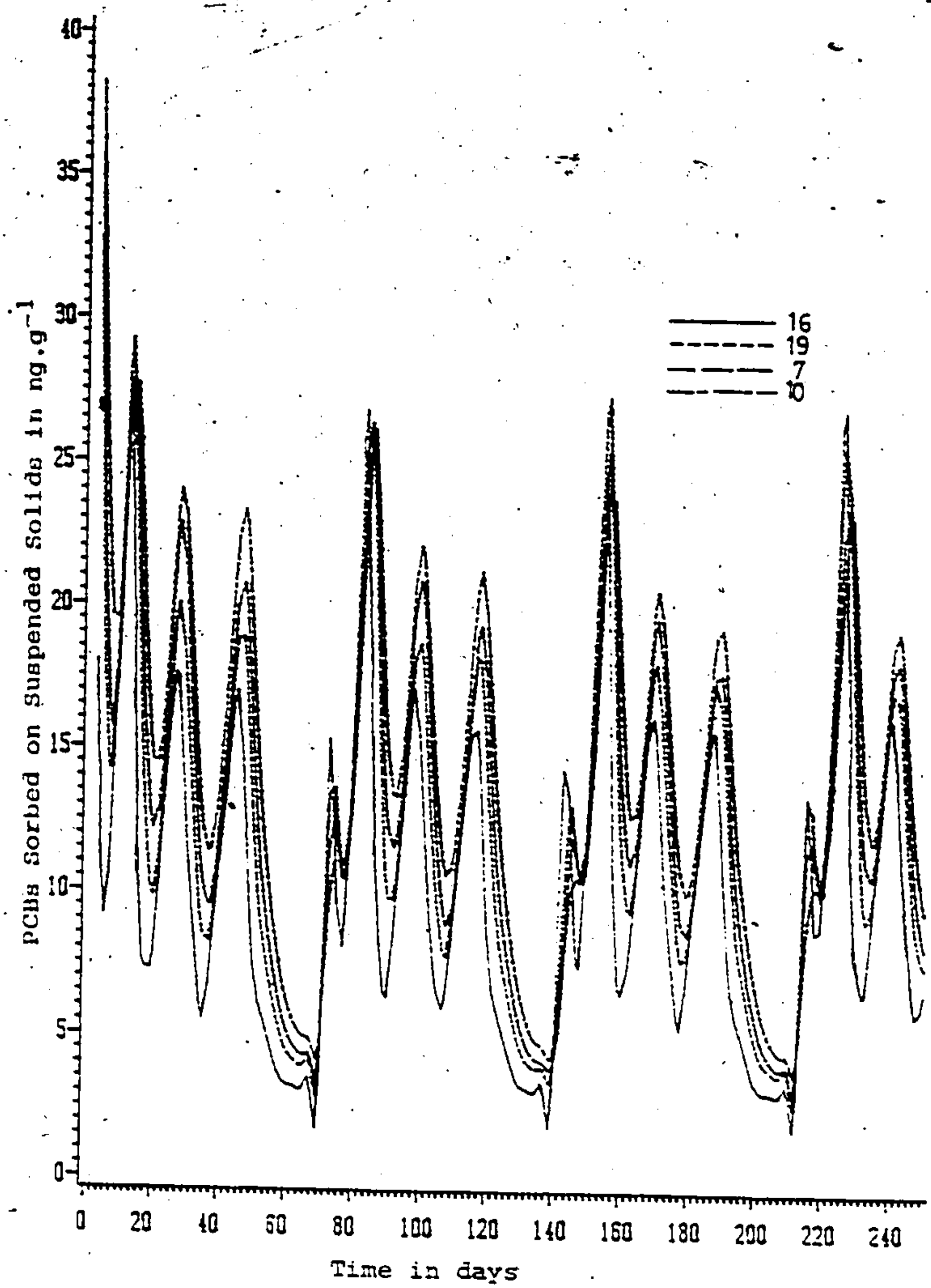

Figure 6.39 PCBs Sorbed onto Suspended Sediments in Water Segments

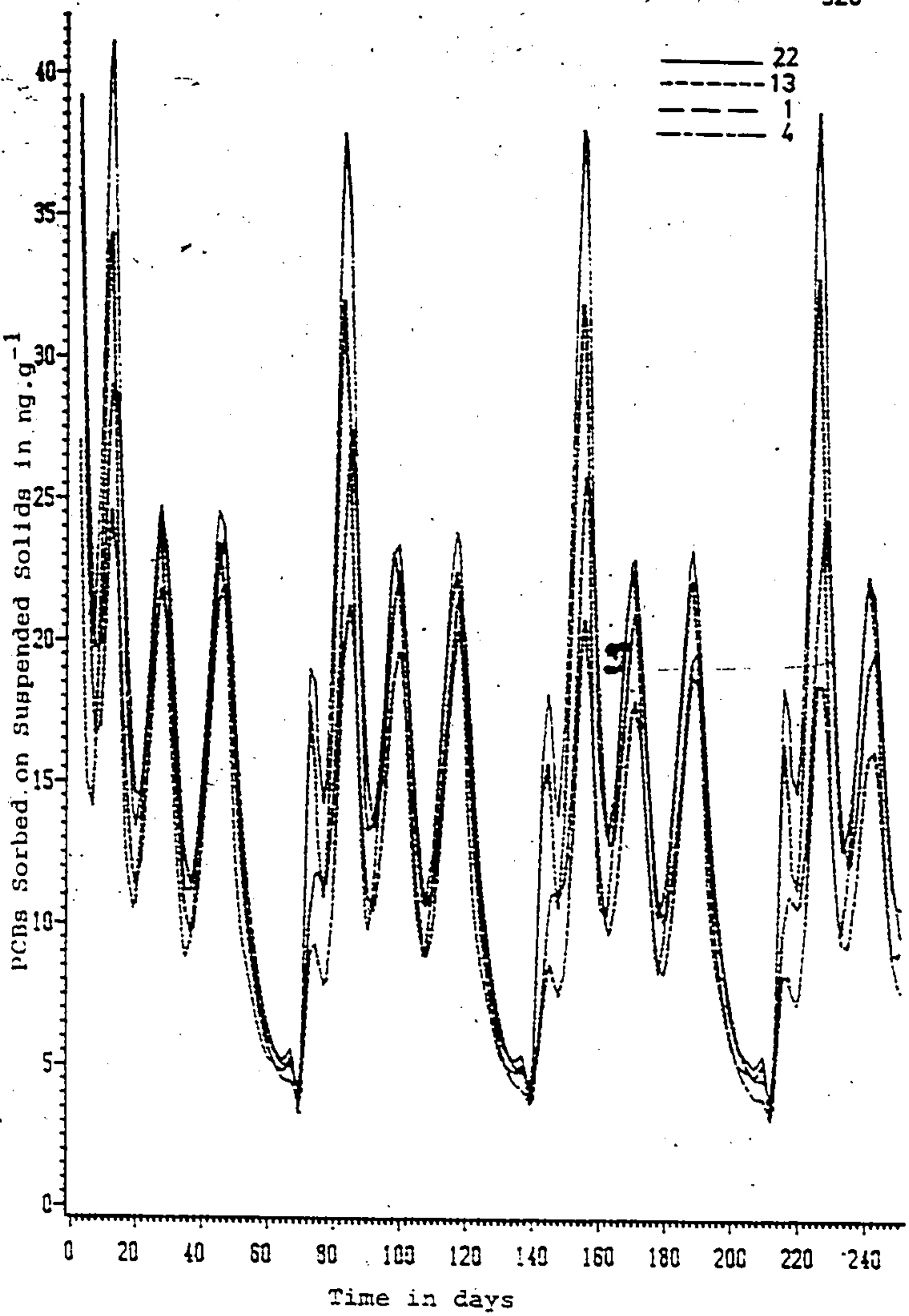

Figure 6.40 PCBs Sorbed onto Suspended Sediments in Water Segments

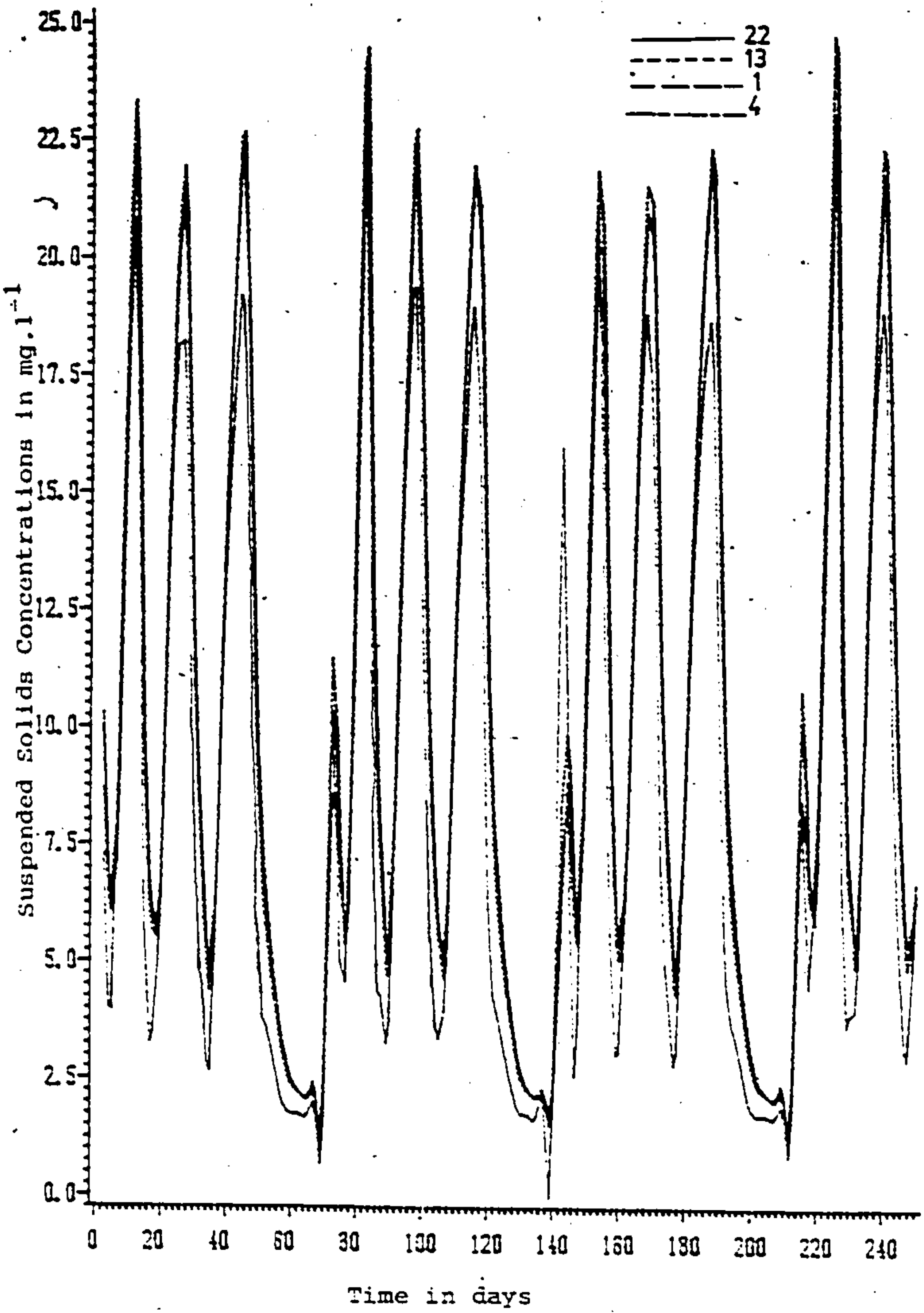

Figure 6.41 Suspended Solids Concentrations in Water Segments

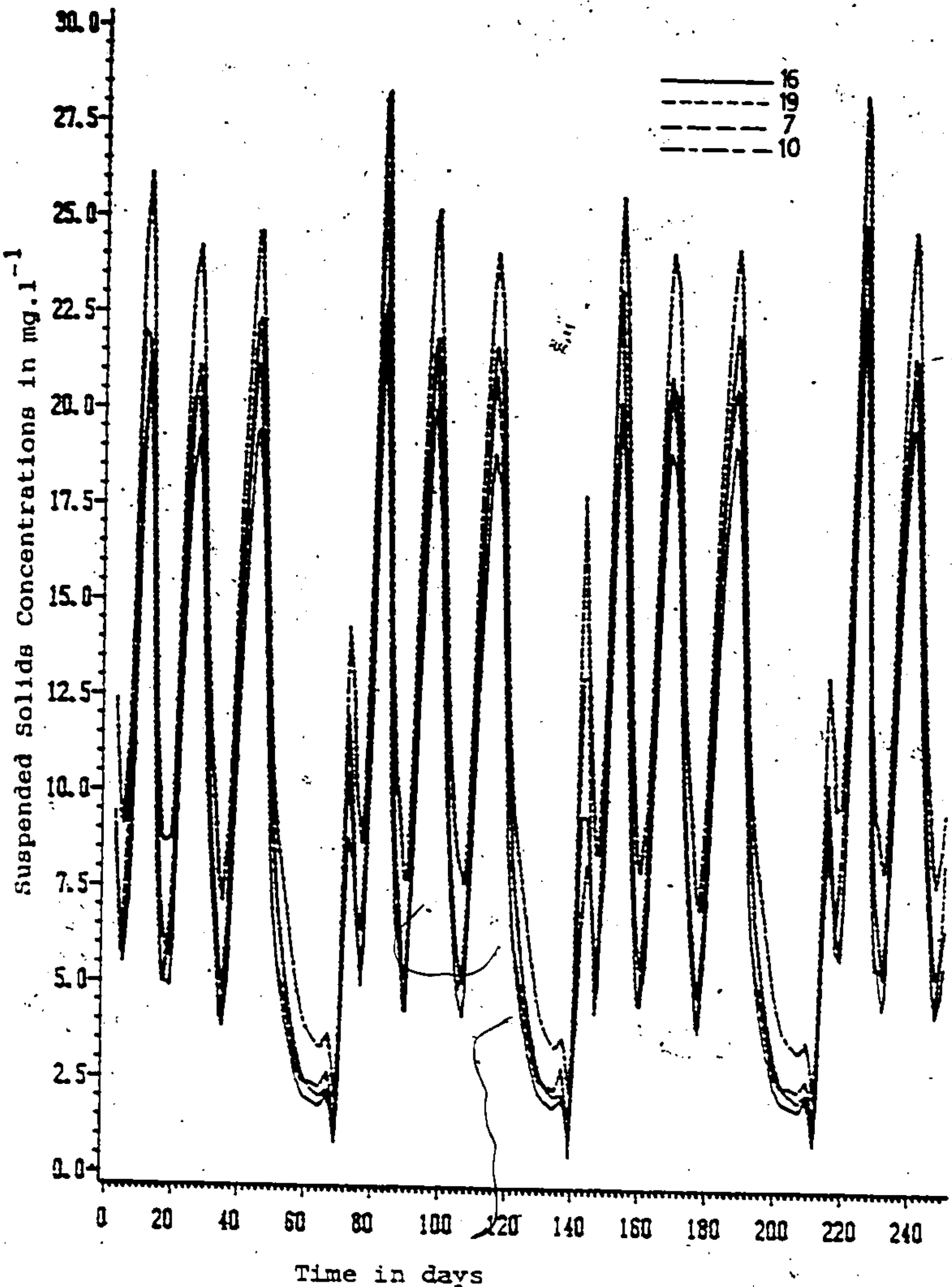

Figure 6.42 Suspended Solids Concentrations in Water Segments.

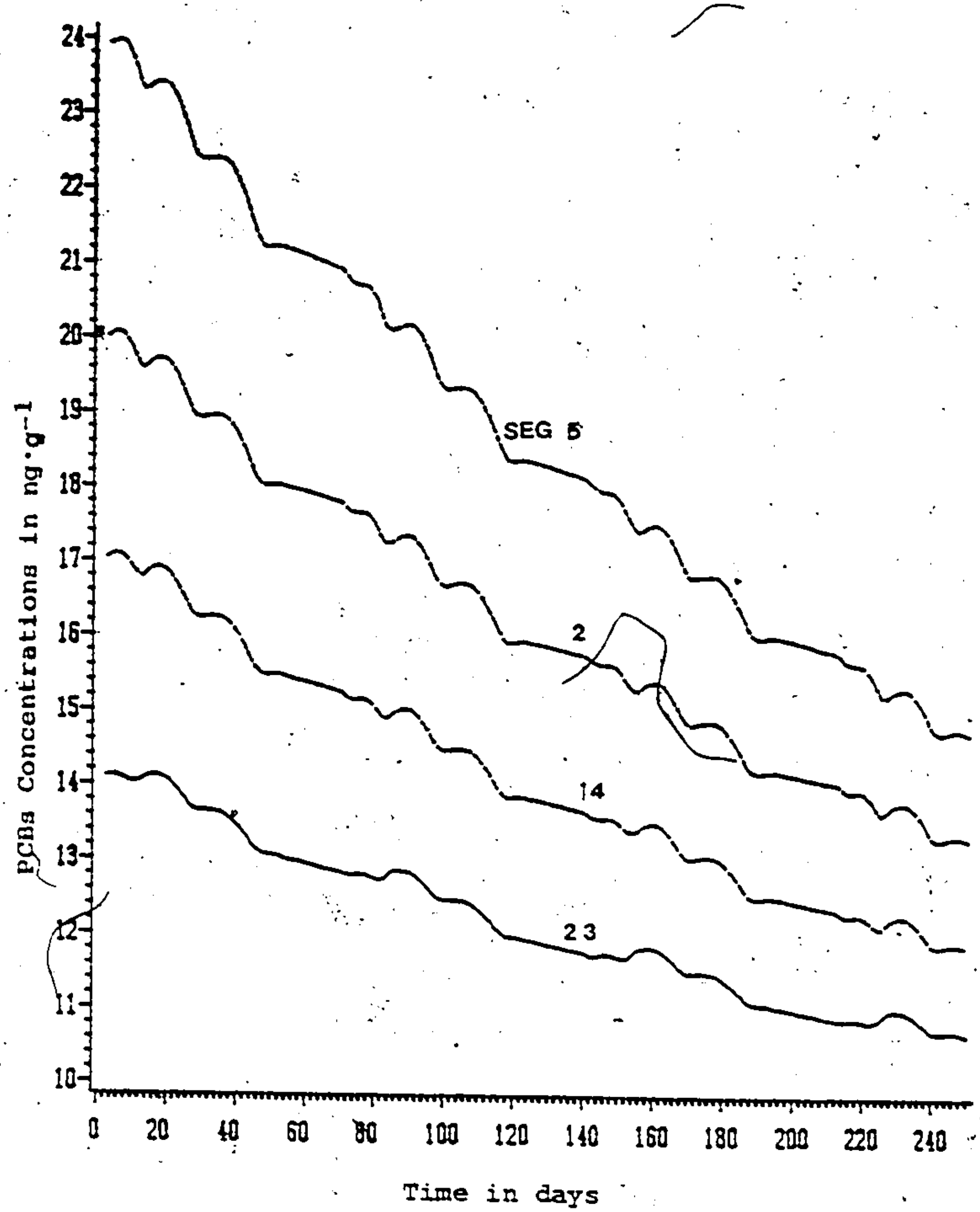

Figure 6.43 PCBs sorbed onto Sediment Bed Segments

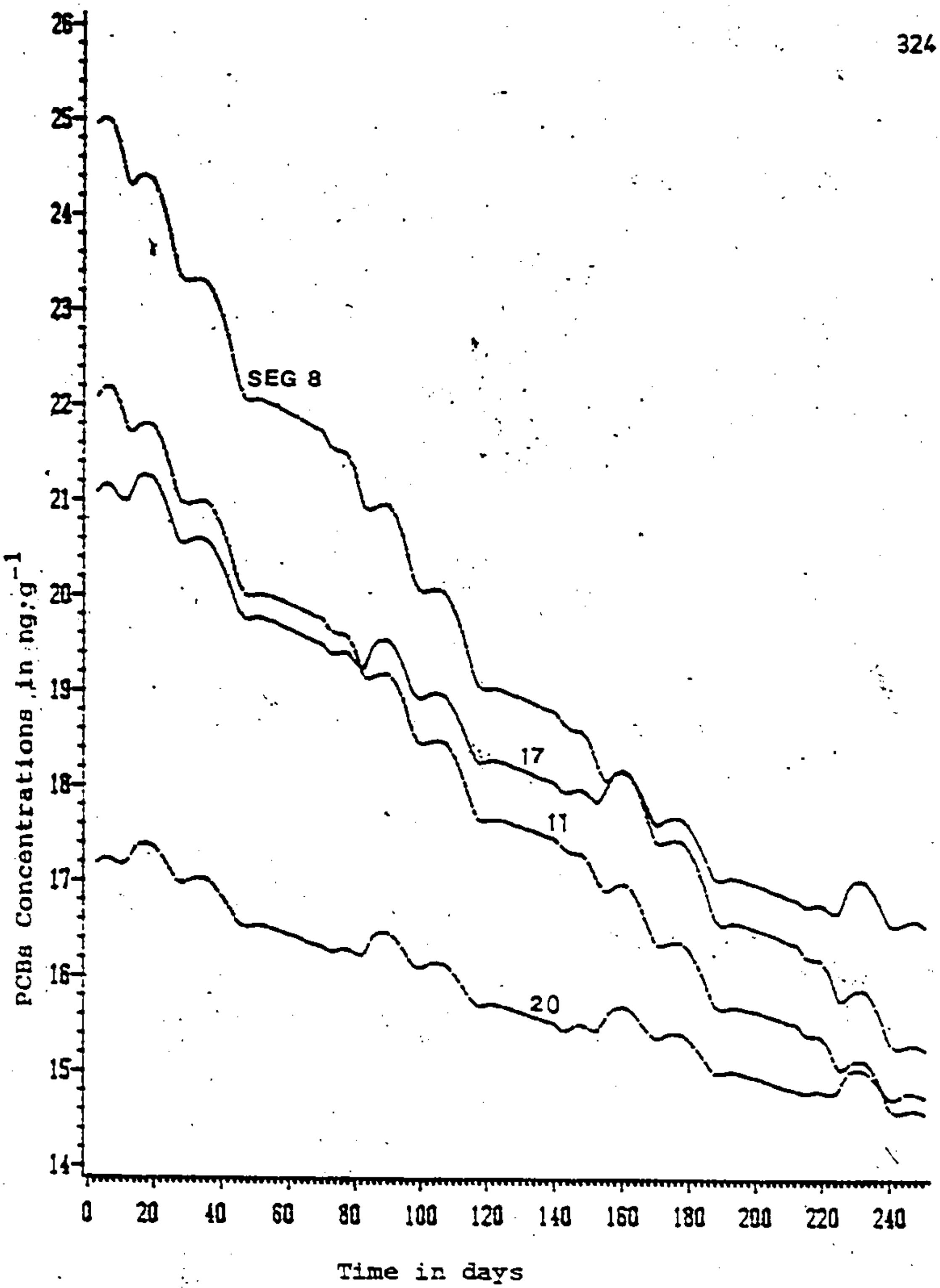

Figure 6.44 PCBs Sorbed onto Bed Sediment Segments

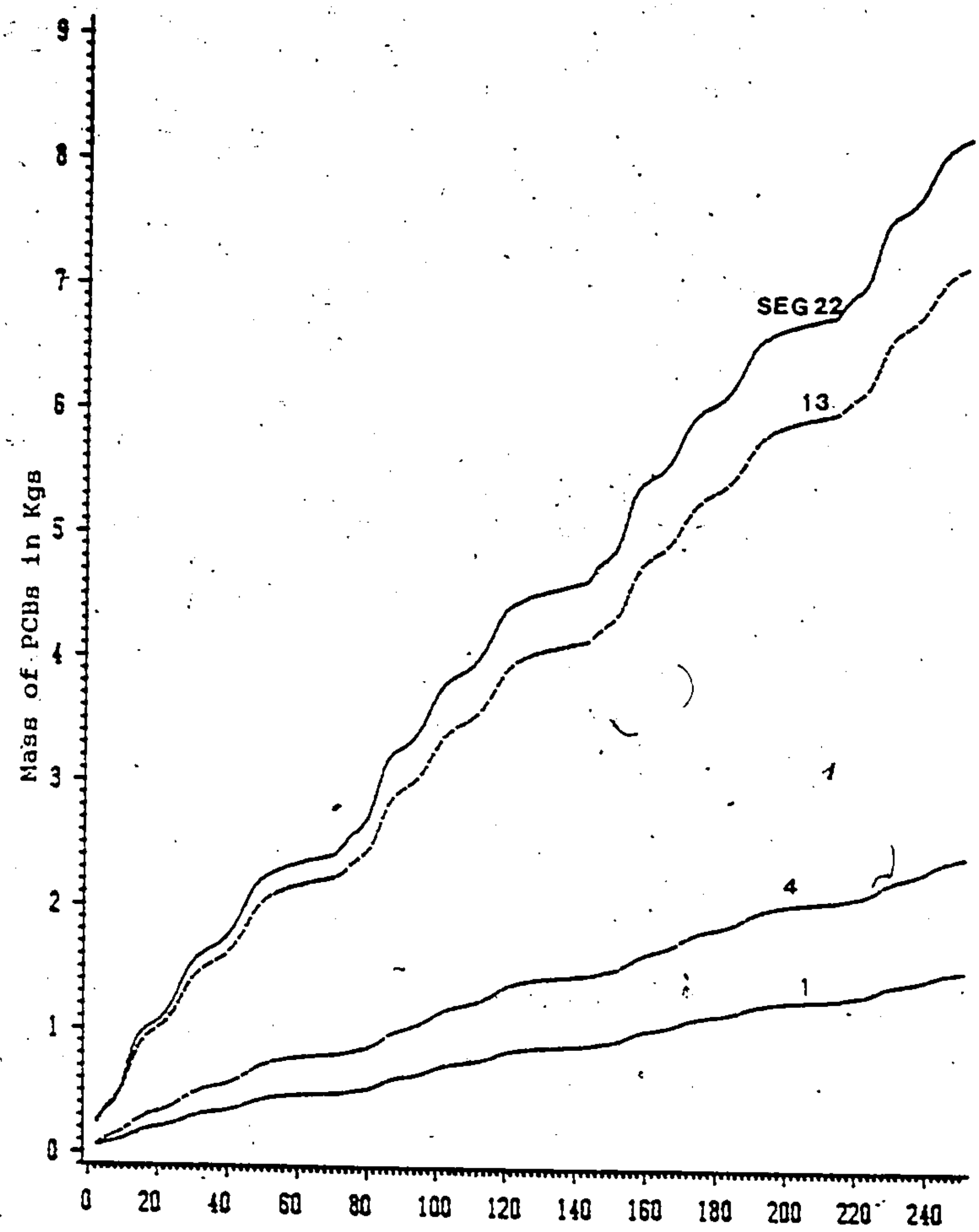

Figure 6.45 Cumulative Mass of PCBs lost from Water Segments by Volatilization

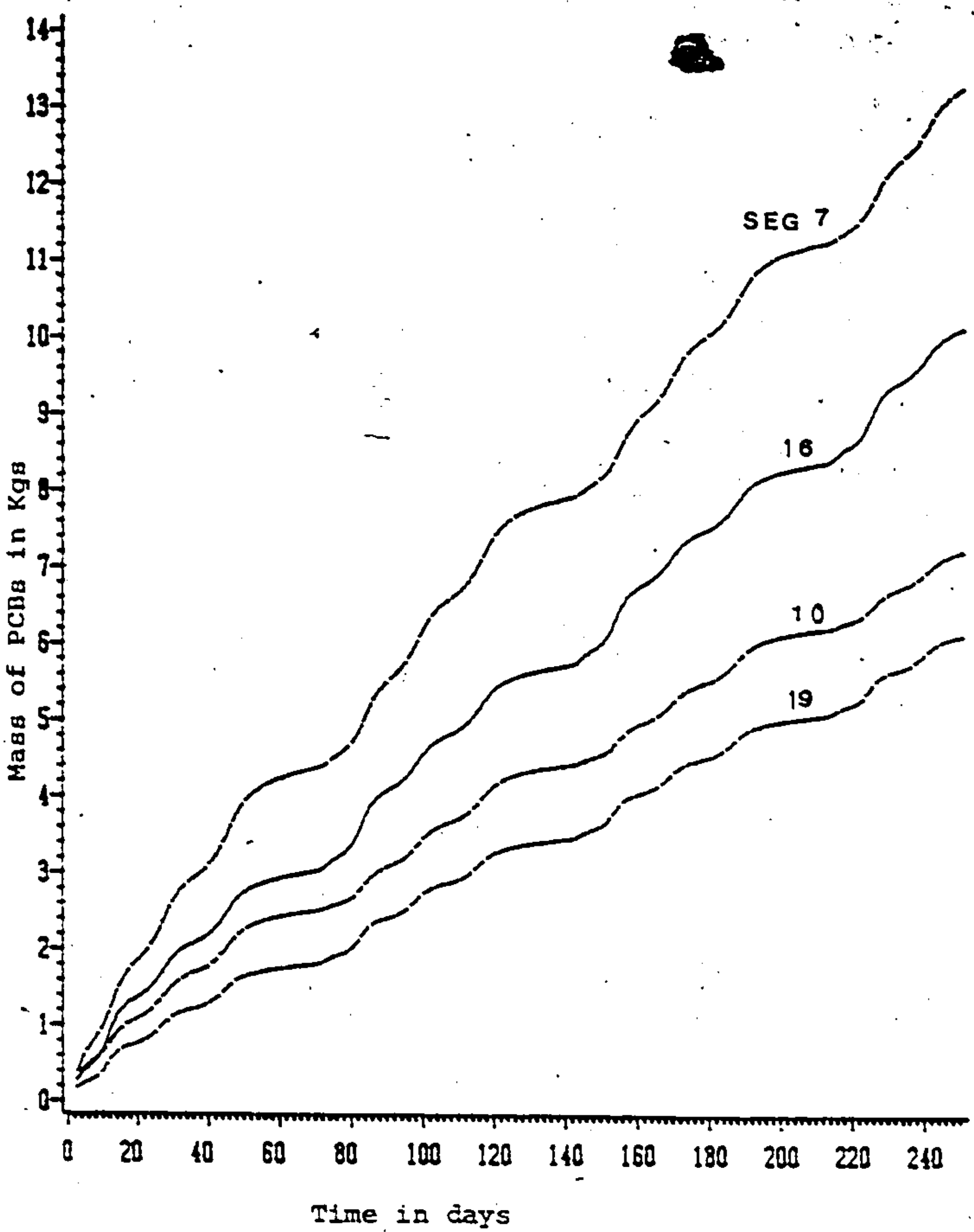

Figure 4.46 Cumulative Mass of PCBs lost from Water Segments by Volatilization

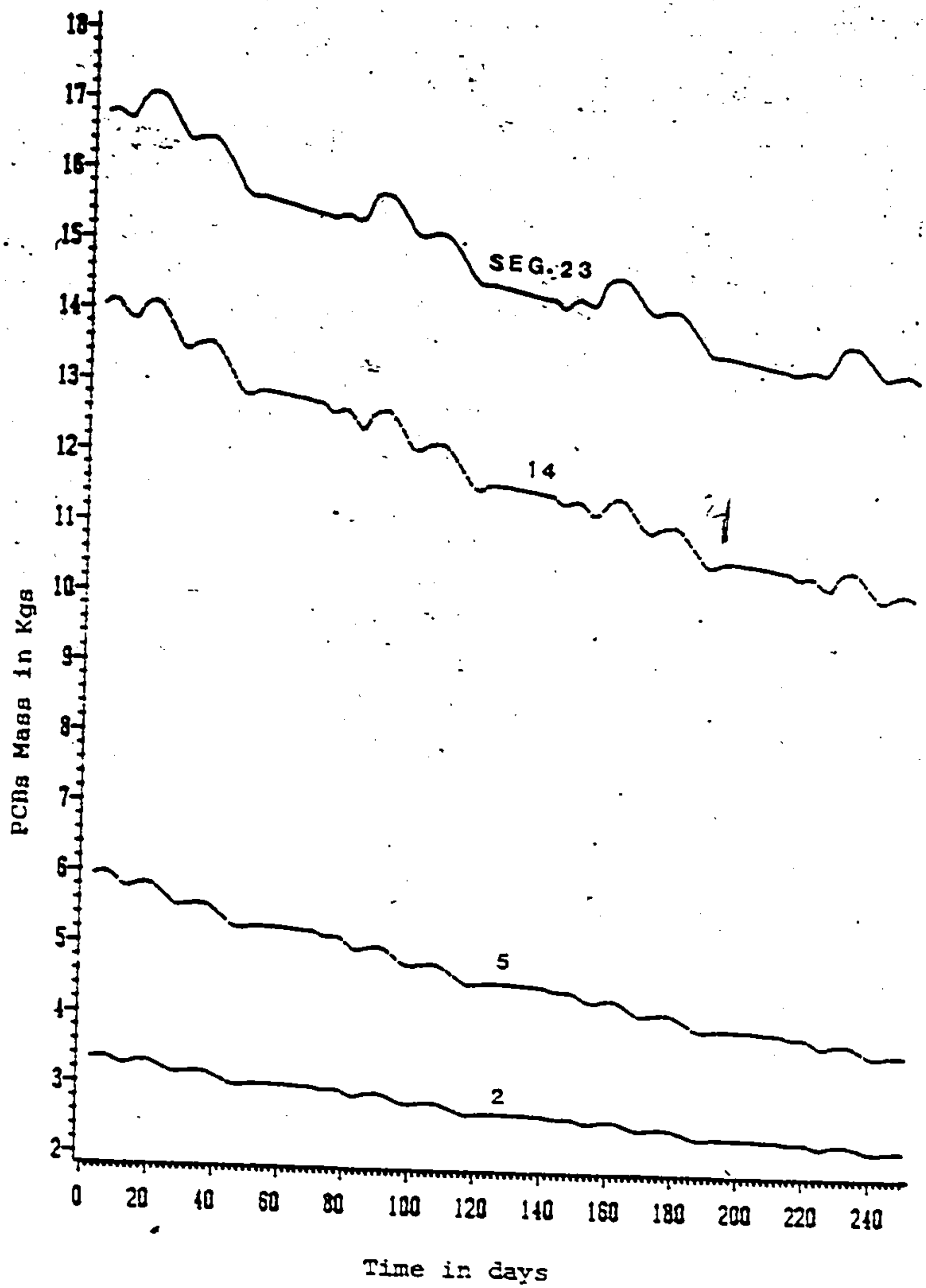

Figure 6.47 Total Mass of PCBs in Surface Bed Segments

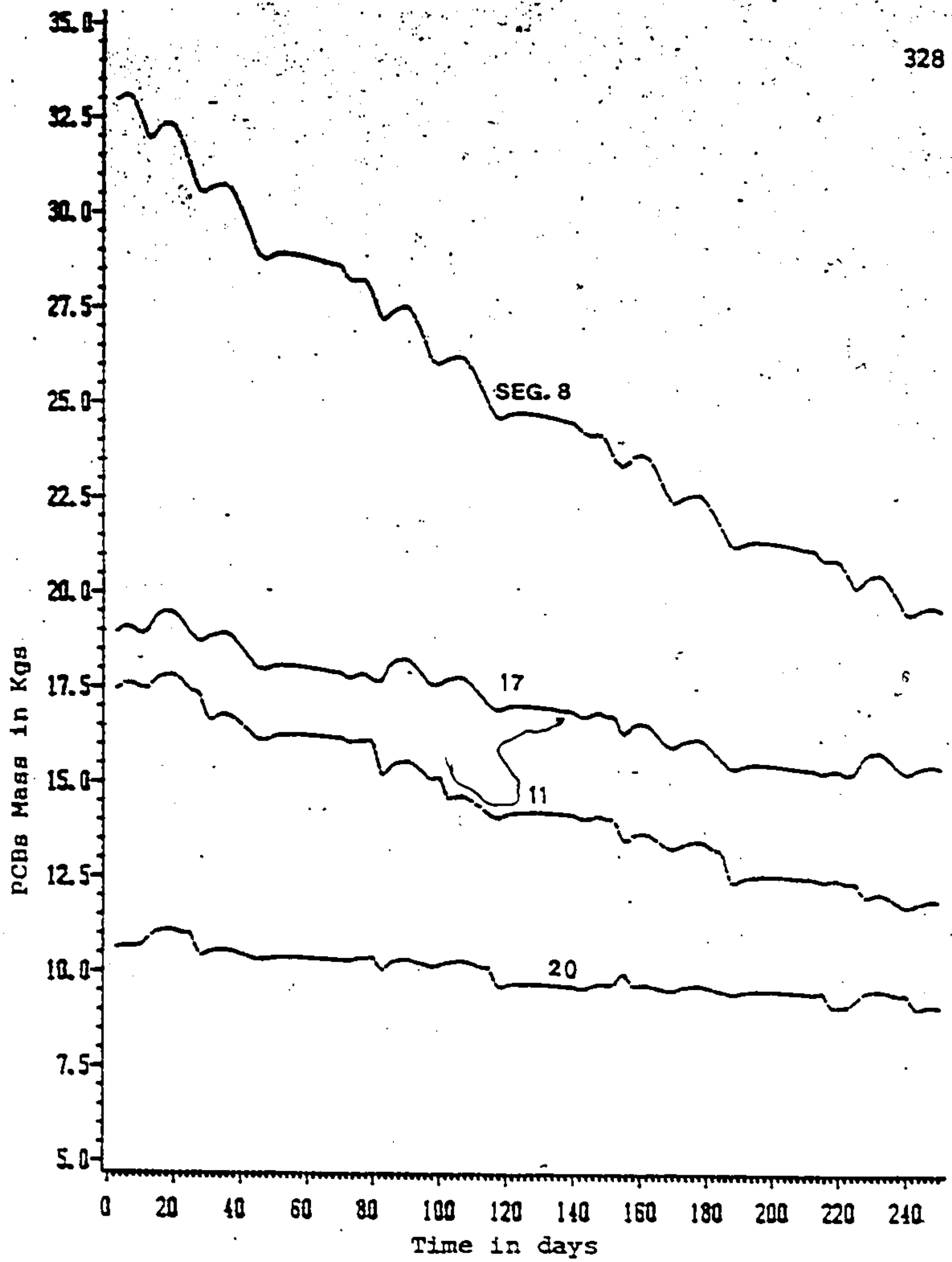

Figure 6.48 Total Mass of PCBs in Surface Bed Segments

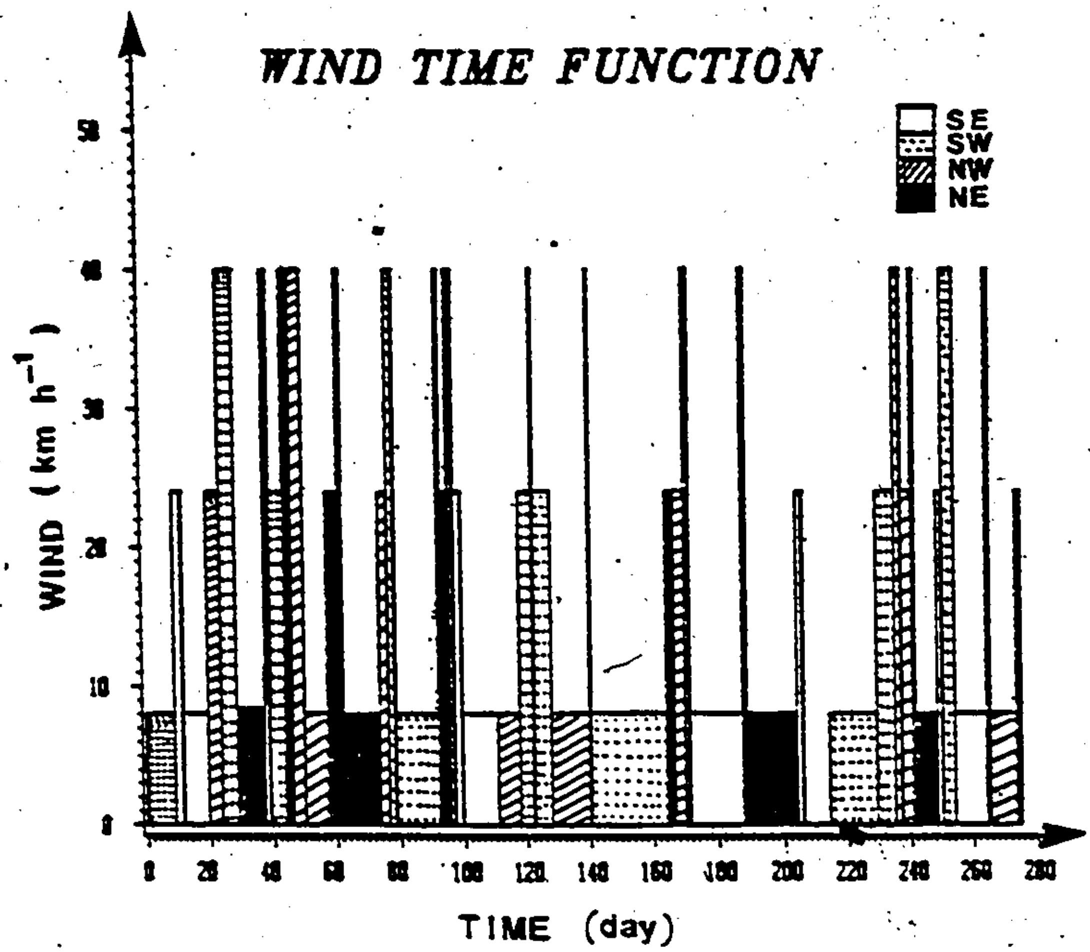

Figure 7.1 Assumed Wind Time Function over Lake St. Clair

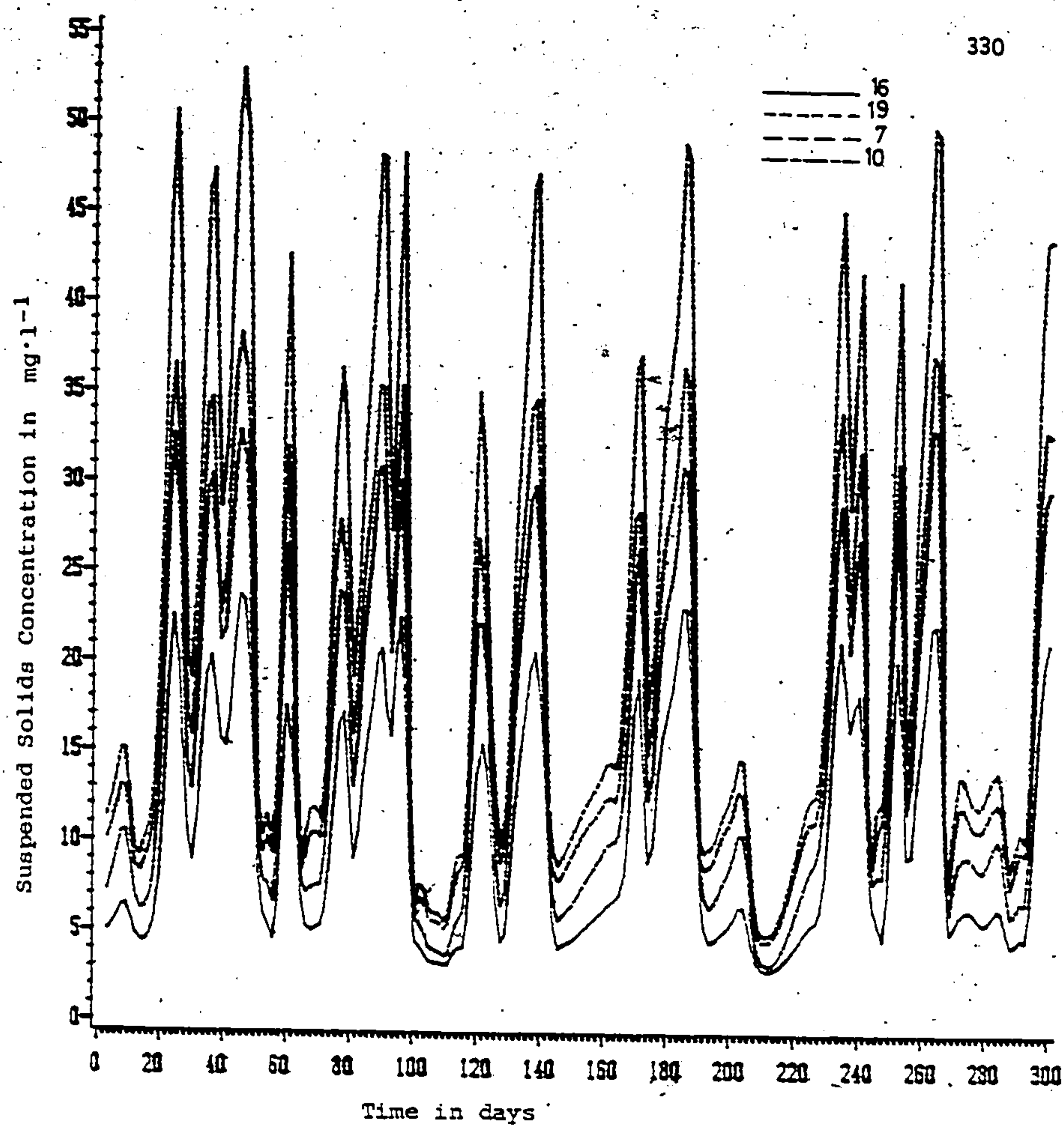

Figure 7.2 Suspended Solids Concentrations in Water Segments in Lake St. Clair.

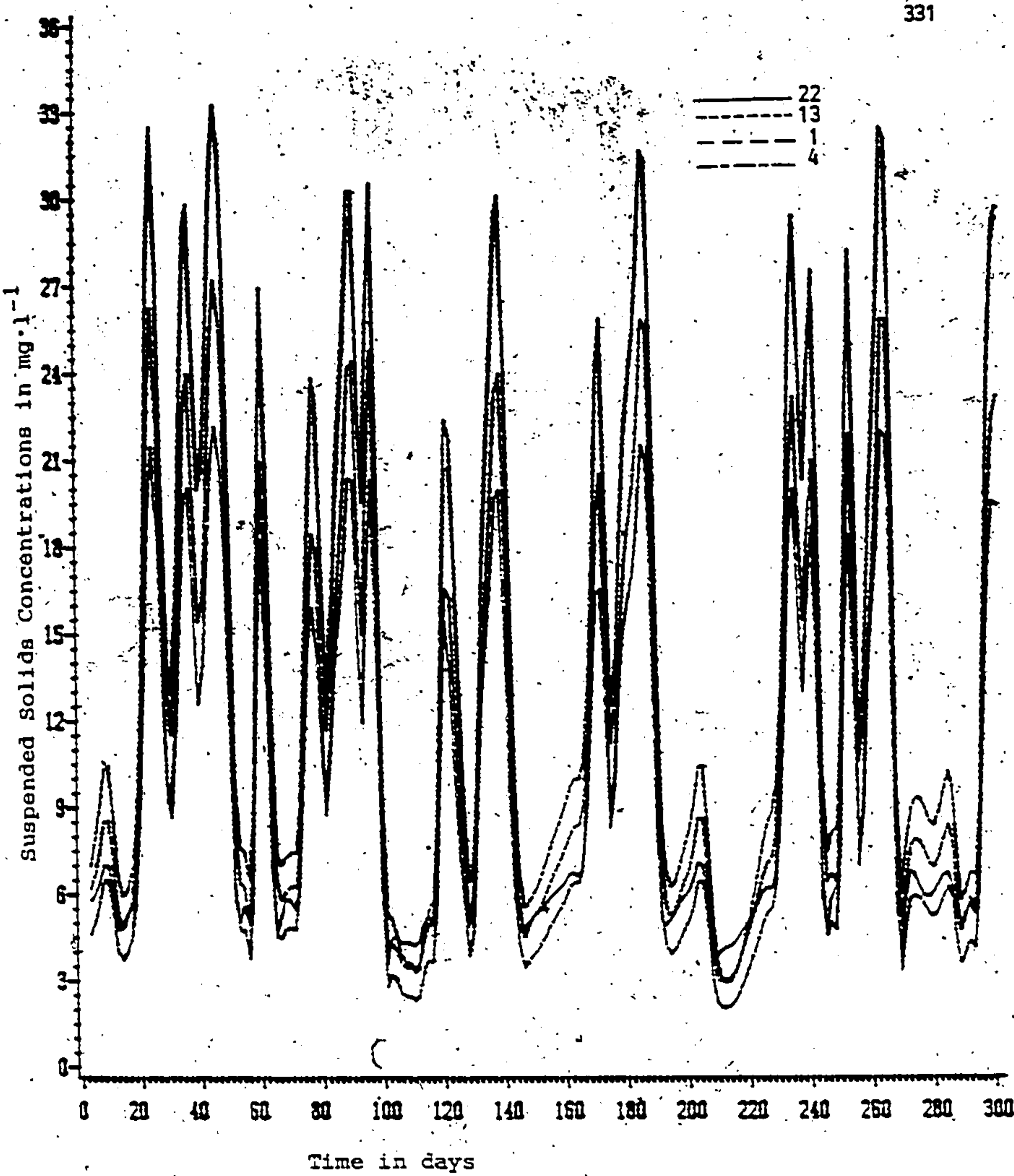

Figure 7.3 Suspended Solids Concentrations in Water Segments in Lake St. Clair

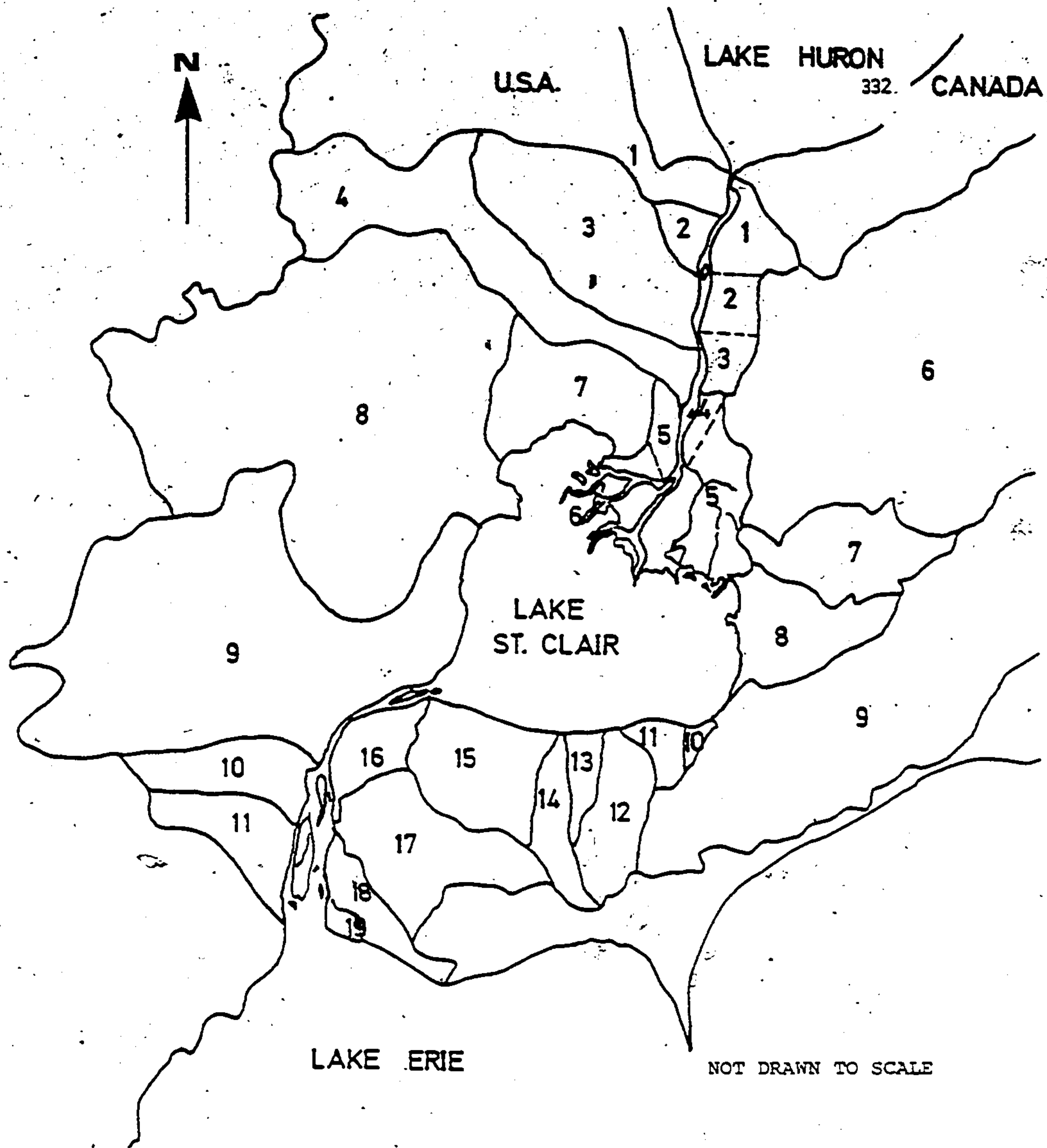

Figure 7.4 The Main Drainage Basins in the Huron - Erie Corridor.

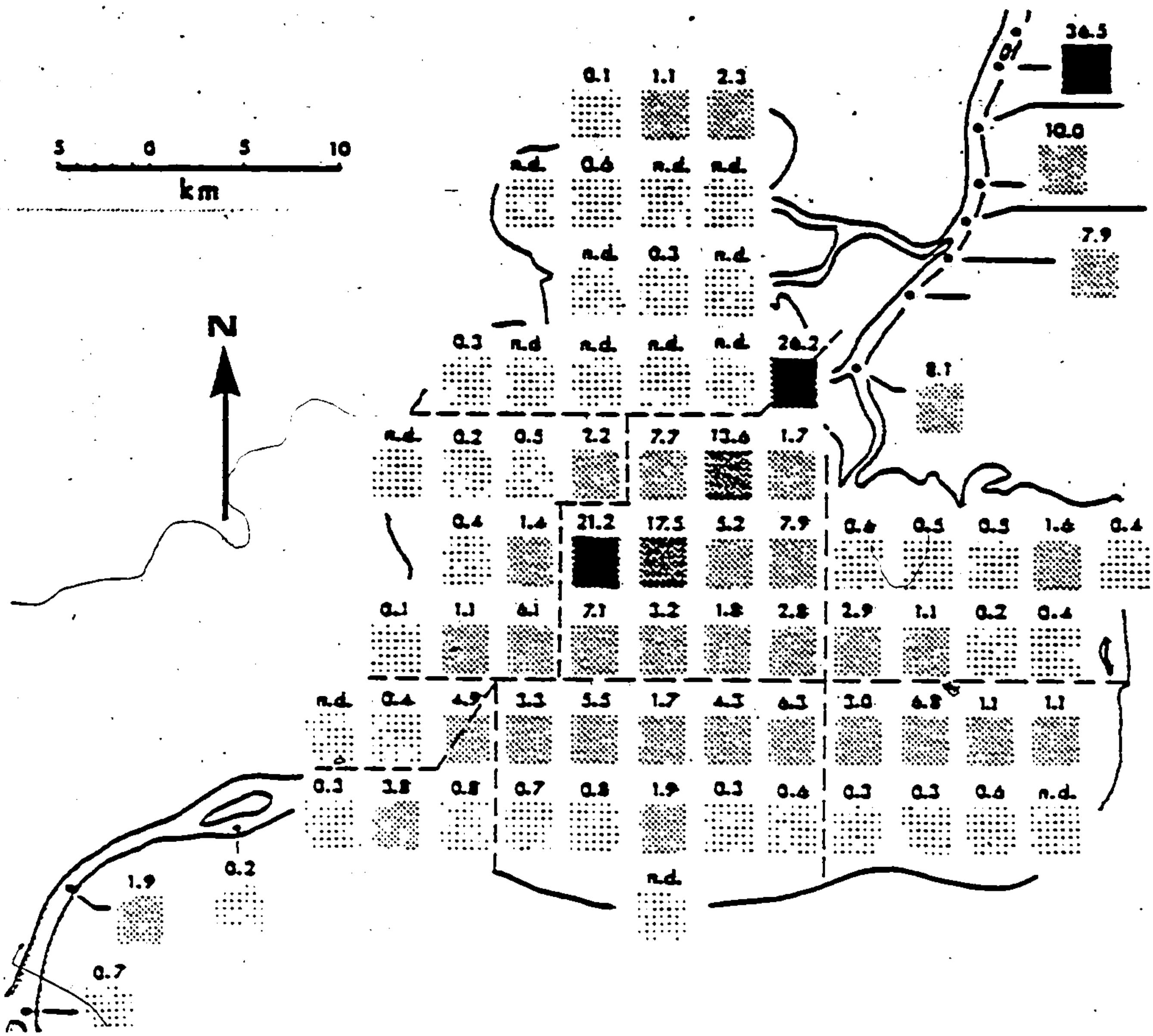

Figure 7.5 The Concentrations of OCS in Bed Sediment in 1984 (After Pugsley et. al, 1985)

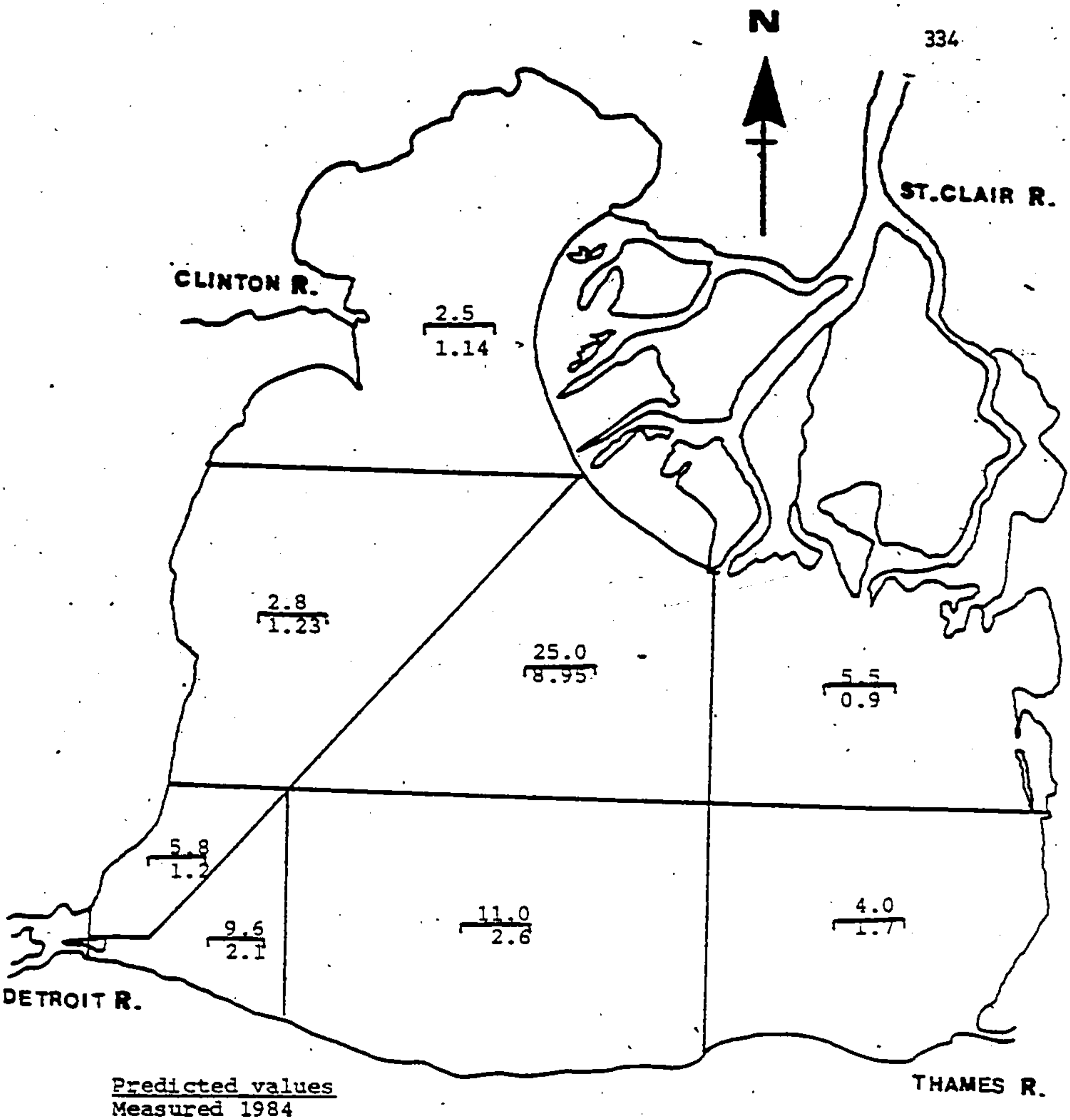

Figure 7.6 Predicted and Measured Concentrations of OCS in Bed Sediments ($ng \cdot g^{-1}$) Based on 2.5 cm surface bed layer

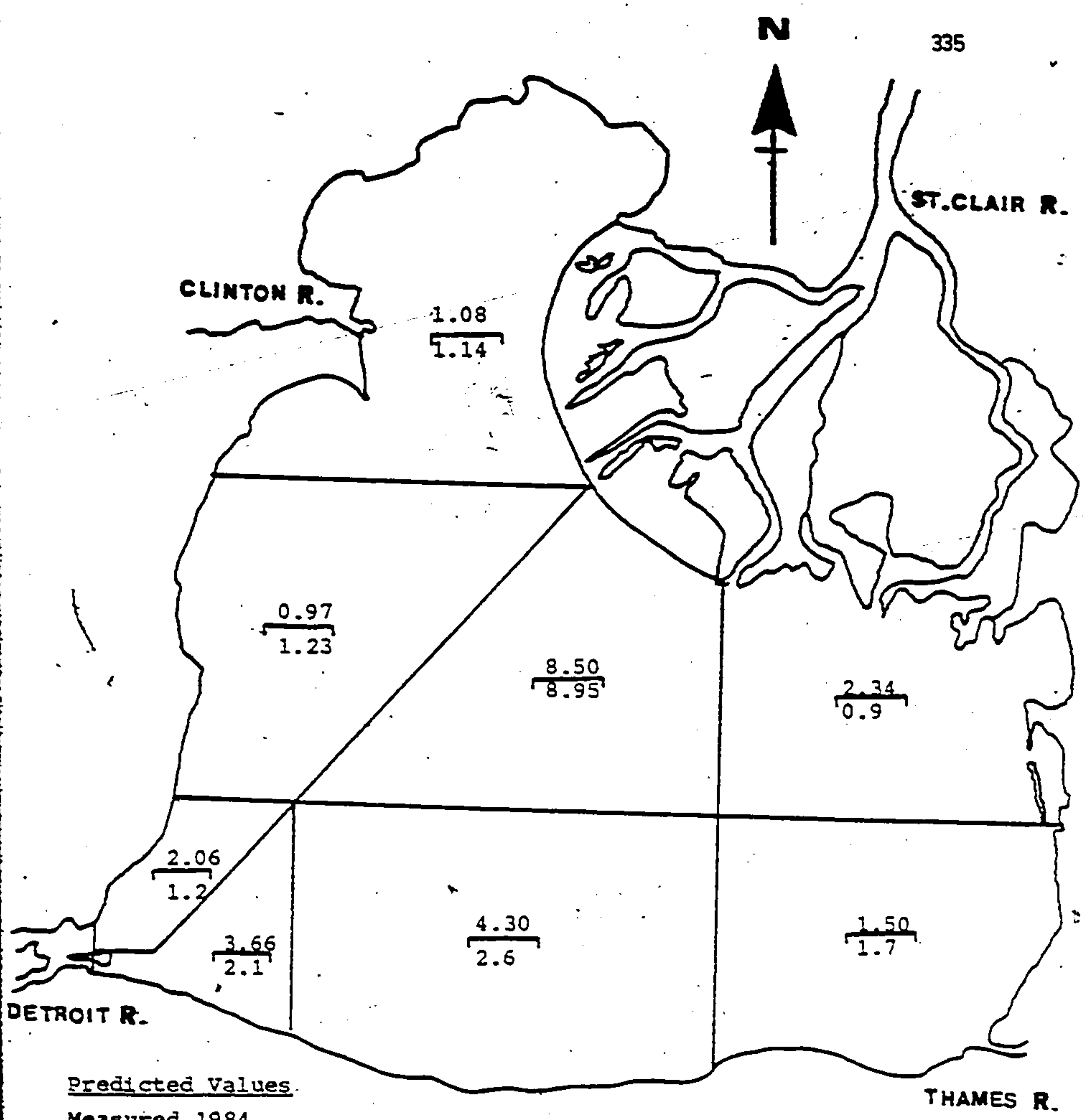

Figure 7.7 Predicted and Measured Concentrations of OCS in Bed Sediments ($ng \cdot g^{-1}$) Bsed on 10 cm surface bed layer

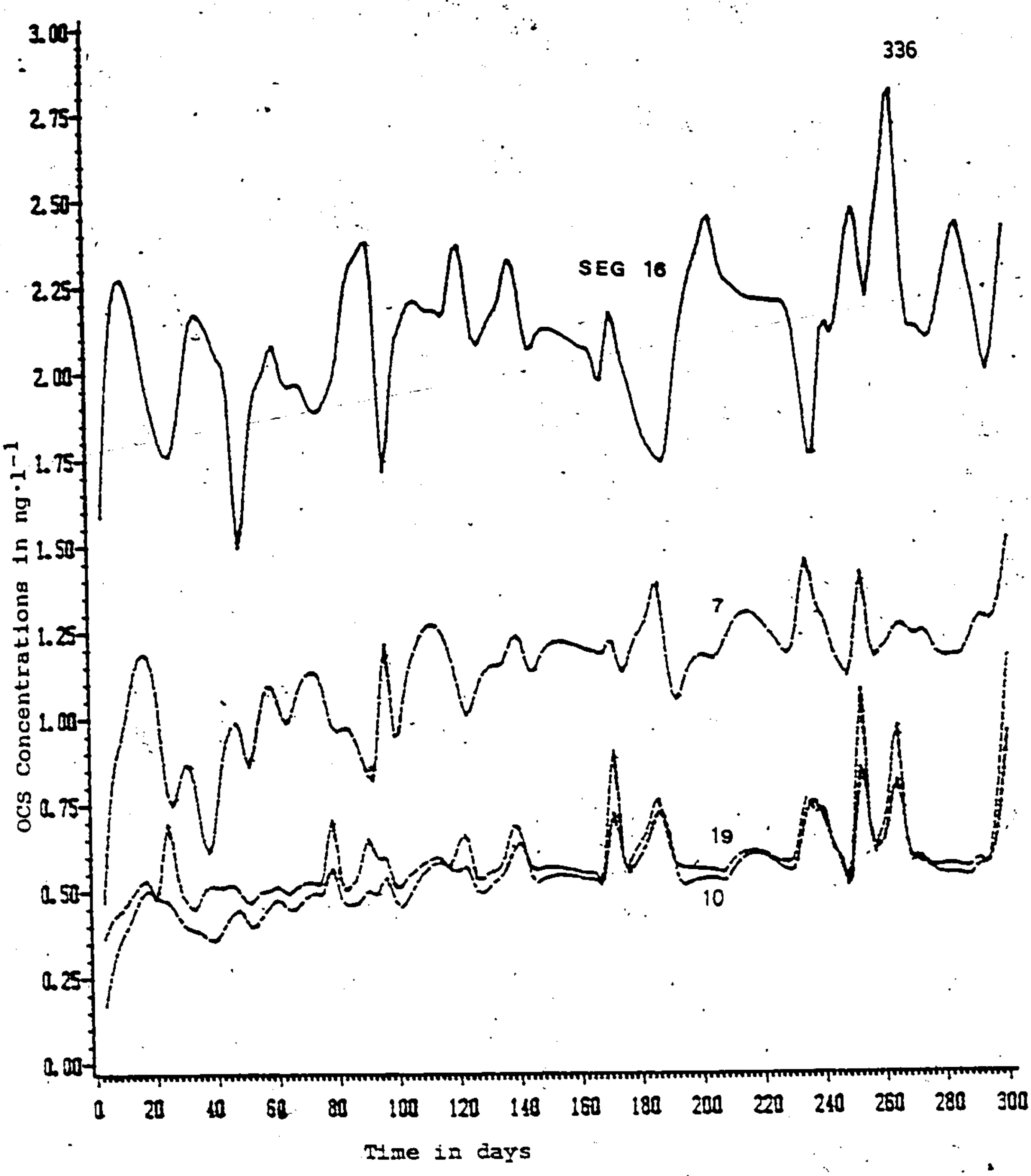

Figure 7.8 Total OCS Concentration in Water Segments in Lake St. Clair

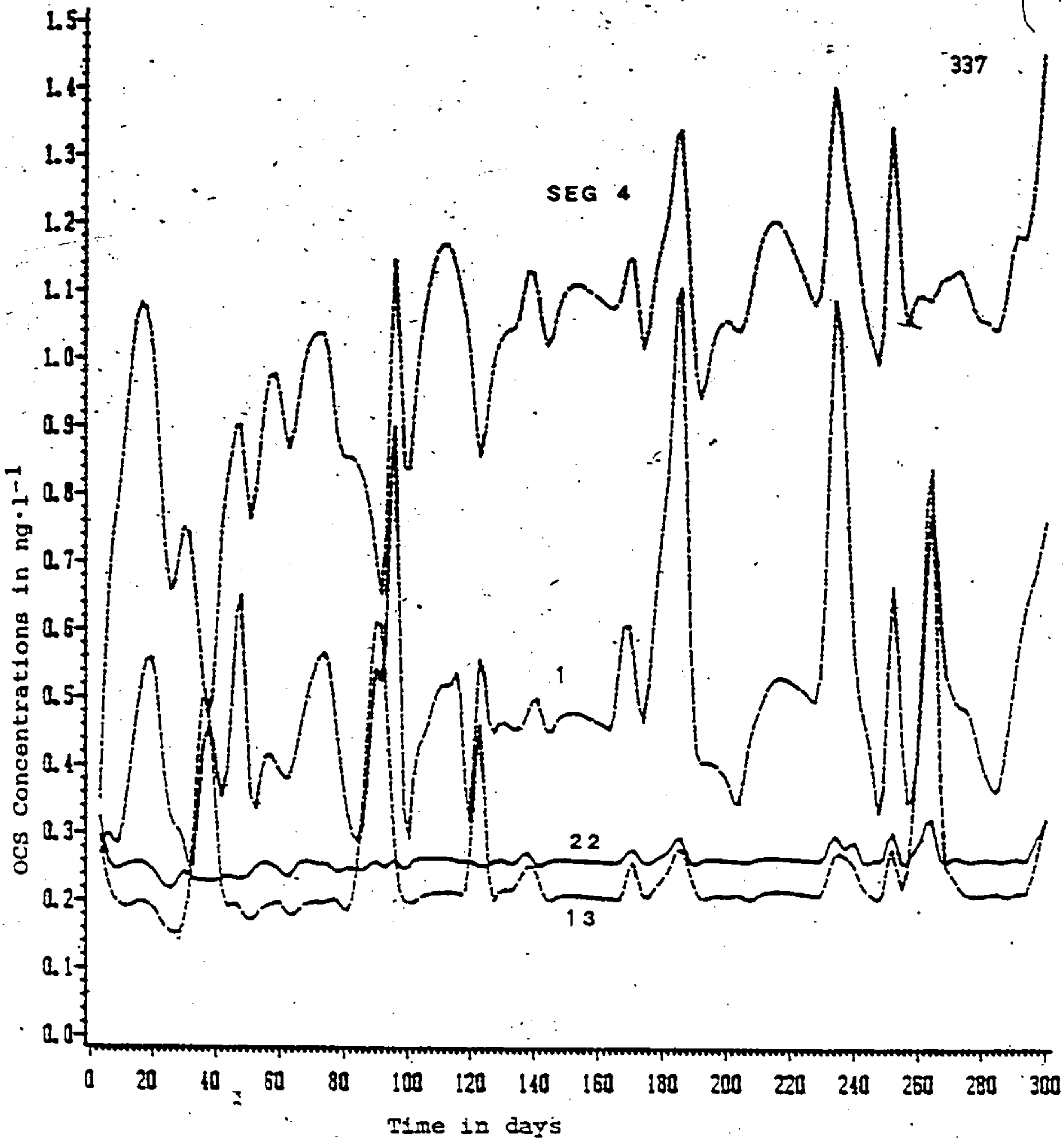

Figure 7.9 Total OCS Concentration in Water Segments in Lake St. Clair.

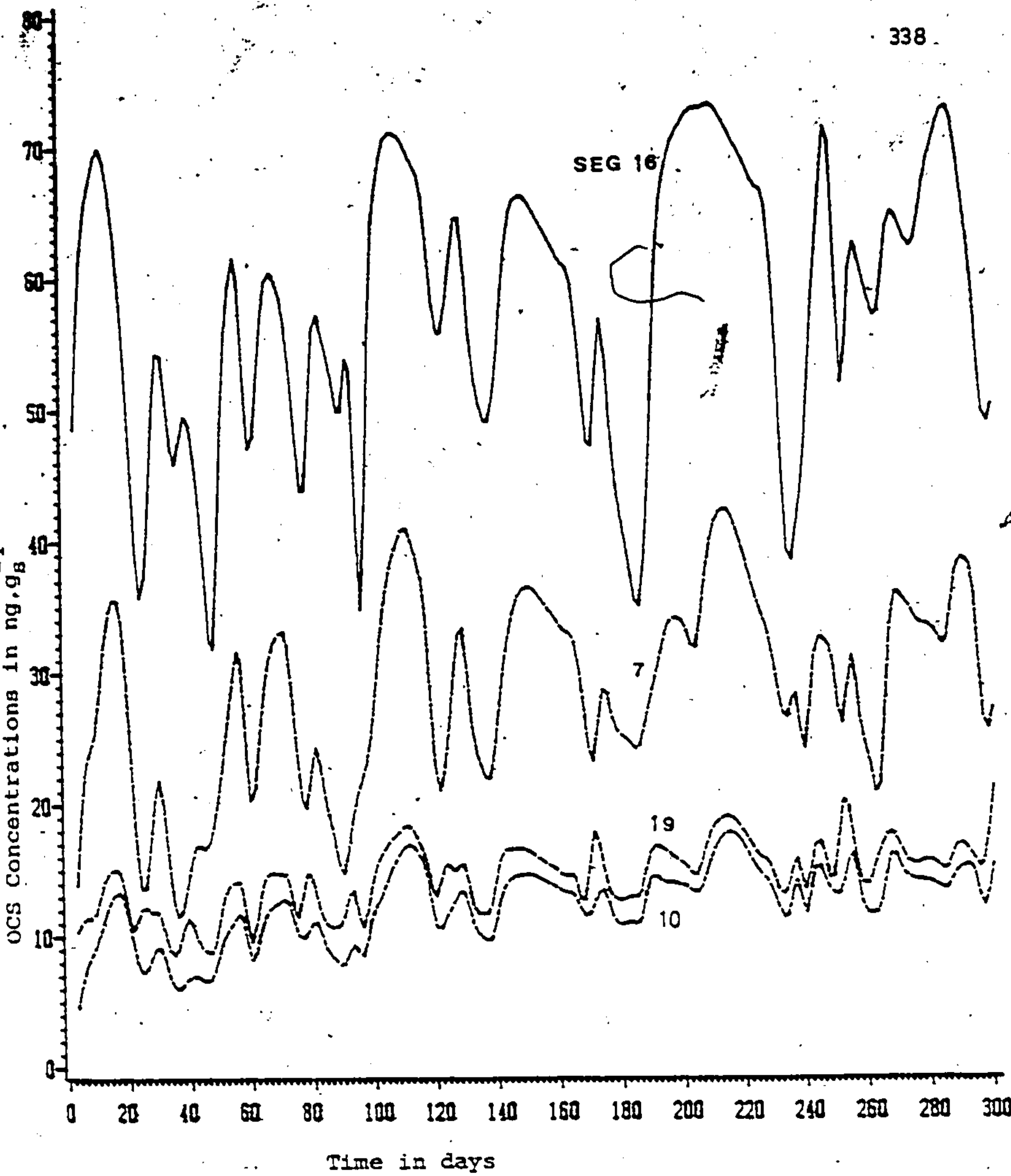

Figure 7.10 OCS Sorbed Onto Suspended Sediments in Water Segments in Lake St. Clair.

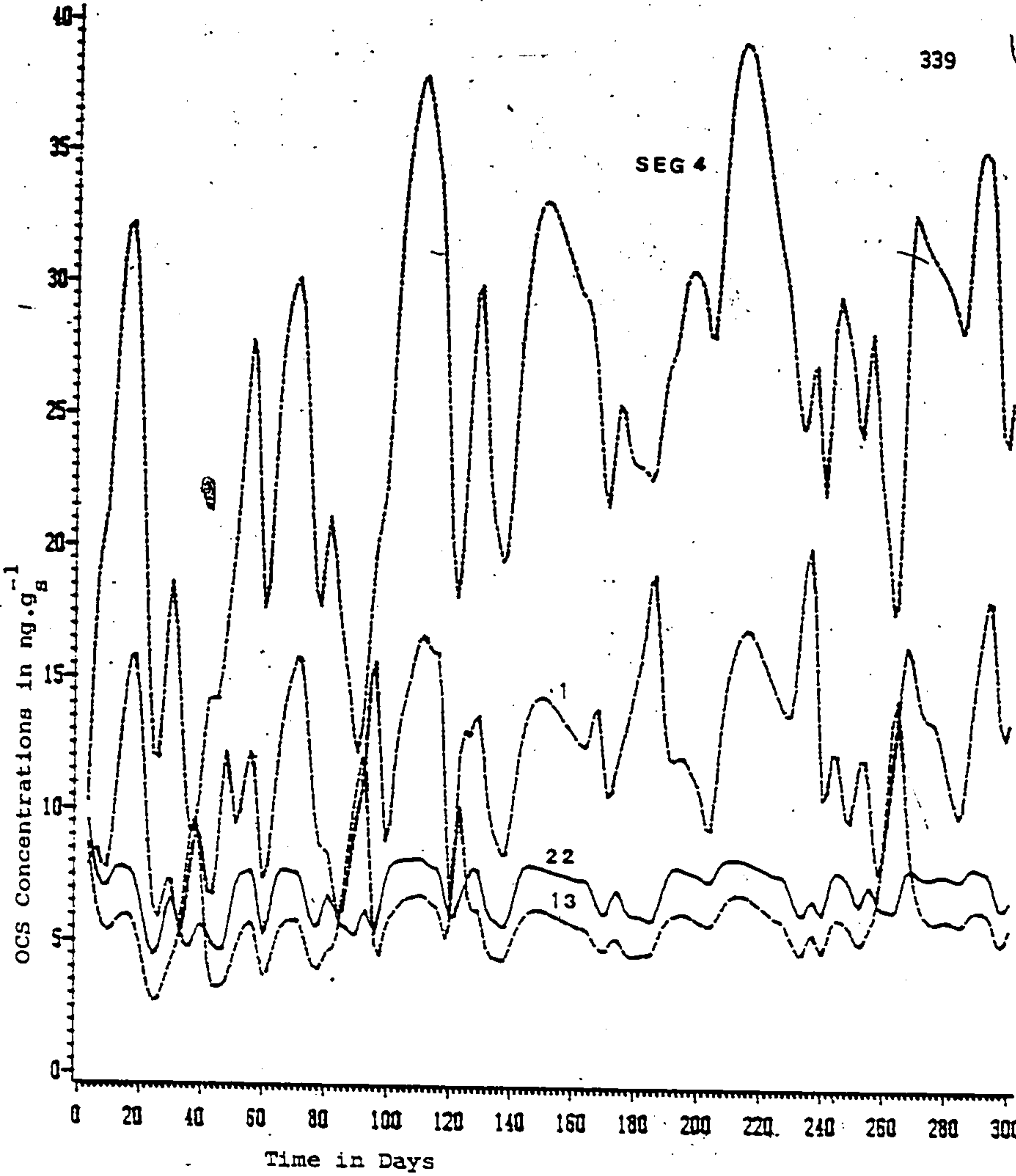

Figure 7.11 OCS Sorbed Onto Suspended Sediments in Water Segments in Lake St. Clair

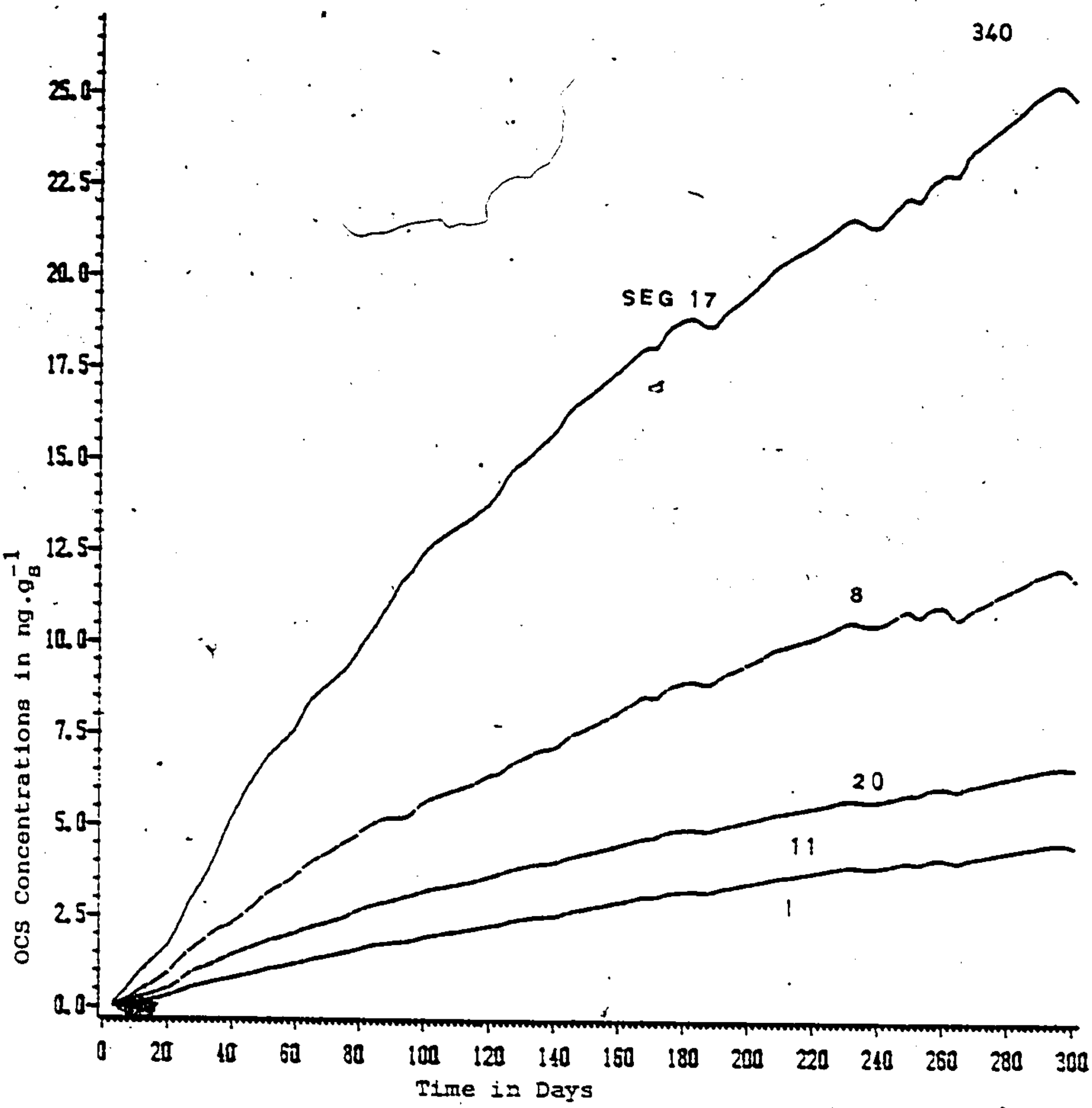

Figure 7.12 OCS Sorbed Onto Sediment Bed Segments in Lake St. Clair

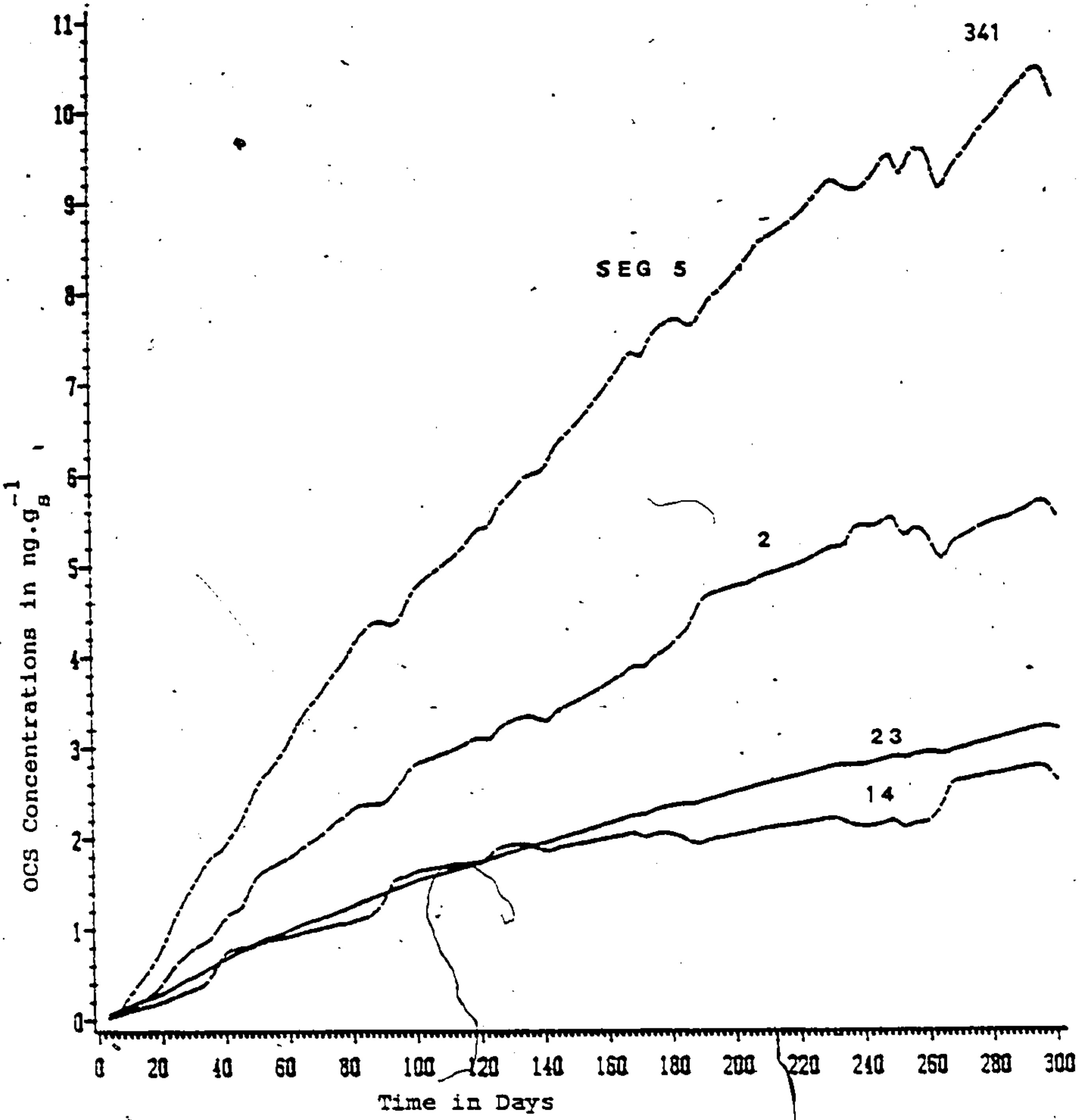

Figure 7.13 OCS Sorbed onto Bed Sediment Segments in Lake St. Clair

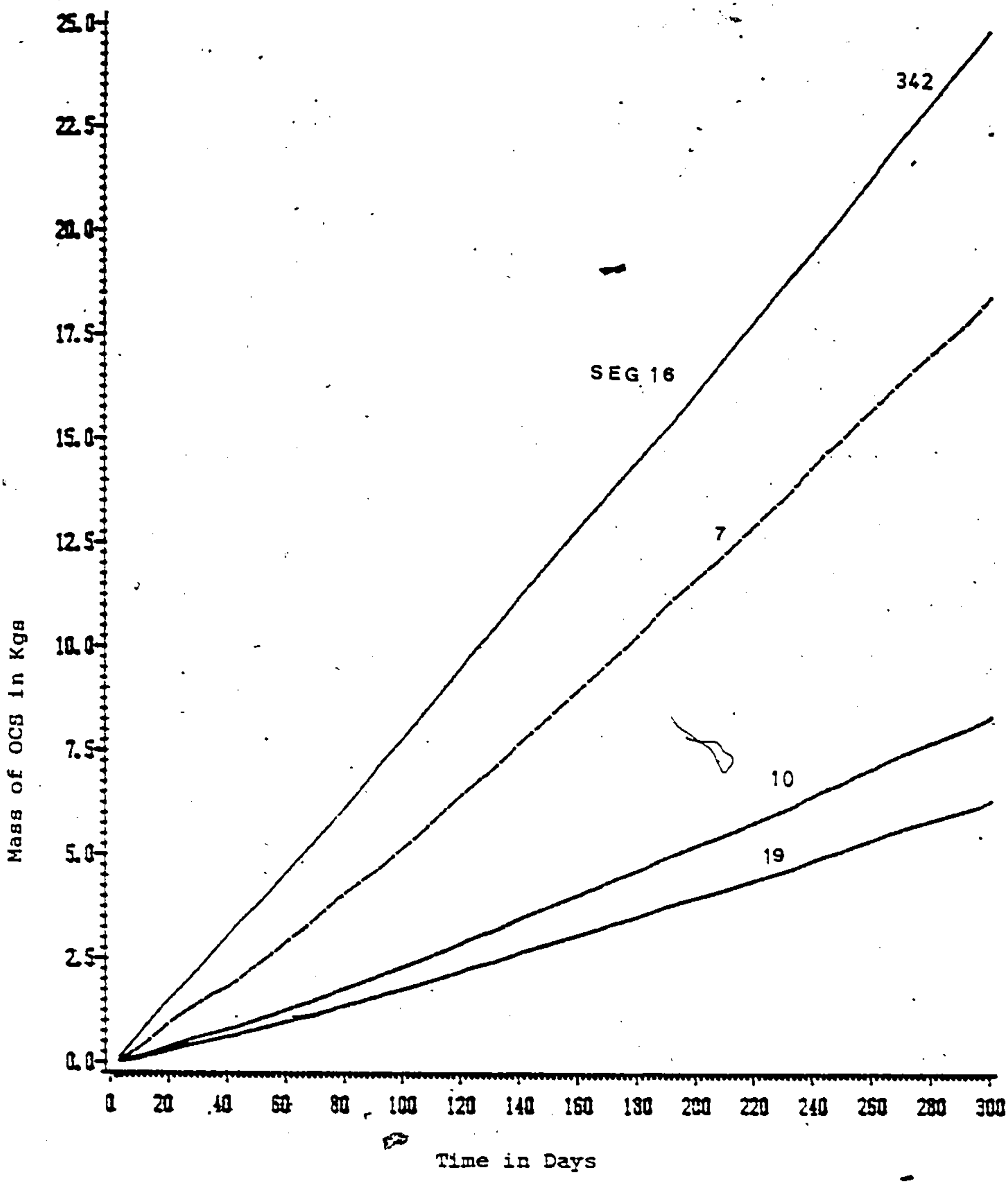

Figure 7.14 Cumulative Mass of OCS Lost from Water Segments by Volatilization in Lake St. Clair

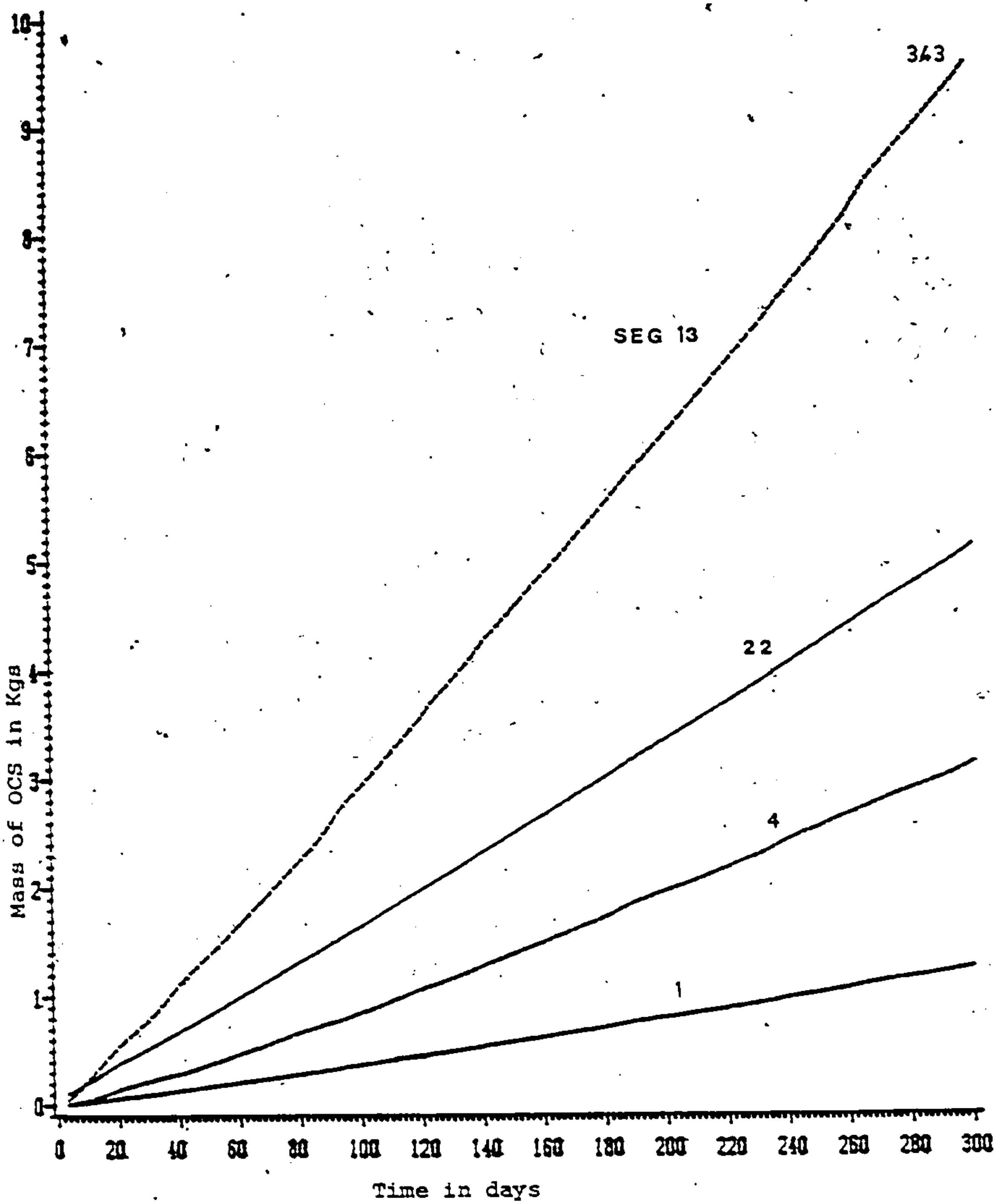

Figure 7.15 Cumulative Mass of PCBs lost from Water Segments by Volatilization in Lake St. Clair

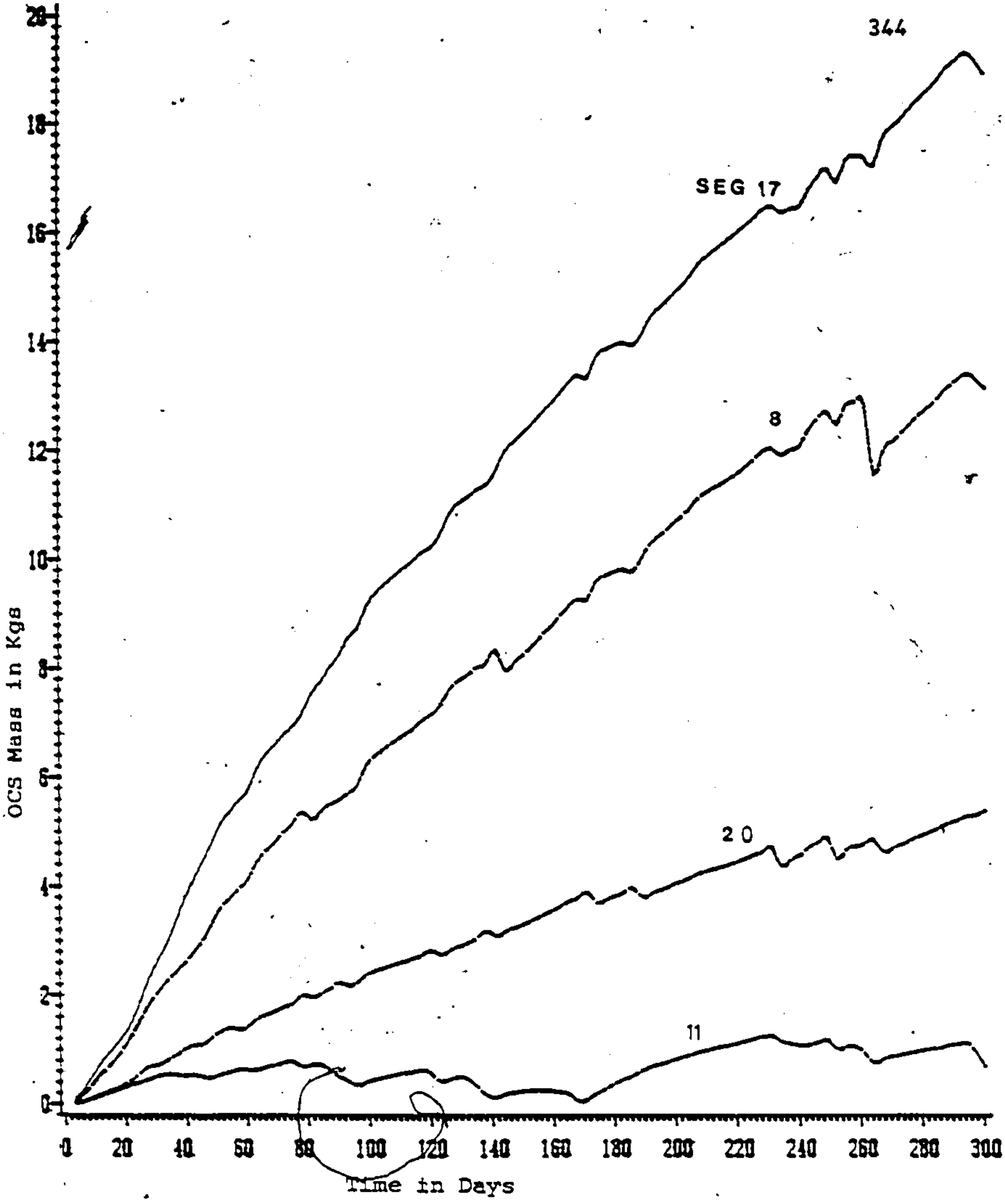

Figure 7.16 Total Mass of OCS in Surface Bed Segments in Lake St. Clair.

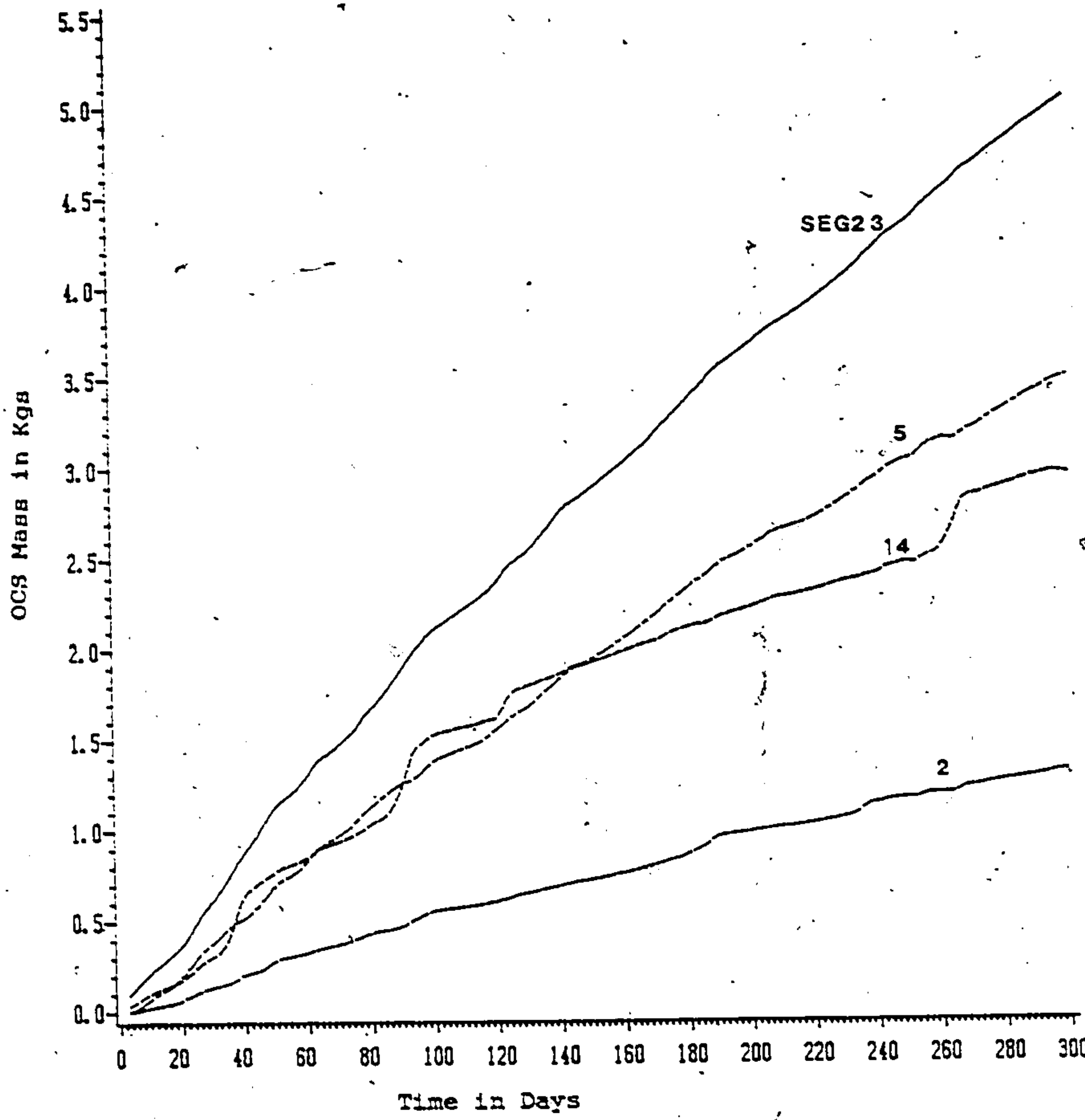

Figure 7.17 Total Mass of OCS in Surface Bed Segments in Lake St. Clair

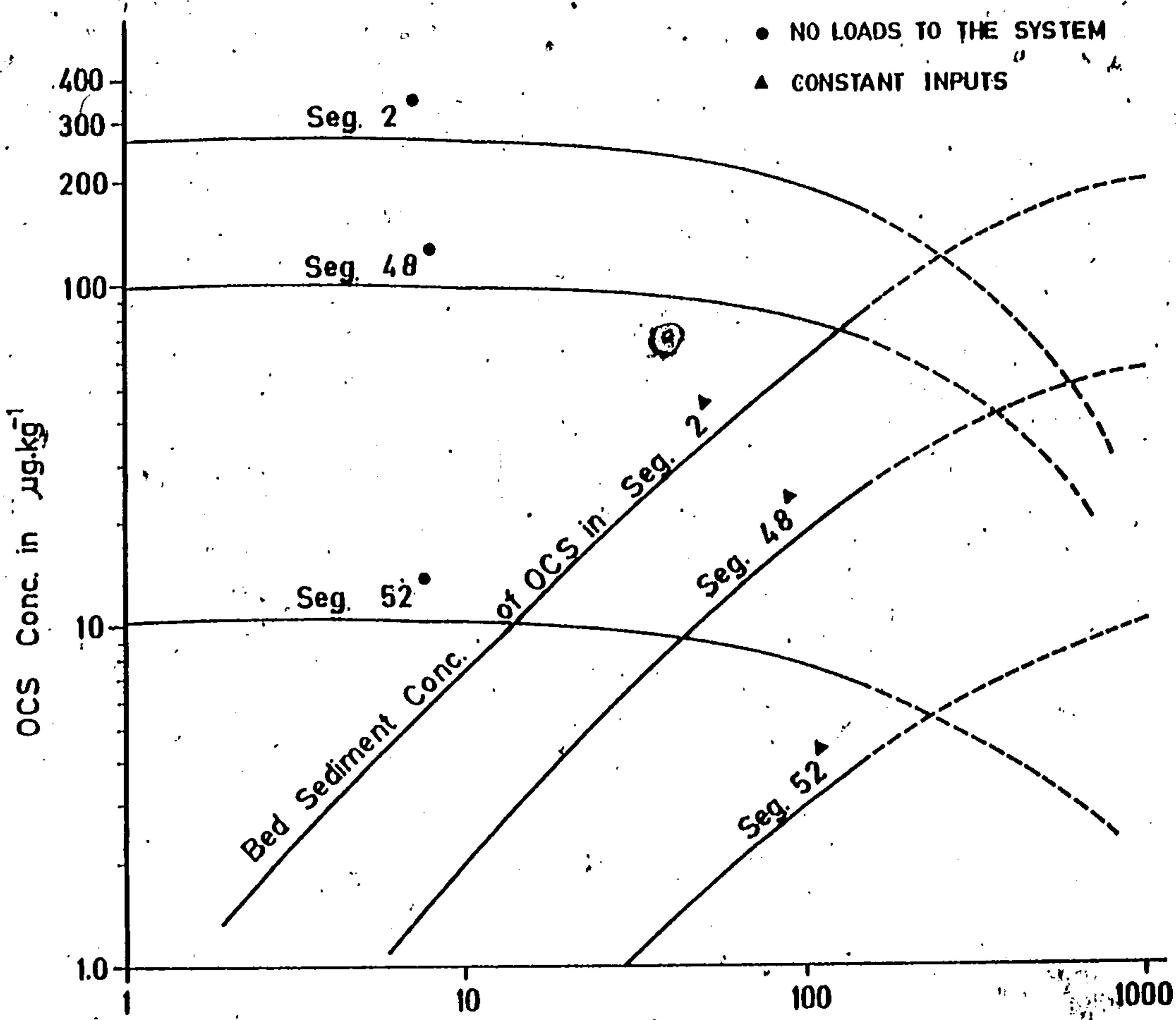

Figure 7.18 Predicted OCS Concentrations in Bed Sediment Along The Canadian Shoreline Segments in St. Clair River

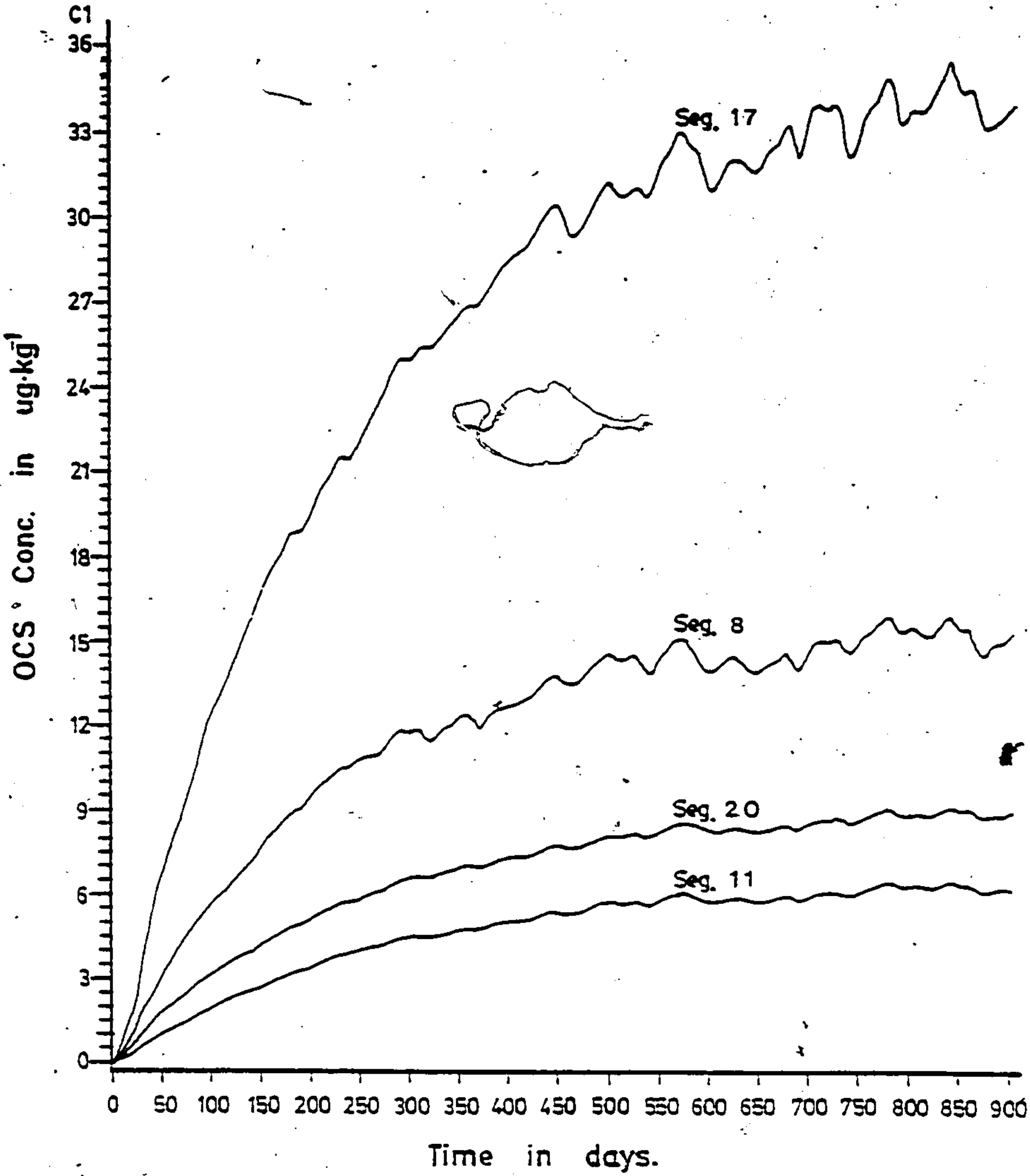

Figure 7.19 Predicted OCS Concentrations in Bed Sediment in Lake St. Clair (Constant Loads)

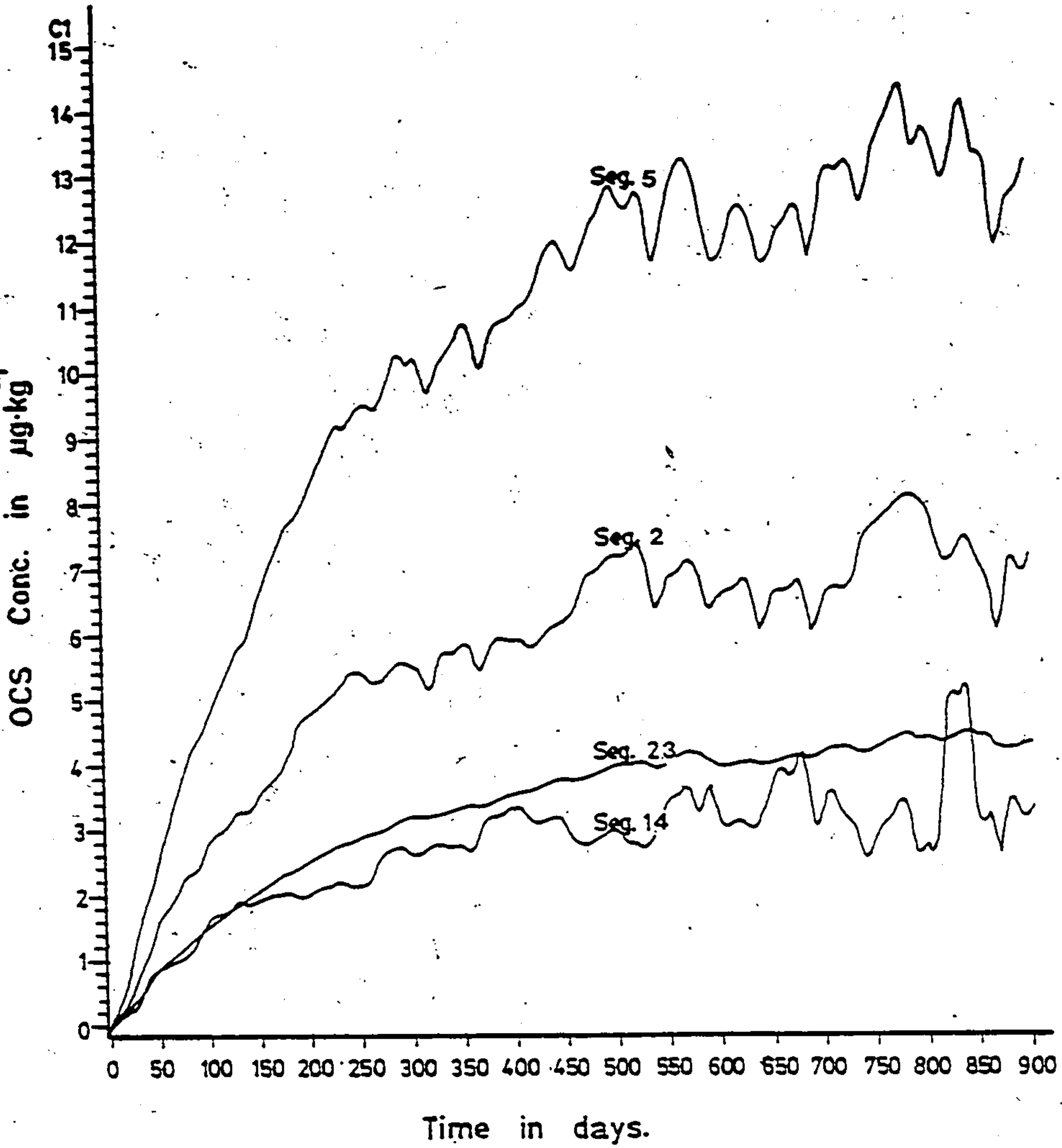

Figure 7.20 Predicted OCS Concentrations in Bed Sediment in Lake St. Clair (Constant Loads)

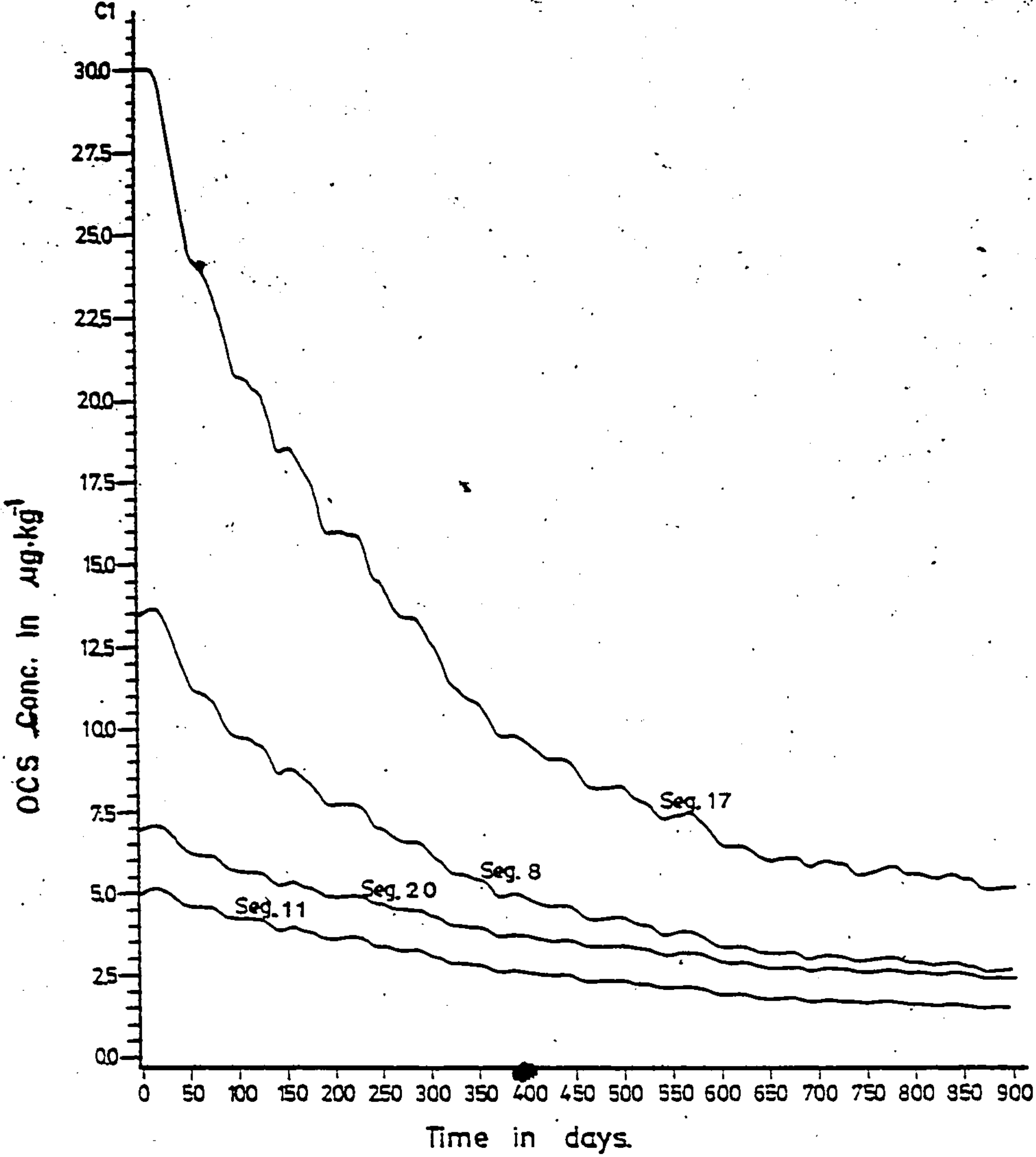

Figure 7.21 Predicted OCS Concentrations in Bed Sediment in Lake St. Clair (No External loads)

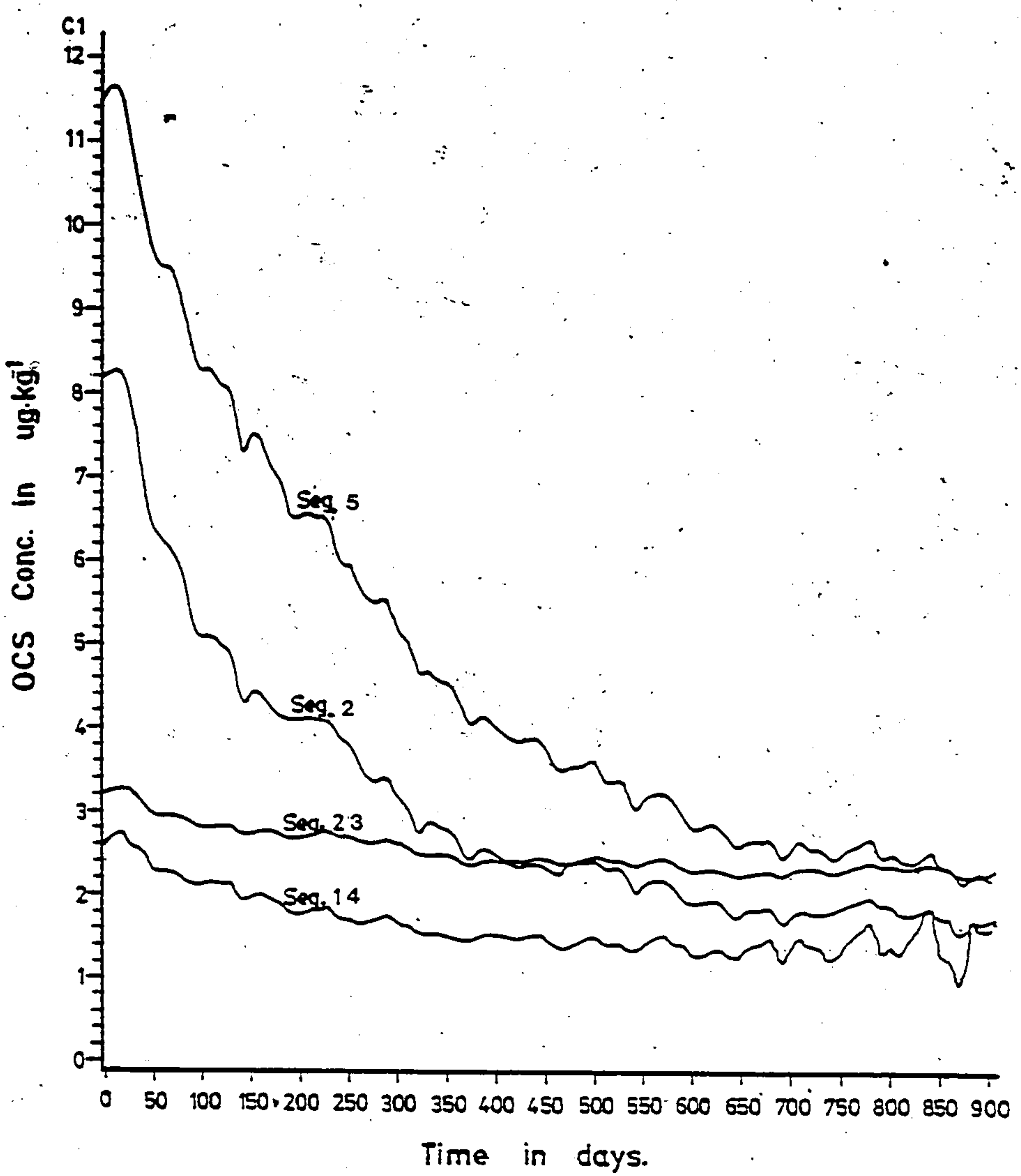

Figure 7.22 Predicted OCS Concentrations in Bed Sediment In Lake St. Clair (No External Loads)

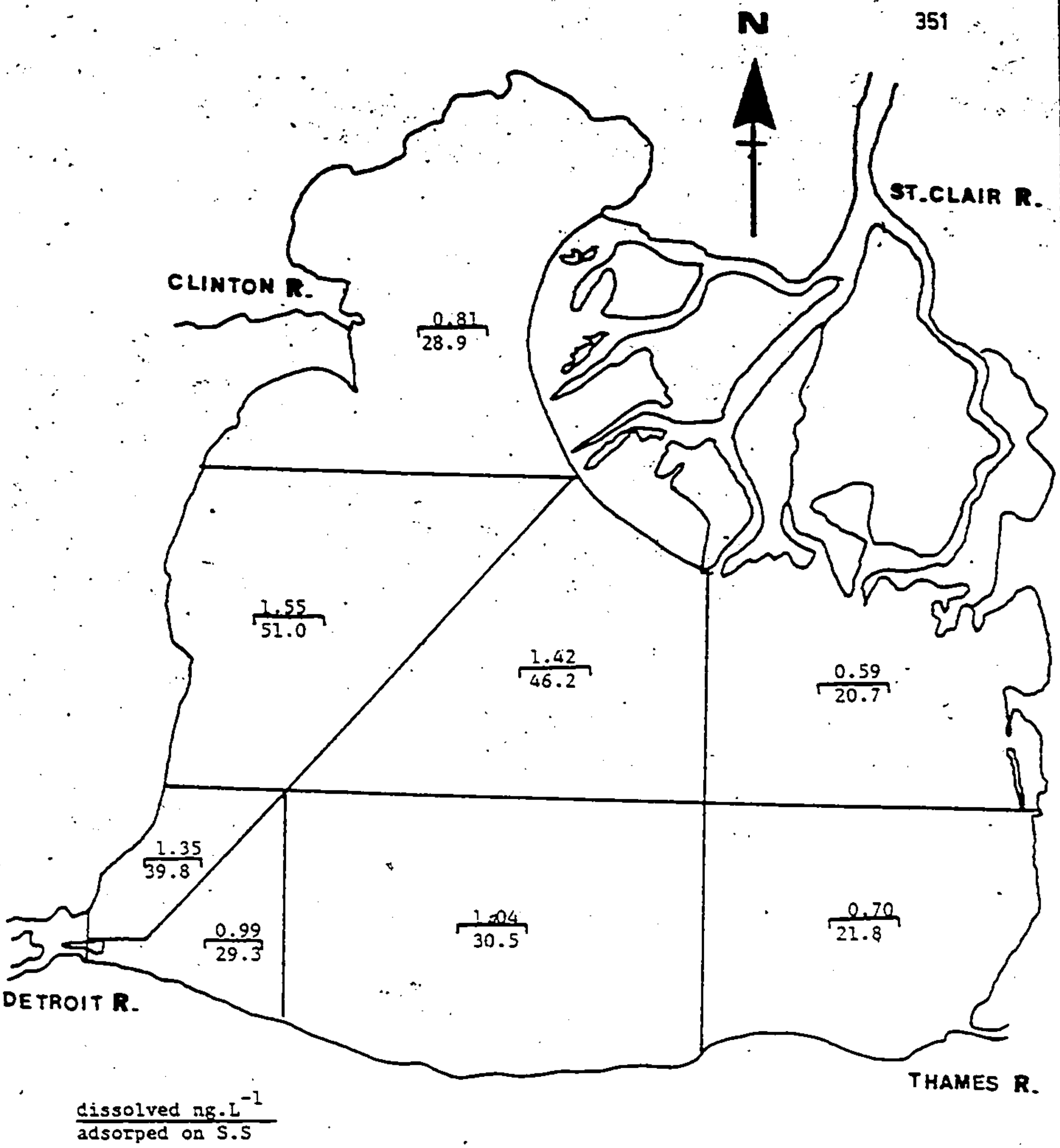

Figure 7.23 Predicted Concentrations of PCBs in Water Segments and on Suspended Solids under Ice Cover in Lake St. Clair

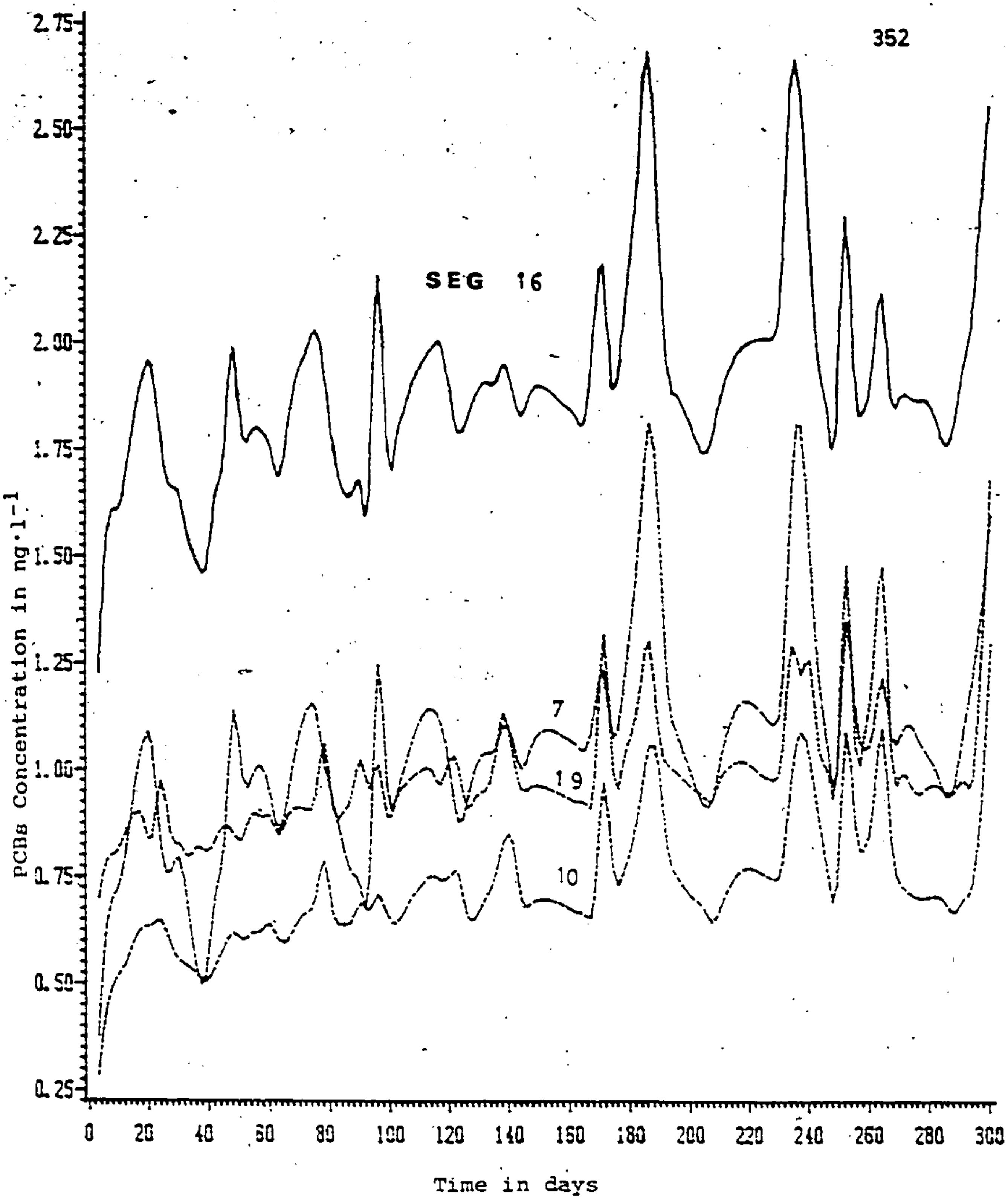

Figure 7.24 Total PCBs Concentration in Water Segments in Lake St. Clair

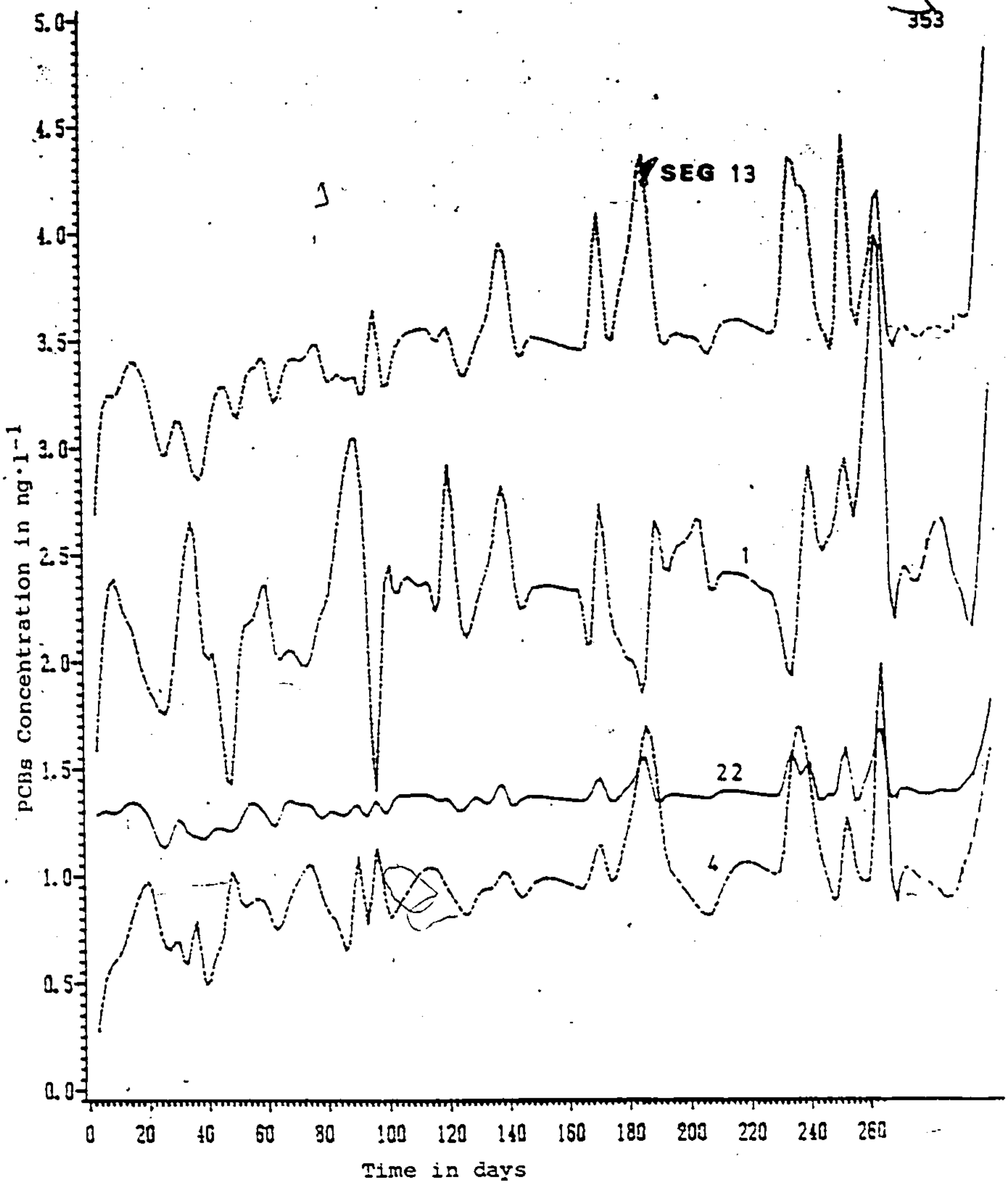

Figure 7.25 Total PCBs Concentration in Water Segments in Lake St. Clair

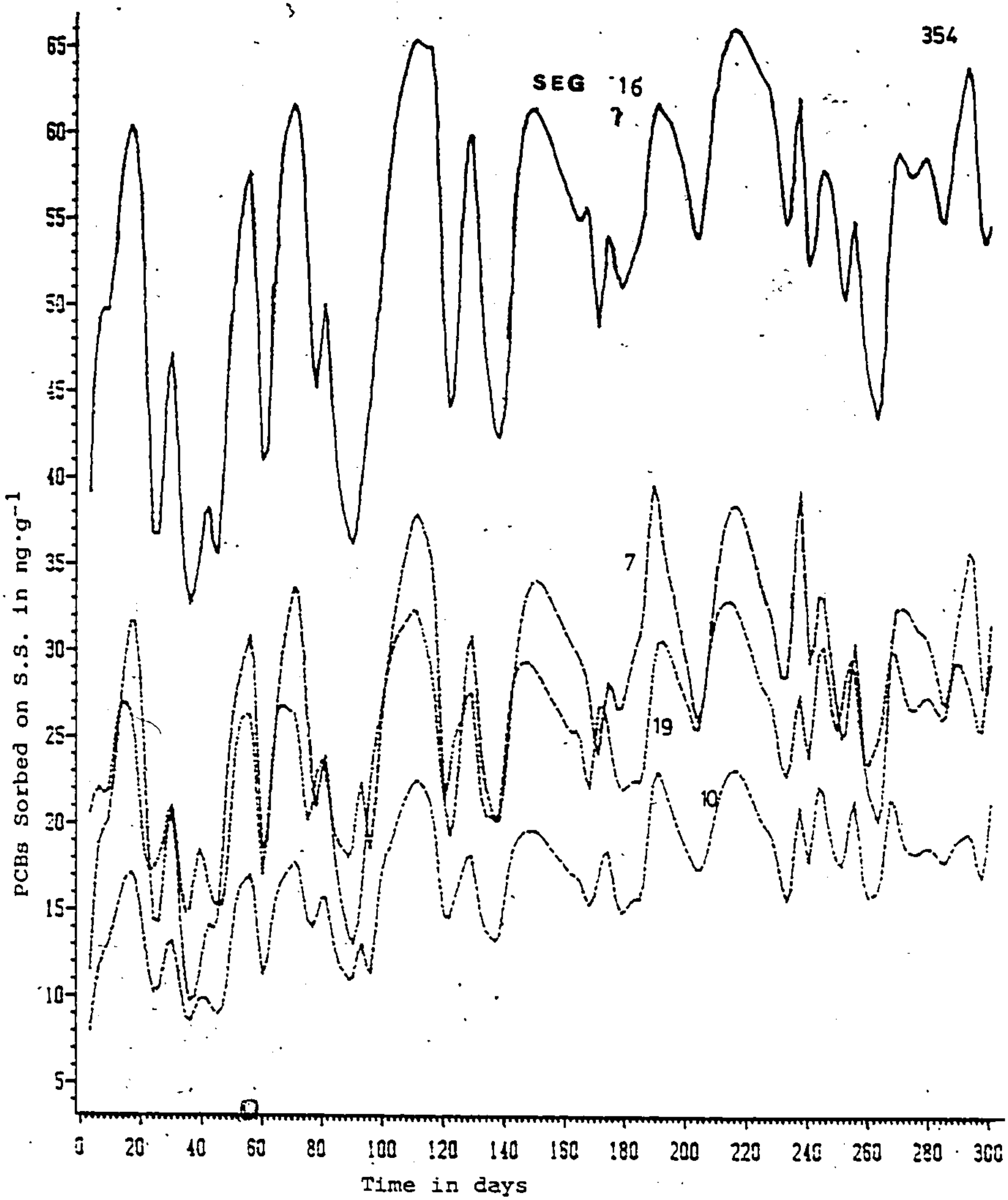

Figure 7.26 PCBs Sorbed onto Suspended Sediments in Water Segments in Lake St. Clair

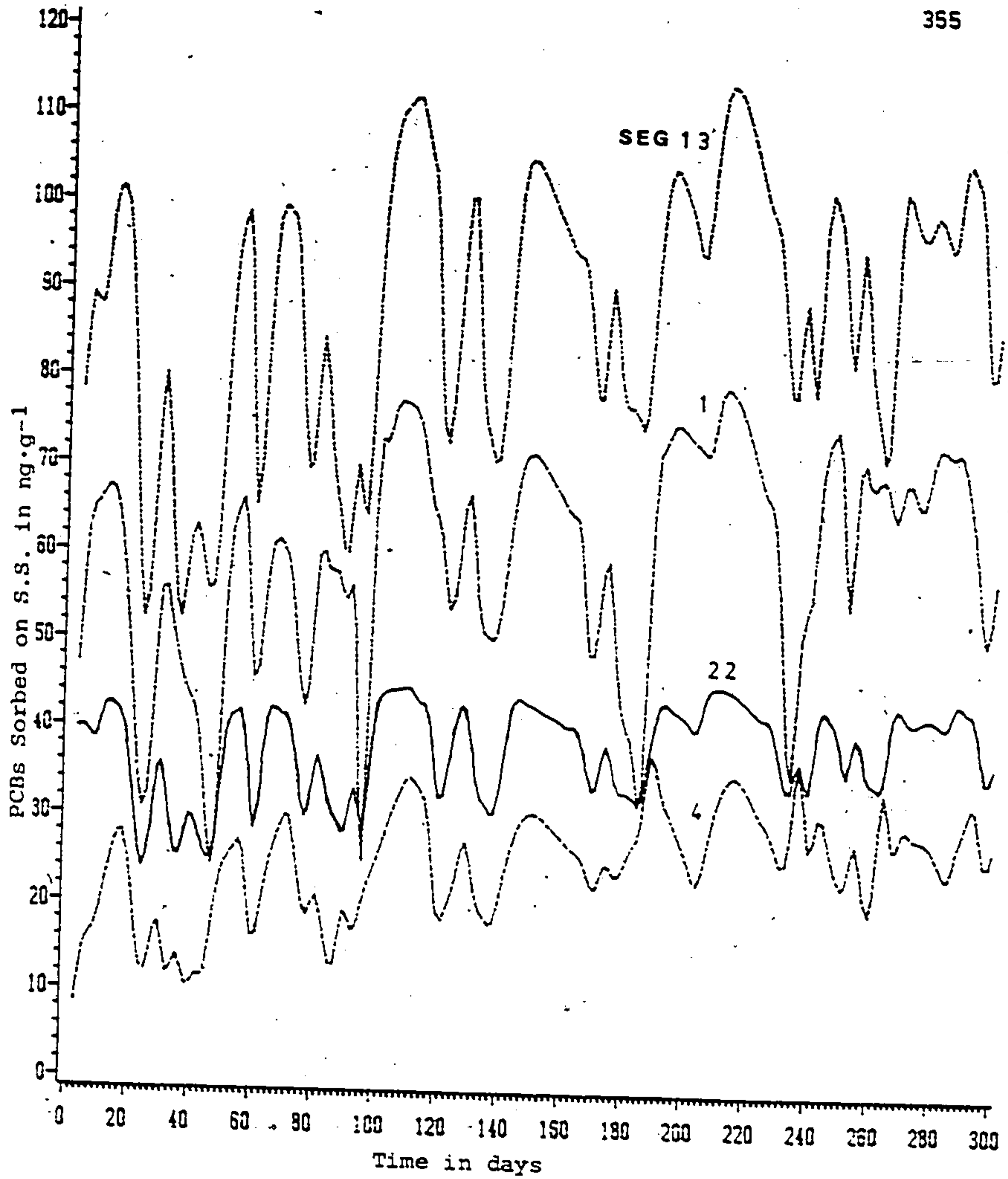

Figure 7.27 PCBs Sorbed onto Suspended Sediments in Water Segments in Lake St. Clair

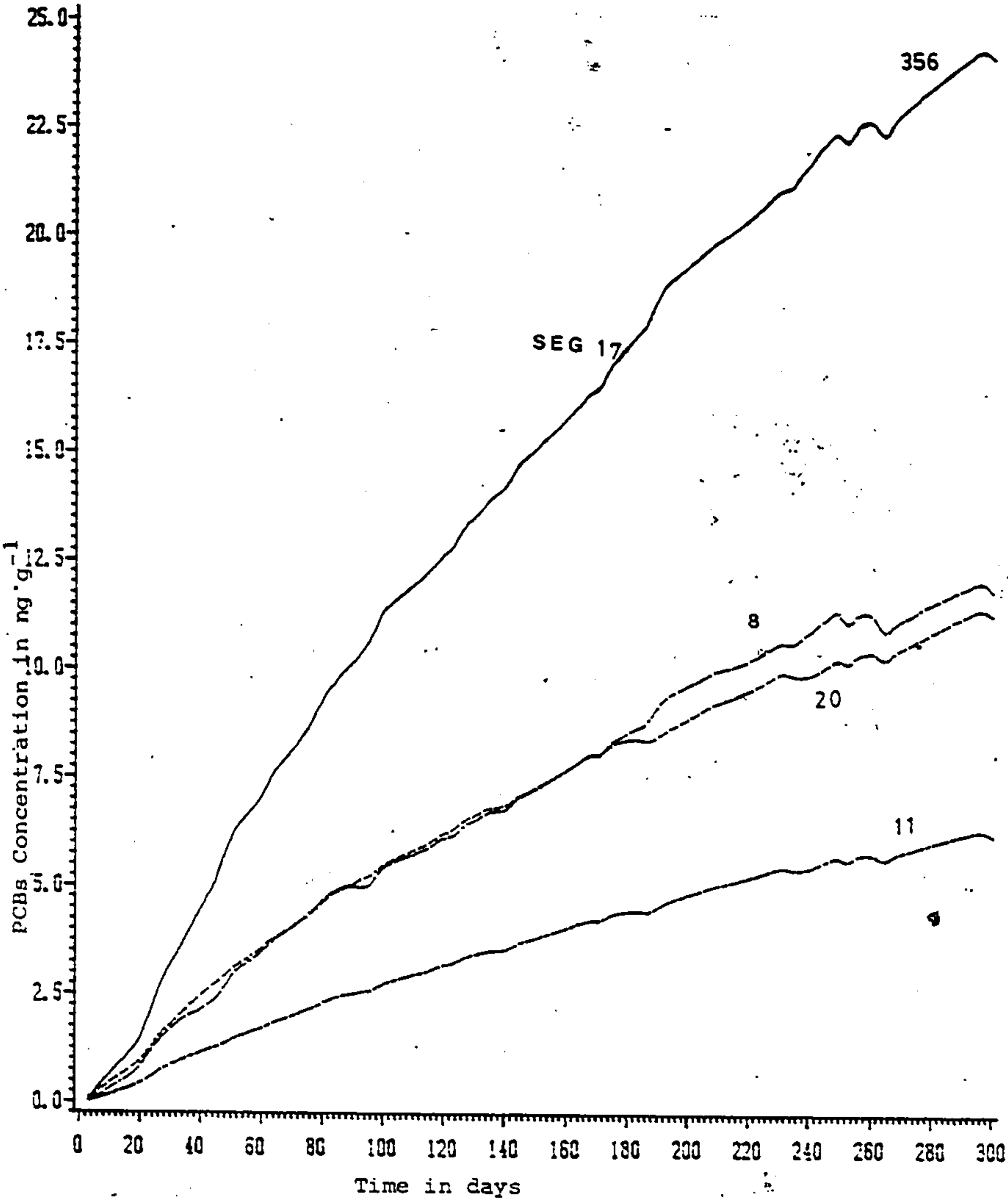

Figure 7.28 PCBs Sorbed onto Sediments in Bed Segments in Lake St. Clair

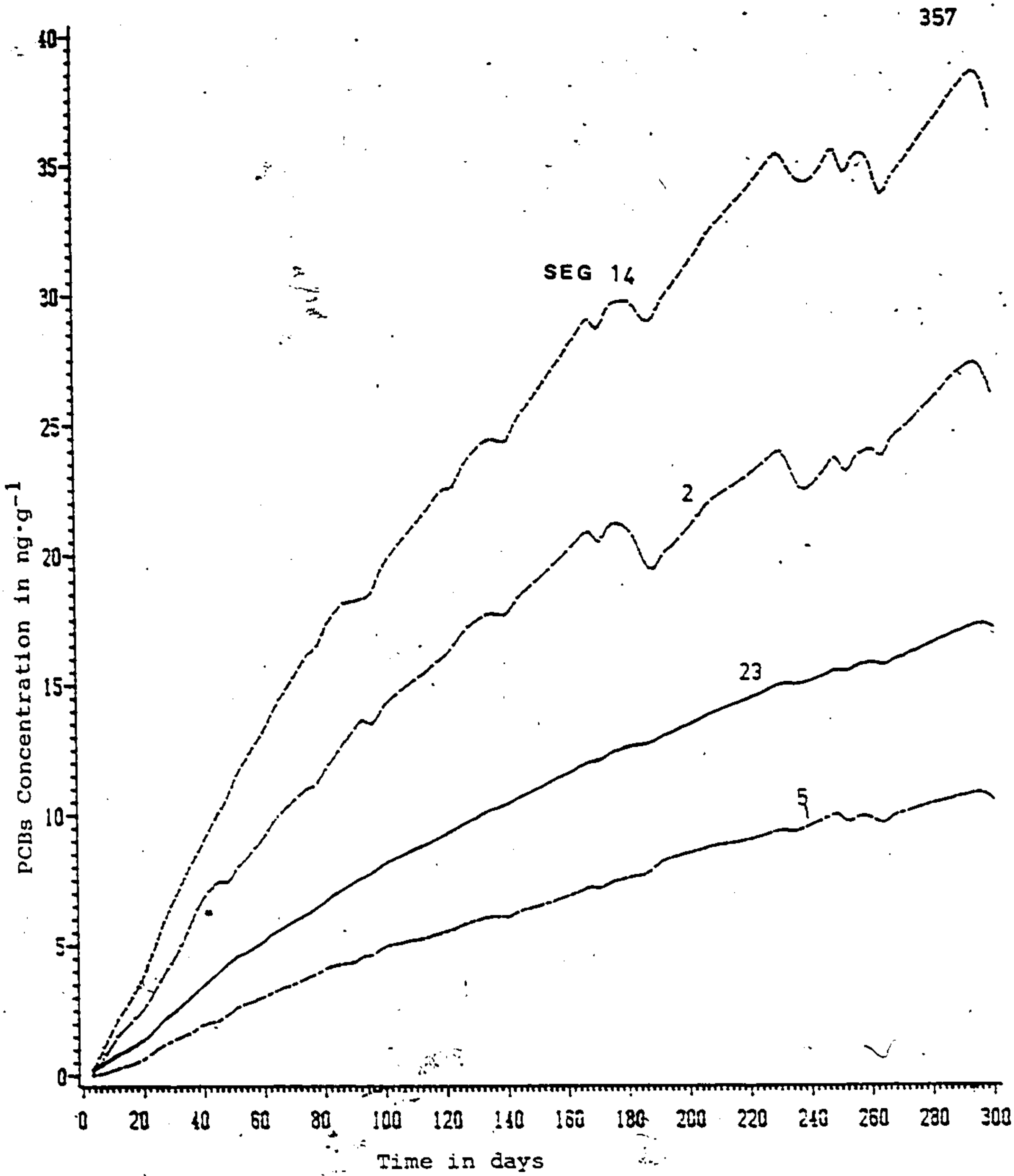

Figure 7.29 PCBs Sorbed onto Sediments in Bed Segments in Lake St. Clair

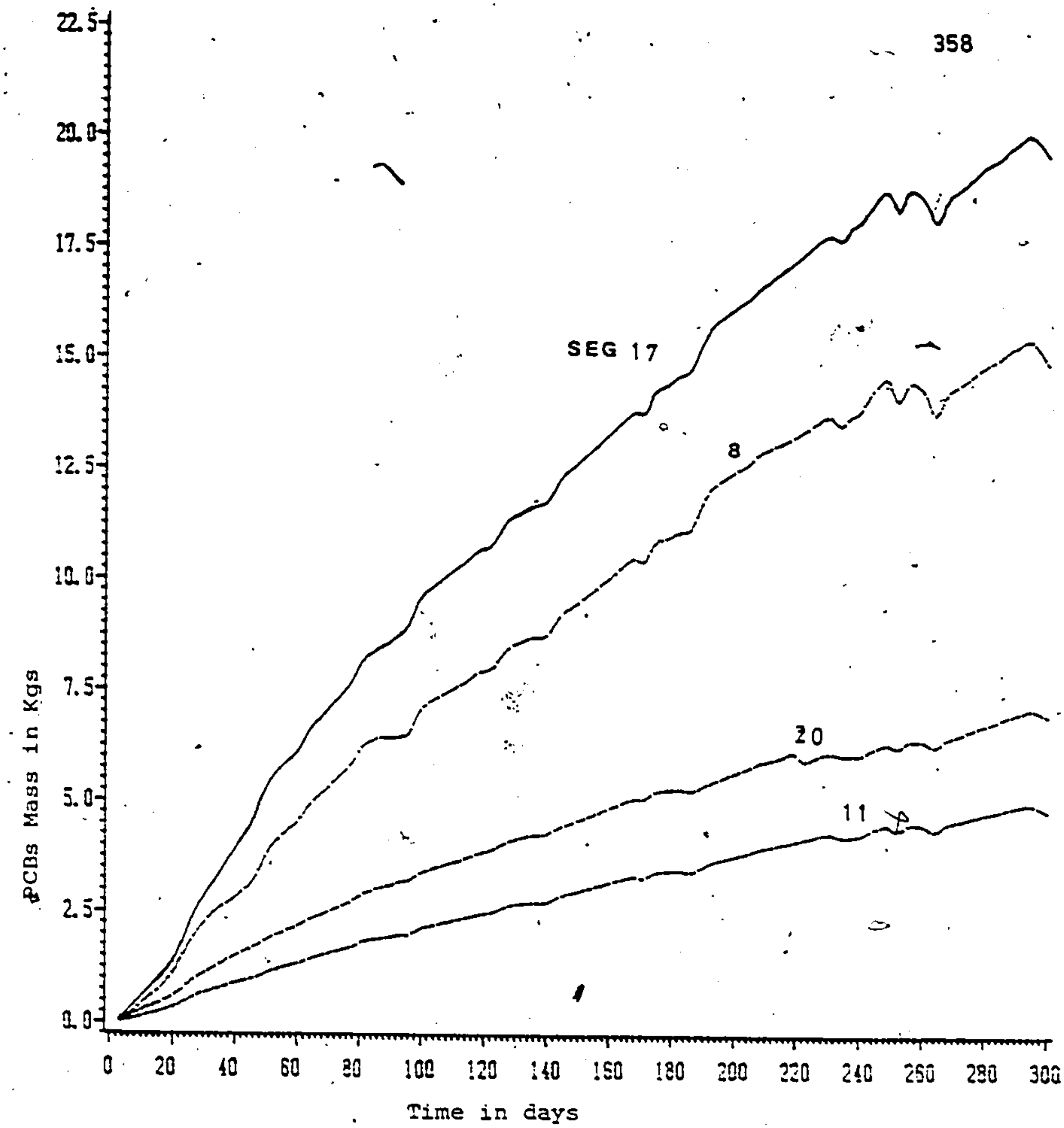

Figure 7.30 Total Mass of PCBs in Surface Bed Segments in Lake St. Clair

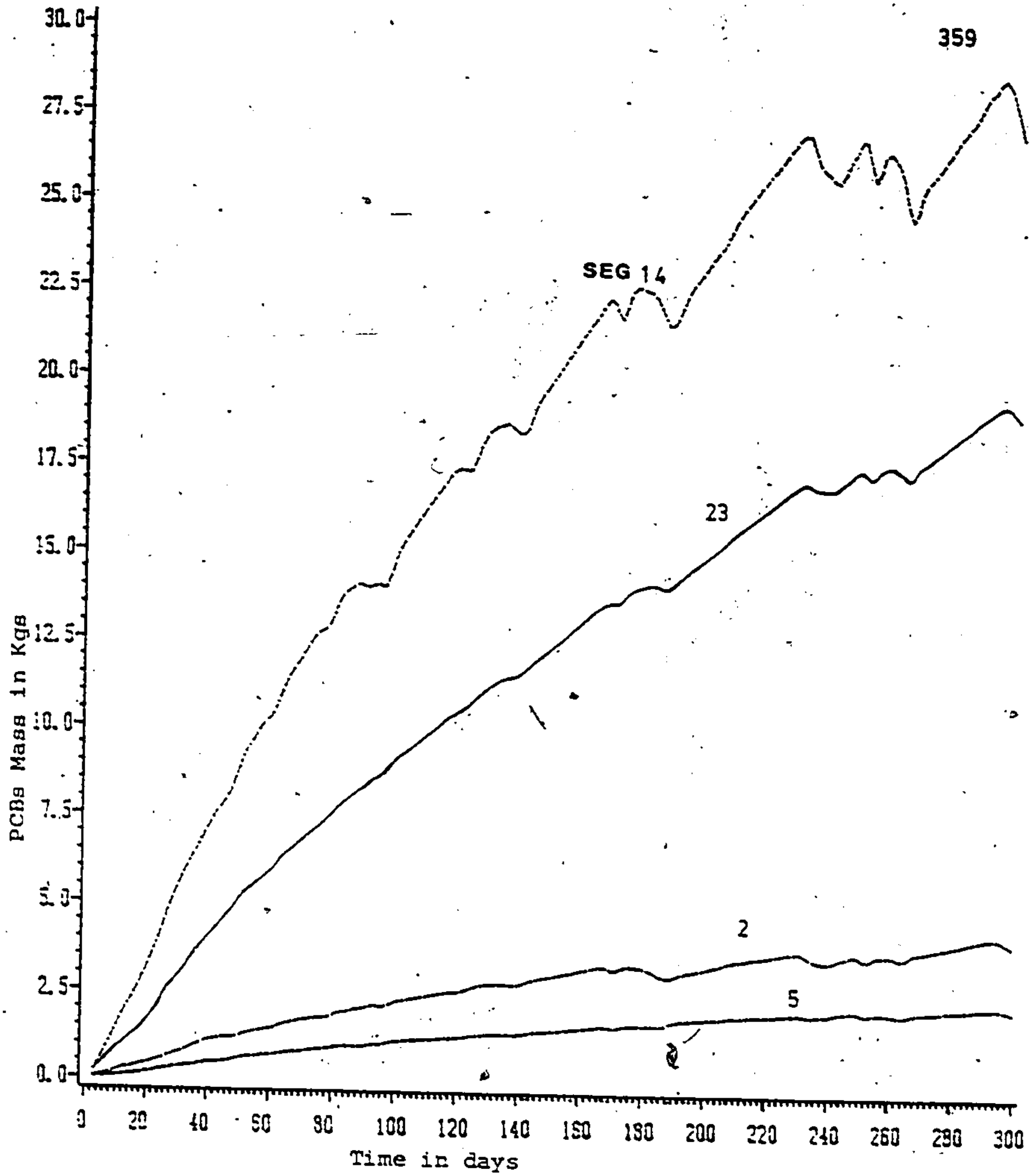

Figure 7.31 Total Mass of PCBs in Surface Bed Segments in Lake St. Clair

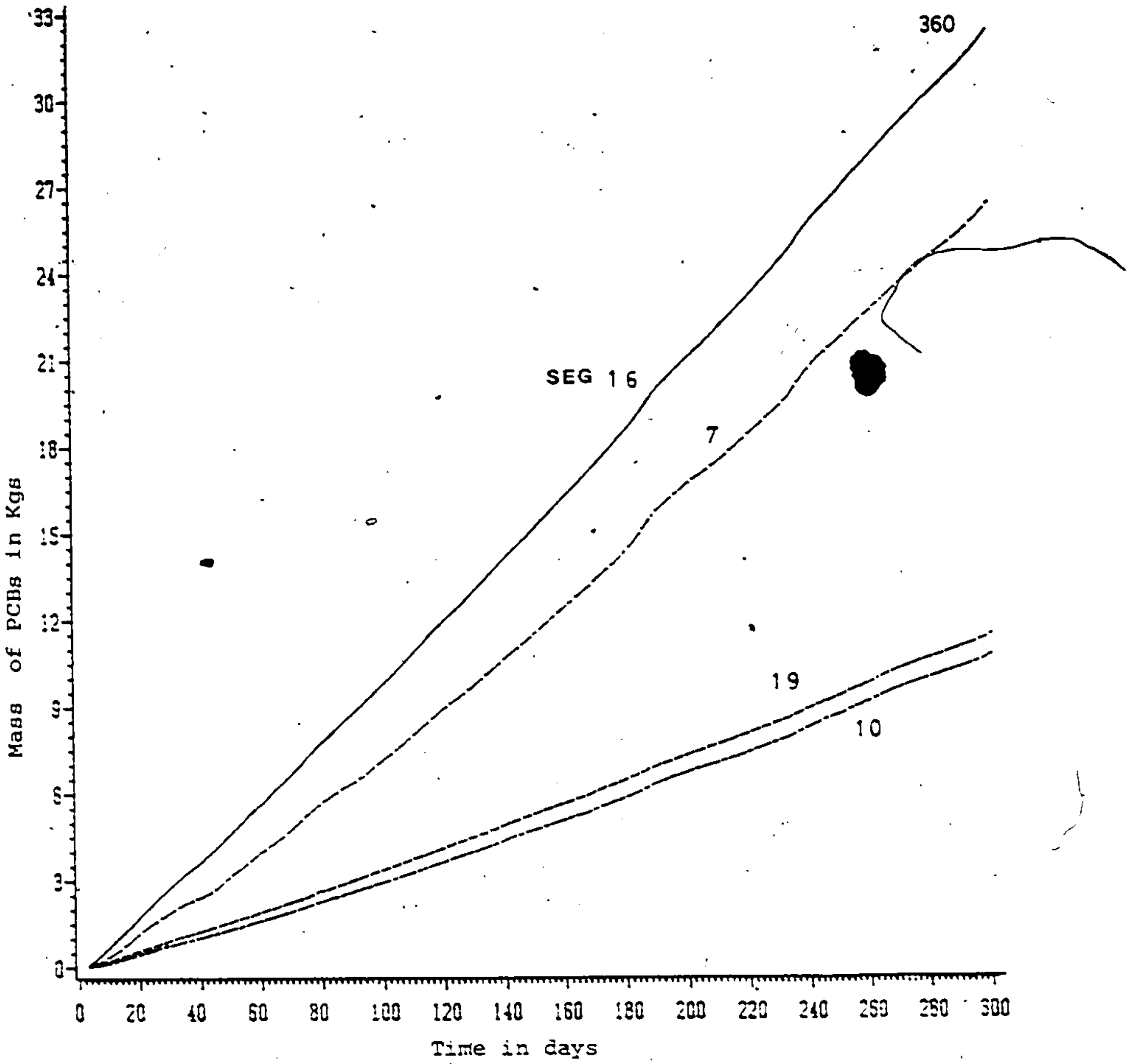

Figure 7.32 Cumulative Mass of PCBs lost from Water Segments by Volatilization in Lake St. Clair

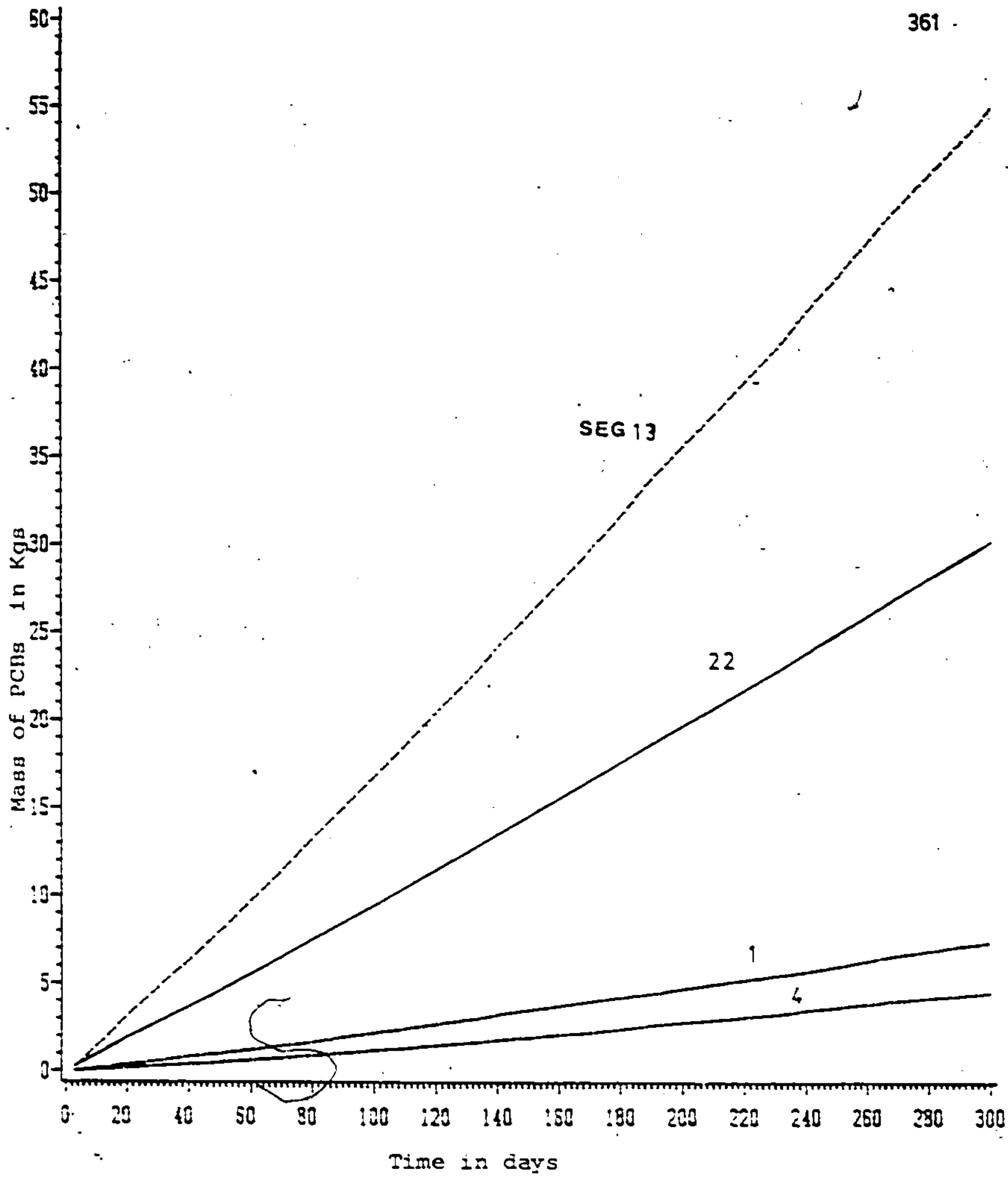

Figure 7.33 Cumulative Mass of PCBs lost from Water Segments by Volatilization in Lake St. Clair

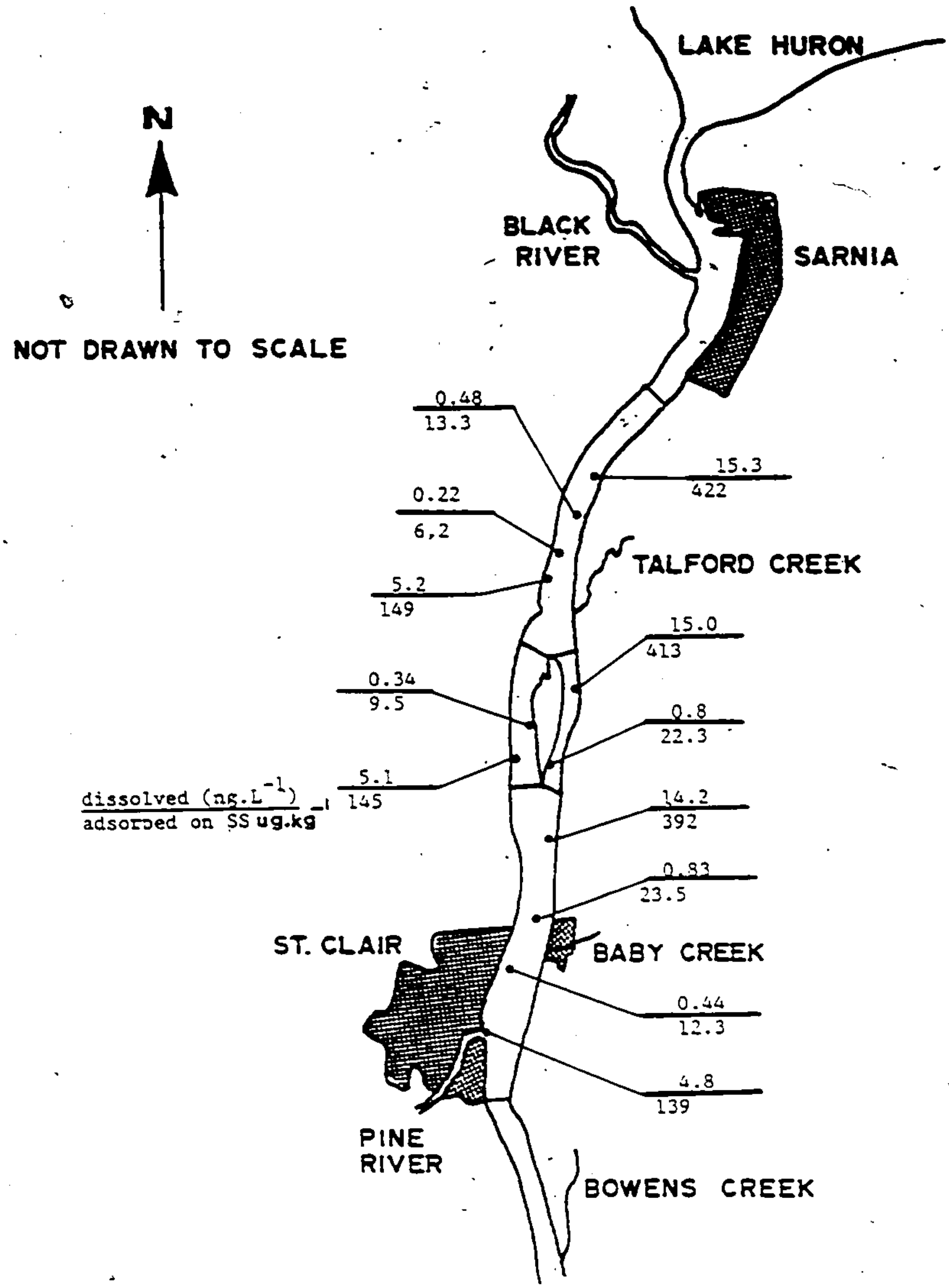

Figure 7.34 Predicted Concentrations of PCBs in Water Segments and on Suspended Solids in St. Clair River

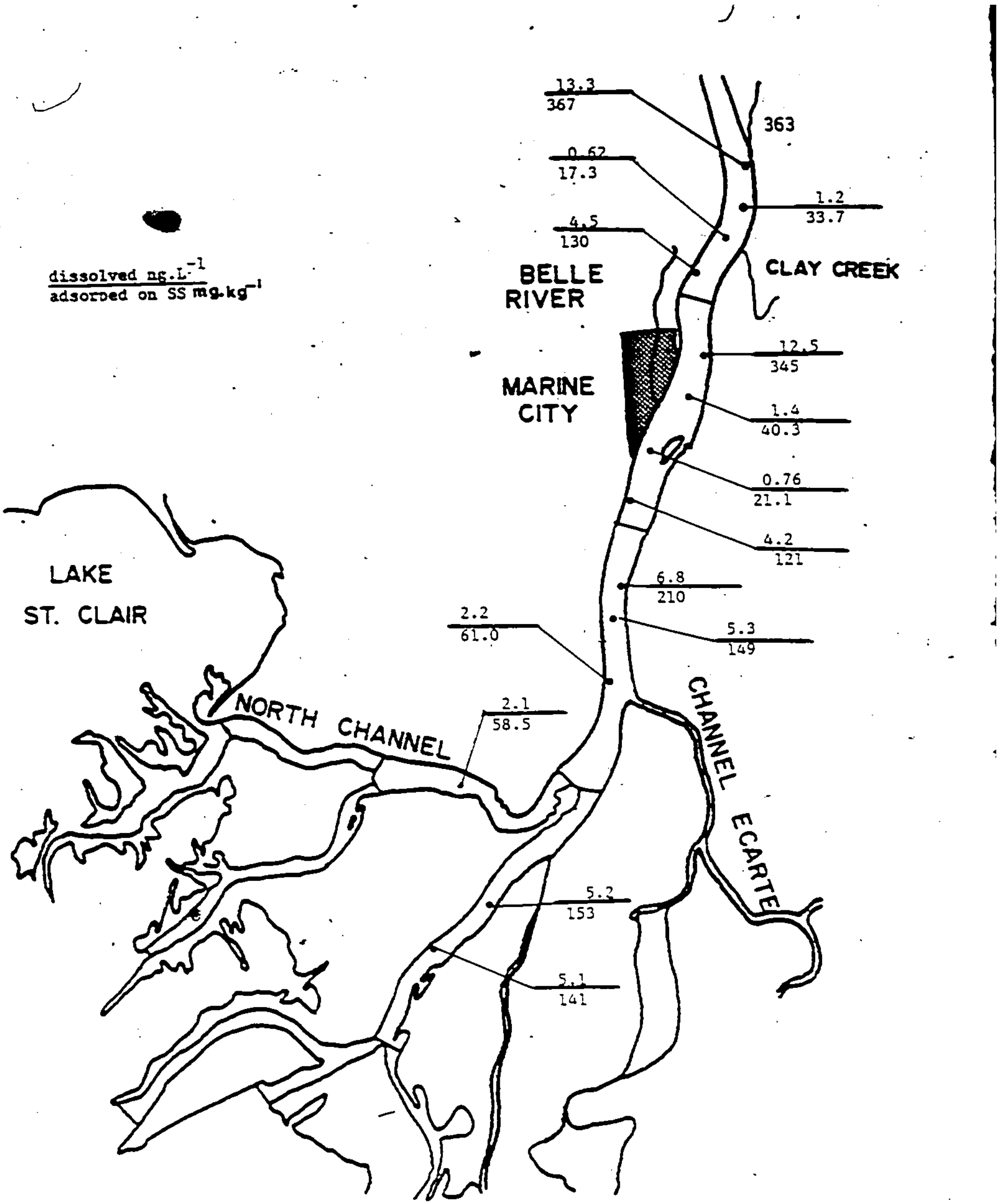

Figure 7.34 (Con't)

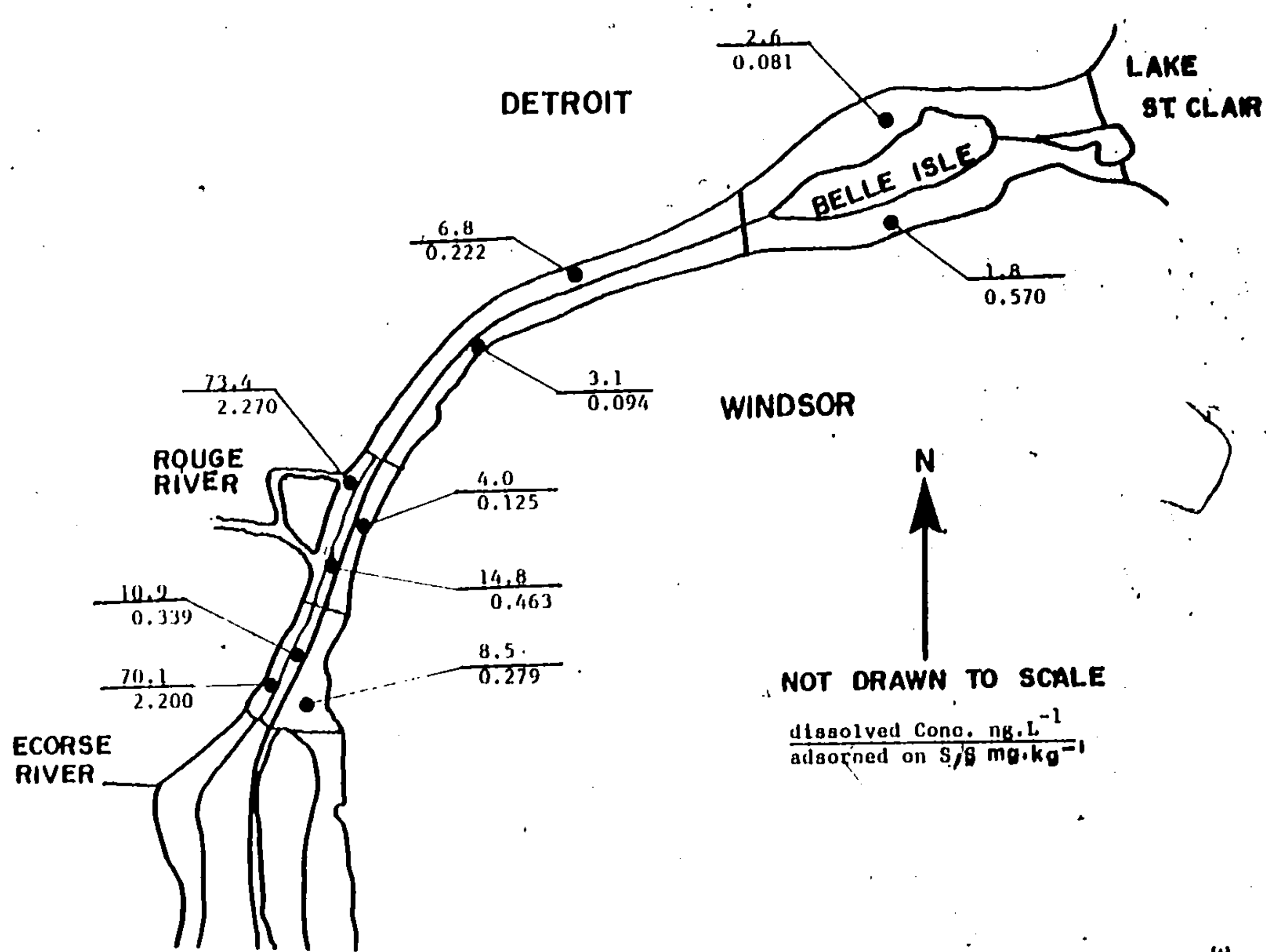

Figure 7.35 Predicted Concentrations of PCBs in Water Segments and on Suspended Solids in the Detroit River

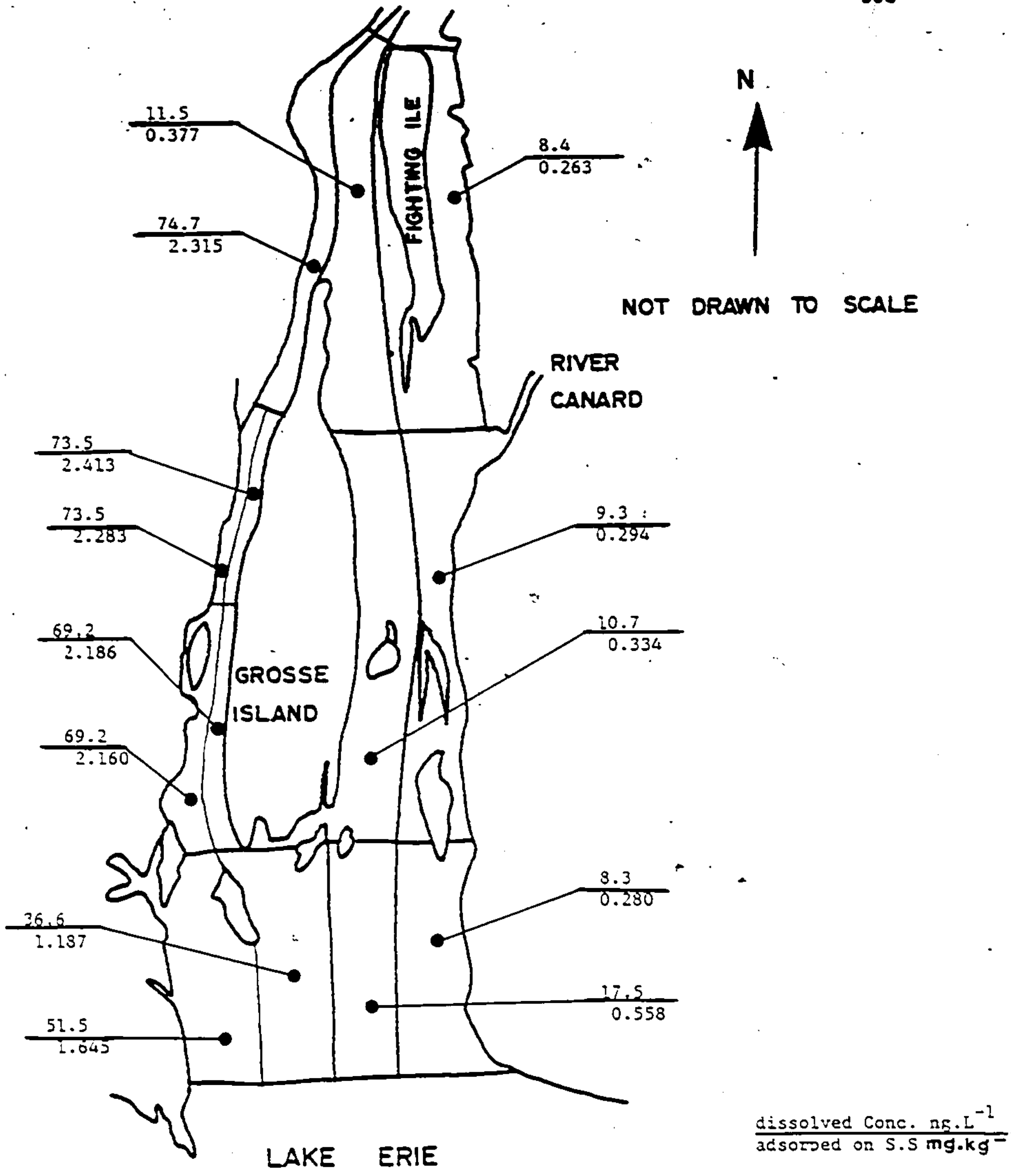

Figure 7.35 (Con't)

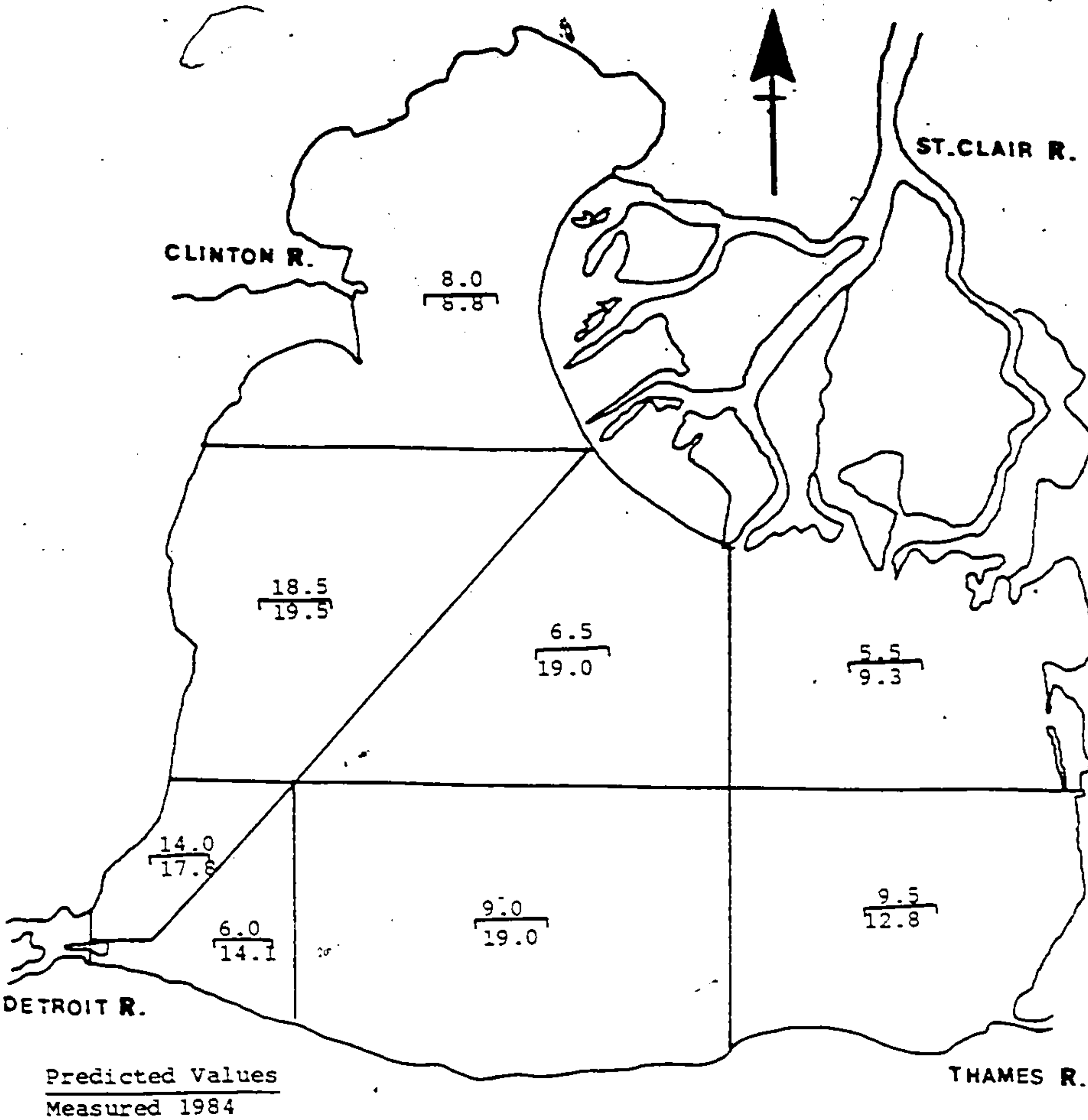

Figure 7.36 Predicted and Measured Concentrations of Lead in Bed Sediments (ug.g^{-1}) in Lake St. Clair

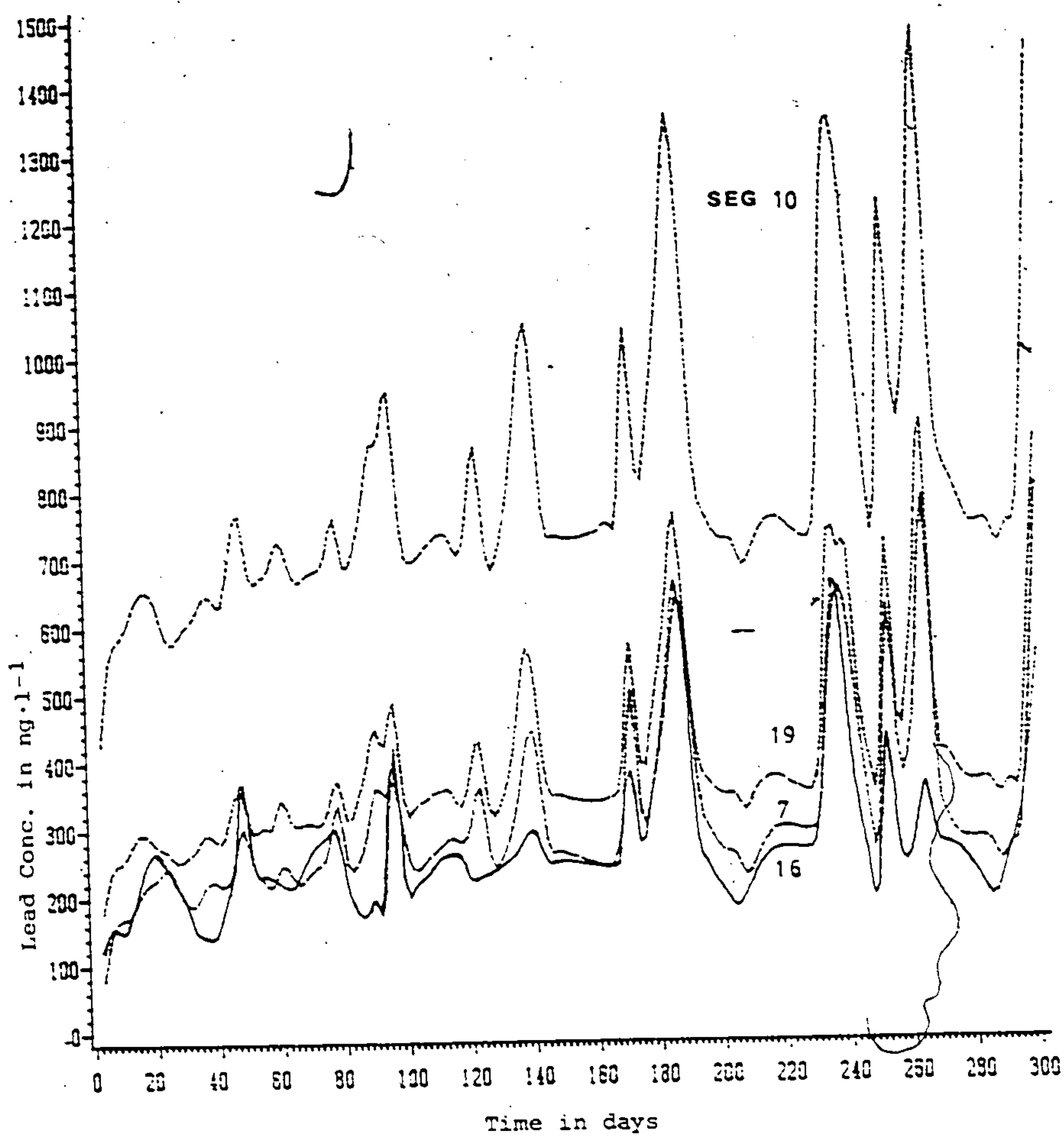

Figure 7.37 Total Lead Concentration in Water Segments in Lake St. Clair

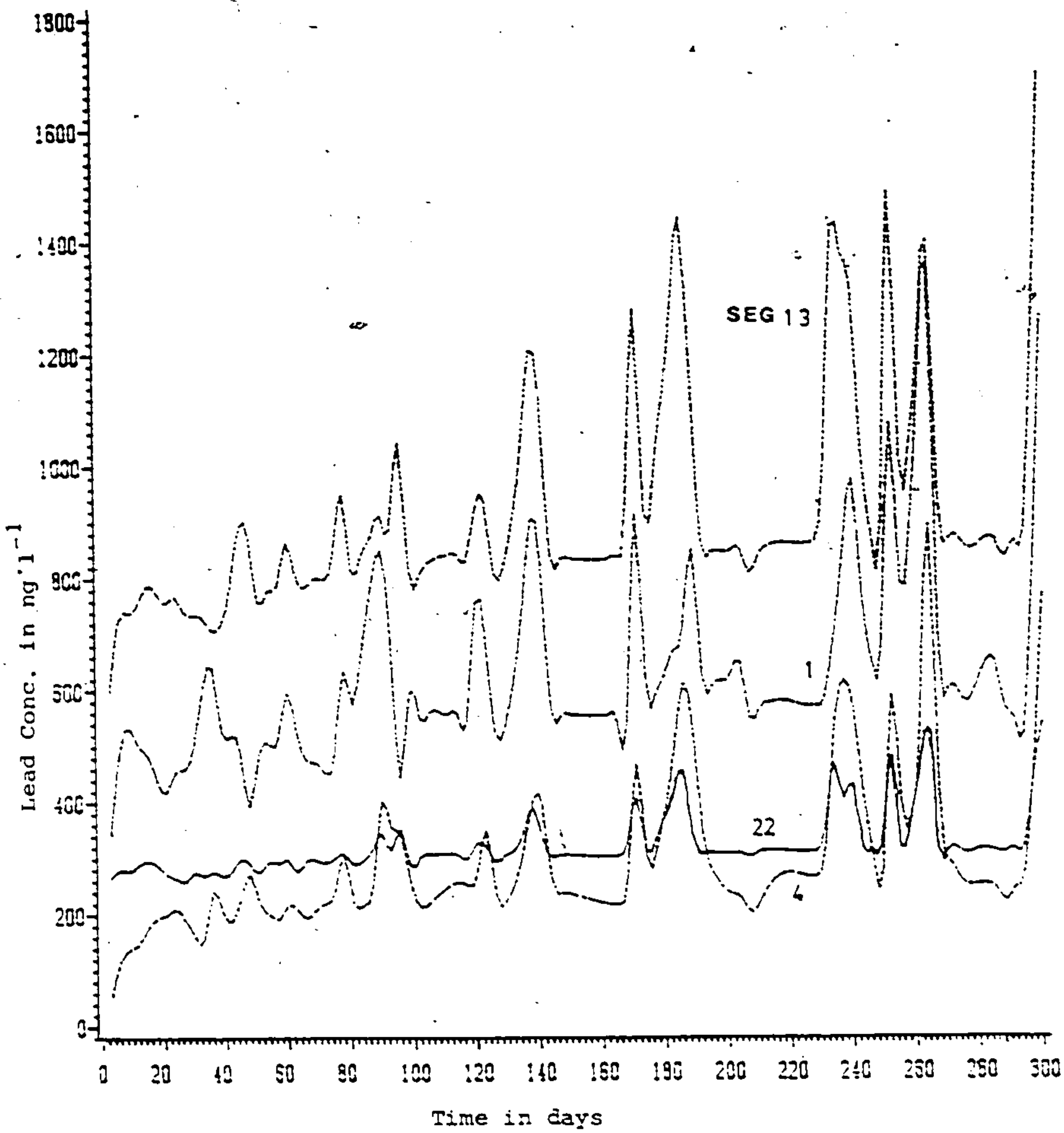

Figure 7.38 Total Lead Concentration in Water Segments in Lake St. Clair

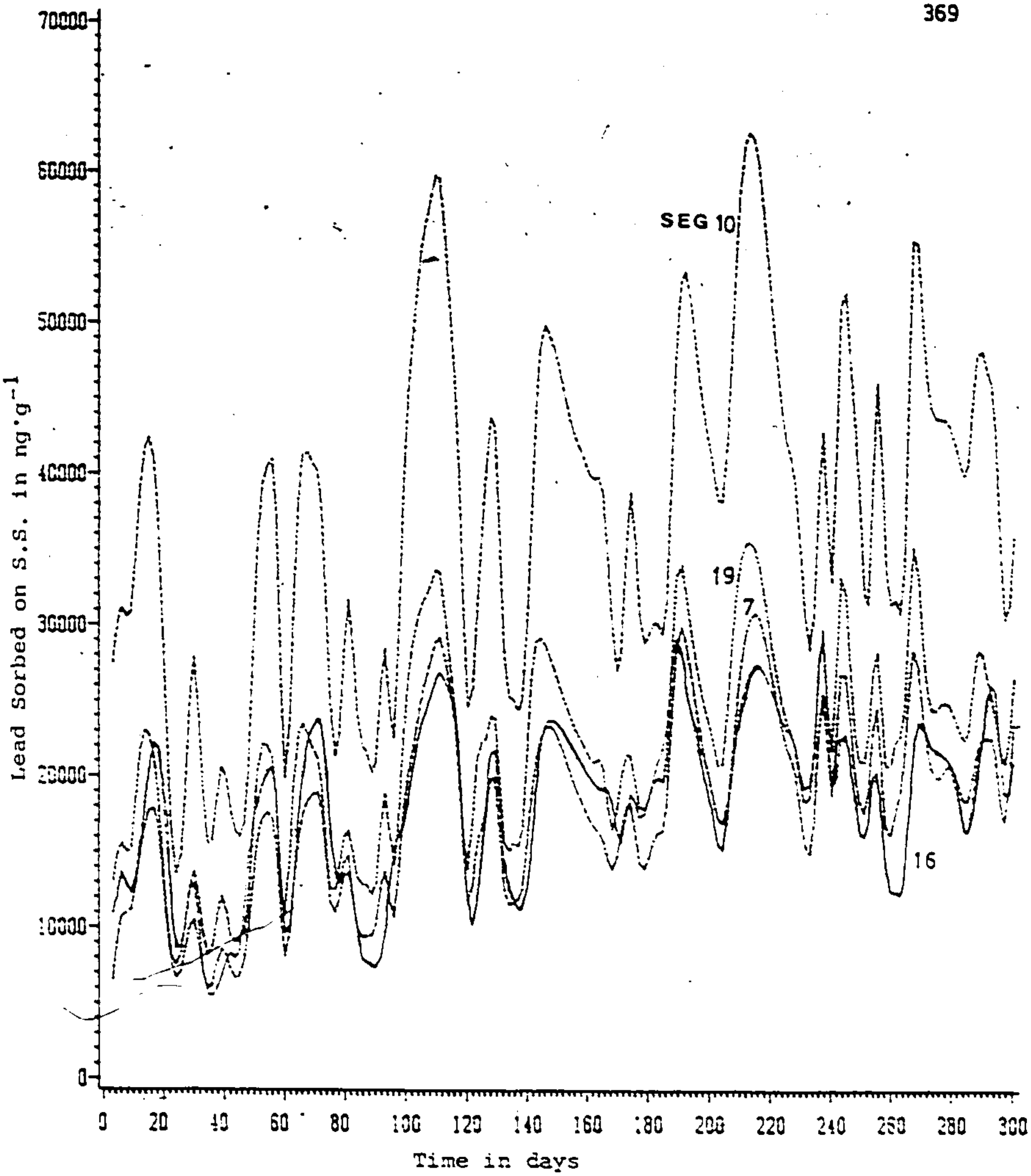

Figure 7.39 Lead Sorbed onto Suspended Sediments in Water Segments in Lake St. Clair

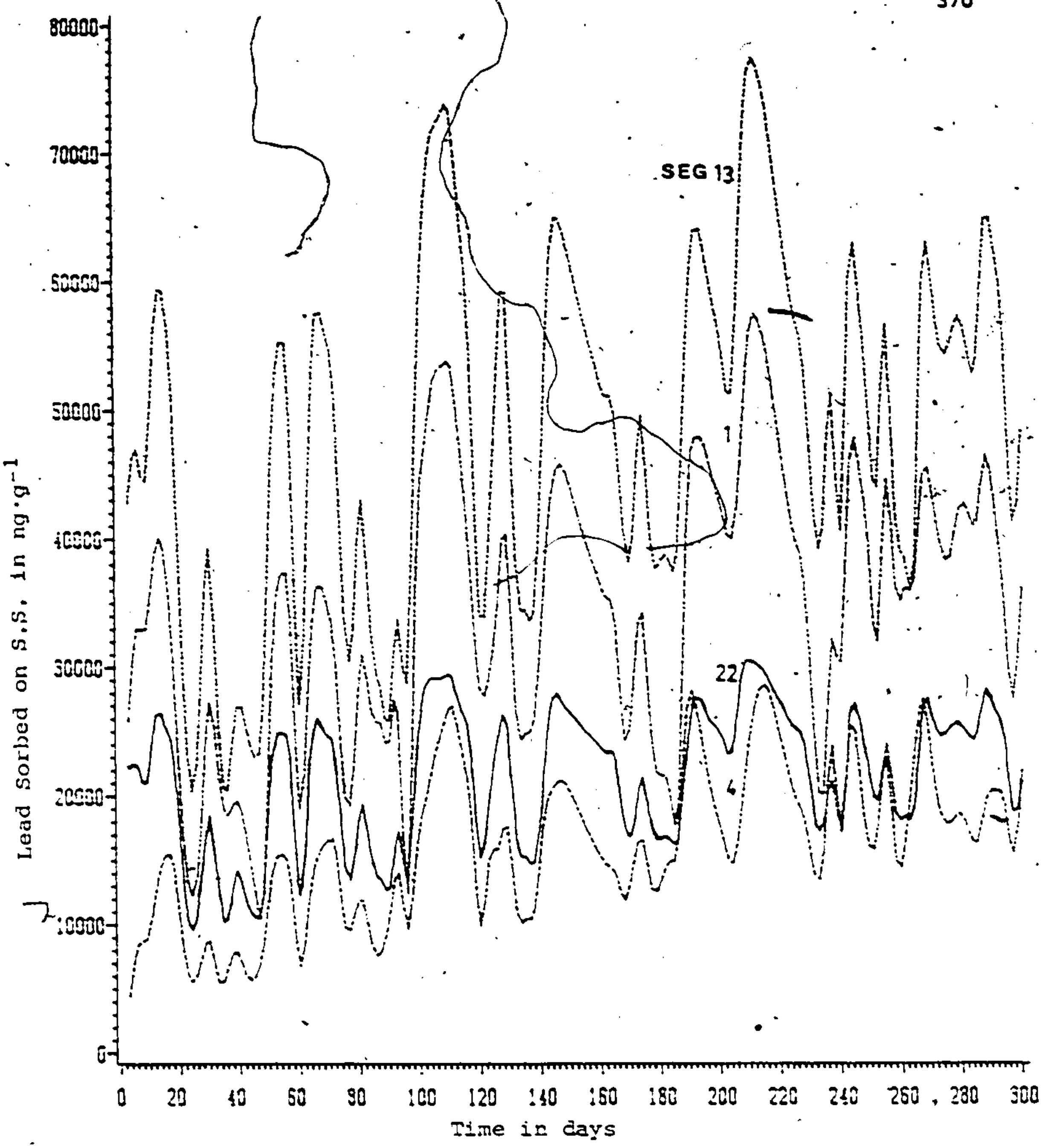

Figure 7.40 Lead Sorbed onto Sediments in Water Segments in Lake St. Clair

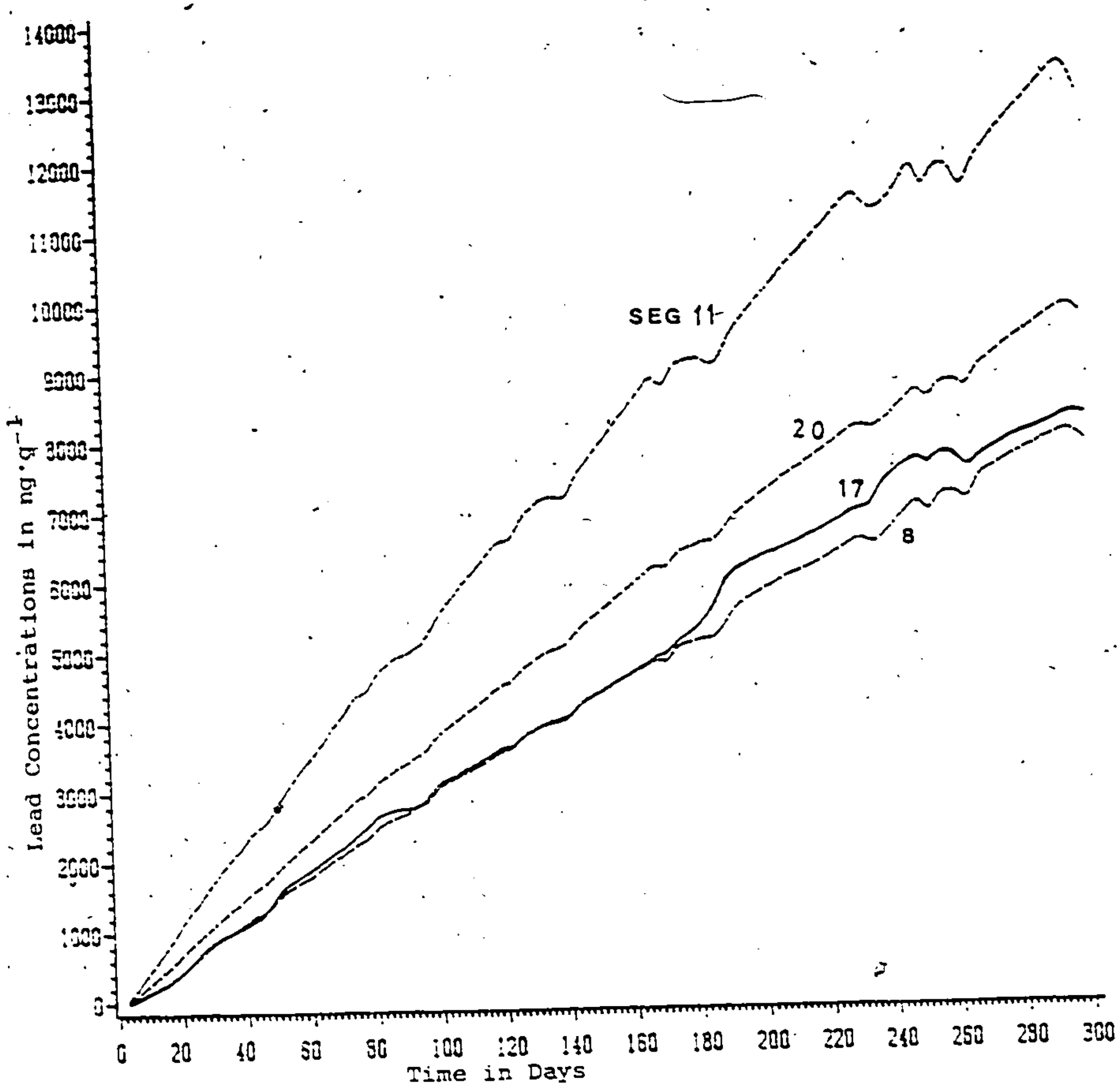

Figure 7.41 Lead Sorbed onto Sediments in Bed Segments in Lake St. Clair

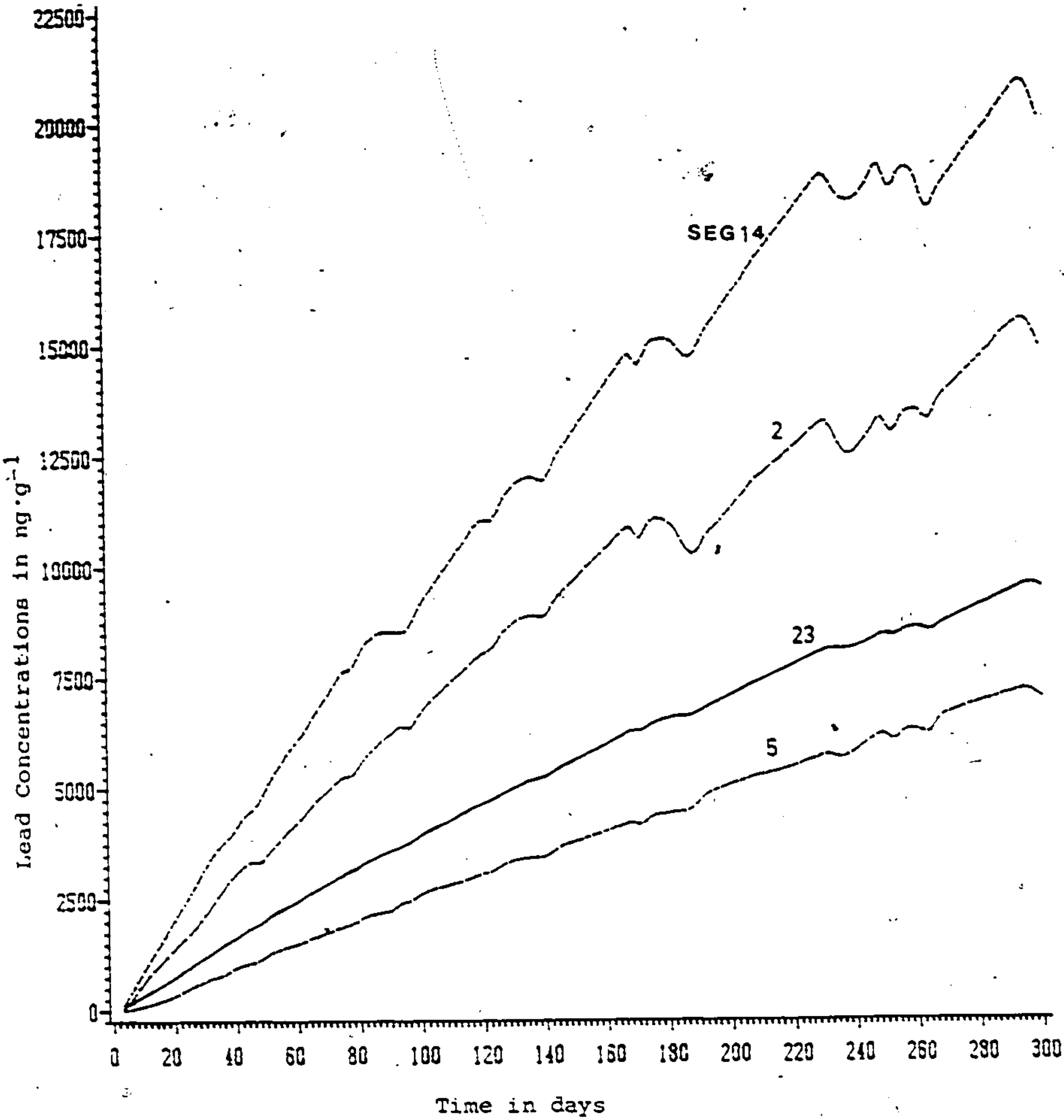

Figure 7.42 Lead Sorbed onto Sediments in Bed Segments in Lake St. Clair

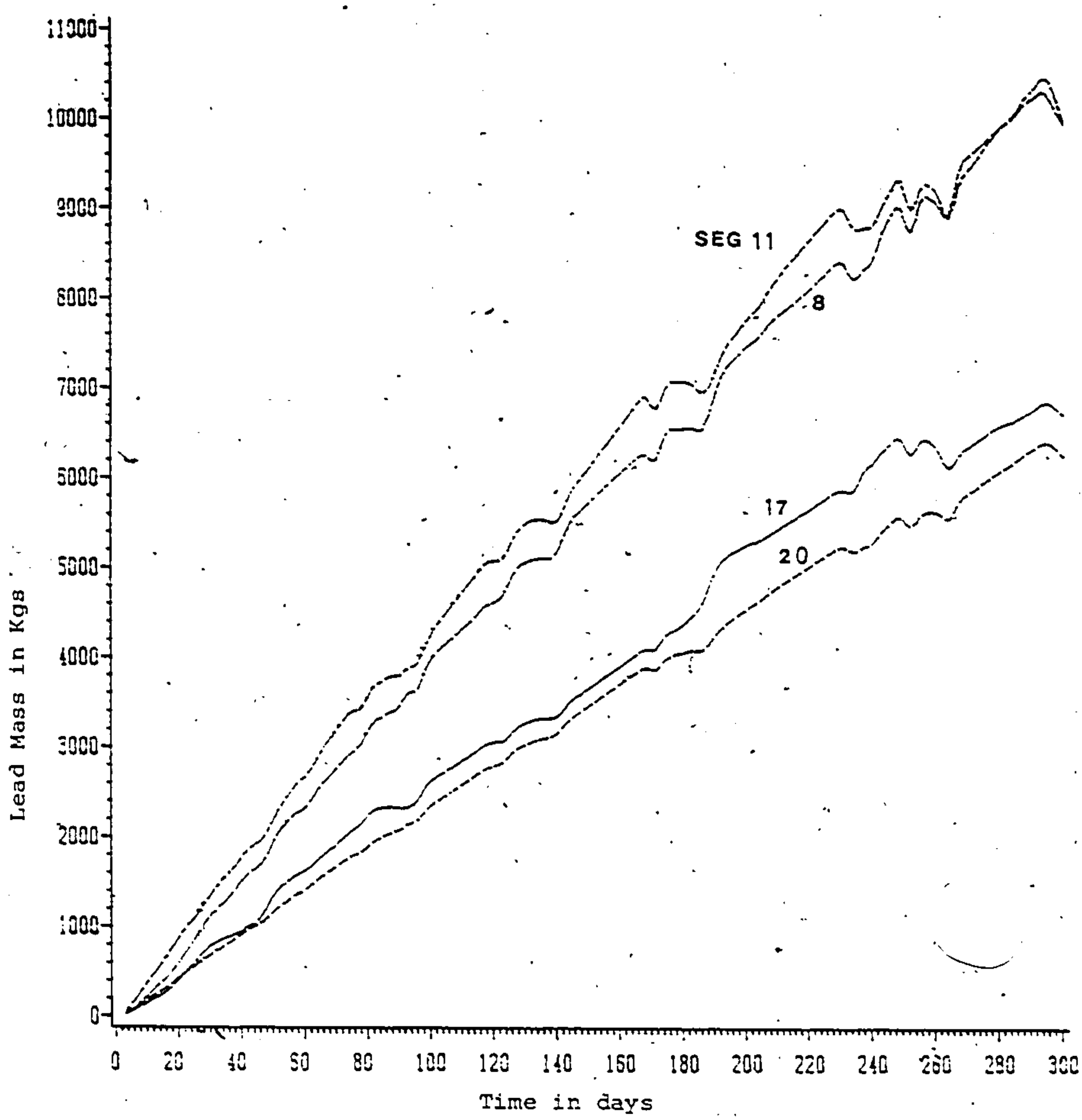

Figure 7.43 Total Mass of Lead in Surface Bed Segments in Lake St. Clair

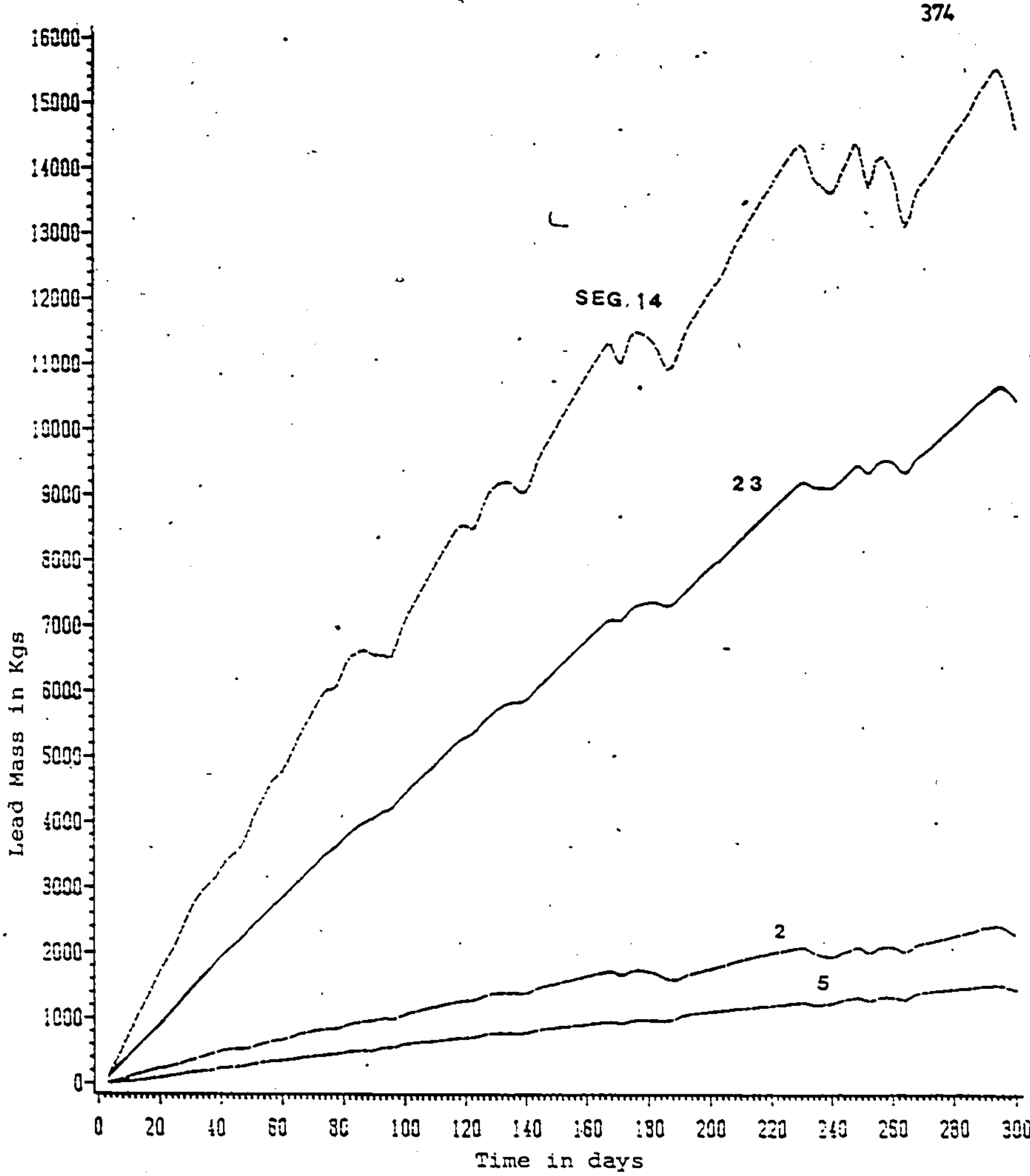

Figure 7.44 Total Mass of Lead in Surface Bed Segments in Lake St. Clair

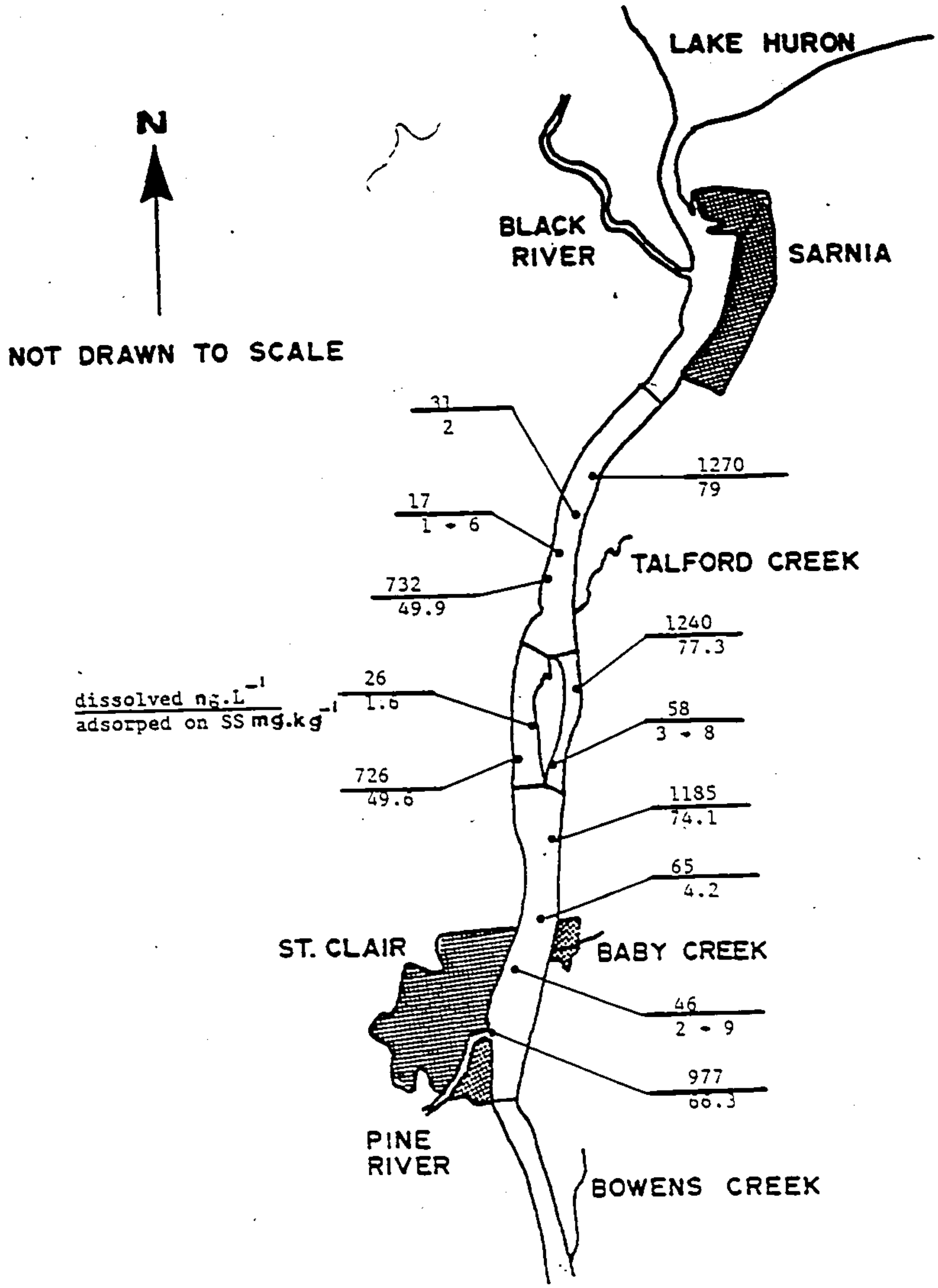

Figure 7.45 Predicted Concentrations of Lead in Water Segments and on Suspended Solids in St. Clair River

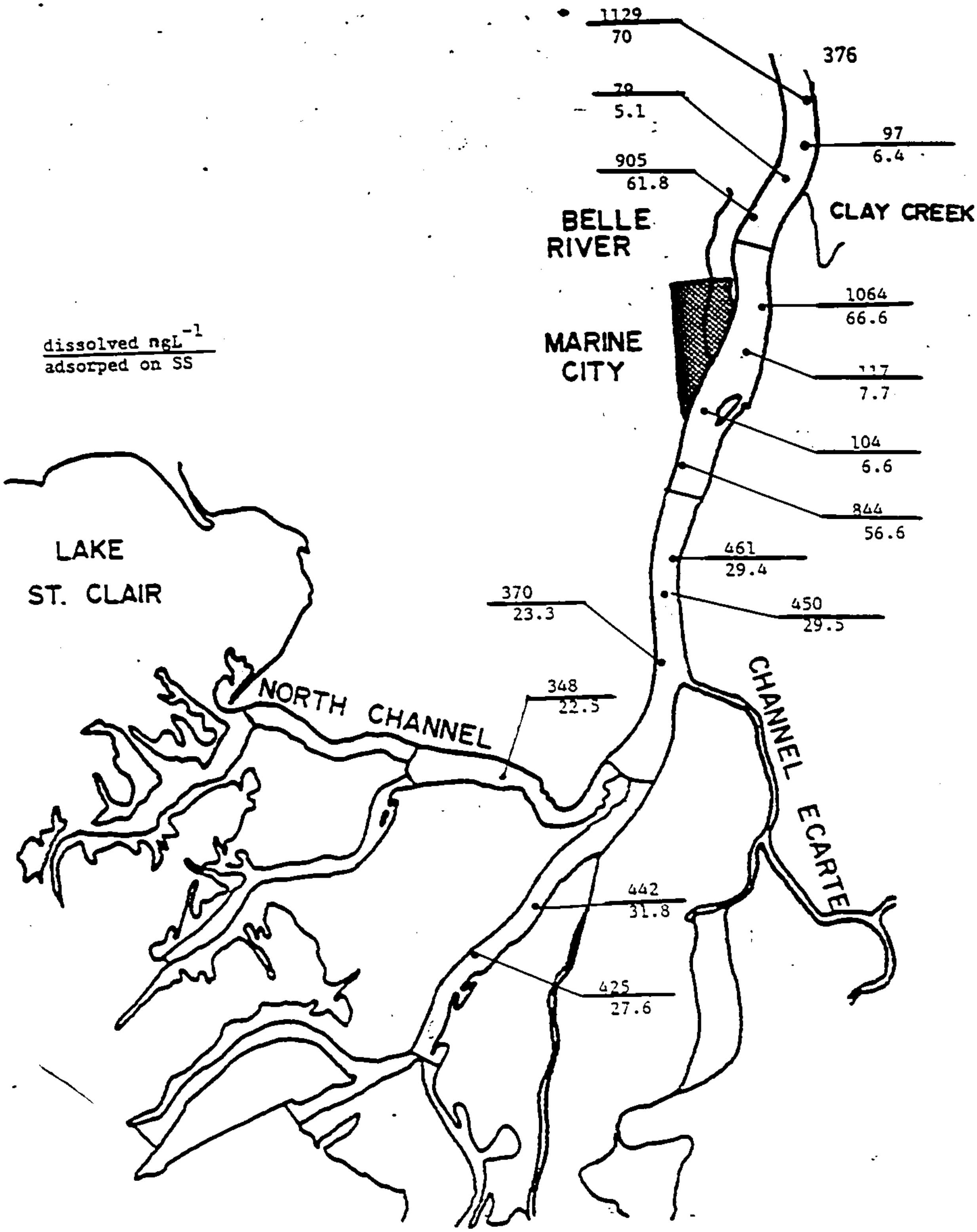

Figure 7.45 (Con't)

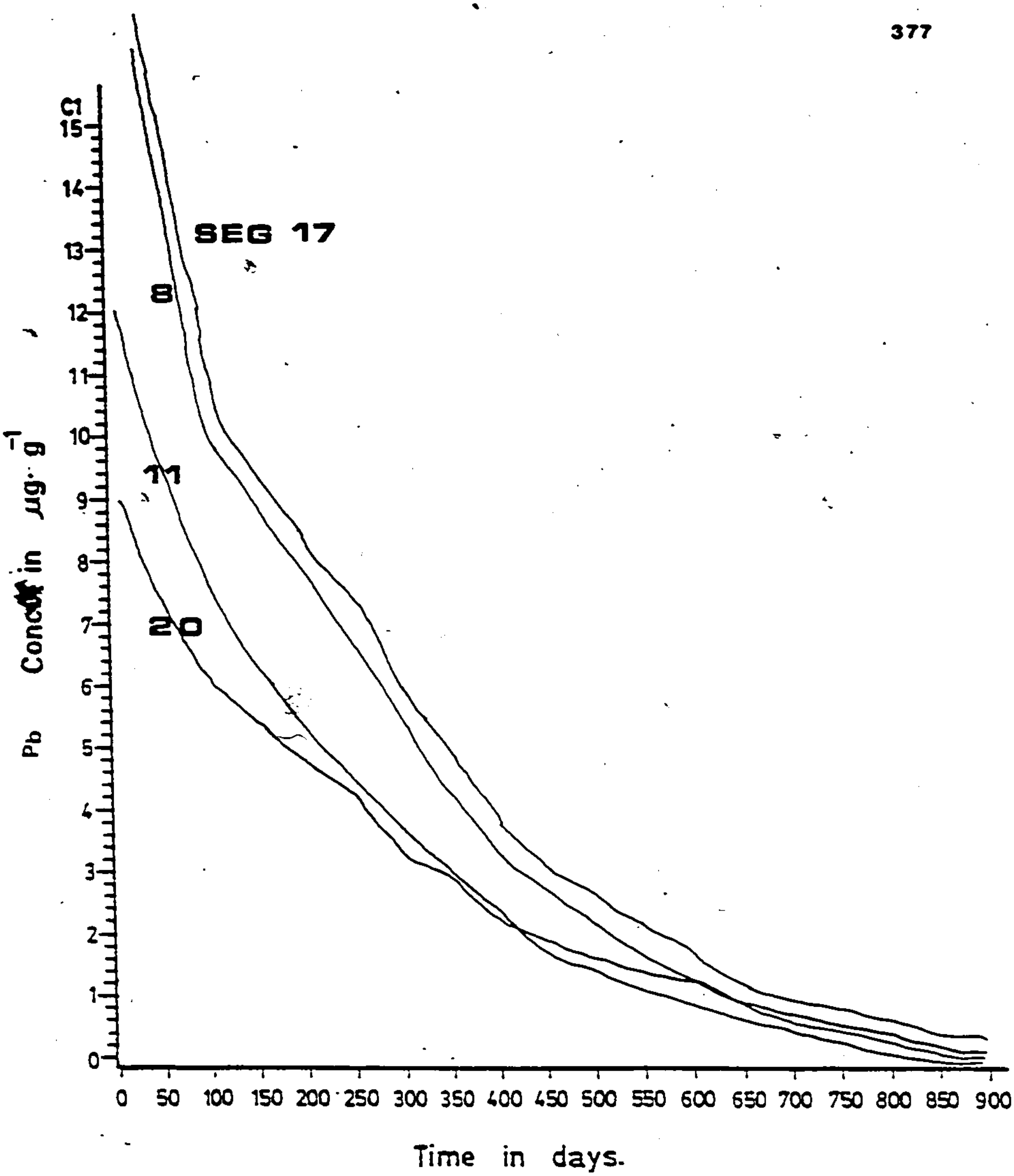

Figure 7.46 Predicted Pb Concentrations in Bed Sediment in Lake St. Clair

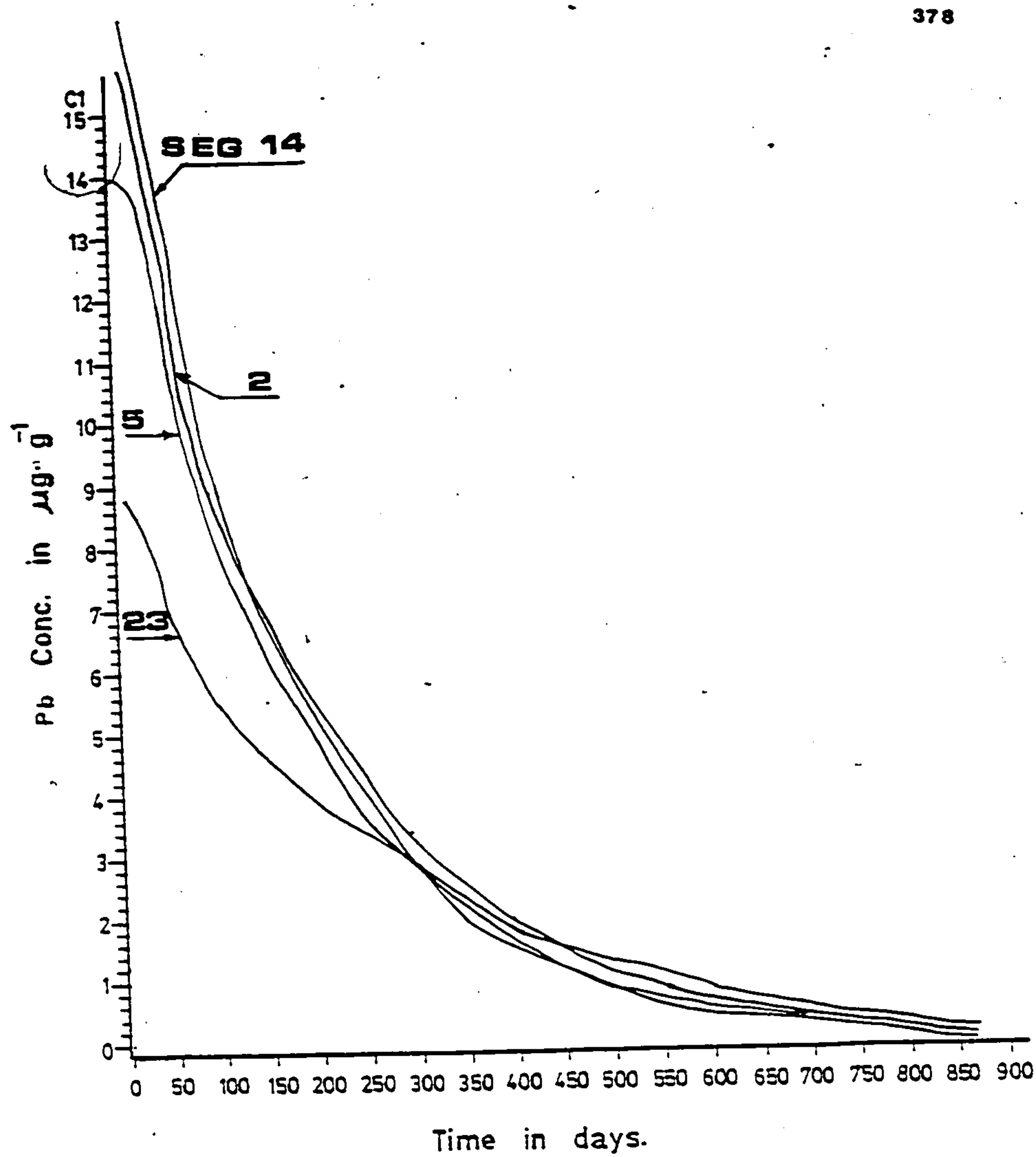

Figure 7.46 Predicted Pb Concentrations in Bed Sediment in Lake St. Clair

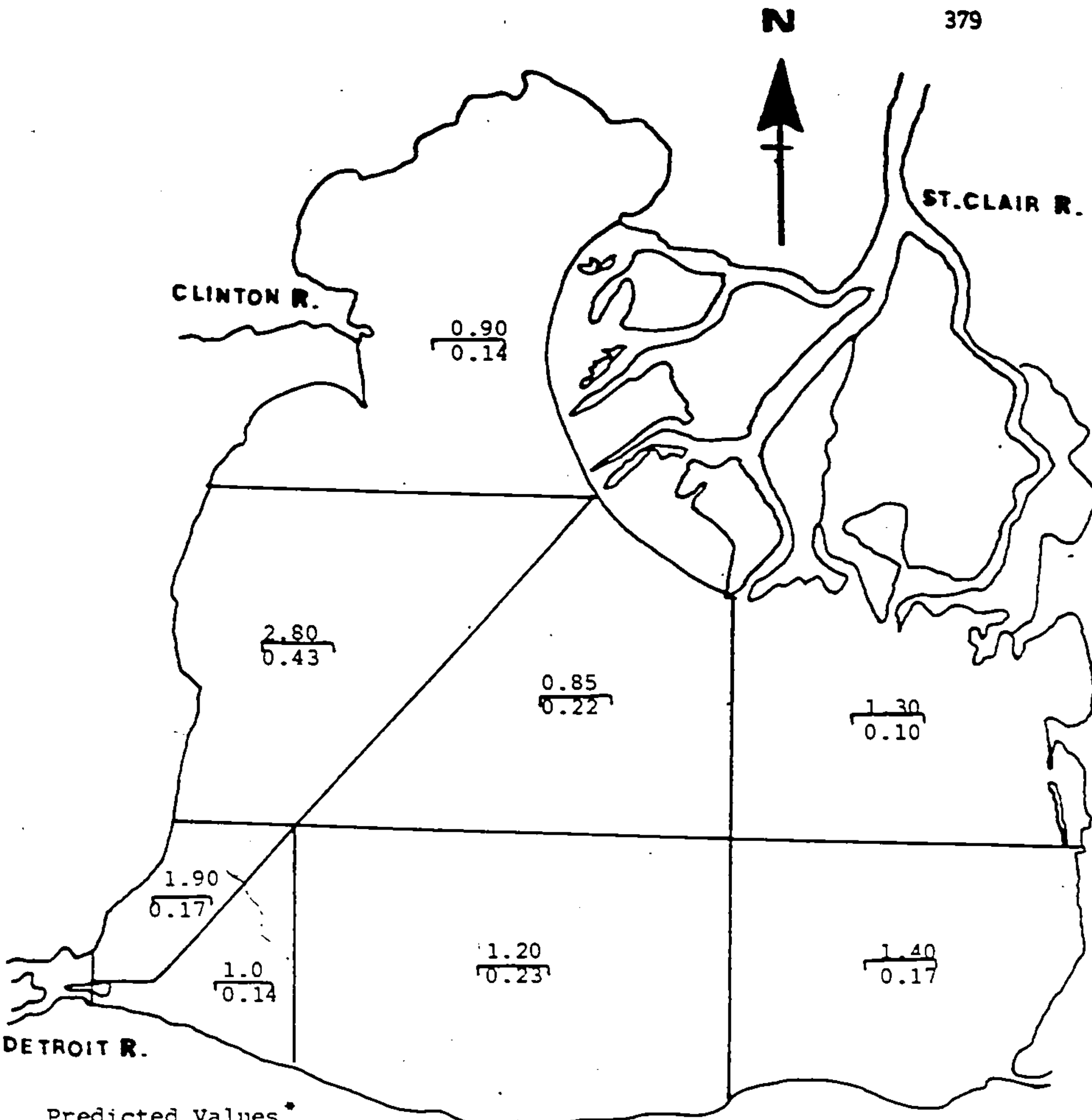

Predicted Values*

Measured 1984**

Figure 7.47 Predicted and Measured Concentrations of Cadmium in Bed Sediments ($ug.g^{-1}$) in Lake St. Clair.

* 2.5 cm active layer

** 10 cm sample depth

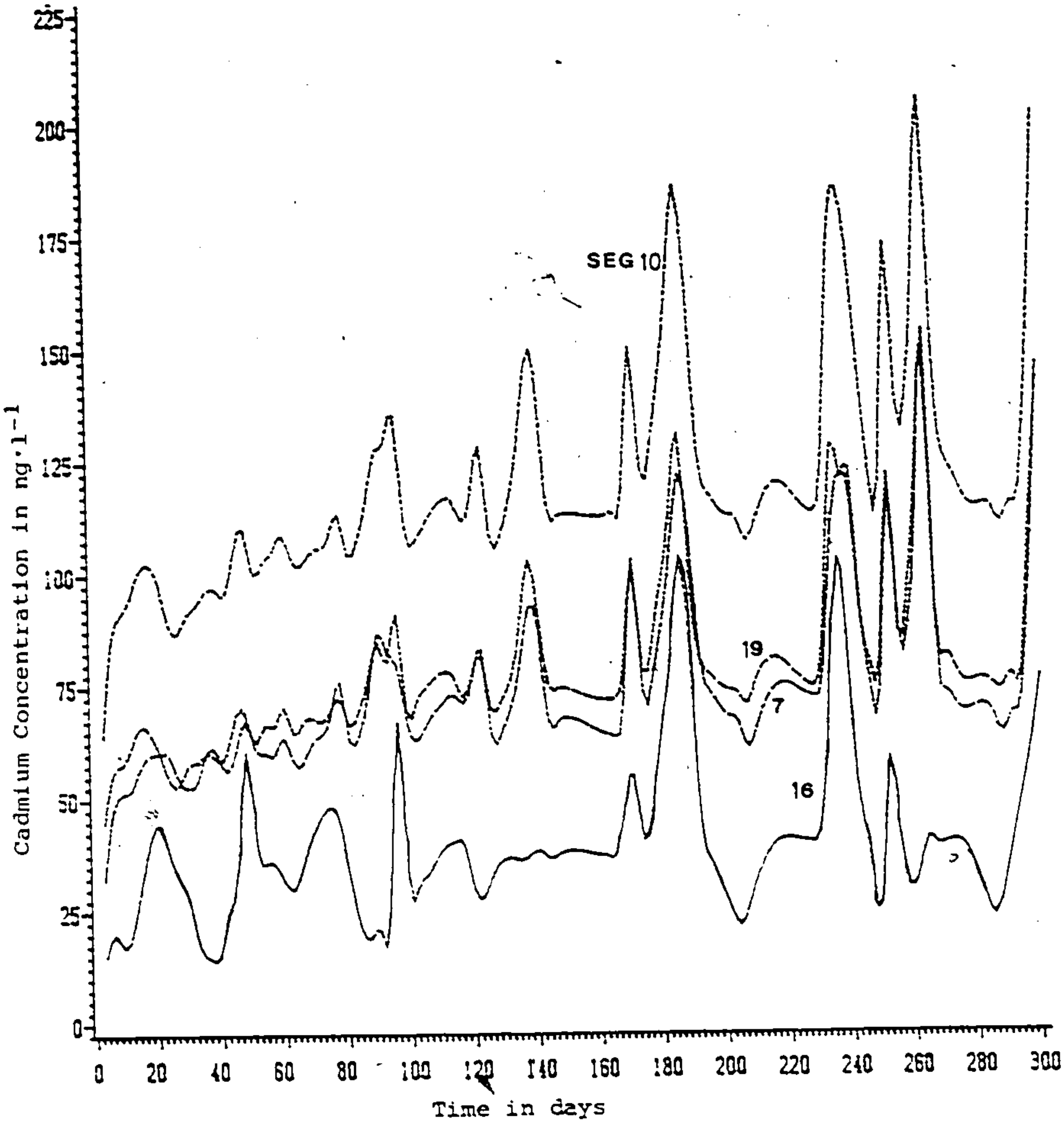

Figure 7.48 Total Cadmium Concentration in Water Segments in Lake St. Clair

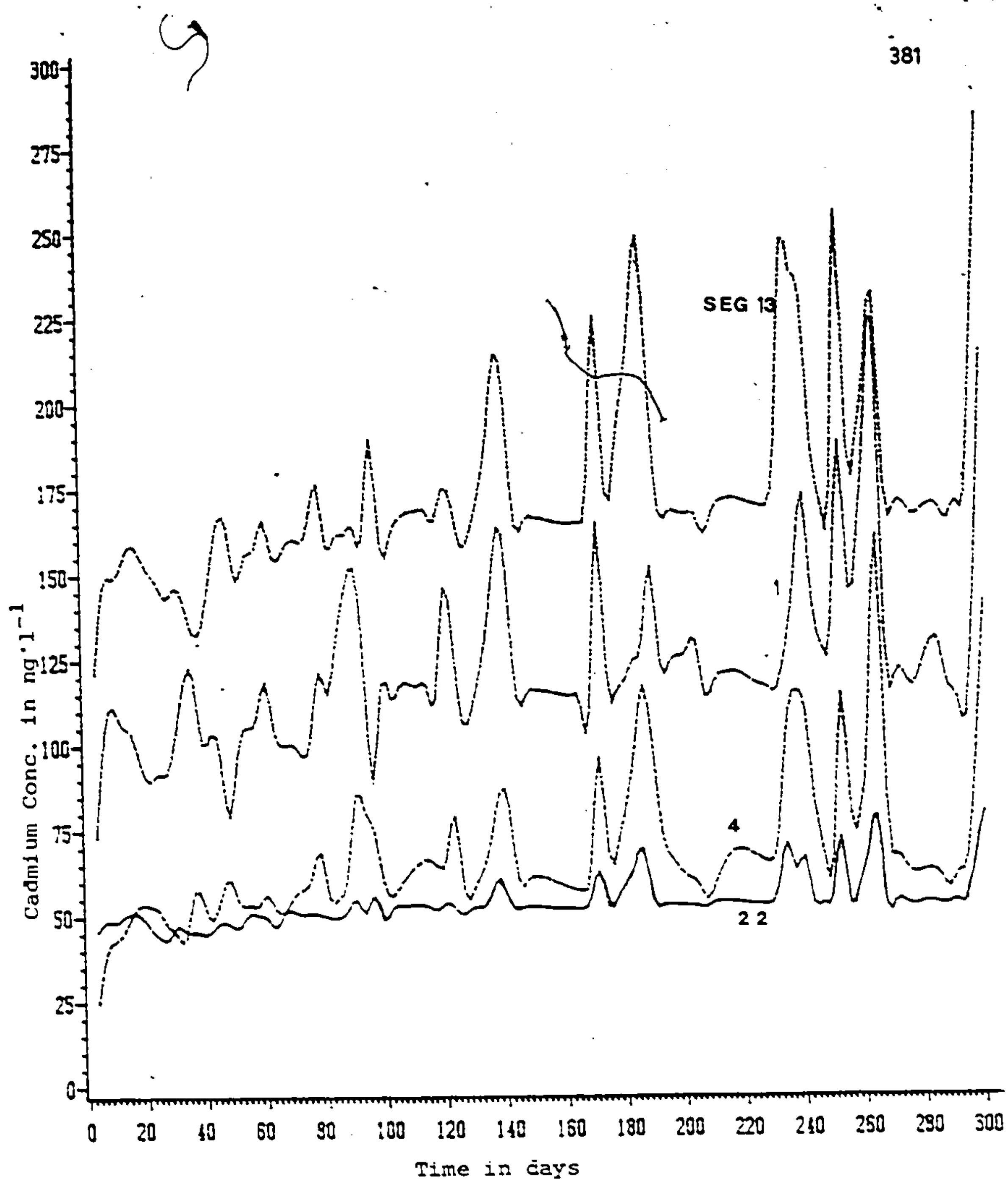

Figure 7.49 Total Cadmium Concentration in Water Segments in Lake St. Clair

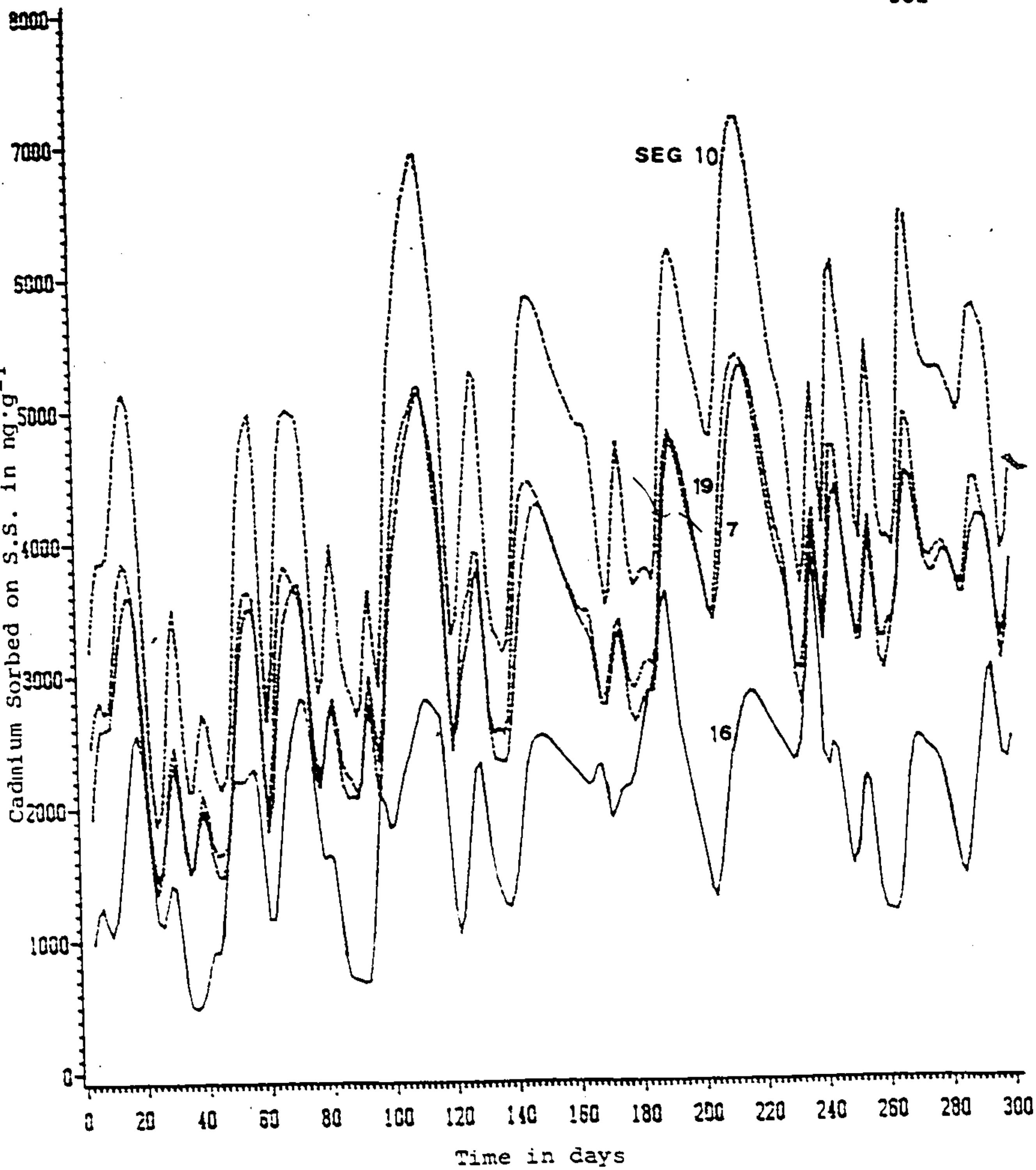

Figure 7.50 Cadmium Sorbed onto Suspended Sediments in Water Segments in Lake St. Clair

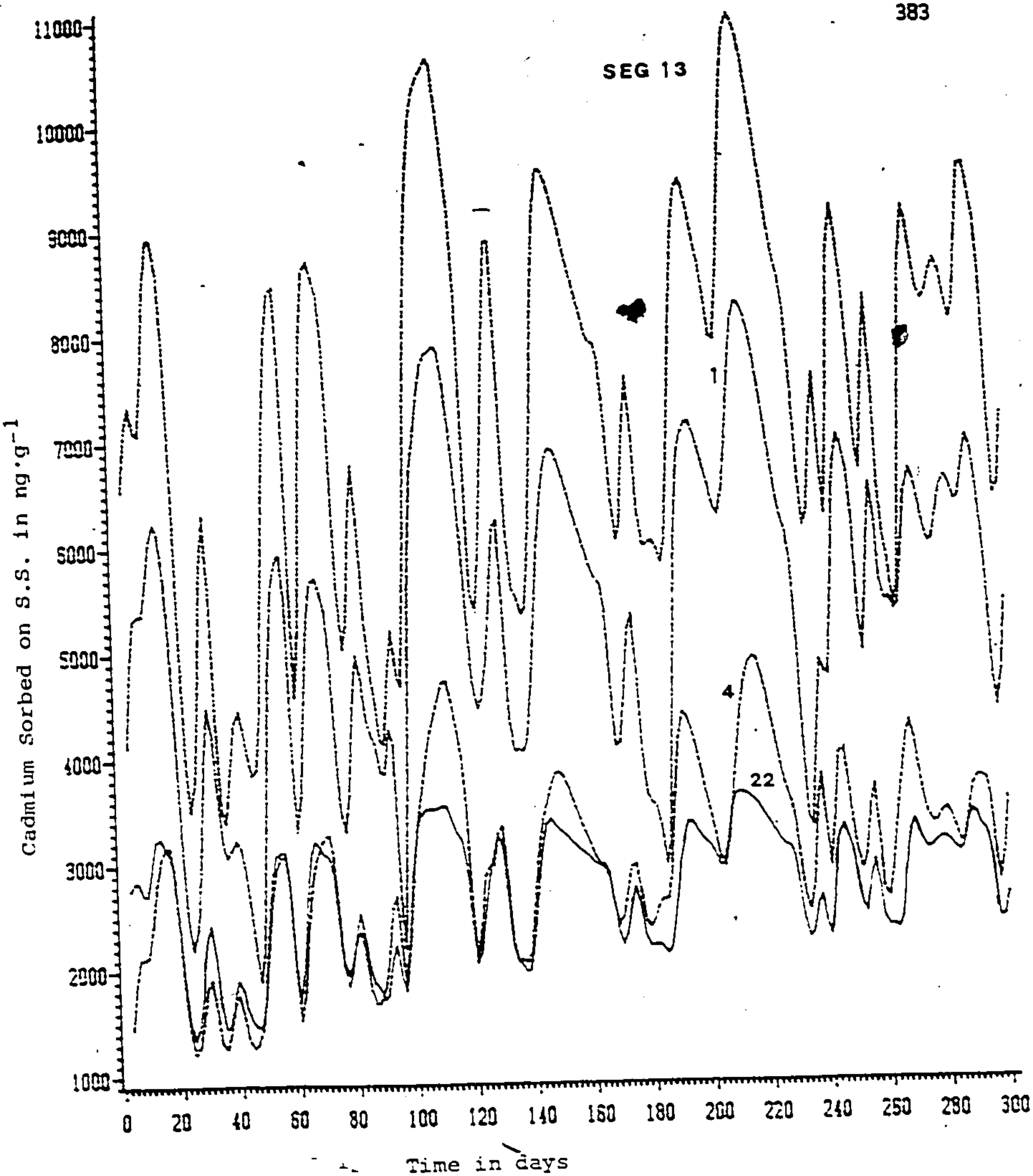

Figure 7.51 Cadmium Sorbed onto Suspended Sediments in Water Segments in Lake St. Clair

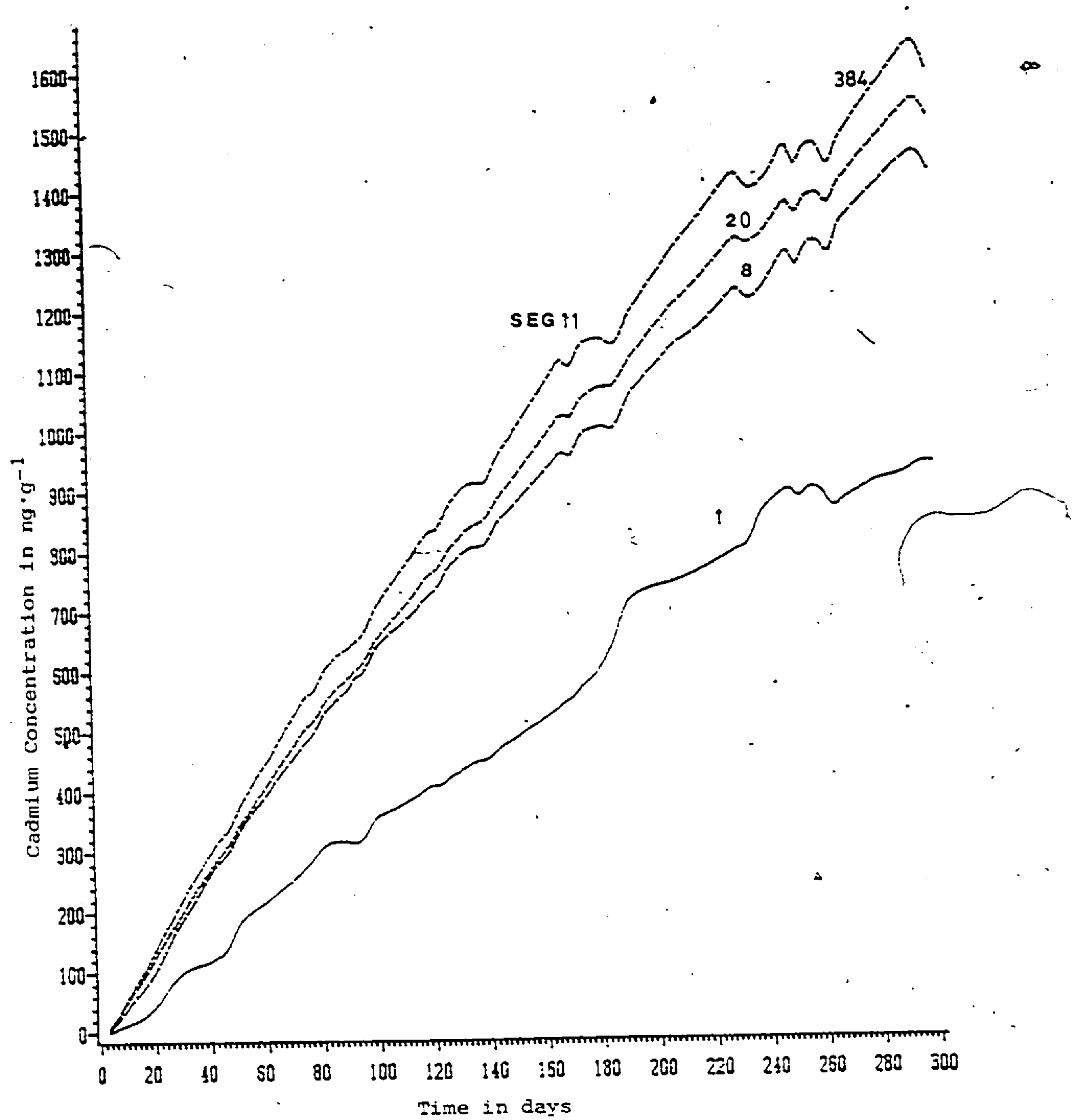

Figure 7.52 Cadmium Sorbed onto Sediments in Bed Segments in Lake St. Clair

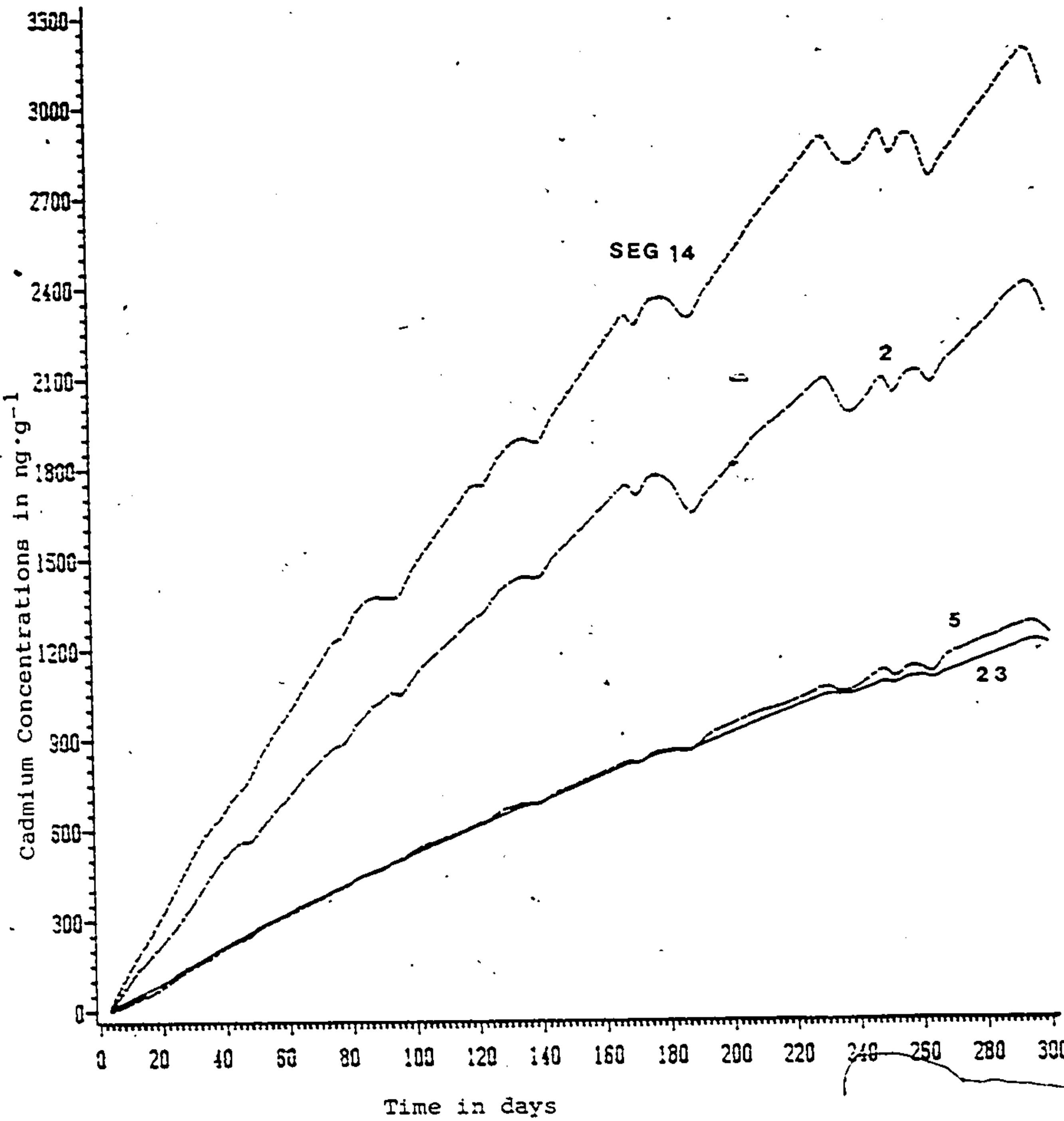

Figure 7.53 Cadmium Sorbed onto Sediment in Bed Segments in Lake St. Clair

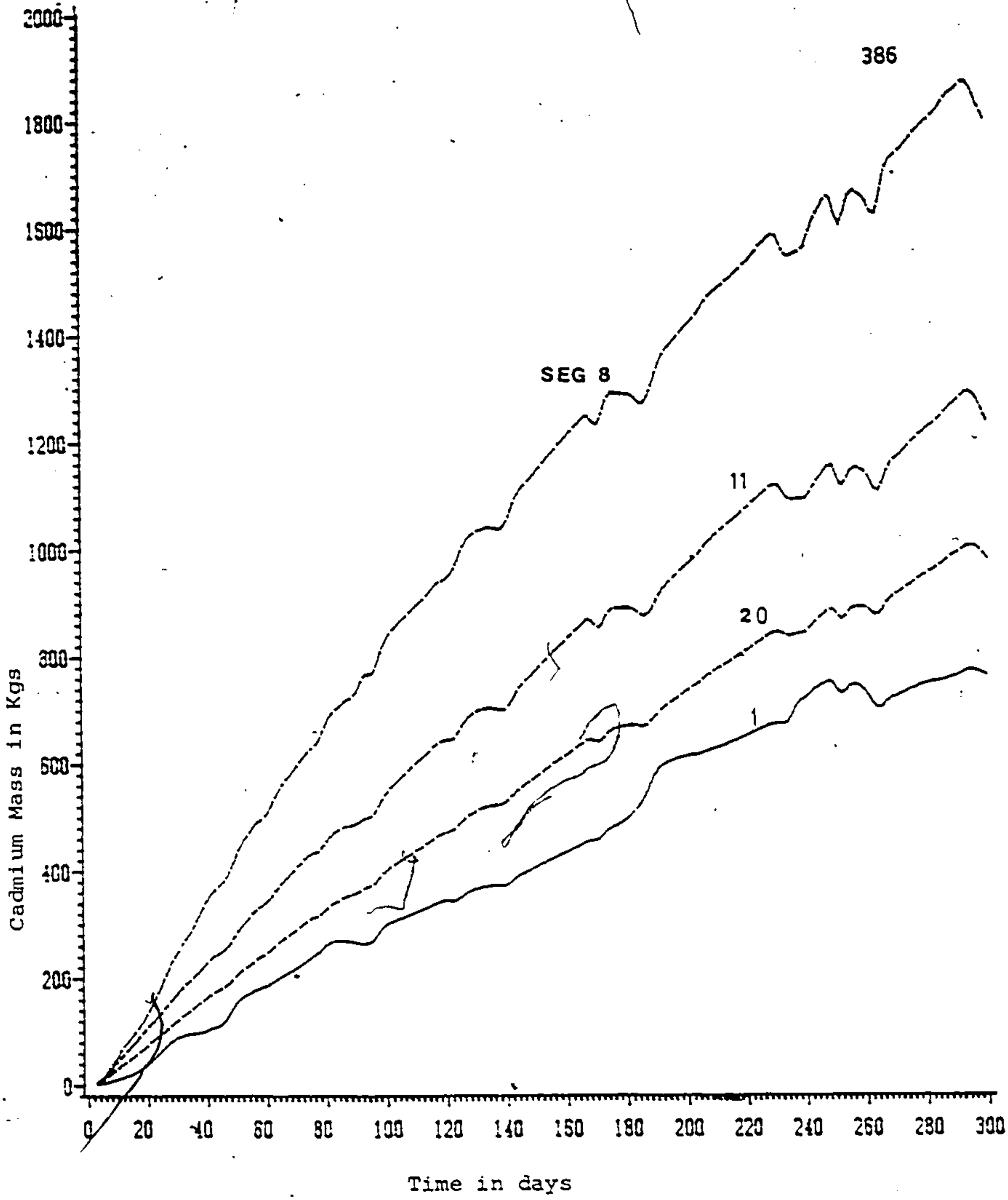

Figure 7.54 Total Mass of Cadmium in Surface Bed Segments in Lake St. Clair

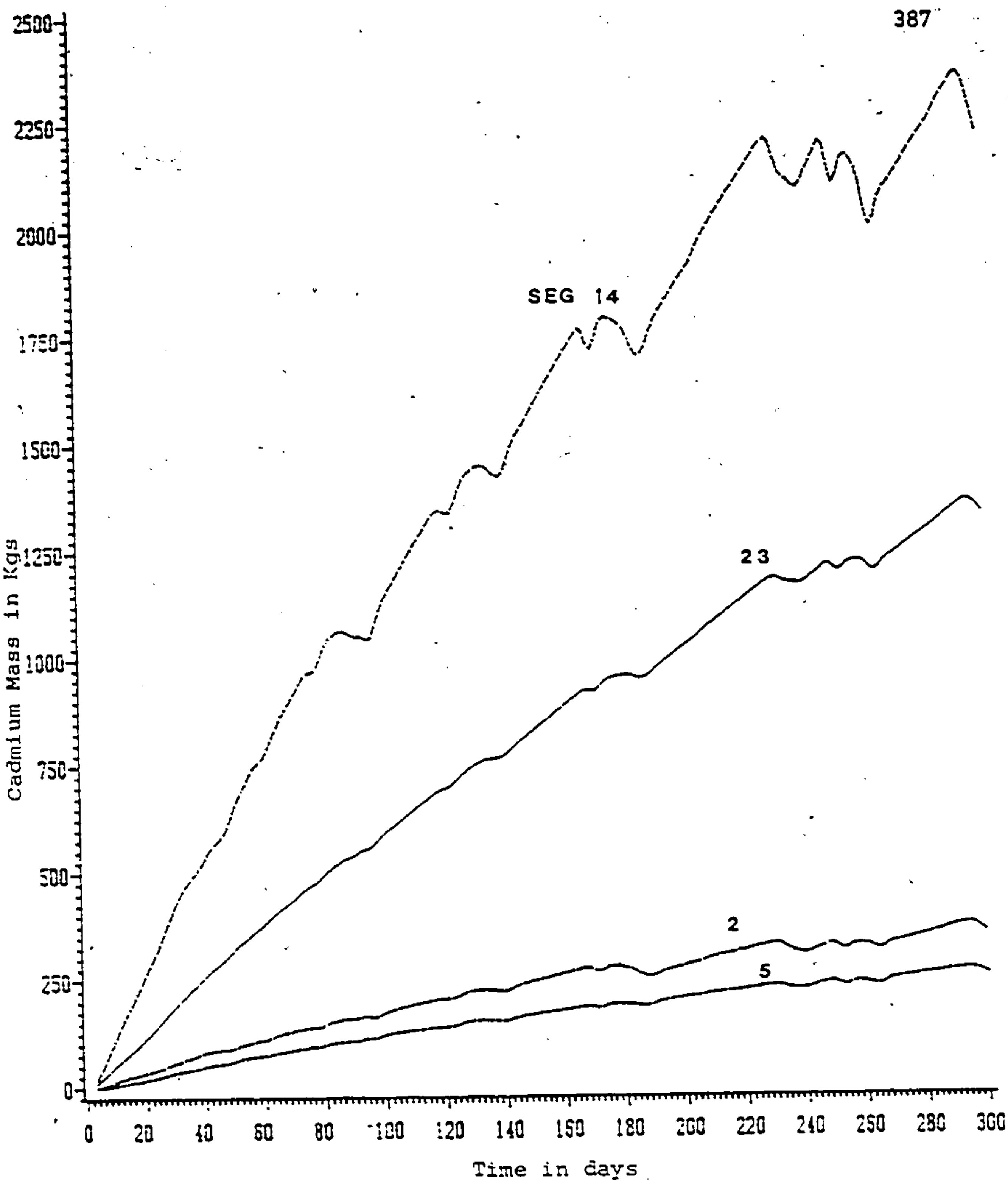

Figure 7.55 Total Mass of Cadmium in Surface Bed Segments in Lake St. Clair

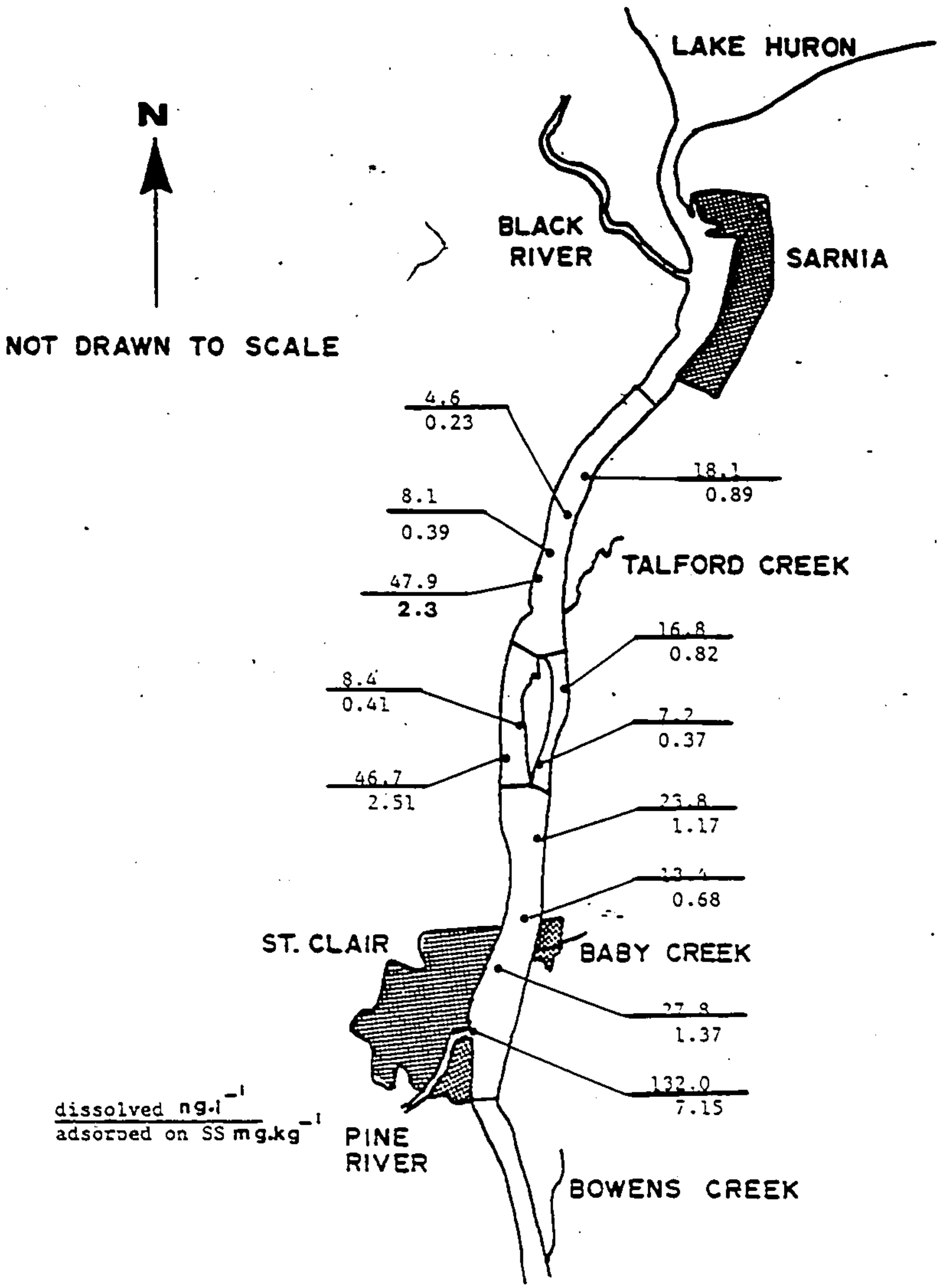

Figure 7.56 Predicted Concentrations of Cadmium in Water Segments and on Suspended Solids in St. Clair River

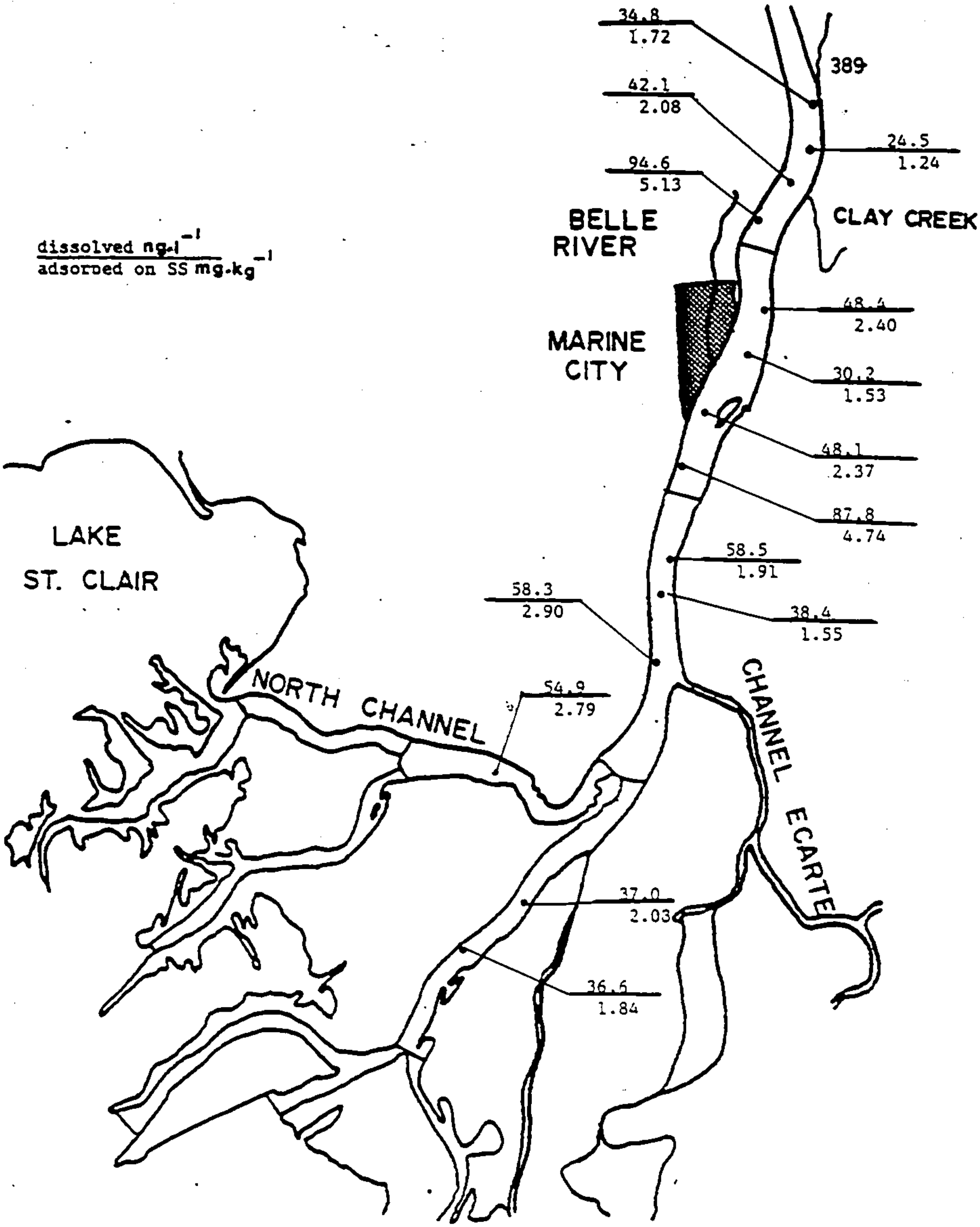

Figure 7.56 (Con't)

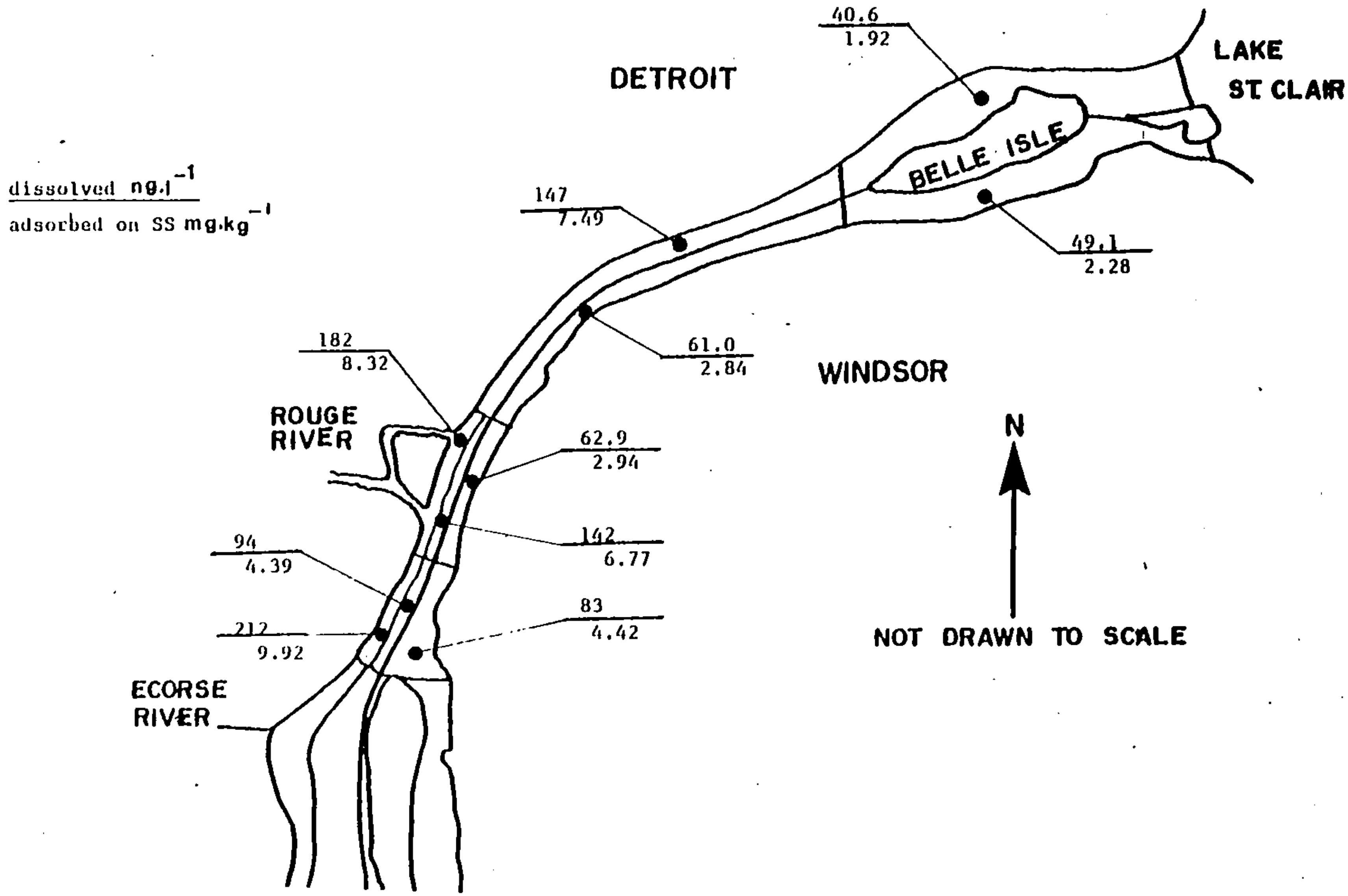

Figure 7.57 Predicted Concentrations of Cadmium in Water Segments and on Suspended Solids in Detroit River

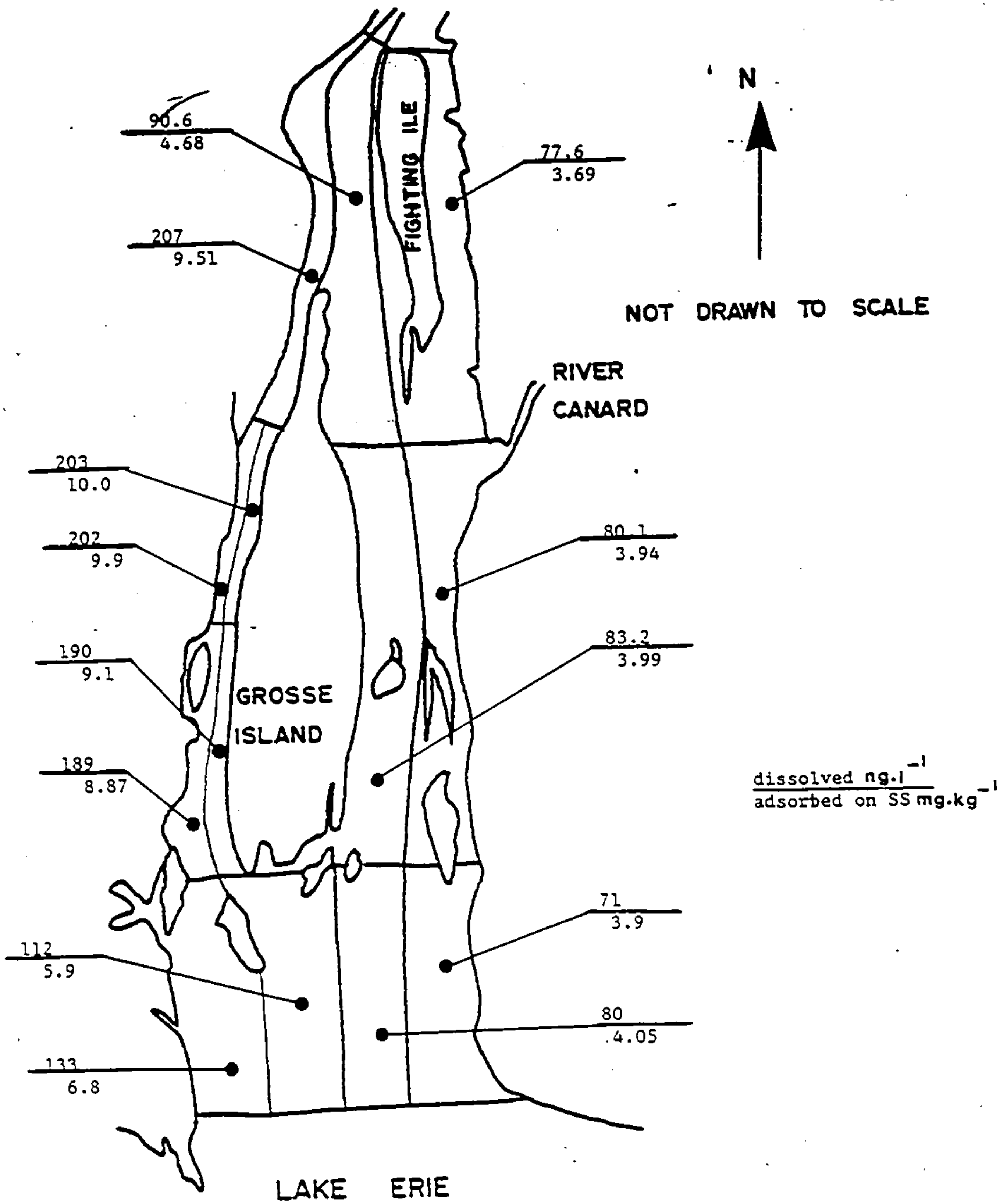

Figure 7.57 (Con't)

APPENDIX E

TABLES

Table 4.1 The Hydraulic Parameters for St. Clair River

Model Reach	Description	Reach Length (m)	Flow Rate $m^3 \cdot s^{-1}$	% of total flow rate	Exponent Coefficient (n_1)
1	Main river up to Stag Island	13410	5285	100.0	0.12
2	East of Stag Island	3050	1600	30.3	0.12
3	West of Stag Island	3050	3683	69.7	0.05
4	Main river up to Chenal Ecarte	26820	5285	100.0	0.15
5	Main river up to Russell Island	2440	5036	95.3	0.15
6	North Channel (1st part)	6100	2785	52.7	0.10
7	South Channel (1st part)	9140	2251	42.6	0.15
8	St. Clair Cutoff (1st part)	1830	2066	39.1	0.15
9	Bassett Channel	6100	185	3.5	0.05
10	North Channel (extension)	4876	1755	33.2	0.05
11	Middle Channel	10360	1030	19.5	0.06
12	South Channel (cont.)	7315	1057	20.0	0.08
13	St. Clair Cutoff (cont.)	2440	1197	22.6	0.10

Table 4.2 HCB Industrial Point Loads into St. Clair River

Outfall No.	Description	Flow $m^3.s^{-1}$	Conc. ng l^{-1} max	Conc. ng l^{-1} min	Total Load in $g.day^{-1}$ max	min	average
1	Extended 80 m	2.30	76	28	15	5.56	10.28
2	shore-based	0.60	39	25	2.02	1.30	1.66
3	--	3.00	9	4	2.33	1.04	1.68
4	--	0.25	13	1	0.28	0.02	0.15
5a	--	0.74	14200	175	908	11.2	460
b	--	0.55	30	---	1.43	---	1.43
c	--	0.19	36200	6330	595	104	350
d	--	0.58	1517	23	76.0	1.15	39
6	--	2.10	32	6	5.80	1.09	3.45
7	--	4.00	55	---	19.0	---	19.0

(Reference: McCorquodale and Ibrahim, 1985.)

Table 4.3 Non Point HCB Loads into St. Clair River.

Tributary	Flow rate $M^3.s^{-1}$	Conc. of HCB in Water $ng_c\ l^{-1}$ max	min	S.S Conc. $mg_s\ l^{-1}$ max	min	HCB on SS $ng_c\ g_s^{-1}$ max	min	loads of HCB $g_c \cdot day^{-1}$ max	min	average
Baby Creek	0.31	0.1	0.1	37	23	1	0.1	0.09	0.09	0.09
Talford	0.67	16	0.1	18	9	147	95	1.08	0.05	0.6
Murphy Drain	0.17	0.1	0.1	51	26	6	2	0.001	0.001	0.001

(Reference: McCorquodale and Ibrahim, 1985.)

Table 4.4 HCB Parameters Required by the TOXIWASP model

Variable	Description	Value	Units	References
BAC1	Bacterial population density in water.	1×10^6	cells ml^{-1}	Paris et al., 1981
BAC2	Bacterial population density in bed sediments.	$1 x 10^7$ to $1 x 10^8$	cells g^{-1}	Wetzel, 1975
KOW	Octanol water partition coefficient.	1×10^6	$l_w \cdot l^{-1}$ oct.	McCorquodale and Ibrahim, 1985
KOC	Organic carbon partition coefficient.	6×10^5	$l_w \cdot Kg^{-1}$ (organic carbon)	McCorquodale and Ibrahim, 1985
MWT	Molecular-weight of the chemical	285	$g \cdot mole^{-1}$	McCorquodale and Ibrahim, 1985
HEN	Henry's Law constant of the toxicant.	5×10^{-3}	$Atm \cdot m^3\ mole^{-1}$	McCorquodale and Ibrahim, 1985
VAP	Vapor pressure of compound	1.09×10^{-5}	torr	McCorquodale and Ibrahim, 1985
SOL	Aqueous solubility of toxicant chemical species	0.03	$mg \cdot l^{-1}$	McCorquodale and Ibrahim, 1985
SED	Concentration of solids in bed	2.33×10^5	$mg \cdot l^{-1}$	Callahan et al., 1979
OCS	Organic carbon content of sediment.	5%	dimensionless	Rodgers, 1981

Table 4.5 The Hydraulic Parameters for Detroit River (K-E) Model

Model Reach	Description	Reach length (m)	Flow Rate $m^3 \cdot S^{-1}$	% of total flow rate	Exponent coefficient n_1
1	North of Peche Island	1250	4672	75	0.12
2	South of Peche Island	1550	1558	25	0.12
3	Main River between Peche and Belle Isle	1100	6230	100	0.10
4	North of Belle Isle	5640	1870	30	0.14
5	South of Belle Isle	5640	4360	70	0.14
6	Main river up to Fighting Island	14000	6230	100	0.10
7	West of Fighting Island	2440	4860	78	0.12
8	West of Grassy Island	1220	2367	38	0.08
9	East of Grassy Island	1220	2492	40	0.10
10	West of Fighting Island up to Grosse Ile	1220	4860	78	0.12
11	West of Grosse Ile	13400	1870	30	0.08
12	East of Grosse Ile	2440	2990	48	0.10
13	East of Fighting Island	7925	1370	22	0.06
14	East of Grosse Ile	4270	4860	78	0.12
15	West of Bois Blanc Island	4880	2803	45	0.08
16	East of Bois Blanc Island	4880	2057	33	0.05

Table 4.6 Suspended Solids and Cadmium Loadings into the Upper Part of Detroit River

Outfall number	Description	S.S $lbs \cdot day^{-1}$	cadmium $lbs \cdot day^{-1}$
U.S. Shoreline			
1	Detroit Water Treatment Plant	60×10^3	100.0
2	Rouge River	62.0×10^3	2.80
3	Ecorse River	18.7×10^3	2.0
Canadian Shoreline			
1	West Windsor Water Treatment Plant	10×10^3	10.0
2	Turkey Creek	10.8×10^3	3.0
3	Canard River	28.5×10^3	2.0

Table 4.7 Cadmium Parameters Required by TOXIWASP Model

Variable	Description	Value	Units	References
BAC1	Bacterial population density in water.	1×10^{6}	cells ml^{-1}	Paris et al., 1981
BAC2	Bacterial population density in bed sediment.	1×10^{7} to 1×10^{8}	cells g^{-1}	Wetzel, 1975
KOW	Octanol water partition coefficient.	6.9×10^{6}	$l_w \cdot l^{-1}$	
KOC	Organic carbon partition coefficient.	4.48×10^{6}	$l_w \cdot Kg^{-1}$ (organic carbon)	Dolan and Bierman, 1982
MWT	Molecular weight of the chemical.	112	$g \cdot mole^{-1}$	
HEN	Henry's Law constant of the toxicant	$3\text{-}1 \times 10^{-5}$	$Atm \cdot m^{3}\ mole^{-1}$	
VAP	Vapor pressure of compound	—	torr	
SOL	Aqueous solubility of toxicant chemical species.	637	$mg \cdot l^{-1}$	
SED	Concentration of solids in bed.	2.33×10^{5}	$mg \cdot l^{-1}$	Callahan et al., 1979
OCS	Organic carbon content of sediment.	5%	dimensionless	Rodgers, 1981

Table 6.1 The Effects of Vertical Eddy Viscosity on the Depth Averaged Velocity in Lake St. Clair

ε $cm^2.s^{-1}$	U $cm.s^{-1}$	V $cm.s^{-1}$	$\sqrt{U^2+V^2}$
0.1	42.0	-60.00	75.00
1.0	39.0	0.56	39.00
10.0	5.7	0.76	5.80
20.0	2.3	0.38	2.30
30.0	0.6	0.21	0.64
40.0	0.4	0.15	0.43
50.0	-0.38	0.09	0.39
80.0	-0.52	0.03	0.52
100.0	-1.10	0.01	1.10

Element No. 36
Latitude 42 20 00 N
Longitude 82 42 30 W
Water depth 6.0 meters

Tx=3-5 Ty=0-0 S=0.3

Table 6.1 continued

$\mathcal{E}$ $cm^2.s^{-1}$	U $cm.s^{-1}$	V $cm.s^{-1}$	$\sqrt{U^2+V^2}$ $cm.s^{-1}$
0.10	-150.0	3.0	150.0
1.0	- 73.0	11.0	74.0
10.0	- 9.2	1.2	9.3
20.0	- 5.8	0.28	5.9
30.0	- 3.5	- 0.52	3.5
40.0	- 3.8	- 0.37	3.8
50.0	- 2.4	- 0.87	2.5
80.0	- 2.9	- 0.70	2.9
100.0	- 1.6	- 1.1	1.9

Element No. 145
Latitude 42 25 30 N
Longitude 82 37 00 W
Water depth 7.0 meters

Tx=3.5 Ty=0.0 , S=0.3

Table 6.2 The Effects of Slip Coefficient on Depth Averaged Velocity in Lake St. Clair

S	U $cm.s^{-1}$	V $cm.s^{-1}$	$\sqrt{U^2+V^2}$
0.0	1.9	0.35	1.9
0.1	3.6	0.46	3.6
0.3	2.3	0.38	2.3
0.6	- 1.2	- 2.5	2.8
0.9	2.0	0.35	2.0
1.2	1.9	0.35	2.0

Element No. 36
Latitude 42 20 00 N
Longitude 82 42.30 W
Water Depth 6.0 meters
Tx=3.5 Ty=0.0 , $\mathcal{E}_n$ =20

Table 6.2 The Effects of Slip Coefficient on Depth Averaged Velocity in Lake St. Clair

S	U $cm.s^{-1}$	V $cm.s^{-1}$	$\sqrt{U^2+V^2}$
0.0	- 4.9	- 0.08	4.9
0.1	- 8.2	1.10	8.3
0.3	- 5.8	0.28	5.9
0.6	- 5.3	0.09	5.3
0.9	- 5.2	0.03	5.2
1.2	- 5.1	- 0.01	5.1

Element No. 145
Latitude 42 25 30 N
Longitude 82 37 00 W
Water Depth 7.0 meters
Tx=3.5 ,Ty=0.0 ,$\mathcal{E}$=20

Table 6.3 Parameters for Lake St. Clair Finite Element Model

No. of elements	284 elements
No. of nodes	173 nodes
Horizontal extents	48 km x-direction 42 km y-direction
Maximum depth	9.0 m
Coriolis parameter	0.0001 rad s^{-1}
Vertical eddy viscosity ε_z	20 cm^2 s^{-1}
Horizontal diffusivity E_H	10^5 cm^2 s^{-1}

	Wind direction	Average wind speed	Wind stresses	
		$m\ s^{-1}$	τ_x (cm^2s^{-2})	τ_y (cm^2s^{-2})
1	NW	8.0	2.0	-2.0
2	NE	8.0	-2.0	-2.0
3	SE	8.0	-2.0	2.0
4	W	8.0	3.0	0.0

River flows and average chloride concentrations during cruise No. 5, July 15 to 24, 1974

Location	Mean flow	Average concentration
	m^3s^{-1}	mg L^{-1}
St. Clair River	5300	—
- North channel (F)	1750	7.46
- Middle channel (G)	1060	7.30
- South channel (D)	1950	7.82
(E)	280	8.52
- Chenal Ecarte (I)	260	8.90
Clinton River and other Michigan streams	50	7.80
Thames River and other Ontario streams	100	14.94
Detroit River	5450	—

Table 6.4 Parameters for the FEM for Suspended Solids in Lake St. Clair

No. of elements 284
Max. depth 9.0 meters
No. of nodes 173 nodes
Vertical eddy viscosity 20 $cm.s^{-1}$
Horizontal diffusivity E_H 10^5 $cm^2.s^{-1}$

Average wind speed during cruise No. 5 6.0 $m.s^{-1}$
Wind direction during cruise No.5 NNE

Average wind speed during cruise No. 6 8.0 $m.s^{-1}$
Wind direction during cruise No. 6 W

River flows and average suspended solids concentrations during cruises No. 5 and 6.

Location	Mean flow $m^3.s^{-1}$	SS concentration cruise No. 5	No. 6
North channel (F)	1750	8.8	4.5
Middle channel (G)	1060	6.2	5.3
South channel (D)	1950	8.0	4.0
(E)	280	9.0	6.0
Chenal Ecorte (I)	260	7.7	1.1
Clinton River	50	3.2	5.0
Thames River	100	15.0	20.0

Table 6.5 Average Concentrations of the Total PCBs in Lake St. Clair, 1970

Water Segment No.	ng/L	Bed Segment No.	ng/g_3	subsurface bed segment	ng/g_s
1	1.50	2	20.0	3	$5x10^{-3}$
4	1.58	5	24.0	6	$5x10^{-3}$
7	1.72	8	25.0	9	$5x10^{-3}$
10	2.42	11	22.0	12	$5x10^{-3}$
13	1.72	14	17.0	15	$5x10^{-3}$
16	1.72	17	21.0	18	$5x10^{-3}$
19	1.95	20	17.0	21	$5x10^{-3}$
22	1.72	23	14.0	24	$5x10^{-3}$

Table 6.6 Estimates of average PCB's and suspended solids loadings during free water surface (1970-1974)

Segment	Loading of PCB's lbs/day Atmospheric	Ind. & Runoff	Total	Suspended solids lbs/day
1	2.81×10^{-3}	------	2.81×10^{-3}	------
4	4.20×10^{-3}	------	4.20×10^{-3}	------
7	2.23×10^{-2}	------	2.23×10^{-2}	------
10	1.32×10^{-2}	5.7×10^{-3}	1.89×10^{-2}	5×10^{5}
13	1.38×10^{-2}	0.867	0.881	1.5×10^{6}
16	1.51×10^{-2}	4.778	4.793	2.0×10^{6}
19	1.03×10^{-2}	0.122	0.132	5×10^{5}
22	1.99×10^{-2}	1.043	1.063	1.5×10^{6}
Total	0.102	6.816	6.918	6.0×10^{6}

Table 6.7 Estimates of average PCBs and suspended solids loading during ice cover (1970–1974)

Segment	Total PCBs lbs day^{-1}	Suspended solids lbs day^{-1}
10	0.05	3.0×10^4
13	0.35	1.0×10^5
16	0.45	1.5×10^5
19	0.05	3.0×10^4
22	0.30	7.0×10^4
Total	1.20	3.8×10^5

Table 6.8 Frequency of occurrence of winds in hours per year.

Wind Speed mph	Wind Direction SE	NE	NW	SW	Total
20-30	98	138	345	373	954
10-20	420	518	518	905	2361
0-10	609	772	952	1338	3671

Table 6.9 Interchange Flow Rates Between Water Segments in CFS for Different steady State Wind Conditions in Lake St. Clair.

Segment Flow		Wind Speed (0-10 mph)				Wind Speed (10-20 mph)				Wind Speed (20-30 mph)				
From	To	NW	SW	SE	NE	NW	SW	SE	NE	NW	SW	SE	NE	Ice Cover
1	0	125457	125457	125457	125457	125457	125457	125457	125457	125457	125457	125457	125457	75294
4	0	61793	61793	61793	61793	61793	61793	61793	61793	61793	61793	61793	61793	37086
4	1	37136	45852	47448	46249	25077	43077	67023	49024	-30850	35150	122950	56950	23564
13	1	88321	79605	78009	79209	100380	82380	58434	76434	156307	90307	2507	68507	51730
7	4	98929	107645	109241	108041	86870	104807	128815	110817	30943	96943	184743	118743	60650
10	7	11060	10381	10737	11632	15042	1621	6971	20392	25802	23408	3788	45420	6488
16	7	87868	97263	98503	96408	71828	103248	121844	90424	5141	73534	180954	73322	54162
0	10	1872	1872	1872	1872	1872	1872	1872	1872	1872	1872	1872	1872	1123
0	19	16852	16852	16852	16852	16852	16852	16852	16852	16852	16852	16852	16852	10114
0	16	69282	69282	69282	69282	69282	69282	69282	69282	69282	69282	69282	69282	41581
0	22	99243	99243	99243	99243	99243	99243	99243	99243	99243	99243	99243	99243	59562
19	10	9188	8509	8865	9760	13170	-251	5099	18520	23930	21536	1916	43548	5365
19	16	7664	8343	7987	7092	3682	17103	11754	-1667	-7077	-4684	14936	-26696	4749
22	13	99243	99243	99243	99243	99243	99243	99243	99243	99243	99243	99243	99243	99243
16	13	-10922	-19638	-21234	-20034	1137	-16863	-40808	-22809	57064	-8936	-96736	-30736	-7832

Table 6.10 PCBs Parameters Required by the TOXIWASP Model.

Variable	Description	Value	Units	References
BAC1	Bacterial population density in water.	$1x10^6$	cells ml^{-1}	Paris et. al., 1981.
BAC2	Bacterial population density in bed sediment.	$1x10^7$ to $1x10^8$	cells g^{-1}	Wetzel, 1975
KOW	Octanol water partition coefficient.	$1x10^6$	$l_w \cdot l_{oct}^{-1}$	Callahan et. al., 1980
KOC	Organic carbon partition coefficient.	$6.3x10^5$	$l_w.Kg^{-1}$ (organic carbon)	Karickhoff et. al.,1979
MWT	Molecular weight of the chemical	320	$g.mole^{-1}$	
HEN	Henry's Law constant of the toxicant.	$3x10^{-4}$	$Atm.m^3\ mole^{-1}$	MacKay et. al., 1983
VAP	Vapor pressure of compound	$7.7x10^{-5}$	torr	MacKay et. al., 1983
SOL	Aqueous solubility of toxicant chemical species.	$8x10^{-3}$	$mg.l^{-1}$	Bidleman et. al., 1983
SED	Concentration of solids in bed.	$2.33x10^5$	$mg.l^{-1}$	Callahan et. al., 1979
OCS	Organic carbon content of sediment.	5%	dimensionless	Rodgers, 1981

Table 7.1 Hydrologic Data for Canadian Streams for the Study Region.

Station No.	Station Description	Drainage Area (Km^2)	Mean Ann. Runoff Depth(m)*	Runoff Vol. $\times 10^{-6}$ $(m^3.y)^{-1}$r	Mean Flow rate $m^3.s^{-1}$	Total Ann. Sedi. load 10^{-3} tons	Suspended Solid Mean Conc. $mg.1^{-1}$	Suspended Solid Av. Load 10^{-3} Kg.day^{-1}
1	Talford Creek	93	0.225	21.13	0.67	0.36	75	4.34
2	Bowens Creek	46	0.213	9.75	0.31	0.16	—	2.00
3	Clay Creek	65	0.213	13.82	0.44	0.24	—	2.85
4	Murphy Creek & Marshy Cr.	77	0.200	5.45	0.17	0.09	—	1.10
5	Total From small streams	231	0.200	46.25	1.47	0.79	—	9.52
6	Sydenham River North	2715	0.230	624.45	19.80	10.64	—	128.31
7	Sydenham River East	242	0.198	47.92	1.52	0.82	—	9.85
8	Rankin Creek & Bayle Drain	232	0.195	45.24	1.43	0.77	—	9.27
9	Thames River	5650	0.270	1525.5	48.37	69.33	200	835.8
10	Total from small streams	17	0.195	3.32	0.11	0.06	75	0.71
11	Tremblay Creek	50	0.195	9.75	0.31	0.17	—	2.00
12	Ruscom Creek	168	0.195	32.76	1.04	0.56	—	6.74
13	Maison & Duck Creek	50	0.195	9.75	0.31	0.17	—	2.00
14	Belle River	105	0.195	20.48	0.65	0.35	—	4.21
15	Puce R., Pke Cr. and Little R.	266	0.195	51.87	1.65	0.89	—	10.70
16	Turkey Creek	124	0.198	24.18	0.76	0.41	—	4.92
17	Canard River	313	0.200	62.60	2.00	1.08	—	12.96

*Estimated from Ontario Atlas

Table 7.2 Hydrologic Data for U.S. Streams in the Study Region.

Station No.	Station Description	Drainage Area Km^2	Ann. Ave. Runoff depth m*	Total Runoff Vol. x 10^{-6} m^3 yr^{-1}	Ann. Ave Flow Rate $m^3.s^{-1}$	Total Ann. Sedi. Load x 10^{-3} Tons	Suspended Solids Av. Conc. mg l^{-1}*	Suspended Solids Av. load Kg.day^{-1} 10^{-3}
1	Black River at Port Huron	1910	0.198	380	12.00	1.38	32	33.2
2	Total from small streams	51	0.210	10.7	0.34	0.04	34	1.0
3	Pine River at St. Clair	510	0.195	99.5	3.15	0.41	36	9.8
4	Belle River at Marine City	540	0.195	103	3.29	0.94	40	11.37
5	Fisher Greek at Algonac	46	0.192	8.9	0.28	0.03	30	0.72
6	Sashaboaw Creek	74	0.198	14.2	0.45	0.06	30	1.5
7	Total from small streams	300	0.190	57.0	1.81	0.23	36	5.62
8	Clinton River	1965	0.250	490	15.58	2.23	40	53.84
9	Rouge River	1180	0.195	230	7.40	1.17	44	28.2
10	Ecorse River	176	0.210	37	1.17	0.17	42	4.24
11	Total from small steams	190	0.220	42	1.33	0.20	42	4.82

* From U.S. Geological Survey Water Data

Table 7.3 OCS Parameters Required by the TOXIWASP model

Variable	Description	Value	Units	References
BAC1	Bacterial population density in water.	$1x10^6$	cells ml^{-1}	Paris et. al., 1981
BAC2	Bacterial population density in bed sediment.	$1x10^7$ to $1x10^8$	cells g^{-1}	Wetzel, 1975
KOW	Octanol water partition coefficient.	$1.9x10^6$	$l_w.l^{-1}oct.$	Veith, et. al., 1979b
KOC	Organic carbon partition coefficient.	$1.2x10^6$	$l_w.Kg^{-1}$(organic carbon)	
MWT	Molecular weight of the chemical.	300	$g.mole^{-1}$	
HEN	Henry's Law constant of the toxicant.	$1x10^{-4}$	$Atm.m^3\ mole^{-1}$	
VAP	Vapor pressure of compound	$4x10^{-5}$	torr	
SOL	Aqueous solubility of toxicant chemical species.	0.02	$mg.l^{-1}$	
SED	Concentration of solids in bed.	$2.33x10^5$	$mg.l^{-1}$	Callahan et. al., 1979
OCS	Organic carbon content of sediment.	5%	dimensionless	Rodgers, 1981

Table 7.4 Pd Parameters Required by the TOXIWASP model

Variable	Description	Value	Units	References
BAC1	Bacterial population density in water.	$1x10^6$	cells ml^{-1}	Paris et. al., 1981
BAC2	Bacterial population density in bed sediment.	$1x10^7$ to $1x10^8$	cells g^{-1}	Wetzel, 1975
KOW	Octanol water partition coefficient.	$13.2x10^6$	$l_w.l^{-1}oct.$	Veith, et. al., 1979b
KOC	Organic carbon partition coefficient.	$8.56x10^6$	$l_w.Kg^{-1}$ (organic carbon)	
MWT	Molecular weight of the chemical.	207	$g.mole^{-1}$	
HEN	Henry's Law constant of the toxicant.	$3.1x10^{-4}$	$Atm.m^3\ mole^{-1}$	
VAP	Vapor pressure of compound	$4x10^{-5}$	torr	
SOL	Aqueous solubility of toxicant chemical species.	637	$mg.l^{-1}$	
SED	Concentration of solids in bed.	$2.33x10^5$	$mg.l^{-1}$	Callahan et. al., 1979
OCS	Organic carbon content of sediment.	5%	dimensionless	Rodgers, 1981

Table 7.5 The Estimated Lead and Cadmium Loading Rates into the Study Area.

Station No.	Station Description	Drainage Area km^2	Population	Pd $lbs.day^{-1}$	Cd $lbs.day^{-1}$
CANADA					
1	Talford Creek	93	71,070	250	4.5
2	Bowens Creek	46	6,660	3	2.2
3	Clay Creek	65	10,046	4	3.1
4	Murphy Creek + Marshy Cr.	77	4,989	2	3.7
5	Total from :all streams	231	2,462	1	11.0
6	Sydenham River North	2715	23,150	10	15
7	Sydenham River East	242	11,506	5	11.6
8	Rankin Creek & Bayle Drain	232	---	--	11.1
9	Thames River	5650	619,204	262	35
10	Total from small steams	17	---	--	0.8
11	Tremblay Creek	50	6,888	3	2.4
12	Ruscom Creek	168	---	--	8.1
13	Moison & Duck Creek	50	4,403	2	2.4
14	Belle River	105	3,568	2	5.0
15	Puce R., Pike Cr. and Little R.	266	10,150	4	12.8
16	Turkey Creek	124	192,083	81	6.0
17	Canard River	313	27,896	12	15.0
USA					
1	Black River at Port Huron	1910	74,800	32	12
2	Total from small streams	51	264,700	112	2.5
3	Pine River at St. Clair	510	138,802	59	24
4	Belle River at Marine City	540	---	--	26
5	Fisher Creek at Algonac	46	---	--	2.2
6	Sashabaw Creek	74	---	--	3.6
7	Total from small streams	300	70,000	30	14
8	Clinton River	1965	1,061,600	450	94
9	Rouge River	1180	2,210,000	935	57
10	Ecorse River	176	275,500	117	8.5
11	Total from small streams	190	32,000	14	9.0

Table 7.6. Comparison of predicted and Measured Contaminants Concentration in Sediments in St. Clair and Detroit Rivers.

Model Segment No.	Predicted OCS Con. on S.S. ng.g^{-1}	Observed Bed Sed. Conc. in Surficial (ng.g^{-1}) Source#1 min	Source#1 max	Source#2 min	Source#2 max	Source#3 min	Source#3 max
St. Clair River							
1	273	0.1	59.8	ns	ns	90	8900
9	266	0.1	79.5	ns	ns	ns	ns
17	253	0.3	24.6	ns	ns	ns	ns
25	238	4.9	26.5	ns	ns	ns	ns
33	224	3.6	36.5	ns	ns	ns	ns
41	97	7.9	10.0	ns	ns	ns	ns
47	91	8.1	26.2	ns	ns	ns	ns
Ave.	206	3.6	37.6	ns	ns	90	8900
Detroit River							
1	17.5	0.2	0.3	ns	ns	ns	ns
5	17.3	--	1.9	ns	ns	ns	ns
9	17.2	ns	ns	ns	ns	ns	ns
15	16.5	--	0.7	ns	ns	ns	ns
21	15.0	0.4	0.8	ns	ns	ns	ns
27	14.3	nd	0.2	ns	ns	ns	ns
39	13.9	--	3.5	ns	ns	ns	ns
Ave.	15.9	0.3	1.23	ns	ns	ns	ns

Model Segment No.	Predicted PCB's Con. on S.S. ng.g^{-1}	Observed Bed Sed. Conc. in Surficial (ng.g^{-1}) Source#1 min	Source#1 max	Source#2 min	Source#2 max	Source#3 min	Source#3 max
St. Clair River							
1	422	2.3	7.6	ns	ns	35	1245
9	413	2.3	20.0	ns	ns	ns	ns
17	392	2.3	7.6	ns	ns	ns	ns
25	367	2.3	7.6	ns	ns	ns	ns
33	345	2.3	7.6	ns	ns	ns	ns
41	210	nd	2.3	ns	ns	ns	ns
47	153	nd	2.3	ns	ns	ns	ns
Ave	329	2.0	7.9	ns	ns	35	1245
Detroit River							
1	57	nd	2.3	ns	ns	nd	36
5	94	--	7.6	ns	ns	70	260
9	125	--	2.3	ns	ns	70	255
15	279	--	7.6	ns	ns	25	55
21	263	--	2.3	ns	ns	nd	55
27	294	2.3	2.3	ns	ns	40	88
39	280	--	7.6	ns	ns	nd	110
Ave	199	2.0	4.6	ns	ns	51	122.7

1. From Great Lakes Report, 1984.
2. From Great Lakes Report, 1985.
3. From MOE Report, 1982.

nd: not detected
ns: no samples
--: one reading

Model Segment No.	Predicted Lead Con. on S.S. ug.g-1	Observed Lead Conc. in Surficial Bed Sed. (ug.g-1) Source≠1 min	max	Source≠2 min	max	Source≠3 min	max
St. Clair River							
1	79.0	9.0	17.0	6.7	393.0	8.0	128
9	77.0	8.4	337.0	5.9	219.0	ns	ns
17	74.1	6.3	76.0	33.0	88.0	ns	ns
25	70.0	19.0	21.0	14.0	35.0	ns	ns
33	66.6	18.5	28.5	9.4	24.0	ns	ns
41	28.4	15.0	57.0	8.7	28.0	ns	ns
47	27.8	9.6	19.0	2.0	12.0	ns	ns
Ave.	60.4	12.2	79.3	11.4	114.0	8.0	128
Detroit River							
1	13.3	12	21	--	32	4.8	79.0
5	23.4	--	103	--	43	56.0	218.0
9	25.7	ns	ns	ns	ns	41.0	65.5
15	52.9	--	14	--	17	17.0	26.0
21	45.1	14	26	ns	ns	3.0	24.0
27	48.8	10	14	ns	ns	9.5	78.0
39	39.4	--	37	--	32	8.5	44.0
Ave.	35.5	12	35.8	--	31.0	20	76.3

Model Segment No.	Predicted Cadmium Con. on S.S. ug.g-1	Observed Conc. in Surficial Bed Sed. (ug.g-1) Source≠1 min	max	Source≠2 min	max	Source≠3 min	max
St. Clair River							
1	0.89	0.05	0.08	0.03	1.80	ns	ns
9	0.82	0.06	0.08	0.08	0.16	ns	ns
17	1.17	0.06	0.18	0.13	0.18	ns	ns
25	1.72	0.07	0.11	0.08	1.60	ns	ns
33	2.40	0.07	0.15	0.09	0.20	ns	ns
41	1.91	0.05	0.06	0.06	0.16	ns	ns
47	2.03	---	0.06	0.02	0.06	ns	ns
Ave.	1.56	0.06	0.103	0.07	0.59	--	--
Detroit River							
1	2.28	0.08	0.14	---	0.22	0.30	0.50
5	2.84	---	0.50	---	0.24	0.30	4.48
9	2.94	---	0.19	ns	ns	0.3	0.63
15	4.42	0.19	0.50	---	0.19	0.3	0.3
21	3.69	0.09	0.12	ns	ns	0.3	0.45
27	3.94	---	0.09	ns	ns	0.35	0.80
39	3.90	---	0.51	---	0.37	0.30	1.30
Ave.	3.43	0.12	0.29	---	0.26	0.31	1.21

APPENDIX F

NOMENCLATURE

A	Cross sectional area
A^*	Coefficient in complex form for Equ. 5.31
A^*_r, A^*_i	The real and imaginary parts of A^*
$A(x,y)$	Coefficient function in local depth (Equ. 5.36)
a	The upwinding coefficient in Equ. 5.64
a_i, a_j, a_k	Constants in Eqs. 5.40, 5.41 and 5.42
a_1, a_2, a_3	Coefficients in Equ. 3.14
B^*	Coefficient in complex form in Equ. 5.31
B^*_r, B^*_i	The real and imaginary parts of B^*
$B(x,y)$	Coefficient function in local depth (Equ. 5.36)
b	Constant in Equ. 2.9
b_i, b_j, b_k	Constants in Eqs. 5.40, 5.41 and 5.42
b_1, b_2, b_3	Empirical constants in Eqs. 3.31, 3.32 and 3.33
C	Contaminant concentration
C_0	Amount of dissolved chemical in water
C_1, C_2	Concentration of chemical and sediment
C_g	Concentration of chemical in the bulk gas phase
C_b	Concentration of bacteria
C_k, C_f	Empirical constants in Equ. 3.33
$C(x,y)$	Coefficient function of local depth in Equ. 5.36

c_i, c_j, c_k	Constants in Eqs. 5.40, 5.41 and 5.42
D	Vertical reference dimension
D_0	The diffusion factor
D'	Dispersion term in Equ. 3.11
E	Longitudinal dispersion in rivers
E_x, E_y, E_z	Coefficients of dispersion in lakes
E'	Local term in Equ. 3.10
E_1	Horizontal Ekman number
E_0	Vertical Ekman number
e ,e ,e	Constants in Equ. 5.76
$\{F\}$	Global forcing vector
$\{F^e\}$	Element forcing vector
f	Coriolis coefficient
f_c, f_w	Constants in Equ. 5.74 and 5.75
f'	Assumed function for Equ. 3.12
G	Source/Sink term in Equ. 5.53
G'	Production of kinetic energy
$\{G\}$	Global forcing vector in FEM
$\{G^e\}$	Element forcing vector
G_0	Source/Sink term in Equ. 5.66
$\{G_0\}$	Global forcing vector in FEM

$\{G_o^e\}$	Element forcing vector
g	The acceleration of gravity
H	The curvilinear length of the streamline
H_o	Henery's law constant
H_1	The downstream part of a streamline Equ. 5.64
h	Mixing depth of water
i	Adjacent segments in Equ. 3.38
ij	Interface between segment j and i
j	Segment number in Equ. 3.38
K	Turbulent kinetic energy
K'	First order reaction coefficient
K_3	First order biodegradation rate constant
K_b	Second order biodegradation rate constant
K_f	Parameter in Equ. 2.10
K_o	Half saturation constant
K_{oc}	Octanal water partition coefficient
K_v	Mass transfer coefficient
K_p	Organic carbon partition coefficient

L	Horizontal reference dimension
L_b	Depth of active sediment bed layer
L_w	Depth of water segment
l	Characteristic mixing length in Equ. 3.38
M	Number of nodes per cross section in a river
m_0	Coefficient in Equ. 2.9
m_1, m_2	Coefficients for coordinate system
N	The shape function for FEM
NE	Number of elements in the FEM
N^*	Coefficient in Equ. 5.24
n	Coefficient in Equ. 5.25
n'	Coefficient in Equ. 2.10
n_0	Manning's roughness factor in Equ. 3.1
n_1	Empirical exponent
P_e	Local Peclet number
P_k, P_ε	Effective production of K and ε
p	Pressure intensity
p_j	Coefficient in Equ. 3.17
p_*	Nondimensional pressure intensity

Q	Water discharge
Q_0	Input discharge assigned at a specified node
Q_1, Q_2	Chemical and sediment net exchange with bed
q_i	Coefficient in Equ. 3.18
R	Surface wind stresses in complex form
$[R]$	Global stiffness matrix in the FEM
$[R^e]$	Element stiffness matrix in the FEM
R_b	Net microbial degradation rate
R_0	Rossby number
R_v	Net volatilization transfer rate
R_x, R_y	Nondimensional wind stresses
RF	Rainfall intensity
R^*	Coefficient in Equ. 5.22
R^*_r, R^*_i	The real and imaginary parts of R^*
r	Local radius of curvature in Equ. 3.1
r_0	Radius of curvature to the middle of the channel
r_j	Coefficient in Equ. 3.19

S_o	Constant slope
S_1, S_2	Empirical constants in Eqs. 3.31 and 3.32
S_j	Coefficient in Equ. 3.20
Sb	Concentration of sediment in bed
Sw	Concentration of sediment in water
s	Slip coefficient at the lake bottom
TR	Raw water turbidity
[T]	Global stiffness matrix
$[T^e]$	Element stiffness matrix
T_B	Bottom Stress
T_c	Current stress
T_x, T_y	Wind stress functions
T_{xz}, T_{bx}	Turbulent stresses in Eqs 3.34 and 3.35
T_s	Surface wind stresses
T_w	Wave stress
T*	Coefficient in Equ. 5.23
T^*_r, T^*_i	The real and imaginary parts of T*
T_o	Channel width

$U(z)$	Vertically averaged longitudinal velocity
U_o	Maximum specific growth rate
u	Horizontal velocity in x-direction
u_b	The x-component of the bottom velocity
u_m	Maximum velocity near the bottom
u_*	Nondimensional horizontal velocity
V	Depth averaged velocity in y-direction
V	Segment volume
V_s	Wind velocity at 4m above water surface
$V*$	Settling velocity of suspended solids
v	Horizontal velocity in y-direction
v_b	The y-component of bottom velocity
v_*	Nondimensional horizontal velocity
W	Horizontal velocity in complex notation
WD	Wind speed in Equ. 5.76
Wb	Deposition velocity of suspended sediment
Ws	Scour velocity of bed segment
W_1, W_2	Mass loading of chemical and sediment
w	Vertical velocity in the z-direction
w_b	Complex bottom currents
w_*	Nondimensional vertical velocity

X	Amount of sorbed chemical per mass of sediment
X_{oc}	Mass fraction of organic carbon in sediment
x	Longitudinal cartesian coordinate
x_*	Nondimensional distance in x-direction
Y	Biomass produced per mass of chemical degraded
Y_*	Nondimensional distance in y-direction
y	Lateral cartesian coordinate
Z	Lateral distance from the shoreline of a river
z	Vertical cartesian coordinate
z_*	Nondimensional distance in z-direction
ε_o	Vertical eddy viscosity coefficient
ε_1	Horizontal eddy viscosity coefficient
ε	Turbulent dissipation rate
ρ	Mean density of water
ρ_o	Mean air density
ψ	Stream function

REFERENCES

Allen, H.E., M.A. Halley, 1980. Assessment of Airborne Inorganic Contaminants in the Great Lakes. Report to the Great Lakes Science Advisory Board of the IJC. 160pp.

Akhtar, W., 1978. Study of mixing in natural streams and air agitated tanks. Ph.D. dissertation, University of Windsor, Windsor, Ontario.

Ambrose, R.B., S.I. Hill and L.A. Mulkey. (1983). User's Manual for the Chemical Transport and Fate Model TOXIWASP. USEPA, ORD, Environmental Research Laboratory, Athens, Georgia, 30613.

Aris, R., 1956. On the dispersion of a solute in a fluid flowing through a tube. Proc. Roy. Soc. (London), A, 235, p67-77.

Ayers, J. C., (1964). Currents and related problems at Metropolitan beach. Lake St.Clair, Great Lakes Res. Div. Spec. Rpt. No. 20, Univ.of Mich., Ann Arbor, Michigan.

Bauer, S. W. and Graf, W. H., 1978. Wind-induced water circulation of Lake Geneva. Proc. 10th Int. Liego Coll. Oct. Hydr. Liege.

Bell, G. L., (1980). Lake St.Clair and St.Clair and Detroit Rivers Chemical and Physical Characteristics Data for 1974. NOAA Tech. Memo. ERL, GLERL-12, National Technical Information Service, Springfield, VA, 22161.

Bengtsson, L., 1973. Mathematical model of wind-induced circulation in a lake. Proc. Int. Symp. on Hydrology of lakes, Helsinki, p 312-320.

Bengtsson, L., 1978. Wind-induced circulation in lakes. Nordic Hydrology, Vol. 9, p 75-94.

Bonham-Carter and J. H. Thomas. (1973). Numerical calculation of steady wind-driven currents in Lake Ontario and the Rochester Embayment. In Proc. 16th Conf. Great Lakes Res.. Int. Assoc. Great Lakes Res.

Bowden, K. F., Kravel, D. P., and R. E. Lewis, 1974. Some features of turbulent diffusion from a continuous source at sea. Adv. Geophys., Vol. 18A, p 315-329.

Chang, H., (1983). Expendature in Curved Open Channels. J. Hyd. Div., ASCE, Vol. 109, No. 7, pp. 1012-1022.

Cheng, R. T. and Tung, C. (1970). Wind Driven Lake Circulation by FEM. Proc. 13th Conf. Great Lakes Res. Int. Assoc. Great Lakes Res.

Christie, I., D. F. Griffiths, A. R. Mitchell and O. C. Zienkiewicz. (1976). Finite Element Methods for Second Order Differential Equations with Significant First Order Derivatives. Int. J. Num. Meth. Enging., Vol. 10, pp. 1389-1396.

Csanady, G. T., 1967. Large-scale motion in the Great Lakes. J. Geophys. Res., Vol. 72, p 4151-4162.

Csanady, G. T., 1968. Wind-driven summer circulation in the Great Lakes. J. Geophys., Res. Vol. 73, p 2579-2589.

Demuren, A. O., and Rodi, W., 1983. Side discharges into open channels: Mathematical model. J. Hyd. Div., ASCE, Vol. 109, No. 12, pp 1707-1722.

Dolan, D. M. and Bierman, V. J., 1982. Mass balance modeling of heavy metals in Saginaw Bay, Lake Huron. J. Great Lakes Res. Int. Ass. Great Lakes Res., Vol. 8, No. 4, pp 676-694.

Durham, R.W. and Oliver, B.G., 1983. History of Lake Ontario Contamination from the Niagara River by Sediment Radiodating and Chlorinated Hydrocarbon Analysis. J Great Lakes Res., Vol.9, pp160-168.

Ekman, V.W., 1905. On the influence of the earth's rotation on ocean currents. Ark. Mat. Astron. Fys. 2(11), 52p.

Environment Canada, 1983. Study in trends in Canadian environmental and water issues concerning Ontario and the Great Lakes region. L. J. D'Amore and Associates Ltd. for CCIW/IWD.

Falkenmark, M., 1973. Dynamic studies in Lake Velen. Int. Hydrological Decade. Sweden, Rep. 31.

Finlayson, B. (1972). The Method of Weighted Residual and Variational Principles. Academic Press.

Fischer, H. B., 1967. The mechanics of dispersion in natural streams. J. Hyd. Div., ASCE, HY6, p 187-216.

Fischer, H. B., 1968. Dispersion predictions in natural streams. J. Sanit. Eng. Div., ASCE, Vol.94, pp 927-943.

Fischer, H. B., 1969. The effect of bends on dispersion in streams. J. Water Resources Research, Vol. 5, No. 2., p 496-506.

Fischer, H. B., 1973. Longitudinal dispersion and transverse mixing in open channel flow. Ann. Rev. Fluid Mech. Vol. 5, pp 59-78.

Fishbein, L., 1973. Mutagens and potential mutagens in the biosphere. The Science of Total Environment, Vol. 2, p 305-371.

Frank, R., Holdrinet, M., Broun, M.E., Thomas, R.L., Kemp, A.L.W.and Jaquet, J.M., (1977).Organochlorine Insecticides and PCBs in Sediment of Lake St.Clair (1970-1974) and Lake Erie (1971).Sci. Total Environm., Vol. 8, 205.

Gallagher, R. H., J. A. Liggett and S. K. T. Chan. (1973).Finite Element Shallow Lake Circulation.J. Hyd. Div., ASCE, Vol. 99, pp. 1083-1096.

Gedney, R. T. and W. Lick, 1972.Wind driven lake currents in Lake Erie. J. Geophys. Res., Vol. 77, p 2714-2723.

Gedney, R. T., 1971.Numerical calculations of wind driven currents in Lake Erie. Ph.D. thesis, Case Western Reserve University, Cleveland, Ohio, 258 pp.

Gupta, S. K. and Tanji, K. K. (1977).Computer Program for Solution of Large, Sparce, Unsymmetric Systems of Linear Equations.Int. J. Num. Meth. Enging., Vol. 11, pp. 1251-1259.

Hamblin, P. F. (1969).Hydraulic and Wind Induced Circulation in a Model of a Great Lake.In Proc. 12th Conf. Great Lakes Res. Int. Assoc. Great Lakes Res.

Hansen, W., 1956. Theorie zur Errechnung des wasserstandes und der stromungen in randmeeren nebst anwendungen. Tellus, Vol. 8, p 287-300.

Heaps, N., 1973. Three-dimensional numerical model of trishsea. Geophys. J. R. Astr. Soc., 35.

Heinrich, J. C. and O. C. Zienkiewcz. (1977). Quadratic Finite Element Schemes for Two-dimensional Convective Transport Problems. Int. J. for Num. Meth. in Enging., Vol. 11, pp. 1831-1844.

Hinze, J.O., 1959. Turbulence. McGraw Hill Co., New York.

Hughes, T. J. (1978). A Simple Scheme for Developing Upwind Finite Elements. Int. J. for Num. Meth. in Enging., Vol. 12, pp. 1359-1365.

Hutton, M., 1982. Cadmium in the European Community a Prospective Assessment of Sources, Human Exposure and Environmental Impact, Monitoring and Assessment. Research Centre, University of London.

Ibrahim, K., and J.A. McCorquodale, 1985. Finite element circulation model for Lake St.Clair. J. Great Lakes Res., Int. Ass. Great Lakes, Vol. 11, No. 3, p 208-222.

Imam, E.H., (1981). Numerical Modelling of Rectangular Clarifiers. Thesis Presented to University of Windsor, Windsor, Ontario, in Partial Fulfillment of the Requirements for the Degree of Doctor of Philosophy.

International Joint Commission, 1980. Annual Report- A Perspective on the problem of hazardous substances in the Great Lakes Basin Ecosystem. Toronto, Ontario.

Jaworski, J.F., 1978. Effects of Lead in the Environment 1978. Quantitative Aspects, NRCC National Res. Council of Canada. No. 16736.

Jelesnianski, C.P., 1967. Numerical computations of storm surges with bottom stress. Mon. Weather Rev., Vol. 95, p 740-756.

Jirka, G. H., Abraham, G., and Harleman, D. R. F., 1975. An assessment of techniques for hydrothermal prediction. Final Report to U.S. Atomic Energy Comm. Dept. Civil Eng. MIT, R. M. Parsons Lab. Rep. No. 203.

Karickhoff, S. W., D. S. Brown, and T. A. Scott. (1979). Sorption of Hydrophobic Pollutants on Natural Sediments. Water Res. 13, pp. 241-248.

Kemp, A.L.W., R.L. Thomas, C.I. Dell and J.M. Jaquet, 1976.J. Fish Res Board Can. 33

Kikkawa, H., S. Ikeda and A. Kitagawa, (1976).Flow and Bed Topography in Curved Open Channels. J. of Hyd. Div., ASCE, Vol. 102, No. 9, pp. 1327-1344.

Kreyszing, Erwin. (1972).Advanced Engineering Mathematics.Third Edition, Wiley, New York, 333 pages.

Kuehl, D.W., E.N. Leonard, K.J. Welch and C.D. Veith, 1980.Identification of hazardous organic chemicals in fish from the Ashtabula River, Ohio and Wabash River, Indiana.Association of official analytical chemists Journal, Vol. 63, p1238-1244.

Laevastu, T. et al., 1974. A vertical integrated hydrodynamical numerical model. Part I of four reports, Env. Prediction Res. Facility, Naval Postgraduate School, Technical Note No 1-74.

Lau, Y.L. and B.G. Krishnappan, (1981).Modeling Transverse Mixing in Natural Streams.J. of Hyd. Div., ASCE, Vol. 107, pp. 207-227.

Leach, J. H. (1980).Limnological Sampling Intensity in Lake St.Clair in Relation to Distribution of Water Masses.J. Great Lakes Res. Int. Assoc. Great Lakes Res.

Liggett, J.A., 1969. Unsteady circulation in shallow homogeneous lakes. J. Hyd. Div., ASCE, Vol. 95, p 1273-1288.

Liggett, J. A. and Hadjitheodorou, C. (1969).Circulation in Shallow Homogeneous Lakes.J. Hyd. Div., ASCE, Vol. 95, pp. 609-620.

Lunde, G. and E.F. Ofstad, 1976. Determination of fat soluble chlorinated compounds in fish. Fresenius-Zeitschrift fur Analytische chemie, Vol. 282, p395-399.

Madsen, O. S., 1977.A realistic model of wind induced Ekman boundary layer. J. Phys. Oceanogr., Vol. 7, p 248-255.

Martin, H.C. and G.F. Carey, 1973.Introduction to finite-element analysis. McGraw-Hill, N.Y.

McCorquodale, J.A., E. Imam, J.K. Bewtra, Y.S. Hamdy, and J.K. Kinkead, (1983).Transport of Pollutants in Natural

Streams.Canadian J. of Civil Engineering, Vol. 10, No. 1, pp. 9-17.

McCorquodale, J.A., and K. Ibrahim, 1983. Niagara river pollution transport . IRI, Ministry of Environment, Toronto, Ont.

McCorquodale, J.A., and K. Ibrahim, 1985. Application of (k-ε) model and TOXIWASP model to the determination of HCB Distribution in the St.Clair River Ecosystem. IRI, Ministry of Environment, Toronto, Ontario.

Motz, L. H., and Benedict, B. A., 1972. Surface jet model for heated discharges. J. Hyd. Div., ASCE, Vol. 98, No. HY1, p 181-199.

Nriagu, J. O., (Ed), 1980. Cadmium in the Environment. John Wil-ey and Sons Inc., New York.

Payre, G., M. D. Brossia and J. Bazinet. (1982).An Upwind Finite Element Method Via Numerical Integration.Int. J. for Num. Meth. in Enging., Vol. 18, pp. 381-396.

Pearce, B. R. and Cooper, C. K. (1981).Numerical Circulation Model for Wind Induced Flow.J. of Hyd. Div., ASCE, Vol. 107.

Phillips, D. W. and Irbe, J. G. (1978).Lake to Land Comparison of Wind, Temperature and Humidity on Lake Ontario During the International Field Year for the Great Lakes (IFYGL). Atmos. Env. Service Rept. CLI-2-77. 4905 Dufferin St., Downsview,Ont. M3H 5T4.

Pinder, G. F. and W. G. Gray. (1977).Finite Element Simulation in Surface and Subsurface Hydrology.Academic Press.

Pugsley, C.W., Paul D.N. Hebert, Gordon W. Wood, George Brotea and Taras W. Obal, 1985. Distribution of Contaminants in Clams amd Sediments From Huron-Erie Corridor. I-PCBs And Octachlorostyrene.J. Great Lakes Research, Int. Ass. Great Lakes, Vol. 11, No.3, p 275-289.

Quinn, F.H., and J.C. Hagman. (1977).Detroit and St.Clair Transient Models.NOAA Tech. Memo. ERL GLERL-14, National Technical Information Service, Springfield, Va. 22151. 45pp.

Rao, P. S. C. and J. M. Davidson., (1980). Estimation of Pesticide Retention and Transformation Parameters Required in nonpoint source Pollution Models. In: Environmental Impact of Nonpoint Source Pollution, M. R. Overcashand J. M. Davidson, Eds. Ann Arbor Science, Ann Arbor, MI. pp. 23-67.

Rastogi, A.K. and Rodi, W., (1978). Predictions of Heat and Mass Transfer in Open Channels. J. of Hyd. Div., ASCE, No. HY3, pp. 397-420.

Richardson, W. L., V. E. Smith, and R. Wethington, 1982. Dynamic mass balance of PCB and suspended solids in Saginaw Bay A Case Study. In: Proceedings of workshop on physical Behaviour of PCBs in the Great Lakes. D. Mackay. (Ed).

Roach, P. J., (1976). Computational Fluid Dynamics. Hermosa Publishers, Albuquerque.

Rodi, W., (1980). Turbulence Models and Their Application in Hydraulics. A State of Art Review, IAHR.

Saffman, P. G., 1977. Problems and progress in the theory of turbulence. Proceedings of structure and mechanics of turbulence II, Springer Verlag, Berlin, p 273-306.

Salmon, J. R., J. A. Liggett and R. H. Gallagher. (1980). Dispersion Analysis in Homogeneous Lakes. Int. J. for Num. Meth. in Enging., Vol. 15, pp. 1627-1642.

Shirazi, M., and Davis, L., 1974. Workbook of thermal plume prediction. Vol. 2, Surface Discharges, Thermal Pollution Branch, Pacific Northwest, Environmental Research Laboratory, USEPA, Corvallis, Ore.

Schwab, D. J. and J. A. Morton. (1984). Estimation of Overlake Wind Speed from Overland Wind Speed; A Comparison of Three Methods. J. Great Lakes Res. Int. Assoc. Great Lakes Res.

Schwab, D. J., Bennentt, J. R. and Jessup, A. T. (1981). A Two Dimensional Lake Circulation Modeling System. NOAA Tech. Memo. ERL, GLERL-38, National Technical Information Service, Springfield, VA, 22161, 79 pp.

Sheng, Y.P., and W. Lick, 1979. The transport and resuspension of sediments in a shallow lake. J. Geoph. Res., Vol. 84, No. C4, p 1809-1826.

Simons, T. J. (1980). Circulation Model of Lakes and Inland Seas. Can. Bull. Fish. Aquat. Sci., 203, Ottawa, Canada.

Simons, T. J. (1971). Development of Numerical Models of Lake Ontario. Proc. Conf. Great Lakes Res. IAGLR. 14, pp. 654-669.

Sternberg, R.W., 1972. Predicting initial motion and bed load transport of sediment particles in the shallow marine environment. In Shelf Sediment Transport, edited by D.P.Swift, Dowden, Hutchin, Ross, Stroudsburg, Pa.

Stolzenbach, K., and Harleman, D. R. F., 1973. Three dimensional heated surface jets. Water Resources Reserch, Vol. 9, No. 1, pp 129-137.

Stone, H. L., and Brain, P. L. T., (1963). Numerical Solution of Convective Transport Problems. American Institute of Chemical Engineering J. Vol. 9, pp 681-688.

Szabo, B., and Lee, G. C. (1969). Derivation of Stiffness Matrices for Problems in Plane Elasticity by Galerkin's Method. Int. J. for Num. Meth. in Enging., Vol. 1, pp. 301-310.

Taylor, G. I., 1921. Diffusion by continuous movements. Proc. London Math. Soc., A-20, pp 196-211.

Taylor, G. I., 1953. Dispersion of soluble matter in solvent flowing slowly through a tube. Proc. Roy. Soc.(London), A, 219, p 186-203.

Taylor, G. I., 1954. The dispersion of matter in turbulent flow through a pipe. Proc. Roy. Soc.(London), A, 223, p 446-468.

Ten Noever de Brouw,M. C., J. H. Koeman and R.H. deVos, 1969. Chlorinated biphenyls in fish, mussels and birds from the river Rhine and the Netherlands coastal area. Nature, p221-1126.

Thomann, R.V. and J. A. Mueller (1983). Steady State Modeling of Toxic Chemicals-Theory and Applicationto PCBs in the Great Lakes and Sagina Bay. In: Mackay et al., (Eds.).

Thomas, J. H., 1975. A theory of steady wind driven currents in shallow water with variable eddy viscosity. J. Phys. Oceanogr., Vol. 5, p 136-142.

Thornley, S., and Hamdy Y., 1984. An Assessment of the bottom fauna and sediments of the Detroit River. Ontario Ministry of the Environment Report, Toronto, Ontario.

US Army Coastal Engineering Research Centre, 1977. Shore Protection Mannual. Vol. 1, Fort Belvoir, Va.

U.S Army Corps of Engineers. (1983). Surface Velocities and Directions in St.Clair River. U.S Army, Detroit District, Great Lakes Hydraulics and Hydrology Branch.

U.S Army Corps of Engineers. (1974). River Current Studies in Detroit River. U.S Army, Detroit District, Great Lakes Hydraulics and Hydrology Branch.

USEPA, 1978. Cadmium Additions to Agricultural Lands Via Commercial Phosphate Fertilizers. A Preliminary Assessment.

Weber, J.B. and Mrozek, 1979 Polychlorinated biphenyls, phytotoxicity, absorption and translocation by plants and inactivation by activated carbon. Bull., Environ. Contamin. Toxical. Vol. 23, p 412-417.

Welander, P., 1959a. Wind Action on a shallow Seas. Tellus, Vol. 9, No. 1, pp. 45-52.

Welander, P., 1959b On the vertical integrated mass transport in the oceans. In B. Bolin (Ed), p 95-101, The atmosphere and the sea in motion. The Rockefeller Inst. Press.

Wu, J., 1969. Wind stress and surface roughness at air sea interface. J. Geophys. Res. Vol. 74, p 444-455.

Yotsukura, N., and Cobb, E. D., (1972). Transverse Diffusion of Solutes in Natural Streams. United States Geological Survey, Professional Paper 582-C.

Yotsukura, N., and Sayre, W. W., (1976). Transferse Mixing in Natural Channels. Water resources Research, Vol. 12, No. 4, pp. 695-704.

Zienkiewicz, O.C., 1977 The finite element method. McGraw Hill Book Company (UK) Limited.

VITA AUCTORIS

The Auther was born on the twenty third of November, 1952, in Port Said, Egypt. In June of 1975 he graduated from Cairo University with his Bachelor's degree in Civil Engineering. In August of the same year he was appointed as an instructor of Civil Engineering at Hydraulics and irrigation Department, Faculty of Engineering, Cairo University, Egypt. Thereupon, he participated as a Graduate Research Assistant in the River Nile Basin System Simulation Studies under Cairo University and Massachusetts Institute of Technology Technological Planning Program.

In June 1980, he graduated with a M.A.Sc. in Civil Engineering, Cairo University. Following this, he shared responsibility as a hydrologist in a comprehensive study to prepare a Flood Prevention Scheme in the Upper Region of Egypt, under the United Nations Development Program (UNDP).

In January of 1982 he came to Canada, and enrolled in a programme leading to the degree of Doctor of Philosophy at University of Windsor, Windsor, Ontario, Canada.